Synthesis and Characterization of M@SiCN Catalysts and their Application in the Synthesis of Renewable Products

Dissertation

zur Erlangung des akademischen Grades
eines Doktors der Naturwissenschaften (Dr. rer. nat.)
im Fach Chemie der Fakultät Biologie, Chemie und Geowissenschaften
der Universität Bayreuth

vorgelegt von

M.Sc. Daniel Forberg

geboren in Karl-Marx-Stadt

Bayreuth, 2016

Die vorliegende Arbeit wurde in der Zeit von November 2012 bis März 2016 in Bayreuth am Lehrstuhl Anorganische Chemie II unter Betreuung von Herrn Professor Dr. Rhett Kempe angefertigt.

Vollständiger Abdruck der von der Fakultät für Biologie, Chemie und Geowissenschaften der Universität Bayreuth genehmigten Dissertation zur Erlangung des akademischen Grades eines Doktors der Naturwissenschaften (Dr. rer. nat.).

Dissertation eingereicht am:	08.04.2016
Zulassung durch die Promotionskommission:	13.04.2016
Wissenschaftliches Kolloquium:	21.11.2016

Amtierender Dekan: Prof. Dr. Stefan Schuster

Prüfungsausschuss:

Prof. Dr. Rhett Kempe	(Erstgutachter)
Prof. Dr. Josef Breu	(Zweitgutacher)
Prof. Dr. Peter Stohriegl	(Vorsitz)
Prof. Dr. Frank Hahn	

„Winners must have two things: Definite goals and burning desire to achieve them."

(Brad Burden)

Für meine Eltern, Heike Knell und Roman Forberg, und meine Oma, Ingrid Fischer.

Table of Contents

Abbreviations IX

1. Zusammenfassung 1

2. Summary 5

3. Introduction 9

4. Synopsis 19

5. Individual Contribution to Joint Publications 35

6. The Synthesis of Pyrroles via Acceptorless Dehydrogenative Condensation of Secondary Alcohols and 1,2-Amino Alcohols Mediated by a Robust and Reusable Catalyst Based on Nanometer-sized Iridium Particles 39

6.1 Introduction 40

6.2 Results and Discussion 41

6.3 Conclusions 45

6.4 Experimental Section 46

6.5 References 46

6.6 Supporting Information 50

7. The Sustainable Synthesis of Indoles, Carbazoles, Quinolines and Acridines via Catalytic Condensation of Phenols and Aminoalcohols or Aminophenols 101

7.1 Introduction 102

7.2 Results and Discussion 104

7.3 References 110

7.4 Supporting Informations 113

8. Single-Catalyst High Weight% Hydrogen Storage in a N-Heterocycle Synthesized From Lignin Hydrogenolysis Products and Ammonia 235

8.1 Introduction 236

8.2 Results and Discussion 237

8.3 Conclusions 241

8.4 Experimental Section 242
8.5 References 243
8.6 Supporting Informations 247
9. List of Publications 265
10. Acknowledgements 267
11. Declaration/Erklärung 271

Abbreviations

12H-NEC	dodecahydro-*N*-ethylcarbazole
ADC	acceptorless dehydrogenative condensation
$Ap^{TMA}H$	(4-methyl-pyridin-2-yl)-(2,4,6-trimethyl-phenyl)-amine
$Ap^{TMS}H$	4-methyl-2-[(trimethylsilyl)-amino]-pyridine
a.u.	arbitrary units
BET	Brunauer-Emmett-Teller
Bn	benzyl
CF-HP ^{129}Xe NMR	continuous-flow, hyperpolarized ^{129}Xe NMR
cod	cis-1,5-cyclooctadiene
DCP	dicumylperoxide
EDX	energy dispersive X-ray spectroscopy
Et	ethyl
FT-IR	fourier transform infrared spectroscopy
GC	gas chromatography
GC-MS	gas chromatography coupled with mass spectroscopy
HAADF	high angle annular dark field
HR-TEM	high resolution transmission electron microscopy
HTT1800	commercially available polysilazane precursor
ICP-OES	inductively coupled plasma optical emission spectrometry
i-Pr	*iso*-propyl
Ir/Al_2O_3	aluminium oxide supported iridium
$[IrAp^{TMA}(cod)]$	idium[(4-methyl-pyridin-2-yl)-(2,4,6-trimethyl-phenyl)amine-(cycloocta-1,5-diene)]
Ir/C	carbon supported iridium

$Ir/CaCO_3$	calcium carbonate supported iridium
Ir@SiCN	silcon carbonitride supported iridium
KO^tBu	potassium *tert*-butoxide
LOHC	liquid organic hydrogen carrier
M@SiCN	silicon carbonitride supported metal
Me	methyl
n-Bu	*n*-butyl
NEC	*N*-ethylcarbazole
NMR	nuclear magnetic resonance
OMe	methoxy
$PdAp^{TMS}_2$	palladium-bis[4-methyl-*N*-(trimethylsilyl)-2-pyridinaminato]
Pd/C	carbon supported palladium
PDC	polymer derived ceramic
Pd@SiCN	silicon carbonitride supported palladium
Pd/SiO_2	silica supported palladium
Ph	phenyl
ppm	parts per million
Ref.	reference
Ru/Al_2O_3	aluminium oxide supported ruthenium
Ru/C	carbon supported ruthenium
Ru@SiCN	silicon carbonitride supported ruthenium
RT	room temperature
SI	supporting information
SiCN	silicon carbonitride
t	time
thf	tetrahydrofuran

TEM	transmission electron microscopy
TGA	thermal gravimetric analysis
wt.%	weight-%
XRD	X-ray diffraction

1. Zusammenfassung

Ziel dieser Arbeit war die Synthese, Charakterisierung und katalytische Anwendung von neuen Metall@SiCN-Katalysatoren. Mittels Salzmetathese und Methanoleliminierung wurden zunächst geeignete Metall-Aminopyridinatokomplexe synthetisiert und diese anschließend mit einem kommerziell erhältlichen Polysilazan zu einem metallmodifizierten, präkeramischen Polymer vernetzt. Durch Pyrolyse unter Stickstoffatmosphäre bei 750 - 1100 °C wurden die jeweiligen M@SiCN-Katalysatoren erhalten (**Abb. 1-1**). Die Natur und die Größe der erhaltenen Nanopartikel waren sowohl von der Pyrolysetemperatur als auch vom Metallgehalt abhängig. Die Charakterisierung der metallhaltigen, keramischen Katalysatoren erfolgte hauptsächlich mittels Pulverdiffraktometrie (XRD), Transelektronenmikroskopie (TEM) und energiedispersiver Röntgenspektroskopie (EDX).

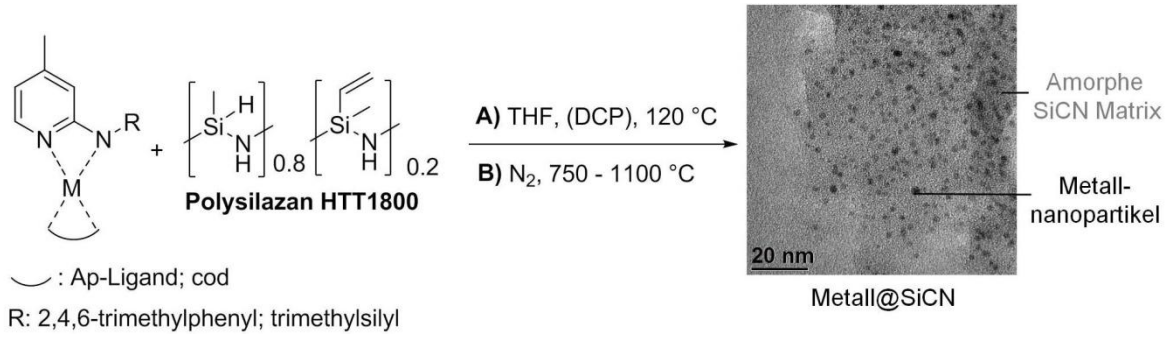

Abb. 1-1: Allgemeine Syntheseroute für die Herstellung von Metall@SiCN-Katalysatoren

Die Überlegenheit von Siliziumcarbonitridmaterialien gegenüber herkömmlichen Katalysatorträgermaterialien zeichnet sich vor allem durch eine hohe mechanische Stabilität und Temperaturbeständigkeit, sowie eine große chemische Robustheit, vor allem im basischen Milieu, aus. Ausgehend von 1,2-Aminoalkoholen und sekundären Alkoholen wurde an unserem Lehrstuhl vor Kurzem eine neue und nachhaltige Pyrrolsynthese entwickelt, welche von einem homogenen Iridiumkatalysator im basischen Milieu katalysiert wird. Um dieses neue Synthesekonzept auf wiederverwendbare Katalysatoren zu überführen, wurde ein neuer Iridiumkatalysator basierend auf dem Trägermaterial Siliziumcarbonitrid hergestellt. Trotz einer hohen Pyrolysetemperatur von 1100 °C und einem hohen Metallgehalt von 18.9 wt.% konnten Iridiumnanopartikel mit einer mittleren Partikelgröße von 1.3 nm generiert werden. Mit diesem neuen Ir@SiCN-Katalysator wurden nach der eben beschriebenen Syntheseroute eine Vielzahl von 2,3-substituierten, 2,3,5-substituierten und polyzyklischen

Pyrrolen dargestellt. In der Summe konnten 23 Pyrrolderivate mit einer akzeptablen Toleranz gegenüber funktionellen Gruppen in sehr guten Ausbeuten von bis zu 93 % isoliert werden. Im Vergleich zu kommerziell erhältlichen, heterogenen Iridiumkatalysatoren zeichnete sich der Ir@SiCN-Katalysator durch eine höhere Aktivität und eine signifikant bessere Wiederverwendbarkeit aus.

Durch Hydrogenolyse von ligninhaltiger Biomasse können verschieden substituierte Phenole erhalten werden, deren nachhaltige Funktionalisierung bzw. Weiterverarbeitung noch immer eine Herausforderung darstellt. Daher haben wir ein Synthesekonzept entwickelt, welches man als Erweiterung der eben beschriebenen Pyrrolsynthese auffassen kann. Phenole werden dabei in einem Dreistufenprozess mit Aminoalkoholen oder Aminophenolen zu Indolen, Carbazolen, Quinolinen und Acridinen kondensiert. Hierfür wurde zuerst ein neuer Nanokompositkatalysator basierend auf der Bildung von sub-nanometer großen Rutheniumpartikeln (Ru@SiCN) synthetisiert. Mit diesem war die milde Hydrierung von Phenolderivaten möglich. Die jeweiligen Zyclohexanole wurden anschließend mittels modifizierten Literaturvorschriften zu Tetrahydropyrrolen, -carbazolen, -pyridinen und -acridinen umgesetzt. Durch eine akzeptorfreie Dehydrierung dieser Produkte konnten die entsprechenden Indole, Quinoline, Carbazole und Acridine generiert werden. Hierfür wurde ein neuer Pd@SiCN-Katalysator mit einer mittleren Palladiumpartikelgröße von 1.8 nm entwickelt, welcher im Vergleich zu kommerziell erhältlichen, heterogenen Pd-Katalysatoren eine deutlich höhere Aktivität aufzeigte. Es konnten 18 Indole, 3 Carbazole, 5 Quinoline und 6 Acridine in sehr guten Ausbeuten von bis zu 93 % isoliert werden. Auch eine Eintopfreaktion, bei welcher der jeweilige Katalysator von der Reaktionsmischung abgetrennt und für die nächste Reaktion durch einen anderen ersetzt wurde, konnte erfolgreich durchgeführt werden. Die Nachhaltigkeit dieser Reaktionssequenz drückt sich nicht nur im Einsatz von wiederverwendbaren Katalysatoren, sondern auch durch die Wasserstoffneutralität aus. Der im ersten Schritt zur Hydrierung benötigte Wasserstoff kann in den zwei darauffolgenden Schritten wiedergewonnen werden.

In einem simultanen Prozess wurde analog zu der in **Abb. 1-1** dargestellten Syntheseroute ein Pd_2Ru@SiCN-Komposit generiert. HR-TEM, HAADF und EDX Untersuchungen bewiesen die Existenz von Pd-Partikeln mit einer durchschnittlichen Partikelgröße von 1.6 nm. Die metallische Rutheniumphase hingegen war homogen verteilt und konnte sowohl in der Matrix als auch bei den Pd-Partikeln nachgewiesen werden. Aufgrund der außerordentlich guten Hydrier- und Dehydrierfähigkeit dieses Katalysatorsystems war eine Anwendung in der

Wasserstoffspeicherung mit der LOHC-Methode (Liquid Organic Hydrogen Carrier) aussichtsreich. Nach erfolgter Systemoptimierung konnte *N*-Ethylcarbazol (NEC) unter milderen Bedingungen als in der Literatur beschrieben zu Dodecahydro-*N*-ethylcarbazol (12H-NEC) hydriert werden. Dieses wurde anschließend akzeptorfrei zu NEC dehydriert. Mit nur einem einzigem Katalysatorsystem konnten so in drei aufeinander folgenden Zyklen reversibel > 5.5 wt.% (> 95 %) Wasserstoff gespeichert werden. Um die Wasserstoffspeicherkapazität zu erhöhen, wurde Phenazin in einem Zweistufenprozess bestehend aus der dehydrierenden Kondensation von 1,2-Zyclohexandiol, ein Hauptprodukt der Hydrogenolyse von Lignin, und Ammoniak sowie einer akzeptorfreien Dehydrierung synthetisiert. Unter Verwendung des Pd_2Ru@SiCN-Katalysators konnte in sieben aufeinanderfolgenden Speicherzyklen Wasserstoff mit 5.8 - 7.1 wt.% gespeichert werden, was einer Effektivität > 80 % entspricht.

2. Summary

The aim of this thesis was the preparation, characterization, and catalytic application of novel metal@SiCN catalysts. For this purpose, aminopyridinato complexes were synthesized by methanol elimination or salt metathesis reactions. The generated complexes were mixed with the commercially available polysilazane HTT1800. A metal modified polysilazane was obtained after crosslinking. The pyrolysis of these materials at 750 – 1100 °C under nitrogen atmosphere resulted in the formation of metallic nano particles embedded in an amorphous silicon carbonitride matrix (**Fig. 2-1**). The size and nature of the metallic nanoparticles were dependend on the metal to silicon ratio and on the pyrolysis temperature. The materials were characterized by powder X-ray diffraction (XRD), transelectron microscopy (TEM), and energy dispersive X-ray spectroscopy (EDX).

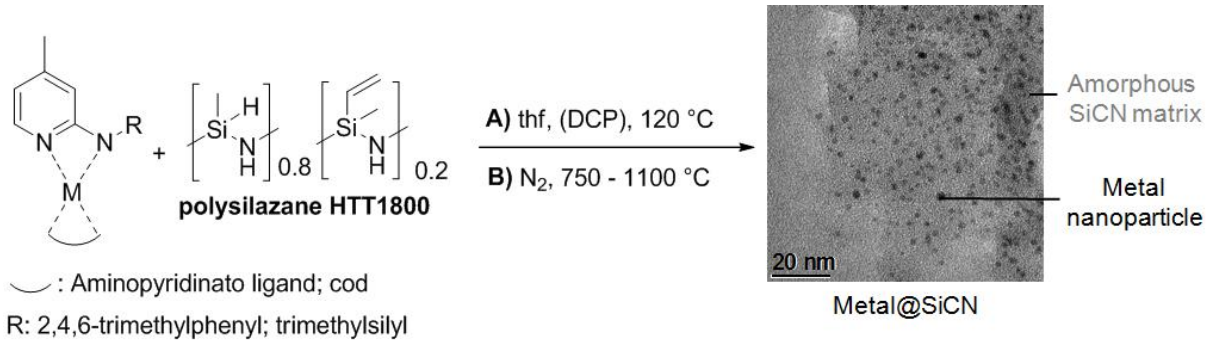

Fig. 2-1: General synthesis route for metal@SiCN catalysts

The comparison with other commercial support materials for heterogeneous catalysts exposed the benefits of SiCN materials like high mechanical and temperature resistance as well as the outstanding chemical inertness especially in strong basic media. A novel and sustainable pyrrole synthesis starting from 1,2-amino alcohols and secondary alcohols catalyzed by a homogeneous iridium catalyst under basic conditions was developed by our group recently. To extend this novel reaction concept towards reusable catalysts, we synthesized a novel silicon carbonitride composite material based on iridium nanoparticles. We were able to generate Ir nanoparticles with a median diameter of 1.3 nm despite a high pyrolysis temperature of 1100 °C and a high metal loading of 18.9 wt.%. This novel Ir@SiCN catalyst was successfully applied in the synthesis of 2,5-substituted and 2,3,5-substituted as well as polycyclic pyrroles. In sum, 23 pyrrole derivatives with an interesting functional group tolerance could be isolated in excellent yields up to 93 %. Furthermore, the Ir@SiCN catalyst

is superior to other commercially available, heterogeneous Ir catalysts especially in terms of reusability.

Phenols are the main lignin hydrogenolysis products and their sustainable functionalization is still challenging. Thus, we developed a novel three step synthesis route which makes a variety of different substance classes accessible by the catalytic functionalization of phenols with amino alcohols or aminophenols. For the efficient and mild hydrogenation of phenols, a novel nano composite catalyst based on silicon carbonitride and sub-nanometer sized ruthenium particles was generated. The prepared cyclohexanols were coupled to tetrahydropyrroles, -carbazoles, -pyridines, and -acridines by modification of literature methodologies using homogeneous and heterogeneous iridium catalysts. The acceptorless dehydrogenation of the cyclohexyl ring(s) attached to the pyrrole or pyridine ring lead to the formation of the corresponding indoles, quinolines, carbazoles, and acridines. Since commercially available, heterogeneous Pd catalysts showed a low activity in catalyzing this reaction, we developed a suitable Pd@SiCN catalyst with a median Pd particle diameter of 1.8 nm. The broad application of this reaction sequence was demonstrated by the isolation of 18 indoles, 3 carbazoles, 5 quinolines, and 6 acridines in excellent combined yields up to 93 % for the final product. Moreover, we proofed the advantageous utilization of reusable catalysts by the performance of a one-pot reaction in which the catalyst was separated from the mixture and the appropriate catalyst for the next reaction was added. The great catalyst reusability as well as the hydrogen neutrality, meaning the hydrogen can be used prior to its generation, emphasizes the sustainability of this synthesis route.

The simultaneous mixture of two metal complexes (Ru and Pd) with the polysilazane and subsequent pyrolysis resulted in the formation of a Pd_2Ru@SiCN composite material. HR-TEM, HAADF and EDX investigations proofed the existence of metallic Pd nano particles with a median diameter of 1.6 nm. The Ru phase was distributed homogeneously and could be detected in the SiCN matrix as well as at the Pd particles. We searched for an application in hydrogen storage with the LOHC (Liquid Organic Hydrogen Carrier) method, since the prepared catalyst combined an excellent hydrogenation ability with great dehydrogenation skills. After optimization of the reaction conditions, we were able to hydrogenate *N*-ethylcarbazole (NEC) under milder conditions as described in literature. The acceptorless dehydrogenation of dodecahydro-*N*-ethylcarbazole (12H-NEC) could be performed at conditions similar to literature. The reversible hydrogen storage with the NEC/12H-NEC system using only one reusable catalyst was performed three times with a hydrogen storage

capacity > 5.5 wt.% (> 95 %). Next, we searched for other N-heterocyclic substances to increase the hydrogen storage capacity. Phenazine could be synthesized sustainably in a two step procedure starting from 1,2-cyclohexanediol, a main hydrogenolysis product of lignin. The coupling of 1,2-cyclohexanediol with ammonia mediated by the Ir@SiCN catalyst and a subsequent dehydrogenation using either Pd@SiCN or Pd_2Ru@SiCN gave phenazine in 74 % yield. The application of phenazine as novel hydrogen carrier was proofed by seven consecutive hydrogen storage cycles using the Pd_2Ru@SiCN catalyst. A storage capacity of 5.8 - 7.1 wt.%, which is synonymous to an storage effectivity of > 80 %, could be achieved.

3. Introduction

Polymer derived ceramic materials (PDC´s) have attracted much interest during the past decades due to their excellent material properties. This material class can be synthesized from preceramic organosilicon polymers containing the elements Si, C, N, O, B, and Al. The result is a nano composite material with binary up to pentanary structures. A classification in oxide ceramics (containing oxygen atoms) and non-oxide ceramics (no presence of oxygen atoms) is established in the literature. The non-oxide PDC´s posses a high resistance towards crystallization and decomposition, an outstanding stability against mechanical creep, corrosion and oxidation as well as an excellent thermal and chemical robustness.[1] Thereby, the molecular synthesis pathway, e.g. for silicon carbonitrides, is an essential benefit (**Fig. 3-1**). The condensation of molecular nitrogen and silicon compounds leads to oligomers or polymers. Their crosslinking reaction and pyrolysis under inert gas atmosphere results in the formation of amorphous SiCN materials.[2] Thus, the final ceramic properties like composition, microstructure, and phase distribution can be adjusted by the molecular structure and the type of the applied polymer (polysilazane).[1a,b] Moreover, the use of silicon-based polymers enables the production of ceramic components such as monoliths, fibers, membranes, coatings, and powders.[3] Non-oxide silicon carbonitride materials can be nano-structured by the use of polyolefin or block copolymer templates or synthesis, by hard and soft as well as by self-sacrificial template methods resulting in the generation of porous materials with a high surface area.[4]

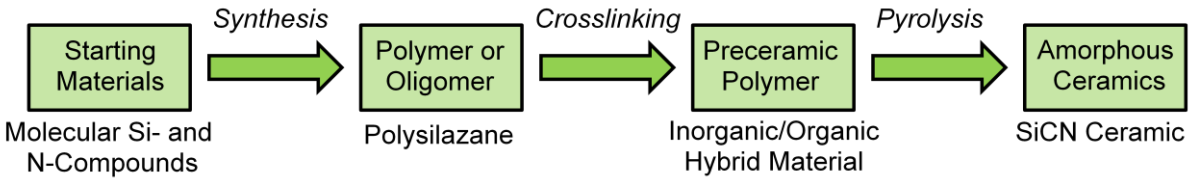

Fig. 3-1: Molecular synthesis route to polymer derived SiCN materials[5]

The incorporation of metallic or intermetallic particles or phases into a silicon carbonitride material leads to a new material class, which combines the properties of ceramics with the characteristics of metals. Thus, improvements in the field of thermic and electric conductivity[6], magnetism[7] or catalytic activity[8,4i] can be expected for such nano composites.[9] The synthesis of transition metal containing non-oxide polymer derived ceramic materials can be achieved by three different techniques.[10] The blending of the

polymer precursor with metal or metal oxide powders limits the size of the metallic particles by the particle size of the used powder. The synthesis from metallopolymers results in the formation of metallic clusters. The metal atoms are bonded to the polymer and thus the particle size can be varied by the nature and amount of the metallic component. Ferrocene-functionalized ceramic precursors have been described as one example but they suffer from several drawbacks like general applicability due to the restricted variety of available precursors and time-consuming synthesis. The modification of the precursor polymers by coordination compounds (metal complexes) seems to be more feasible.[8e] Nevertheless, the selection of the suitable coordination compound is crucial. Metal carbonyls are toxic and volatile and metal amides or alkyls suffer from sufficient stability, which goes along with a decrease in the reaction potential towards the polymer precursor as well as from a lack of availability for late transition metals.[8e] The application of aminopyridinato complexes[11] includes a lot of advantages like the good compatibility to polysilazanes and high solubility in organic solvents. Due to the low coordination numbers and strained binding modes, these complexes offer a high reactivity with respect to crosslinking and/or transmetalation to the polysilazane. Furthermore, they are easily available for almost all transition metals and are accessible in multigram scale. The elemental composition of the aminopyridinato ligands and the polysilazanes are identical and thus a contamination of the final ceramic with "alien" atoms is excluded a priori. In summary, the modification of polysilazanes with aminopyridinato complexes offers a safe and general approach for the generation of metal nanoparticles in a silicon carbonitride matrix.

Due to the robust nature of SiCN materials and the possible generation of small metal nanoparticles, the application of such nano composites as heterogeneous catalysts seems to be feasible and was intensively investigated during the last years. The whole synthesis concept and process was developed with the metal copper and the formed Cu@SiCN materials were applied in the oxidation of cycloalkanes.[8a] Pd_2Si nanoparticles could be generated by pyrolysis at 1100 °C and were proofed to be catalytically active in the selective hydrogenation of ketones and aldehydes to the corresponding alcohols.[8b] The incorporation of nickel resulted in simultaneous formation of nickel nanoparticles and microporosity at a pyrolysis temperature of 600 °C to form nickel modified polymer carbon hybrides. The porosity and phase distribution was investigated by solid state NMR and CF-HP ^{129}Xe NMR spectroscopy and the materials were highly active in the selective hydrogenation of alkynes to alkenes.[8c] The utilization of polyethylene as sacrificial filler accesses the formation of porous SiCN materials, active metallic nanoparticles, and, depending on the used metal, turbostratic or

multiwalled carbon nanotubes at the same time.[8d] SCHWARZ *et al.* synthesized a mesoporous SiCN containing material by impregnation of activated carbon and subsequent oxidative removal of the carbon template. The impregnation with Pd resulted in a catalyst, which is very efficient in the total oxidation of methane.[8e] Another mesoporous SiCN catalyst for methane oxidation was prepared by the WIESNER group using poly(isoprene-*block*-dimethylaminoethylmethacrylate) as structure-directing agent.[4i]

The increase in air pollution and the occurrence of global warming due to continuously growing, anthropogenic CO_2 emissions let Germany try to hold the pioneering task in the energy revolution of the western countries. Up to now, the percentage of fossil fuels in the energy consumption of Germany still amounts 80 % with mineral oil as the only decreasing feedstock regarding short-term availability.[12] Therefore, the current fossil fuel based energy technologies have to be changed towards a more sustainable way of living. Most of the renewable energy sources like solar, wind, and geothermal energy are suffering from an intermittent character, which hinders the integration in our current energy supply system.[13] As a consequence, new energy storage systems have to be developed to satisfy the changing supply and demand of energy. Due to its high energy density, which is about three times higher than that of petroleum, hydrogen is claimed as a possible and environmentally friendly energy carrier since 40 years.[14] The low density of molecular hydrogen results in a challenging storage since there are significant technical and safety concerns regarding cryogenic liquid and compressed hydrogen.[15] The physical storage of hydrogen in porous materials like metal organic frameworks usually requires high hydrogen pressures and sufficient storage can only be achieved at low temperatures, which limits the application and leads to an increase in costs.[15b] The storage in molecular hydrogen carriers offers a great diversity of potential compounds (see chapter 8). Here, liquid organic hydrogen carriers (LOHC) are promising since the hydrogen can be bonded and released reversibly without CO or CO_2 emissions and the liquid nature enables the usage of the existent transportation system for fossil fuels.[13,16] N-Heterocycles seem to be an interesting substance class. They possess a sufficient storage capacity and the presence of nitrogen atoms allows lower dehydrogenation temperatures as compared to the corresponding cycloalkanes.[17] The reversible hydrogen storage with homogeneous catalysts was successfully applied using 2,6-dimethylpyridine[18] and 2,6-dimethyl-1,5-naphthyridine[19] as substrates. Regarding the sustainability aspect, the application of one reusable, heterogeneous catalyst system for both, hydrogenation and dehydrogenation reactions, would be reasonable. Furthermore, a suitable N-heterocycle

possessing a high storage capacity and a sustainable production, e.g. from lignocellulosic biomass, would be essential.

However, not only the future energy supply but also the production of fine chemicals may be critical with mineral oil running out. At the time, the chemical industry is mainly based on hydrocarbons and oil crack products coming from fossil fuels and chemicals are produced by oxidation and functionalization steps. Therefore, new synthesis concepts based on novel and renewable feedstocks have to be developed to replace fossil fuels. Here, the most promising feedstock is biomass, especially lignocellulose, which is abundantly available, inexpensive, and not in competition to the food chain.[20] The transformation of biomass into pyrolysis oils or bio-oils and upgrading by catalytic hydrogenation and hydrogenolysis steps generates a number of different platform chemicals like alcohols, carboxylic acids or aldehydes.[21] The defunctionalization and deoxygenation of these highly oxidized chemicals will be an important task for future chemists (**Fig. 3-2**).[22]

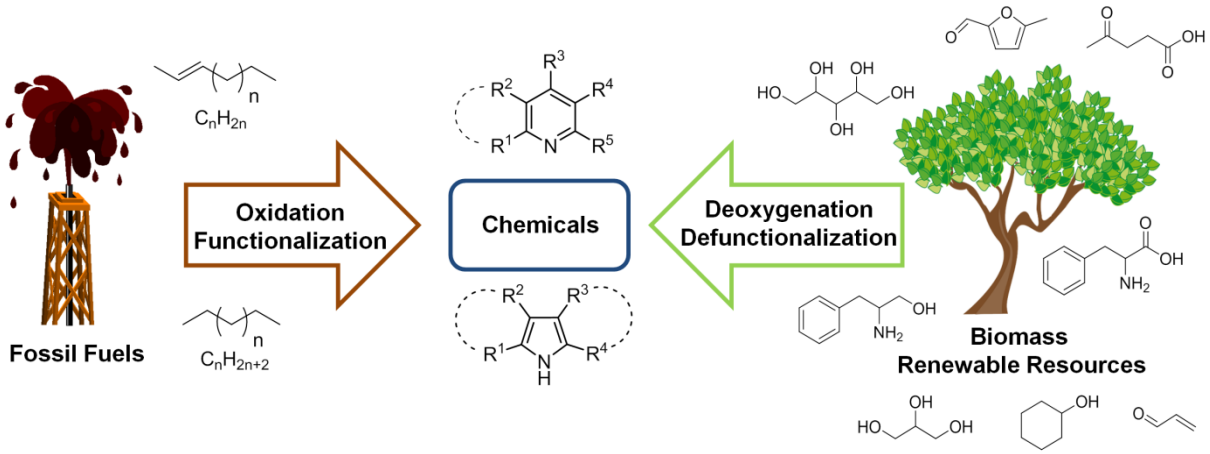

Fig. 3-2: Production of fine chemicals from fossil fuels and renewable resources

With this background, a promising catalytic synthesis concept called “borrowing hydrogen” or “hydrogen autotransfer” (BH/HA) was developed to react alcohols with amines to form an alkylated amine.[23] Using homogeneous catalysts, unreactive alcohols are transferred to the corresponding carbonyl compounds, which condensates with an amine to form the imine. Further hydrogenation with the hydrogen parked at the catalyst gives the functionalized amine product (**Fig. 3-3, A**).[24] The suppression of the final hydrogenation step by elimination of the molecular hydrogen gives access to the imine intermediates.[25] When amino alcohols are used as amine component, further condensation and dehydrogenation steps can lead to the formation of N-heteroaromatic products (**Fig. 3-3, B**). In summary, this novel synthesis concept links alcohols with 1,2-amino alcohols to form pyrroles with liberation of hydrogen

and water as useful and non-toxic by-products.[26] The application of 1,3-amino alcohols instead of 1,2-amino alcohols generates pyridines and quinolines with the liberation of three equivalents of hydrogen.[27] Pyrimidines can be synthesized from alcohols and ammonia generating up to four equivalents of H_2.[28] For such transformations, homogeneous iridium and ruthenium catalysts have been used, which may have the advantage of a high activity and great functional group tolerance but suffer from a lack of reusability.

The main topic of this thesis was the extension of such sustainable synthesis concepts towards reusable catalyst systems, which is challenging due to the strong basic conditions required. The valorization of alcohols derived from renewable resources to fine chemicals (e.g. pyrroles and pyridines) as well as the storage of hydrogen in a N-heterocycle synthesized from a main lignin hydrogenolysis product using robust and reusable M@SiCN catalysts was successfully applied.

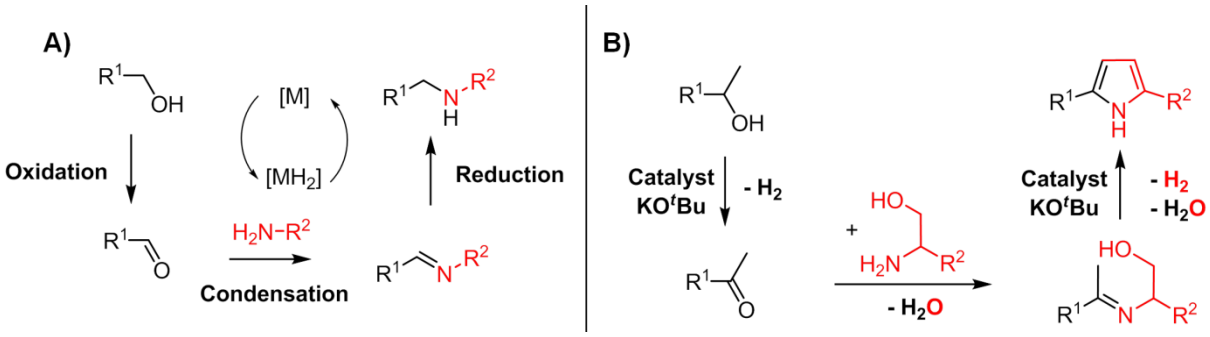

Fig. 3-3: Novel reaction concepts for the valorization of alcohols with amines and amino alcohols. A) BH/HA mechanism**. B)** Sustainable pyrrole synthesis from secondary alcohols and 1,2-amino alcohols.

[1] a) Polymer derived Ceramics - From Nano-Structure to Applications, ed. P. Colombo, R. Riedel, G. D. Soraru, H.-J. Kleebe, DEStech Publications, Pennsylvania, 2010. b) P. Colombo, G. Mera, R. Riedel, G. D. Soraru, *J. Am. Ceram. Soc.* **2010**, *93*, 1805. c) E. Ionescu, H.-J. Kleebe, R. Riedel, *Chem. Soc. Rev.* **2012**, *41*, 5032 and references cited therein.

[2] a) E. Kroke, Y. L. Li, C. Konetschny, E. Lecomte, C. Fasel, R. Riedel, *Mater. Sci. Eng. R* **2000**, *26*, 97. b) D. Seyferth, G. H. Wiseman, *J. Am. Ceram. Soc.* **1984**, *67*, C132.

[3] E. Ionescu, *Polymer-Derived Ceramics* in Ceramics Science and Technology, Set (eds R. Riedel and I.-W. Chen), Wiley-VCH Verlag GmbH & Co. KGaA, Weinheim, Germany (2013) and references cited therein.

[4] a) J.-K. Ewert, C. Denner, M. Friedrich, G. Motz, R. Kempe, *Nanomaterials* **2015**, *5*, 425. b) Y. Shi, Y. Wan, D. Zhao, *Chem. Soc. Rev.* **2011**, *40*, 3854. c) M. Kamperman, C. B. Garcia, P. Du, H. Ow, U. Wiesner, *J. Am. Chem. Soc.* **2014**, *126*, 14708. d) S. K. T. Pillai, W. P. Kretschmer, C. Denner, G. Motz, M. Hund, A. Fery, M. Trebbin, S. Förster, R. Kempe, *Small* **2013**, *9*, 984. e) C. T. Nguyen, P. H. Hoang, J. Perumal, D. P. Kim, *Chem. Commun.* **2011**, *47*, 3484. f) Z. Xiao, A. Wang, D.-P. Kim, *J. Mater. Chem.* **2010**, *20*, 2853. g) B. H. Jones, T. P. Lodge, *J. Am. Chem. Soc.* **2009**, *131*, 1676. h) Q. D. Nghiem, D. J. Kim, D. P. Kim, *Adv. Mater.* **2007**, *19*, 2351. i) J. Yan, L. Y. Hong, A. J. Wang, D. P. Kim, *Solid State Phenom.* **2007**, *124-126*, 727. i) M. Kamperman, A. Burns, R. Weissgraeber, N. van Vegten, S. C. Warren, S. M. Gruner, A. Baiker, U. Wiesner, *Nano Lett.* **2009**, *9*, 2756.

[5] G. Glatz, *From Aminopyridinato Complexes via Metal Containing SiCN Precursor Ceramics to Heterogeneous Recyclable Oxidation Catalysts.* Dissertation, Universität Bayreuth, **2009**.

[6] a) H.-Y. Ryu, R. Raj, *J. Am. Ceram. Soc.* **2007**, *90*, 295. b) H.-Y. Ryu, Q. Wang, R. Raj, *J. Am. Ceram. Soc.* **2010**, *93*, 1668. c) R.-G. Duan, F. D. Kuntz, A. K. Mukherjee, US Patent 10453879 (**2003**).

[7] a) R. Hauser, A. Francis, R. Theismann, R. Riedel, *J. Mater. Sci.* **2008**, *43*, 4042. b) S. I. Andronenko, A. Leo, I. Stiharu, S. K. Misra, *Appl. Magn. Reson.* **2010**, *39*, 347. c) S. I. Andronenko, I. Stiharu, D. Menard, C. Lacroix, S. K. Misra, *Appl. Magn. Reson.* **2010**, *38*, 385. d) A. Saha, S. R. Shah, R. Raj, S. E. Russek, *J. Mater. Res.* **2003**, *18*, 2549. e) X. Yan, X. N. Cheng, G. C. Han, R. Hauser, R. Riedel, *Key Eng. Mater.* **2007**, *353–358*, 1485. f) X. Yan, X. N. Cheng, C. S. Li, R. Hauser, R. Riedel, *Mater. Sci. Forum* **2007**, *546–549*, 2269. g) Y. Li, Z. Zheng, C. Reng, Z. Zhang, W. Gao, S. Yang, Z. Xie, *Appl. Organomet. Chem*. **2003**, *17*, 120. h) M. S. Bazarjani, M. M. Müller, H.-J. Kleebe, Y. Jüttke, I. Voigt, M. B. Yazdi, L. Alff, R. Riedel, A. Gurlo, *ACS Appl. Mater. Interfaces* **2014**, *6*, 12270. i) A. Francis, E. Ionescu, C. Fasel, R. Riedel, *Inorg. Chem.* **2009**, *48*, 10078.

[8] a) G. Glatz, T. Schmalz, T. Kraus, F. Haarmann, G. Motz, R. Kempe, *Chem. - Eur. J.* **2010**, *16*, 4231. b) M. Zaheer, G. Motz, R. Kempe, *J. Mater. Chem.* **2011**, *21*, 18825.

c) M. Zaheer, C. D. Keenan, J. Hermannsdörfer, E. Roessler, G. Motz, J. Senker, R. Kempe, *Chem. Mater.* **2012**, *24*, 3952. d) T. Schmalz, T. Kraus, M. Günthner, C. Liebscher, U. Glatzel, R. Kempe, G. Motz, *Carbon* **2011**, *49*, 3065. e) S. Schwarz, M. Friedrich, G. Motz, R. Kempe, *Z. Anorg. Allg. Chem.* **2015**, *641*, 2266.

[9] G. Mera, M. Gallei, S. Bernard, E. Ionescu, *Nanomaterials* **2015**, *5*, 468.

[10] M. Zaheer, T. Schmalz, G. Motz, R. Kempe, *Chem. Soc. Rev.* **2012**, *41*, 5102.

[11] a) R. Kempe, *Eur. J. Inorg. Chem.* **2003**, 791. b) G. Glatz, S. Demeshko, G. Motz, R. Kempe, *Eur. J. Inorg. Chem.* **2009**, 1385. c) S. Deeken, G. Motz, R. Kempe, *Z. Anorg. Allg. Chem.* **2007**, *633*, 320. d) A. Spannenberg, P. Arndt, R. Kempe, *Angew. Chem.* **1998**, *110*, 824; *Angew. Chem., Int. Ed.* **1998**, *37*, 832. e) A. Spannenberg, A. Tillack, P. Arndt, R. Kirmse, R. Kempe, *Polyhedron* **1998**, *17*, 845. f) S. Deeken, S. Proch, E. Casini, H. F. Braun, C. Mechtler, C. Marschner, G. Motz, R. Kempe, *Inorg. Chem.* **2006**, *45*, 1871. g) G. Glatz, G. Motz, R. Kempe, *Z. Anorg. Allg. Chem.* **2008**, *634*, 2897.

[12] a) http://www.bgr.bund.de/DE/Themen/Energie/energie_node.html, access on 16.03.2016; b) N.Armaroli, V. Balzani, *Angew. Chem. Int. Ed.* **2007**, *46*, 52.

[13] D. Teichmann, W. Arlt, P. Wasserscheid, R. Freymann, *Energy Environ. Sci*. **2011**, *4*, 2767.

[14] J. O'M. Bockris, *Science* **1972**, *176*, 1323.

[15] a) A. Sartbaeva, V. L. Kuznetsov, S. A. Wells, P. P. Edwards, *Energy Environ. Sci.* **2008**, *1*, 79. b) U. Eberle, M. Felderhoff, F. Schüth, *Angew. Chem., Int. Ed.* **2009**, *48*, 6608.

[16] Z. Jiang, Q. Pan, J. Xu, T. Fang, *Int. J. Hydrogen Energ*. **2014**, *39*, 17442.

[17] a) E. Clot, O. Eisenstein, R. H. Crabtree, *Chem. Commun.* **2007**, *2007*, 2231. b) R. H. Crabtree, *Energy Environ. Sci.* **2008**, *1*, 134.

[18] S. Chakraborty, W. W. Brennessel, W. D. Jones, *J. Am. Chem. Soc*. **2014**, *136*, 8564.

[19] K.-I. Fujita, Y. Tanaka, M. Kobayashi, R. Yamaguchi, *J. Am. Chem. Soc.* **2014**, *136*, 4829.

[20] a) C. O. Tuck, E. Pérez, I. T. Horváth, R. A. Sheldon, M. Poliakoff, *Science* **2012**, *337*, 695.

[21] a) T. P. Vispute, H. Zhang, A. Sanna, R. Xiao, G. W. Huber, *Science* **2010**, *330*, 1222. b) C. Li, X. Zhao, A. Wang, G. W. Huber, T. Zhang, *Chem. Rev*. **2015**, *115*, 11559.

[22] M. J. Gilkey, B. Xu, *ACS Catal.* **2016**, *6*, 1420.

[23] a) R. Grigg, T. R. B. Mitchell, S. Sutthivaiyakit, N. Tongpenyai, *J. Chem. Soc. Chem. Commun.* **1981**, *12*, 611. b) Y. Watanabe, Y. Tsuji, Y. Ohsugi, *Tetrahedron Lett*. **1981**, *22*, 2667.

[24] a) A. J. A. Watson, J. M. J. Williams, *Science* **2010**, *329*, 635. b) G. Guillena, D. J. Ramón, M. Yus, *Chem. Rev.* **2010**, *110*, 1611. c) S. Bähn, S. Imm, L. Neubert, M. Zhang, H. Neumann, M. Beller, *ChemCatChem* **2011**, *3*, 1853. d). M. Pera-Titus, F. Shi, *ChemSusChem* **2014**, *7*, 720. e) S. Pan, T. Shibata, *ACS Catal.* **2015**, *3*, 704. f) K.-i. Shimizu, *Catal. Sci. Technol.* **2015**, *5*, 1412.

[25] a) B. Gnanaprakasam, J. Zhang, D. Milstein, *Angew. Chem., Int. Ed.* **2010**, *49*, 1468. b) A. Maggi, R. Madsen, *Organometallics* **2012**, *31*, 451. c) Y. Shiraishi, M. Ikeda, D. Tsukamoto, S. Tanaka, T. Hiraia, *Chem. Commun.* **2011**, *47*, 4811. d) M. A. Esteruelas, N. Honczek, M. Oliván, E. Onate, M. Valencia, *Organometallics* **2011**, *30*, 2468. e) J. M. Pérez, R. Cano, M. Yus, D. J. Ramón, *Eur. J. Org. Chem.* **2012**, *24*, 4548. f) J. W. Rigoli, S. A. Moyer, S. D. Pearce, J. M. Schomaker, *Org. Biomol. Chem.* **2012**, *10*, 1746. g) L. Tang, H. Sun, Y. Li, Z. Zha, Z. Wang, *Green Chem.* **2012**, *14*, 3423. h) G. Zhang, S. K. Hanson, *Org. Lett.* **2013**, *15*, 650.

[26] a) S. Michlik, R. Kempe, *Nat. Chem.* **2013**, *5*, 140. b) C. Gunanathan, D. Milstein, *Science* **2013**, *341*, 1229712. c) D. Srimani, Y. Ben-David, D. Milstein, *Angew. Chem., Int. Ed*. **2013**, *52*, 4012. d) M. Zhang, X. Fang, H. Neumann, M. Beller, *J. Am. Chem. Soc.* **2013**, *135*, 11384. e) D. Forberg, J. Obenauf, M. Friedrich, S.-M. Hühne, W. Mader, G. Motz, R. Kempe, *Catal. Sci. Technol.* **2014**, *4*, 4188.

[27] a) S. Michlik, R. Kempe, *Angew. Chem., Int. Ed.* **2013**, *52*, 6326. b) D. Srimani, Y. Ben-David, D. Milstein, *Chem. Commun*. **2013**, *49*, 6632. c) S. Ruch, T. Irrgang, R. Kempe, *Chem. Eur. J.* **2014**, *20*, 13279. d) B. Pan, B. Liu, E. Yue, X. Yang, Z. Wang, W.-H. Sun, *ACS Catal.* **2016**, *6*, 1247.

[28] N. Deibl, K. Ament, R. Kempe, *J. Am. Chem. Soc.* **2015**, *137*, 12804.

4. Synopsis

During the past years our group was engaged in the synthesis of novel, metal-containing ceramic materials starting from preceramic polymers such as polysilazanes. Thereby, suitable aminopyridinato complexes for almost all transition metals were prepared and the synthesis process to the final metal containing ceramic material was developed. The benefits of such metal aminopyridinato complexes were proofed to be the high reactivity towards the NH functions of the polysilazane, the good solubility in organic solvents, the absence of "alien" elements and the contribution of the ligand to the ceramic yield. During the preparation process the metal (Cu and Pd) transmetalates from the complex to the polysilazane by elimination of the ligand and crosslinking can be achieved either by the complex itself or by the addition of a radical initiator and photolytic or thermic energy. After pyrolysis of the metal modified polymer the formation of metallic (Cu) or intermetallic (Pd_2Si) phases could be observed. Moreover, high metal loadings up to 13.7 wt.% could be achieved and the materials were proofed to be catalytically active in oxidation (Cu) and hydrogenation (Pd_2Si) reactions.

The big particle size and the improvable catalytic activity of the generated copper and palladium silicide nanoparticles let us focus on the metal iridium. Therefore, a suitable iridium complex ([$IrAp^{TMA}$(cod)], **Fig. 4-1, II**) was synthesized from the aminopyridinato ligand **I** and (1,5-cyclooctadiene)methoxyiridium dimer by methanol elimination (**Fig. 4-1 A, left**). It was found, that this complex was able to crosslink the polysilazane HTT1800 without addition of a radical initiator during removal of the solvent to form an orange solid. Pyrolysis of this metal containing preceramic polymer under nitrogen atmosphere at 1100 °C resulted in the final amorphous Ir@SiCN ceramic nano composite material (**Fig. 4-1 A, right**). Powder XRD analysis confirmed the existence of the metallic cubic crystalline Ir phase and the broad reflexes indicated a small particle size of 1.3 nm which could be confirmed by TEM and HR-TEM analysis (**Fig. 4-1 B, C**).

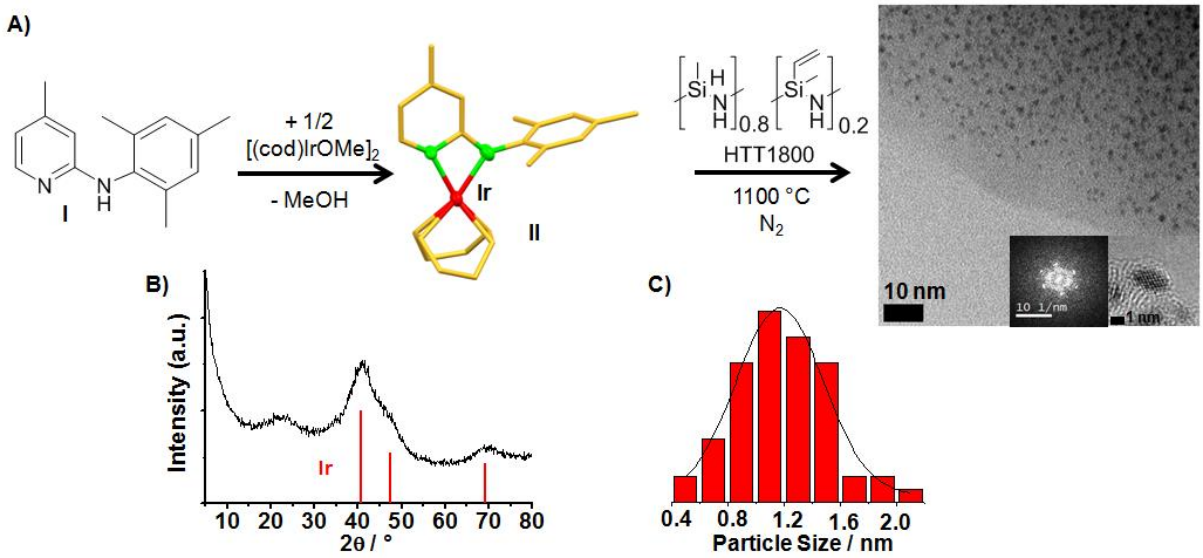

Fig. 4-1: Synthesis and characterization of the Ir@SiCN catalyst. A) Synthesis of [IrAp^{TMA}(cod)] **II** from the aminopyridinato ligand **I**. Pyrolysis after addition of the polysilazane HTT1800 with TEM picture and HR-TEM analysis. **B)** Powder XRD. **C)** Particle size distribution.

The high activity of this catalyst regarding the hydrogenation of ketones and aldehydes to the corresponding alcohols let us focus on more ambitious organic transformations. Silicon carbonitride materials are known to possess a high stability against oxidation and an outstanding robustness under harsh chemical conditions especially in a strong basic environment. Thus, the synthesis of pyrroles from secondary alcohols and 1,2-amino alcohols (**Fig. 3-3, B**), which was developed with a homogeneous Ir catalyst by our group, seemed interesting to us.

For preliminary investigations, the reaction of 2-aminobutan-1-ol and 1-phenylethanol was chosen as model reaction. After optimization of the reaction conditions (amino alcohol to alcohol ratio, temperature, solvent, catalyst loading) the role of the base was found to be critical. The use of KO^{t}Bu gave the highest yield of 2-ethyl-5-phenyl-1*H*-pyrrole (73 %) but resulted in a significant self-condensation of 1-phenylethanol after the first oxidation step. Therefore cycloheptanol was chosen as alternative alcohol source and all parameters, especially the alcohol to base ratio, were adjusted a second time resulting in a GC yield of 96 % with a catalyst loading of 0.33 mol% or 1.27 wt.% active iridium. Having the right reaction conditions in hand, the protocol was applied to several substrates. Firstly, 1-phenylethanol was used as a constant building block and the variation of the 1,2-amino alcohol, which is limited by the natural occurrence of the corresponding amino acids, gave six different 2,5-substituted pyrroles with isolated yields between 59 % and 93 %. The

modification of the secondary alcohol yielded seven products with isolated yields up to 81 %. Thereby, sulfur containing and olefinic functional groups were tolerated by the catalyst. The C-alkylation step can also take place at a secondary aliphatic carbon atom, which was proofed by the synthesis of various 2,3,5-substituted pyrroles in 36 % to 90 % yields. The usage of cyclic alcohols results in the formation of polycyclic pyrroles and variation of the ring size generated smaller and larger rings attached at the pyrrole. In summary, 23 2,5-substituted, 2,3,5-substituted as well as polycyclic pyrroles could be isolated with yields up to 93 % having an attractive functional group tolerance (**Fig. 4-2**).

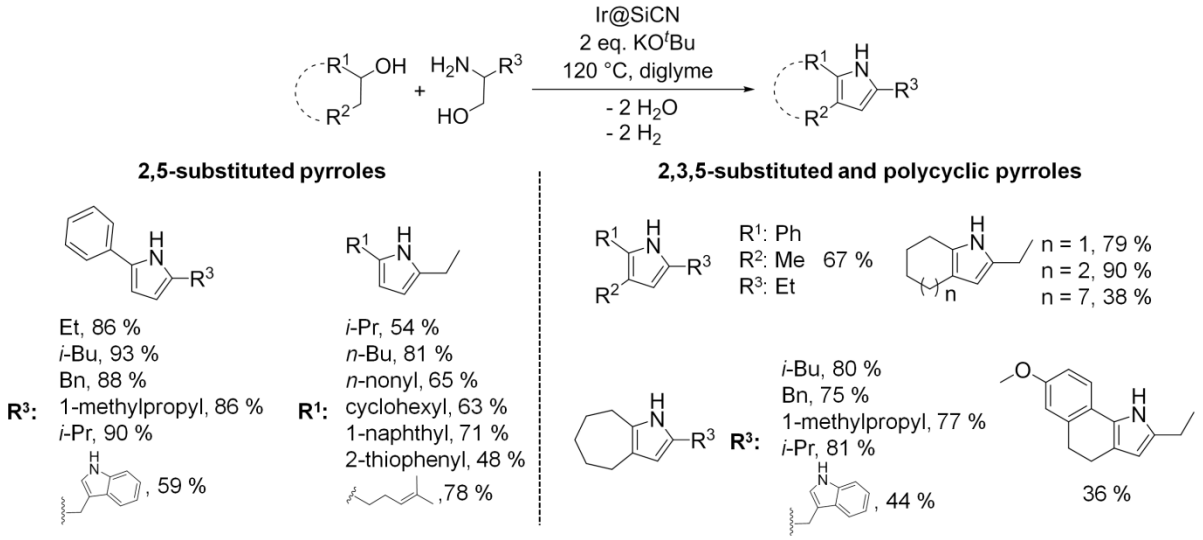

Fig. 4-2: Synthesized 2,5- and 2,3,5-substituted as well as polycyclic pyrroles by Ir@SiCN catalyzed reaction of secondary alcohols with 1,2-amino alcohols

A comparison to other commercially available, heterogeneous iridium catalysts showed the superiority of our catalyst system under the given reaction conditions. None of the other applied catalysts was able to catalyze the reaction adequately and besides they suffered from a high activity loss in the second run. The Ir@SiCN catalyst was applied eight consecutive times to the reaction of cycloheptanol with 2-amino-1-butanol to form 2-ethyl-1,5,6,7,8,9-hexahydrocyclohepta[*b*]pyrrole in 85 % – 93 % yield. This clearly underlined the robustness and excellent reusability of the prepared Ir@SiCN catalyst.

Delighted and inspired by the great applicability of the Ir@SiCN catalyst in organic transformations, we tried to extend this novel sustainable synthesis concept towards the functionalization of phenols with amino alcohols or amino phenols. We established a reaction sequence containing hydrogenation as well as multiple dehydrogenation and condensation steps. In the first step, the phenols were hydrogenated and in the second step an acceptorless dehydrogenative condensation (ADC) led to polycyclic compounds combining saturated and

aromatic rings. At last, an acceptorless dehydrogenation results in the purely unsaturated N-heterocyclic products. Therefore, we firstly searched for suitable catalytic systems, which were able to catalyze the corresponding reaction step most efficiently. For this purpose, we designed a novel Ru@SiCN as well as Pd@SiCN catalyst for the hydrogenation and dehydrogenation step, respectively. The ADC step was found to be mediated best using either a reusable Ir@SiCN or a homogenous PN_5P-Ir-Pincer catalyst. So, the generation of several polycyclic N-heterocycles like pyrroles, indoles, carbazoles, pyridines, quinolines, and acridines could be successfully applied (**Fig. 4-3**). All these structural motifs are frequently present in natural products, pharmaceuticals, several material classes like conductive polymers and find a rising application as molecular hydrogen carrier for the storage of energy.

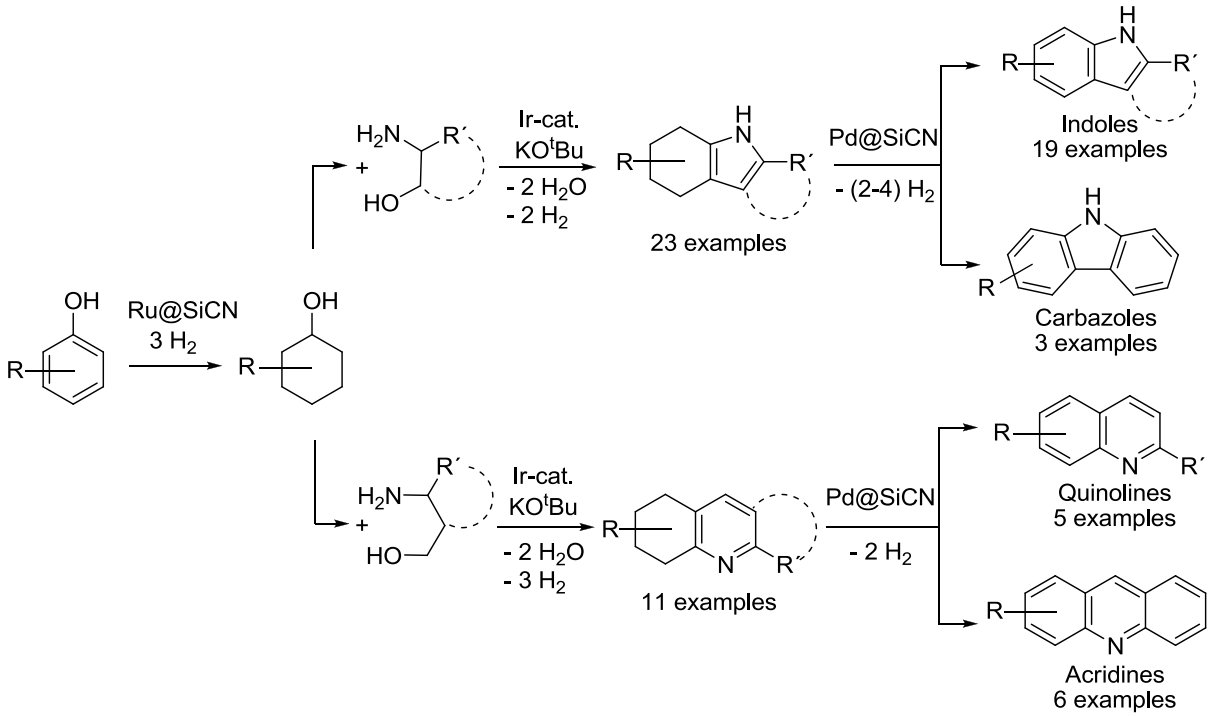

Fig. 4-3: Catalytic condensation of phenols and amino alcohols to polycyclic aromatic compounds – synthesis of pyrroles, indoles, carbazoles, pyridines, quinolines, and acridines.

Firstly, a novel Ru@SiCN catalyst was developed to achieve an improved hydrogenation activity towards aromatic compounds as compared to the Ir@SiCN system. We chose bis(2-methylallyl)(1,5-cyclooctadiene)ruthenium(II) as coordination compound since it is commercially available and should fulfill the requirements for the synthesis process. The complex was solved in thf and HTT1800 was added followed by crosslinking using dicumylperoxide (DCP) as radical initiator at 120 °C (**Fig. 4-4, A**). The resulting brown solid had to be pyrolyzed under nitrogen atmosphere at a maximum temperature of 900 °C as the formation of ruthenium silicides was observed at 1000 °C and 1100 °C. Analysis of the final

material by powder XRD revealed only one broad reflex at a 2θ value of 35 – 45 ° indicating very small Ru particles (**Fig. 4-4, D**). The size of the Ru nanoparticles was estimated by Debye-Scherrer equation to be 0.9 – 1.1 nm, which was verified by HR-TEM analysis. Analysis of the FFT resulted in a d-spacing of 205.6 ± 1.7 pm, which is in accordance to the theoretical value of 204.9 pm for the (101)-reflex of hexagonal crystalline ruthenium. Furthermore, a specific surface area (Brunauer-Emmett-Teller model [BET]) of 208 m²/g was observed (**Fig. 4-4, C**).

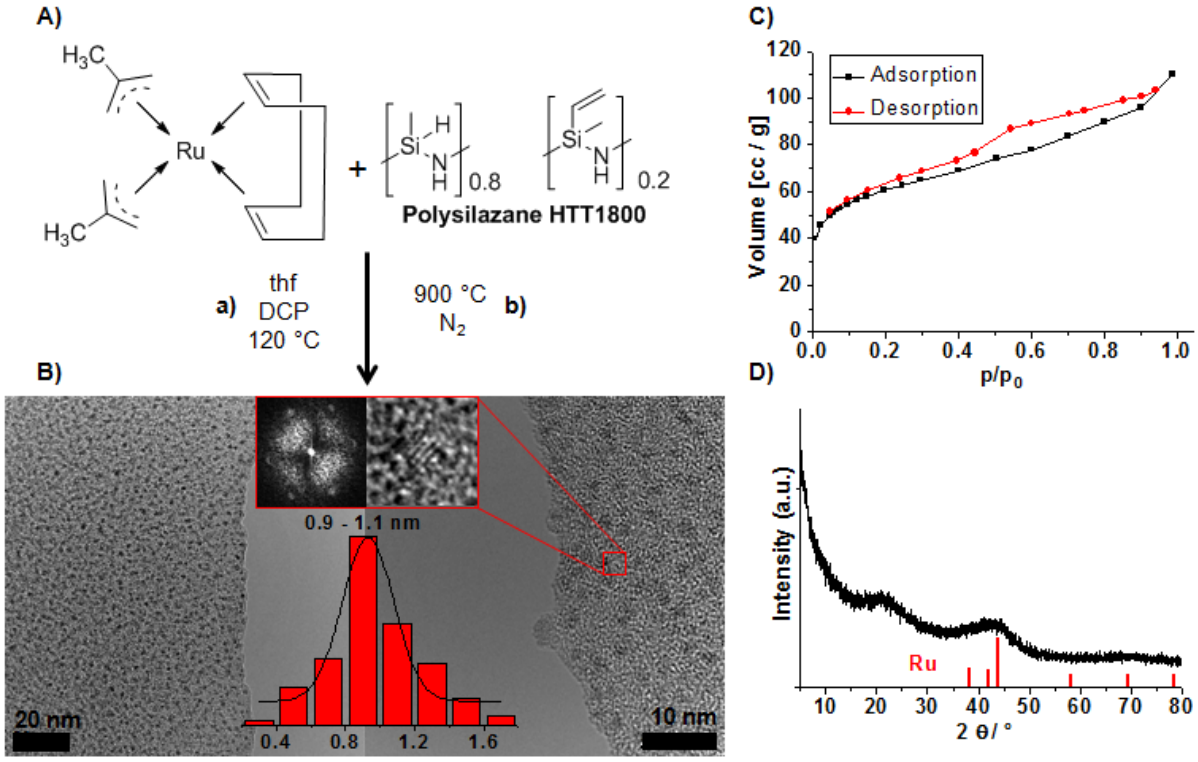

Fig. 4-4: Synthesis of the Ru@SiCN catalyst. A) Catalyst synthesis. **B)** HR-TEM pictures with magnification of one Ru particle and FFT; Particle size distribution. **C)** BET analysis**. D)** Powder XRD analysis.

This novel Ru nano composite catalyst was found to be highly active in the hydrogenation of aromatic compounds. Firstly, the superiority of the Ru@SiCN catalyst towards other, commercially available, heterogeneous iridium, ruthenium, and palladium catalysts was proven (**Tab. 1, left**). We justify the application of Ru in this step with the significantly higher hydrogenation activity as compared to Ir and Pd catalysts prepared with the same method. Next, a number of different phenols were hydrogenated at mild conditions with a metal loading of only 0.03 mol% active Ru (**Tab. 1, right**). An up-screening of the reaction was also possible resulting in the hydrogenation of 11.4 g (100 mmol) phenolic compounds within 24 h with a catalyst loading of only 0.01 mol%.

Tab. 1: Catalyst screening for phenol hydrogenation[a] (left) and hydrogenation of phenolic compounds[b] (right)

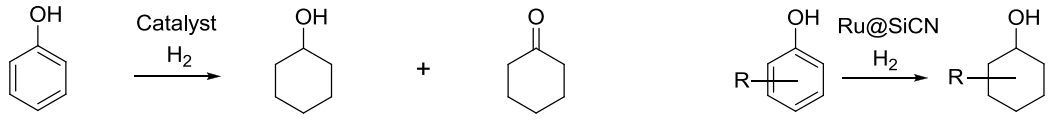

Catalyst	Yield (Cyclohexanol) [%][c]	Yield (Cyclohexanone) [%][c]	R	Yield (Cyclohexanols) [%][d]
Ru@SiCN	80	0		
Ru/C (5 %)	34	0	H	> 99
Ru/Al_2O_3 (5 %)	15	0	H[e]	97[f]
Pd/C (10 %)	3	3	1-methyl	> 99
Pd/SiO_2 (5 %)	0	0	1-ethyl	> 99
Ir/C (1 %)	3	0	4-methyl	> 99
Ir/Al_2O_3 (1 %)	3	0	4-*tert*-butyl	> 99
$Ir/CaCO_3$ (5 %)	12	0	3,5-dimethyl	92
Ir@SiCN	18	0	2-amino[g]	98
Pd@SiCN	10	22		

[a] Reaction conditions: T = 50 °C, $p(H_2)$ = 3 bar, 1 mmol phenol, $V(H_2O)$ = 1 mL, t = 5 h, 0.03 mol% active metal referring to 5 mg Ru@SiCN. [b] Reaction conditions: T = 50 °C, $p(H_2)$ = 20 bar, 1 mmol substrate, $V(H_2O)$ = 1 mL, t = 20 h, 0.03 mol% active metal referring to 5 mg Ru@SiCN. [c] Yields determined by GC using cyclopentanol as internal standard. [d] Yields determined by GC using dodecane as internal standard. [e] 100 mmol substrate, 50 °C, $p(H_2)$ = 20 bar, 200 mg Ru@SiCN catalyst (0.01 mol% active metal), 10 mL water, 24 h. [f] Yield of isolated product. [g] 80 °C, $p(H_2)$ = 50 bar, 24 h, 20 mg catalyst (0.12 mol% active Ru).

The hydrogenated phenols were now available for the coupling reaction with amino alcohols to form N-heterocylcic products (**Fig. 4-5, A**). 1,5,6,7,8-Pentahydro-cyclohexa[*b*]pyrroles could be prepared by two different methodologies: The first one required the homogenous PN_5P-Ir-Pincer catalyst **I** and a reaction flask equipped with a semi-permeable membrane as reported by MICHLIK *et al.* (**Fig. 4-5, B;** Ref. 26a in chapter 3) and the second method made use of the reusable Ir@SiCN **II** catalyst as presented previously in **Fig. 4-1** (**Fig. 4-5, C**). For the homogeneous catalyst, the reaction conditions were optimized by increasing the catalyst loading to 0.3 mol% and the oil bath temperature to 105 °C. The reusable Ir@SiCN catalyst only required a slightly higher oil bath temperature of 130 °C. It is notable, that both catalysts showed a negligible difference in the synthesis of most of the products.

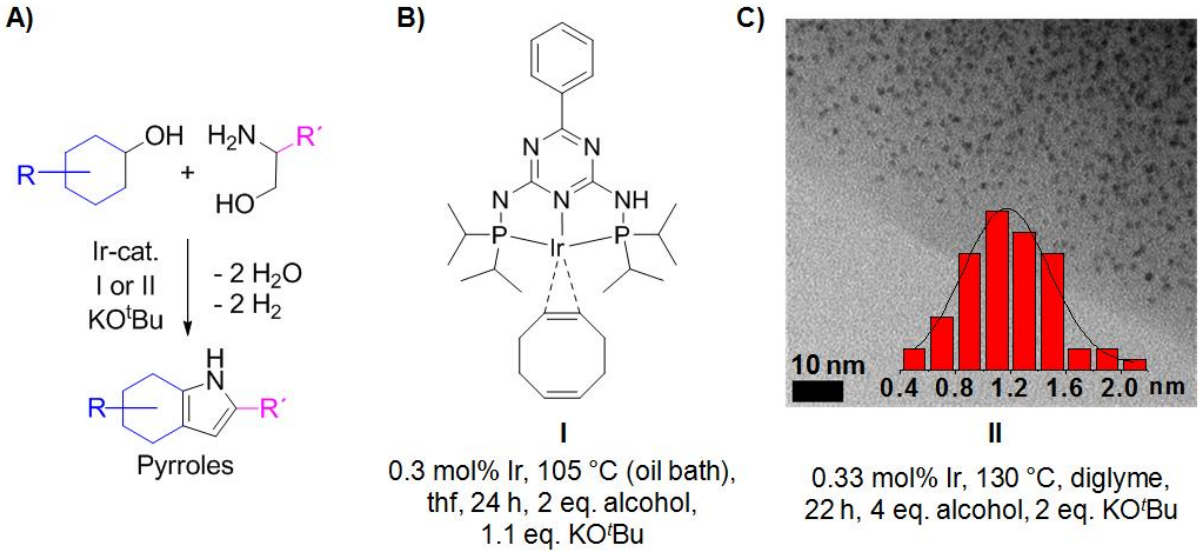

Fig. 4-5: Catalytic synthesis of 1,5,6,7,8-pentahydro-cyclohexa[*b*]pyrroles. A) Reaction scheme. **B)** (PN_5P-Ir) catalyst (cat **I**). **C)** Ir@SiCN catalyst (cat **II**).

Having the optimized reaction conditions in hand, we synthesized different 1,5,6,7,8-pentahydro-cyclohexa[*b*]pyrroles (**Tab. 2, 1a-h, 2a-e, 3a-d, 4a-c**). Thereby, the most efficient catalyst for the corresponding synthesis was used. Firstly, we used 2-amino-3-phenyl-propan-1-ol as constant building block and applied different substituted cyclohexanols to isolate eight pyrroles in 48 – 82 % yield (**Tab. 2, 1a-h**). Next, we varied the 1,2-amino alcohol compound, which is limited by the natural occurrence of the corresponding amino acids, yielding five products in moderate to good yields (**Tab. 2, 2a-e**). The use of 2-aminocyclohexanol as 1,2-amino alcohol compound allowed the variation of the secondary alcohol. Here (**Tab. 2, 3a-d**), four products were prepared in good yields with one of them containing an olefin group (**3d**). Tricyclic pyrroles and carbazoles are accessible by applying cyclic alcohols in moderate to excellent yields (**Tab. 2, 4a-c; 5a-c**).

Tab. 2: Synthesis of 1,5,6,7,8-pentahydro-cyclohexa[*b*]pyrroles (1a-h, 2a-e, 3a-d, 4a-c) and 1,2,3,4,5,6,7,8-octahydrocarbazoles (5a-c)

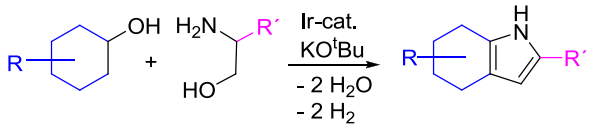

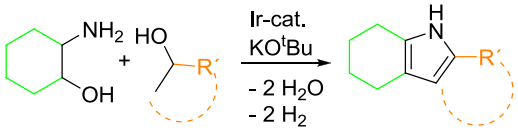

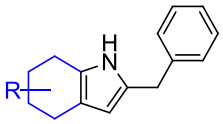

1a: R = H, 82 %; cat I

1b: R = 7-methyl, 57 %; cat II

1c: R = 5-methyl, 63 %; cat I

1d: R = 7-ethyl, 63 %; cat II

1e: R = 5-*tert*-butyl, 48 %; cat I

1f: R = 4,6-dimethyl, 66 %; cat II

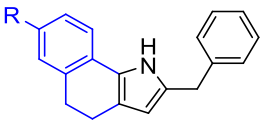

1g: R = H, 82 %; cat I

1h: R = OMe, 61 %; cat II

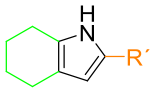

3a: R´= phenyl, 76 %; cat I

3b: R´= *n*-hexyl, 76 %; cat I

3c: R´= 4-methoxyphenyl, 74 %; cat I

3d: R´= methylpent-3-enyl, 79 %; cat II

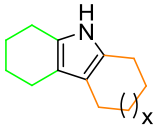

4a: x = 2, 96 %; cat I

4b: x = 3, 95 %; cat I

4c: x = 7, 53 %; cat I

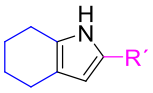

2a: R´= ethyl, 78 %; cat II

2b: R´= *sec*-butyl, 76 %; cat I

2c: R´= *iso*-butyl, 69 %; cat I

2d: R´= *iso*-propyl, 52 %; cat II

2e: R´=  , 49 %; cat II

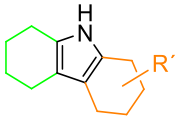

5a: R´= H, 85 %; cat I

5b: R´= 3-methyl, 70 %; cat I

5c: R´= benzo[*a*], 57 %; cat I

The application of 1,3-amino alcohols allowed the synthesis of pyridines and tetrahydroacridines by elimination of three equivalents of hydrogen (**Fig. 4-6, A**). Here again, one could either use a homogenous PN_5P-CF_3-Ir-pincer catalyst **III** as reported by MICHLIK *et al.* (**Fig. 4-6, B;** Ref. 27a in chapter 3) or the reusable Ir@SiCN catalyst **II** as presented previously in **Fig. 4-1** (**Fig. 4-6, C**). The reaction temperature and the catalyst loading for the reusable catalyst **II** were optimized to 140 °C and 0.5 mol% active metal, respectively. We were able to isolate 2,3-cyclohexenopyridines by variation of the amino alcohol in moderate to good yields (**Tab. 3, 6a-e**). The use of 2-aminobenzylalcohol enabled the synthesis of 1,2,3,4-tetrahydroacridines as further substance class (**Tab. 3, 7a-f**). It is notable, that the products **6b-e** and the acridines (**7a-f**) were only accessible in good yields using the reusable Ir@SiCN catalyst **II**.

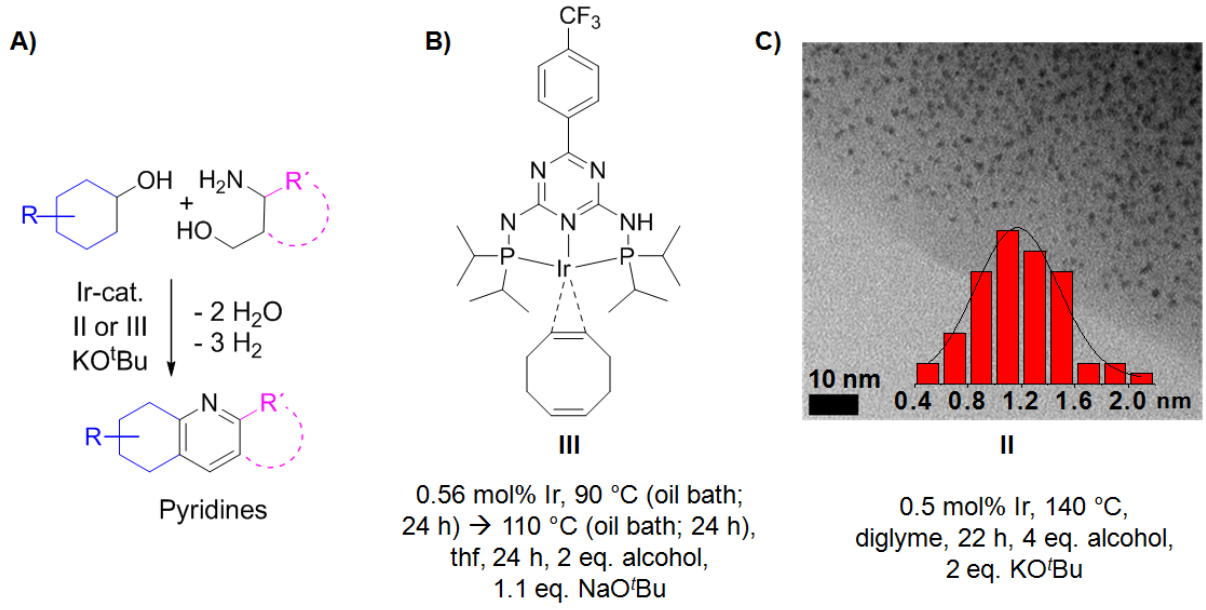

Fig. 4-6: Catalytic synthesis of 2,3-cyclohexenopyridines. A) Reaction scheme. **B)** (PN_5P-CF_3-Ir) catalyst (cat **III**). **C)** Ir@SiCN catalyst (cat **II**).

The dehydrogenation of the fused cyclohexyl ring would extend the substrate broadness of this synthesis route towards indoles, carbazoles, quinolines, and acridines. An acceptorless dehydrogenation by elimination of the molecular hydrogen would provide the opportunity to run the whole synthesis, from phenol to the final aromatic product, hydrogen neutral meaning the liberated hydrogen can be used prior to its generation.

Tab. 3: Catalytic synthesis of 2,3-cyclohexenopyridines (6a-e) and 1,2,3,4-tetrahydroacridines (7a-f)

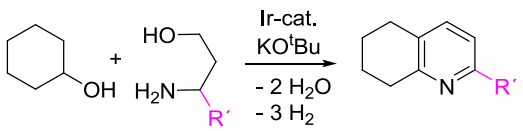

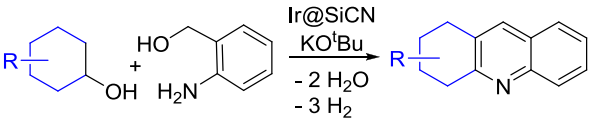

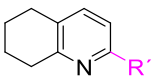

6a: R´= H, 65 %; cat III

6b: R´= $C_{11}H_{23}$, 84 %; cat II

6c: R´= *p*-tolyl, 79 %; cat II

6d: R´= 3,4-dimethoxyphenyl, 85 %; cat II

6e: R´= pyridine-3-yl, 66 %; cat II

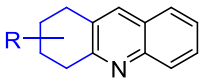

7a: R = H, 83 %; cat II

7b: R = 2-*tert*-butyl, 92 %; cat II

7c: R = 2-methyl, 70 %; cat II

7d: R = 4-methyl, 72 %; cat II

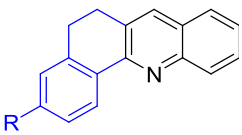

7e: R = H, 93 %; cat II

7f: R = OMe, 83 %; cat II

Therefore, we generated a nano composite catalyst based on palladium nanoparticles and silicon carbonitride. The $Pd(Ap^{TMS})_2$ complex was synthesized by salt metathesis reaction of dichloro(1,5-cyclooctadiene)palladium(II) and lithiated 4-methyl-2-((trimethylsilyl)amido)-

pyridine. A solution of $Pd(Ap^{TMS})_2$, polysilazane HTT1800 and 3 wt.% DCP in thf was crosslinked at 120 °C during evaporation of the solvent. The resulting Pd modified preceramic polymer was pyrolyzed under nitrogen atmosphere at 750 °C generating the Pd@SiCN catalyst (**Fig. 4-7, A**). Here, a higher pyrolysis temperature resulted in agglomeration of the Pd particles, which affected the catalytic activity negatively. The existence of the metallic Pd phase was verified by powder XRD analysis. The reflexes at 2θ values of 40.1, 46.3 and 67.8 ° can be assigned to the (111), (200) and (220) reflexes of cubic crystalline palladium (**Fig. 4-7, B**). The median particle size was calculated to be 2.0 nm, which is in accordance to the result of the TEM analysis (1.8 nm; **Fig. 4-7, C**).

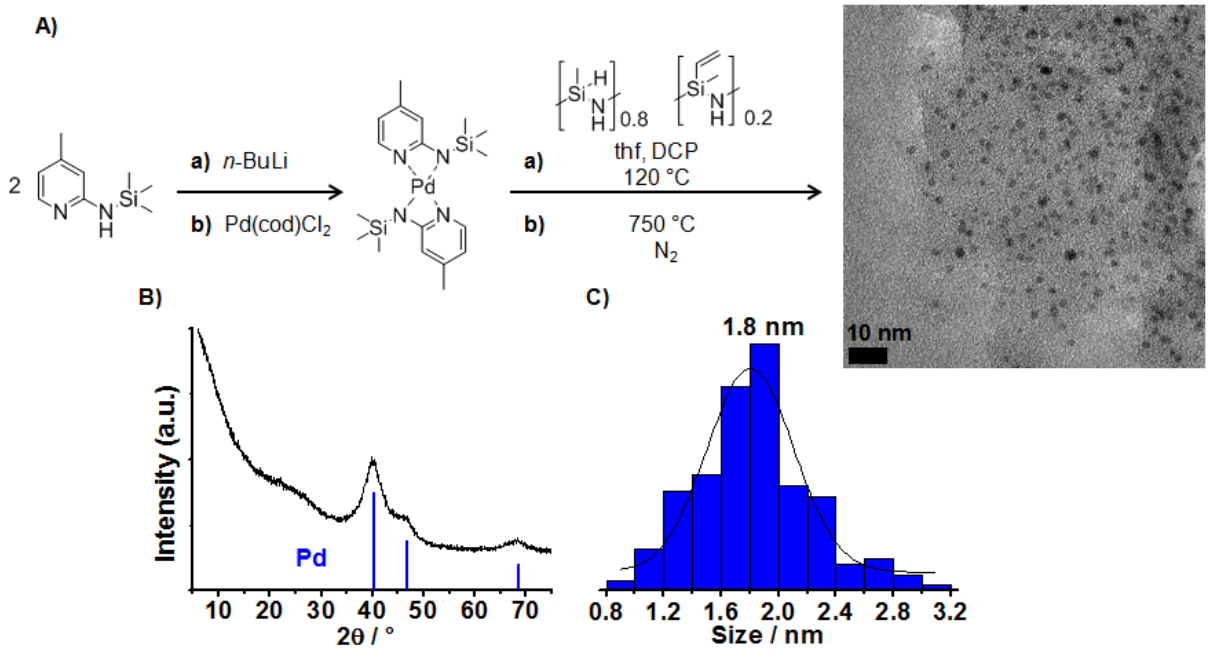

Fig. 4-7: Synthesis and characterization of the Pd@SiCN catalyst. A) Synthesis starting from the $Ap^{TMS}H$ ligand. **B)** Powder XRD. **C)** Particle size distribution.

Having the most active Pd@SiCN catalyst found, we tested its ability in the acceptorless dehydrogenation reaction of the products presented in **Tab. 2** and **Tab. 3**. It was found, that an oil bath temperature of 180 °C (reaction temperature was 170 °C) was ideal to dehydrogenate the 1,5,6,7,8-pentahydro-cyclohexa[*b*]pyrroles to the corresponding indoles with isolated yields > 90 % (**Tab. 4, 1i-p, 2f-j, 3e-g, 4d-f**). The dehydrogenation of the 1,2,3,4,5,6,7,8-octahydrocarbazoles to the corresponding carbazoles required a slightly higher reaction temperature of 180 °C (**Tab. 4, 5d-f**). Quinolines and acridines could be prepared at 200 °C (metal bath temperature) in excellent isolated yields (**Tab. 4, 6f-j; 7g-l**). The percentages in brackets are presenting the combined, isolated yields for all three reaction steps (hydrogenation, ADC coupling and dehydrogenation), which was > 46 % for the indoles,

between 53 % and 81 % for the carbazoles, higher than 58 % for the quinolines, and 65 – 88 % for the acridines.

Tab. 4: Acceptorless dehydrogenation of 1,5,6,7,8-pentahydro-cyclohexa[*b*]pyrroles (1i-p, 2f-j, 3e-g, 4d-f), 1,2,3,4,5,6,7,8-octahydrocarbazoles (5d-f), 5,6,7,8-tetrahydroquinolines (6f-j) and 1,2,3,4-tetrahydroacridines (7g-l)

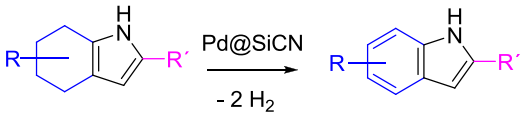

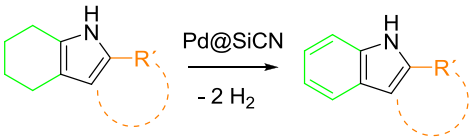

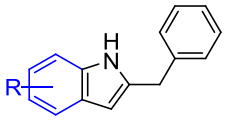

1i: R = H, > 99 % (79 %)
1j: R = 7-methyl, > 99 % (54 %)
1k: R = 5-methyl, > 99 % (61 %)
1l: R = 7-ethyl, > 99 % (61 %)
1m: R = 5-*tert*-butyl, 99 % (46 %)
1n: R = 4,6-dimethyl, 98 % (63 %)

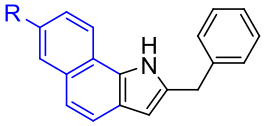

1o: R = H, 99 % (79 %)
1p: R = OMe, 99 % (59 %)

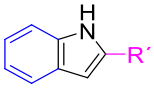

2f: R´= ethyl, > 99 % (76 %)
2g: R´= *sec*-butyl, 95 % (70 %)
2h: R´= *iso*-butyl, 90 % (60 %)
2i: R´= *iso*-propyl, 96 %

2j: R´= , 90 % (48 %)

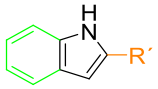

3e: R´= phenyl, 99 % (73 %)
3f: R´= *n*-hexyl, 99 % (73 %)
3g: R´= 4-methoxyphenyl, 97 % (70 %)

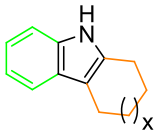

4d: x = 2, > 99 % (93 %)
4e: x = 3, 97 % (89 %)
4f: x = 7, > 99 % (50 %)

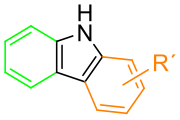

5d: R´= H, 98 % (81 %)
5e: R´= 3-methyl, 97 % (70 %)
5f: R´= benzo[*a*], 96 % (53 %)

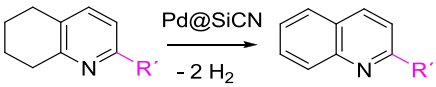

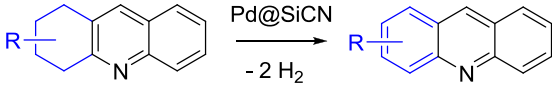

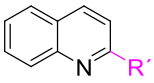

6f: R´= H, 92 % (58 %)
6g: R´= $C_{11}H_{23}$, 88 % (72 %)
6h: R´= *p*-tolyl, 94 % (72 %)
6i: R´= 3,4-dimethoxyphenyl, 93 % (77 %)
6j: R´= pyridine-3-yl, 97 % (62 %)

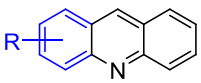

7g: R = H, 98 % (79 %)
7h: R = 2-*tert*-butyl, 97 % (87 %)
7i: R = 2-methyl, > 99 % (68 %)
7j: R = 4-methyl, 93 % (65 %)

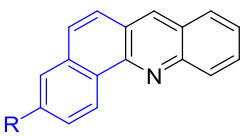

7k: R = H, 98 % (88 %)
7l: R = OMe, 98 % (79 %)

At last we made the effort to run this synthesis route in a one-pot procedure without isolating the intermediates to underline the advantageous use of the reusable silicon carbonitride catalysts (**Fig. 4-8**). Phenol was hydrogenated in thf and the Ru@SiCN catalyst was separated by centrifugation. The supernatant cyclohexanol solution was added to a mixture of 2-aminobenzylalcohol, KO^{t}Bu, diglyme, and Ir@SiCN. After evacuation and flushing with argon for three times, the mixture was stirred at 140 °C (oil bath temperature) for 22 h. By the addition of water, the ADC catalyst (Ir@SiCN) went into the water phase and could thus be easily removed. The organic products were extracted with diethylether. Afterwards, the Pd@SiCN catalyst was added and the low boiling solvents were removed under reduced pressure. Dehydrogenation at 190 °C reaction temperature gave acridine in isolated yields between 79 % and 84 % after column chromatography. The catalysts were purified by centrifugation and the procedure was repeated three times to show the great reusability of the M@SiCN catalysts.

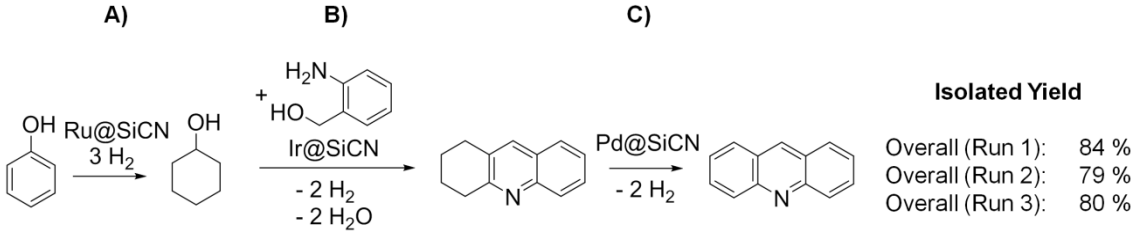

Fig. 4-8: One-pot synthesis of acridine starting from phenol and 2-aminopyridine

Inspired by the great hydrogenation activity of the Ru@SiCN catalyst and the proven applicability of the Pd@SiCN catalyst for acceptorless dehydrogenation reactions, we attemted to combine these two active species on one single support material. The fact that both metals are crystallizing in different crystal systems suggested the formation of separated nanoparticles instead of bimetallic ones. Furthermore, the N atoms in the support should avoid an aggregation of the metal nanoparticles via coordinative saturation of single metal ions or atoms. In addition, the presence of N atoms in the support should achieve strong metal nanoparticles-support interactions. Thus, we proofed this theories by simply mixing the commercially available bis(2-methylallyl)(1,5-cyclooctadiene)ruthenium(II) complex **1** and the synthesized Pd(Ap^{TMS})$_2$ complex **2** with the polysilazane HTT1800 and crosslinked the mixture at 110 °C for 24 h (**Fig. 4-9, A**). The resulting brown solid was pyrolysed under N_2 atmosphere at 750 °C to give the silicon carbonitride composite material containing the two different metal species. Analysis of the microstructure of the catalyst by TEM analysis showed the formation of particles with a median diameter of 1.6 nm. Investigations by powder XRD analysis could not reveal the nature of the metallic particles (**Fig. 4-9, B+C**).

Therefore, we performed high angle annular dark field (HAADF) microscopy and EDX measurements to gain further insight in the nature and composition of the catalyst. The existence of metallic Pd particles was indicated by EDX and could be confirmed by HR-TEM analysis. The Ru phase was distributed homogenously in the whole material and could be detected all over the matrix as well as at the Pd particles (**Fig. 4-9, D-G**).

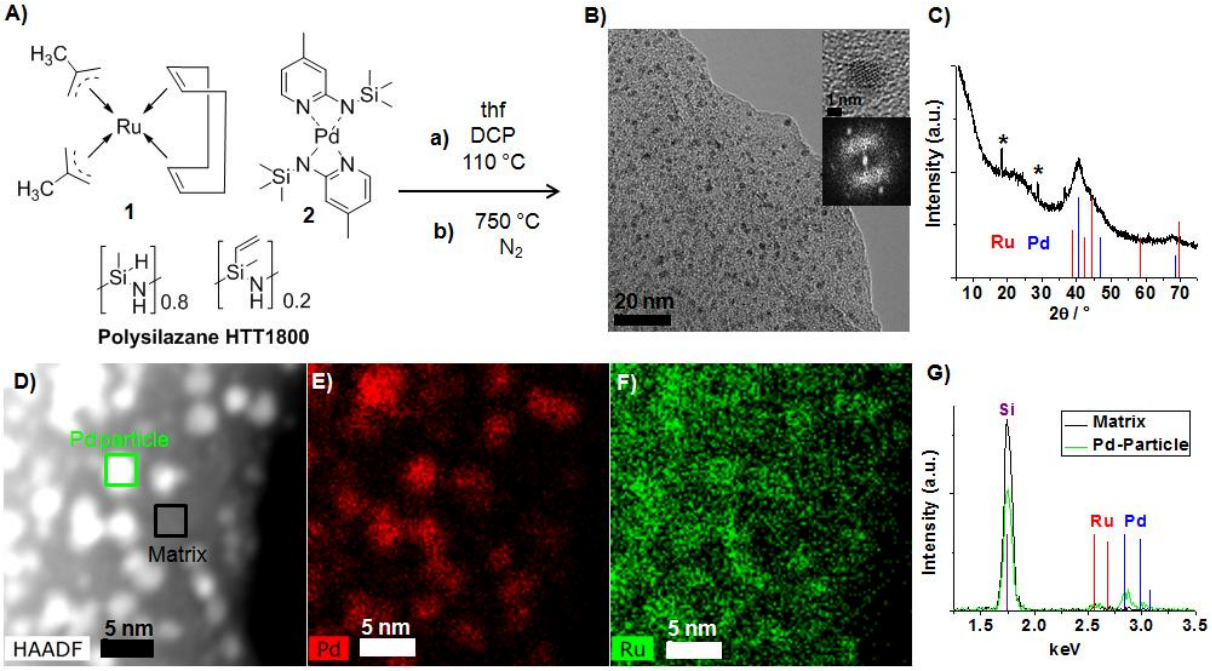

Fig. 4-9: Synthesis and characterization of the Pd_2Ru@SiCN catalyst. A) Synthesis procedure. **B)** TEM picture with magnification of one Pd particle and FFT. **C)** Powder XRD. **D)** HAAF picture. **E)** EDX mapping of Pd. **F)** EDX mapping of Ru. **G)** EDX analysis of the matrix and Pd particle.

Next, we tested the material in the hydrogenation of *N*-ethylcarbazole (NEC) and acceptorless dehydrogenation of dodecahydro-*N*-ethylcarbazole (12H-NEC). Firstly, we optimized the Pd to Ru ratio and found that a ratio of 2 gave the most active catalyst for both reactions. A comparison of the catalytic activity of the Pd_2Ru@SiCN catalyst with other commercially available, heterogeneous Ru and Pd catalysts and mixtures of them revealed the superiority of our catalyst system (**Fig. 4-10, A+B**). After optimization of the reaction conditions to 110 °C and 20 bar H_2 pressure, which is milder than the conditions reported in the literature for the hydrogenation reaction, and 190 °C for the acceptorless dehydrogenation, we applied the catalyst in three consecutive hydrogen storage cycles with the NEC system. Thereby, the storage capacity was > 5.5 wt.% (95 %) during the whole experiment illustrating the great reusability of the Pd_2Ru@SiCN catalyst (**Fig. 4-10, C**).

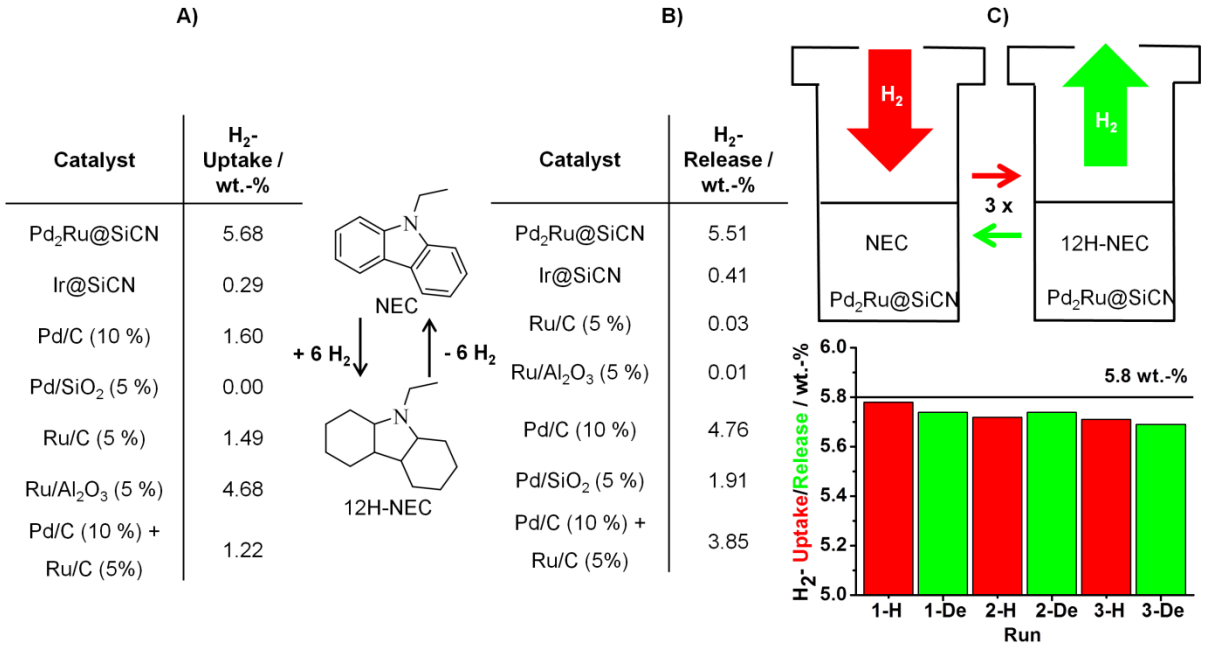

Fig. 4-10: Hydrogen storage with the NEC system. A) Hydrogenation of NEC to 12H-NEC; 110 °C, p(H_2) = 20 bar, 1 mmol NEC, 0.52 mol% active metal, 36 h. **B)** Dehydrogenation of 12H-NEC to NEC; 181 °C, 2 mmol 12H-NEC, 0.52 mol% active metal, 7 h. **C)** Catalyst reusability and reversible hydrogen storage in NEC: 1.0 g (5.12 mmol) *N*-ethylcarbazole, 200 mg Pd_2Ru@SiCN (0.52 mol% active metal); Hydrogenation: 110 °C, 20 bar H_2, 36 h; Dehydrogenation: 181 °C, 20 h. The hydrogen uptake and release values were calculated by GC and GC-MS analysis and are based on the former step. The maximum theoretical hydrogen uptake or release is 5.8 wt.%.

The reversible storage of hydrogen with the NEC system catalyzed by only one reusable catalyst system was achieved for the first time but the maximum hydrogen storage capacity is limited to 5.8 wt.%. This value exceeds the current DOE target of 5.5 wt.% for the year 2017 but will not be enough to satisfy future requirements. Furthermore, the used N-heterocycle should be synthesized from renewable resources such as lignin to enhance the sustainability. Lignin, a three-dimensional polymer, composes 15 – 30 % of the lignocellulosic biomass, which is abundantly available and indigestible. 1,2-Dialkoxybenzenes are the main building blocks of the lignin structure (**Fig. 4-11, green cycles**). It is reported in the literature, that the selective C-O bond cleavage via catalytic hydrogenolysis and subsequent hydrogenation gives 1,2-dihydroxycyclohexane as useful platform chemical product. The previously presented reusable Ir@SiCN catalyst was able to react 1,2-dihydroxycyclohexane with ammonia applying the BH/HA methodology to the corresponding diamine or 2-aminocyclohexanol, which then undergoes further dehydrogenation to form 1,2,3,4,6,7,8,9-octahydrophenazine in 74 % isolated yield (**Fig. 4-11, A**). The acceptorless dehydrogenation of octahydrophenazine

to phenazine either by Pd@SiCN or by Pd_2Ru@SiCN quantitatively yields a suitable material for hydrogen storage applications. Next, we applied phenazine in seven consecutive hydrogen storage cycles. The hydrogenation was performed by solving phenazine in a dioxane/water mixture at 115 °C and 50 bar H_2 pressure. After removal of the solvent, the residual tetradecahydrophenazine(s) were dehydrogenated under argon atmosphere at 190 °C using a small amount of diglyme as solvent. The hydrogen uptake/release was higher than 5.8 wt.% (80 %) for all seven cycles showing the excellent reusability of the catalyst (**Fig. 4-11, B**).

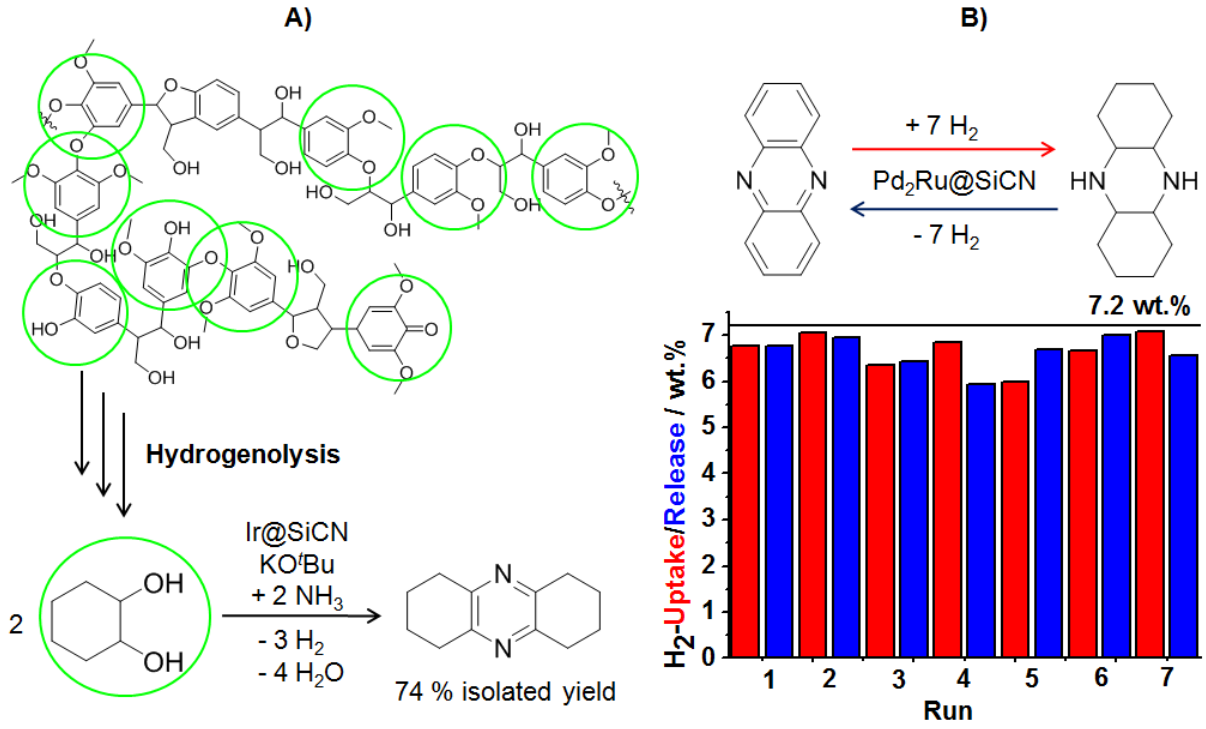

Fig. 4-11: Sustainable synthesis of 1,2,3,4,6,7,8,9-octahydrophenazine from 1,2-dihydroxycyclohexane and ammonia and its use as a reversible hydrogen carrier. A) Synthesis of octahydrophenazine from 1,2-cyclohexanediol and ammonia mediated by Ir@SiCN. **B)** Reversible hydrogen storage catalyzed by Pd_2Ru@SiCN.

5. Individual Contribution to Joint Publications

The results presented in this thesis were obtained in collaboration with others and are published or submitted as indicated below. In the following, the contributions of all the co-authors to the different publications are specified. The asterisk denotes the corresponding author.

5.1 Chapter 6

This work is published in Catalysis Science & Technology (*Catal. Sci. Technol.* **2014**, *4*, 4188-4192.), with the title

"The synthesis of pyrroles *via* acceptorless dehydrogenative condensation of secondary alcohols and 1,2-amino alcohols mediated by a robust and reusable catalyst based on nanometer-sized iridium particles".

Authors: Daniel Forberg, Johannes Obenauf, Martin Friedrich, Sven-Martin Hühne, Werner Mader, Günter Motz, Rhett Kempe*

I synthesized and characterized all the presented pyrrole compounds. Furthermore, the Ir@SiCN catalyst was prepared and characterized by me. Johannes Obenauf did the single X-ray analysis of the [IrAp^{TMA}(cod)] complex and solved the crystal structure. Martin Friedrich and Sven-Martin Hühne performed the HR-TEM measurements of the Ir@SiCN catalyst. Werner Mader provided the HR-TEM instrument. The publication was written by me and Rhett Kempe who supervised the work. Rhett Kempe and I designed and planed all the experiments. Moreover, Rhett Kempe and Günter Motz were involved in scientific discussions and corrections of the manuscript.

5.2 Chapter 7

This work is submitted to Science and is out for review with the title:

"The Sustainable Synthesis of Indoles, Carbazoles, Quinolines and Acridines via Catalytic Condensation of Phenols and Aminoalcohols or Aminophenols".

Authors: Daniel Forberg, Muhammad Zaheer, Martin Friedrich, Wilfried Assenmacher, Werner Mader, Tobias Schmidt, Rodrigo Q. Albuquerque, Stephan Kümmel, Rhett Kempe*

I synthesized and characterized all the organic products as well as all the used catalysts. Rhett Kempe and I designed and planed all the experiments. Furthermore, the manuscript was written by Rhett Kempe and me. Martin Friedrich and Wilfried Assenmacher performed the HR-TEM measurements and helped with the interpretation of the results. The HR-TEM instrument was provided by Werner Mader. Tobias Schmidt, Rodrigo Q. Albuquerque, and Stephan Kümmel did the theoretical analysis of the Pd@SiCN catalyst and wrote that part of the manuscript. Muhammad Zaheer did some preliminary work regarding the Pd@SiCN catalyst. Rhett Kempe was involved in scientific discussions and corrections of the manuscript and supervised the work.

5.3 Chapter 8

This work is submitted to Nature Communications and is out for review with the title:

"Single-catalyst high weight% hydrogen storage in a N-heterocycle synthesized from lignin hydrogenolysis products and ammonia".

Authors: Daniel Forberg, Martin Friedrich, Nobuyoshi Miyajima, Rhett Kempe*

I synthesized and characterized all the catalysts and products and performed all the analysis regarding product characterization and H_2 storage determination. Furthermore, Rhett Kempe and I wrote the manuscript and designed and planed all the experiments. Martin Friedrich performed the HR-TEM measurements and helped with the analysis and interpretation of the TEM and HR-TEM results. Nobuyoshi Miyajima did the HAADF and EDX measurements. Rhett Kempe was involved in scientific discussions and corrections of the manuscript and supervised the work.

Now this work is published as:

D. Forberg, T. Schwob. M. Zaheer, M. Friedrich, N. Miyajima, R. Kempe, *Nat. Commun.* **2016**, *7*, 13201.

6. The Synthesis of Pyrroles via Acceptorless Dehydrogenative Condensation of Secondary Alcohols and 1,2-Amino Alcohols Mediated by a Robust and Reusable Catalyst Based on Nanometer-sized Iridium Particles

Daniel Forberg[a], Johannes Obenauf,[a] Martin Friedrich,[a] Sven-Martin Hühne,[b] Werner Mader,[b] Günter Motz[c] and Rhett Kempe*,[a]

[a] Lehrstuhl für Anorganische Chemie II, Universität Bayreuth, Universitätsstraße 30, 95440 Bayreuth, Germany. E-Mail: kempe@uni-bayreuth.de

[b] Lehrstuhl für Anorganische Materialforschung, Universität Bonn, 53117 Bonn, Germany.

[c] Lehrstuhl für Keramische Werkstoffe, Universität Bayreuth, 95440 Bayreuth, Germany.

Published in: *Catal. Sci. Technol.* **2014**, *4*, 4188-4192.

Abstract

Pyrroles are important compounds with several applications in medicine and material science. They can be synthesized sustainably from secondary alcohols and amino alcohols. Hydrogen and water are liberated in the course of this reaction. Here, we present that this sustainable catalytic pyrrole synthesis can be mediated efficiently by a novel iridium nanoparticle catalyst. The catalyst synthesis starts from molecular precursors, an N-ligand stabilized Ir complex and a commercially available polysilazane. The generation of nanometer-sized iridium particles was achieved (due to the presence of N atoms in the support). The robust nature of the support allows reuse of the catalyst. The scope of the reaction was verified by the synthesis of 23 pyrrole derivatives (up to 93 % isolated yield). Thus, an attractive functional group tolerance (e.g. amines and olefins) could be observed. Commercially

available heterogeneous Ir catalysts are inefficient in this pyrrole synthesis and extremely limited in terms of reusability.

6.1 Introduction

Pyrroles are important compounds. The pyrrole motif is an essential part of the structure of hemoglobin and chlorophyll.[1] Furthermore, pyrroles are important in medical applications due to their antibacterial,[2] antitumor[3] and antifungal[4] properties. In addition, they have applications in molecular optics[5] as conducting polymers[6] and in solar cells[7] and batteries;[8] they can also be used as antioxidant agents[9] and gas sensors.[10] Due to the importance of this substance class, there is a need for an extensive improvement in the present synthetic methods and for the development of new (catalytic) synthesis protocols.[11,12] With this background, a novel catalytic pyrrole synthesis was developed recently by several groups (Milstein, Saito and us, **Scheme 1**).[13] In this regard, 1,2-amino alcohols and secondary alcohols are selectively connected to diversely functionalized pyrroles via acceptorless dehydrogenation (hydrogen is liberated) and condensation steps.[14,15] A similar pyrrole synthesis was developed by Beller's group.[16] The use of 1,3-amino alcohols allows the generation of regioselectively substituted pyridine derivatives.[17] Here, three equivalents of H_2 are liberated per pyridine molecule. These synthesis protocols are especially interesting due to their sustainability aspect: the products can be obtained from renewable resources which are abundant and not in competition with the food chain.[15a,18,19]

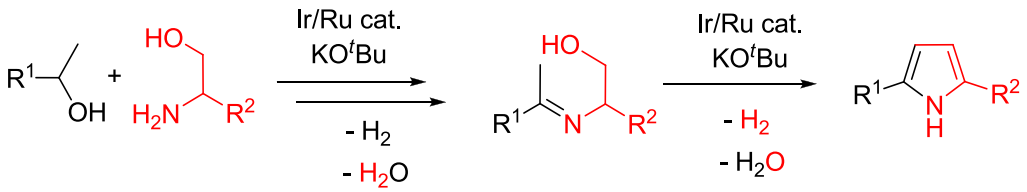

Scheme 1: Synthesis of pyrroles from secondary alcohols and 1,2-amino alcohols under elimination of water and hydrogen

Up to now, homogeneous iridium and ruthenium catalysts have been used for this pyrrole synthesis. The extension of this sustainable synthesis concept towards reusable catalysts seems a desirable goal to us. It looks especially challenging since the synthesis takes place under rather strong basic conditions. Many classic heterogeneous catalysts might not be stable under these conditions. Silicon carbonitride (SiCN) appears to us as a suitable catalyst support material due to its chemical inertness.[20] Furthermore, the N atoms of the support may provide the active sites needed for the protonation and deprotonation steps during alcohol

dehydrogenation.[21] A few examples of M@SiCN catalysts were already reported to be active and selective in oxidation and hydrogenation reactions.[22] However, such iridium catalysts are unknown.

Here, we present the efficient synthesis of pyrrole derivatives starting from secondary alcohols and 1,2-amino alcohols (**Scheme 1**) mediated by a novel recyclable nanocomposite catalyst. Nanometer-sized iridium particles (Ø = 1.3 nm) could be generated at high temperatures and at high metal loadings in a chemically inert support (amorphous SiCN). The Ir catalyst introduced here is reusable and more efficient than (commercially available) iridium nanoparticle catalysts.

6.2 Results and Discussion

The synthesis of the applied Ir@SiCN catalyst is shown schematically in **Fig. 1a**. The application of **II** in the Ir@SiCN catalyst synthesis is based on the solvent compatibility of complex **II** and the used polysilazane (HTT1800, Clariant Advanced Materials), the high reactivity of **II** with respect to the crosslinking of the silazane and the possible production of **II** in a multigram scale. The inexpensive and commercially available polysilazane HTT1800 was added to a THF solution of complex **II**, wherein an increase in viscosity indicates crosslinking of the polysilazane. Hydrosilylation and dehydrocoupling were identified as the most relevant crosslinking reactions (FT-IR measurements and analysis of the released hydrogen gas *via* GC). After removal of the solvent, the sample was pyrolyzed under a nitrogen atmosphere at 1100 °C. ICP-OES measurements revealed 18.9 wt% Ir. Powder XRD was carried out to confirm the amorphous nature of the SiCN matrix as well as the presence of metallic iridium nanoparticles (**Fig. 1b**). The broad reflexes at 2θ values of 40.7°, 47.2° and 69.1° can be assigned to the (111), (200) and (220) reflexes of cubic crystalline iridium. The broadness of the reflexes indicates very small sizes of iridium particles which were calculated to be 1.2 nm. The existence of an Ir–SiCN nanocomposite was also confirmed by transmission electron spectroscopy (TEM) (**Fig. 1a**; ESI†). The particles are distributed homogeneously over the whole nitride matrix. An average particle size of 1.3 nm was determined by TEM (**Fig. 1c**), which is in agreement with the results of the XRD investigation. Analysis by HRTEM also confirmed the existence of crystalline iridium nanoparticles (ESI).

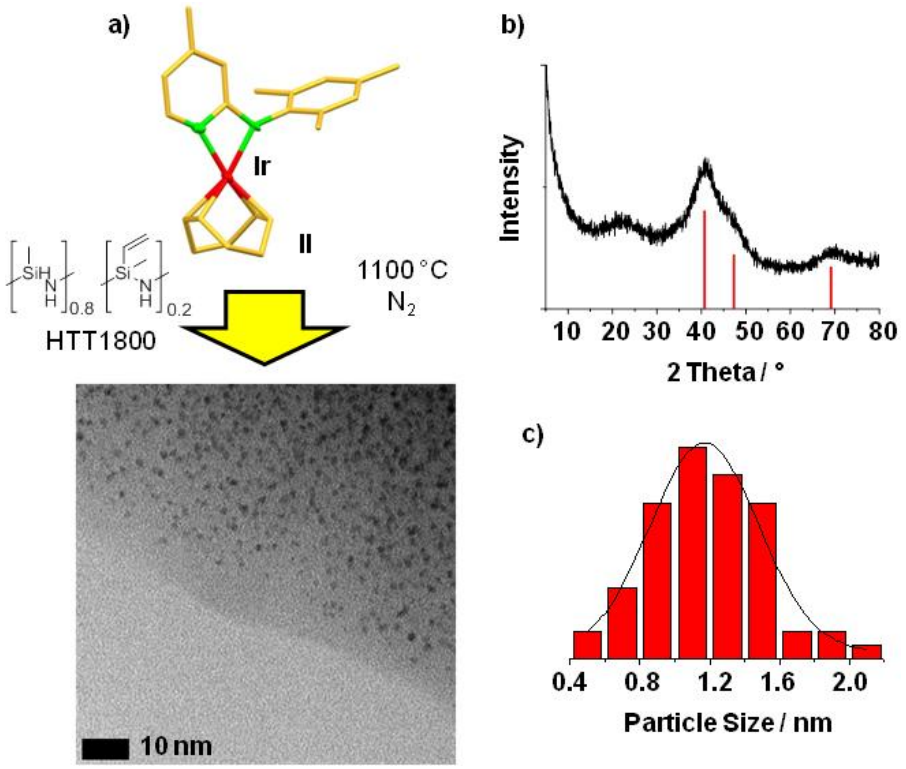

Fig. 1 a) Synthesis of the Ir@SiCN catalyst. The novel aminopyridinato iridium complex II (for its synthesis, see the ESI) crosslinks the commercially available polysilazane HTT1800 then undergoes pyrolysis under a nitrogen atmosphere at 1100 °C, resulting in Ir@SiCN nanocomposites. The coordinative saturation of the iridium particles by the N atoms of the support material allows the formation of homogeneously distributed nanometer-sized Ir particles. **b) Powder XRD** (red: reflexes of cubic crystalline iridium). **c) Particle size distribution.** For the HRTEM image, see the ESI.

The reaction of 2-aminobutan-1-ol and 1-phenylethanol was chosen as the model reaction to investigate the optimal reaction parameters. The ratio of amino alcohol to alcohol and the influence of the base were explored first. The highest yield could be obtained by using KO^{t}Bu as a base. At 120 °C (oil bath temperature; 115 °C inside) and with bis(2-methoxylethyl)ether (diglyme) as the solvent, the maximum yield was 73 %. Here, the use of base leads to significant self-condensation of 1-phenylethanol (after oxidation). Hence, the alcohol to base ratio was optimized and the yield could be increased to 96 % (determined by GC) with an iridium loading of 0.33 mol% (or 1.27 wt.%).

Next, we applied other heterogeneous iridium catalysts to underline the need for the novel Ir@SiCN catalyst (**Fig. 2**). Neither Ir@MIL-101,[23] Ir/$CaCO_3$, Ir/Al_2O_3 nor Ir/C was able to catalyze the synthesis of **1a** adequately or better using the same amount of active iridium. In contrast to our Ir@SiCN nanocomposite catalyst, the tested commercially available catalysts suffered from a significant activity loss in the second run. The most active commercial

catalyst (Ir/C) shows a significant activity loss in the second run (47 % of the conversion of the first run). The activity loss of the other commercial catalysts in the second run is even higher.

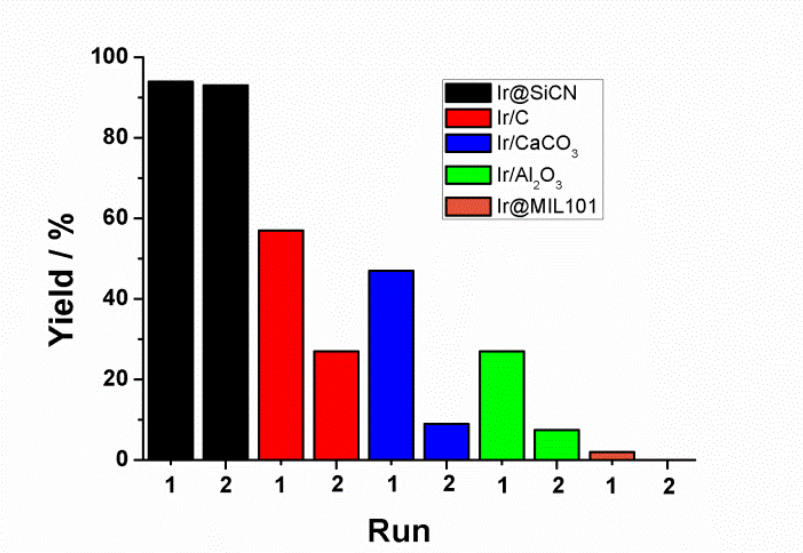

Fig. 2 Screening of different heterogeneous iridium catalysts under identical conditions using the same amount of active Ir. Yields were determined by GC.

With the optimized reaction conditions in hand, the potential of the Ir@SiCN catalyst regarding the substrate scope was investigated. Various amino alcohols were reacted with 1-phenylethanol. The isolated yields were between 93 % (**1b**) and 86 % (**1a,d**). It was also possible to introduce an indol group (**Table 1, entry 5**). Next, the substrate scope with regard to the secondary alcohol was studied. Therefore, 2-amino-1-butanol was used as a constant building block. The catalyst system showed high regioselectivity towards the formation of 2,5-disubstituted pyrroles when aliphatic alcohols like 2-hexanol were used. Only traces of the 2,4-disubstituted pyrrole could be found. The alkylation of a terminal CH_3 group is significantly faster than that of a CH_2 group at the β-position. Aliphatic alcohols with different lengths (**Table 1, entry 8 and 9**), branched alcohols (**Table 1, entry** 7), 1-cyclohexylethanol (**Table 1, entry 10**) and 1-(1-naphthyl)ethanol (**Table 1, entry 11**) were applied successfully. Furthermore, our recyclable catalyst tolerates sulfur-containing functional groups (**Table 1, entry 12**) and olefin functions (**Table 1, entry 13**). The C-alkylation step can also take place at a secondary aliphatic carbon atom. As an example, 5-ethyl-3-methyl-2-phenyl-1*H*-pyrrole (**2a**) was synthesized in 67 % yield. The application of cyclic alcohols results in bicyclic pyrroles like 2-ethyl-1,5,6,7,8,9-hexahydrocyclohepta[*b*]pyrrole (**2b**), which was accessible in 90 % yield. The variation of the amino alcohol yielded bicyclic pyrroles in isolated yields between 75 % (**2d**) and 81 % (**2g**). The variation of the alcohol building block resulted in the

generation of smaller (**Table 2, entry 8 and 10**) and larger (**Table 2, entry 9**) rings attached to the pyrroles.

Table 1 Synthesis of 2,5-disubstituted pyrroles from secondary alcohols and 1,2-amino alcohols[a].

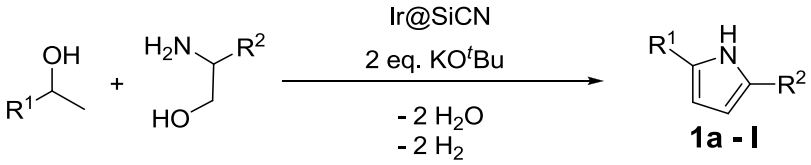

Entry	Product		Yield [%][b]
1	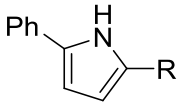	**1a** R = Et	86
2		**1b** R = i-Bu	93
3		**1c** R = Bn	88
4		**1d** R = 1-methylpropyl	86
5		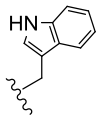 **1e** R =	59
6		**1f** R = i-Pr	90
7	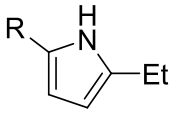	**1g** R = i-Pr	54
8		**1h** R = n-Bu	81
9		**1i** R = n-nonyl	65
10[c]		**1j** R = cylcohexyl	63
11		**1k** R = 1-naphtyl	71
12		**1l** R = 2-thiophenyl	48
13		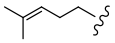 **1m** R =	78

[a] Reaction conditions: 1,2-amino alcohol (6 mmol), secondary alcohol (24 mmol), KOtBu (12 mmol), Ir@SiCN catalyst (0.33 mol% Ir), 6 mL diglyme, 24 h at 120 °C oil bath temperature. [b] Isolated yield. [c] 130 °C.

The multiple recycling of our Ir@SiCN catalyst was investigated with the parameters from **Table 2**. The reaction of cycloheptanol and 2-amino-1-butanol was chosen as the model reaction and the yields of **2b** were determined by GC. The catalyst was separated by centrifugation and washed with water and acetone after each run. Within 8 runs, the yields were between 85 and 93 % (see the ESI). This emphasizes the very good robustness of the catalyst system introduced here.

Table 2 Synthesized 2,3,5-trisubstituted pyrroles[a]

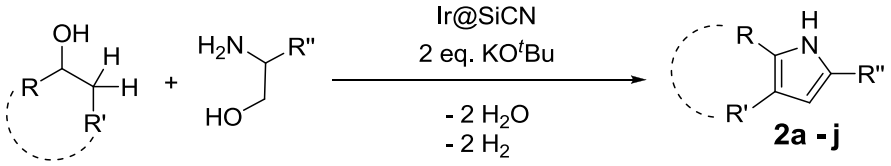

Entry	Product		Yield [%][b]
1[c]	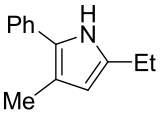	**2a**	67
2[d]		**2b** R = Et	90
3		**2c** R = i-Bu	80
4		**2d** R = Bn	75
5	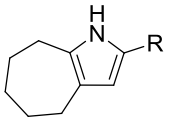	**2e** R = 1-methylpropyl	77
6		**2f** R = 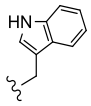	44
7		**2g** R = i-Pr	81
8[e]	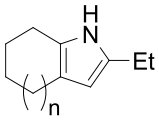	**2h** n = 1	79
9		**2i** n = 7	38
10[f]	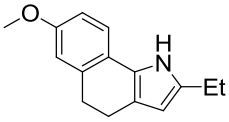	**2j**	36

[a] **Reaction conditions:** 1,2-amino alcohol (6 mmol), secondaryl alcohol (24 mmol), KO^{t}Bu (12 mmol), Ir@SiCN catalyst (0.33 mol% Ir), 6 mL diglyme, 24 h at 120 °C oil bath temperature. [b] Isolated yield. [c] 135 °C. [d] Large batch (4x). [e] 130 °C. [f] 125 °C.

6.3 Conclusions

In summary, we presented the efficient synthesis of regioselectively substituted pyrroles starting from secondary alcohols and amino alcohols catalyzed by an Ir nanoparticle catalyst under (relatively) mild conditions. The used SiCN support enables the generation of nanometer-sized Ir particles and the robust nature of that support results in very good reusability of the catalyst under basic conditions. Other Ir nanoparticle catalysts show lower activity and very limited reusability. The Ir@SiCN catalyst, an easy-to-handle and airstable powder, promises versatile applications in sustainable organic synthesis especially if the addition of strong bases is required to mediate the reactions.

6.4 Experimental Section

Catalyst synthesis

1.0 g of HTT1800 (Clariant Advanced Chemicals) was added to a solution of 817 mg of [Ir(Ap^{TMA})cod] (for synthesis, see the ESI) in 15 mL of THF. The solvent was removed under reduced pressure and the remaining dark orange solid was pyrolyzed under a nitrogen atmosphere at 1100 °C (holding time 1 h; see the ESI).

General method for synthesis of 2,5-disubstituted pyrroles

200 mg of Ir@SiCN, 6 mmol of 1,2-aminoalcohol, 24 mmol of secondary alcohol, 12 mmol of KO^{t}Bu and 5 mL of bis(2-methoxylethyl)ether were heated at an oil bath temperature of 120 °C for 24 h using a pressure tube with a pressure-equalizing device (bubble counter). After cooling, the mixture was extracted with diethyl ether (3x), dried over Na_2SO_4 and then the solvents were removed under reduced pressure at 60 °C. The products were isolated by column chromatography on silica gel eluting with pentane/Et_2O (for details, see the ESI).

Acknowledgements

The authors thank the Deutsche Forschungsgemeinschaft (SFB 840 and KE 756/23-1) for financial support.

6.5 References

[1] J. A. Joule and K. Mills, *Heterocyclic Chemistry*, Wiley, Chichester, 5th edn, 2010.

[2] a) S. D. Joshi, Y. More, H. M. Vagdevi, V. P. Vaidya, G. S. Gadaginamath and V. H. Kulkarni, *Med. Chem. Res.*, 2012, **22**, 1073. b) R. W. Bürli, D. McMinn, J. A. Kaizerman, W. Hu, Y. Ge, Q. Pack, V. Jiang, M. Gross, M. Garcia and R. Tanaka, *Bioorg. Med. Chem. Lett.*, 2004, **14**, 1253.

[3] a) T.-L. Su, T.-C. Lee and R. Kakadiya, *Eur. J. Med. Chem.*, 2013, **69**, 609. b) N. Amishiro, S. Nagamura, E. Kobayashi, A. Okamoto, K. Gomi, M. Okabe and H. Saito, *Bioorg. Med. Chem.*, 2000, **8**, 1637. c) N. Amishiro, S. Nagamura, E. Kobayashi, A. Okamoto, K. Gomi and H. Saito, *Chem. Pharm. Bull.*, 1999, **47**, 1393.

[4] a) M. K. Kathiravan, A. B. Salake, A. S. Chothe, P. B. Dudhe, R. P. Watode, M. S. Mukta and S. Gadhwe, *Bioorg. Med. Chem.*, 2012, **20**, 5678. b) M.-Z. Wang, H. Xu,

T.-W. Liu, Q. Feng, S.-J. Yu, S.-H. Wang and Z.-M. Li, *Eur. J. Med. Res.*, 2011, **46**, 1463.

[5] S.-S. P. Chou and Y.-H. Yeh, *Tetrahedron Lett.*, 2001, **42**, 1309.

[6] J. R. Reynolds, P. A. Poropatic and R. L. Toyooka, *Macromolecules*, 1987, **20**, 958.

[7] a) S. Qu and H. Tian, *Chem. Commun.*, 2012, **48**, 3039. b) A. Hagfeldt, G. Boschloo, L. Sun, L. Kloo and H. Pettersson, *Chem. Rev.*, 2010, **110**, 6595.

[8] a) L. Zhu, Y. Shen, M. Sun, J. Qian, Y. Cao, X. Ai and H. Yang, *Chem. Commun.*, 2013, **49**, 11370. b) H. Nishide and K. Oyaizu, *Science*, 2008, **319**, 737.

[9] D. Wang, X. Hu and G. Zhao, *Int. J. Food Sci. Tech.*, 2008, **43**, 1880.

[10] B. P. J. D. L. Costello, P. Evans, N. Guernion, N. M. Ratcliffe, P. S. Sivanand and G. C. Teare, *Synthetic Metals*, 2000, **114**, 181.

[11] Recent metal catalyzed examples: (a) M.-N. Zhao, Z.-H. Ren, Y.-Y. Wang and Z.-H. Guan, *Org. Lett.*, 2014, **16**, 608. (b) L. Ran, Z.-H. Ren, Y.-Y. Wang and Z.-H. Guan, *Green Chem.*, 2014, **16**, 112. (c) S. Peng, L. Wang, J. Huang, S. Sun, H. Guo and J. Wang, *Adv. Syn. Catal.*, 2013, **355**, 2550. (d) S. Pan and T. Shibata, *ACS Catal.*, 2013, **3**, 704. (e) N. Thies, M. Gerlach and E. Haak, *Eur. J. Org. Chem.*, 2013, **32**, 7354. (f) J. Liu, Z. Fang, Q. Zhang, Q. Liu and X. Bi, *Angew. Chem., Int. Ed.*, 2013, **52**, 6953. (g) Z. Shi, M. Suri and F. Glorius, *Angew. Chem., Int. Ed.*, 2013, **52**, 4892. (h) T. Miura, K. Hiraga, T. Biyajima, T. Nakamuro and M. Murakami, *Org. Lett.*, 2013, **15**, 3298. (i) B. Pan, C. Wang, D. Wang, F. Wu and B. Wan, *Chem. Commun.*, 2013, **49**, 5073. (j) Z. Chen, B. Lu, Z. Ding, K. Gao and N. Yoshikai, *Org. Lett.*, 2013, **15**, 1966. (k) J. B. Bharate, R. Sharma, S. Aravinda, V. K. Gupta, B. Singh, S. B. Bharate and R. A. Vishwakarma, *RSC Adv.*, 2013, **3**, 21736. (l) T. J. Donohoe, J. F. Bower and L. K. M. Chan, *Org. Biomol. Chem.*, 2012, **10**, 1322. (m) N. Schley, G. Dobereiner and R. H. Crabtree, *Organomet.*, 2011, **30**, 4174. (n) M. Yamagishi, K. Nishigai, T. Hata and H. Urabe, *Org. Lett.*, 2011, **13**, 4873. (o) M. P. Huestis, L. Chan, D. R. Stuart and K. Fagnou, *Angew. Chem.*, 2011, **123**, 1374. (p) E. P. J. Ng, Y.-F. Wang and S. Chiba, *Synlett*, 2011, **6**, 783. (q) B. M. Trost, J.-P. Lumb and J. M. Azzarelli, *J. Am. Chem. Soc.*, 2011, **133**, 740. (r) Q. Cai, F. Zhou, T. Xu, L. Fu and K. Ding, *Org. Lett.*, 2011, **13**, 340. (s) S. Maiti, S. Biswas and U. Jana, *J. Org. Chem.*, 2010, **75**, 1674. (t) T. J. Donohoe, N. J. Race, J. F. Bower and C. K. A. Callens, *Org. Lett.*, 2010, **12**, 4094. (u) T. Sasada, T. Sawada, R. Ikeda, N. Sakai and T. Konakahara, *Eur. J. Org. Chem.*, 2010, **2010**, 4237. (v) W. Liu, H. Jiang and L. Huang, *Org. Lett.*, 2010, **12**, 312. (w) D. R. Stuart, P. Alsabeh, M. Kuhn and K. Fagnou, *J. Am. Chem. Soc.*, 2010, **132**, 18326.

(x) M. Lin, L. Hao and R. D. Ma, *Synlett*, 2010, **15**, 2345. (z) K. Taguchi, S. Sakaguchi and Y. Ishii, *Tetrahedron Lett.*, 2005, **46**, 4539.

[12] For recent nonmetal catalyzed examples see ESI (6).

[13] (a) S. Michlik and R. Kempe, *Nat. Chem.*, 2013, **5**, 140. (b) K. Iida, T. Miura, J. Ando and S. Saito, *Org. Lett.*, 2013, **15**, 1436. (c) D. Srimani, Y. Ben-David and D. Milstein, *Angew. Chem., Int. Ed.*, 2013, **52**, 4012.

[14] C. Gunanathan and D. Milstein, *Science*, 2013, **341**, 249.

[15] For recent examples of dehydrogenative condensation please see: (a) T. Hille, T. Irrgang and R. Kempe, *Chem. - Eur. J.*, 2014, **20**, 5569. (b) S. Musa, S. Fronton, L. Vaccaro and D. Gelman, *Organometallics*, 2013, **32**, 3069. (c) G. Zhang and S. K. Hanson, *Org. Lett.*, 2013, **15**, 650. (d) K. S. Sandhya and C. H. Suresh, *Organometallics*, 2013, **32**, 2926. (e) H. Li, X. Wang, M. Wen and Z.-X. Wang, *Eur. J. Inorg. Chem.*, 2012, **31**, 5011. (f) L. Tang, H. Sun, Y. Li, Z. Zha and Z. Wang, *Green Chem.*, 2012, **14**, 3423. (g) J. W. Rigoli, S. A. Moyer, S. D. Rearce and J. M. Schomaker, *Org. Biomol. Chem.*, 2012, **10**, 1746. (h) A. Maggi and R. Madsen, *Organometallics*, 2012, **31**, 451. (i) A. C. Marr, *Catal. Sci. Technol.*, 2012, **2**, 279. (j) M. A. Esteruelas, N. Honczek, M. Olivàn, E. Oñate and M. Valencia, *Organometallics*, 2011, **30**, 2468. (k) C. Gunanathan and D. Milstein, *Acc. Chem. Res.*, 2011, **44**, 588. (l) C. Xu, L. Y. Goh and S. A. Pullarkat, *Organometallics*, 2011, **30**, 6499. (m) B. Gnanaprakasam, J. Zhang and D. Milstein, *Angew. Chem., Int. Ed.*, 2010, **49**, 1468. (n) D. Milstein, *Top. Catal.*, 2010, **53**, 915.

[16] (a) M. Zhang, X. Fang, H. Neumann and M. Beller, *J. Am. Chem. Soc.*, 2013, **135**, 11384. (b) J. Schranck, A. Tlili and M. Beller, *Angew. Chem., Int. Ed.*, 2013, **52**, 7642. (c) M. Zhang, H. Neumann and M. Beller, *Angew. Chem.*, 2013, **125**, 625.

[17] (a) D. Srimani, Y. Ben-David and D. Milstein, *Chem. Commun.*, 2013, **49**, 6632. (b) S. Michlik and R. Kempe, *Angew. Chem., Int. Ed.*, 2013, **52**, 6326. S. Ruch, T. Irrgang and R. Kempe, *Chem. - Eur. J.*, 2014, DOI: 10.1002/chem.201402952.

[18] C. O. Tuck, E. Pérez, I. T. Horváth, R. A. Sheldon and M. Poliakoff, *Science*, 2012, **337**, 695.

[19] T. P. Vispute, H. Zhang, A. Sanna, R. Xiao and G. W. Huber, *Science*, 2010, **330**, 1222.

[20] M. Zaheer, T. Schmalz, G. Motz and R. Kempe, *Chem. Soc. Rev.*, 2012, **41**, 5102.

[21] S. Qu, Y. Dang, C. Song, M. Wen, K.-W. Huang and Z.-X. Wang, *J. Am. Chem. Soc.*, 2014, **136**, 4974.

[22] (a) M. Zaheer, J. Hermannsdörfer, W. P. Kretschmer, G. Motz and R. Kempe *ChemCatChem*, 2014, **6**, 91. (b) M. Zaheer, C. D. Keenan, J. Hermannsdörfer, E. Roessler, G. Motz, J. Senker and R. Kempe, *Chem. Mater.*, 2012, **24**, 3952; (c) M. Zaheer, G. Motz and R. Kempe, *J. Mater. Chem.*, 2011, **21**, 18825; (d) G. Glatz, T. Schmalz, T. Kraus, F. Haarmann, G. Motz and R. Kempe, *Chem. - Eur. J.*, 2010, **16**, 4231; (e) M. Kamperman, A. Burns, R. Weissgraeber, N. van Vegten, S. C. Warren, S. M. Gruner, A. Baiker and U. Wiesner, *Nano Lett.*, 2009, **9**, 2756.

[23] (a) J. Hermannsdörfer, M. Friedrich and R. Kempe, *Chem. - Eur. J.*, 2013, **19**, 13652. (b) J. Hermannsdörfer, M. Friedrich, N. Miyajima, R. Q. Albuquerque, S. Kümmel and R. Kempe, *Angew. Chem., Int. Ed.*, 2012, **51**, 11473. (c) J. Hermannsdörfer and R. Kempe, *Chem. - Eur. J.*, 2011, **17**, 8071.

6.6 Supporting Information

6.6.1 General Considerations

All reactions were carried out in a dry argon or nitrogen atmosphere using standard Schlenk or glove box techniques. Halogenated solvents were dried over P_2O_5, and nonhalogenated solvents were dried over sodium benzophenone ketyl. Deuterated solvents were ordered from Cambridge Isotope Laboratories, vented, stored over molecular sieves and distilled. All chemicals were purchased from commercial sources with purity over 95 % and used without further purification. Polysilazane "KiON HTT 1800" was purchased from Clariant Advanced Materials GmbH, Frankfurt (Germany) and used without further purification. NMR spectra were received using an INOVA 300 or 400 MHz spectrometer at 298 K. Chemical shifts are reported in ppm relative to the deuterated solvent. Elemental analyses were carried out on a Vario elementar EL *III*. X-ray crystal structure analyses were performed with a STOE-STADIVARI diffractometer [λ(Mo-K_α) = 0.71073 Å] equipped with an Oxford Cryostream low-temperature unit. Structure solution and refinement were accomplished with SIR-97 and SHELXL-2014[1,2]. GC analyses were carried out on an Agilent 6890N Network GC system equipped with a HP-5 column (30 m x 0.32 μm x 0.25 μm) using *n*-dodecane as internal standard. GC/MS analyses were carried out on an Agilent 7890A/MSD 5975C system equipped with a HP-5MS column (30 m x 0.32 μm x 0.25 μm). Ceramisation was carried out under nitrogen atmosphere in a high temperature furnace (Gero, Germany). All X-ray powder diffractograms were recorded by using a STOESTADE-P-diffractometer (CuK_α-Strahlung, 1.54178 Å) in θ-2θ-geometry and with a position sensitive detector. Transmission electron microscopy (TEM) was carried out by using a Varian LEO 9220 (200 kV) instrument. The sample was suspended in chloroform and sonicated for 5 min. Subsequently a drop of the suspended sample was placed on a grid (Plano S 166-3) and allowed to dry. High resolution transmission electron microscopy (HR-TEM) was carried out by using a Philips CM300 FEG/UT (300 kV) instrument. The sample was suspended in chloroform and sonicated for 2 min. Subsequently a drop of the suspended sample was placed on a grid with lacy carbon film and allowed to dry. EDX measurements were carried out by using a Zeiss Field-Emission-Scanning-Electron-Microscope (FESEM) „LEO 1530 GEMINI". The acceleration voltage was 1 – 5 kV. FT-IR measurements were performed using a Perkin-Elmer FTIR-spectrum 100. TGA measurements were carried out under nitrogen atmosphere by using a Netzsch 409 C instrument (5 °Cmin^{-1} heating rate up to 1000 °C). Milling of the catalyst was performed in a ball mill "Pulverisette 0" (Fritsch, Germany) for 15 min. ChemBET

measurements were carried out by using a ChemBET Pulsar TPR/TPD instrument from Quantachrome. N_2 sorption was measure using a Nova2000e (Quantachrome). ICP-OES measurements were carried out by using a Vista-pro radical model from Varian.

6.6.2 Catalyst Synthesis

Synthesis of (4-methyl-pyridin-2-yl)-(2,4,6-trimethyl-phenyl)-amine $Ap^{TMA}H$ **I**:

(4-Methyl-pyridin-2-yl)-(2,4,6-trimethyl-phenyl)-amine $Ap^{TMA}H$ was synthesized according to a published procedure.[3] To 13.3 g (105 mmol) of 2-chloro-4-methylpyridine 17.77 g (103.5 mmol) of 2,4,6-trimethylaniline hydrochloride were added to get a mash. After stirring at 180 °C for 26 h the residue was dissolved in 50 mL of water and made alkaline with Na_2CO_3. The mixture was extracted three times with 75 mL of CH_2Cl_2 and dried over Na_2SO_4. Subsequent removing of the solvent yielded a residue which was dissolved in 200 mL of a hot 1:1 mixture of hexane and diethyl ether and filtered. After removal of the solvent the solid was re-crystallized in diethyl ether to give colourless crystals (9.26 g = 40.9 mmol = 39 %).

^{1}H NMR (400 MHz, C_6D_6, 298 K): δ = 8.11 (d, 1H, J_{H-H} = 17 Hz); 6.77 (s, 1H); 6.20 (d, 1H, J_{H-H} = 17 Hz); 5.89 (s, 1H); 2.18 (s, 6H); 2.15 (s, 3H); 1.72 (s, 3H) ppm.

Synthesis of iridium[(4-methyl-pyridin-2-yl)-(2,4,6-trimethyl-phenyl)-amine(cyclooctadiene)] [$IrAp^{TMA}$(cod)] **II**:

1.657 g (2.5 mmol) bis(1,5-cyclooctadien)-di-μ-methoxydiiridium were added to a solution of 1.132 g (5 mmol) $Ap^{TMA}H$ in 100 mL THF and stirred over night at room temperature. The solvent was removed *in vacuo* and the residue was extracted with either hexane or diethyl ether. The solvent was concentrated *in vacuo* and stored in a freezer at -30 °C yielding [$IrAp^{TMA}$(cod)] as orange crystals. (1.155 g = 2.20 mmol = 88 %).

^{1}H NMR (400 MHz, D_8-THF, 298 K): δ = 7.18 (d, 1H, J_{H-H} = 5.52 Hz); 6.79 (s, 2H); 5.87 (d, 1H, J_{H-H} = 5.52 Hz); 5.08 (s, 1H); 3.84 (m, 2H); 3.51 (m, 2H); 2.30 (s, 6H); 2.14 - 2.24 (m, 7H); 1.97 (s, 3H); 1.46 (m, 4H) ppm. ^{13}C NMR (103 MHz, CD_2Cl_2, 298 K): δ = 178.6, 152.9, 142.8, 139.9, 135.2, 134.2, 129.0, 109.5, 106.2, 65.3, 59.7, 32.7, 22.3, 21.1, 18.6 ppm.

Elemental analysis (%) for $C_{23}H_{29}IrN_2$ calcd: C 52.55, H 5.56, N 5.33; found: C 52.54, H 5.54, N 5.39.

Single X-ray data:

Compound	**[IrAp^{TMA}(cod)]**
Formula	$C_{23}H_{29}IrN_2$
Formula weight	525.68
Crystal system	triclinic
Space group	*P-1*
a [Å]	7.8138(3)
b [Å]	14.5845(5)
c [Å]	19.1054(7)
α [°]	68.745(3)
β [°]	87.157(3)
γ [°]	75.844(3)
Cell volume [Å^3]	1965.70(13)
Z	4
Crystal size [mm^3]	0.211x0.188x0.186
Habit	block
Colour	orange
Density [gcm^{-3}]	1.776
T [K]	133(2)
Theta range	1.555 – 28.973
Unique reflections	41743
Observed reflections [I > 2s(I)]	28827
Parameters	478
wR_2 (all data)	0.1450
R [I > 2s(I)]	0.0941

CCDC: 1014360

Ceramization:

Under vigorous stirring 1.0 g HTT1800 was added drop wise to a solution of 817 mg (1.55 mmol) [IrAp^{TMA}(cod)] in 15 mL THF. The solvent was removed slowly under reduced pressure and the resulting orange-brown solid was pyrolyzed under N_2 atmosphere with the following program:

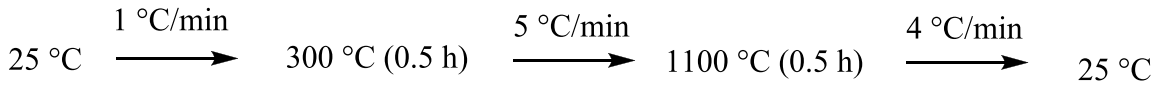

The ceramic yield was 72 %. After ball milling for 15 minutes, the catalyst was pre-treated by applying 20 bar H_2 for 3 days in an aqueous suspension.

6.6.3 Characterization of Ir@SiCN Catalyst

FT-IR Measurements:

FT-IR measurements were carried out to study the crosslinking of polysilazane HTT1800 and [IrAp^{TMA}(cod)] (**Fig. 1**).

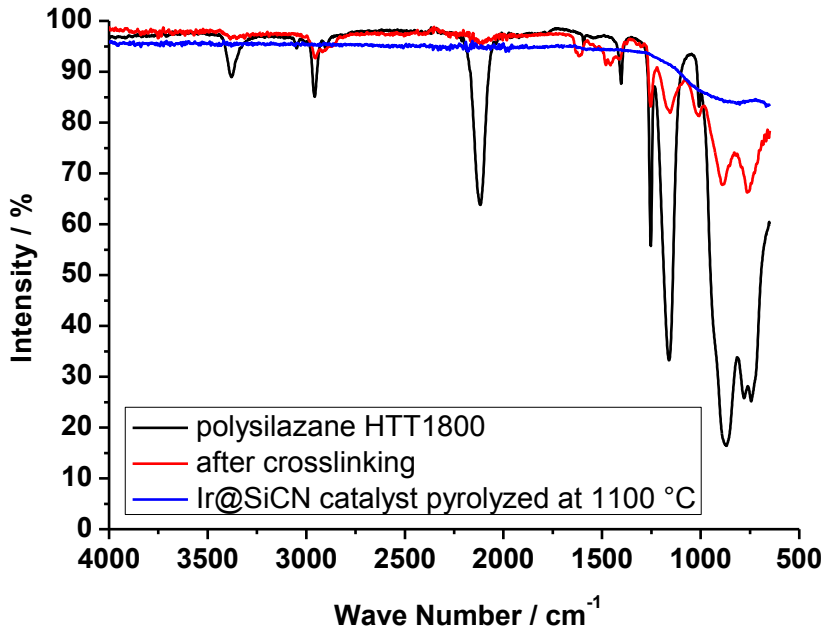

Fig. 1: FT-IR study of the Ir@SiCN nano composite synthesis

^{1}H NMR Spectroscopy:

60 mg HTT1800 was added to a solution of 50 mg [IrAp^{TMA}(cod)] in 2 mL THF. The solvent was removed under reduced pressure and the mixture became solid. The "green body" was extracted with 1 mL of C_6D_6. ^{1}H NMR measurement indicate the presence of only traces of HTT1800 and [IrAp^{TMA}(cod)].

TEM Measurements:

TEM measurements an overview over the the Ir@SiCN catalyst to show the homogenously distributed very small nanometer sized Ir particles (**Fig. 2, left**). Furthermore HR-TEM

measurements were performed to verify the metallic nature of the Ir particles by analysis of the FFT (**Fig. 2, right**).

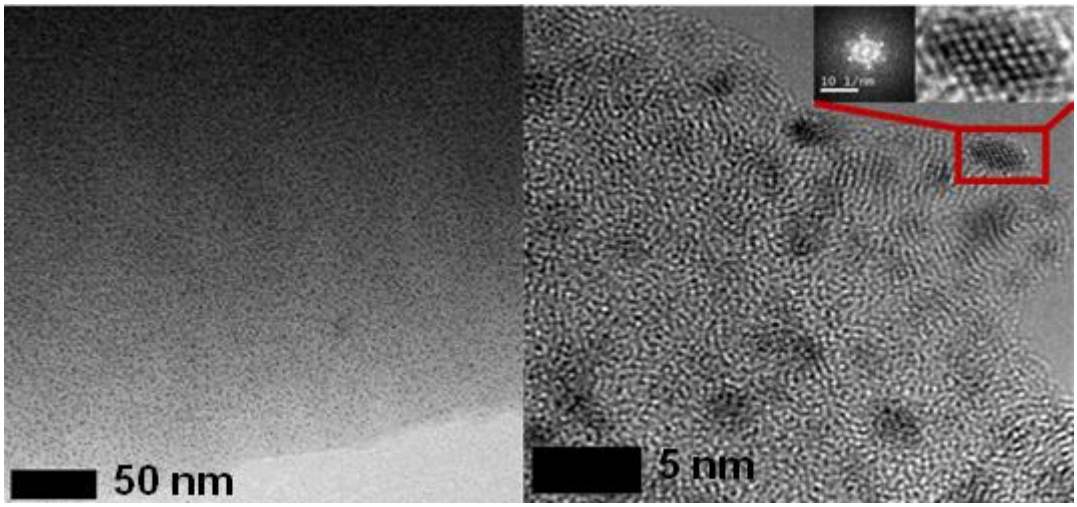

Fig. 2: TEM analysis of the Ir@SiCN catalyst. left: overview; right: HR-TEM.

ICP-OES-Analysis:

50 mg of the sample was solved in 1.5 mL HNO_3 (65 %, distilled), 4.5 mL HCl (32 %, p.a.) and 1 mL HF (40 %) and heated in the microwave at 170 °C for 7 min (80 % power), at 180 °C for 7 min (85 % power) and at 195 °C for 20 min (90 % power).

Result: 18.9 wt% Ir content

Powder XRD Analysis:

Powder XRD analysis was applied to verify the existence of Ir nanoparticles and to prove the amorphous character of the SiCN support (**Fig. 3**). Reference card for cubic crystalline Iridium was 00-046-1044.[4]

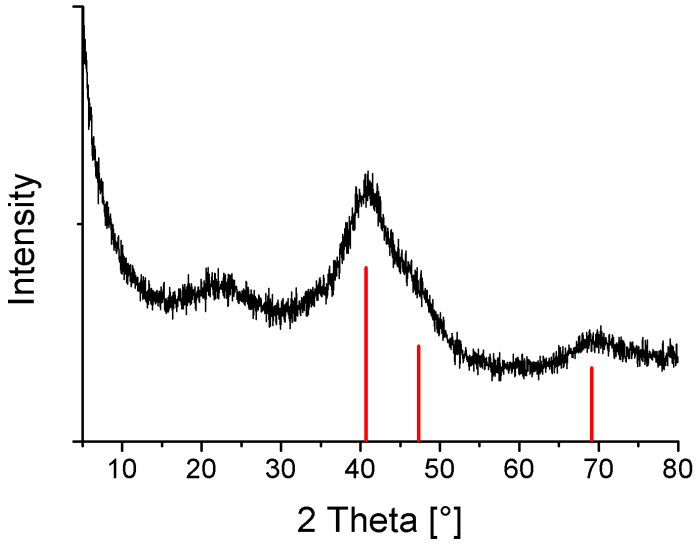

Fig. 3: Powder XRD analysis of the Ir@SiCN catalyst (red: Reflexes of cubic crystalline iridium; reference card: 00-046-1044)

EDX Measurement:

Iridium as well as all other elements of the SiCN support could be detected (**Fig. 4**).

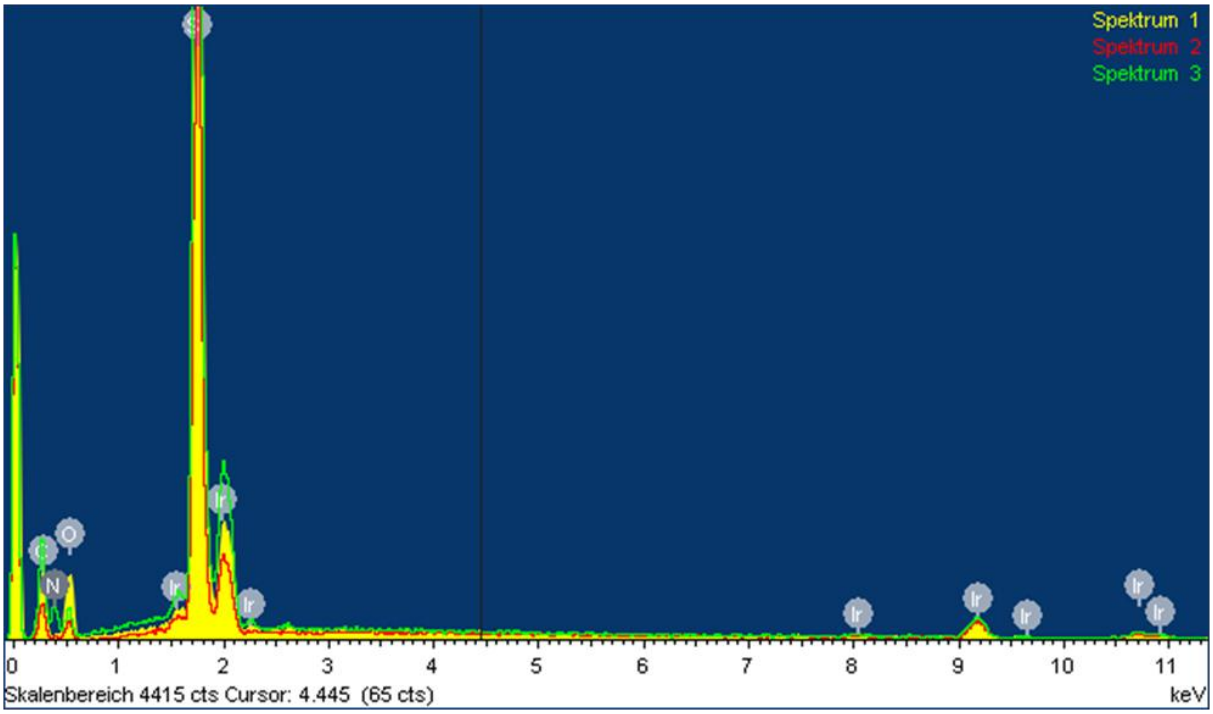

Fig. 4: EDX mapping of the Ir@SiCN catalyst

ChemBET Measurements:

182 mg of the Ir@SiCN catalyst was pre-treated under helium and nitrogen atmosphere at 500 °C for 3 hours. After cooling the sample to RT, hydrogen gas was added portion wise using a 50 µL injection loop. Analysis of the results was performed with the free version of the program fytik 0.9.8.[5]

Metal dispersion on surface of Ir@SiCN catalyst: 6.61 %

N_2 Sorption

N_2 sorption experiments revealed no porosity of the Ir@SiCN nano composite as synthesized.

Reusability of the Ir@SiCN Catalyst:

200 mg Ir@SiCN, cycloheptanol (2892 µL, 24.0 mmol), 2-amino-butan-1-ol (565 µL, 6.0 mmol), 4 mL diglyme and KO^{t}Bu (1.37 g, 12.0 mmol) were stirred in a pressure tube equipped with a pressure equalization device for 24 h at 120 °C. The mixture was quenched with 3 mL water and extracted 2 times with 15 mL diethyl ether. The extract was dried over Na_2SO_4 and the yield of 2-ethyl-1,5,6,7,8,9-hexahydro-cyclohepta[*b*]pyrrole was determined by GC. The catalyst was recovered by centrifugation, washed with water (1x) and acetone (2x) and used for the next run. The results are shown in **Fig. 5**.

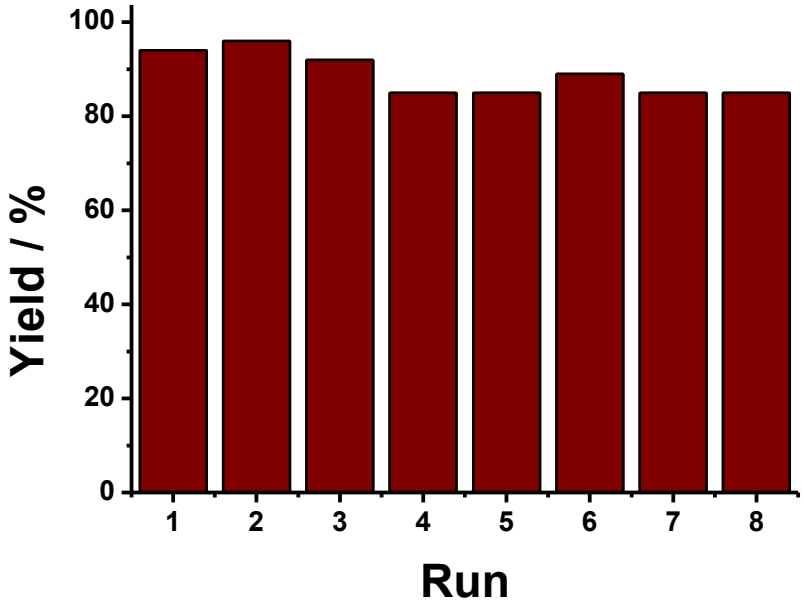

Fig. 5: Reusability of the Ir@SiCN catalyst; the catalyst was recovered after each run

Leaching Experiments:

1: 200 mg Ir@SiCN catalyst and 1.374 mg KOtBu were stirred in 6 mL diglyme at 120 °C for 20 h. The solid catalyst was centrifugated and the supernatant basic solution was used as "catalyst" for pyrrole synthesis:

565 µL (6.0 mmol), 2-amino-1-butanol and 2904 µL (24.0 mmol) 1-phenylethanol were added to the centrifugate and stirred at 120 °C (oil bath temperature) for 24 h. After extraction with diethyl ether the product 2-ethyl-5-phenyl-1*H*-pyrrole could not be detected by GC.

2: 50 mg Ir@SiCN catalyst and 300 mg KO^{t}Bu were stirred in 3 mL H_2O at 120 °C (pressure tube) for 19 h. The solid catalyst was centrifugated and the supernatant solution analysed by ICP-OES (see ICP-OES analysis). 0.02 % of the applied Iridium could be found.

Use of other (commercial) heterogeneous iridium catalysts

Ir/C (1 wt.-%; 50 % water wet), Ir/Al_2O_3 (1 wt.-%) and Ir/$CaCO_3$ (5 wt.-%) were received from Alfa Aesar and used without further treatment or purification. Ir@MIL101 (5 wt.-%) was prepared in our group by chemical vapour deposition. The amount of active metal was the same as in 200 mg of the above used Ir@SiCN catalyst.

Ir/C:

508 mg Ir/C, 1-phenylethanol (2904 µL, 24.0 mmol), 2-amino-butan-1-ol (565 µL, 6.0 mmol), 6 mL diglyme, and KO^{t}Bu (1.37 g, 12.0 mmol) were heated at 120 °C (oil bath temperature) for 24 h. After extraction with diethyl ether the yield was determined by GC. The catalyst was recovered by centrifugation, washed with water (1x) and acetone (2x) and used for one more run.

Ir/Al_2O_3:

254 mg Ir/Al_2O_3, 1-phenylethanol (2904 µL, 24.0 mmol), 2-amino-butan-1-ol (565 µL, 6.0 mmol), 6 mL diglyme, and KO^{t}Bu (1.37 g, 12.0 mmol) were heated at 120 °C (oil bath temperature) for 24 h. After extraction with diethyl ether the yield was determined by GC. The catalyst was recovered by centrifugation, washed with water (1x) and acetone (2x) and used for one more run.

Ir/$CaCO_3$:

50 mg Ir/$CaCO_3$, 1-phenylethanol (2904 µL, 24.0 mmol), 2-amino-butan-1-ol (565 µL, 6.0 mmol), 6 mL diglyme, and KO^{t}Bu (1.37 g, 12.0 mmol) were heated at 120 °C (oil bath temperature) for 24 h. After extraction with diethyl ether the yield was determined by GC. The catalyst was recovered by centrifugation, washed with water (1x) and acetone (2x) and used for one more run.

Ir@MIL101:

50.8 mg Ir@MIl101, 1-phenylethanol (2904 µL, 24.0 mmol), 2-amino-butan-1-ol (565 µL, 6.0 mmol), 6 mL diglyme, and KO^{t}Bu (1.37 g, 12.0 mmol) were heated at 120 °C (oil bath temperature) for 24 h. After extraction with diethyl ether the yield was determined by GC.

6.6.4 Screening Reactions

General Screening Procedure:

In a pressure tube catalyst, solvent, alcohol, amino alcohol and base were combined. The pressure tube was closed with a semi-permeable membrane, added to a pressure equalizer, heated to the desired temperaure and stirred for 24 h. The reaction mixture was cooled to room temperature under argon atmosphere and 1 mL of water as well as 5 mL diethyl ether were added. *n*-Dodecane was added as internal standard and after shaking, a small fraction of the organic phase was analyzed by GC. The following reaction was investigated.

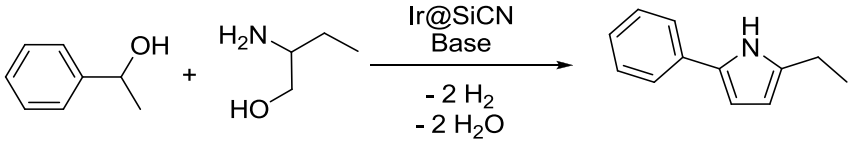

Supplementary Table 1: Alcohol ratio

Amino Alcohol / Secondary Alcohol [eq.]	Yield [%]
1 : 3	**34**
1 : 2	**51**
1 : 1.5	**54**
1 : 1.1	**53**
1.1 : 1	**61**
1.5 : 1	**68**
2 : 1	**45**
3 : 1	**55**

Reaction conditions: 1.1 eq. KO^{t}Bu (according to secondary alcohol), 1.5 mL diglyme, 50 mg (0.33 mol%) Ir@SiCN catalyst, 24 h, 120 °C (oil bath temperature) (reaction connected to a pressure equalisation). Yields were determined by GC analyses with *n*-dodecane as internal standard.

Supplementary Table 2: Temperature screening

Temperature [°C] (Oil Bath)	Yield [%]
90	**33**
105	**42**
120	**68**
130	**68**
150	**54**

Reaction conditions: 1 eq. 2-amino-1-butanol (1 mmol, 94.1 µL), 1.5 eq. 1–phenylethanol (1.5 mmol, 181.4 µL), 1.1 eq. KO^{t}Bu (according to secondary alcohol), 1.5 mL diglyme, 50 mg (0.33 mol%) Ir@SiCN catalyst, 24 h (reaction connected to a pressure equalisation). Yields were determined by GC analyses with *n*-dodecane as internal standard.

Supplementary Table 3: Solvent screening

Solvent	Yield [%]
THF	**12**
Diglyme	**68**
Dioxane	**41**
Toluene	**56**
Water	**0**

Reaction conditions: 1 eq. 2-amino-1-butanol (1 mmol, 94.1 µL), 1.5 eq. 1–phenylethanol (1.5 mmol, 181.4 µL), 1.1 eq. KO^{t}Bu (according to secondary alcohol), 1.5 mL solvent, 50 mg (0.33 mol%) Ir@SiCN catalyst, 120 °C or reflux, 24 h (reaction connected to a pressure equalisation). Yields were determined by GC analyses with *n*-dodecane as internal standard.

Supplementary Table 4: Solvent Amount

Amount Diglyme [mL]	Yield [%]
3	**50**
1.5	**68**
0.5	**64**

Reaction conditions: 1 eq. 2-amino-1-butanol (1 mmol, 94.1 µL), 1.5 eq. 1–phenylethanol (1.5 mmol, 181.4 µL), 1.1 eq. KO^{t}Bu (according to secondary alcohol), 50 mg (0.33 mol%) Ir@SiCN catalyst, 120 °C (oil bath temperature), 24 h (reaction connected to a pressure equalisation). Yields were determined by GC analyses with *n*-dodecane as internal standard.

Supplementary Table 5: Base screening

Base	Yield [%]
KO^tBu	**68**
NaO^tBu	**58**
KOH	**61**
KH	**45**
K_2CO_3	**0**

Reaction conditions: 1 eq. 2-amino-1-butanol (1 mmol, 94.1 µL), 1.5 eq. 1–phenylethanol (1.5 mmol, 181.4 µL), 1.1 eq. base (according to secondary alcohol), 1.5 mL diglyme, 50 mg (0.33 mol%) Ir@SiCN catalyst, 120 °C (oil bath temperature), 24 h (reaction connected to a pressure equalisation). Yields were determined by GC analyses with *n*-dodecane as internal standard.

Supplementary Table 6: Amount of KO^tBu

Base Amount According to Secondary Alcohol [eq.]	Yield [%]
2	**34**
1.5	**50**
1.1	**68**
1	**73**
0.9	**72**
0.8	**66**
0.5	**57**
0.1	**12**
0	**0**

Reaction conditions: 1 eq. 2-amino-1-butanol (1 mmol, 94.1 µL), 1.5 eq. 1–phenylethanol (1.5 mmol, 181.4 µL), 1.5 mL diglyme, 50 mg (0.37 mol%) Ir@SiCN catalyst, 120 °C (oil bath temperature), 24 h (reaction connected to a pressure equalisation). Yields were determined by GC analyses with *n*-dodecane as internal standard.

Supplementary Table 7: Screening of catalyst loading

Catalyst Loading [mol-%]	Yield [%]
0.33	**68**
0.66	**73**
1.98	**66**

Reaction conditions: 1 eq. 2-amino-1-butanol (1 mmol, 94.1 µL), 1.5 eq. 1–phenylethanol (1.5 mmol, 181.4 µL), 1.0 eq. KO^{t}Bu (according to secondary alcohol), 1.5 mL diglyme, 120 °C (oil bath temperature), 24 h (reaction connected to a pressure equalisation). Yields were determined by GC analyses with *n*-dodecane as internal standard.

Screen-Up & Optimization of Base to Alcohol Ratio:

The consumption of 1-phenylethanol in conjunction with high amounts of base was always 90-100 %. Therefore the base to alcohol ratio had to be optimized to increase the yield of the desired product. Therefore the amount of KO^{t}Bu was decreased to 0.5 eq. according to the alcohol:

Supplementary Table 8: Temperature screening II

Temperature [°C] (Oil Bath)	Yield [%]
100 (42 h)	**20**
120	**68**
130	**72**

Reaction conditions: 1 eq. 2-amino-1-butanol (6 mmol, 565 µL), 1.5 eq. 1–phenylethanol (9 mmol, 1088 µL), 0.5 eq. KO^{t}Bu (according to secondary alcohol), 300 mg (0.33 mol%) Ir@SiCN catalyst, 9 mL diglyme, 24 h (reaction connected to a pressure equalisation). Yields were determined by GC analyses with *n*-dodecane as internal standard. The increase in conversion from 120 to 130 °C seemed minor and a temperature of 120 °C was regarded as optimal in terms of a good functional group tolerance.

Supplementary Table 9: Solvent Amount II

Amount Diglyme [mL]	Yield [%]
6	**74**
9	**68**
12	**53**

Reaction conditions: 1 eq. 2-amino-1-butanol (6 mmol, 565 µL), 1.5 eq. 1–phenylethanol (9 mmol, 1088 µL), 0.5 eq. KO^{t}Bu (according to secondary alcohol), 300 mg (0.33 mol%) Ir@SiCN catalyst, 120 °C (oil bath temperature), 24 h (reaction connected to a pressure equalisation). Yields were determined by GC analyses with *n*-dodecane as internal standard.

Supplementary Table 10: Screening of catalyst loading II

Catalyst Loading [mol%]	Yield [%]
0.12	**58**
0.33	**68**
0.50	**75**

Reaction conditions: 1 eq. 2-amino-1-butanol (6 mmol, 565 µL), 1.5 eq. 1–phenylethanol (9 mmol, 1088 µL), 0.5 eq. KO^{t}Bu (according to secondary alcohol), 120 °C (oil bath temperature), 6 mL diglyme, 24 h (reaction connected to a pressure equalisation). Yields were determined by GC analyses with *n*-dodecane as internal standard. A catalyst loading of 0.33 mol% seemed the optimum in terms of high conversion and low catalyst loading.

Supplementary Table 11: Alcohol ratio

Amino Alcohol / Secondary Alkohol [eq.]	Yield [%]
1.5 : 1	**68**
2 : 1	**74**
4 : 1	**96**

Reaction conditions: 0.5 eq. KO^{t}Bu (according to secondary alcohol), 200 mg (0.33 mol%) Ir@SiCN catalyst, 120 °C (oil bath temperature), 6 mL diglyme, 24 h (reaction connected to a pressure equalisation). Yields were determined by GC analyses with *n*-dodecane as internal standard.

6.6.5 Characterization of the Pyrrole Products

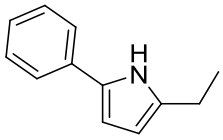

1a: 2-ethyl-5-phenyl-1*H*-pyrrole:

200 mg Ir@SiCN, 1-phenylethanol (2904 µL, 24.0 mmol), 2-amino-butan-1-ol (565 µL, 6.0 mmol), 6 mL diglyme, KO^{t}Bu (1.37 g, 12.0 mmol), 24 h at 120 °C (oil bath temperature). Purification by column chromatography 40:1 pentane: Et_2O; Yield: 0.887 g = 5.18 mmol = 86 % as colourless solid. M($C_{12}H_{13}N$) = 171.24 gmol^{-1}.

^{1}H NMR (300 MHz, CD_2Cl_2, 298 K): δ = 8.25 (s_br, 1H), 7.48-7.44 (m, 2H), 7.40-7.34 (m, 2H), 7.22-7.16 (m, 1H), 6.44-6.42 (m, 1H), 6.00-5.98 (m, 1H), 2.70 (q, *J* = 7.5 Hz, 2H), 1.30 (t, *J* = 7.5 Hz, 3H) ppm. ^{13}C NMR (75 MHz, CD_2Cl_2, 298 K): δ = 136.3, 133.6, 130.8, 129.4, 126.1, 123.7, 106.7, 106.5, 21.5, 14.1 ppm. MS (EI, m/z): 171.1 (M^+).

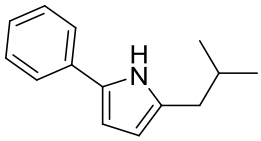

1b: 2-isobutyl-5-phenyl-1*H*-pyrrole:

200 mg Ir@SiCN, 1-phenylethanol (2904 µL, 24.0 mmol), 2-amino-4-methylpentan-1-ol (767 µL, 6.0 mmol), 6 mL diglyme, KO^{t}Bu (1.37 g, 12.0 mmol), 24 h at 120 °C (oil bath temperature). Purification by column chromatography 50:1 pentane: Et_2O; Yield: 1.113 g = 5.58 mmol = 93 % as colourless solid. M($C_{14}H_{17}N$) = 199.29 gmol^{-1}.

^{1}H NMR (300 MHz, CD_2Cl_2, 298 K): δ = 8.19 (s_br, 1H), 7.46-7.43 (m, 2H), 7.37-7.32 (m, 2H), 7.19-7.14 (m, 1H), 6.42-6.40 (m, 1H), 5.96-5.94 (m, 1H), 2.51 (d, *J* = 7.2 Hz, 2H), 1.96-1.83 (m, 1H), 0.97 (d, *J* = 6.6 Hz, 6H) ppm. ^{13}C NMR (75 MHz, CD_2Cl_2, 298 K): δ = 133.9, 133.6, 130.7, 129.4, 126.0, 123.6, 108.5, 106.6, 37.8, 29.8, 22.7 ppm. MS (EI, m/z): 199.2 (M^+).

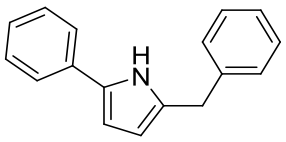

1c: 2-benzyl-5-phenyl-1*H*-pyrrole:

200 mg Ir@SiCN, 1-phenylethanol (2904 µL, 24.0 mmol), 2-amino-3-phenylpropan-1-ol (907 mg, 6.0 mmol), 6 mL diglyme, KO^{t}Bu (1.37 g, 12.0 mmol), 24 h at 120 °C (oil bath temperature). Purification by column chromatography 80:1 → 10:1 pentane: Et_2O; Yield: 1.234 g = 5.29 mmol = 88 % as colourless solid. M($C_{17}H_{15}N$) = 233.31 gmol^{-1}.

^{1}H NMR (300 MHz, CD_2Cl_2, 298 K): δ = 8.18 (s_br, 1H), 7.42-7.38 (m, 2H), 7.35-7.23 (m, 7H), 7.18-7.13 (m, 1H), 6.43-6.41 (m, 1H), 6.03-6.01 (m, 1H), 4.02 (s, 2H) ppm. ^{13}C NMR (75 MHz, CD_2Cl_2, 298 K): δ = 140.2, 133.3, 132.9, 131.8, 129.3, 129.1, 129.1, 127.0, 126.3, 123.8, 109.0, 106.6, 34.7 ppm. MS (EI, m/z): 233.2 (M^+).

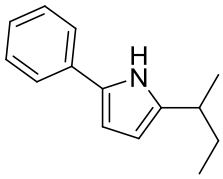

1d: 2-sec-butyl-5-phenyl-1*H*-pyrrole:

200 mg Ir@SiCN, 1-phenylethanol (2904 µL, 24.0 mmol), 2-amino-3-methylpentan-1-ol (703 mg, 6.0 mmol), 6 mL diglyme, KO^{t}Bu (1.37 g, 12.0 mmol), 24 h at 120 °C (oil bath temperature). Purification by column chromatography 50:1 pentane: Et_2O; Yield: 1.025 g = 5.14 mmol = 86 % as colourless oil. M($C_{14}H_{17}N$) = 199.29 gmol^{-1}.

^{1}H NMR (300 MHz, CD_2Cl_2, 298 K): δ = 8.24 (s_br, 1H), 7.51-7.47 (m, 2H), 7.42-7.36 (m, 2H), 7.24-7.18 (m, 1H), 6.48-6.46 (m, 1H), 6.03-6.01 (m, 1H), 2.82-2.71 (m, 1H), 1.80-4.57 (m, 2H), 1.33 (d, *J* = 6.9 Hz, 3H), 0.98 (t, *J* = 7.2 Hz, 3H) ppm. ^{13}C NMR (75 MHz, CD_2Cl_2, 298 K): δ = 139.9, 133.7, 130.6, 129.4, 126.1, 123.7, 106.4, 106.2, 35.0, 30.8, 20.6, 12.2 ppm. MS (EI, m/z): 199.1 (M^+).

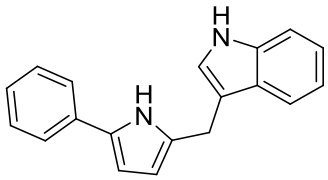

1e: 3-(5-phenyl-1*H*-pyrrol-2-ylmethyl)-1*H*-indole:

200 mg Ir@SiCN, 1-phenylethanol (2892 µL, 24.0 mmol), 2-amino-3-(1*H*-indol-3-yl)-propan-1-ol (1.14 g, 6.0 mmol), 6 mL diglyme, KO^{t}Bu (1.37 g, 12.0 mmol), 24 h at 120 °C (oil bath temperature). Purification by column chromatography 15:1 → 8:1 → 4:1 pentane: Et_2O; Yield: 0.964 g = 3.54 mmol = 59 % as colourless solid. M($C_{19}H_{16}N_2$) = 272.34 gmol^{-1}.

^{1}H NMR (300 MHz, CD_2Cl_2, 298 K): δ = 8.24 (s_br, 1H), 8.13 (s_br, 1H), 7.57-7.54 (m, 1H), 7.41-7.35 (m, 3H), 7.32-7.27 (m, 2H), 7.22-7.06 (m, 4H), 6.45-6.43 (m, 1H), 6.10-6.08 (m, 1H), 4.17 (s, 2H) ppm. ^{13}C NMR (75 MHz, CD_2Cl_2, 298 K): δ = 137.1, 133.5, 133.3, 131.2, 129.3, 127.8, 126.1, 123.7, 123.0, 122.7, 120.0, 119.3, 114.2, 111.7, 108.3, 106.6, 24.5 ppm. MS (EI, m/z): 272.2 (M^+).

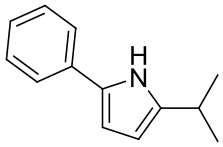

1f: 2-isopropyl-5-phenyl-1*H*-pyrrole:

200 mg Ir@SiCN, 1-phenylethanol (2904 µL, 24.0 mmol), 2-amino-3-methyl-butan-1-ol (619 mg, 6.0 mmol), 6 mL diglyme, KO^{t}Bu (1.37 g, 12.0 mmol), 24 h at 120 °C (oil bath temperature). Purification by column chromatography 90:1 → 25:1 pentane: Et_2O; Yield: 0.998 g = 5.39 mmol = 90 % as colourless oil. M($C_{13}H_{15}N$) = 185.26 gmol^{-1}.

^{1}H NMR (300 MHz, CD_2Cl_2, 298 K): δ = 8.23 (s_br, 1H), 7.49-7.45 (m, 2H), 7.40-7.35 (m, 2H), 7.22-7.16 (m, 1H), 6.44-6.42 (m, 1H), 6.00-5.98 (m, 1H), 3.06-2.93 (m, 1H), 1.33 (d, *J* = 6.9 Hz, 6H) ppm. ^{13}C NMR (75 MHz, CD_2Cl_2, 298 K): δ = 141.0, 133.6, 130.7, 129.4, 126.1, 123.8, 106.4, 105.5, 27.8, 23.1 ppm. MS (EI, m/z): 185.2 (M^+).

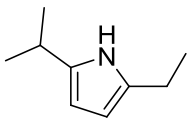

1g: 2-ethyl-5-isopropyl-1*H*-pyrrole:

200 mg Ir@SiCN, 3-methyl-butan-2-ol (2580 µL, 24.0 mmol), 2-amino-butan-1-ol (565 µL, 6.0 mmol), 6 mL diglyme, KO^{t}Bu (1.37 g, 12.0 mmol), 24 h at 120 °C (oil bath temperature). Purification by column chromatography 40:1→ 20:1 pentane: Et_2O; Yield: 0.446 g = 3.25 mmol = 54 % as colourless oil. M($C_9H_{15}N$) = 137.22 gmol^{-1}.

^{1}H NMR (300 MHz, CD_2Cl_2, 298 K): δ = 7.65 (s_br, 1H), 5.82-5.80 (m, 2H), 2.95-2.86 (m, 1H), 2.62 (q, *J* = 7.8 Hz, 2H), 1.28-1.23 (m, 9H) ppm. ^{13}C NMR (75 MHz, $CDCl_3$, 298 K): δ = 137.4, 132.5, 103.6, 102.6, 27.0, 22.7, 20.8, 13.5 ppm. MS (EI, m/z): 137.2 (M^+).

elemental analysis (%) for $C_9H_{15}N$ calcd: C 78.77, H 11.02, N 10.21; found: C 79.21, H 11.44, N 10.30.

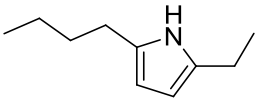

1h: 2-ethyl-5-butyl-1*H*-pyrrole:

200 mg Ir@SiCN, 2-hexanol (3024 µL, 24.0 mmol), 2-amino-butan-1-ol (565 µL, 6.0 mmol), 6 mL diglyme, KO^{t}Bu (1.37 g, 12.0 mmol), 24 h at 120 °C (oil bath temperature). Purification by column chromatography 100:1 → 20:1 pentane: Et_2O; Yield: 0.734 g = 4.85 mmol = 81 % as colourless oil. M($C_{10}H_{17}N$) = 151.25 gmol^{-1}.

^{1}H NMR (300 MHz, CD_2Cl_2, 298 K): δ = 7.70 (s_br, 1H), 5.76-5.74 (m, 2H), 2.63-2.54 (m, 4H), 1.65-1.55 (m, 2H), 1.47-1.34 (m, 2 H), 1.24 (t, *J* = 7.5 Hz, 3H), 0.97 (t, *J* = 7.5 Hz, 3H) ppm. ^{13}C NMR (75 MHz, CD_2Cl_2, 298 K): δ = 133.0, 131.7, 105.1, 104.4, 32.7, 28.0, 23.1, 21.4, 14.3, 14.2 ppm. MS (EI, m/z): 151.1 (M^+).

elemental analysis (%) for $C_{10}H_{77}N$ calcd: C 79.41, H 11.33, N 9.26; found: C 79.81, H 11.10, N 8.71.

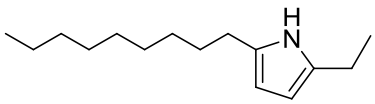

1i: 2-ethyl-5-nonyl-1*H*-pyrrole:

200 mg Ir@SiCN, 2-undecanol (4992 µL, 24.0 mmol), 2-amino-butan-1-ol (565 µL, 6.0 mmol), 6 mL diglyme, KO^{t}Bu (1.37 g, 12.0 mmol), 24 h at 120 °C (oil bath temperature). Purification by column chromatography 70:1 → 30:1 pentane: Et_2O; Yield: 0.867 g = 3.92 mmol = 65 % as colourless solid. M($C_{15}H_{27}N$) = 221.38 gmol^{-1}.

^{1}H NMR (300 MHz, CD_2Cl_2, 298 K): δ = 7.66 (s_br, 1H), 5.73-5.70 (m, 2H), 2.61-2.50 (m, 4H), 1.63-1.54 (m, 2H), 1.40-1.24 (m, 12H), 1.21 (t, *J* = 7.8 Hz, 3H), 0.90 (t, *J* = 6.9 Hz, 3H) ppm. ^{13}C NMR (75 MHz, CD_2Cl_2, 298 K): δ = 132.9, 131.7, 105.0, 104.3, 32.5, 30.5, 30.2, 30.1, 30.0, 29.9, 28.3, 23.3, 21.4, 14.5, 14.2 ppm. MS (EI, m/z): 221.2 (M^+).

elemental analysis (%) for $C_{15}H_{27}N$ calcd: C 81.38, H 12.29, N 6.33; found: C 81.37, H 12.78, N 6.38.

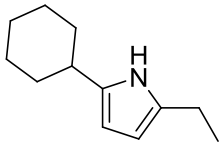

1j: 2-ethyl-5-cyclohexyl-1*H*-pyrrole:

200 mg Ir@SiCN, 1-cyclohexyl-1-ethanol (3316 µL, 24.0 mmol), 2-amino-butan-1-ol (565 µL, 6.0 mmol), 6 mL diglyme, KO^{t}Bu (1.37 g, 12.0 mmol), 24 h at 120 °C (oil bath temperature). Purification by column chromatography 80:1 → 20:1 pentane : Et_2O; Yield: 0.663 g = 3.74 mmol = 63 % as light yellow oil. M($C_{12}H_{19}N$) = 177.29 gmol^{-1}.

^{1}H NMR (300 MHz, CD_2Cl_2, 298 K): δ = 7.68 (s_br, 1H), 5.73-5.69 (m, 2H), 2.57 (q, *J* = 7.5 Hz, 2H), 2.51-2.45 (m, 1H), 2.00-1.90 (m, 2H), 1.84-1.68 (m, 3H), 1.45-1.26 (m, 5 H), 1.21 (t, *J* = 7.5 Hz, 3H) ppm. ^{13}C NMR (75 MHz, CD_2Cl_2, 298 K): δ = 137.1, 132.6, 104.1, 103.1, 37.4, 34.0, 27.0, 26.8, 21.4, 14.1 ppm. MS (EI, m/z): 177.2 (M^+).

elemental analysis (%) for $C_{12}H_{19}N$ calcd: C 81.30, H 10.80, N 7.90; found: C 81.27, H 10.71, N 8.05.

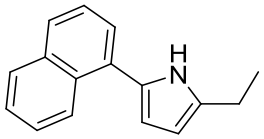

1k: 2-ethyl-5-(naphthalene-1-yl)-1*H*-pyrrole:

200 mg Ir@SiCN, (±)-1-(1-naphthyl)ethanol (4.13 g, 24.0 mmol), 2-amino-butan-1-ol (565 µL, 6.0 mmol), 5 mL diglyme, KO^{t}Bu (1.37 g, 12.0 mmol), 24 h at 120 °C (oil bath temperature). Purification by column chromatography 10:1 → 2:1 pentane : Et_2O; Yield: 0.942 g = 4.26 mmol = 71 % as yellow oil. M($C_{16}H_{15}N$) = 221.12 gmol^{-1}.

^{1}H NMR (300 MHz, CD_2Cl_2, 298 K): δ = 8.41-8.36 (m, 1H), 8.23 (s_br, 1H), 7.93-7.88 (m, 1H), 7.82-7.76 (m, 1H), 7.55-7.47 (m, 4H), 6.42-6.40 (m, 1H), 6.10-6.08 (m, 1H), 2.75 (q, *J* = 7.5 Hz, 2H), 1.34 (t, *J* = 7.5 Hz, 3H) ppm. ^{13}C NMR (75 MHz, CD_2Cl_2, 298 K): δ = 135.9, 134.7, 132.4, 131.7, 129.2, 128.9, 127.4, 126.7, 126.4, 126.3, 126.1, 125.9, 110.2, 106.2, 21.5, 14.1 ppm. MS (EI, m/z): 222.1 (M^+).

elemental analysis (%) for $C_{16}H_{15}N$ calcd: C 86.84, H 6.83, N 6.33; found: C 87.03, H 6.96, N 6.66.

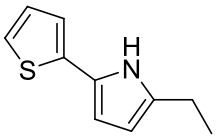

1l: 2-ethyl-5-(thiophen-2-yl)-1*H*-pyrrole:

200 mg Ir@SiCN, 1-(thiophen-yl)ethanol (2643 µL, 24.0 mmol), 2-amino-butan-1-ol (565 µL, 6.0 mmol), 6 mL diglyme, KO^{t}Bu (1.37 g, 12.0 mmol), 24 h at 130 °C (oil bath temperature). Purification by column chromatography 20:1 →15:1 pentane: Et_2O; Yield: 0.511 g = 2.90 mmol = 48 % as yellow oil. M($C_{10}H_{11}NS$) = 177.27 gmol^{-1}.

^{1}H NMR (300 MHz, CD_2Cl_2, 298 K): δ = 8.11 (s_br, 1H), 7.13-7.10 (m, 1H), 7.02-6.97 (m, 2H), 6.28-6.26 (m, 1H), 5.92-5.90 (m, 1H), 2.65 (q, *J* = 7.5 Hz, 2 H), 1.27 (t, *J* = 7.5 Hz, 3H) ppm. ^{13}C NMR (75 MHz, CD_2Cl_2, 298 K): δ = 137.3, 136.1, 128.2, 125.5, 122.4, 120.4, 107.2, 106.6, 21.4, 14.1 ppm. MS (EI, m/z): 177.1 (M^+).

elemental analysis (%) for $C_{10}H_{11}NS$ calcd: C 67.76, H 6.25, N 7.90; found: C 68.18, H 6.57, N 7.86.

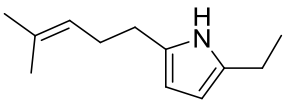

1m: 2-ethyl-5-(4-methyl-pent-3-enyl)-1*H*-pyrrole:

200 mg Ir@SiCN, 6-methyl-5-hepten-2-ol (3664 µL, 24.0 mmol), 2-amino-butan-1-ol (565 µL, 6.0 mmol), 6 mL diglyme, KO^{t}Bu (1.37 g, 12.0 mmol), 24 h at 130 °C (oil bath temperature). Purification by column chromatography 70:1 → 30:1 pentane: Et_2O; Yield: 0.834 g = 4.70 mmol = 78 % as light yellow oil. M($C_{12}H_{19}N$) = 177.29 gmol^{-1}.

^{1}H NMR (300 MHz, CD_2Cl_2, 298 K): δ = 7.70 (s_br, 1H), 5.73-5.69 (m, 2H), 5.23-5.17 (m, 1H), 2.60-2.53 (m, 4H), 2.27 (q, *J* = 7.5 Hz, 2H), 1.71 (s, 3H), 1.60 (s, 3H), 1.20 (t, *J* = 7.5 Hz, 3H) ppm. ^{13}C NMR (75 MHz, CD_2Cl_2, 298 K): δ = 133.1, 132.9, 131.4, 105.2, 104.4, 29.0, 28.4, 26.0, 21.4, 18.0, 14.2 ppm. MS (EI, m/z): 177.2 (M^+).

elemental analysis (%) for $C_{12}H_{19}N$ calcd: C 81.30, H 10.80, N 7.90; found: C 81.49, H 10.78, N 8.11.

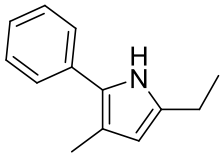

2a: 5-ethyl-3-methyl-2-phenyl-1*H*-pyrrole:

200 mg Ir@SiCN, 1-phenylpropanol (3288 µL, 24.0 mmol), 2-amino-butan-1-ol (565 µL, 6.0 mmol), 6 mL diglyme, KO^{t}Bu (1.37 g, 12.0 mmol), 24 h at 135 °C (oil bath temperature). Purification by column chromatography 50:1 → 20:1 pentane : Et_2O; Yield: 0.740 g = 3.99 mmol = 67 % as colourless oil. M($C_{13}H_{15}N$) = 185.26 gmol^{-1}.

^{1}H NMR (300 MHz, CD_2Cl_2, 298 K): δ = 7.91 (s_br, 1H), 7.41-7.35 (m, 4H), 7.22-7.16 (m, 1H), 5.83-5.82 (m, 1H), 2.63 (q, *J* = 7.5 Hz, 2H), 2.22 (s, 3H), 1.25 (t, *J* = 7.5 Hz, 3H) ppm. ^{13}C NMR (75 MHz, CD_2Cl_2, 298 K): δ = 134.7, 134.6, 129.2, 126.7, 126.2, 125.8, 116.8, 109.2, 21.4, 14.1, 13.0 ppm. MS (EI, m/z): 185.1 (M^+).

elemental analysis (%) for $C_{13}H_{15}N$ calcd: C 84.28, H 8.16, N 7.56; found: C 84.76, H 7.63, N 7.13.

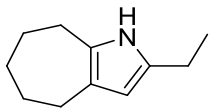

2b: 2-ethyl-1,5,6,7,8,9-hexahydro-cyclohepta[*b*]pyrrole:

800 mg Ir@SiCN, cycloheptanol (11568 µL, 96.0 mmol), 2-amino-butan-1-ol (2260 µL, 24.0 mmol), 16 mL diglyme, KO^{t}Bu (5.48 g, 48.0 mmol), 24 h at 120 °C (oil bath temperature). Purification by column chromatography 40:1 → 20:1 pentane: Et_2O; Yield: 3.516 g = 21.54 mmol = 90 % as colourless solid. M($C_{11}H_{17}N$) = 163.26 gmol^{-1}.

^{1}H NMR (300 MHz, C_6D_6, 298 K): δ = 6.45 (s_br, 1H), 5.80 (d, *J* = 3.0 Hz, 1H), 2.66-2.62 (m, 2H), 2.39-2.27 (m, 4H), 1.71-1.64 (m, 4H), 1.63-1.56 (m, 2H), 1.07 (t, *J* = 7.5 Hz, 3H) ppm. ^{13}C NMR (75 MHz, C_6D_6, 298 K): δ = 129.1, 127.9, 121.2, 107.1, 32.6, 30.0, 29.4, 29.1, 28.7, 21.1, 14.3 ppm. MS (EI, m/z): 163.1 (M^+).

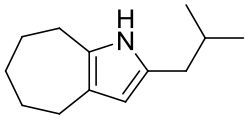

2c: 2-isobutyl-1,5,6,7,8,9-hexahydro-cyclohepta[*b*]pyrrole:

200 mg Ir@SiCN, cycloheptanol (2892 µL, 24.0 mmol), 2-amino-4-methylpentan-1-ol (767 µL, 6.0 mmol), 6 mL diglyme, KO^{t}Bu (1.37 g, 12.0 mmol), 24 h at 120 °C (oil bath temperature). Purification by column chromatography 50:1→15:1 pentane: Et_2O; Yield: 0.913 g = 4.77 mmol = 80 % as colourless solid. M($C_{13}H_{21}N$) = 191.31 gmol^{-1}.

^{1}H NMR (300 MHz, CD_2Cl_2, 298 K): δ = 7.40 (s_br, 1H), 5.57 (d, *J* = 2.7 Hz, 1H), 2.62-2.58 (m, 2H), 2.50-2.46 (m, 2H), 2.33 (d, *J* = 6.9 Hz, 2H), 1.81-1.72 (m, 3H), 1.70-1.59 (m, 4H), 0.91 (d, *J* = 6.6 Hz, 6H) ppm. ^{13}C NMR (75 MHz, CD_2Cl_2, 298 K): δ = 128.8, 127.6, 121.6, 108.5, 37.6, 32.6, 30.1, 29.9, 29.6, 29.0, 28.9, 22.8 ppm. MS (EI, m/z): 191.2 (M^+).

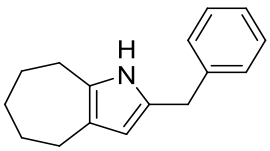

2d: 2-benzyl-1,5,6,7,8,9-hexahydro-cyclohepta[*b*]pyrrole:

200 mg Ir@SiCN, cycloheptanol (2892 µL, 24.0 mmol), 2-amino-3-phenylpropan-1-ol (907 mg, 6.0 mmol), 6 mL diglyme, KO^{t}Bu (1.37 g, 12.0 mmol), 24 h at 120 °C (oil bath temperature). Purification by column chromatography 30:1 → 10:1 pentane: Et_2O; Yield: 1.007 g = 4.47 mmol = 75 % as colourless solid. M($C_{16}H_{19}N$) = 225.33 gmol^{-1}.

^{1}H NMR (300 MHz, CD_2Cl_2, 298 K): δ = 7.40 (s_br, 1H), 7.36-7.31 (m, 2H), 7.27-7.22 (m, 3H), 5.66-5.64 (m, 1H), 3.86 (s, 2H), 2.61-2.51 (m, 4H), 1.81-1.78 (m, 2H), 1.70-1.63 (m, 4H) ppm. ^{13}C NMR (75 MHz, CD_2Cl_2, 298 K): δ = 141.0, 129.9, 129.1, 129.0, 126.8, 126.7, 121.8, 109.0, 34.6, 32.6, 30.1, 29.6, 28.9, 28.8 ppm. MS (EI, m/z): 225.2 (M^+).

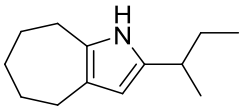

2e: 2-sec-butyl-1,5,6,7,8,9-hexahydro-cyclohepta[*b*]pyrrole:

200 mg Ir@SiCN, cycloheptanol (2892 µL, 24.0 mmol), 2-amino-3-methylpentan-1-ol (703 mg, 6.0 mmol), 6 mL diglyme, KO^{t}Bu (1.37 g, 12.0 mmol), 24 h at 120 °C (oil bath temperature). Purification by column chromatography 50:1→15:1 pentane: Et_2O; Yield: 0.881 g = 4.61 mmol = 77 % as colourless solid. M($C_{13}H_{21}N$) = 191.31 gmol^{-1}.

^{1}H NMR (300 MHz, CD_2Cl_2, 298 K): δ = 7.44 (s_br, 1H), 5.59 (d, *J* = 3.0 Hz, 1H), 2.64-5.59 (m, 2H), 2.57-2.48 (m, 3H), 1.83-1.75 (m, 2H), 1.70-1.60 (m, 4H), 1.58-1.41 (m, 2H), 1.19 (d, *J* = 7.2 Hz, 3H), 0.90 (t, *J* = 7.5 Hz, 3H) ppm. ^{13}C NMR (75 MHz, CD_2Cl_2, 298 K): δ = 133.7, 128.6, 121.3, 106.2, 34.6, 32.6, 30.8, 30.1, 29.7, 29.1, 28.9, 20.5, 12.3 ppm. MS (EI, m/z): 191.2 (M^+).

elemental analysis (%) for $C_{13}H_{21}N$ calcd: C 81.61, H 11.06, N 7.32; found: C 81.38, H 11.00, N 7.34.

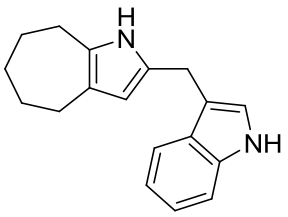

2f: 2-((1H-indol-3-yl)methyl)-1,4,5,6,7,8-hexahydrocyclohepta[b]pyrrole:

200 mg Ir@SiCN, cycloheptanol (2904 µL, 24.0 mmol), 2-amino-3-(1H-indol-3-yl)-propan-1-ol (1.14 g, 6.0 mmol), 6 mL diglyme, KOtBu (1.37 g, 12.0 mmol), 24 h at 120 °C (oil bath temperature). Purification by column chromatography 10:1 → 2:1 pentane: Et_2O and removement of cycloheptanol by vacuum distillation at 90 °C; Yield: 0.694 g = 2.63 mmol = 44 % as orange solid. M(C18H20N2) = 264.36 gmol-1.

^{1}H NMR (300 MHz, CD_2Cl_2, 298 K): δ = 8.06 (s_br, 1H), 7.58-7.55 (m, 1H), 7.45 (s_br, 1H), 7.39-7.37 (m, 1H), 7.22-7.17 (m, 1H), 7.12-7.04 (m, 2H), 5.75-5.74 (m, 1H), 4.01 (s, 2H), 2.56-2.50 (m, 4H), 1.82-1.74 (m, 2H), 1.70-1.59 (m, 4H) ppm. ^{13}C NMR (75 MHz, CD_2Cl_2, 298 K): δ = 137.0, 129.3, 127.9, 127.0, 122.8, 122.5, 121.7, 119.8, 119.4, 114.8, 111.7, 108.2, 32.6, 30.1, 29.6, 29.0, 28.8, 24.1 ppm. MS (EI, m/z): 264.1 (M^+).

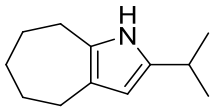

2g: 2-isopropyl-1,5,6,7,8,9-hexahydro-cyclohepta[*b*]pyrrole:

200 mg Ir@SiCN, cycloheptanol (2904 µL, 24.0 mmol), 2-amino-3-methyl-butan-1-ol (619 mg, 6.0 mmol), 6 mL diglyme, KO^{t}Bu (1.37 g, 6.0 mmol), 24 h at 120 °C (oil bath temperature). Purification by column chromatography 60:1 → 40:1 pentane: Et_2O; Yield: 0.863 g = 4.87 mmol = 81 % as colourless solid. M($C_{12}H_{19}N$) = 177.29 gmol^{-1}.

^{1}H NMR (300 MHz, CD_2Cl_2, 298 K): δ = 7.47 (s_br, 1H), 5.59 (d, *J* = 3.0 Hz, 1H), 2.88-2.74 (m, 1H), 2.63-5.59 (m, 2H), 2.51-2.47 (m, 2H), 1.86-1.75 (m, 2H), 1.69-1.60 (m, 4H), 1.20 (d, *J* = 6.9 Hz, 6H) ppm. ^{13}C NMR (75 MHz, CD_2Cl_2, 298 K): δ = 134.8, 128.7, 121.3, 105.6, 32.6, 30.1, 29.6, 29.0, 28.8, 27.4, 23.2 ppm. MS (EI, m/z): 177.2 (M^+).

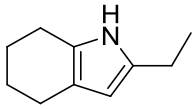

2h: 2-ethyl-1,5,6,7,8-pentahydro-cyclohexa[*b*]pyrrole:

200 mg Ir@SiCN, cyclohexanol (2529 µL, 24.0 mmol), 2-amino-butan-1-ol (565 µL, 6.0 mmol), 6 mL diglyme, KO^{t}Bu (1.37 g, 12.0 mmol), 24 h at 130 °C (oil bath temperature). Purification by column chromatography 40:1→10:1 pentane: Et_2O; Yield: 0.710 g = 4.76 mmol = 79 % as colourless oil. M($C_{10}H_{15}N$) = 149.23 gmol^{-1}.

^{1}H NMR (300 MHz, CD_2Cl_2, 298 K): δ = 7.45 (s_br, 1H), 5.59 (d, *J* = 2.4 Hz, 1H), 2.56-5.50 (m, 4H), 2.45-2.41 (m, 2H), 1.83-1.68 (m, 4H), 1.20 (t, *J* = 7.5 Hz, 3H) ppm. ^{13}C NMR (75 MHz, CD_2Cl_2, 298 K): δ = 132.7, 125.4, 117.0, 103.9, 24.6, 24.2, 23.5, 23.2, 21.4, 14.5 ppm. MS (EI, m/z): 149.1 (M^+).

elemental analysis (%) for $C_{10}H_{15}N$ calcd: C 80.48, H 10.13, N 9.39; found: C 80.52, H 10.25, N 9.10.

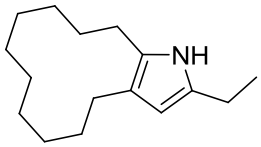

2i: 2-ethyl-4,5,6,7,8,9,10,11,12,13-decahydro-1H-cyclododeca[b]pyrrole:

200 mg Ir@SiCN, cyclododecanol (4.42 g, 24.0 mmol), 2-amino-butan-1-ol (565 µL, 6.0 mmol), 6 mL diglyme, KO^{t}Bu (1.37 g, 12.0 mmol), 24 h at 120 °C (oil bath temperature). Purification by column chromatography 40 : 1 pentane : Et_2O; Yield: 0.477 g = 2.04 mmol = 34 % as colourless oil. M($C_{16}H_{27}N$) = 233.39 gmol^{-1}.

^{1}H NMR (300 MHz, CD_2Cl_2, 298 K): δ = 7.44 (s_br, 1H), 5.68-5.67 (m, 1H), 2.63-2.56 (m, 4H), 2.41 (t, *J* = 6.0 Hz, 2H), 1.72-1.62 (m, 4H), 1.53-1.39 (m, 8H), 1.34-1.29 (m, 4H), 1.25 (t, *J* = 7.5 Hz, 3H) ppm. ^{13}C NMR (75 MHz, CD_2Cl_2, 298 K): δ = 132.8, 127.0 120.4, 104.6, 29.7, 28.8, 25.5, 25.3, 25.3, 25.2, 23.0, 23.0, 22.6, 21.5, 21.5, 14.2 ppm. MS (EI, m/z): 233.2 (M^+).

elemental analysis (%) for $C_{16}H_{27}N$ calcd: C 82.34, H 11.66, N 6.00; found: C 82.34, H 11.59, N 6.09.

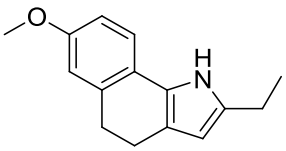

2j: 2-ethyl-7-methoxy-4,5-dihydro-1*H*-benzo[*g*]indole:

200 mg Ir@SiCN, 6-methoxy-1,2,3,4-tetrahydronaphthalene-1-ol (4.28 g, 24.0 mmol), 2-amino-butan-1-ol (565 µL, 6.0 mmol), 6 mL diglyme, KO^{t}Bu (1.37 g, 12.0 mmol), 24 h at 125 °C (oil bath temperature). Purification by column chromatography pentane : Et_2O 20:1 → 2:1; Yield: 0.492 g = 2.16 mmol = 36 % as viscous yellow oil. M($C_{15}H_{17}NO$) = 227.30 gmol^{-1}.

^{1}H NMR (300 MHz, CD_2Cl_2, 298 K): δ = 8.27 (s_br, 1H), 7.11-7.08 (m, 1H), 6.92-6.91 (m, 1H), 6.80-6.77 (m, 1H), 5.94-5.93 (m, 1H), 3.87 (s, 3H), 3.01-2.96 (m, 2H), 2.81-2.70 (m, 4H), 1.37 (t, *J* = 7.8 Hz, 3H) ppm. ^{13}C NMR (75 MHz, CD_2Cl_2, 298 K): δ = 157.5, 136.9, 135.1, 126.7, 123.8, 119.3, 119.2, 115.3, 111.7, 104.9, 55.7, 31.1, 22.6, 21.7, 14.4 ppm. MS (EI, m/z): 227.0 (M^+).

elemental analysis (%) for $C_{15}H_{17}NO$ calcd: C 79.26, H 7.54, N 6.16; found: C 79.32, H 7.28, N 5.35.

1a:

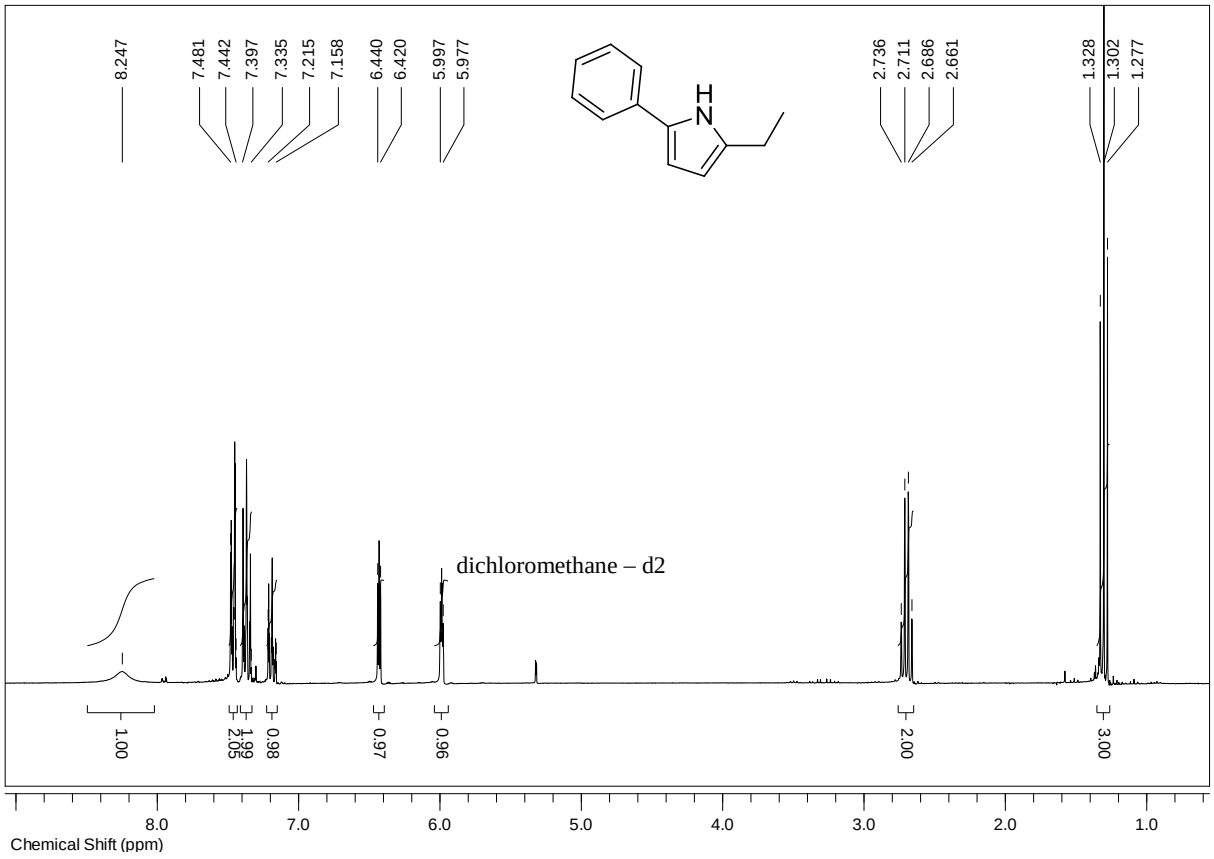
8.247
7.481
7.442
7.397
7.335
7.215
7.158
6.440
6.420
5.997
5.977
2.736
2.711
2.686
2.661
1.328
1.302
1.277
H
N
dichloromethane – d2
1.00
2.05
1.99
0.98
0.97
0.96
2.00
3.00
8.0
7.0
6.0
5.0
4.0
3.0
2.0
1.0
Chemical Shift (ppm)

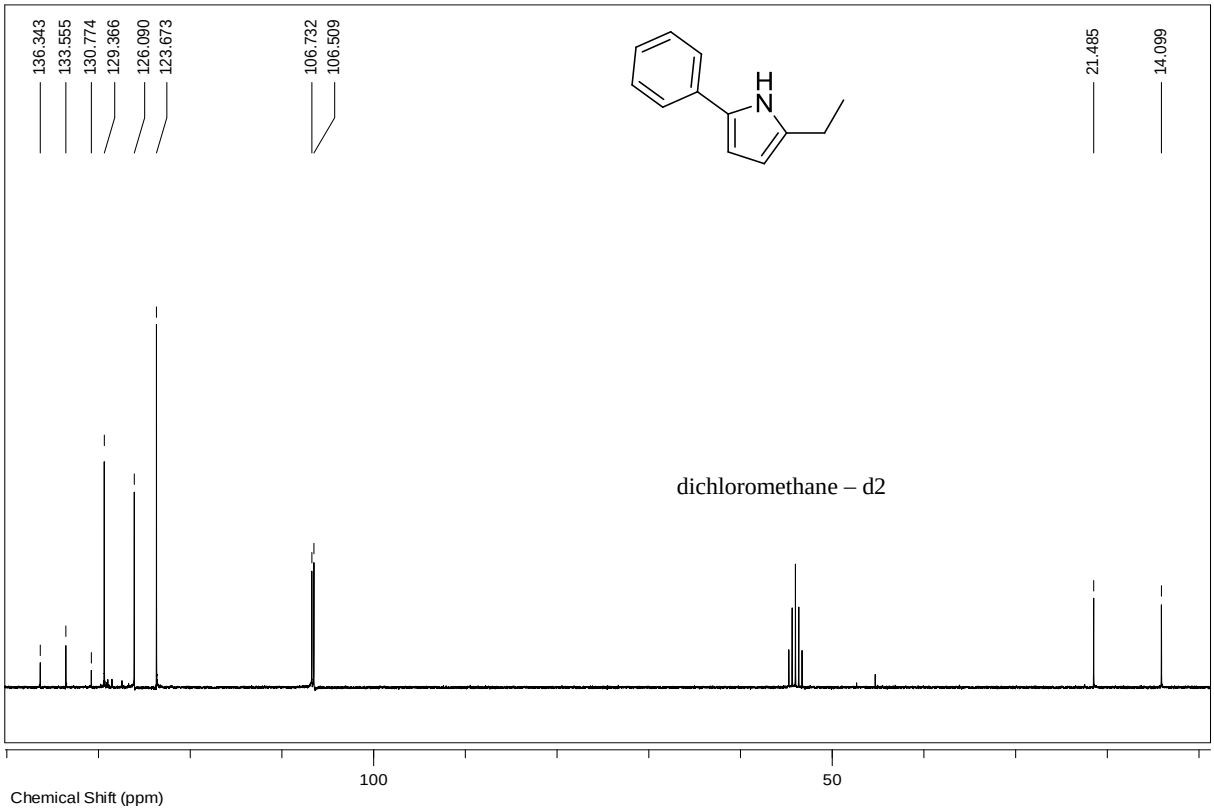
136.343
133.555
130.774
129.366
126.090
123.673
106.732
106.509
21.485
14.099
H
N
dichloromethane – d2
100
50
Chemical Shift (ppm)

1b:

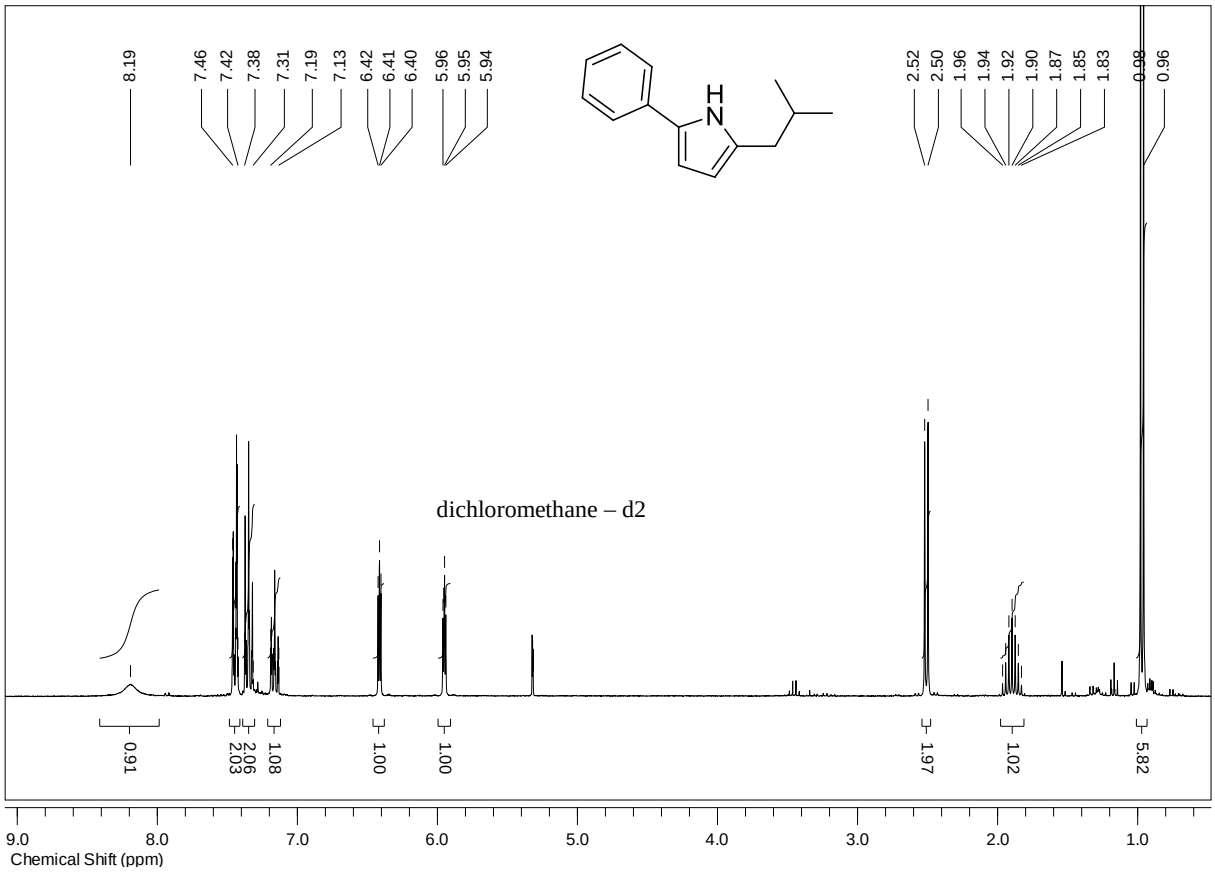
8.19
7.46
7.42
7.38
7.31
7.19
7.13
6.42
6.41
6.40
5.96
5.95
5.94
2.52
2.50
1.96
1.94
1.92
1.90
1.87
1.85
1.83
0.98
0.96
H
N
dichloromethane – d2
0.91
2.03
2.06
1.08
1.00
1.00
1.97
1.02
5.82
9.0
8.0
7.0
6.0
5.0
4.0
3.0
2.0
1.0
Chemical Shift (ppm)

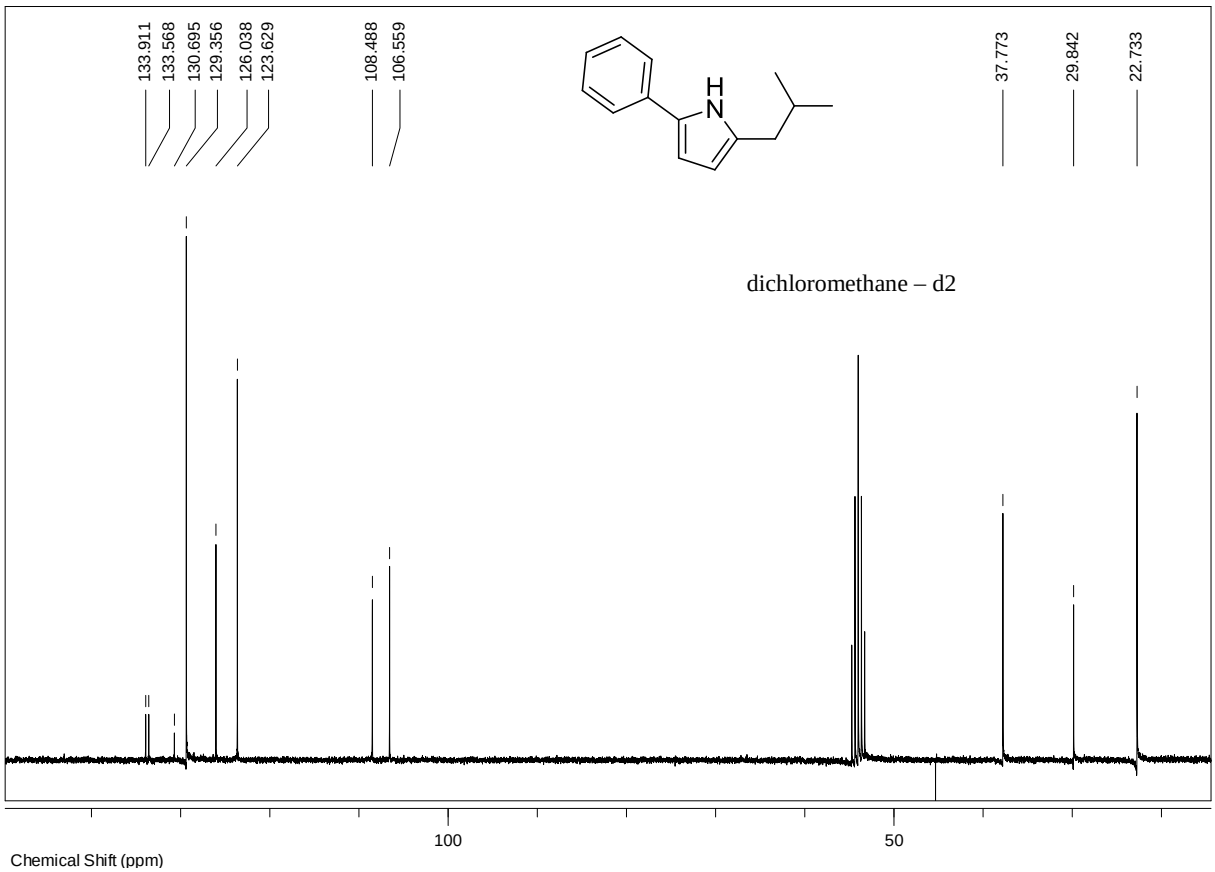
133.911
133.568
130.695
129.356
126.038
123.629
108.488
106.559
37.773
29.842
22.733
H
N
dichloromethane – d2
100
50
Chemical Shift (ppm)

1c:

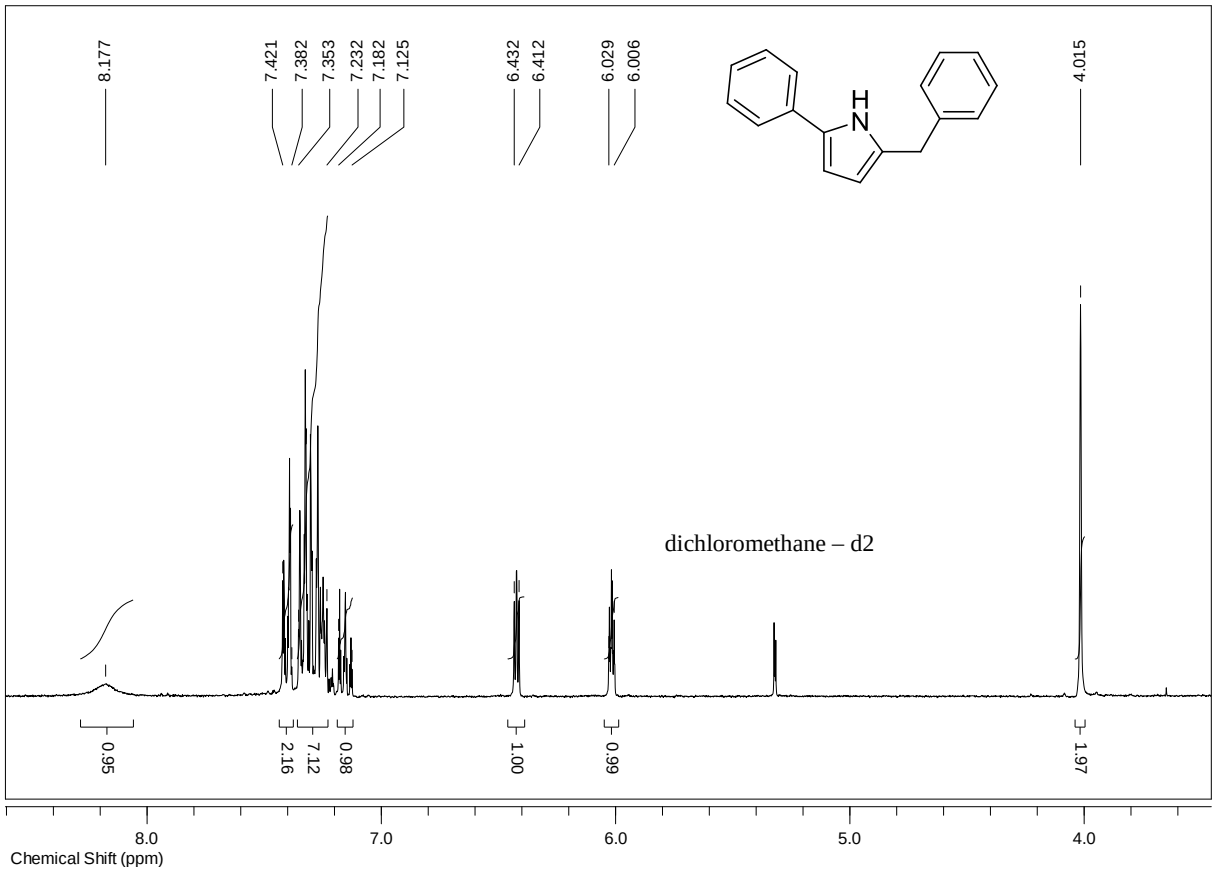
8.177
7.421
7.382
7.353
7.232
7.182
7.125
6.432
6.412
6.029
6.006
4.015
H
N
dichloromethane – d2
0.95
2.16
7.12
0.98
1.00
0.99
1.97
8.0
7.0
6.0
5.0
4.0
Chemical Shift (ppm)

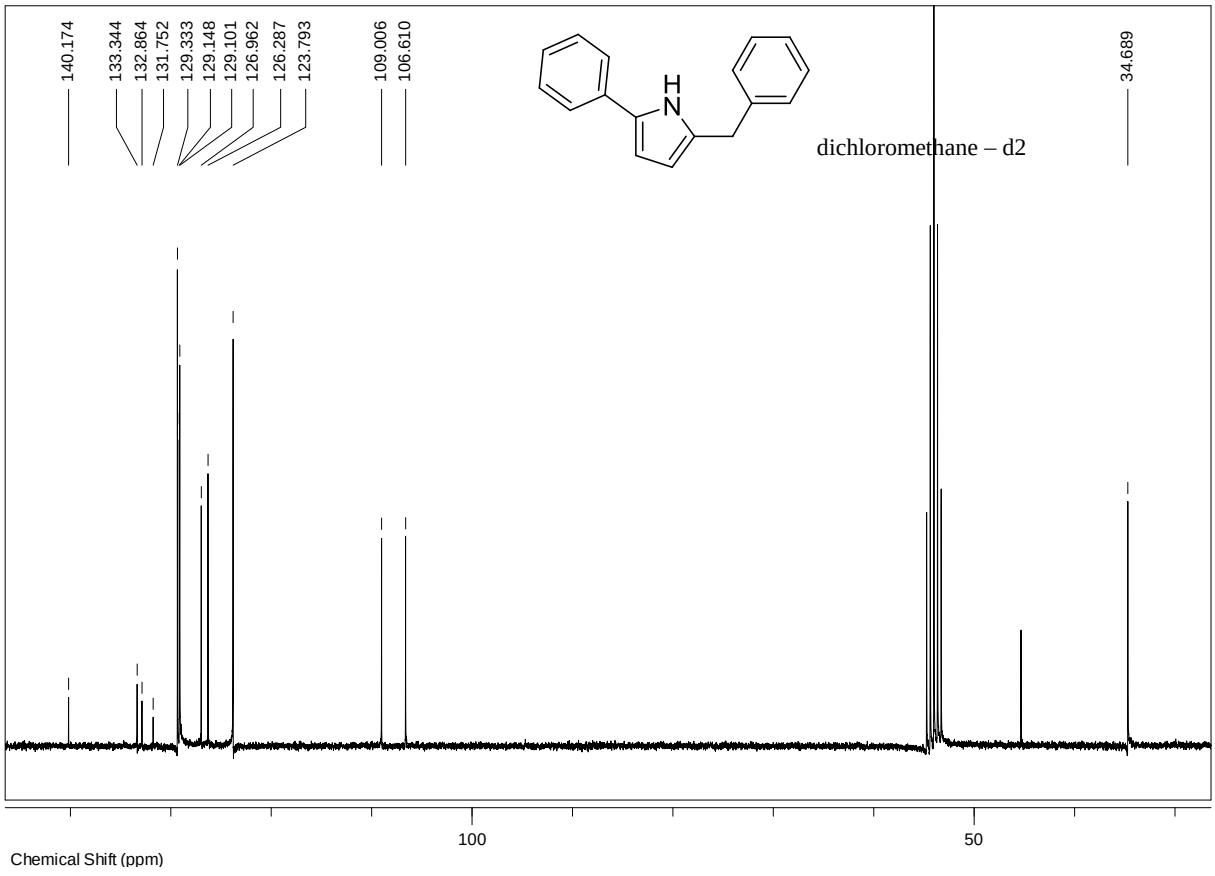
140.174
133.344
132.864
131.752
129.333
129.148
129.101
126.962
126.287
123.793
109.006
106.610
34.689
H
N
dichloromethane – d2
100
50
Chemical Shift (ppm)

1d:

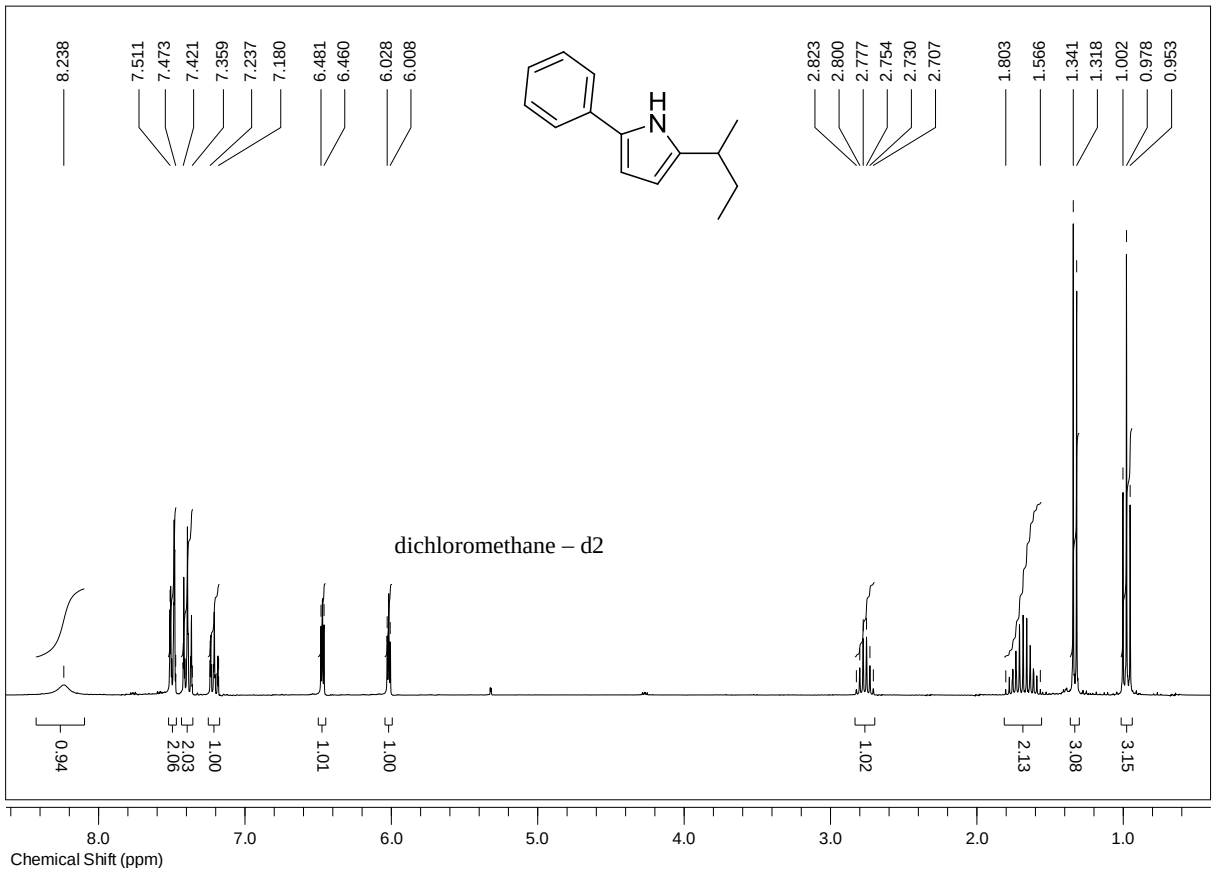
8.238
7.511
7.473
7.421
7.359
7.237
7.180
6.481
6.460
6.028
6.008
2.823
2.800
2.777
2.754
2.730
2.707
1.803
1.566
1.341
1.318
1.002
0.978
0.953
H
N
dichloromethane – d2
0.94
2.06
2.03
1.00
1.01
1.00
1.02
2.13
3.08
3.15
8.0
7.0
6.0
5.0
4.0
3.0
2.0
1.0
Chemical Shift (ppm)

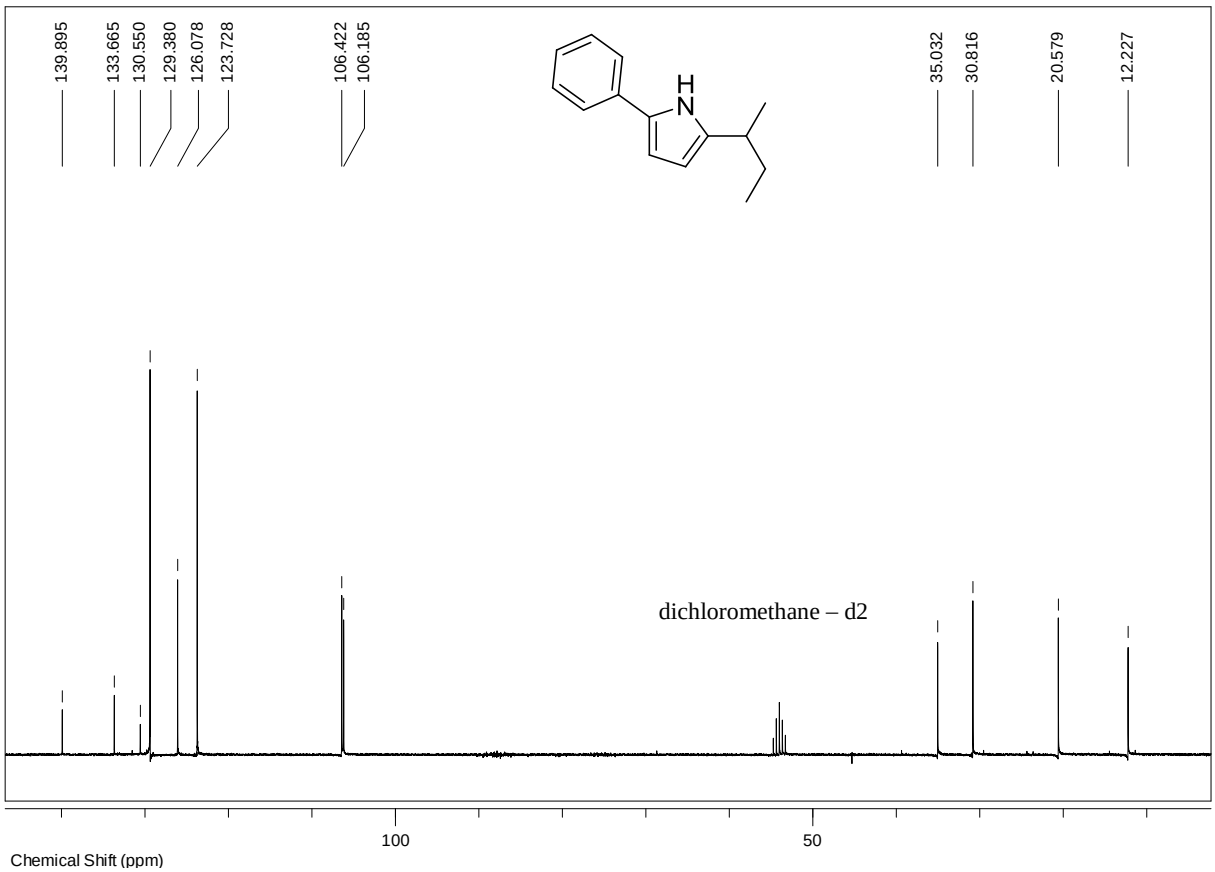
139.895
133.665
130.550
129.380
126.078
123.728
106.422
106.185
35.032
30.816
20.579
12.227
H
N
dichloromethane – d2
100
50
Chemical Shift (ppm)

1e:

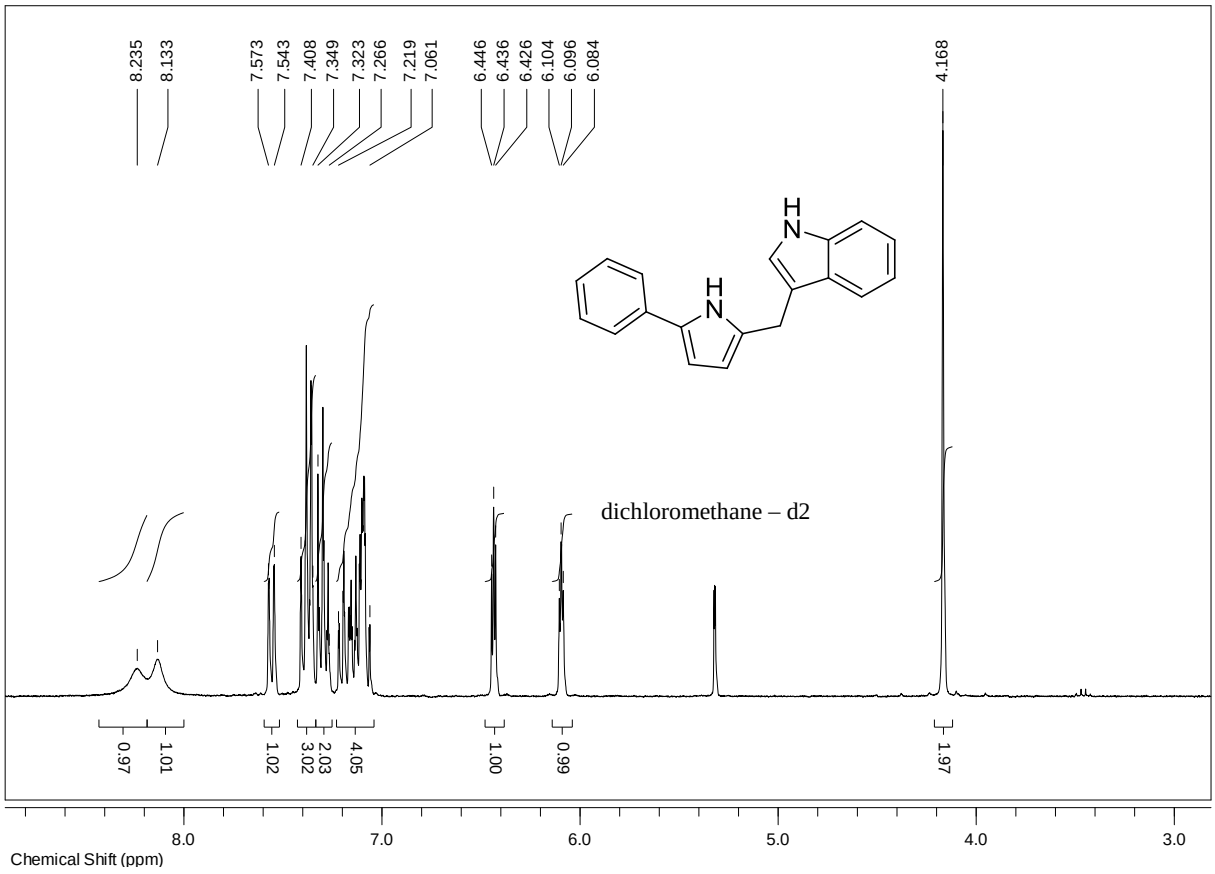
8.235
8.133
7.573
7.543
7.408
7.349
7.323
7.266
7.219
7.061
6.446
6.436
6.426
6.104
6.096
6.084
4.168
H
N
H
N
dichloromethane – d2
0.97
1.01
1.02
3.02
2.03
4.05
1.00
0.99
1.97
8.0
7.0
6.0
5.0
4.0
3.0
Chemical Shift (ppm)

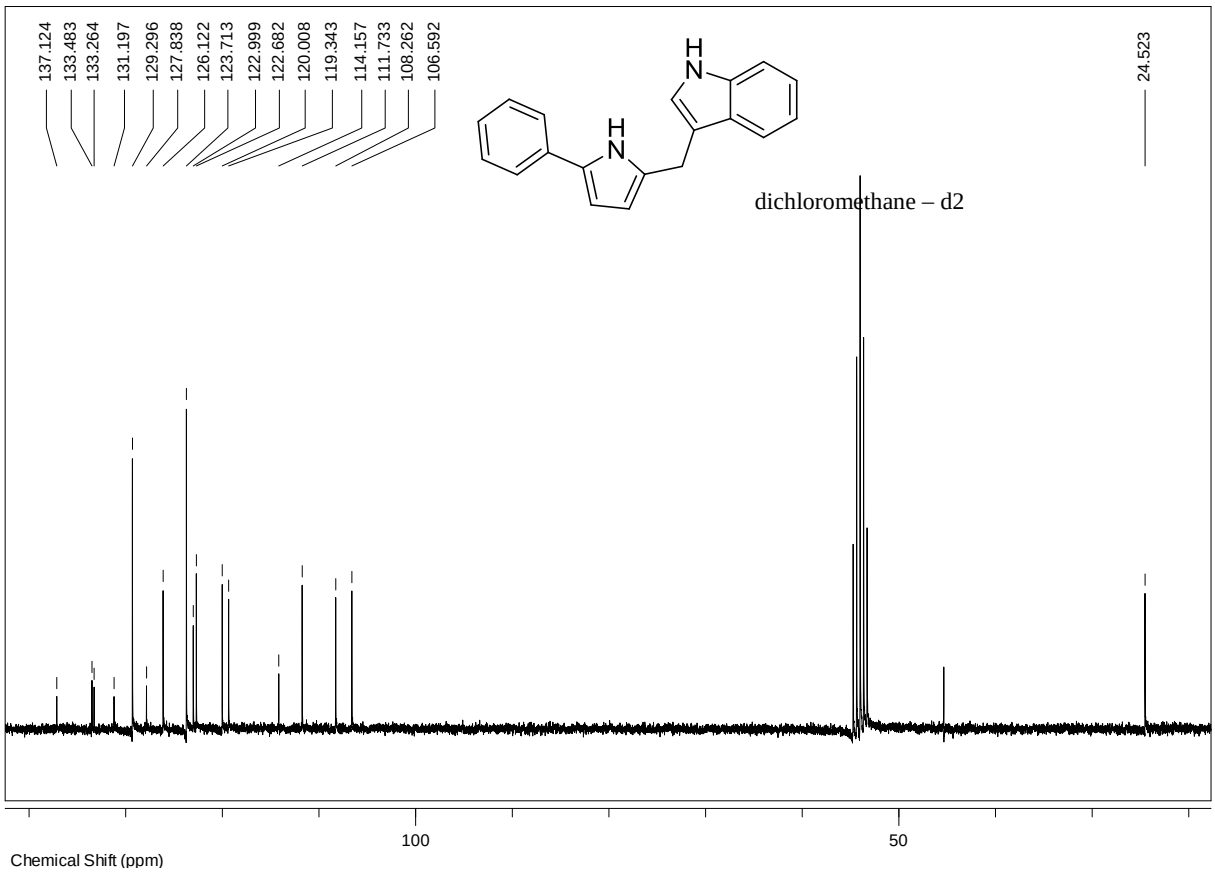
137.124
133.483
133.264
131.197
129.296
127.838
126.122
123.713
122.999
122.682
120.008
119.343
114.157
111.733
108.262
106.592
24.523
H
N
H
N
dichloromethane – d2
100
50
Chemical Shift (ppm)

1f:

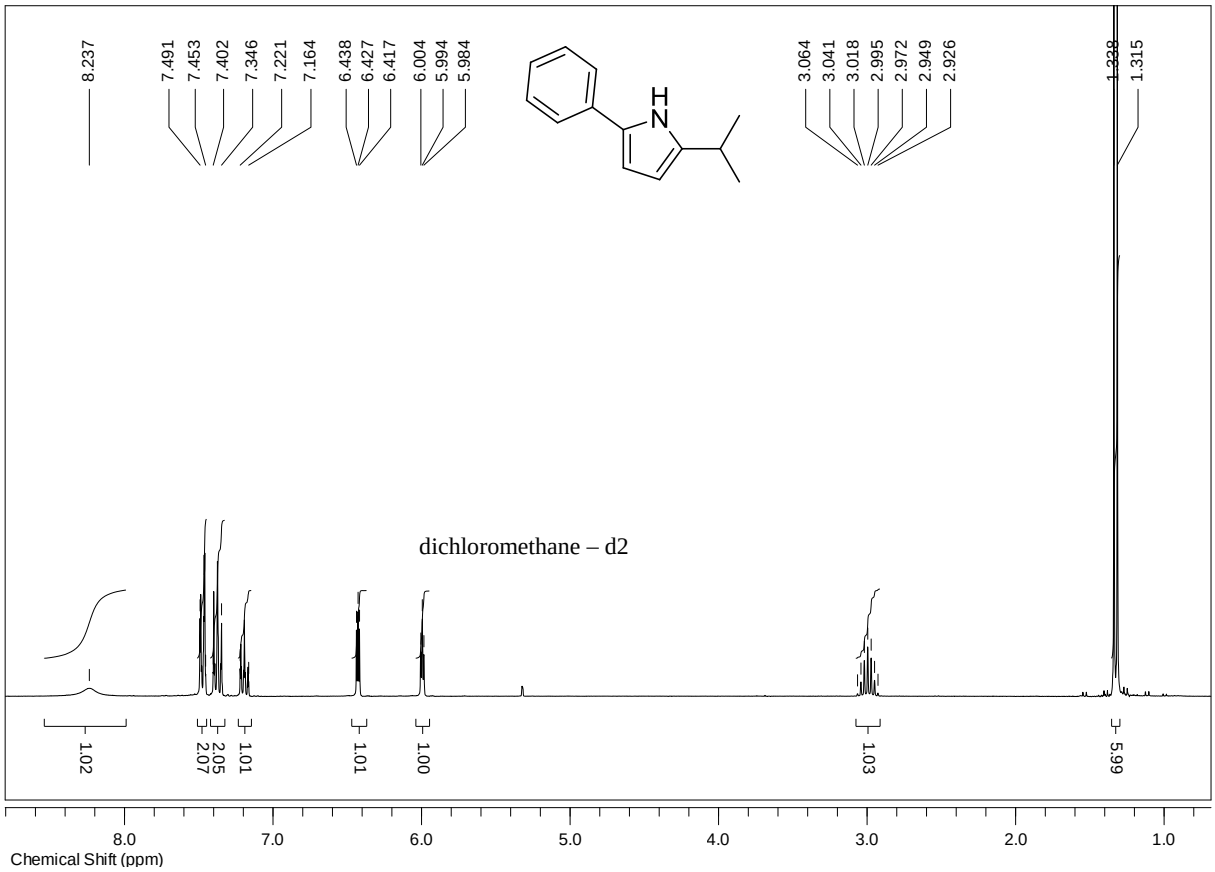
8.237
7.491
7.453
7.402
7.346
7.221
7.164
6.438
6.427
6.417
6.004
5.994
5.984
3.064
3.041
3.018
2.995
2.972
2.949
2.926
1.338
1.315
H
N
dichloromethane – d2
1.02
2.07
2.05
1.01
1.01
1.00
1.03
5.99
8.0
7.0
6.0
5.0
4.0
3.0
2.0
1.0
Chemical Shift (ppm)

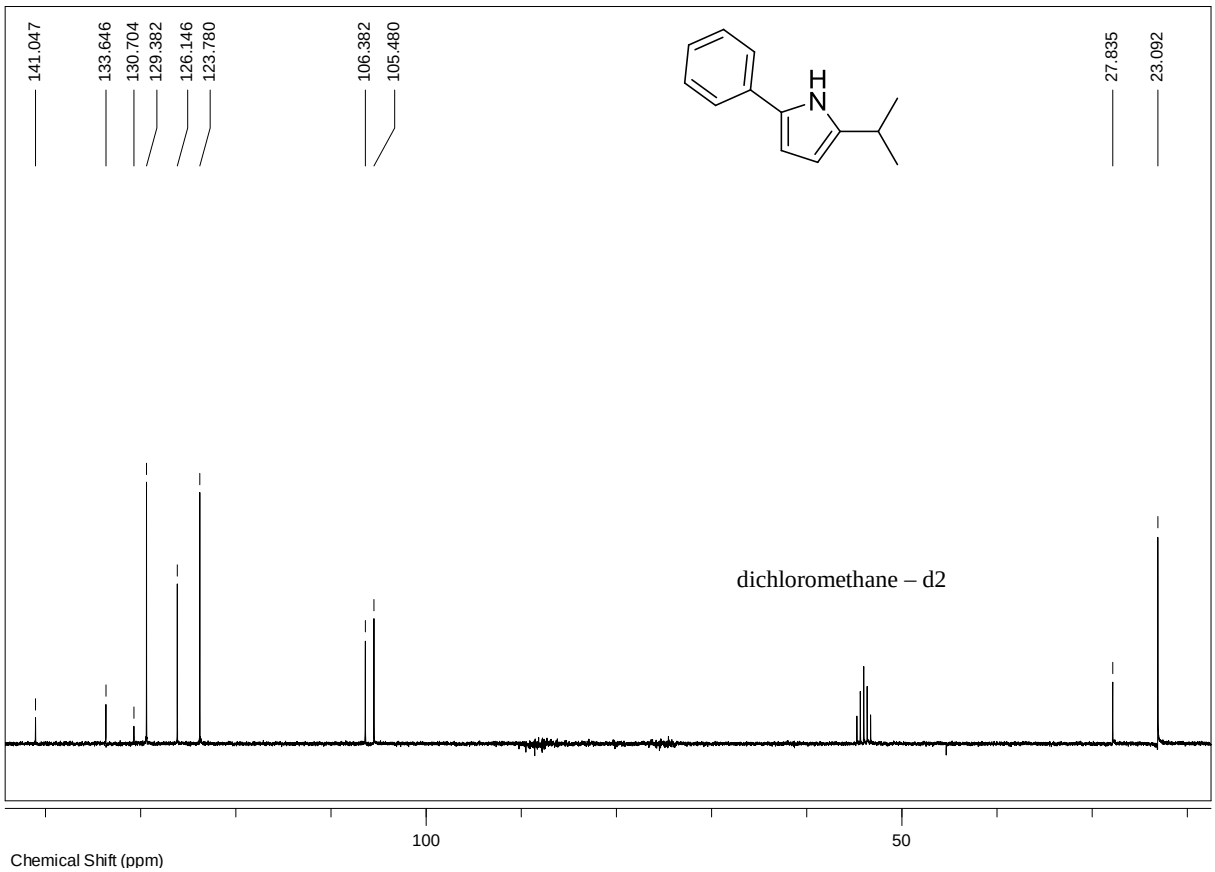
141.047
133.646
130.704
129.382
126.146
123.780
106.382
105.480
27.835
23.092
H
N
dichloromethane – d2
100
50
Chemical Shift (ppm)

1g:

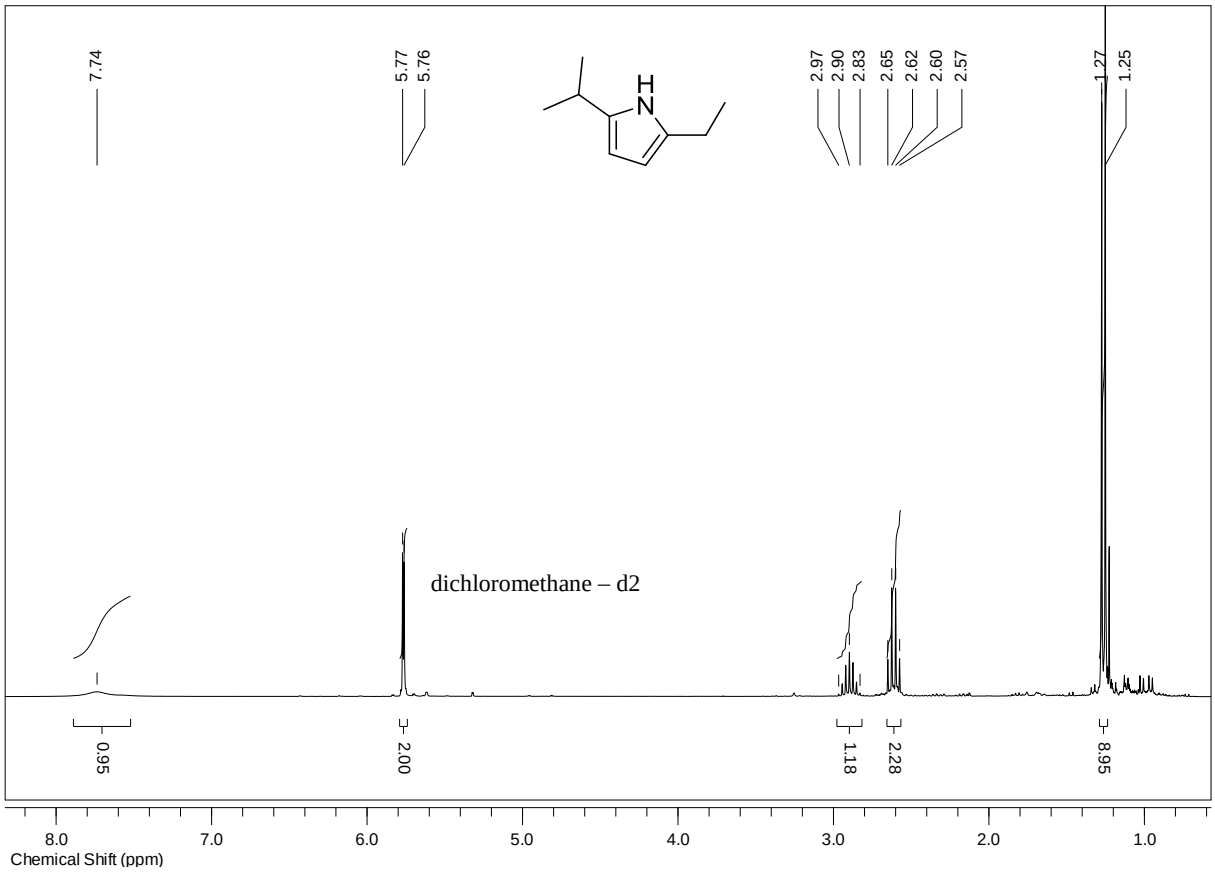
7.74
5.77
5.76
2.97
2.90
2.83
2.65
2.62
2.60
2.57
1.27
1.25
dichloromethane – d2
0.95
2.00
1.18
2.28
8.95
8.0
7.0
6.0
5.0
4.0
3.0
2.0
1.0
Chemical Shift (ppm)

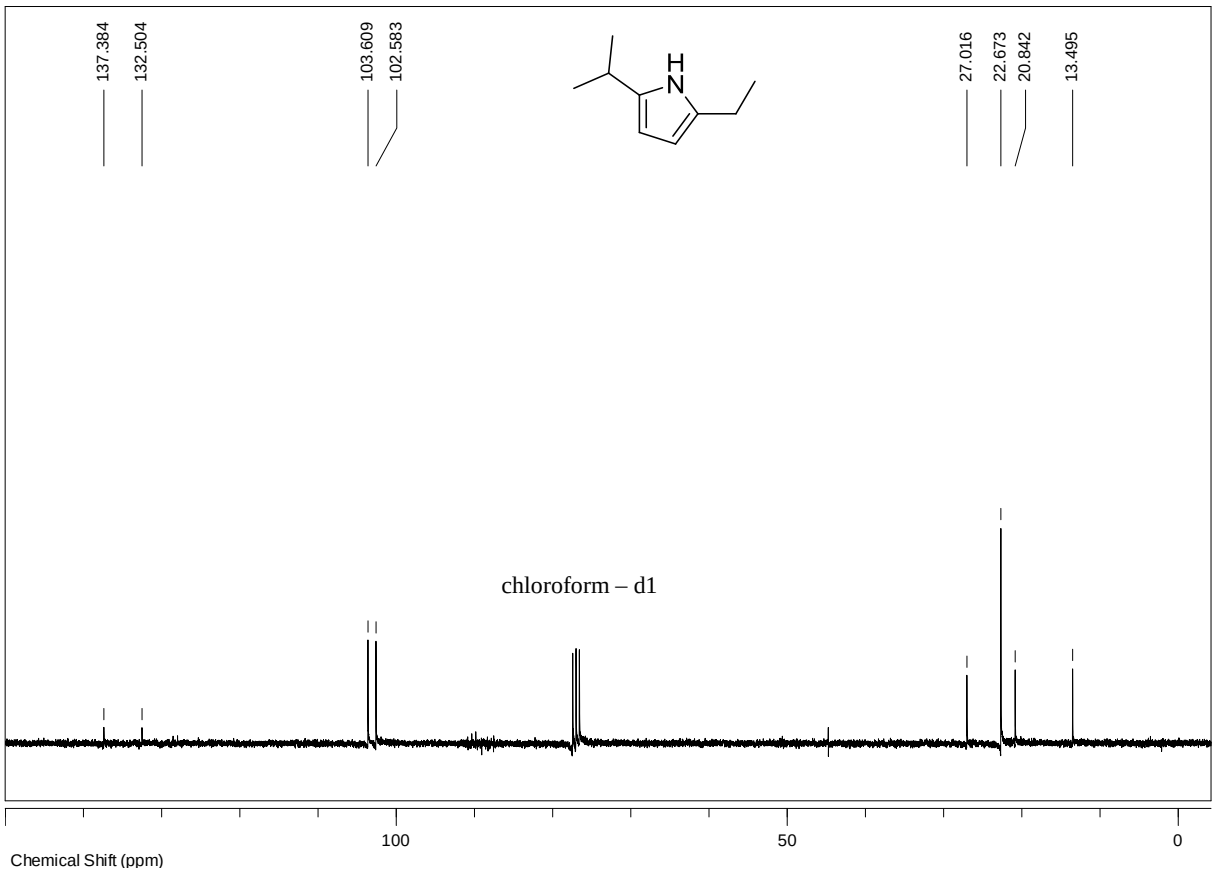
137.384
132.504
103.609
102.583
27.016
22.673
20.842
13.495
chloroform – d1
100
50
0
Chemical Shift (ppm)

1h:

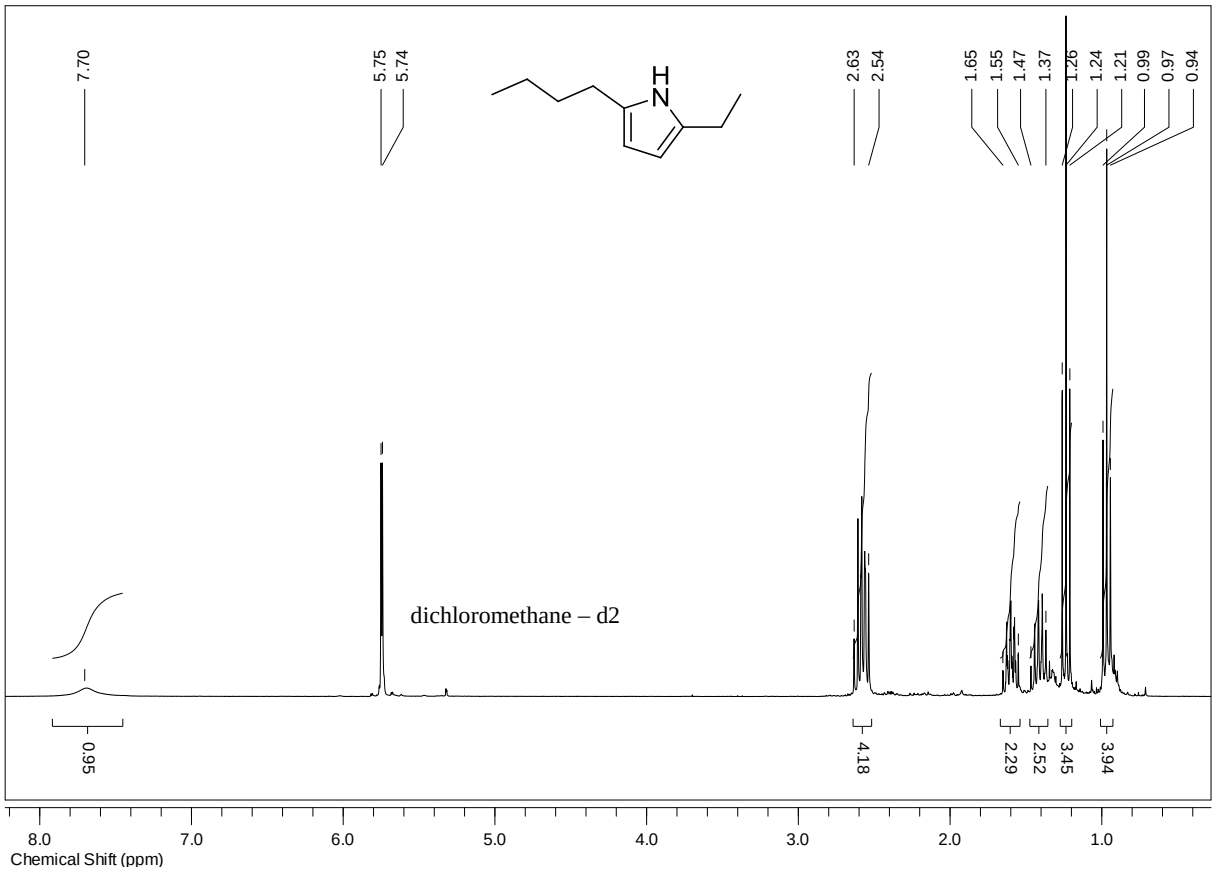
7.70
5.75
5.74
2.63
2.54
1.65
1.55
1.47
1.37
1.26
1.24
1.21
0.99
0.97
0.94
dichloromethane – d2
0.95
4.18
2.29
2.52
3.45
3.94
8.0
7.0
6.0
5.0
4.0
3.0
2.0
1.0
Chemical Shift (ppm)

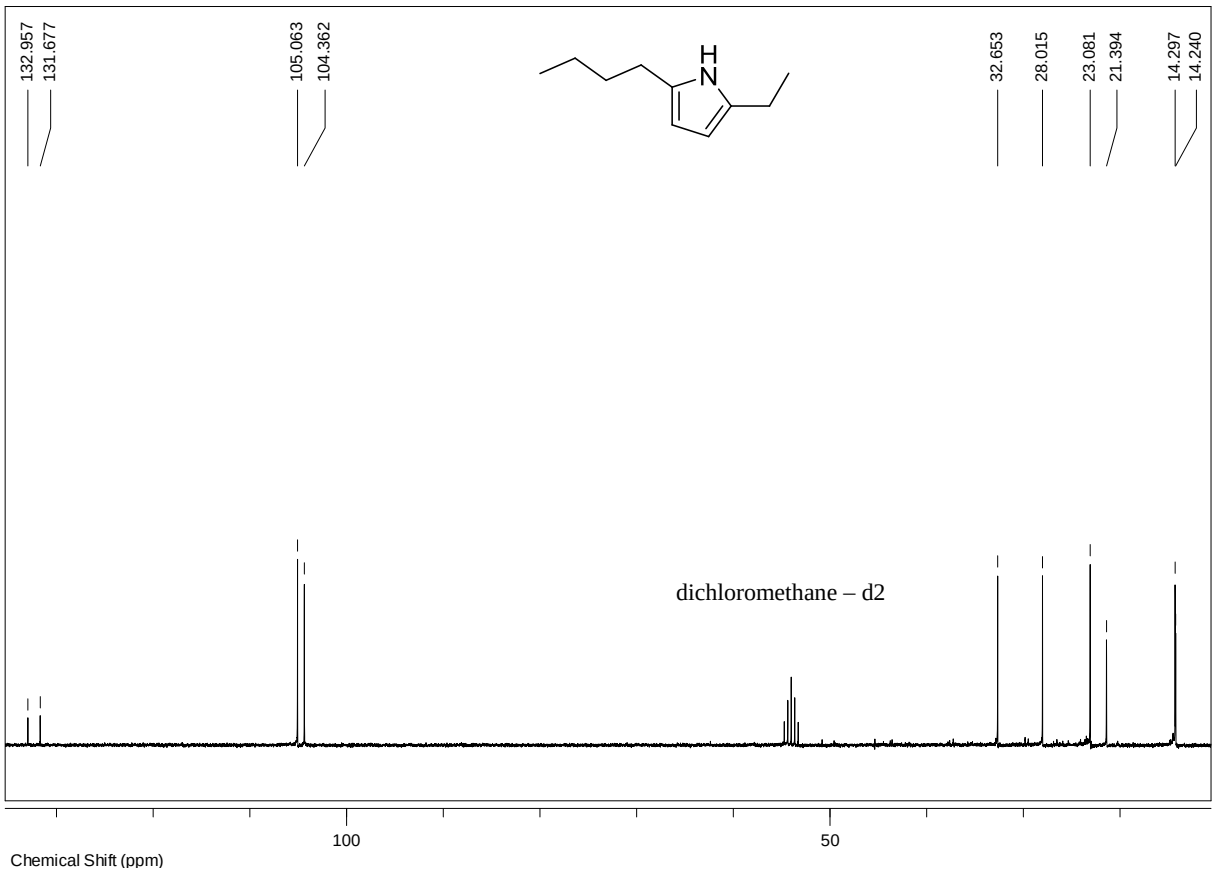
132.957
131.677
105.063
104.362
32.653
28.015
23.081
21.394
14.297
14.240
dichloromethane – d2
100
50
Chemical Shift (ppm)

1i:

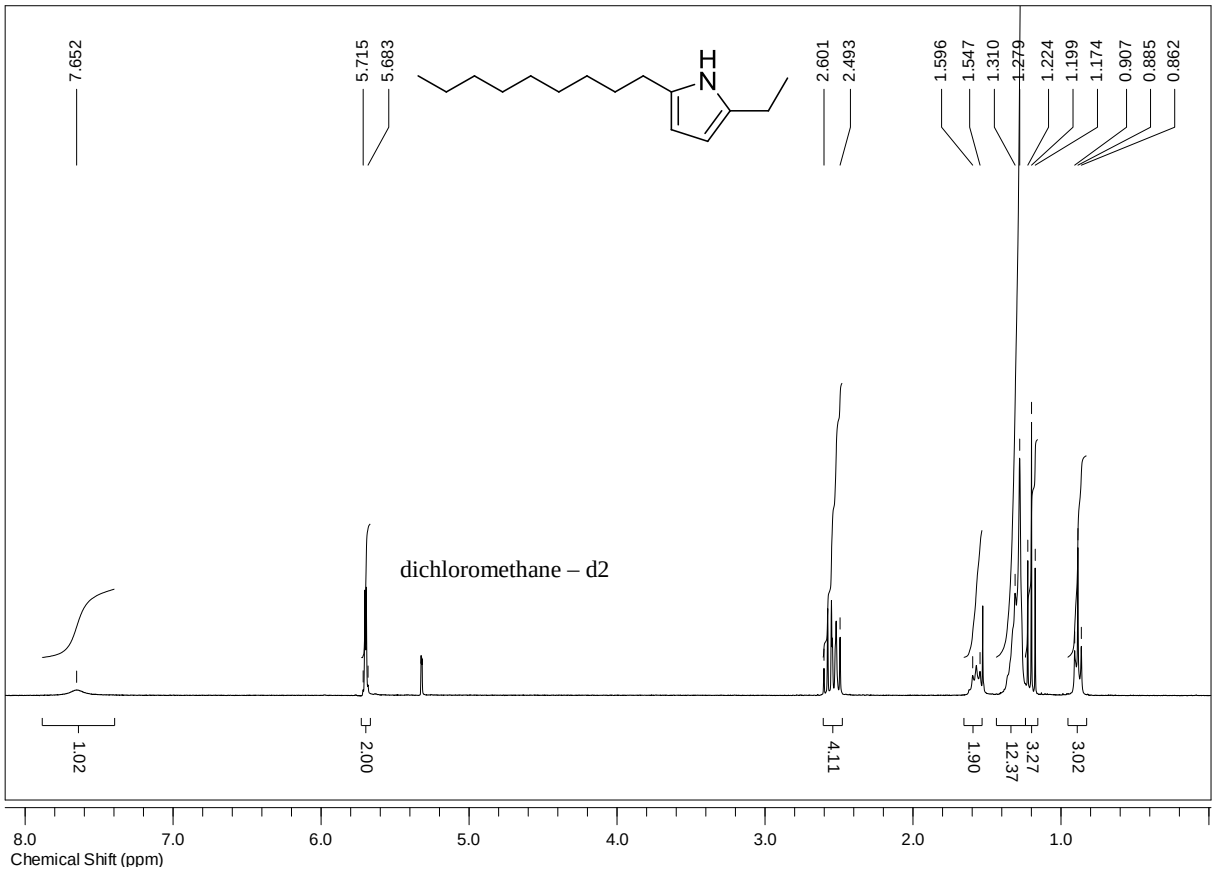
7.652
5.715
5.683
2.601
2.493
1.596
1.547
1.310
1.279
1.224
1.199
1.174
0.907
0.885
0.862
dichloromethane – d2
1.02
2.00
4.11
1.90
12.37
3.27
3.02
8.0
7.0
6.0
5.0
4.0
3.0
2.0
1.0
Chemical Shift (ppm)

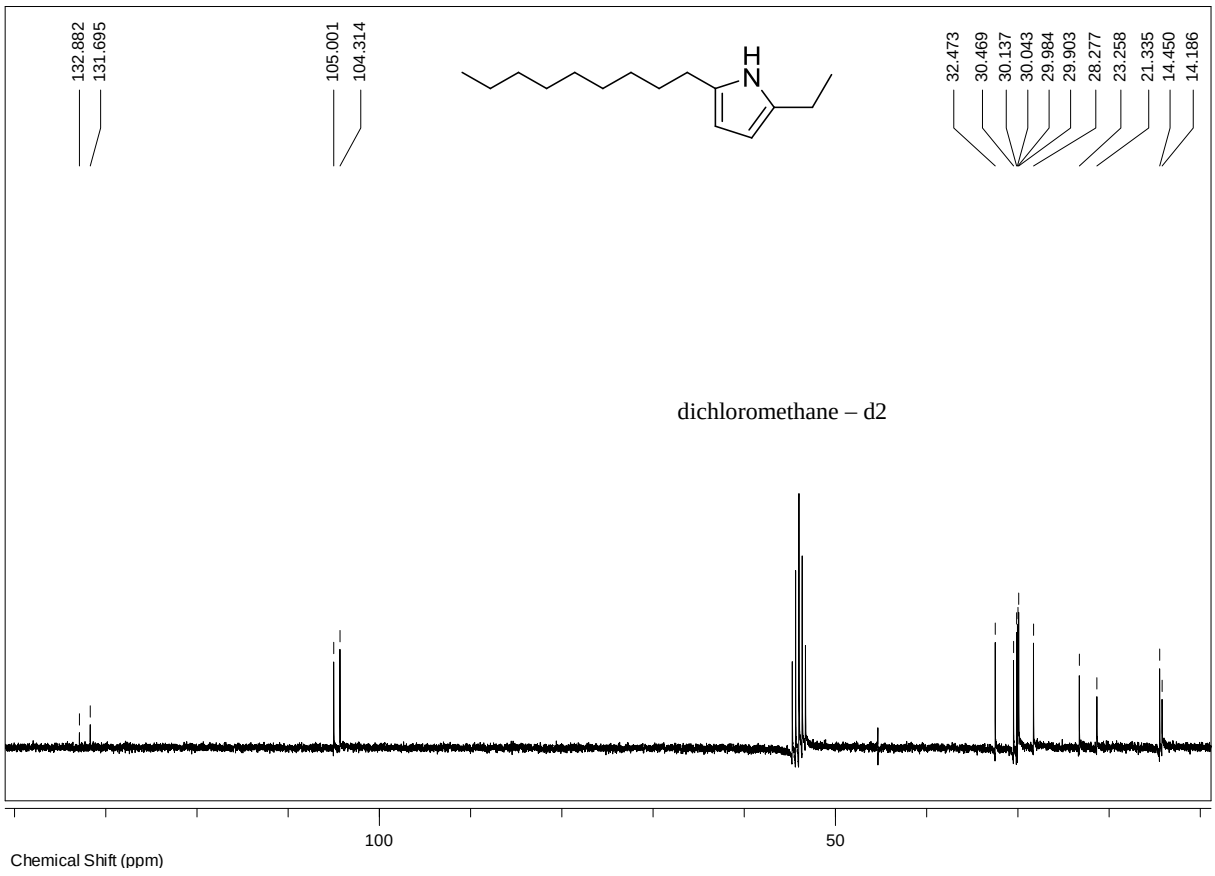
132.882
131.695
105.001
104.314
32.473
30.469
30.137
30.043
29.984
29.903
28.277
23.258
21.335
14.450
14.186
dichloromethane – d2
100
50
Chemical Shift (ppm)

1j:

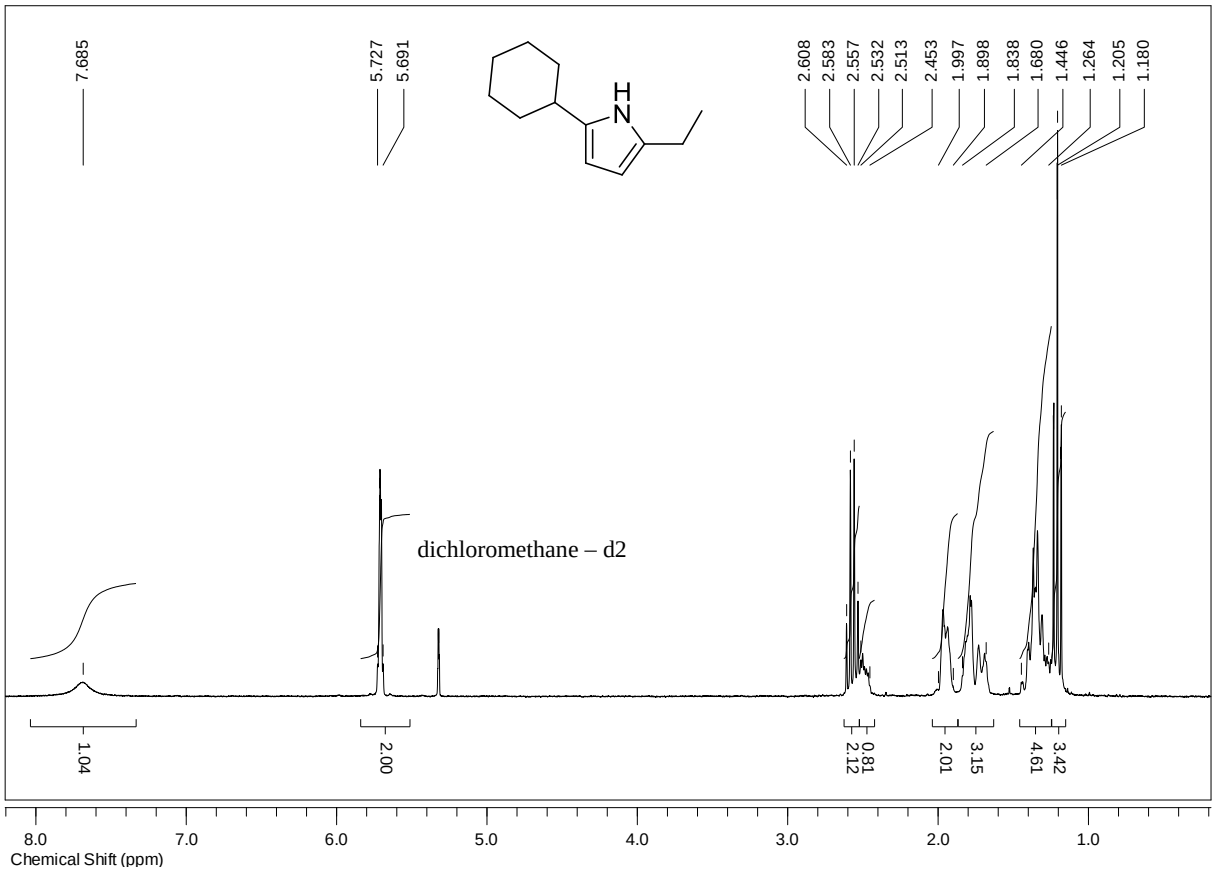
7.685
5.727
5.691
2.608
2.583
2.557
2.532
2.513
2.453
1.997
1.898
1.838
1.680
1.446
1.264
1.205
1.180
H
N
dichloromethane – d2
1.04
2.00
2.12
0.81
2.01
3.15
4.91
3.42
8.0
7.0
6.0
5.0
4.0
3.0
2.0
1.0
Chemical Shift (ppm)

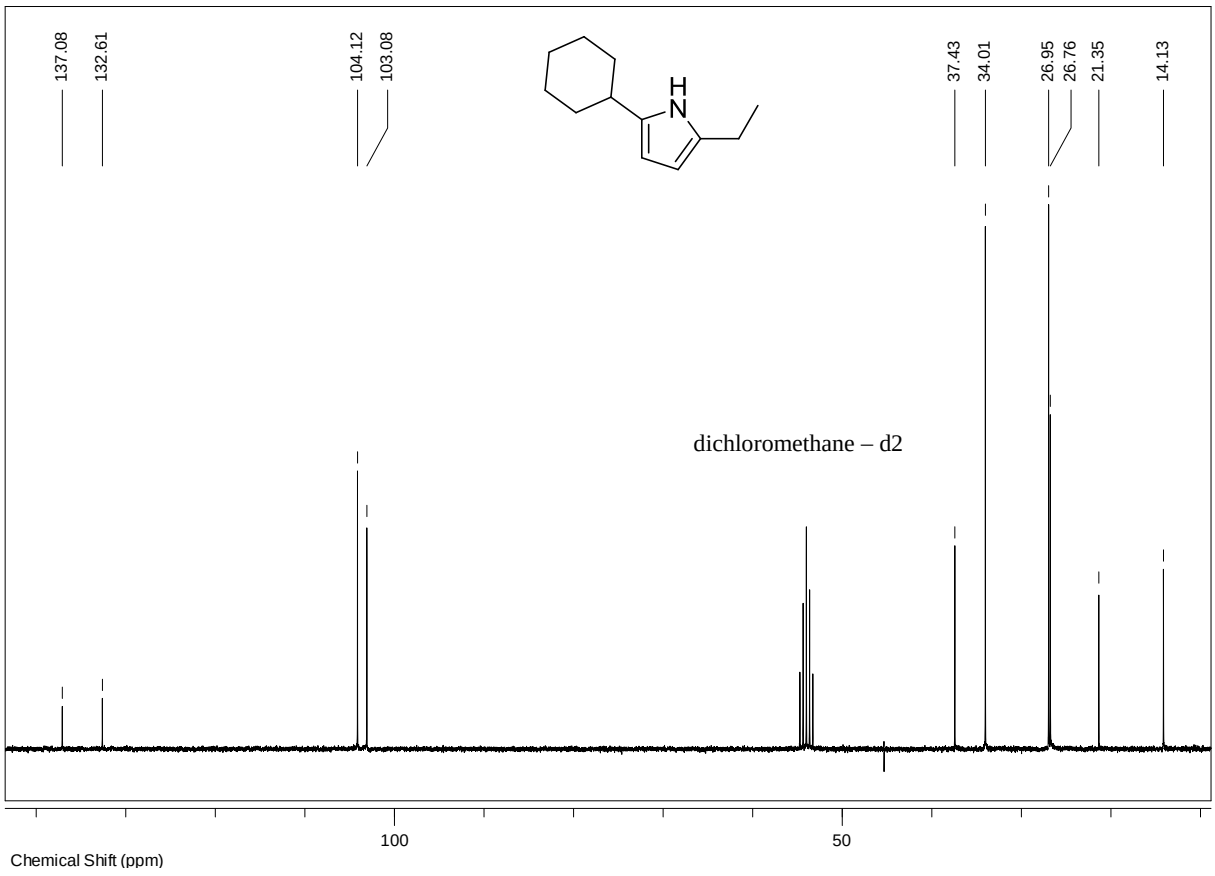
137.08
132.61
104.12
103.08
37.43
34.01
26.95
26.76
21.35
14.13
H
N
dichloromethane – d2
100
50
Chemical Shift (ppm)

1k:

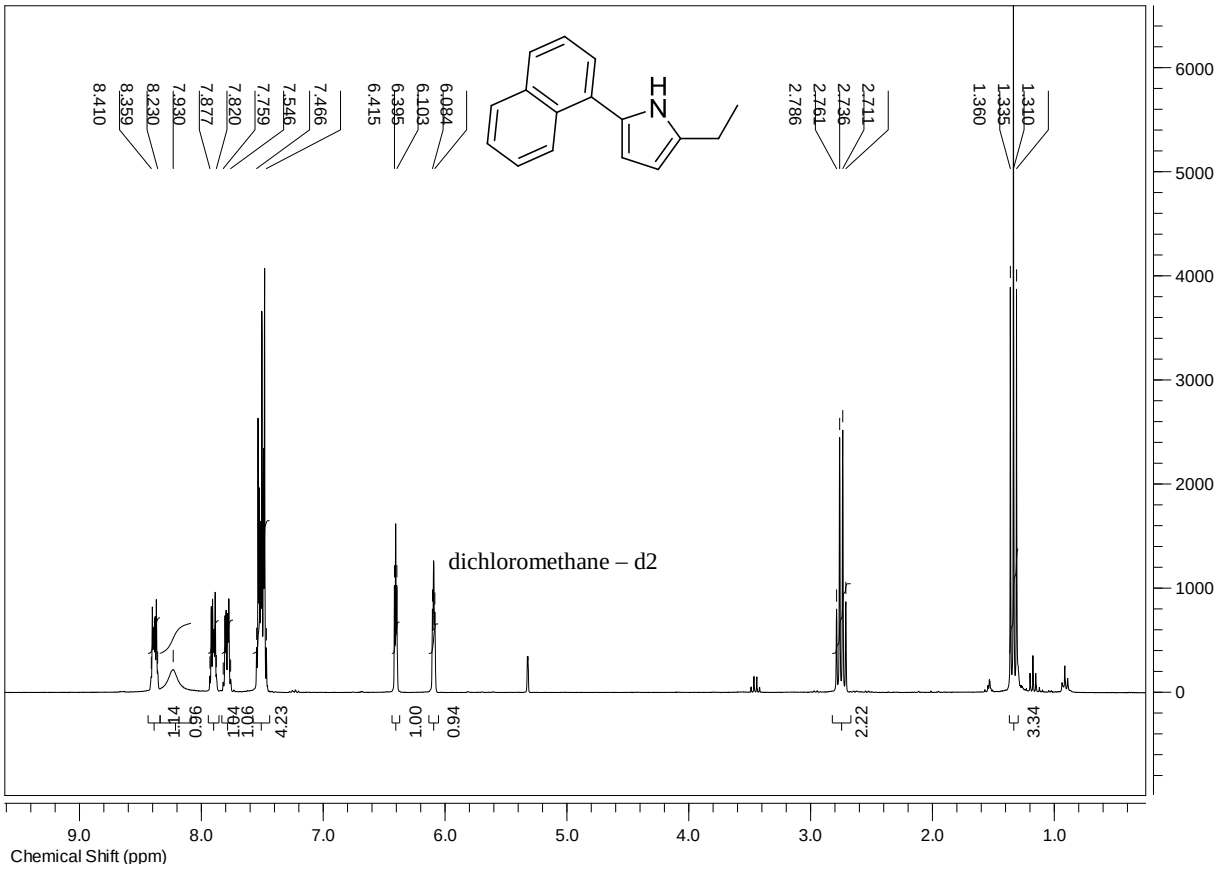
8.410
8.359
8.230
7.930
7.877
7.820
7.759
7.546
7.466
6.415
6.395
6.103
6.084
2.786
2.761
2.736
2.711
1.360
1.335
1.310
dichloromethane – d2
1.14
0.96
1.04
1.06
4.23
1.00
0.94
2.22
3.34
9.0
8.0
7.0
6.0
5.0
4.0
3.0
2.0
1.0
Chemical Shift (ppm)

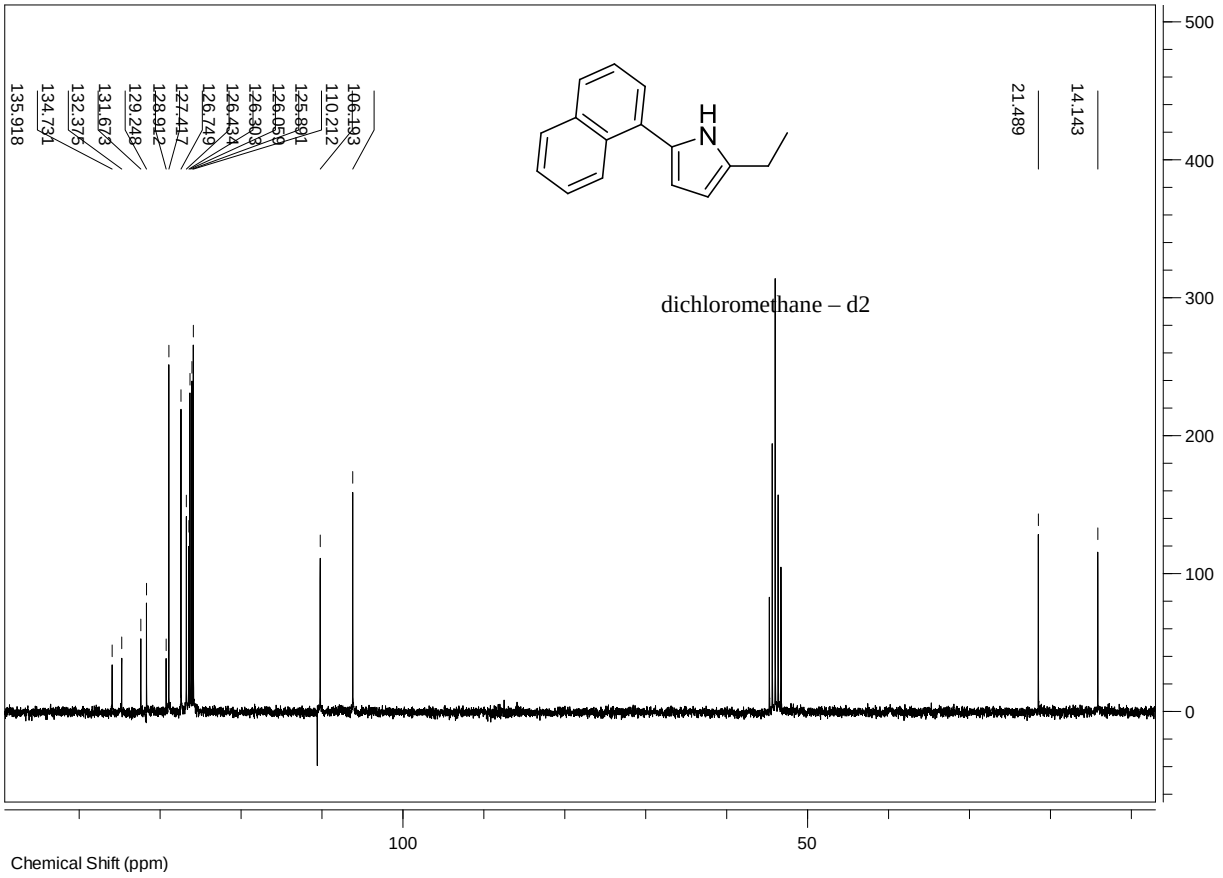
135.918
134.731
132.375
131.673
129.248
128.912
127.417
126.749
126.434
126.303
126.059
125.891
110.212
106.193
21.489
14.143
dichloromethane – d2
100
50
Chemical Shift (ppm)

1l:

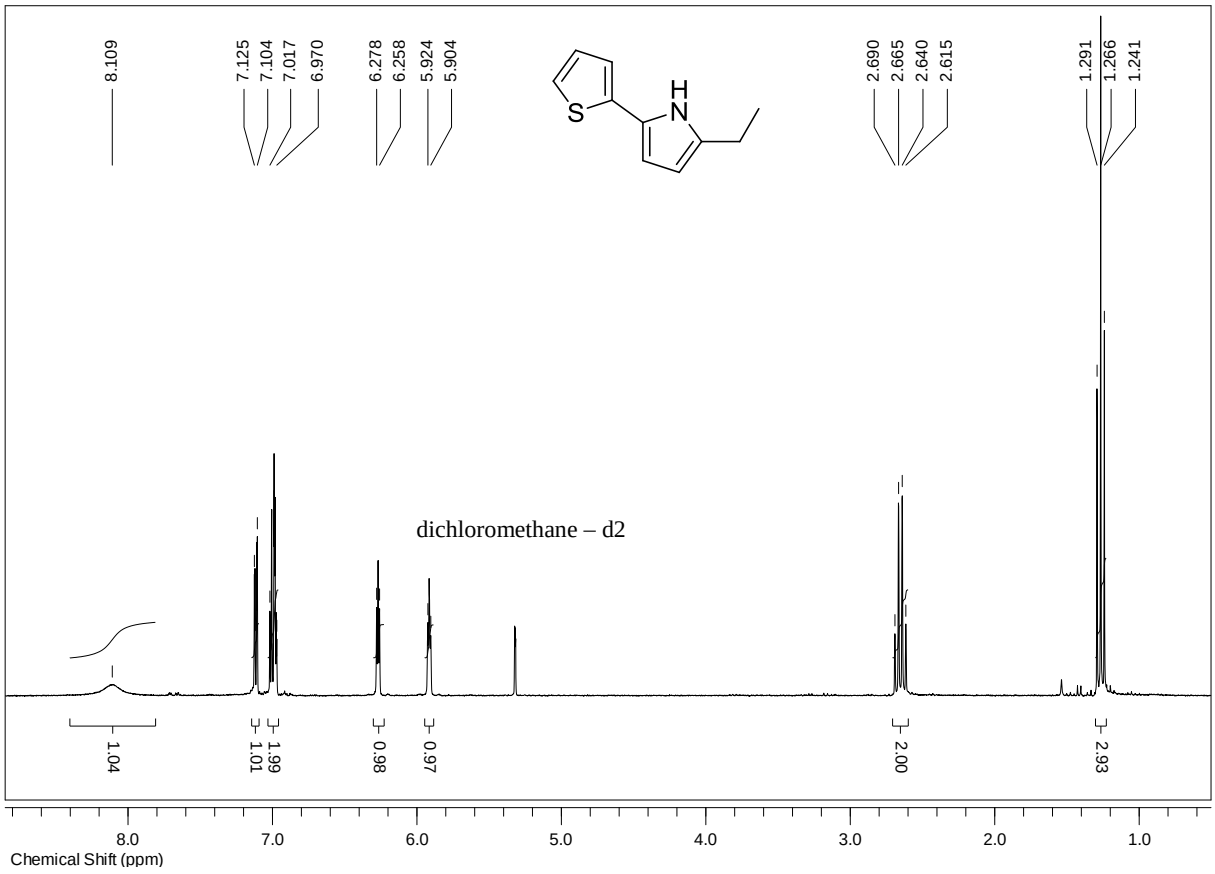
8.109
7.125
7.104
7.017
6.970
6.278
6.258
5.924
5.904
2.690
2.665
2.640
2.615
1.291
1.266
1.241
S
H
N
dichloromethane – d2
1.04
1.01
1.99
0.98
0.97
2.00
2.93
8.0
7.0
6.0
5.0
4.0
3.0
2.0
1.0
Chemical Shift (ppm)

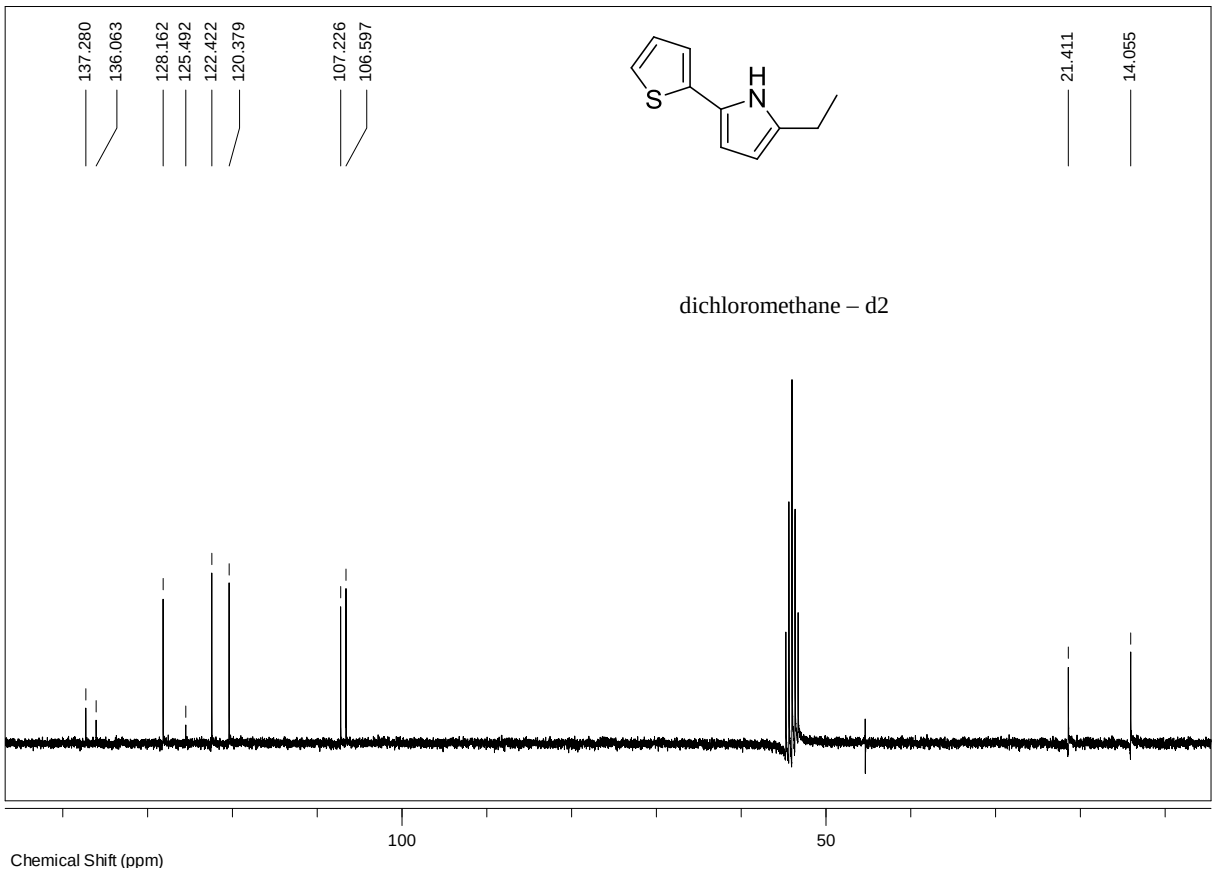
137.280
136.063
128.162
125.492
122.422
120.379
107.226
106.597
21.411
14.055
S
H
N
dichloromethane – d2
100
50
Chemical Shift (ppm)

1m:

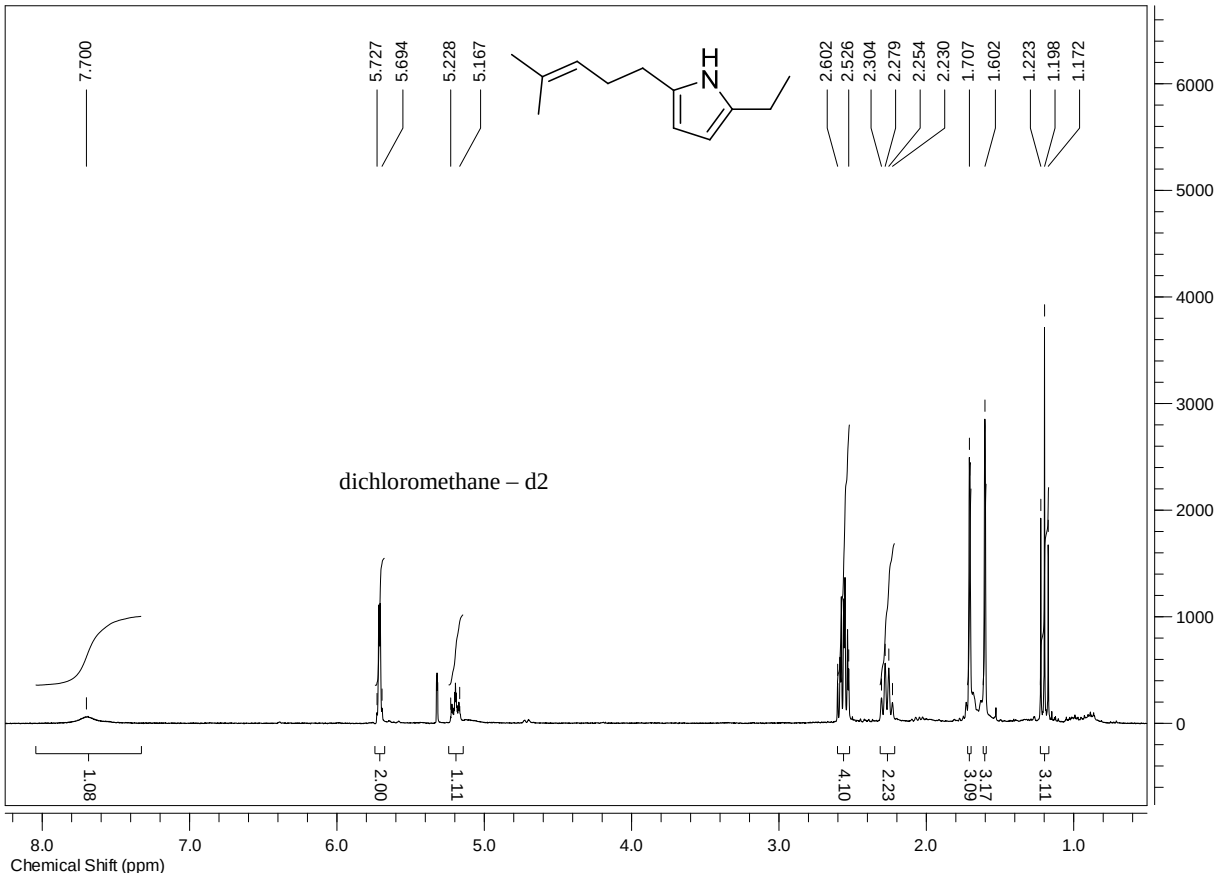
7.700
5.727
5.694
5.228
5.167
2.602
2.526
2.304
2.279
2.254
2.230
1.707
1.602
1.223
1.198
1.172
dichloromethane – d2
1.08
2.00
1.11
4.10
2.23
3.09
3.17
3.11
Chemical Shift (ppm)

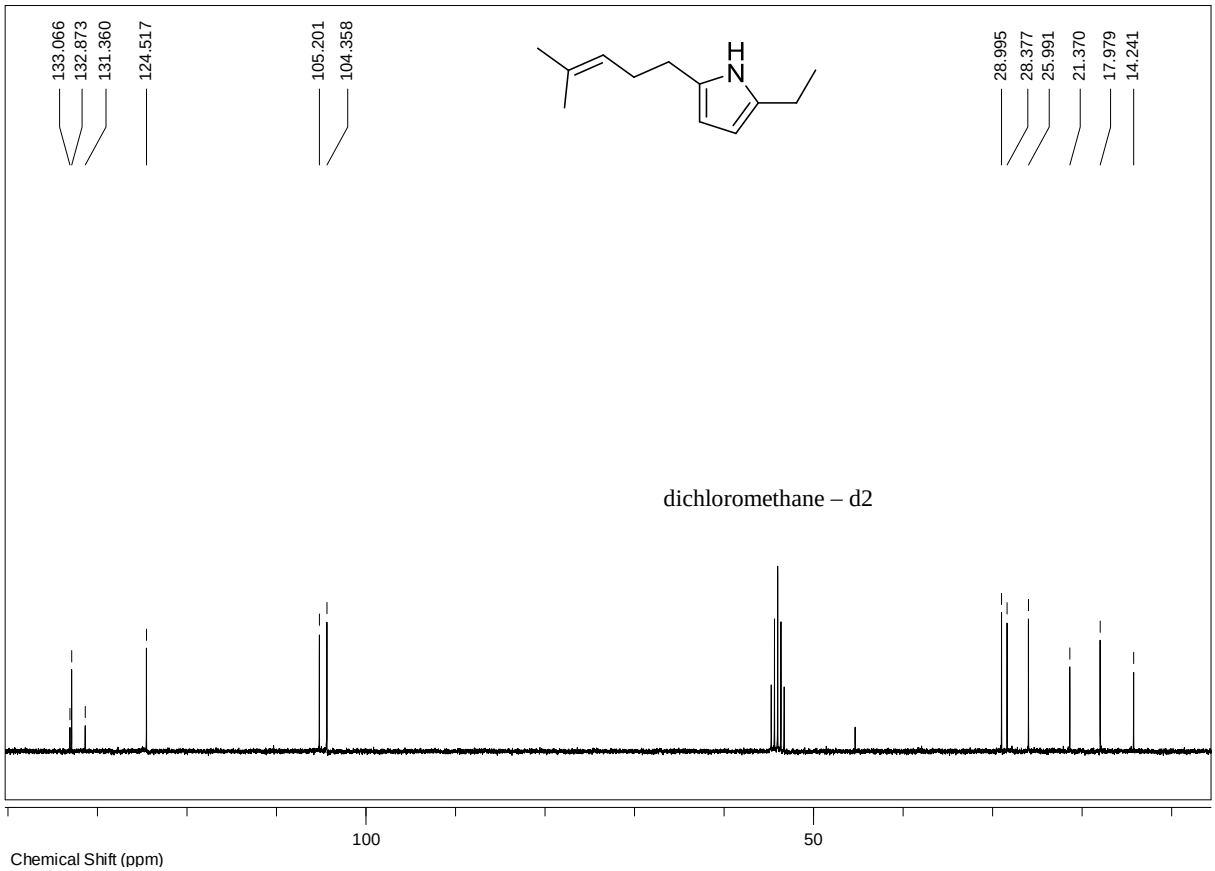
133.066
132.873
131.360
124.517
105.201
104.358
28.995
28.377
25.991
21.370
17.979
14.241
dichloromethane – d2
Chemical Shift (ppm)

2a:

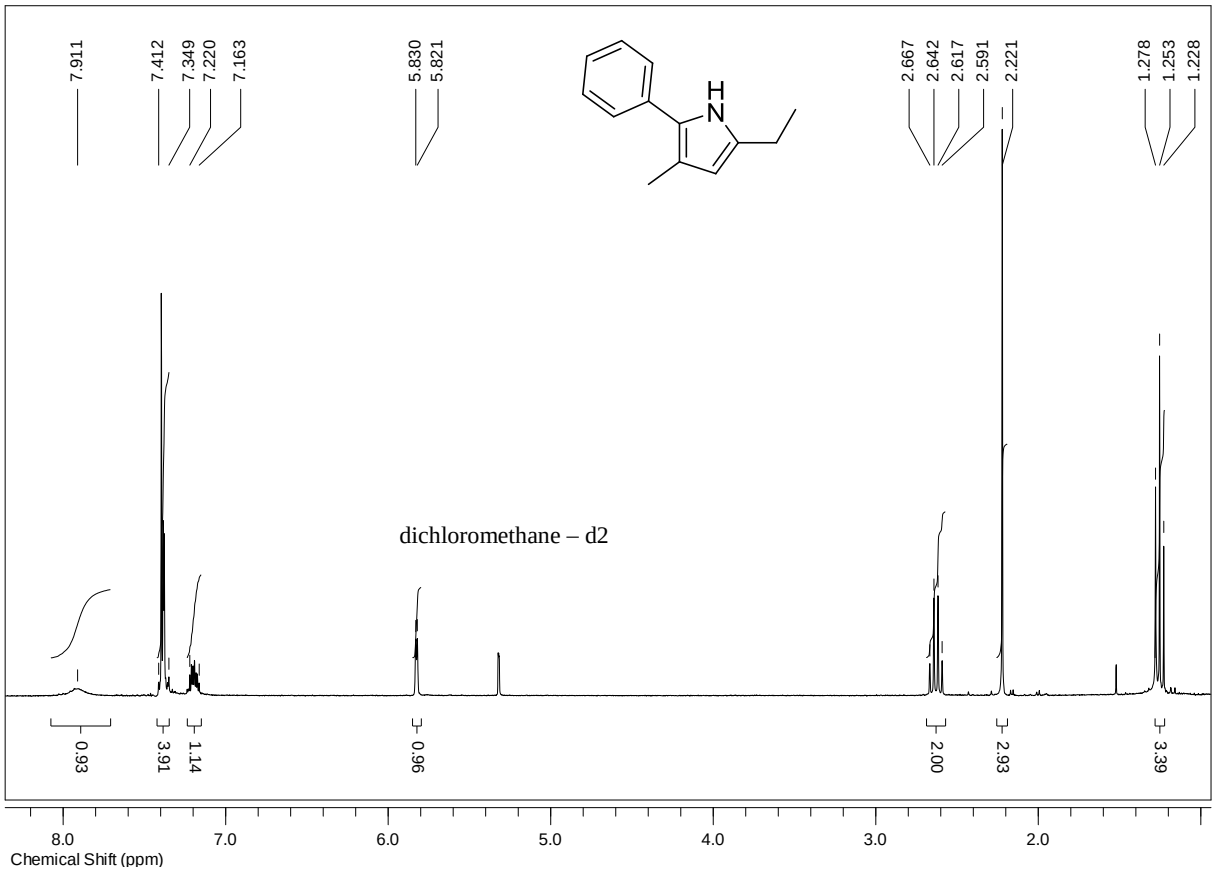
7.911
7.412
7.349
7.220
7.163
5.830
5.821
2.667
2.642
2.617
2.591
2.221
1.278
1.253
1.228
H
N
dichloromethane – d2
0.93
3.91
1.14
0.96
2.00
2.93
3.39
8.0
7.0
6.0
5.0
4.0
3.0
2.0
Chemical Shift (ppm)

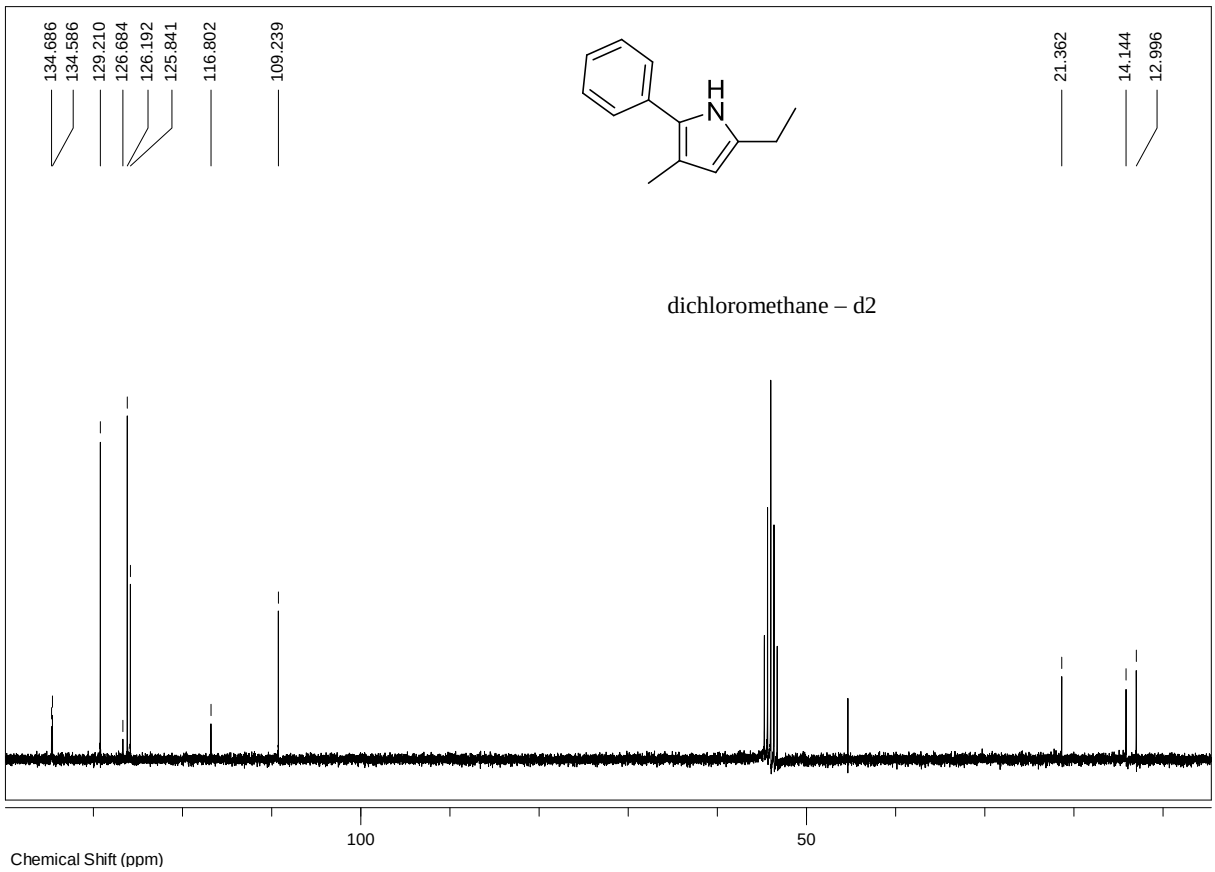
134.686
134.586
129.210
126.684
126.192
125.841
116.802
109.239
21.362
14.144
12.996
H
N
dichloromethane – d2
100
50
Chemical Shift (ppm)

2b:

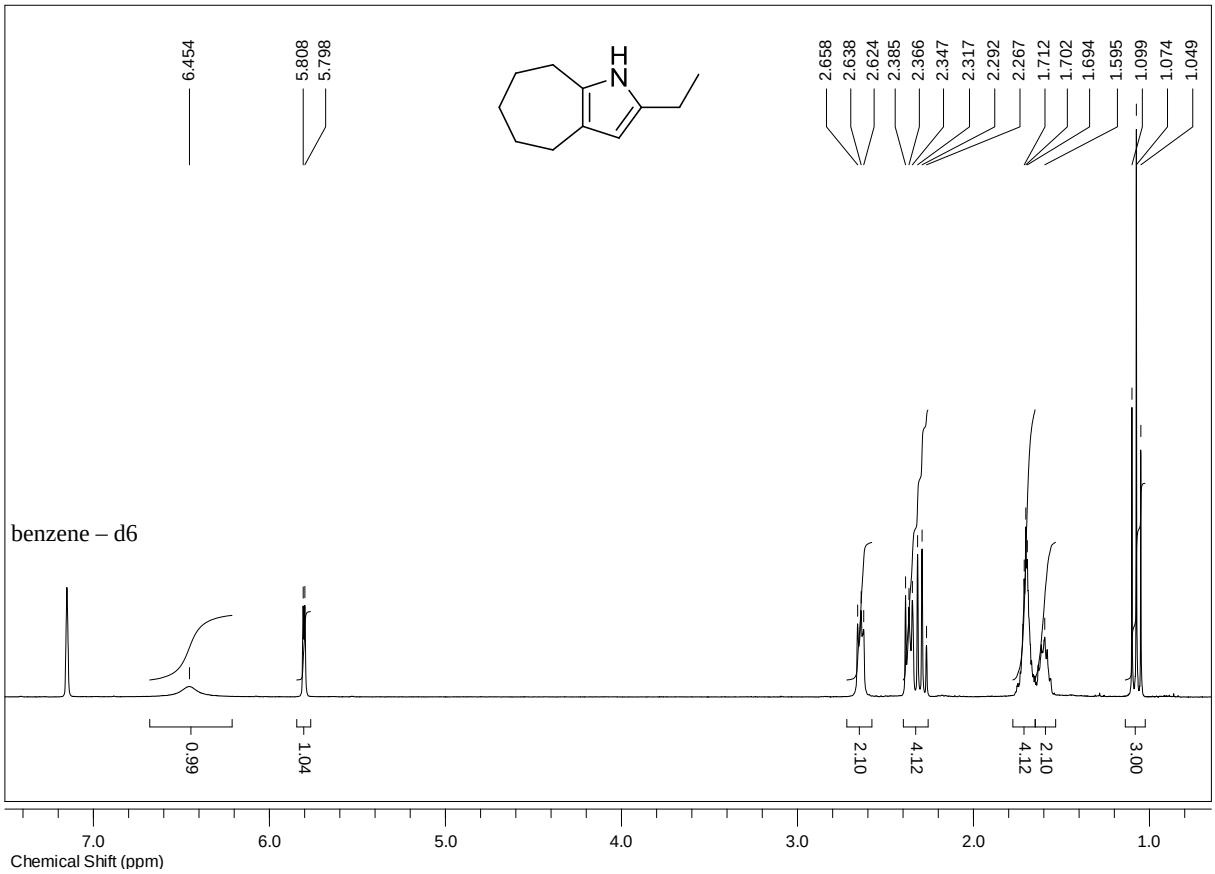
6.454
5.808
5.798
2.658
2.638
2.624
2.385
2.366
2.347
2.317
2.292
2.267
1.712
1.702
1.694
1.595
1.099
1.074
1.049
benzene – d6
0.99
1.04
2.10
4.12
4.12
2.10
3.00
7.0
6.0
5.0
4.0
3.0
2.0
1.0
Chemical Shift (ppm)

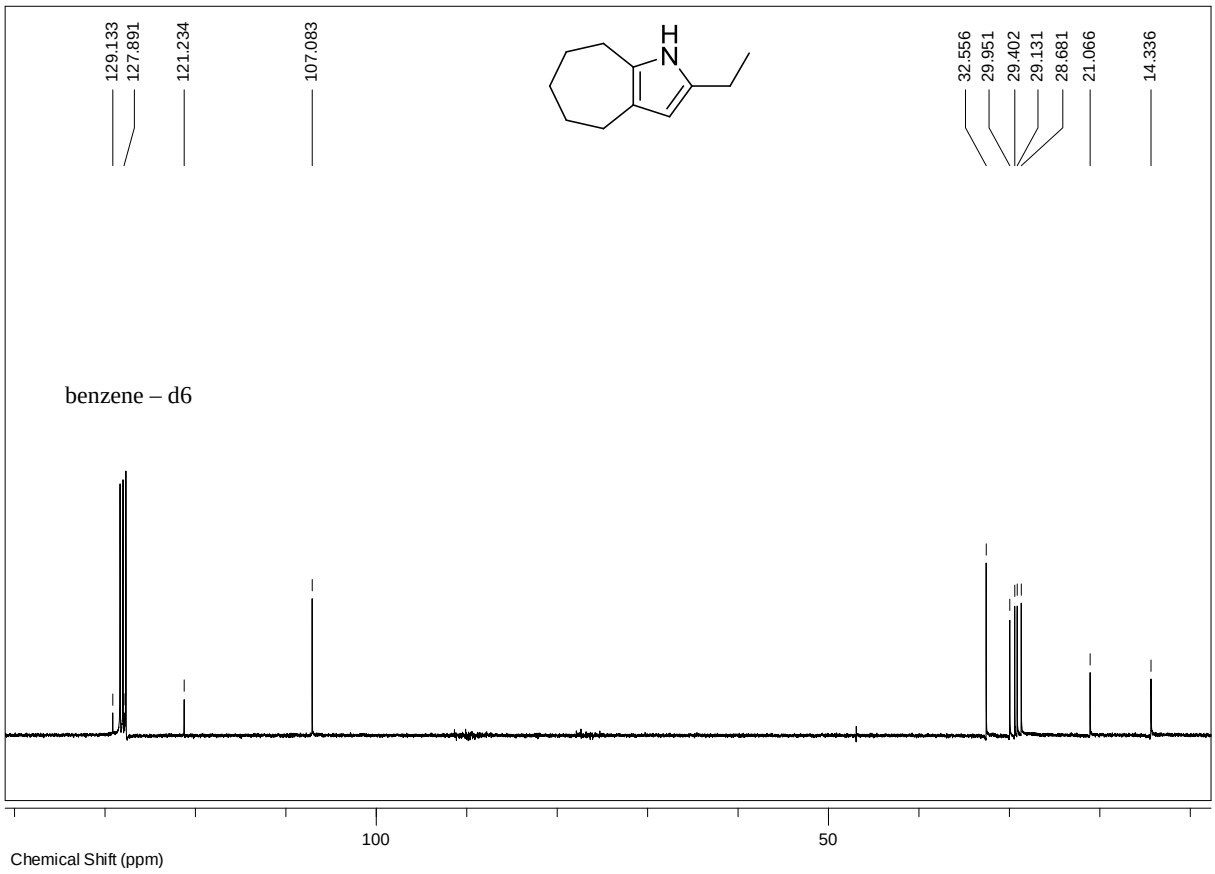
129.133
127.891
121.234
107.083
32.556
29.951
29.402
29.131
28.681
21.066
14.336
benzene – d6
100
50
Chemical Shift (ppm)

2c:

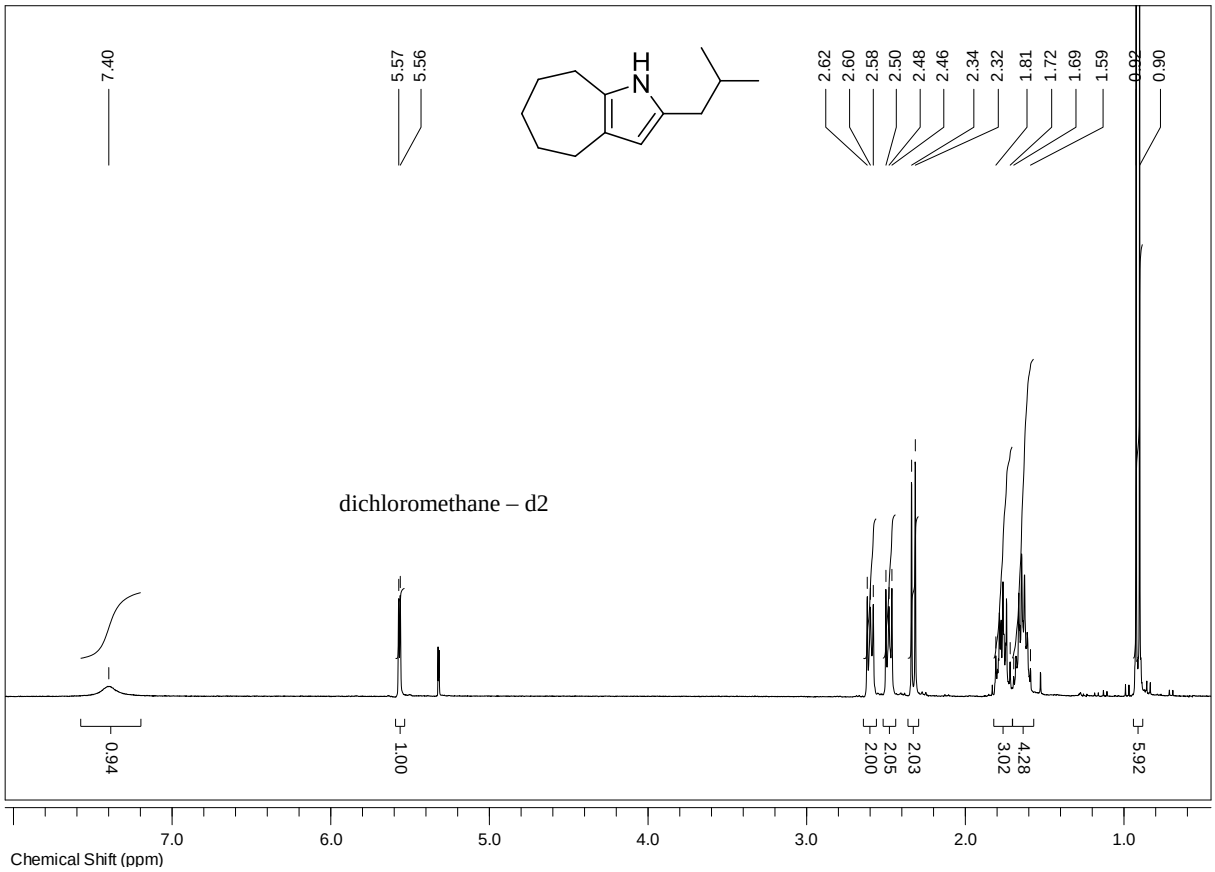
7.40
5.57
5.56
2.62
2.60
2.58
2.50
2.48
2.46
2.34
2.32
1.81
1.72
1.69
1.59
0.92
0.90
dichloromethane – d2
0.94
1.00
2.00
2.05
2.03
3.02
4.28
5.92
7.0
6.0
5.0
4.0
3.0
2.0
1.0
Chemical Shift (ppm)

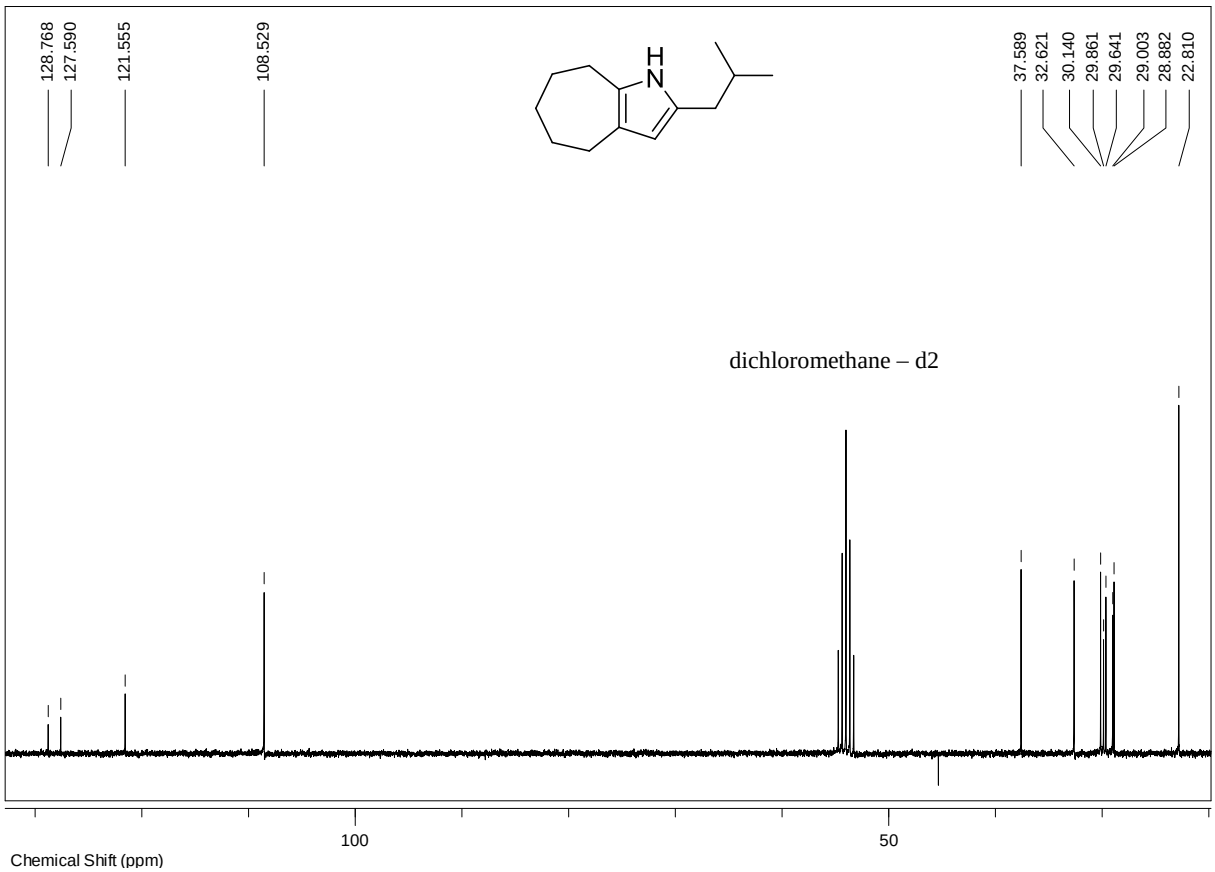
128.768
127.590
121.555
108.529
37.589
32.621
30.140
29.861
29.641
29.003
28.882
22.810
dichloromethane – d2
100
50
Chemical Shift (ppm)

2d:

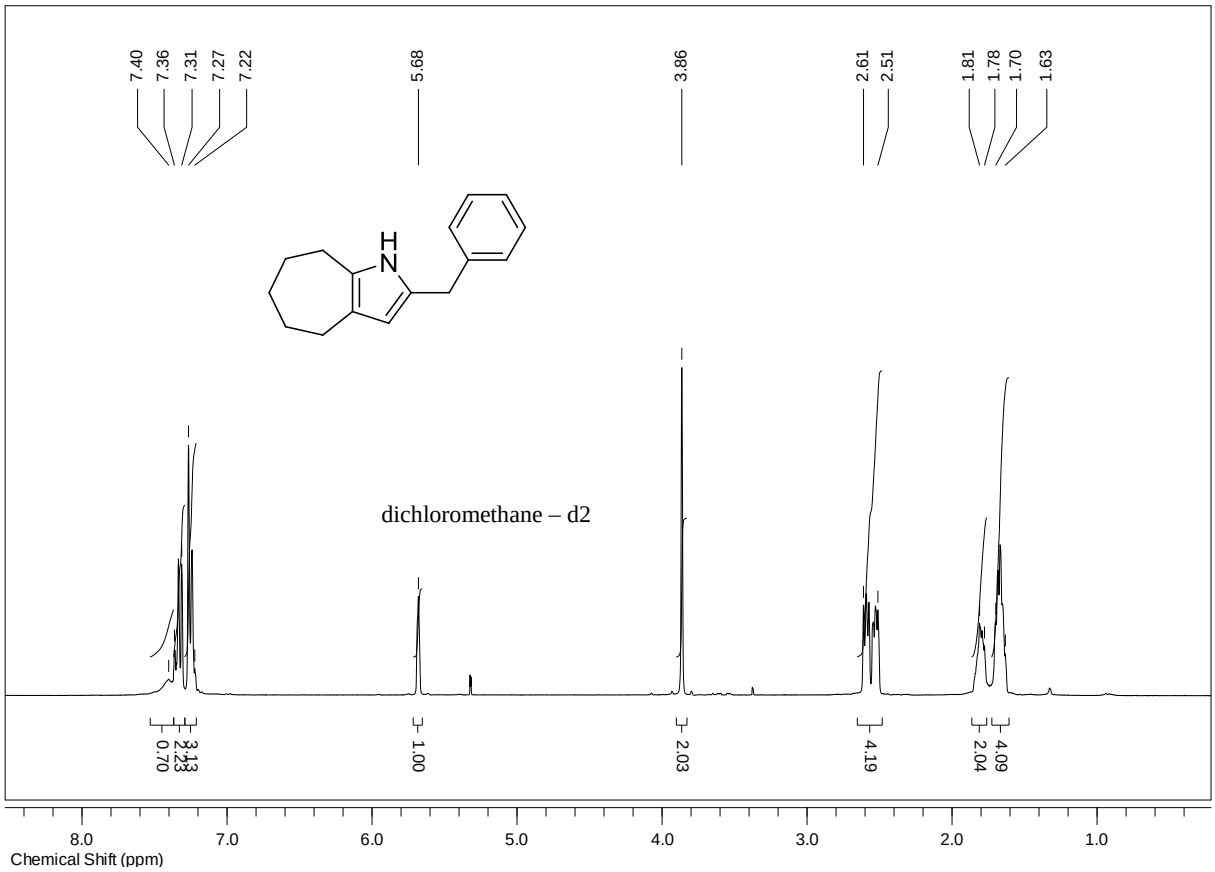
7.40
7.36
7.31
7.27
7.22
5.68
3.86
2.61
2.51
1.81
1.78
1.70
1.63
H
N
dichloromethane – d2
0.70
2.23
2.13
1.00
2.03
4.19
2.04
4.09
8.0
7.0
6.0
5.0
4.0
3.0
2.0
1.0
Chemical Shift (ppm)

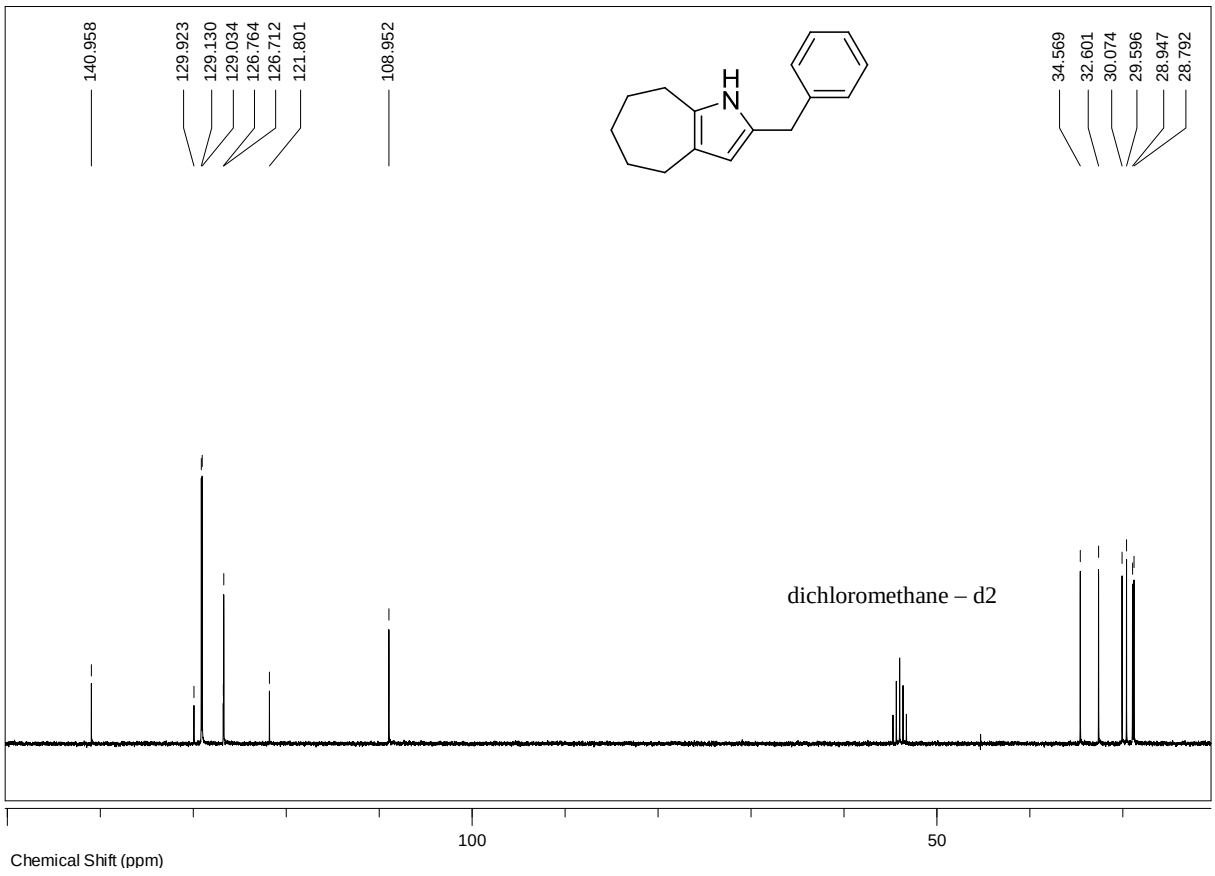
140.958
129.923
129.130
129.034
126.764
126.712
121.801
108.952
H
N
34.569
32.601
30.074
29.596
28.947
28.792
dichloromethane – d2
100
50
Chemical Shift (ppm)

2e:

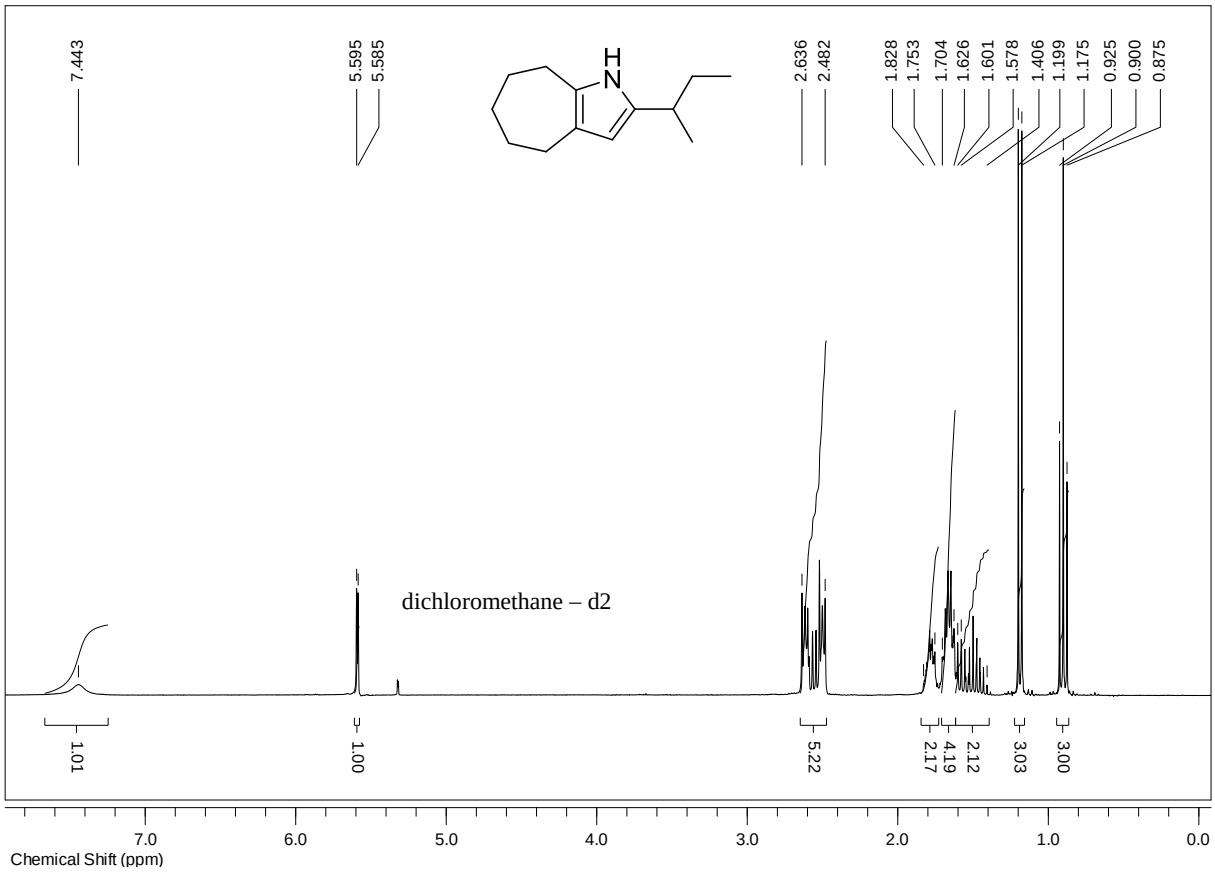
7.443
5.595
5.585
2.636
2.482
1.828
1.753
1.704
1.626
1.601
1.578
1.406
1.199
1.175
0.925
0.900
0.875
dichloromethane – d2
1.01
1.00
5.22
2.17
6.19
2.12
3.03
3.00
7.0
6.0
5.0
4.0
3.0
2.0
1.0
0.0
Chemical Shift (ppm)

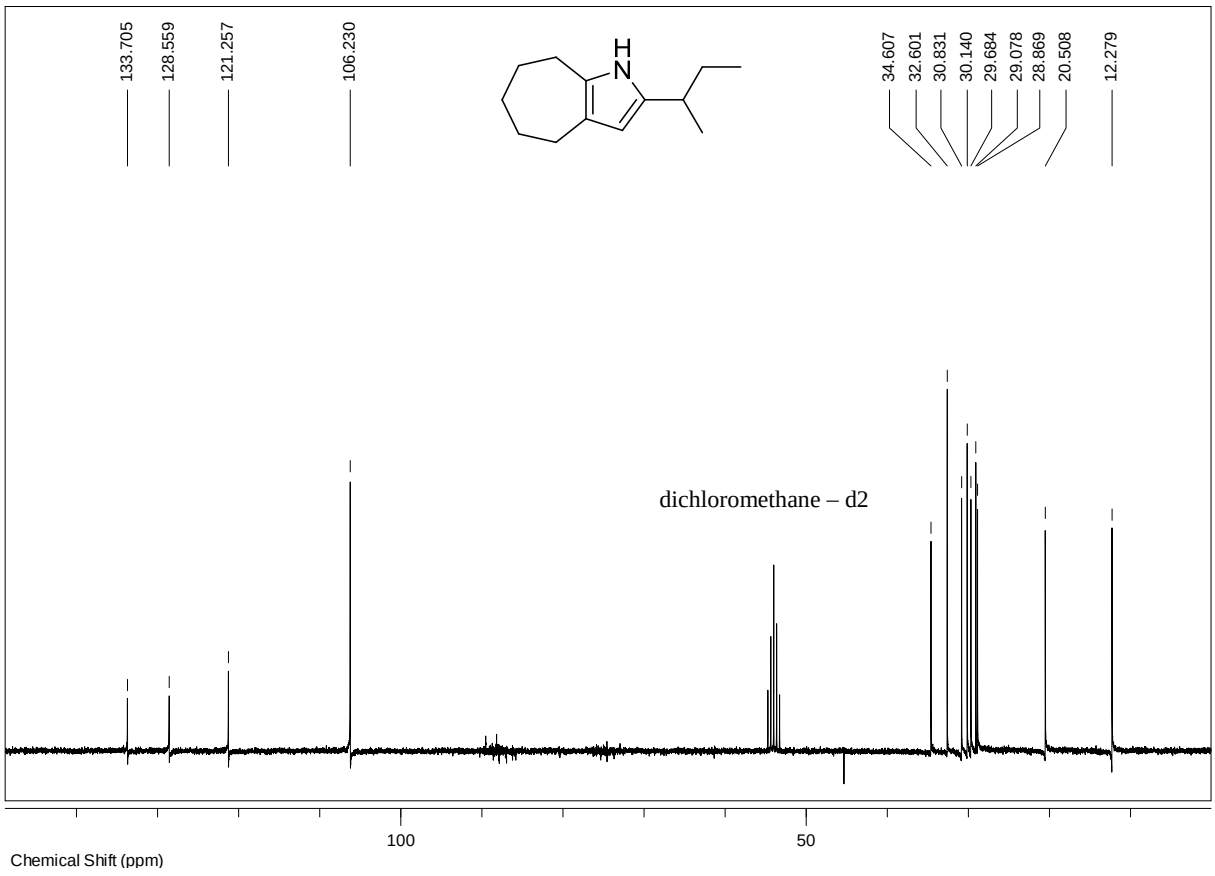
133.705
128.559
121.257
106.230
34.607
32.601
30.831
30.140
29.684
29.078
28.869
20.508
12.279
dichloromethane – d2
100
50
Chemical Shift (ppm)

2f:

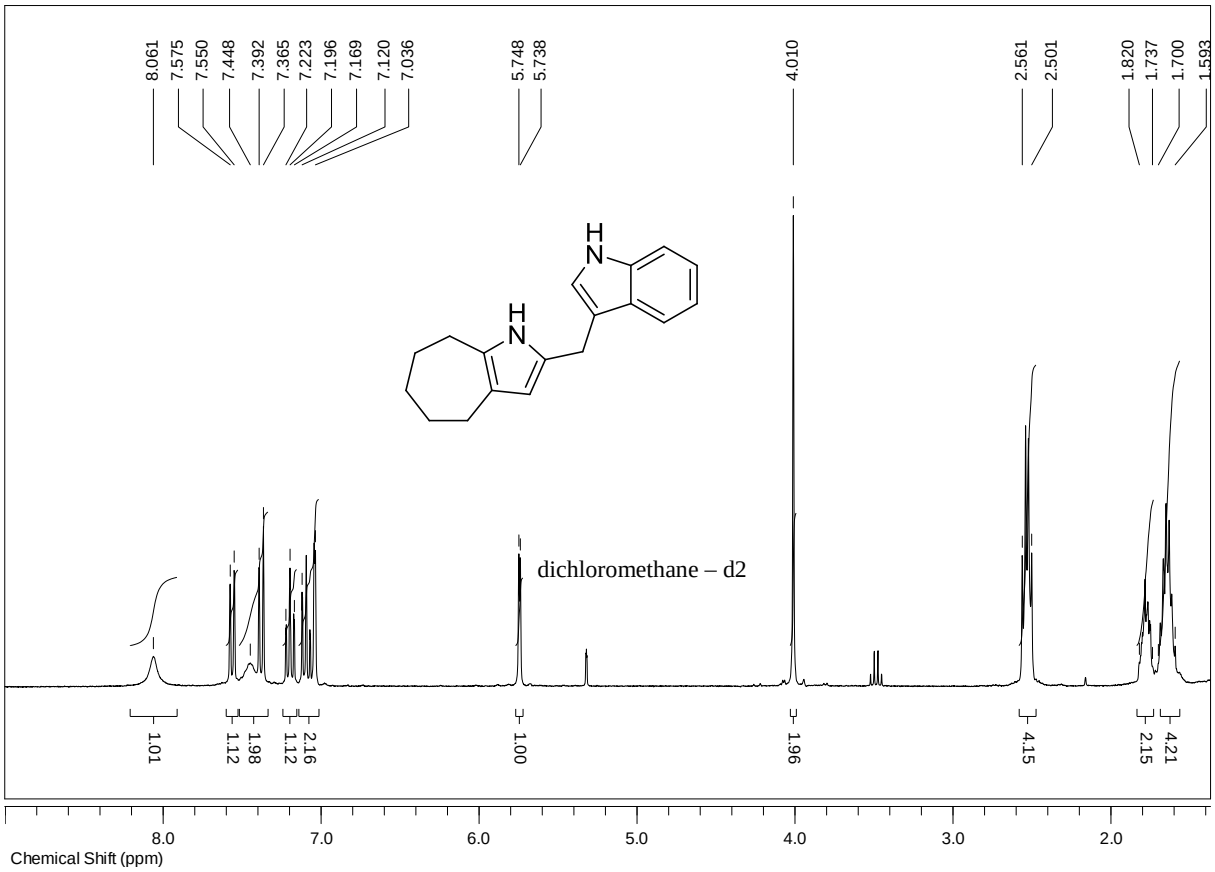
8.061
7.575
7.550
7.448
7.392
7.365
7.223
7.196
7.169
7.120
7.036
5.748
5.738
4.010
2.561
2.501
1.820
1.737
1.700
1.593
dichloromethane – d2
1.01
1.12
1.98
1.12
2.16
1.00
1.96
4.15
2.15
4.21
8.0
7.0
6.0
5.0
4.0
3.0
2.0
Chemical Shift (ppm)

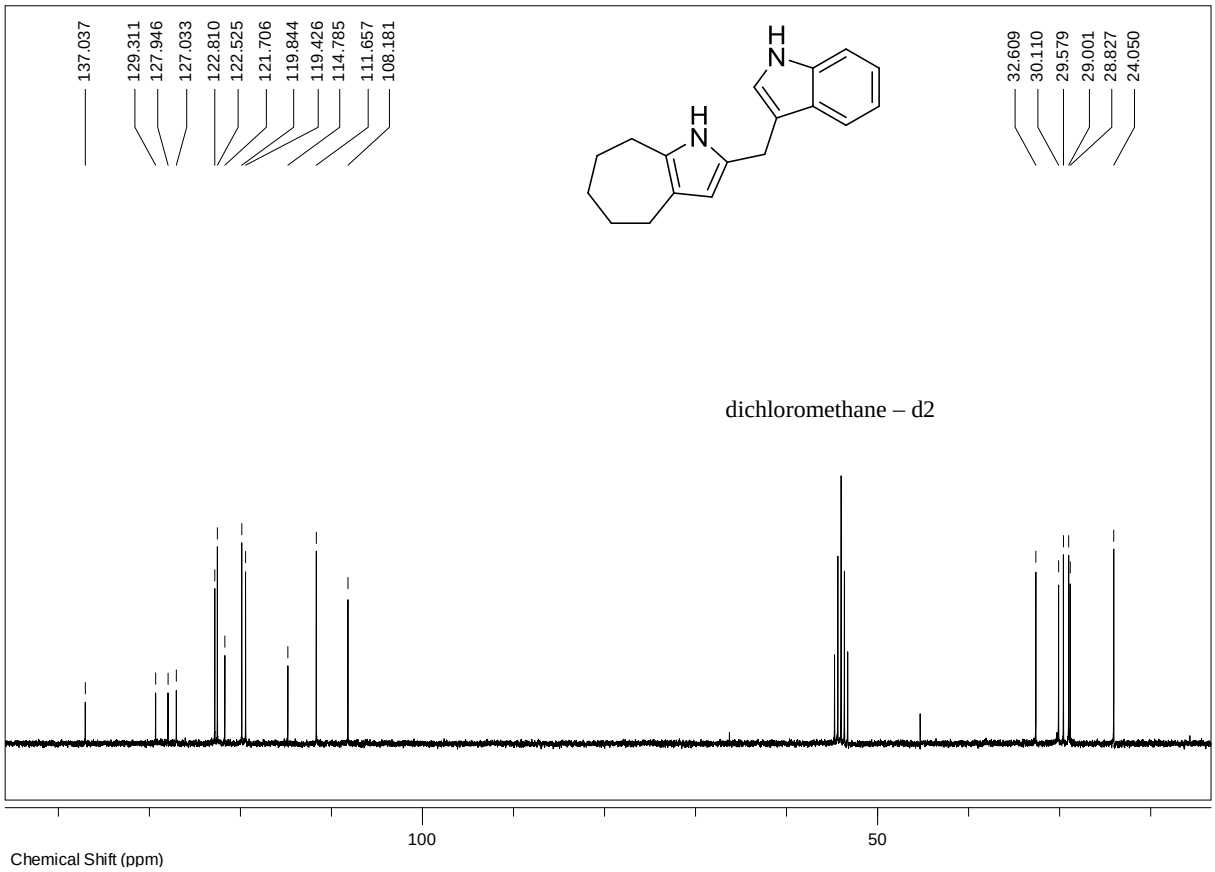
137.037
129.311
127.946
127.033
122.810
122.525
121.706
119.844
119.426
114.785
111.657
108.181
32.609
30.110
29.579
29.001
28.827
24.050
dichloromethane – d2
100
50
Chemical Shift (ppm)

2g:

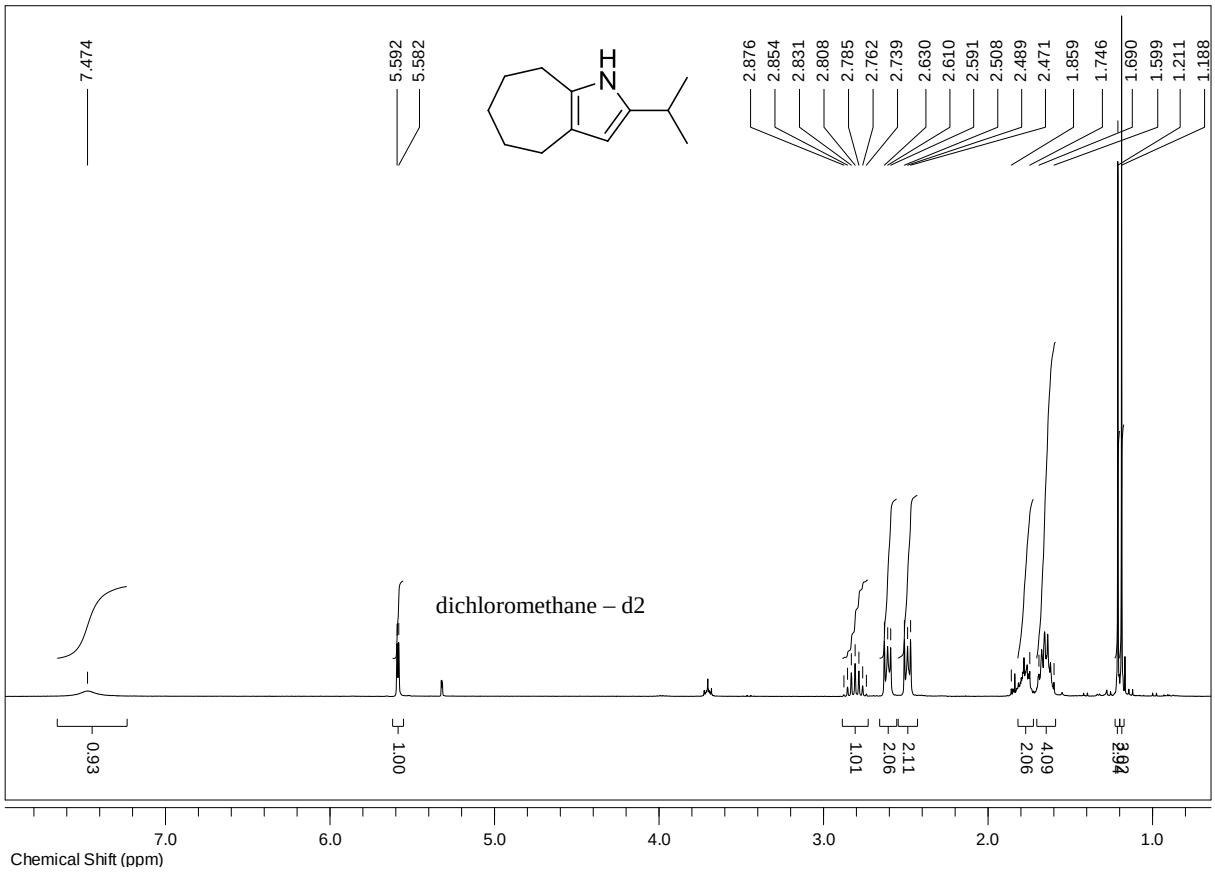
7.474
5.592
5.582
2.876
2.854
2.831
2.808
2.785
2.762
2.739
2.630
2.610
2.591
2.508
2.489
2.471
1.859
1.746
1.690
1.599
1.211
1.188
dichloromethane – d2
0.93
1.00
1.01
2.06
2.11
2.06
4.09
3.84
7.0
6.0
5.0
4.0
3.0
2.0
1.0
Chemical Shift (ppm)

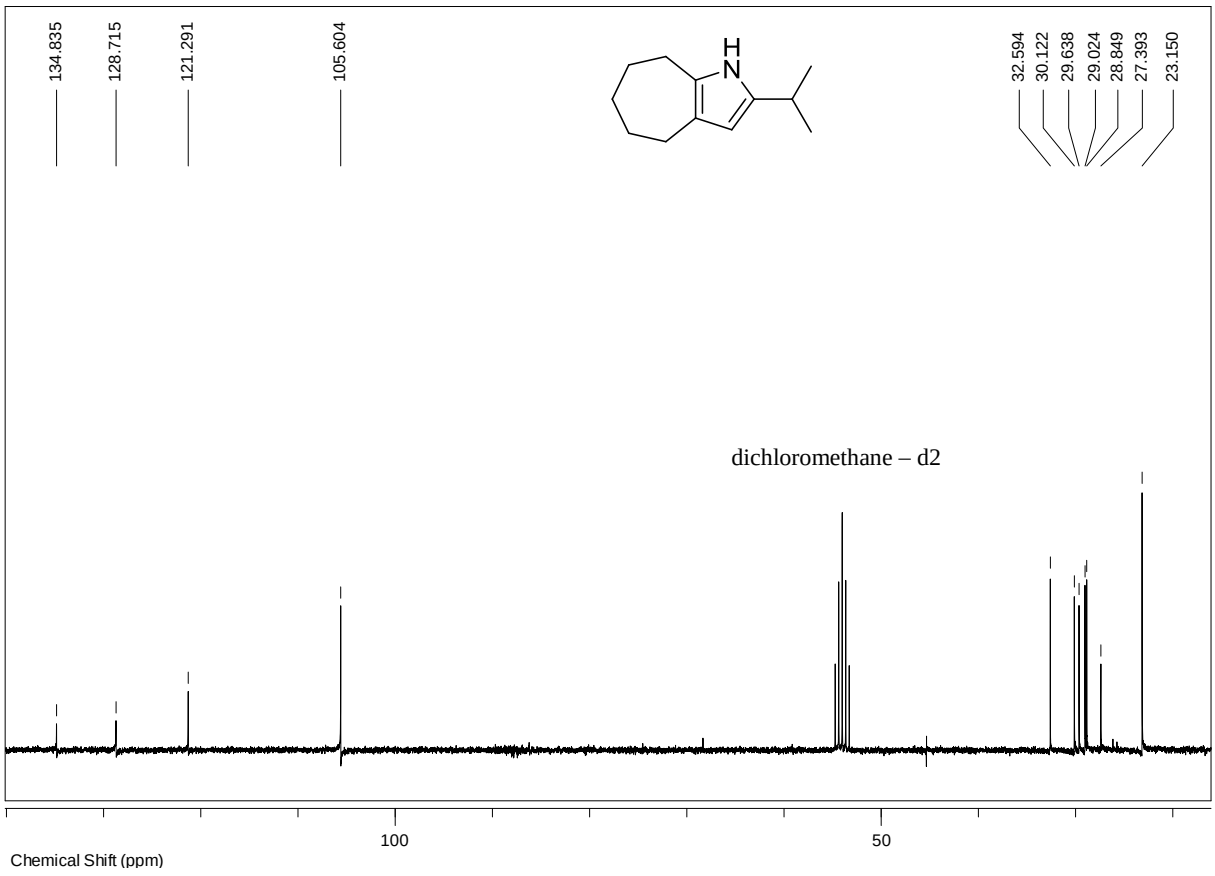
134.835
128.715
121.291
105.604
32.594
30.122
29.638
29.024
28.849
27.393
23.150
dichloromethane – d2
100
50
Chemical Shift (ppm)

2h:

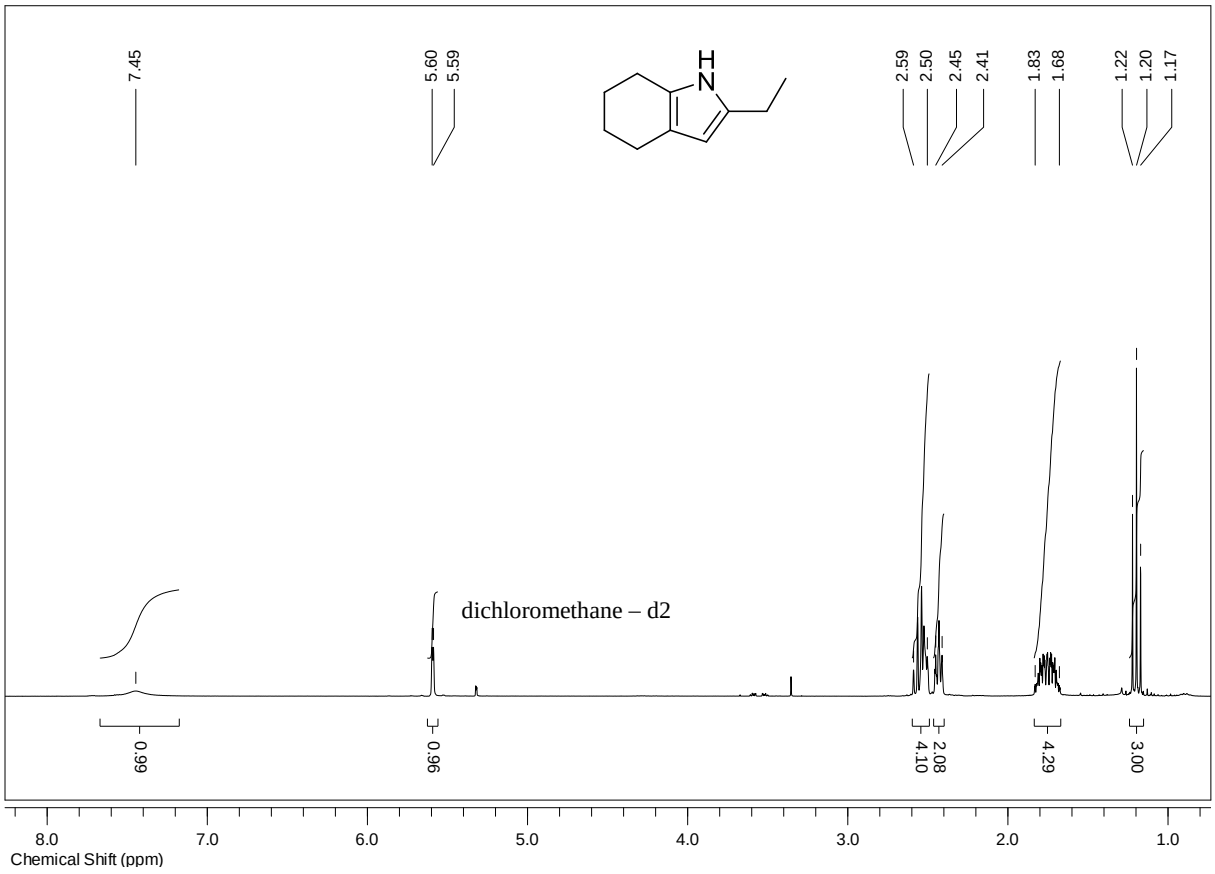
7.45
5.60
5.59
2.59
2.50
2.45
2.41
1.83
1.68
1.22
1.20
1.17
dichloromethane – d2
0.99
0.96
4.10
2.08
4.29
3.00
8.0
7.0
6.0
5.0
4.0
3.0
2.0
1.0
Chemical Shift (ppm)

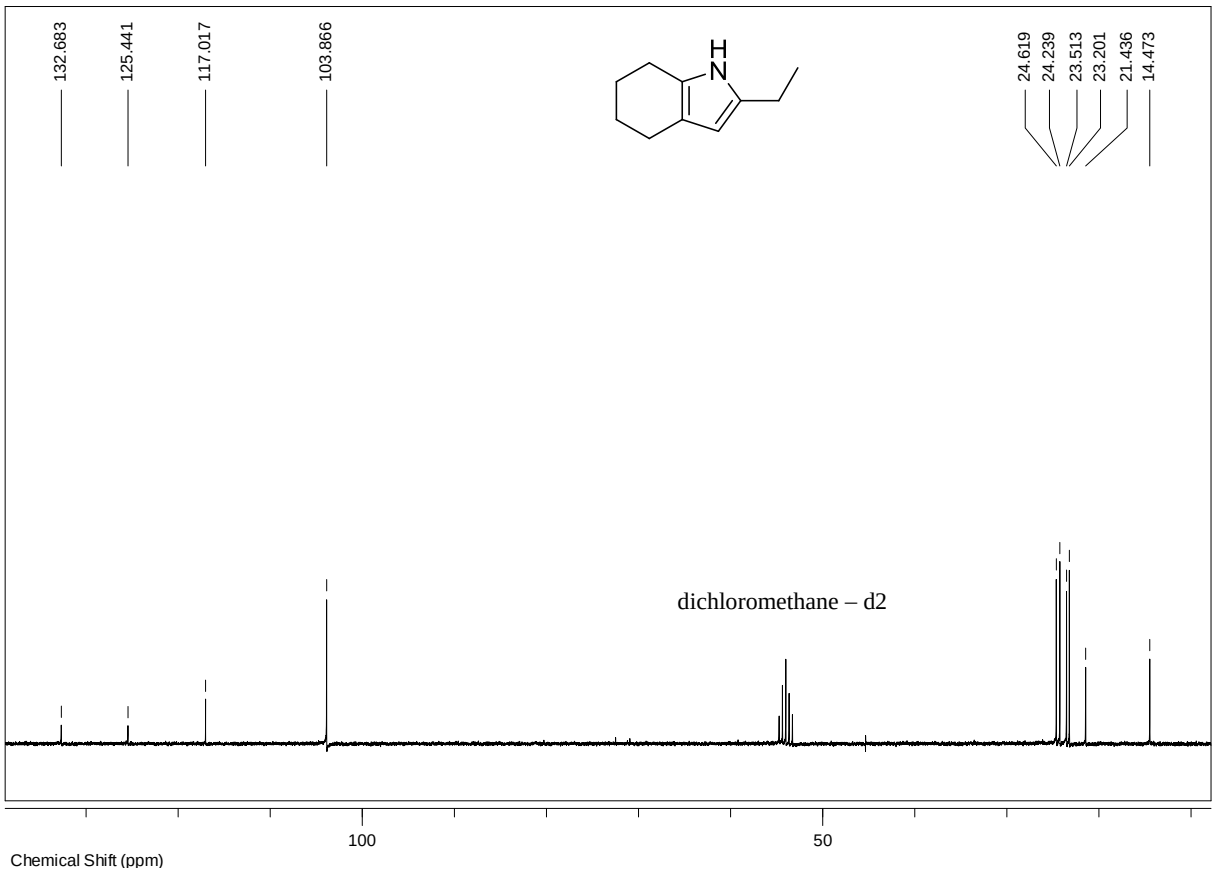
132.683
125.441
117.017
103.866
24.619
24.239
23.513
23.201
21.436
14.473
dichloromethane – d2
100
50
Chemical Shift (ppm)

2i:

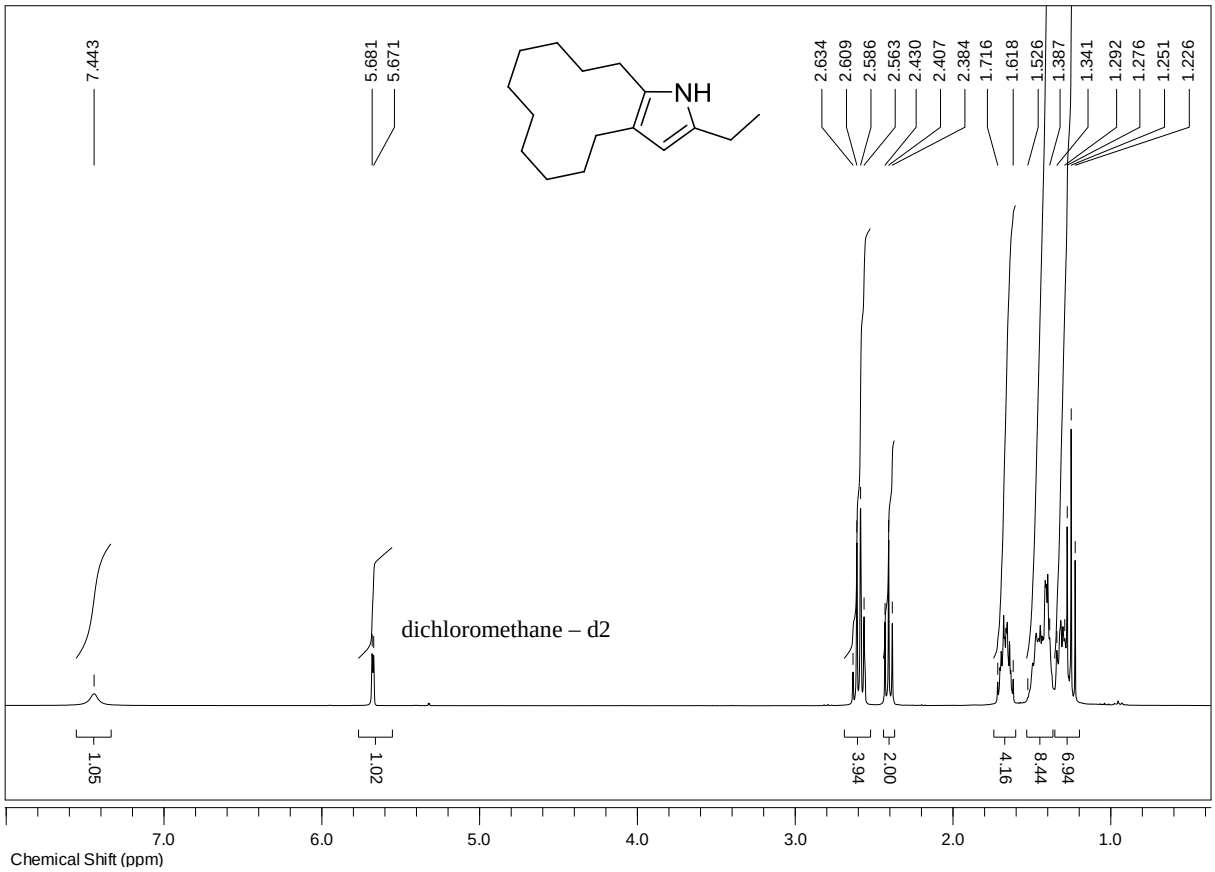
7.443
5.681
5.671
NH
2.634
2.609
2.586
2.563
2.430
2.407
2.384
1.716
1.618
1.526
1.387
1.341
1.292
1.276
1.251
1.226
dichloromethane – d2
1.05
1.02
3.94
2.00
4.16
8.44
6.94
7.0
6.0
5.0
4.0
3.0
2.0
1.0
Chemical Shift (ppm)

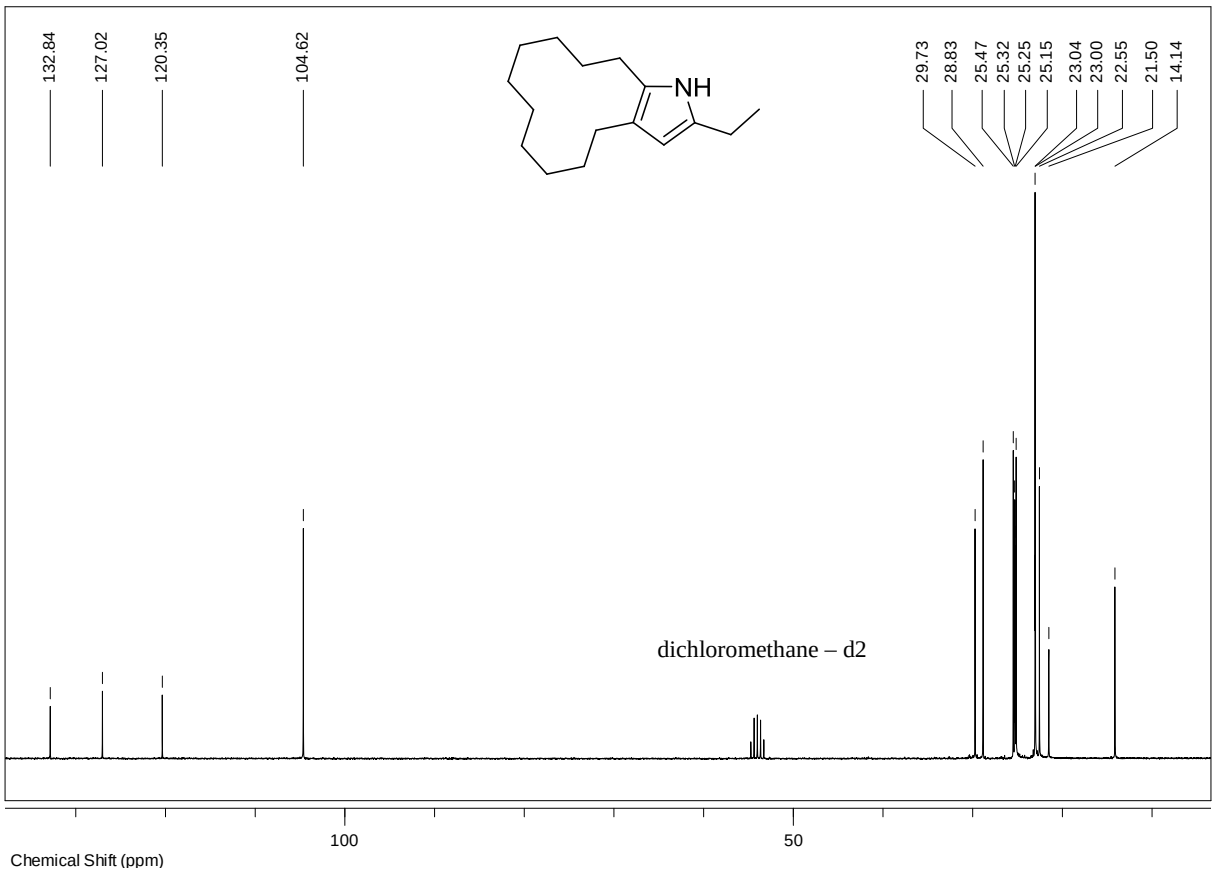
132.84
127.02
120.35
104.62
NH
29.73
28.83
25.47
25.32
25.25
25.15
23.04
23.00
22.55
21.50
14.14
dichloromethane – d2
100
50
Chemical Shift (ppm)

2j:

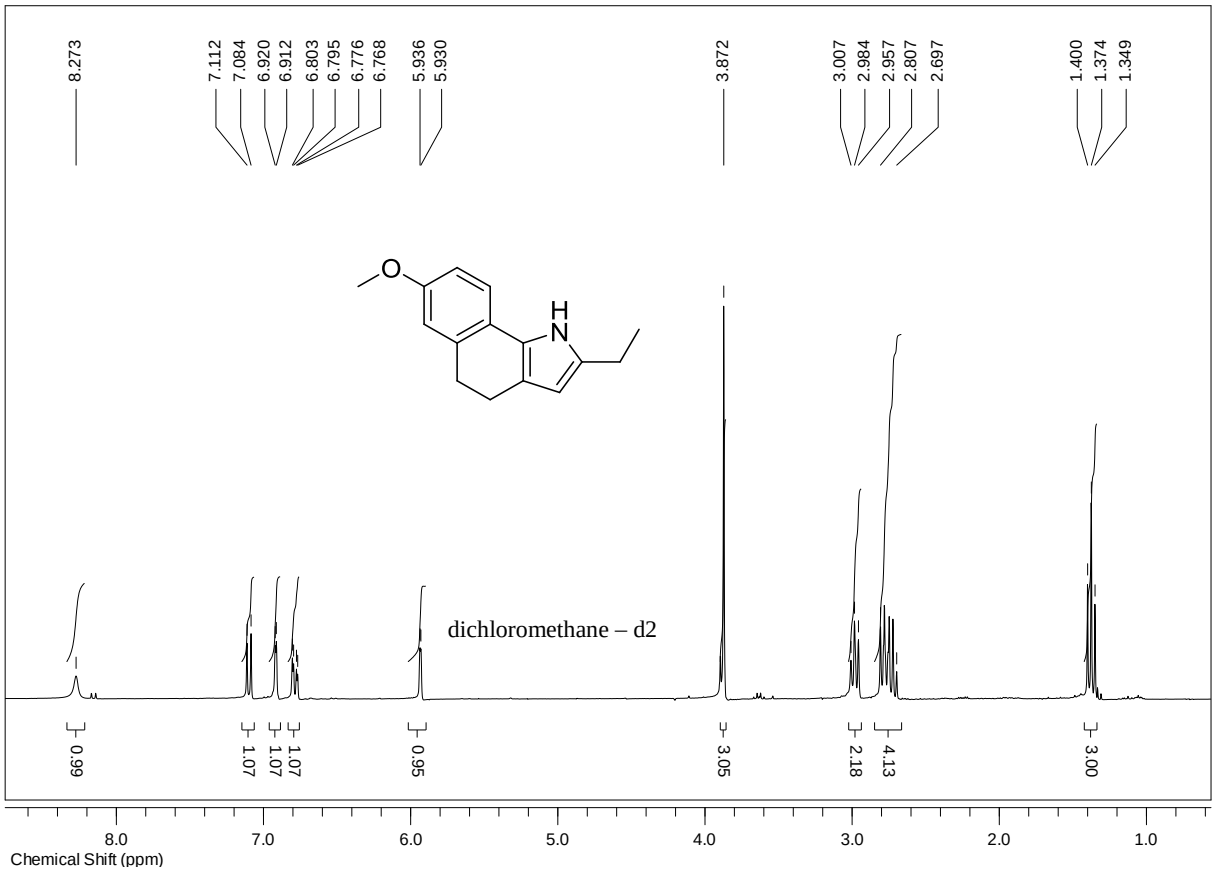
8.273
7.112
7.084
6.920
6.912
6.803
6.795
6.776
6.768
5.936
5.930
3.872
3.007
2.984
2.957
2.807
2.697
1.400
1.374
1.349
O
H
N
dichloromethane – d2
0.99
1.07
1.07
1.07
0.95
3.05
2.18
4.13
3.00
8.0
7.0
6.0
5.0
4.0
3.0
2.0
1.0
Chemical Shift (ppm)

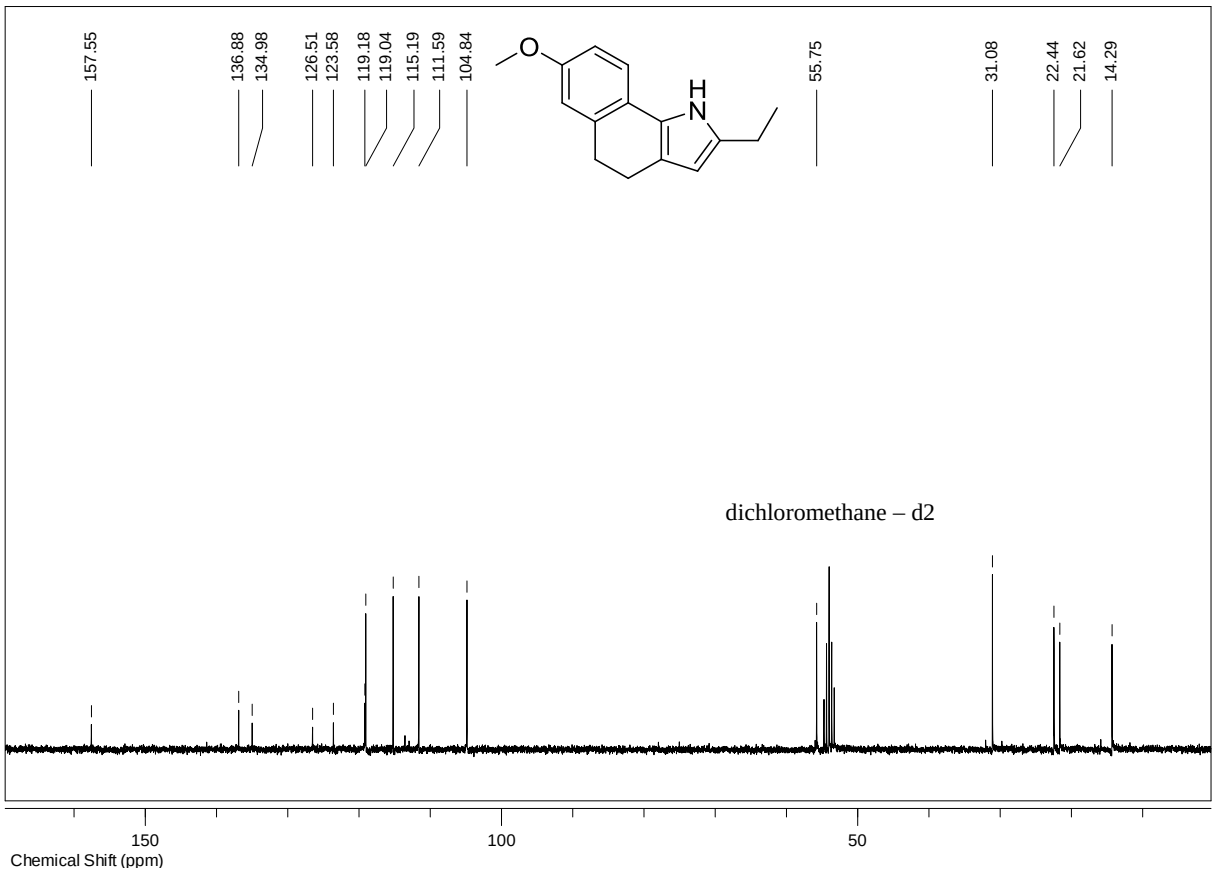
157.55
136.88
134.98
126.51
123.58
119.18
119.04
115.19
111.59
104.84
O
H
N
55.75
31.08
22.44
21.62
14.29
dichloromethane – d2
150
100
50
Chemical Shift (ppm)

6.6.6 References

[1] A. Altomare, M. C. Burla, M. Camalli, G. L. Cascarano, C. Giacovazzo, A. Guagliardi, A. G. G. Moliterni, G. Polidori, R. Spagna, J. Appl. Crystallogr., 1999, **32**, 115.

[2] G. M. Sheldrick, *Acta Crystallogr., Sect. A: Found Crystallogr.*, 2008, **64**, 112.

[3] G. Glatz, T. Irrgang, R. Kempe, *Z. Kristallogr. NCS*, 2007, **222**, 265.

[4] A. Kern, W. Eysel, Mineralogisch-Petrograph. Inst., Univ. Heidelberg, Germany, ICDD Grant-in-Aid, 1993.

[5] M. Wojdyr, J. *Appl. Cryst.*, 2010, **43**, 1126.

[6] Recent nonmetal catalyzed examples: (a) R. Yan, X. Kang, X. Zhou, X. Li, X. Liu, L. Xiang, Y. Li, G and J. Huang, *Org. Chem.*, 2014, **79**, 465. (b) M.-N. Zhao, Z.-H. Ren, Y.-Y. Wang and Z.-H. Guan, *Chem. - Eur. J.*, 2014, **20**, 1839. (c) J. Zhang, C. Xing, B. Tiwari, Y and R. Chi, *J. Am. Chem. Soc.*, 2013, **135**, 8113. (d) F.-J. Duan, J.-C. Ding, H.-J. Deng, D.-B. Chen, J.-X. Chen, M.-C. Liu and H.-Y. Wu, *Chinese Chem. Lett.*, 2013, **24**, 793. (e) S. Rakshit, F. W. Patureau and F. Glorius, *J. Am. Chem. Soc.*, 2010, **132**, 9585.

7. The Sustainable Synthesis of Indoles, Carbazoles, Quinolines and Acridines via Catalytic Condensation of Phenols and Aminoalcohols or Aminophenols

Daniel Forberg[a], Muhammad Zaheer[a], Martin Friedrich[a], Wilfried Assenmacher[b], Werner Mader[b], Tobias Schmidt[c], Rodrigo Q. Albuquerque[c], Stephan Kümmel[c], Rhett Kempe[a]

[a] Lehrstuhl für Anorganische Chemie II – Katalysatordesign, Universität Bayreuth, 95440 Bayreuth, Germany. E-mail: kempe@uni-bayreuth.de

[b] Lehrstuhl für Anorganische Materialforschung, Universität Bonn, 53117 Bonn, Germany

[c] Lehrstuhl für Theoretische Physik IV, Universität Bayreuth, 95440 Bayreuth, Germany

Abstract

The conservation of our global element resources is a challenge of the utmost urgency. Since aliphatic and aromatic alcohols are accessible from abundant indigestible kinds of biomass, first and foremost lignocellulose, the development of novel chemical reactions converting alcohols into important classes of compounds is a particularly attractive carbon conservation and CO_2-emission reduction strategy. Herein, we report a conceptually novel sustainable synthesis of polycyclic aromatic N-heterocycles: the catalytic condensation of phenols and aminoalcohols or aminophenols. This reaction proceeds via hydrogenation and multiple dehydrogenation–condensation steps, mediated by novel reusable catalysts in a most efficient manner. The scope of the concept is exemplarily demonstrated by the synthesis of indoles, carbazoles, quinolines and acridines, the structural motifs of which figure prominently in many important natural products, drugs and materials.

One sentence summary: Biomass derived building blocks can be linked via a novel catalytic condensation reaction to important azaarene motifs found in many natural products, drugs and materials.

7.1 Introduction

The sustainable use of the resources of our planet has become a necessity and one of the great challenges of our time. For chemistry, with its enormous demand for carbon, the move away from the currently dominating technologies consuming oil and related fossil resources towards more sustainable strategies is indispensable in the longer term. An attractive alternative carbon source, if responsibly chosen, is biomass. Lignocellulose, a class of biomass that is abundantly available, barely used and indigestible[1] can be converted to aliphatic alcohols via pyrolysis and hydrogenation steps[2]. Phenols can be obtained from just lignin via aryl ether hydrogenolysis[3]. Thus, alcohols can be regarded as the sustainable alternative to oil crack products, which are the basis of many of the chemical compounds produced today. Consequently, the development of novel reactions that convert alcohols to important classes of compounds is a central topic in chemistry[4]. Catalysis, with its capacity to accelerate specific reaction pathways, is a promising tool to discover and hone such reactions. Sustainable or green reactions of this type will be even more appealing if the scope of methodologies already in place can be significantly extended rather than abandoned and replaced by an altogether different technology. Such a new extended chemistry should encourage and accelerate the move away from the current fossil-based chemistry we are still exploiting.

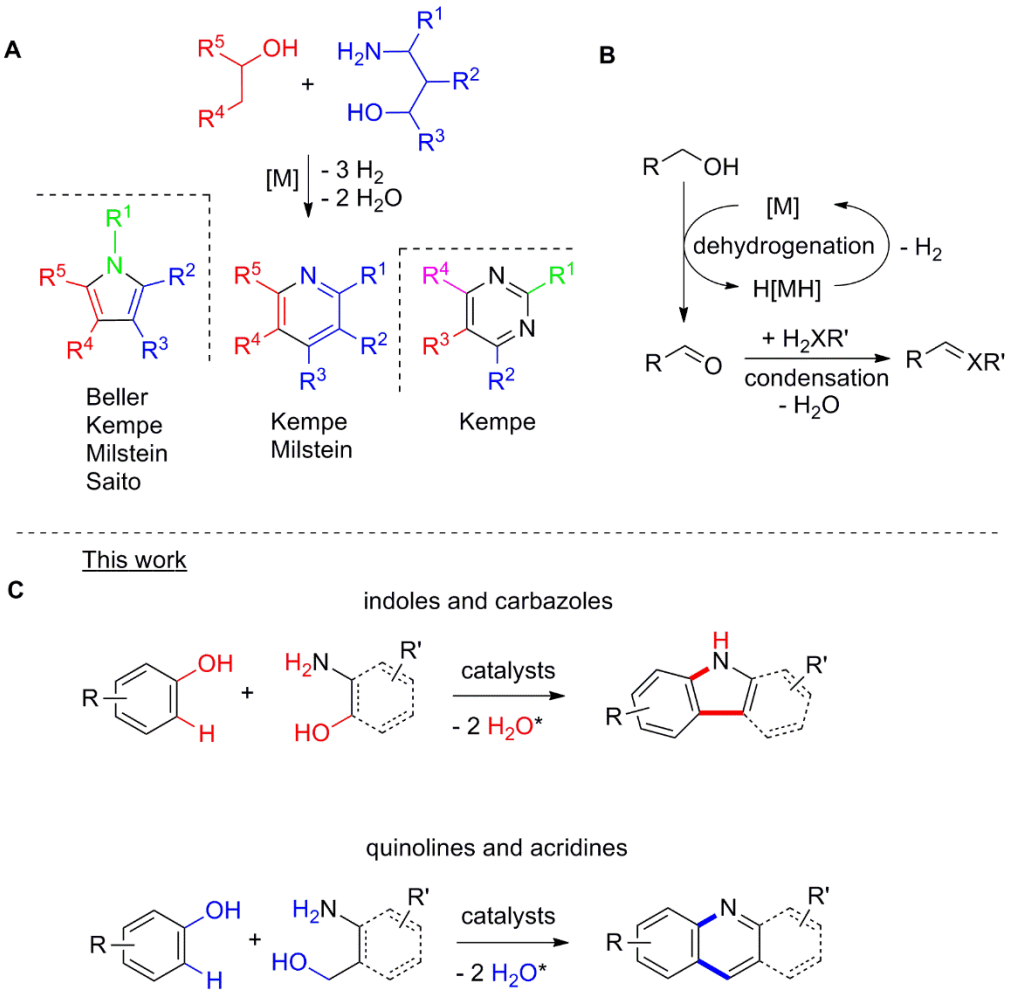

Figure 1. Sustainable catalytic synthesis of aromatic N-heterocycles and the novel synthesis of polycyclic azaarenes disclosed here. A) Known sustainable two-, three-, and four-component reactions linking alcohols to important aromatic N-heterocyclic compounds. The synthetic pathway is shown for the pyridine synthesis (R = substituents). **B)** The combination of dehydrogenation and condensation permits the selective formation of C-C and C-N multiple bonds in these coupling reactions. The alcohols are deoxygenated in the condensation step, while the dehydrogenation step leads to aromatization ([M] = transition metal catalysts; X = CH or N). **C)** Catalytic reaction of phenols and aminoalcohols or aminophenols to polycyclic aromatic compounds disclosed here – sustainable synthesis of indoles, carbazoles, quinolines and acridines via catalytic condensation (*in addition, H_2 is liberated in some reactions; indoles and aciridines 1 equiv. and quinolines 2 equiv.).

A concept has been introduced recently by which the combination of dehydrogenation and condensation steps permits the synthesis of important aromatic N-heterocycles, such as pyrroles[4,5,6,7,8,9], pyridines[10,11,12], pyrimidines[13] and others[14,15,16,17], starting from alcohols (**Figure 1, A**)[18,19]. In this concept, condensation steps deoxygenate the alcohols and dehydrogenations enable aromatization (**Figure 1, B**). The liberation of H_2 in the course of these reactions is appealing to us, because it allows for novel synthesis concepts where

additional steps dovetail with the liberation of hydrogen and use it for reductive substrate activation before it is released.

Herein, we report on a novel concept of a sustainable synthesis in which phenols are catalytically functionalized by reaction with aminoalcohols or aminophenols (**Figure 1, C**). This process involves hydrogenation as well as multiple dehydrogenation and condensation steps. We exemplarily applied this concept to the synthesis of indoles, carbazoles, quinolines and acridines to demonstrate its broad scope. We first hydrogenate the phenols. In the next step, a dehydrogenation–condensation sequence is applied giving rise to polycyclic compounds combining saturated and aromatic rings. Finally, dehydrogenation leads to purely aromatic polycyclic N-heterocyclic compounds. The reaction proceeds via polycyclic pyrrole and pyridine intermediates, interesting compounds which can be isolated if desired. The overall reaction may be run without isolation of the intermediates by just adding or removing the catalyst for the anticipated reaction step. We developed efficient reusable catalysts for this purpose. The concept is also suitable to meet the challenges associated with aryl ether hydrogenolysis, a key step of lignin valorization[3], by feeding the hydrogenated phenols into the reactions discussed herein. The target polycyclic aromatic N-heterocycles have a wide range of conceivable applications in medicine and materials science. Indoles, which feature a "privileged structure" due to their biosynthesis from sugars and amino acids, frequently show a high degree of bioactivity when part of pharmaceuticals, fragrances, agrochemicals and dye pigments[20]. Carbazoles are used as antitumor drugs[21] and in organic solar cell applications[22].

7.2 Results and Discussion

The simple condensation of phenols and aminophenols to carbazoles becomes explicable by presuming a reaction sequence, as shown in **Figure 2, A**. In the first step, the two starting phenols are hydrogenated. The resulting cyclohexanols could undergo an acceptorless dehydrogenative condensation (ADC)[4] to afford an octahydrocarbazole intermediate which, in turn, is dehydrogenated to give the final carbazole product. To run such reaction sequences as a hassle-free procedure without the need for isolating intermediates, easy to separate reusable catalysts would be advantageous. Based on the recently made progress in ADC reactions and the many catalysts described to mediate such reactions[4-14], we focused, firstly, on the development of efficient hydrogenation and dehydrogenation catalysts. A comparison of commercially available ruthenium (Ru), palladium (Pd) and iridium (Ir) catalysts revealed

only low conversions (maximum 34 %) under the conditions given: hydrogenation of phenol at 50 °C applying 3 bar H_2 pressure for 5 h with a catalyst loading of 0.03 mol% active metal (**Figure 2, B**). Since Ru catalysts showed the highest activity and very small metal nanoparticles had previously been generated in a silicon carbonitride (SiCN) matrix[23], we now developed a Ru-SiCN nanocomposite catalyst (Ru@SiCN). This Ru@SiCN catalyst achieved 80 % conversion for the hydrogenation of phenol under the screening conditions given and was, thus, identified as the most active catalyst under scrutiny.

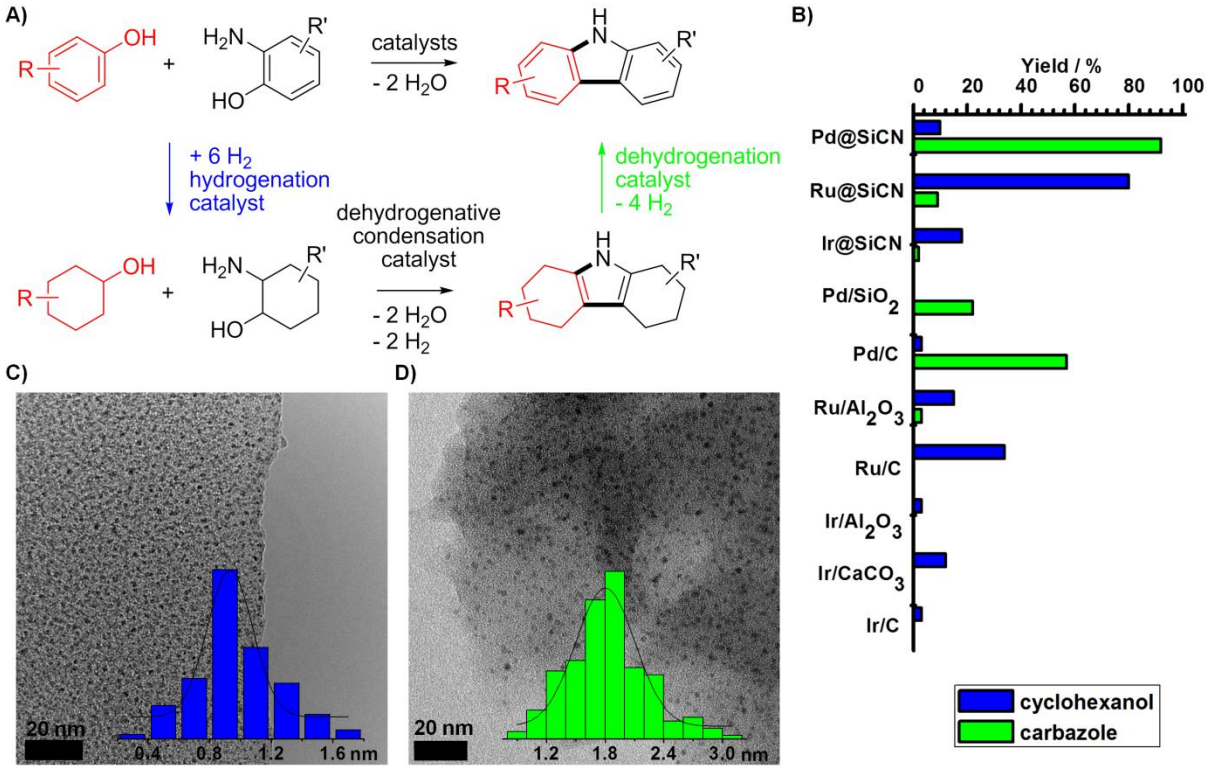

Figure 2. Proposed reaction sequence for the catalytic condensation of phenols and aminophenoles to carbazoles, and catalyst identification for the necessary dehydrogenation and the hydrogenation step. A) The condensation of phenols and aminophenols via hydrogenation and multiple dehydrogenation/condensation steps. **B)** Identification of an efficient hydrogenation and dehydrogenation catalyst. Reaction conditions: hydrogenation of phenol: 1 mmol phenol, 50 °C, 3 bar H_2, 0.03 mol% active Ru, 1 mL H_2O, 5 h. Dehydrogenation of octahydrocarbazole: 1 mmol substance, 0.75 mL diglyme, 0.18 mol% active metal, 190 °C, Ar flow (4-6 mL/min). **C)** TEM analysis and Ru nanoparticle distribution of the Ru@SiCN catalyst. **D)** TEM analysis and Pd nanoparticle distribution of the Pd@SiCN catalyst.

Ru@SiCN was synthesized in a two-step procedure. The commercially available allyl-cycloocta-1,5-diene Ru complex $[(C_3H_5)_2Ru(C_8H_{12})]$ and the commercially available polysilazane HTT 1800 were mixed in tetrahydrofuran, followed by crosslinking using dicumylperoxide and solvent evaporation at 120 °C. Secondly, pyrolysis of the crosslinked

Ru-polymer at 900 °C under a nitrogen atmosphere generated a porous Ru-SiCN nanocomposite. A specific surface area (Brunauer-Emmett-Teller model) of 208 m²/g (metal mediated porosity[24] was observed. Transmission electron microscopy (TEM) revealed metallic nanoparticles homogenously distributed in the SiCN matrix, a mean particle size below 1 nm and a narrow particle size distribution. The existence of the metallic Ru phase was verified by high-resolution TEM. A d-spacing of 205.6 ± 1.7 pm is in accordance with the theoretical value of 204.9 pm for the (101)-reflex of hexagonal crystalline Ru. Similar to Ru@SiCN, a palladium-SiCN nano composite catalyst (Pd@SiCN) was identified as the most active dehydrogenation catalyst (**Figure 2, B**). For its synthesis, a Pd aminopyridinato complex was employed as the Pd-precursor[25]. The existence of Pd nanoparticles with a mean diameter of 1.8 nm could be verified by powder X-ray diffraction and TEM analysis. In addition, we examined the electronic structure of Pd@SiCN with a combination of methods strategy. This involved, firstly, the determination of the atomic coordinates in a classical MD simulation of a 3 nm Pd particle embedded in SiCN. Next, we calculated the electronic density of states (DOS) for subsystems of increasing size at the Pd-SiCN interface with first principles density functional theory. We systematically varied the amount of exact exchange in the exchange-correlation approximation to make sure that we obtained a realistic impression of the d-electron contribution to the DOS. Please see the Supplementary Materials for details. The calculations clearly indicate that Pd retains its electronic structure if embedded in the SiCN matrix. The latter can, therefore, be seen as a support that efficiently stabilizes the metal nanoparticles, while preserving the electronic structure features that are beneficial to catalysis.

Having efficient catalysts for the hydrogenation and the dehydrogenation step available, we studied the scope of the novel catalytic condensation concept. We used Ir catalysts, preferentially a reusable Ir@SiCN catalyst[9] or PN_5P-pincer catalysts[4], both introduced by our group recently, for the ADC step. Firstly, different phenols were coupled with 2-amino-3-phenylpropan-1-ol to synthesize indoles with different substituents at the six-membered ring of this important structural motive. We also isolated the pyrrole intermediates, which could then be dehydrogenated to the corresponding indoles at 172 °C (**Table 1, 1a-h**). Maximum overall yields of 79 % could be obtained. The overall yield is usually determined by the ADC step, meaning that the corresponding pyrroles were isolated in similar yields. By keeping phenol as the constant building block and varying the 1,2-aminoalcohol, different substituents at the five-membered ring were introduced. Five indoles (and the corresponding pyrrole intermediates) could be obtained in good isolated yields up to 76 % (**Table 1, 1i-m**). The

utilization of 2-aminophenol as the phenol building block permits the introduction of substituents at the five-membered ring of the indole motive via abundantly available secondary alcohols. Three examples of products were isolated in overall yields between 70 and 73 % (**Table 1, 1n-p**). The use of cyclic alcohols in combination with 2-aminophenol allowed the synthesis of tricyclic indoles. Different ring sizes could be applied and indoles in very good to excellent yields were obtained: 93 % for the eight- and 89 % for the seven-membered ring (**Table 1, 1q-s**). The 12-membered ring compound (decahydro-5*H*-cyclododeca[*b*]indole) could still be isolated in 50 % overall yield. As mentioned above (**Figure 2, A**), the combination of phenols and 2-amino-phenols generates carbazoles as an example of a further substance class addressable with our synthesis concept. The dehydrogenation of the octahydrocarbazole intermediates required a slightly higher reaction temperature of 190 °C and gave an almost quantitative yield for the dehydrogenation step. Carbazole was isolated in an overall yield of 81 % and 11*H*-benzo[*a*]carbazole in 51 % (**Table 1, 2a,c**). 3-Methylcarbazole is a common precursor for carbazole alkaloids in plants[21], and could be isolated in 70 % (**Table 1, 2b)**. The formation of quinolines and acridines becomes feasible by applying 1,3- instead of 1,2-aminoalcohols. The reaction conditions for the ADC reaction step were optimized at first. To our delight, the reusable Ir@SiCN catalyst was more efficient than the homogeneous Ir pincer catalyst. A somewhat higher catalyst loading than that used for the indole and carbazole synthesis and a reaction temperature of 140 °C were necessary to mediate the ADC step. The functionalization of phenol with various 1,3-aminoalcohol components resulted in the formation of quinolines in overall isolated yields of 58 – 77 % (**Table 1, 3a-e**). Again, the pyridine intermediates could be isolated in similar yields. The utilization of 2-aminobenzylalcohol resulted in the formation of acridines (**Table 1, 4a-f**).

Table 1. Synthesis of indoles, carbazoles, quinolines and acridines[a)]

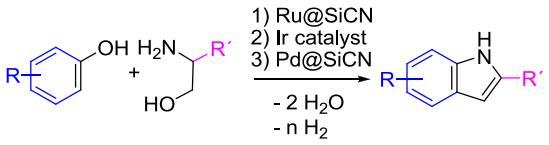

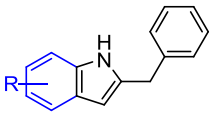

1a: R = H; 79 %
1b: R = 7-methyl; 54 %
1c: R = 5-methyl; 61 %
1d: R = 7-ethyl; 61 %
1e: R = 5-*tert*-butyl; 46 %
1f: R = 4,6-dimethyl; 63 %

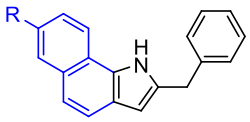

1g: R = H; 79 %
1h: R = methoxy; 59 %

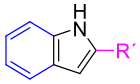

1i: R´= ethyl; 76 %
1j: R´= *sec*-butyl; 70 %
1k: R´= isobutyl; 60 %
1l: R´= isopropyl; 48 %

1m: R´= ; 43 %

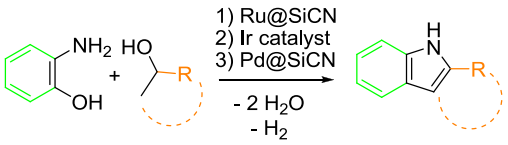

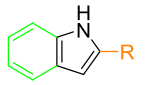

1n: R = phenyl; 73 %
1o: R = *n*-hexyl; 73 %
1p: R = 4-methoxyphenyl; 70 %

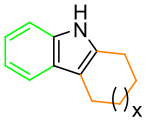

1q: x = 2; 93 %
1r: x = 3; 89 %
1s: x = 7; 50 %

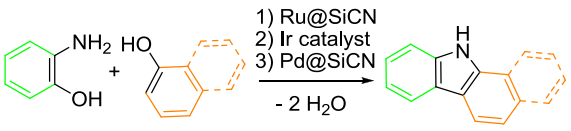

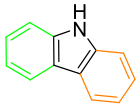

2a: 81 %

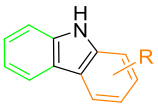

2b: R = 3-Me; 70 %

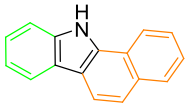

2c: 53 %

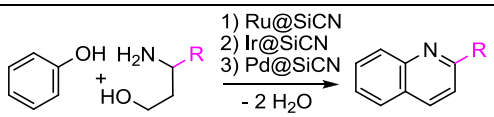

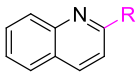

3a: R = H; 58 %
3b: R = $C_{11}H_{23}$; 72 %
3c: R = p-tolyl; 72 %
3d: R = 3,4-dimethoxyphenyl; 77 %
3e: R = pyridine-3-yl; 62 %

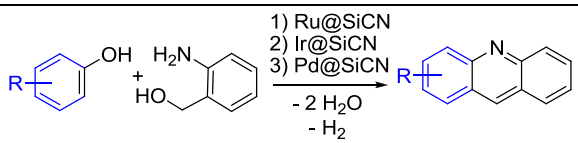

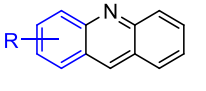

4a: R = H; 79 %
4b: R = 2-*tert*-butyl; 87 %
4c: R = 2-methyl; 68 %
4d: R = 4-methyl; 65 %

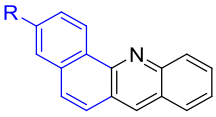

4e: R = H, 88 %
4f: R = methoxy, 79 %

Reaction conditions: Step 1: Hydrogenation of phenol using Ru@SiCN. Step 2: ADC reaction of the cyclohexanol from step 1 and 1,2- or 1,3-aminoalcohol to the corresponding intermediate pyrrole, pyridine, tetrahydrocarbazole or tetrahydroacridine product. Step 3: Acceptorless dehydrogenation using Pd@SiCN at 170 – 190 °C. a) Overall isolated yields.

Since it is possible to apply reusable catalysts for most of the reaction steps, the overall reaction sequence can be performed without isolating the intermediate products (**Figure 3**).

The hydrogenation of phenol is now performed in tetrahydrofuran, since the presence of water is detrimental to the second step involving condensation reactions. The Ru@SiCN catalyst was separated by centrifugation and a mixture of Ir@SiCN catalyst, KO^{t}Bu, diglyme and 2-aminobenzylalcohol was added to the cyclohexanol solution. The mixture was evacuated and flushed with argon three times and stirred at 140 °C for 22 h. Water was added to more easily remove the ADC catalyst (Ir@SiCN). The Pd@SiCN catalyst was added to the organic phase and the low boiling solvents were evaporated. The acceptorless dehydrogenation at elevated temperature finally yielded the acridine product in overall yields between 79 and 84 %. The catalysts for all reaction steps were purified by centrifugation and the entire procedure was repeated three times to demonstrate the reusability of the Ru@SiCN, Ir@SiCN and Pd@SiCN catalysts (**Figure 3**).

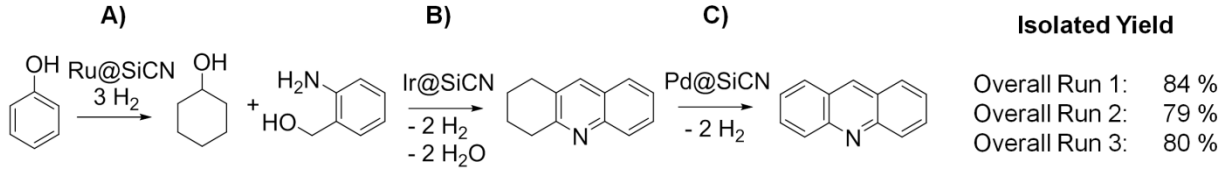

Figure 3. Direct synthesis of acridine without isolation of any of the intermediates and reusability of the employed catalysts. A) 12 mmol, 25 mg (0.096 mol% active metal) Ru@SiCN, 1.5 mL THF, p(H_2) = 20 bar, T = 50 °C, 24 h. The catalyst was removed by centrifugation and the supernatant solution was added to **B)** 3 mmol 2-aminobenzylalcohol, 6 mmol KO^{t}Bu, 3 mL diglylme, 150 mg (0.50 mol% active metal) Ir@SiCN, T = 140 °C, 20 h. Catalyst was removed by addition of water and the organic phase was collected. After adding the mixture to 100 mg (0.12 mol% active metal) Pd@SiCN, the solvents were removed under reduced pressure and then heated at 190 °C for 36 h at an slight Ar flow of 4 – 6 mL/min.

Acknowledgments: We acknowledge financial support from the Deutsche Forschungsgemeinschaft, KE 756/23-2 and SFB 840, B1.

Supplementary Materials:

Materials and Methods
Figures S1-S11
Tables S1-S5
References [25-42]

7.3 References

[1] C. O. Tuck, E. Pérez, I. T. Horváth, R. A. Sheldon, M. Poliakoff, Valorization of biomass: Deriving more value from waste. *Science* **337**, 695-699 (2012).

[2] T. P. Vispute, H. Zhang, A. Sanna, R. Xiao, G. W. Huber, Renewable chemical commodity feedstocks from integrated catalytic processing of pyrolysis oils. *Science* **330**, 1222-1227 (2010).

[3] M. Zaheer, R. Kempe, Hydogenolysis of aryl ethers: a key step in lignin valorization to valuable chemicals. *ACS Catal*. **5**, 1675-1684 (2015).

[4] S. Michlik, R. Kempe, A sustainable catalytic pyrrole synthesis. *Nat. Chem*. **5**, 140-144 (2013).

[5] K. Iida, T. Miura, J. Ando, S. Saito, The dual role of ruthenium and alkali base catalysts in enabling a conceptually new shortcut to N-unsubstituted pyrroles through unmasked α-amino aldehydes. *Org. Lett.* **15**, 1436-1439 (2013).

[6] D. Srimani, Y. Ben-David, D. Milstein, Direct synthesis of pyrroles by dehydrogenative coupling of β-aminoalcohols with secondary alcohols catalyzed by ruthenium pincer complexes. *Angew. Chem., Int. Ed*. **52**, 4012-4015 (2013).

[7] M. Zhang, X. Fang, H. Neumann, M. Beller, General and regioselective synthesis of pyrroles via ruthenium-catalyzed multicomponent reactions. J. *Am. Chem. Soc.* **135**, 11384-11388 (2013).

[8] M. Zhang, H. Neumann, M. Beller, Selective ruthenium-catalyzed three-component synthesis of pyrroles. *Angew. Chem., Int. Ed*. **125**, 625-629 (2013).

[9] D. Forberg, *et al*., The synthesis of pyrroles via acceptorless dehydrogenative condensation of secondary alcohols and 1,2-amino alcohols mediated by a robust and reusable catalyst based on nanometer-sized iridium particles. *Catal. Sci. Technol.* **4**, 4188-4192 (2014).

[10] S. Michlik, R. Kempe, Regioselectively functionalized pyridines from sustainable resources. *Angew. Chem.* **125**, 6450-6454 (2013); *Angew. Chem. Int. Ed.* **52**, 6326-6329 (2013).

[11] D. Srimani, B.-D. Yehoshoa, D. Milstein, Direct synthesis of pyridines and quinolines by coupling of γ-amino-alcohols with secondary alcohols liberating H_2 catalyzed by ruthenium pincer complexes. *Chem. Commun.* **49**, 6632-6634 (2013).

[12] B. Pan, *et al.*, A ruthenium catalyst with unprecedented effectiveness for the coupling cyclization of γ-amino alcohols and secondary alcohols. *ACS Catal.* **6**, 1247-1253 (2016).

[13] N. Deibl, K. Ament, R. Kempe, A sustainable multicomponent pyrimidine synthesis. *J. Am. Chem. Soc.* **137**, 12804-12807 (2015).

[14] S. Ruch, T. Irrgang, R. Kempe, New iridium catalysts for the selective alkylation of amines by alcohols under mild conditions and for the synthesis of quinolines by acceptor-less dehydrogenative condensation. *Chem. Eur. J.* **20**, 13279-13285 (2014).

[15] T. Hille, T. Irrgang, R. Kempe, The synthesis of benzimidazoles and quinoxalines from aromatic diamines and alcohols by iridium-catalyzed acceptorless dehydrogenative alkylation. *Chem. Eur. J.* **20**, 5569 – 5572 (2014).

[16] B. Xiong, Y. Li, W. Lv, Z. Tan, H. Jiang, M. Zhang, Ruthenium-catalyzed staightforward synthesis of 1,2,3,4-tetrahydronaphthyridines via selective transfer hydrogenation of pyridyl ring with alcohols. *Org. Lett.* **17**, 4054−4057 (2015).

[17] S. M. A. Siddiki, K. Kon, A. S. Touchy, K.-i. Shimizu, Direct synthesis of quinazolinones by acceptorless dehydrogenative coupling of o-aminobenzamide and alcohols by heterogeneous Pt catalysts. *Catal. Sci. Technol.* **4**, 1716-1719 (2014).

[18] The contributions were inspired by work of Ishii and coworkers: K. Taguchi, S. Sakaguchi, Y. Ishii, Synthesis of quinolines from amino alcohol and ketones catalyzed by $[IrCl(cod)]_2$ or $IrCl_3$ under solvent-free conditions. *Tetrahedron. Lett.* **46**, 4539-4542 (2005).

[19] The contributions were inspired by work of Crabtree and coworkers: N. D. Schley, G. E. Dobereiner, R. H. Crabtree, Oxidative synthesis of amides and pyrroles via dehydrogenative alcohol oxidation by ruthenium diphosphine diamine complexes. *Organometallics* **30**, 4174-4179 (2011).

[20] M. Bandini, A. Eichholzer, Catalytic functionalization of indoles in a new dimension. *Angew. Chem., Int. Ed.* **48**, 9608-9644 (2009).

[21] A. W. Schmidt, K. R. Reddy, H.-J. Knölker, Occurence, biogenesis, and synthesis of biologically active carbazole alkaloids. *Chem. Rev.* **112**, 3193-3328 (2012).

[22] Y.-J. Cheng, S.-H. Yang, C.-S. Hsu, Synthesis of conjugated polymers for organic solar cell applications. *Chem. Rev.* **109**, 5868-5923 (2009).

[23] The N atoms in the support avoid aggregation of the metal nanoparticles via coordinative saturation of single metal ions or atoms. In addition, the presence of N atoms in the support achieve strong metal nanoparticles-support interactions:
M. Zaheer, T. Schmalz, G. Motz, R. Kempe, Polymer derived non-oxide ceramics modified with late transition metals. *Chem. Soc. Rev*. **41**, 5102-5116 (2012).

[24] M. Zaheer, *et al*., Robust microporous monoliths with integrated catalytically active metal sites investigated by hyperpolarized ^{129}Xe NMR. *Chem. Mater.* **24**, 3952-3963 (2012).

[25] A. Spannenberg, P. Arndt, R. Kempe, Yttrate-mediated ligand transfer and direct synthesis as a route to amidopalladium complexes. *Angew. Chem., Int. Ed.* **37**, 832-835 (1998).

7.4 Supporting Informations

7.4.1 General Considerations

All reactions were carried out in a dry argon or nitrogen atmosphere using standard Schlenk or glove box techniques. Halogenated solvents were dried over P_2O_5, and nonhalogenated solvents were dried over sodium benzophenone ketyl. Deuterated solvents were ordered from Cambridge Isotope Laboratories, vented, stored over molecular sieves and distilled. All chemicals were purchased from commercial sources with purity over 95 % and used without further purification. Polysilazane "KiON HTT 1800" was purchased from Clariant Advanced Materials GmbH, Frankfurt (Germany) and used without further purification. NMR spectra were received using an INOVA 300 MHz spectrometer at 298 K. Chemical shifts are reported in ppm relative to the deuterated solvent. Elemental analyses were carried out on a Vario elementar EL *III*. X-ray crystal structure analyses were performed with a STOE-STADIVARI diffractometer [λ(Mo-K_α) = 0.71073 Å] equipped with an Oxford Cryostream low-temperature unit. Structure solution and refinement were accomplished with SIR-97 and SHELXL-2014[25,26]. GC analyses were carried out on an Agilent 6890N Network GC system equipped with a HP-5 column (30 m x 0.32 mm x 0.25 µm) using *n*-dodecane as internal standard. GC/MS analyses were carried out on an Agilent 7890A/MSD 5975C system equipped with a HP-5MS column (30 m x 0.32 mm x 0.25 µm). Ceramization was carried out under nitrogen atmosphere in a high temperature furnace (Gero, Germany). All X-ray powder diffractograms were recorded by using a STOESTADE-P-diffractometer (CuK_α-Strahlung, 1.54178 Å) in θ-2θ-geometry and with a position sensitive detector. Transmission electron microscopy (TEM) was carried out by using a Varian LEO 9220 (200 kV) instrument. The sample was suspended in chloroform and sonicated for 5 min. Subsequently a drop of the suspended sample was placed on a grid (Plano S 166-3) and allowed to dry. High resolution transmission electron microscopy (HR-TEM) was carried out by using a Philips CM300 FEG/UT (300 kV) instrument. The sample was suspended in chloroform and sonicated for 2 min. Subsequently a drop of the suspended sample was placed on a grid with lacy carbon film and allowed to dry. EDX measurements were carried out by using a Zeiss Field-Emission-Scanning-Electron-Microscope (FESEM) „LEO 1530 GEMINI". The acceleration voltage was 1 – 5 kV. FT-IR measurements were performed using a Perkin-Elmer FTIR-spectrum 100. Milling of the catalyst was performed in a ball mill "Pulverisette 0" (Fritsch, Germany) for 15 min. ChemBET measurements were carried out by using a ChemBET Pulsar TPR/TPD instrument from Quantachrome. N_2 sorption was measure using a Nova2000e

(Quantachrome). ICP-OES measurements were carried out by using a Vista-pro radical model from Varian. Ir/C (1 wt.-%; 50 % water wet), Ir/Al_2O_3 (1 wt.-%) and $Ir/CaCO_3$ (5 wt.-%) were received from Alfa Aesar and used without further treatment or purification. The catalysts Pd/SiO_2 (5 %) and Ru/C (5 %) were purchased from ABCR, Pd/C (10 %) was purchased from Merck and the Ru/Al_2O_3 (5 %) catalyst was obtained from Alfa Aesar. All these catalysts were used without further activation or purification.

7.4.2 Catalyst Synthesis

Synthesis of the Ir@SiCN Catalyst

The used Ir@SiCN catalyst was synthesized, characterized and used as reported[27].

Synthesis of the Pd@SiCN Catalyst

Synthesis of 4-Methyl-2-((trimethylsilyl)amino)pyridine $Ap^{TMS}H$

4-Methyl-2-((trimethylsilyl)-amino)pyridine $Ap^{TMS}H$ was synthesized according to a published procedure in 92 % yield[28].

Synthesis of Palladiumaminopyridinato Complex $Pd(Ap^{TMS})_2$

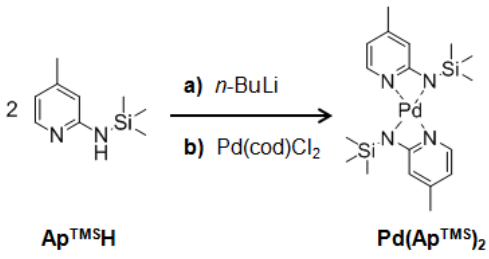

$Ap^{TMS}H$ **$Pd(Ap^{TMS})_2$**

Scheme 1: Synthesis of $Pd(Ap^{TMS})_2$ via salt metathesis reaction

The palladium complex $Pd(Ap^{TMS})_2$ was synthesized according to a published procedure in 53 % yield[29].

^{1}H NMR (300 MHz, $CDCl_3$, 298 K): δ = 7.31 (d, 1H, *J* = 8.7 Hz), 5.84 (d, 1H, *J* = 8.7 Hz), 5.71 (s, 1H), 2.10 (s, 3H), 0.19 (s, 9H) ppm. ^{13}C NMR (75 MHz, $CDCl_3$, 298 K): δ = 175.9, 148.8, 143.1, 110.9, 108.1, 21.6, 1.7 ppm.

Ceramization

Under vigorous stirring 183 mg HTT1800 was added drop wise to a solution of 66 mg (0.14 mmol) $Pd(Ap^{TMS})_2$ and 5 mg dicumylperoxid (2.7 wt.-%) in 1 mL thf. The reaction vial was immediately placed in a pre-heated oil bath at 110 °C for 24 h. After cooling down the solvent was removed under reduced pressure and the brown-black solid was pyrolyzed under N_2 atmosphere with the following heating program:

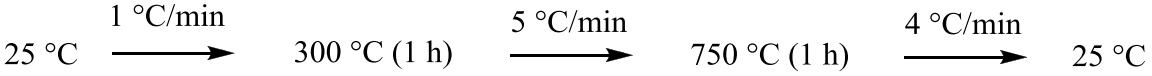

The ceramic yield was 78 %. After ball milling for 15 minutes, the catalyst was pre-treated by stirring in an aqueous solution of NaOH (c = 1 mol/l) at 60 °C for 12 h.

ICP-OES Analysis

50 mg of the sample was solved in 1.5 mL HNO_3 (65 %, distilled), 4.5 mL HCl (32 %, p.a.) and 1 mL HF (40 %) and heated in the microwave at 170 °C for 7 min (80 % power), at 180 °C for 7 min (85 % power) and at 195 °C for 20 min (90 % power).

Result: 8.31 wt.-% Pd content

ChemBET Measurement

90 mg of the Pd@SiCN catalyst was pre-treated under helium and nitrogen atmosphere at 400 °C for 3 hours. After cooling the sample to RT, hydrogen gas (5 % in N_2) was added portion wise using a 250 µL injection loop. Analysis of the results was performed with the free version of the program fytik 0.9.8[30].

Metal dispersion on the surface of Pd@SiCN catalyst: 4.60 %.

N_2 Sorption

N_2 sorption experiments revealed no porosity of the Pd@SiCN nano composite as synthesized.

Powder XRD Analysis

The result of the powder XRD analysis is shown in **Fig. S1**. The 2θ values of 40.1°, 46.3° and 67.8° can be assigned to the (111), (200) and (220) reflexes of cubic crystalline palladium.

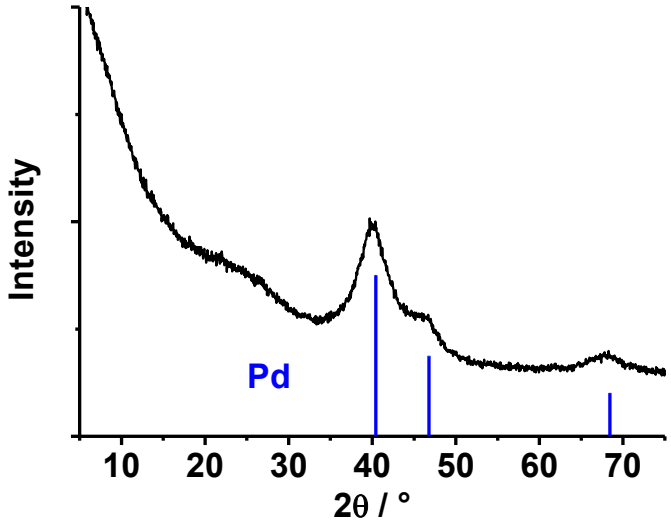

Fig. S1: Powder XRD analysis of the Pd@SiCN catalyst (blue: Reflexes of cubic crystalline palladium; reference card: 00-001-1201)

TEM Analysis

Fig. S2 shows the homogeneous distribution of the Pd nanoparticles in the amorphous SiCN matrix.

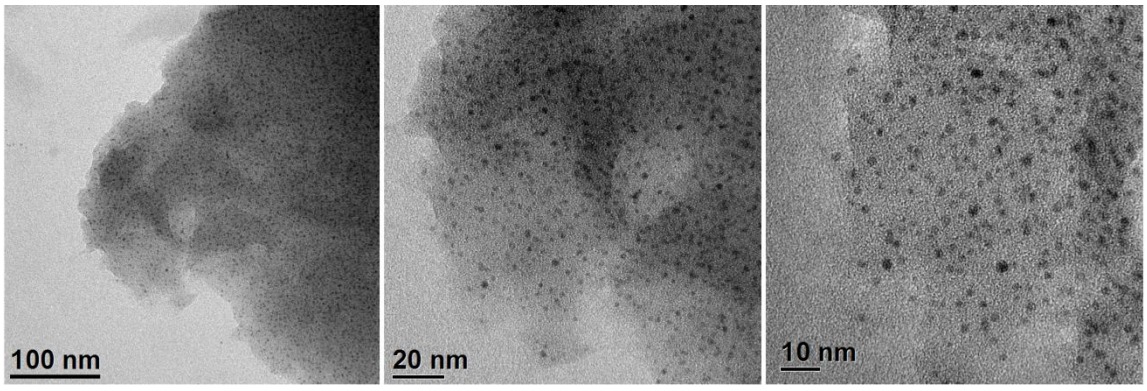

Fig. S2: TEM measurements of the Pd@SiCN catalyst

Size of the Pd Nanoparticles

The size of the palladium nanoparticles were measured with the program "ImageJ". The median particle diameter was measured to be 1.8 nm (**Fig. S3**).

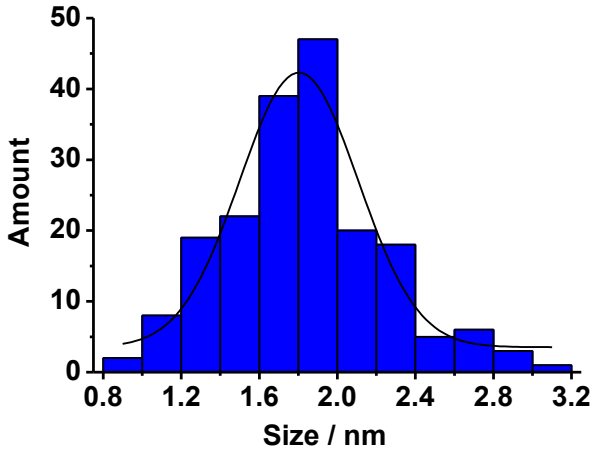

Fig. S3: Histogram of the measured palladium nanoparticles

Computational Details

Obtaining theoretical insight into the electronic structure of systems such as SiCN is very challenging. The large number of atoms and electrons excludes the possibility to straightforwardly perform first principle calculations. Therefore, we approached the problem of obtaining insight into Pd@SiCN by combining different techniques. We first investigated the structure of a system that is close to the experimental situation via molecular dynamics (MD) simulations. A Pd particle with 586 atoms was embedded in a matrix consisting of 2240 Si, 1904 C and 2140 N Atoms. The ratio of atoms was chosen such that it resembles a typical experimental situation. The MD simulations used the embedded-atom method[31] to calculate the interaction within the Pd atoms in the NP, the Terso-potential[32,33,34] for modelling the SiCN support, and a Lennard-Jones potential between the particles. The Pd particle was created as a cutout from the bulk crystal structure, embedded in the SiCN matrix, and annealed at a low temperature of 10 K. This procedure was chosen because our MD is just intended to generate an atomic configuration that is close to the experimental one and that we can use as a first input to the density functional theory (DFT) calculations that will give us information about the electronic structure. As seen in panel **a** of **Fig. S5**, the embedded Pd particle is somewhat deformed. At the base it is approximately 1.5 nm wide, its height is

about 3 nm. The important observation though is that the Pd particle clearly retains a facetted structure. It thus captures the decisive features of the experimental situation.

Insight into the electronic structure which governs catalytic properties can be gained by analyzing the electronic density of states (DOS)[35,36]. Such information cannot be obtained from MD, but requires a method that takes the electrons into account explicitly. Due to the system size, density functional theory (DFT) is the best suited method. Yet, a system with 6780 atoms, many of them of a metal with a substantial number of valence electrons, is much too large for a DFT calculation, even on a modern computer cluster. Therefore, we computed the density of states (DOS) for representative subsystems. We chose a reference point on the interface between Pd particle and SiCN matrix and computed the DOS taking into account all atoms within a certain radius about the reference point. The radii were chosen such that the ratio of SiCN to Pd was (almost) the same in each of the calculations. The red sphere in panel **a** of **Fig. S5** indicates one such subsystem sphere, with a radius of 8 Å. Also for the subsystems the calculations remain a computational challenge, e.g., requiring to take into account 1940 electrons explicitly for the 8 Å sphere. However, the calculations could be converged. We confirmed that with increasing size of the subsystem sphere, the essential electronic structure properties converged. **Fig. S4** shows the DOS integrated from the highest occupied eigenvalue downwards over a region of 1 electron Volt, i.e., integrated over the energetic vicinity of the Fermi level, for subsystems of increasing size. We see that this number converges for subsystem spheres of radii of about 7 Å. Therefore, the 8 Å sphere can be expected to give a reasonably reliable impression of the electronic DOS of the Pd@SiCN system.

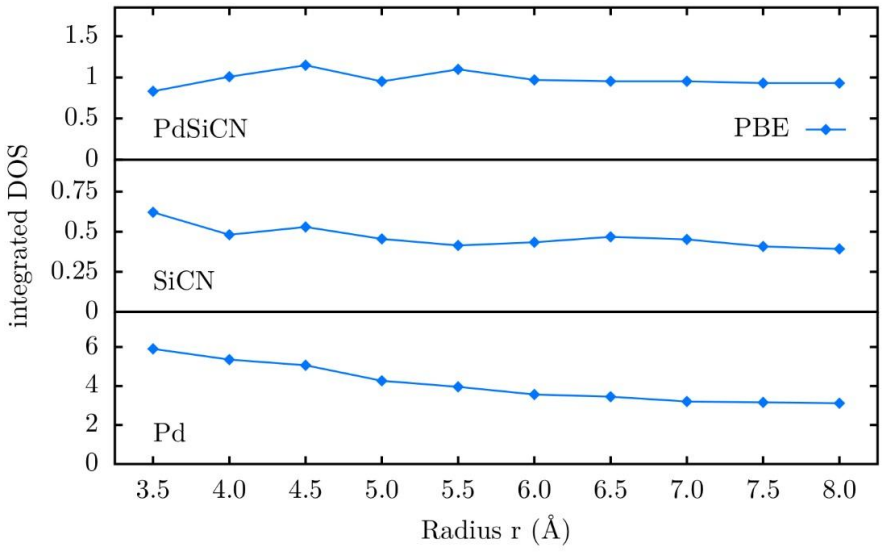

Fig. S4: Convergence of the integrated DOS with increasing subsystem sphere radius.

Thus, we can obtain insight into the electronic structure of the Pd@SiCN system by analyzing sufficiently large subsystems. Panel **b** in **Fig. S5** shows the electronic DOS for a subsystem sphere of 5.5 Å, panel **c** the one for a sphere of 8 Å, using the PBE functional[37] for the exchange-correlation energy. The DFT calculations were performed with the Turbomole program package[38]. The accuracy of the used resolution of the identity and the basis set were checked. A TZVPP basis was used for the DOS calculations. In each case we computed the DOS for the combined Pd@SiCN system (black line), the DOS for just the Pd atoms with all SiCN atoms removed (red line), and the DOS for just the SiCN atoms with all Pd atoms removed (blue line). One clearly sees that the DOS in the chemically most relevant range, i.e., the energetically high lying region close to the Fermi level, is undoubtedly dominated by the DOS from the Pd atoms: The structure and height of the black line is close to the one of the red line. This trend is already observed in panel **b**, but becomes yet clearer for the larger subsystem **c**. We verified that our conclusion that Pd retains its electronic structure properties in the SiCN matrix does not depend on the chosen xc approximation by repeating the calculations for the smaller subsystems with the PBE0[39] and the BHLYP hybrid functional[40]. The latter are computationally much more expensive due to the exact exchange contributions, but the exact exchange can be expected to cancel an important part of the one-electron self-interaction that may displace the d-states. From this perspective it is an important and reassuring finding that the hybrid calculations fully confirm the trends seen with the PBE functional.

In summary we can therefore conclude from the calculations that Pd retains its electronic structure even when embedded in the SiCN matrix and therefore keeps it favorable catalytic properties.

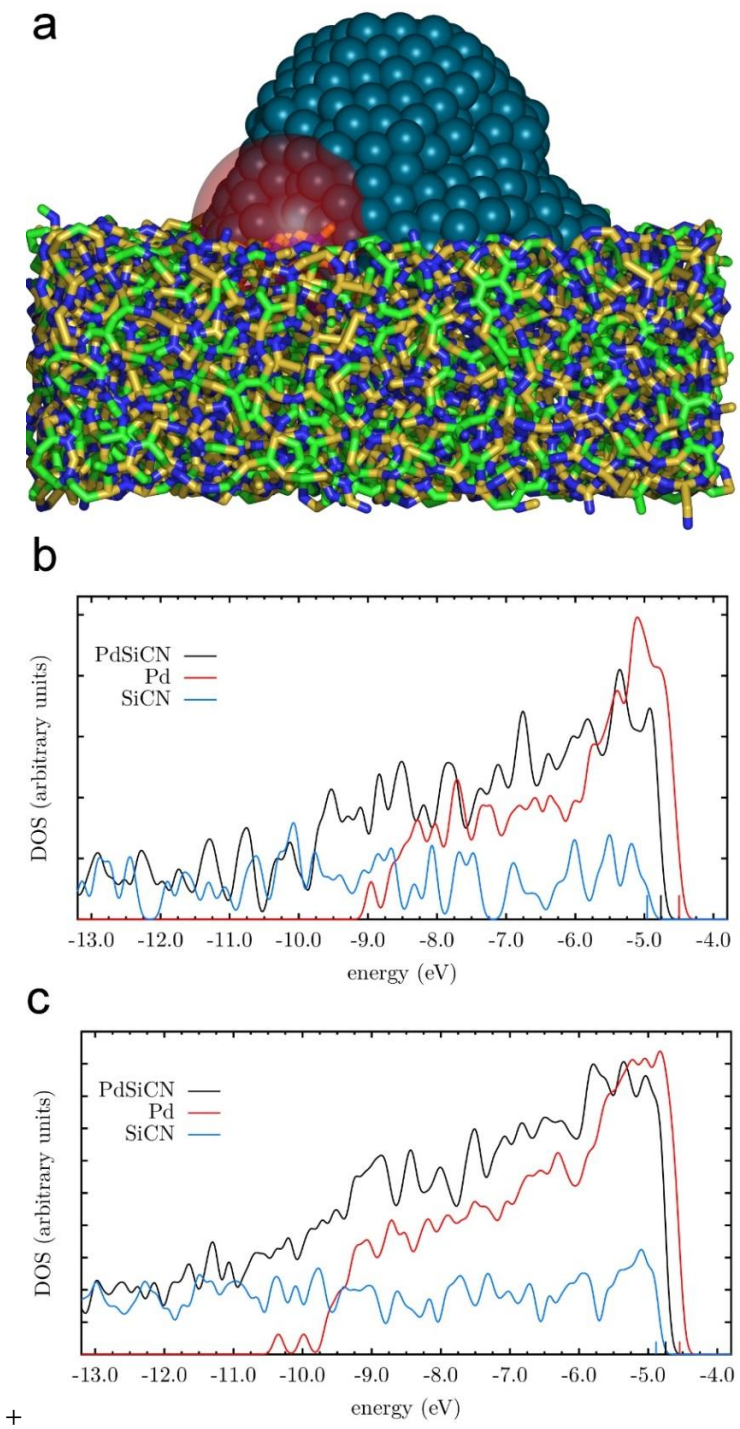

Fig. S5: Structure and density of States for Pd in SiCN. Panel a: Molecular dynamics structure of a Pd particle embedded in a SiCN matrix. The red sphere indicates the spherical sub system referred to in panel **c**. **Panel b:** Electronic density of states for a spherical cut out with radius 5.5 Å. Black: Combined Pd@SiCN system. Red: Pd only. Blue: SiCN only. **Panel c:** Electronic density of states for a spherical cut out with radius 8 Å; color coding as in panel **b**. Clearly the combined density of states is dominated by Pd in the energetically high lying, i.e. chemically relevant, range. This trend increases with increasing system size. Thus, Pd keeps its chemical character and beneficial properties when the NPs are embedded in the SiCN matrix.

Synthesis of the Ru@SiCN Catalyst:

The bis(2-methylallyl)(1,5-cyclooctadiene)ruthenium(II) complex was purchased from the company "Sigma Aldrich" and used without further purification.

Ceramization

Under vigorous stirring 0.552 g (638 µL) HTT1800 was added drop wise to a solution of 274 mg (0.86 mmol) bis(2-methylallyl)(1,5-cyclooctadiene)ruthenium(II) and 15 mg dicumylperoxid (2.7 wt.-%) in 6 mL thf. Half of the solvent was removed slowly under reduced pressure and the resulting solution was crosslinked at 120 °C for 24 h. After removal of the solvent the brown-black solid was pyrolyzed under N_2 atmosphere with the following heating program:

$$25\ °C \xrightarrow{1\ °C/min} 300\ °C\ (1\ h) \xrightarrow{5\ °C/min} 900\ °C\ (1\ h) \xrightarrow{4\ °C/min} 25\ °C$$

The ceramic yield was 81 %. After ball milling for 15 minutes, the catalyst was pre-treated by stirring in an aqueous solution of NaOH (c = 1 mol/l) at 60 °C for 12 h.

ICP-OES Analysis

25 mg of the sample was solved in 1.5 mL HNO_3 (65 %, distilled), 4.5 mL HCl (32 %, p.a.) and 1 mL HF (40 %) and heated in the microwave at 170 °C for 7 min (80 % power), at 180 °C for 7 min (85 % power) and at 195 °C for 20 min (90 % power).

Result: 9.68 wt% Ru content.

ChemBET Measurement

59 mg of the Ru@SiCN catalyst was pre-treated under helium and nitrogen atmosphere at 450 °C for 3 hours. After cooling the sample to RT, hydrogen gas was added portion wise using a 50 µL injection loop. Analysis of the results was performed with the free version of the program fytik 0.9.8[30].

Metal dispersion on the surface of Ru@SiCN catalyst: 6.16 %.

N_2 Sorption

The BET surface area was calculated to be 208 m^2/g (**Fig. S6**).

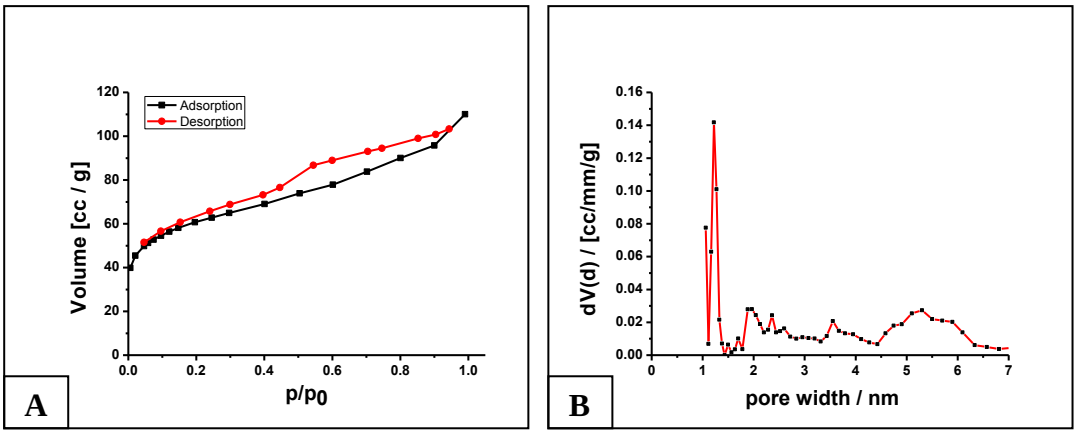

Fig. S6: N_2 sorption analysis of the Ru@SiCN catalyst. (A) Nitrogen sorption isotherme. **(B)** Calculated pore size distribution.

Powder XRD Analysis

The result of the powder XRD analysis is shown in **Fig. S7**. The size of the Ru nanoparticles was calculated to be 0.9-1.1 nm.

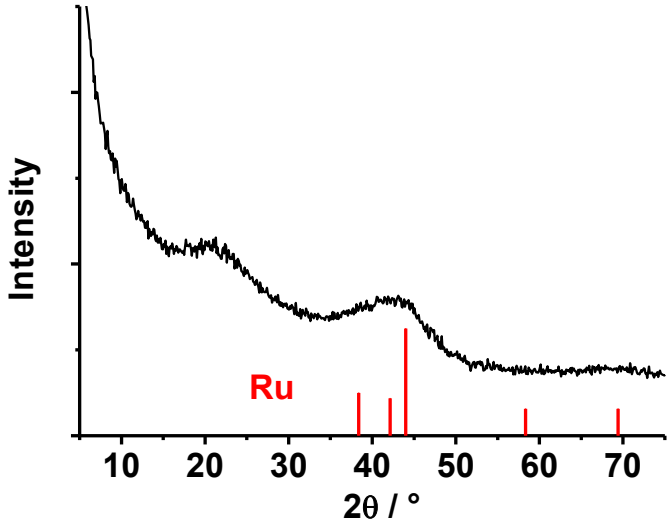

Fig. S7: Powder XRD analysis of the Ru@SiCN catalyst (red: Reflexes of hexagonal crystalline ruthenium; reference card: 00-001-1253)

HR-TEM Analysis

The Ru@SiCN catalyst was analyzed by TEM and HR-TEM to reveal the nature of the particles (**Fig. S8**). Analysis of the FFT resulted in a d-spacing of 205.6 ± 1.7 pm is in accordance with the theoretical value of 204.9 pm for the (101)-reflex of hexagonal crystalline ruthenium.

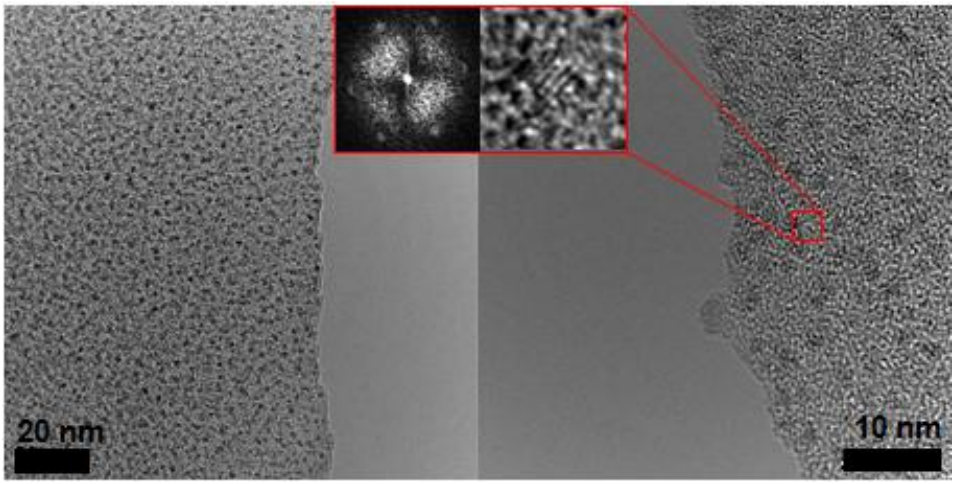

Fig. S8: HR-TEM analysis of the Ru@SiCN catalyst. left & right: HR-TEM picture. middle: Magnification of one Ru nanoparticle with the corresponding FFT.

Size of the Ru Nanoparticles

The size of the ruthenium nanoparticles were measured with the program "ImageJ". The median particle diameter was calculated to be 0.93 nm (**Fig. S9**).

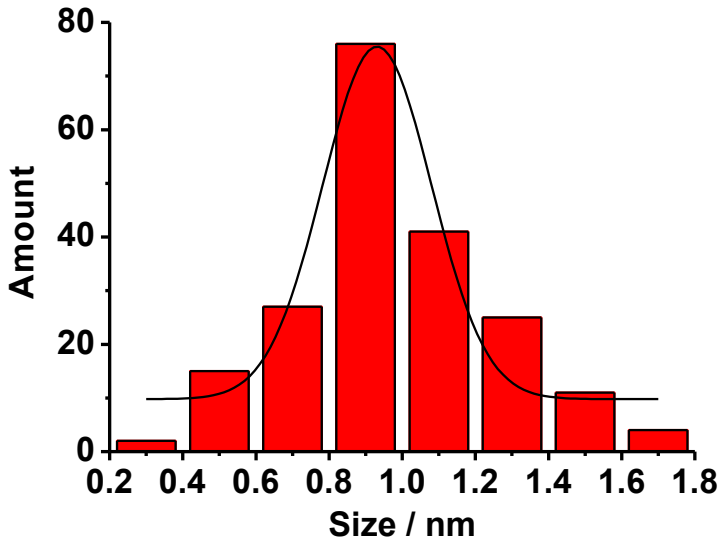

Fig. S9*:* Histogram of the measured ruthenium nanoparticles

7.4.3 Catalysis

Hydrogenation of Phenolic Compounds

Phenol could be hydrogenated at 50 °C and 3 bar H_2 pressure within 24 h using only 0.03 mol% active Ru. A comparison to other commercial catalysts with a reaction time of 5 h is given in **Tab. S1**.

Tab. S1: Comparison of Ru@SiCN to commercial catalysts in the hydrogenation of phenole[a)]

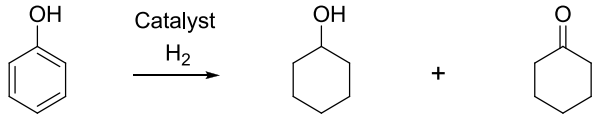

Catalyst	Yield[b)] [%]	Yield[b)] [%]
Ru@SiCN	80	0
Ru/C (5 %)	34	0
Ru/Al_2O_3 (5 %)	15	0
Pd/C (10 %)	3	3
Pd/SiO_2 (5 %)	0	0
Ir/C (1 %)	3	0
Ir/Al_2O_3 (1 %)	3	0
$Ir/CaCO_3$ (5 %)	12	0
Ir@SiCN	18	0
Pd@SiCN	10	22

a) 1 mmol substrate, 50 °C, p(H_2) = 3 bar, 0.03 mol% active metal referring to 5 mg Ru@SiCN, 1 mL H_2O, 5 h. b) Yields were determined by GC using cyclopentanol as internal standard.

The conditions and results of the hydrogenation of pheno lic compounds can be found in **Tab. S2**.

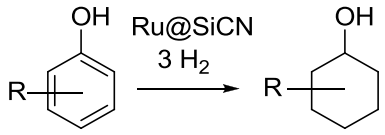

Tab. S2: Hydrogenation of phenolic compounds[a)]

No.	R	Yield [%][b)]
1[c)]	none	> 99
2[d)]	none	97[e)]
3	1-methyl	> 99
4	1-ethyl	> 99
5	4-methyl	> 99
6	4-*tert*-butyl	> 99
7	3,5-dimethyl	92
8[f)]	2-amino	98

a) 1 mmol substrate, 50 °C, p(H_2) = 20 bar, 5 mg Ru@SiCN catalyst (0.03 mol% active metal), 1 mL water, 20 h. b) Yields determined by GC and GC-MS using dodecane as internal standard. c) 50 °C, 3 bar H_2 pressure, 24 h. d)100 mmol substrate, 50 °C, p(H_2) = 20 bar, 200 mg Ru@SiCN catalyst (0.01 mol% active metal), 10 mL water, 24 h. The reactor was pressured again to 20 bar after half of the reaction time. e) Yield of isolated product. f) 80 °C, p(H_2) = 50 bar, 24 h, 20 mg catalyst (0.12 mol% active Ru).

Up-scaling:

Into a reaction glass vial fitted with a magnetic stirring bar, 121 mmol (11.4 g) phenol, 200 mg Ru@SiCN catalyst (0.01 mol% ruthenium), 3 mL tetrahydrofuran and 2 mL water were added. The reaction vial was then placed in a 300 mL Parr autoclave and flushed three times with hydrogen. The autoclave was then pressured with 20 bar hydrogen and the reaction was stirred for 20 h at 50 °C. After half of the reaction time, the hydrogen pressure was again adjusted to 20 bar. After 20 h the hydrogen pressure was released and the sample was extracted five times with diethyl ether. After removal of the solvent under reduced pressure the crude product was obtained in > 95 % yield and analyzed by GC and GC-MS. The hydrogenation of 3,5-dimethylphenol required 80 °C on large scale for full conversion.

Synthesis of Tetrahydropyrroles and Dehydrogenation to Indoles

ADC Coupling:

All pyrrole products were synthesized by modified published procedures using the heterogeneous Ir@SiCN catalyst[27] or the homogeneous PN_5P-Ir-Pincer catalyst (**Fig. S10**)[41].

Heterogeneous[27]:

In a glove box, 200 mg Ir@SiCN, cyclohexanol (24.0 mmol), 1,2-amino alcohol (6.0 mmol), 6 mL diglyme and KO^{t}Bu (1.37 g, 12.0 mmol) were given in Schlenk tube. A pressure equalization device was added and the mixture was heated at 130 °C (oil bath temperature) for 24 h. After cooling to RT, 3 mL water and dodecane as internal standard were added and the product was extracted with diethyl ether (2x). Purification by column chromatography or crystallization resulted in the pure product.

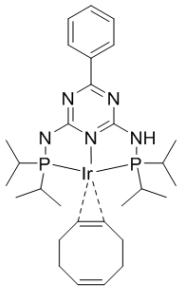

I

Fig. S10: Homogeneous PN_5P-Ir-Pincer catalyst used for pyrrole and carbazole synthesis

Homogeneous[41]:

In a glove box 2.0 mL catalyst **I** (0.02 mmol, 0.01 M in thf), cyclohexanol (20 mmol), 1,2-amino alcohol (10 mmol), 10 mL thf and KO^{t}Bu (11 mmol) were given in a pressure tube and sealed with a semi-permeable membrane. The tube was heated at 105 °C (oil bath temperature) for 22 h. After cooling to RT 3 mL water and dodecane as internal standard were added. The product was extracted with diethyl ether (2x) and purified by column chromatography or crystallization.

Acceptorless Dehydrogenation:

Screening of reaction temperature and catalyst loading:

A reaction temperature of 172 °C (180 °C oil bath temperature) and a catalyst loading of 0.18 mol% (50 mg) was found to be optimal (**Tab. S3**).

Tab. S3: Optimization of reaction temperature and catalyst loading

Temperature (Oil Bath) [°C]	Catalyst Weight [mg]	GC-Yield [%]
150	50	12
160	50	21
170	50	88
180	50	99
180	30	93
180	10	68

Reaction conditions: 1.0 mmol (211 mg) 2-benzyl-4,5,6,7-tetrahydro-1*H*-indole, Pd@SiCN catalyst (50 mg = 0.18 mol% active metal), 0.75 mL diglyme, slight Ar flow (4-6 mL/min), 20 h.

Typical Procedure:

In a 10 mL Schlenk tube 50 mg (0.18 mol% active metal) Pd@SiCN, 1.0 mmol substrate and 0.75 mL diglyme were evacuated and flushed with argon for three times. A slight argon flow of 4-6 mL/min was adjusted and the mixture was stirred for 20 h at 180 °C (oil bath temperature). After cooling to RT the catalyst was separated by centrifugation and washed with acetone two times. The organic phases were combined and the solvent was removed under reduced pressure at 60 °C giving the pure product. If required, further purification was achieved by either column chromatography or crystallization.

Synthesis of 1a:

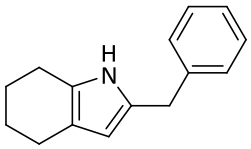

4H-1a: 2-benzyl-4,5,6,7-tetrahydro-1*H*-indole

2.0 mL Catalyst **I** (0.02 mmol, 0.01 M in thf), cyclohexanol (2109 µL, 20 mmol), 2-amino-3-phenylpropan-1-ol (1.51 g, 10 mmol), 10 mL thf, KO^{t}Bu (1.24 g, 11 mmol), 22 h at 105 °C. Purification by column chromatography 30:1 → 15:1 pentane : diethyl ether. Yield: 1.74 g = 8.24 mmol = 82 %. M($C_{15}H_{17}N$) = 211.30 gmol^{-1}.

^{1}H NMR (300 MHz, $CDCl_3$, 298 K): δ = 7.34-7.30 (m, 2H), 7.26-7.21 (m, 3H), 5.71 (s, 1H), 3.92 (s, 2H), 2.48-2.46 (m, 4H), 1.79-1.72 (m, 4H) ppm. ^{13}C NMR (75 MHz, $CDCl_3$, 298 K): δ = 139.7, 128.9, 128.8, 128.5, 126.3, 126.1, 116.8, 105.5, 34.3, 23.8, 23.4, 22.8, 22.7 ppm. MS (EI, m/z): 211.0 (M^+).

elemental analysis (%) for $C_{15}H_{17}N$ calcd: C 85.26, H 8.11, N 6.63; found: C 84.33, H 8.33, N 6.51

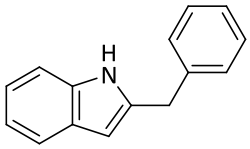

1a: 2-benzyl-1*H*-indole

Yield: quantitative as light brown solid. M($C_{15}H_{13}N$) = 207.27 gmol^{-1}.

^{1}H NMR (300 MHz, CD_2Cl_2, 298 K): δ = 7.91 (s_br, 1H), 7.55-7.53 (m, 1H), 7.38-7.23 (m, 6H), 7.14-7.04 (m, 2H), 6.32 (s, 1H), 4.14 (s, 2H) ppm. ^{13}C NMR (75 MHz, CD_2Cl_2, 298 K): δ = 139.3, 138.7, 136.8, 129.3, 129.2, 129.2, 127.2, 121.7, 120.3, 120.1, 110.97, 101.2, 35.1 ppm. MS (EI, m/z): 207.0 (M^+).

elemental analysis (%) for $C_{15}H_{13}N$ calcd: C 82.72, H 7.64, N 9.65; found: C 82.76, H 8.07, N 8.38.

The overall yield combining all three steps for product **1a** was 79 %.

Synthesis of 1b:

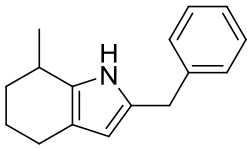

4H-1b: 2-benzyl-7-methyl-4,5,6,7-tetrahydro-1*H*-indole

150 mg Ir@SiCN, 2-methylcyclohexanol (2.74 g, 24.0 mmol), 2-amino-3-phenylpropan-1-ol (906 mg, 6.0 mmol), 5 mL diglyme, KO^{t}Bu (1.37 g, 12.0 mmol), 24 h at 135 °C (oil bath temperature). Purification by column chromatography 40:1→10:1 pentane: Et_2O; Yield: 0.766 g = 3.40 mmol = 57 % as light orange oil. M($C_{16}H_{19}N$) = 225.15 gmol^{-1}.

^{1}H NMR (300 MHz, $CDCl_3$, 298 K): δ = 7.39 (s_br, 1H), 7.37-7.23 (m, 5H), 5.72-5.71 (m, 1H), 3.96 (s, 2H), 2.81-2.75 (m, 1H), 2.51-2.48 (m, 2H), 1.99-1.83 (m, 2H), 1.73-1.61 (m, 1H), 1.47-1.37 (m, 1H), 1.17 (d, *J* = 6.6 Hz, 3H) ppm. ^{13}C NMR (75 MHz, $CDCl_3$, 298 K): δ = 139.7, 131.1, 128.9, 128.7, 128.5, 126.3, 116.5, 105.5, 34.3, 32.6, 28.3, 23.1, 22.6, 20.5 ppm. MS (EI, m/z): 225.2 (M^+).

elemental analysis (%) for $C_{16}H_{19}N$ calcd: C 85.28, H 8.50, N 6.22; found: C: 84.89, H: 8.70, N: 6.20.

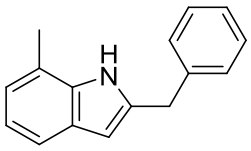

1b: 2-benzyl-7-methyl-1*H*-indole

Yield: quantitative as yellow oil. M($C_{16}H_{15}N$) = 221.12 gmol^{-1}.

^{1}H NMR (300 MHz, $CDCl_3$, 298 K): δ = 7.78 (s_br, 1H), 7.50-7.47 (m, 1H), 7.42-7.38 (m, 2H), 7.34-7.29 (m, 3H), 7.11-7.06 (m, 1H), 7.01-6.99 (m, 1H), 6.40-6.39 (m, 1H), 4.20 (s, 2H), 2.47 (s, 3H) ppm. ^{13}C NMR (75 MHz, $CDCl_3$, 298 K): δ = 138.6, 137.3, 135.8, 128.7, 128.6, 128.2, 126.6, 121.9, 119.9, 119.6, 117.7, 101.8, 34.7, 16.6 ppm. MS (EI, m/z): 221.1 (M^+). HRMS (ESI): calcd. for $C_{16}H_{16}N$ $[M+H]^+$: 222.12772; found: 222.12773.

The overall yield combining all three steps for product **1b** was 54 %.

Synthesis of 1c:

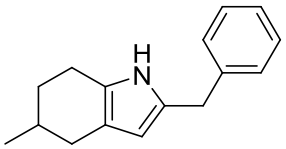

4H-1c: 2-benzyl-5-methyl-4,5,6,7-tetrahydro-1*H*-indole

2.0 mL Catalyst **I** (0.02 mmol, 0.01 M in thf), 4-methylcyclohexanol (2496 µL, 20 mmol), 2-amino-3-phenylpropan-1-ol (1.51 g, 10 mmol), 10 mL thf, KO^{t}Bu (1.24 g, 11 mmol), 22 h at 105 °C. Purification by column chromatography 40:1 → 10:1 pentane : diethyl ether. Yield: 1.42 g = 6.31 mmol = 63 % as light yellow oil. M($C_{16}H_{19}N$) = 225.15 (M^+).

150 mg Ir@SiCN, 4-methylcyclohexanol (2997 µL, 24.0 mmol), 2-amino-3-phenylpropan-1-ol (906 mg, 6.0 mmol), 5 mL diglyme, KO^{t}Bu (1.37 g, 12.0 mmol), 24 h at 135 °C (oil bath temperature). Purification by column chromatography 40:1→10:1 pentane: Et_2O; Yield: 0.766 g = 3.40 mmol = 57 % as light yellow oil. M($C_{16}H_{19}N$) = 225.15 gmol^{-1}.

^{1}H NMR (300 MHz, $CDCl_3$, 298 K): δ = 7.42-7.31 (m, 5H), 5.78 (s, 1H), 3.99 (s, 2H), 2.68-2.59 (m, 3H), 2.23-2.15 (m, 1H), 1.94-1.83 (m, 2H), 1.59-1.46 (m, 1H), 1.14 (d, *J* = 6.3 Hz, 3H) ppm. ^{13}C NMR (75 MHz, $CDCl_3$, 298 K): δ = 139.7, 129.0, 128.7, 128.5, 126.2, 125.8, 116.8, 105.4, 34.3, 34.7, 31.4, 30.1, 22.4, 21.8 ppm. MS (EI, m/z): 225.2 (M^+). HRMS (ESI): calcd. for $C_{16}H_{20}N$ $[M+H]^+$: 226.15902; found: 226.15903.

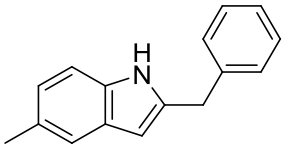

1c: 2-benzyl-5-methyl-1*H*-indole

Yield: quantitative as colorless solid. M($C_{16}H_{15}N$) = 221.12 gmol^{-1}.

H NMR (300 MHz, $CDCl_3$, 298 K): δ = 7.66 (s_br, 1H), 7.35-7.24 (m, 6H), 7.14 (d, *J* = 8.4 Hz, 1H), 6.95 (d, *J* = 8.1 Hz, 1H), 6.26 (s, 1H), 4.12 (s, 2H), 2.44 (s, 3H) ppm. ^{13}C NMR (75 MHz, $CDCl_3$, 298 K): δ = 138.6, 137.8, 134.6, 128.9, 128.9, 128.8, 128.7, 126.7, 122.8, 119.7, 110.1, 100.7, 34.7, 21.4 ppm. MS (EI, m/z): 221.1 (M^+)

elemental analysis (%) for $C_{16}H_{15}N$ calcd: C 86.84, H 6.83, N 6.33; found: C 86.20, H 6.59, N 6.34.

The overall yield combining all three steps for product **1c** was 61 %.

Synthesis of 1d:

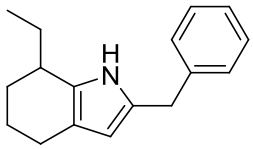

4H-1d: 2-benzyl-7-ethyl-4,5,6,7-tetrahydro-1*H*-indole

2.0 mL Catalyst **I** (0.02 mmol, 0.01 M in thf), 2-ethylcyclohexanol (2.56 g, 20 mmol), 2-amino-3-phenylpropan-1-ol (1.51 g, 10 mmol), 10 mL thf, KO^{t}Bu (1.24 g, 11 mmol), 22 h at 105 °C. Purification by column chromatography 40:1 → 10:1 pentane : diethyl ether. Yield: 1.40 g = 5.85 mmol = 58 %. M($C_{17}H_{21}N$) = 239.17 gmol^{-1}.

150 mg Ir@SiCN, 2-ethylcyclohexanol (3.07 g, 24.0 mmol), 2-amino-3-phenylpropan-1-ol (906 mg, 6.0 mmol), 3 mL diglyme, KO^{t}Bu (1.37 g, 12.0 mmol), 24 h at 135 °C (oil bath temperature). Purification by column chromatography 40:1→10:1 pentane: Et_2O; Yield: 0.850 g = 3.78 mmol = 63 % as light orange oil. M($C_{17}H_{21}N$) = 239.17 gmol^{-1}.

^{1}H NMR (300 MHz, $CDCl_3$, 298 K): δ = 7.39 (s_br, 1H), 7.39-7.34 (m, 2H), 7.30-7.26 (m, 3H), 5.75 (s, 1H), 3.98 (s, 2H), 2.68-2.56 (m, 1H), 2.53-2.49 (m, 2H), 2.02-1.85 (m, 2H), 1.75-1.61 (m, 2H), 1.54-1.40 (m, 2H), 0.99 (t, *J* = 7.2 Hz, 3H) ppm. ^{13}C NMR (75 MHz, $CDCl_3$, 298 K): δ = 139.7, 130.3, 128.8, 128.7, 128.5, 126.2, 116.8, 105.5, 35.0, 34.3, 28.8, 17.8, 23.1, 22.3, 11.6 ppm. MS (EI, m/z): 239.2 (M^+). HRMS (ESI): calcd. for $C_{17}H_{22}N$ $[M+H]^+$: 240.17075; found: 240.17423.

elemental analysis (%) for $C_{17}H_{21}N$ calcd: C 85.30, H 8.84, N 5.85; found: C: 84.95, H: 9.17, N: 5.99.

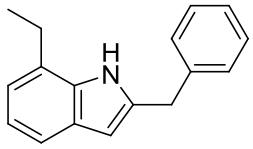

1d: 2-benzyl-7-ethyl-1*H*-indole

Yield: quantitative as yellow-brown oil. M($C_{17}H_{17}N$) = 235.14 gmol^{-1}.

^{1}H NMR (300 MHz, $CDCl_3$, 298 K): δ = 7.81 (s_br, 1H), 7.50-7.48 (m, 1H), 7.42-7.38 (m, 2H), 7.34-7.29 (m, 3H), 7.15-7.10 (m, 1H), 7.06-7.03 (m, 1H), 6.40 (s, 1H), 4.21 (s, 2H), 2.84 (q, *J* = 7.5 Hz, 2H), 1.39 (t, *J* = 7.5 Hz, 3H) ppm. ^{13}C NMR (75 MHz, $CDCl_3$, 298 K): δ = 128.6, 137.2, 135.1, 128.7, 128.6, 128.4, 126.6, 125.8, 120.0, 119.8, 117.7, 101.8, 34.7, 23.9, 13.7 ppm. MS (EI, m/z): 235.2 (M^+).

HRMS (ESI): calcd. for $C_{17}H_{18}N$ $[M+H]^+$: 236.1395; found: 236.1434.

elemental analysis (%) for $C_{17}H_{17}N$ calcd: C 86.77, H 7.28, N 5.95; found: C 85.65, H: 7.37, N: 5.93.

The overall yield combining all three steps for product **1d** was 61 %.

Synthesis of 1e:

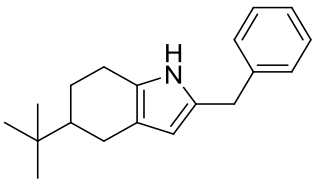

4H-1e: 2-benzyl-5-*tert*-butyl-4,5,6,7-tetrahydro-1*H*-indole

2.0 mL Catalyst **I** (0.02 mmol, 0.01 M in thf), 4-*tert*-butylcyclohexanol (3.13 g, 20 mmol), 2-amino-3-phenylpropan-1-ol (1.51 g, 10 mmol), 10 mL thf, KO^{t}Bu (1.24 g, 11 mmol), 22 h at 105 °C. Purification by column chromatography 20:1 → 8:1 pentane : diethyl ether. Yield: 1.920 g = 7.19 mmol = 72 %. M($C_{19}H_{25}N$) = 267.20 gmol^{-1}.

150 mg Ir@SiCN, 4-*tert*-butylcyclohexanol (3.75 g, 24.0 mmol), 2-amino-3-phenylpropan-1-ol (906 mg, 6.0 mmol), 3 mL diglyme, KO^{t}Bu (1.37 g, 12.0 mmol), 24 h at 135 °C (oil bath temperature). Purification by column chromatography 20:1→8:1 pentane: Et_2O; Yield: 0.770 g = 2.87 mmol = 48 % as light orange oil. M($C_{19}H_{25}N$) = 267.20 gmol^{-1}.

^{1}H NMR (300 MHz, $CDCl_3$, 298 K): δ = 7.34-7.21 (m, 6H), 5.72-5.71 (m, 1H), 3.93 (s, 2H), 2.58-2.53 (m, 3H), 2.29-2.21 (m, 1H), 2.00-1.96 (m, 1H), 1.49-1.36 (m, 2H), 0.93 (s, 9H) ppm. ^{13}C NMR (75 MHz, $CDCl_3$, 298 K): δ = 139.7, 129.3, 128.8, 128.5, 126.3, 126.2, 117.3, 105.7, 45.8, 34.4, 32.5, 27.5, 24.9, 24.2, 23.6 ppm. MS (EI, m/z): 267.1 (M^+).

HRMS (ESI): calcd. for $C_{19}H_{26}N$ $[M+H]^+$: 268.20205; found: 268.20566.

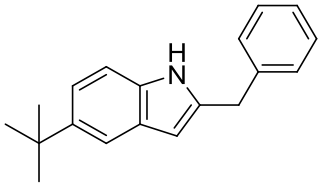

1e: 2-benzyl-5-*tert*-butyl-1*H*-indole

Reaction time: 36 h. Yield: quantitative as yellow-brown oil. M($C_{19}H_{21}N$) = 263.17 gmol^{-1}.

^{1}H NMR (300 MHz, $CDCl_3$, 298 K): δ = 7.68 (s_br, 1H), 7.62 (s, 1H), 7.39-7.19 (m, 7H), 6.35 (s, 1H), 4.14 (s, 2H), 1.44 (s, 9H) ppm. ^{13}C NMR (75 MHz, $CDCl_3$, 298 K): δ = 142.6, 138.7, 137.8, 134.4, 128.8, 128.6, 128.5, 126.6, 119.5, 115.9, 109.9, 101.1, 34.7, 34.5, 31.9 ppm. MS (EI, m/z): 263.1 (M^+).

HRMS (ESI): calcd. for $C_{19}H_{22}N$ $[M+H]^+$: 264.17075; found: 264.17447.

The overall yield combining all three steps for product **1e** was 46 %.

Synthesis of 1f:

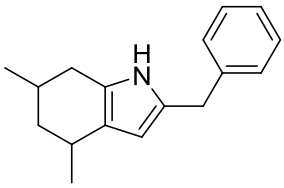

4H-1f: 2-benzyl-4,6-dimethyl-4,5,6,7-tetrahydro-1*H*-indole

150 mg Ir@SiCN, 3,5-dimethylcyclohexanol (3.07 g, 24.0 mmol), 2-amino-3-phenylpropan-1-ol (906 mg, 6.0 mmol), 3 mL diglyme, KO^{t}Bu (1.37 g, 12.0 mmol), 24 h at 135 °C (oil bath temperature). Purification by column chromatography 20:1 pentane: Et_2O; Yield: 0.953 g = 3.98 mmol = 66 % as light yellow oil. M($C_{17}H_{21}N$) = 239.17 gmol^{-1}.

^{1}H NMR (300 MHz, $CDCl_3$, 298 K): δ = 7.34-7.21 (m, 6H), 5.80-5.79 (m, 1H), 3.93 (s, 2H), 2.73-2.61 (m, 1H), 2.54-2.48 (m, 1H), 2.16-2.07 (m, 1H), 1.98-1.79 (m, 2H), 1.16 (d, *J* = 6.9 Hz, 3H), 1.04 (d, *J* = 6.3 Hz, 3H), 1.05-1.02 (m, 1H) ppm. ^{13}C NMR (75 MHz, $CDCl_3$, 298 K): δ = 139.7, 128.9, 128.8, 128.5, 126.2, 125.8, 122.6, 103.8, 42.6, 34.4, 31.3, 30.3, 29.3, 22.4, 21.4 ppm. MS (EI, m/z): 239.1 (M^+).

elemental analysis (%) for $C_{17}H_{21}N$ calcd: C 85.30, H 8.84, N 5.85; found: C 84.84, H 8.83, N 6.03.

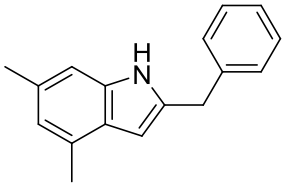

1f: 2-benzyl-4,6-dimethyl-1*H*-indole

Yield: 98 % as yellow-brown oil. M($C_{17}H_{17}N$) = 235.14 gmol^{-1}.

^{1}H NMR (300 MHz, $CDCl_3$, 298 K): δ = 7.63 (s_br, 1H), 7.41-7.29 (m, 5H), 6.91 (s, 1H), 6.81 (s, 1H), 6.34 (s, 1H), 4.14 (s, 2H), 2.56 (s, 3H), 2,47 (s, 3H) ppm. ^{13}C NMR (75 MHz, $CDCl_3$, 298 K): δ = 138.8, 136.3, 131.1, 129.0, 128.7, 128.6, 128.5, 126.6, 126.2, 121.7, 108.1, 99.4, 34.7, 21.6, 18.7 ppm. MS (EI, m/z): 235.1 (M^+). HRMS (ESI): calcd. for $C_{17}H_{18}N$ $[M+H]^+$: 236.14337; found: 236.14317.

elemental analysis (%) for $C_{17}H_{17}N$ calcd: C 86.77, H 7.28, N 5.95; found: C 85.50, H 7.08, N 6.22.

The overall yield combining all three steps for product **1f** was 63 %.

Synthesis of 1g:

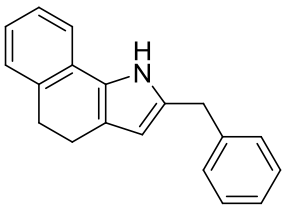

2H-1g: 2-benzyl-4,5-dihydro-1*H*-benzo[*g*]indole

2.0 mL Catalyst **I** (0.02 mmol, 0.01 M in thf), 1,2,3,4-tetrahydronaphthalen-1-ol (2.96 g, 20.0 mmol), 2-amino-3-phenylpropan-1-ol (1.51 g, 10.0 mmol), 10 mL thf, KO^{t}Bu (1.24 g, 11.0 mmol), 22 h at 105 °C. Purification by column chromatography 20:1 → 1:1 pentane : diethyl ether. Yield: 1.85 g = 7.14 mmol = 72 %. M($C_{19}H_{17}N$) = 259.14 gmol^{-1}.

^{1}H NMR (300 MHz, CD_2Cl_2, 298 K): δ = 8.05 (s_br, 1H), 7.40-7.26 (m, 4H), 7.22-7.15 (m, 2H), 7.08-7.02 (m, 2H), 5.92 (s, 1H), 4.02 (s, 2H), 2.94 (t, *J* = 8.1 Hz, 2H), 2.72 (t, *J* = 8.1 Hz, 2H) ppm. ^{13}C NMR (75 MHz, CD_2Cl_2, 298 K): δ = 140.3, 135.0, 132.4, 129.9, 129.1, 128.7, 126.9, 126.9, 125.0, 121.2, 118.3, 107.3, 34.8, 30.5, 22.4 ppm. MS (EI, m/z): 259.1 (M^+).

elemental analysis (%) for $C_{19}H_{17}N$ calcd: C 87.99, H 6.61, N 5.40; found: C 87.57, H 6.75, N 5.36.

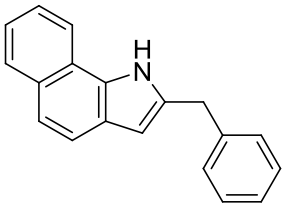

1g: 2-benzyl-1*H*-benzo[*g*]indole

Yield: quantitative as colorless solid. M($C_{19}H_{15}N$) = 257.33 gmol^{-1}.

^{1}H NMR (300 MHz, $CDCl_3$, 298 K): δ = 8.70 (s_br, 1H), 7.95-7.91 (m, 2H), 7.68-7.65 (m, 1H), 7.53-7.48 (m, 2H), 7.43-7.26 (m, 5H), 6.49-6.47 (m, 1H), 4.26 (s, 2H) ppm. ^{13}C NMR (75 MHz, $CDCl_3$, 298 K): δ = 139.6, 136.8, 131.0, 130.5, 129.3, 129.3, 129.2, 129.0, 127.2, 125.8, 125.0, 123.9, 121.9, 120.9, 119.8, 103.2, 35.1 ppm. MS (EI, m/z): 257.1 (M^+).

elemental analysis (%) for $C_{19}H_{15}N$ calcd: C 88.68, H 5.88, N 5.44; found: C 88.84, H 6.04, N 5.34.

The overall yield combining all three steps for product **1g** was 79 %.

Synthesis of 1h:

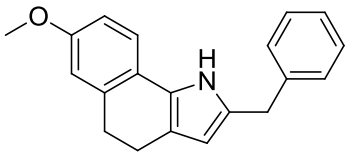

2H-1h: 2-benzyl-7-methoxy-4,5-dihydro-1*H*-benzo[*g*]indole

175 mg Ir@SiCN, 6-methoxy-1,2,3,4-tetrahydronaphthalen-1-ol (4.26 g, 24.0 mmol), 2-amino-3-phenylpropan-1-ol (906 mg, 6.0 mmol), 3 mL diglyme, KO^{t}Bu (1.37 g, 12.0 mmol), 24 h at 135 °C (oil bath temperature). Purification by column chromatography 5:1→2:1 pentane: Et_2O; Yield: 1.053 g = 3.642 mmol = 61 % as colorless solid. M($C_{20}H_{19}NO$) = 289.15 gmol^{-1}.

^{1}H NMR (300 MHz, $CDCl_3$, 298 K): δ = 7.82 (s_br, 1H), 7.37-7.23 (m, 5H), 6.97-6.94 (m, 1H), 6.78-6.77 (m, 1H), 6.70-6.66 (m, 1H), 5.87-5.86 (m, 1H), 4.01 (s, 2H), 3.79 (s, 3H), 2.93-2.87 (m, 2H), 2.72-2.67 (m, 2H) ppm. ^{13}C NMR, 75 MHz, $CDCl_3$, 298 K): δ = 157.0, 139.4, 136.4, 130.6, 128.7, 128.7, 128.6, 127.1, 126.5, 122.8, 118.7, 114.7, 111.1, 106.7, 55.3, 34.4, 30.5, 21.8 ppm. MS (EI, m/z): 289.1 (M^+).

elemental analysis (%) for $C_{20}H_{19}NO$ calcd: C 83.01, H 6.62, N 4.84; found: 82.88, H 6.06, N 4.77.

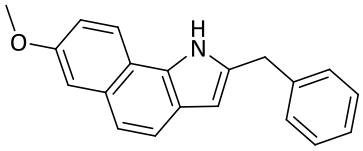

1h: 2-benzyl-7-methoxy-1*H*-benzo[*g*]indole

180 °C reaction temperature. Yield: quantitative as colorless solid. M($C_{20}H_{17}NO$) = 287.36 gmol^{-1}.

^{1}H NMR (300 MHz, $CDCl_3$, 298 K): δ = 8.60 (s_br, 1H), 7.83 (d, *J* = 9 Hz, 1H), 7.61 (d, *J* = 8.7 Hz, 1H), 7.41-7.23 (m, 7H), 7.14 (dd, *J* = 2.7 Hz, *J* = 8.8 Hz, 1H), 8.42-8.41 (m, 1H), 4.21 (s, 2H), 3.91 (s, 3H) ppm. ^{13}C NMR (75 MHz, $CDCl_3$, 298 K): δ = 156.6, 139.8, 136.1, 131.8, 131.5, 129.3, 129.2, 127.1, 123.7, 121.5, 121.4, 120.1, 117.4, 117.0, 108.5, 103.1, 55.8, 35.1 ppm. MS (EI, m/z): 287.0 (M^+).

elemental analysis (%) for $C_{20}H_{17}NO$ calcd: C 83.59, H 5.96, N 4.87; found: C 82.95, H 6.02, N 4.65.

The overall yield combining all three steps for product **1h** was 59 %.

Synthesis of 1i:

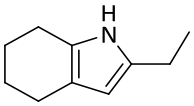

4H-1i: 2-ethyl-4,5,6,7-tetrahydro-1*H*-indole

200 mg Ir@SiCN, cyclohexanol (2529 µL, 24.0 mmol), 2-amino-butan-1-ol (565 µL, 6.0 mmol), 6 mL diglyme, KO^{t}Bu (1.37 g, 12.0 mmol), 24 h at 130 °C (oil bath temperature). Purification by column chromatography 40:1→10:1 pentane: Et_2O; Yield: 0.710 g = 4.76 mmol = 79 % as colorless oil. M($C_{10}H_{15}N$) = 149.23 gmol^{-1}.

^{1}H NMR (300 MHz, CD_2Cl_2, 298 K): δ = 7.45 (s_br, 1H), 5.59 (d, *J* = 2.4 Hz, 1H), 2.56-5.50 (m, 4H), 2.45-2.41 (m, 2H), 1.83-1.68 (m, 4H), 1.20 (t, *J* = 7.5 Hz, 3H) ppm. ^{13}C NMR (75 MHz, CD_2Cl_2, 298 K): δ = 132.7, 125.4, 117.0, 103.9, 24.6, 24.2, 23.5, 23.2, 21.4, 14.5 ppm. MS (EI, m/z): 149.1 (M^+).

elemental analysis (%) for $C_{10}H_{15}N$ calcd: C 80.48, H 10.13, N 9.39; found: C 80.52, H 10.25, N 9.10.

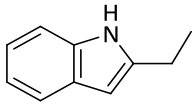

1i: 2-ethyl-1*H*-indole

Yield: quantitative as light brown oil. M($C_{10}H_{11}N$) = 145.20 gmol^{-1}.

^{1}H NMR (300 MHz, CD_2Cl_2, 298 K): δ = 7.93 (s_br, 1H), 7.55-7.52 (m, 1H), 7.31-7.29 (m, 1H), 7.15-7.05 (m, 2H), 6.26 (s, 1H), 2.79 (q, *J* = 7.5 Hz, 2H), 1.36 (t, *J* = 7.5 Hz, 3H) ppm. ^{13}C NMR (75 MHz, CD_2Cl_2, 298 K): δ = 142.2, 136.5, 129.4, 121.3, 120.1, 119.9, 110.8, 98.9, 21.9, 13.6 ppm. MS (EI, m/z): 145.0 (M^+).

elemental analysis (%) for $C_{10}H_{11}N$ calcd: C 82.72, H 7.64, N 9.65; found: C 82.31, H 8.05, N 8.64.

The overall yield combining all three steps for product **1i** was 76 %.

Synthesis of 1j:

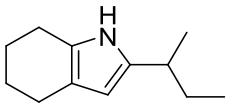

4H-1j: 2-*sec*-butyl-4,5,6,7-tetrahydro-1*H*-indole

2.0 mL Catalyst **I** (0.02 mmol, 0.01 M in thf), cyclohexanol (2109 µL, 20 mmol), 2-amino-3-methylpropan-1-ol (1.17 g, 10 mmol), 10 mL thf, KO^{t}Bu (1.24 g, 11 mmol), 22 h at 105 °C. Purification by column chromatography 40:1 → 10:1 pentane : diethyl ether. Yield: 1.41 g = 7.96 mmol = 80 %. M($C_{12}H_{19}N$) = 177.15 gmol^{-1}.

^{1}H NMR (300 MHz, $CDCl_3$, 298 K): δ = 7.42 (s_br, 1H), 5.68-5.67 (m, 1H), 2.69-2.59 (m, 1H), 2.58-2.54 (m, 2H), 2.52-2.48 (m, 2H), 1.68-1.71 (m, 4H), 1.69-1.60 (m, 1H), 1.59-1.44 (m, 1H), 1.24 (d, *J* = 7.2 Hz, 3H), 0.95 (t, *J* = 7.2 Hz, 2H) ppm. ^{13}C NMR (75 MHz, $CDCl_3$, 298 K): δ = 136.0, 124.9, 116.4, 102.6, 34.2, 30.2, 23.8, 23.5, 22.9, 22.7, 19.9, 12.0 ppm. MS (EI, m/z): 177.2 (M^+).

elemental analysis (%) for $C_{12}H_{19}N$ calcd: C 81.30, H 10.80, N 7.90; found: C 81.03, H 10.95, N 7.69.

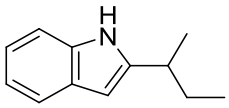

1j: 2-*sec*-butyl-1*H*-indole

Yield: 95 % as brown oil. M($C_{12}H_{15}N$) = 173.12 gmol^{-1}.

^{1}H NMR (300 MHz, $CDCl_3$, 298 K): δ = 7.86 (s_br, 1H), 7.58 (d, *J* = 7.5 Hz, 1H), 7.36 (d, *J* = 7.5 Hz, 1H), 7.18-7.09 (m, 2H), 6.29-6.28 (m, 1H), 2.91-2.79 (m, 1H), 1.81-1.63 (m, 2H), 1.37 (d, *J* = 6.9 Hz, 3H), 0.96 (t, *J* = 7.2 Hz, 3H) ppm. ^{13}C NMR (75 MHz, $CDCl_3$, 298 K): δ = 144.7, 135.6, 128.6, 120.8, 119.8, 119.5, 110.3, 98.2, 34.8, 29.9, 20.0, 11.8 ppm. MS (EI, m/z): 173.2 (M^+).

elemental analysis (%) for $C_{12}H_{15}N$ calcd: C 83.19, H 8.73, N 8.08; found: C 82.71, H 8.98, N 7.77.

The overall yield combining all three steps for product **1j** was 70 %.

Synthesis of 1k:

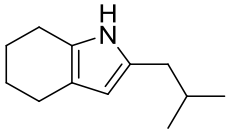

4H-1k: 2-isobutyl-4,5,6,7-tetrahydro-1*H*-indole

2.0 mL Catalyst **I** (0.02 mmol, 0.01 M in thf), cyclohexanol (2109 µL, 20 mmol), 2-amino-4-methylpentan-1-ol (1332 µL, 10 mmol), 10 mL thf, KO^{t}Bu (1.24 g, 11 mmol), 22 h at 105 °C. Purification by column chromatography 60:1 → 10:1 pentane : diethyl ether. Yield: 1.37 g = 7.73 mmol = 77 %. M($C_{12}H_{19}N$) = 177.15 gmol^{-1}.

^{1}H NMR (300 MHz, $CDCl_3$, 298 K): δ = 7.41 (s_br, 1H), 5.70-5.69 (m, 1H), 2.60-2.51 (m, 4H), 2.44 (d, *J* = 6.9 Hz, 2H), 1.90-1.74 (m, 5H), 0.99 (d, *J* = 6.3 Hz, 6H) ppm. ^{13}C NMR (75 MHz, $CDCl_3$, 298 K): δ = 129.8, 125.0, 116.6, 105.0, 37.4, 29.2, 23.8, 23.5, 22.9, 22.7, 22.6 ppm. MS (EI, m/z): 177.2 (M^+).

elemental analysis (%) for $C_{12}H_{19}N$ calcd: C 81.30, H 10.80, N 7.90; found: C 81.21, H 10.79, N 7.99.

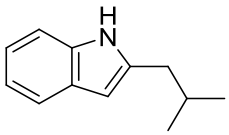

1k: 2-isobutyl-1*H*-indole

Yield: 90 % by additional purification by column chromatography (pentane : diethyl ether = 10 : 1) as orange oil. M($C_{12}H_{15}N$) = 173.12 gmol^{-1}.

^{1}H NMR (300 MHz, $CDCl_3$, 298 K): δ = 7.77 (s_br, 1H), 7.62-7.60 (m, 1H), 7.33-7.31 (m, 1H), 7.21-7.12 (m, 2H), 6.30-6.29 (m, 1H), 2.64 (d, *J* = 7.2 Hz, 2H), 2.02 (h, *J* = 6.9 Hz, 1H), 1.04 (d, *J* = 6.9 Hz, 6H) ppm. ^{13}C NMR (75 MHz, $CDCl_3$, 298 K): δ = 138.9, 135.7, 128.8, 120.8, 119.7, 119.5, 110.3, 100.4, 37.7, 28.9, 22.5 ppm. MS (EI, m/z): 173.1 (M^+).

elemental analysis (%) for $C_{12}H_{15}N$ calcd: C 83.19, H 8.73, N 8.08; found: C 82.80, H: 8.94, N: 7.79.

The overall yield combining all three steps for product **1k** was 60 %.

Synthesis of 1l:

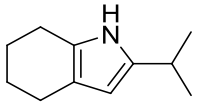

4H-1l: 2-isopropyl-4,5,6,7-tetrahydro-1*H*-indole

2.0 mL Catalyst **I** (0.02 mmol, 0.01 M in thf), cyclohexanol (2109 µL, 20 mmol), 2-amino-3-methylbutan-1-ol (1.03 g, 10 mmol), 10 mL thf, KO^{t}Bu (1.24 g, 11 mmol), 22 h at 105 °C. Purification by column chromatography 50:1 → 10:1 pentane : diethyl ether. Yield: 0.883 g = 5.41 mmol = 54 %. M($C_{11}H_{17}N$) = 163.14 gmol^{-1}.

^{1}H NMR (300 MHz, $CDCl_3$, 298 K): δ = 7.58 (s_br, 1H), 5.84-5.83 (m, 1H), 3.02 (h, *J* = 6.6 Hz, 1H), 2.72-2.63 (m, 4H), 1.97-1.90 (m, 4H), 1.40 (d, *J* = 6.6 Hz, 1H) ppm. ^{13}C NMR (75 MHz, $CDCl_3$, 298 K): δ = 137.0, 125.0, 116.3, 101.9, 27.0, 23.8, 23.4, 22.8, 22.7, 22.6 ppm. MS (EI, m/z): 163.2 (M^+).

elemental analysis (%) for $C_{11}H_{17}N$ calcd: C 80.93, H 10.50, N 8.58; found: C 80.77, H 10.55, N 8.29.

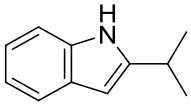

1l: 2-isopropyl-1*H*-indole

Yield: 96 % as brown oil. M($C_{11}H_{13}N$) = 159.10 gmol^{-1}.

^{1}H NMR (300 MHz, $CDCl_3$, 298 K): δ = 7.89 (s_br, 1H), 7.59 (d, *J* = 7.5 Hz, 1H), 7.32 (d, *J* = 7.5 Hz, 1H), 7.19-7.09 (m, 2H), 6.29 (s, 1H), 3.08 (h, *J* = 6.9 Hz, 1H), 1.39 (d, *J* = 6.9 Hz, 6 H) ppm. ^{13}C NMR (75 MHz, $CDCl_3$, 298 K): δ = 145.9, 135.7, 128.6, 121.0, 119.9, 119.5, 110.3, 97.3, 27.6, 22.4 ppm. MS (EI, m/z): 159.1 (M^+).

elemental analysis (%) for $C_{11}H_{13}N$ calcd: C 82.97, H 8.23, N 8.80; found: C 82.67, H 8.26, N 8.53.

The overall yield combining all three steps for product **1l** was 48 %.

Synthesis of 1m:

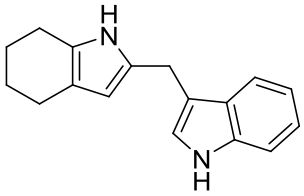

4H-1m: 3-((4,5,6,7-tetrahydro-1*H*-indol-2-yl)methyl)-1*H*-indole

158 mg Ir@SiCN, cyclohexanol (1995 µL, 18.92 mmol), 2-amino-3-(1*H*-indol-3-yl)propan-1-ol (900 mg, 4.73 mmol), 3 mL diglyme, KO^{t}Bu (1.08 g, 9.49 mmol), 24 h at 135 °C (oil bath temperature). Purification by column chromatography 5:1→1:1 pentane: Et_2O; Yield: 0.573 g = 2.29 mmol = 49 % as light red solid. M($C_{17}H_{18}N_2$) = 250.15 gmol^{-1}.

^{1}H NMR (300 MHz, $CDCl_3$, 298 K): δ = 7.85 (s_br, 1H), 7.69 (d, *J* = 7.5 Hz, 1H), 7.41 (s_br, 1H), 7.39 (d, *J* = 7.5 Hz, 1H), 7.33-7.28 (m, 1H), 7.24-7.19 (m, 1H), 7.00-6.99 (m, 1H), 5.91-5.90 (m, 1H), 4.15 (s, 2H), 2.62-2.59 (m, 2H), 2.54-2.50 (m, 2H), 1.91-1.79 (m, 4H) ppm. ^{13}C NMR (75 MHz, $CDCl_3$, 298 K): δ = 136.2, 129.1, 127.4, 125.4, 122.4, 122.0, 119.4, 118.9, 116.7, 113.8, 111.1, 104.5, 23.8, 23.7, 23.4, 22.9, 22.6 ppm. MS (EI, m/z): 250.2 (M^+).

HRMS (ESI): calcd. for $C_{17}H_{19}N_2$ $[M+H]^+$: 251.15427; found: 251.15428.

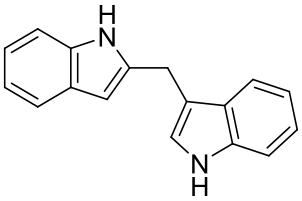

1m: 3-((1H-indol-2-yl)methyl)-1H-indole

Yield: 90 % as red solid by recrystallization from diethyl ether. M($C_{17}H_{14}N_2$) = 246.12 gmol^{-1}.

^{1}H NMR (300 MHz, $CDCl_3$, 298 K): δ = 7.90 (s_br, 1H), 7.82 (s_br, 1H), 7.62-7.56 (m, 2H), 7.39-7.36 (m, 1H), 7.28-7.23 (m, 1H), 7.23-7.13 (m, 4H), 6.98 (s, 1H), 6.44 (s, 1H), 4.29 (s, 2H) ppm. ^{13}C NMR (75 MHz, $CDCl_3$, 298 K): δ = 138.3, 136.4, 135.9, 128.8, 127.2, 122.6, 122.3, 120.9, 119.8, 119.7, 119.5, 119.0, 112.7, 111.2, 110.5, 100.0, 24.4 ppm. MS (EI, m/z): 246.1 (M^+).

HRMS (ESI): calcd. for $C_{17}H_{15}N_2$ $[M+H]^+$: 247.11905; found: 247.12253.

The overall yield combining all three steps for product **1m** was 43 %.

Synthesis of 1n:

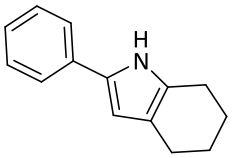

4H-1n: 2-phenyl-4,5,6,7-tetrahydro-1*H*-indole

2.0 mL Catalyst **I** (0.02 mmol, 0.01 M in thf), 1-phenyl-1-ethanol (1826 µL, 15.22 mmol), 2-aminocyclohexanol (875 mg, 7.61 mmol), 10 mL thf, KO^{t}Bu (943 mg, 8.40 mmol), 22 h at 105 °C. Purification by column chromatography 40:1 → 5:1 → 1:1 pentane : diethyl ether. Yield: 1.14 g = 5.78 mmol = 76 % as light colorless/light pink solid. M($C_{14}H_{15}N$) = 197.28 gmol^{-1}.

^{1}H NMR (300 MHz, $CDCl_3$, 298 K): δ = 7.93 (s_br, 1H), 7.44-7.41 (m, 2H), 7.36-7.31 (m, 2H), 7.18-7.13 (m, 1H), 6.29-6.28 (m, 1H), 2.67-2.63 (m, 2H), 2.58-2.54 (m, 2H), 1.91-1.75 (m, 4H) ppm. ^{13}C NMR (75 MHz, $CDCl_3$, 298 K): δ = 133.2, 130.2, 128.7, 128.5, 125.5, 123.3, 118.9, 105.2, 23.8, 23.4, 23.0, 22.9 ppm. MS (EI, m/z): 197.0 (M^+).

elemental analysis (%) for $C_{14}H_{15}N$ calcd: C 85.24, H 7.66, N 7.10; found: C 84.96, H 7.55, N 6.51.

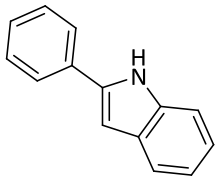

1n: 2-phenyl-1*H*-indole

Yield: quantitative as colorless solid. M($C_{14}H_{11}N$) = 193.24 gmol^{-1}.

^{1}H NMR (300 MHz, $CDCl_3$, 298 K): δ = 8.33 (s_br, 1H), 7.69-7.63 (m, 3H), 7.48-7.40 (m, 3H), 7.36-7.31 (m, 1H), 7.23-7.11 (m, 2H), 6.84-6.82 (m, 1H) ppm. ^{13}C NMR (75 MHz, $CDCl_3$, 298 K): δ = 137.8, 136.8, 132.3, 129.2, 129.0, 127.7, 125.1, 122.3, 120.6, 120.2, 110.9, 99.9 ppm. MS (EI, m/z): 193.0 (M^+).

elemental analysis (%) for $C_{14}H_{11}N$ calcd: C 87.01, H 5.74, N 7.25; found: C 86.90, H 5.88, N 6.88.

The overall yield combining all three steps for product **1n** was 73 %.

Synthesis of 1o:

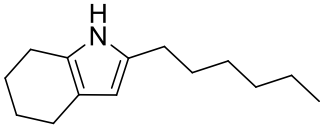

4H-1o: 2-hexyl-4,5,6,7-tetrahydro-1*H*-indole

2.0 mL Catalyst **I** (0.02 mmol, 0.01 M in thf), 2-octanol (2418 µL, 15.22 mmol), 2-aminocyclohexanol (875 mg, 7.61 mmol), 10 mL thf, KO^{t}Bu (0.94 g, 8.37 mmol), 22 h at 105 °C. Purification by column chromatography 80:1 → 20:1 pentane : diethyl ether. Yield: 1.19 g = 5.80 mmol = 76 %. M($C_{14}H_{23}N$) = 205.18 gmol^{-1}.

^{1}H NMR (300 MHz, $CDCl_3$, 298 K): δ = 7.41 (s_br, 1H), 5.68-5.67 (m, 1H), 2.58-2.48 (m, 6H), 1.84-1.72 (m, 4H), 1.67-1.57 (m, 2H), 1.44-1.31 (m, 6H), 0.92 (t, *J* = 6 Hz, 3H) ppm. ^{13}C NMR (75 MHz, $CDCl_3$, 298 K): δ = 131.1, 125.1, 116.7, 103.9, 31.7, 29.8, 29.2, 27.9, 23.9, 23.5, 22.9, 22.7, 22.6, 14.1 ppm. MS (EI, m/z): 205.2 (M^+).

elemental analysis (%) for $C_{14}H_{23}N$ calcd: C 81.89, H 11.29, N 6.82; found: C 81.15, H 11.06, N 6.65.

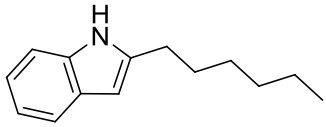

1o: 2-hexyl-1*H*-indole

Yield: 99 % as brown oil. M($C_{14}H_{19}N$) = 201.15 gmol^{-1}.

^{1}H NMR (300 MHz, $CDCl_3$, 298 K): δ = 7.84 (s_br, 1H), 7.56-7.53 (m, 1H), 7.31-7.26 (m, 1H), 7.15-7.05 (m, 2H), 6.25 (s, 1H), 2.76 (t, *J* = 7.5 Hz, 2H), 1.80-1.68 (m, 2H), 1.46-1.28 (m, 6H), 0.91 (t, *J* = 6.9 Hz, 3H) ppm. ^{13}C NMR (75 MHz, $CDCl_3$, 298 K): δ = 140.0, 135.7, 128.8, 120.8, 119.6, 119.4, 110.3, 99.2, 31.6, 29.1, 29.0, 28.1, 22.6, 14.1 ppm. MS (EI, m/z): 201.2 (M^+).

elemental analysis (%) for $C_{14}H_{19}N$ calcd: C 83.53, H 9.51, N 6.96; found: C 83.45, H 9.29, N 6.92.

The overall yield combining all three steps for product **1o** was 73 %.

Synthesis of 1p:

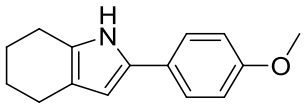

4H-1p: 2-(4-methoxyphenyl)-4,5,6,7-tetrahydro-1*H*-indole

2.0 mL Catalyst **I** (0.02 mmol, 0.01 M in thf), 1-(4-methoxyphenyl)ethanol (2148 µL, 15.22 mmol), 2-aminocyclohexanol (875 mg, 7.61 mmol), 10 mL thf, KO^{t}Bu (943 mg, 8.40 mmol), 22 h at 105 °C. Purification by crystallization from diethyl ether. Yield: 1.27 g = 5.60 mmol = 74 % as light yellow solid. M($C_{15}H_{17}NO$) = 227.30 gmol^{-1}.

^{1}H NMR (300 MHz, $CDCl_3$, 298 K): δ = 7.89 (s_br, 1H), 7.36 (d, *J* = 8.7 Hz, 2H), 6.90 (d, *J* = 8.7 Hz, 2H), 6.19-6.18 (m, 1H), 3.83 (s, 3H), 2.66-2.62 (m, 2H), 2.58-2.54 (m, 2H), 1.91-1.76 (m, 4H) ppm. ^{13}C NMR (75 MHz, $CDCl_3$, 298 K): δ = 157.8, 130.3, 127.7, 126.4, 124.8, 118.6, 114.2, 104.0, 55.2, 23.8, 23.4, 22.9, 22.8 ppm. MS (EI, m/z): 227.2 (M^+).

elemental analysis (%) for $C_{15}H_{17}NO$ calcd: C 79.26, H 7.54, N 6.16; found: C 78.62, H 7.30, N 5.97.

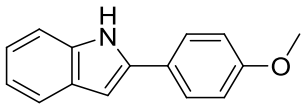

1p: 2-(4-methoxyphenyl)-1*H*-indole

Yield: 97 % as colorless solid by recrystallization from diethyl ether. M($C_{15}H_{13}NO$) = 223.27 $gmol^{-1}$.

^{1}H NMR (300 MHz, THF-d_8, 298 K): δ = 10.39 (s_br, 1H), 7.68 (d, *J* = 8.4 Hz, 2H), 7.47-7.45 (m, 1H), 7.30-7.28 (m, 1H), 7.03-6.91 (m, 2H), 6.96 (d, *J* = 8.4 Hz, 2H), 6.66-6.65 (m, 1H), 3.80 (s, 3H) ppm. ^{13}C NMR (75 MHz, THF-d_8, 298 K): δ = 160.5, 139.3, 138.6, 130.8, 127.3, 126.9, 122.0, 120.8, 120.2, 115.2, 111.6, 98.8, 55.7 ppm. MS (EI, m/z): 223.1 (M^+).

elemental analysis (%) for $C_{15}H_{13}NO$ calcd: C 80.69, H 5.87, N 6.27; found: C 80.28, H 5.69, N 6.19.

The overall yield combining all three steps for product **1p** was 70 %.

Synthesis of 1q:

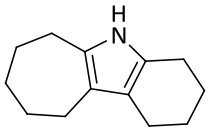

4H-1q: 1,2,3,4,5,6,7,8,9,10-decahydrocyclohepta[*b*]indole

2.0 mL Catalyst **I** (0.02 mmol, 0.01 M in thf), cycloheptanol (1834 µL, 15.22 mmol), 2-aminocyclohexanol (875 mg, 7.61 mmol), 10 mL thf, KO^{t}Bu (943 mg, 8.40 mmol), 22 h at 105 °C. Purification by column chromatography 40:1 → 10:1 pentane : diethyl ether. Yield: 1.38 g = 7.29 mmol = 96 % as light yellow oil. M($C_{13}H_{19}N$) = 189.30 $gmol^{-1}$.

^{1}H NMR (300 MHz, $CDCl_3$, 298 K): δ = 7.23 (s_br, 1H), 2.67-2.64 (m, 2H), 2.56-2.40 (m, 6H), 1.82-1.71 (m, 10H) ppm. ^{13}C NMR (75 MHz, $CDCl_3$, 298 K): δ = 128.2, 122.9, 118.9, 116.7, 31.9, 29.2, 29.1, 28.0, 25.3, 23.6, 23.3, 22.5, 21.3 ppm. MS (EI, m/z): 189.2 (M^+).

elemental analysis (%) for $C_{13}H_{19}N$ calcd: C 82.48, H 10.12, N 7.40; found: C 82.17, H 9.91, N 6.97.

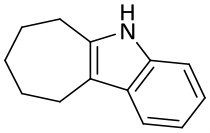

1q: 5,6,7,8,9,10-hexahydrocyclohepta[*b*]indole

Yield: quantitative as colorless solid. M($C_{13}H_{15}N$) = 185.26 gmol^{-1}.

^{1}H NMR (300 MHz, $CDCl_3$, 298 K): δ = 7.67 (s_br, 1H), 7.52-7.47 (m, 1H), 7.30-7.24 (m, 1H), 7.14-7.06 (m, 2H), 2.86-2.83 (m, 4H), 1.96-1.89 (m, 2H), 1.81-1.76 (m, 4H) ppm. ^{13}C NMR (75 MHz, $CDCl_3$, 298 K): δ = 137.4, 134.2, 129.2, 120.6, 119.0, 117.6, 113.7, 110.1, 31.8, 29.6, 28.7, 27.5, 24.6 ppm. MS (EI, m/z): 185.2 (M^+).

elemental analysis (%) for $C_{13}H_{15}N$ calcd: C 84.28, H 8.16, N 7.56; found: C 84.09, H 8.10, N 7.34.

The overall yield combining all three steps for product **1q** was 93 %.

Synthesis of 1r:

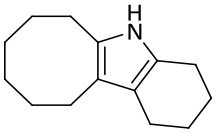

4H-1r: 2,3,4,5,6,7,8,9,10,11-decahydro-1*H*-cycloocta[*b*]indole

2.0 mL Catalyst **I** (0.02 mmol, 0.01 M in thf), cyclooctanol (2004 µL, 15.22 mmol), 2-aminocyclohexanol (875 mg, 7.61 mmol), 10 mL thf, KO^{t}Bu (943 mg, 8.40 mmol), 22 h at 105 °C. Purification by column chromatography 80:1 → 20:1 pentane : diethyl ether. Yield: 1.38 g = 6.79 mmol = 95 % as light yellow oil. M($C_{14}H_{21}N$) = 203.17 gmol^{-1}.

^{1}H NMR (300 MHz, $CDCl_3$, 298 K): δ = 7.20 (s_br, 1H), 2.28-2.62 (m, 2H), 2.55-2.48 (m, 4H), 2.40-2.37 (m, 2H), 1.83-1.72 (m, 4H), 1.64-1.56 (m, 4H), 1.54-1.42 (m, 4H) ppm. ^{13}C NMR (75 MHz, $CDCl_3$, 298 K): δ = 126.2, 123.5, 116.6, 116.2, 29.6, 29.3, 25.9, 25.8, 25.7, 23.7, 23.5, 22.7, 22.5, 21.2 ppm. MS (EI, m/z): 203.0 (M^+).

elemental analysis (%) for $C_{14}H_{21}N$ calcd: C 82.70, H 10.41, N 6.89; found: C 82.56, H 10.42, N 6.75.

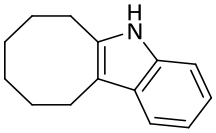

1r: 6,7,8,9,10,11-hexahydro-5*H*-cycloocta[*b*]indole

Yield: 97 % as colorless solid. M($C_{14}H_{17}N$) = 199.29 $gmol^{-1}$.

^{1}H NMR (300 MHz, $CDCl_3$, 298 K): δ = 7.70 (s_br, 1H), 7.51-7.47 (m, 1H), 7.30-7.27 (m, 1H), 7.13-7.05 (m, 2H), 2.89-2.83 (m, 4H), 1.81-1.70 (m, 4H), 1.52-1.39 (m, 4H) ppm. ^{13}C NMR (75 MHz, $CDCl_3$, 298 K): δ = 135.6, 135.0, 128.6, 120.6, 118.9, 117.6, 111.7, 110.2, 29.6, 29.5, 26.0, 25.9, 22.1, 22.1 ppm. MS (EI, m/z): 199.2 (M^+).

elemental analysis (%) for $C_{14}H_{17}N$ calcd: C 84.37, H 8.60, N 7.03; found: C 83.64, H 8.54, N 6.80.

The overall yield combining all three steps for product **1r** was 89 %.

Synthesis of 1s:

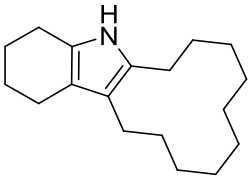

4H-1s: 2,3,4,5,6,7,8,9,10,11,12,13,14,15-tetradecahydro-1*H*-cyclododeca[*b*]indole

2.0 mL Catalyst **I** (0.02 mmol, 0.01 M in thf), cyclododecanol (3.69 g, 20 mmol), 2-amino-3-phenylpropan-1-ol (1.51 g, 10 mmol), 10 mL thf, KO^{t}Bu (1.24 g, 11 mmol), 22 h at 105 °C. Purification by column chromatography 50:1 → 10:1 pentane : diethyl ether. Yield: 1.385 g = 5.34 mmol = 53 %. M($C_{18}H_{29}N$) = 259.23 (M^+).

150 mg Ir@SiCN, cyclododecanol (4.42 g, 24.0 mmol), 2-amino-3-phenylpropan-1-ol (906 mg, 6.0 mmol), 3 mL diglyme, KO^{t}Bu (1.37 g, 12.0 mmol), 24 h at 135 °C (oil bath temperature). GC-Yield: 44 %.

^{1}H NMR (300 MHz, $CDCl_3$, 298 K): δ = 7.26 (s_br, 1H), 2.57-2.36 (m, 8H), 1.88-1.71 (m, 4H), 1.67-1.56 (m, 4H), 1.52-1.44 (m, 4H), 1.37-1.25 (m, 8H) ppm. ^{13}C NMR (75 MHz, $CDCl_3$, 298 K): δ = 126.8, 124.9, 117.5, 116.1, 28.3, 28.1, 25.0, 24.8, 24.8, 24.2, 23.8, 23.4, 22.7, 22.5, 22.2, 22.1, 21.9, 21.2 ppm. MS (EI, m/z): 259.2 (M^+).

HRMS (ESI): calcd. for $C_{18}H_{30}N$ $[M+H]^+$: 260.23727; found: 260.23728.

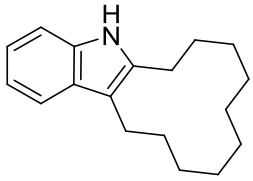

1s: 6,7,8,9,10,11,12,13,14,15-decahydro-5*H*-cyclododeca[*b*]indole

Yield: quantitative as colorless solid. M($C_{18}H_{25}N$) = 255.20 $gmol^{-1}$.

^{1}H NMR (300 MHz, $CDCl_3$, 298 K): δ = 7.68 (s_br, 1H), 7.60 (d, *J* = 7.2 Hz, 1H), 7.29 (d, *J* = 7.2 Hz, 1H), 7.19-7.09 (m, 2H), 2.82-2.75 (m, 4H), 1.91-1.75 (m, 4H), 1.52-1.50 (m, 4H), 1.39-1.26 (m, 8H) ppm. ^{13}C NMR (75 MHz, $CDCl_3$, 298 K): δ = 135.7, 128.6, 120.9, 118.8, 112.2, 110.1, 27.7, 27.4, 24.8, 24.8, 24.7, 24.0, 22.6, 22.5, 22.1, 21.2 ppm. MS (EI, m/z): 255.1 (M^+).

HRMS (ESI): calcd. for $C_{18}H_{26}N$ $[M+H]^+$: 256.20597; found: 256.20598.

The overall yield combining all three steps for product **1s** was 50 %.

Synthesis of Carbazoles

ADC Coupling:

All carbazoles were prepared by modification of a literature method using the homogeneous iridium PN_5P-Ir-Pincer catalyst **I** (**Fig. S10**)[41].

Typical Procedure:

In a glove box 2.0 mL catalyst **I** (0.02 mmol, 0.01 M in thf), cyclohexanol (15.22 mmol), 1,2-amino alcohol (7.61 mmol), 10 mL thf and KO^{t}Bu (8.37 mmol) were given in a pressure tube and sealed with a semi-permeable membrane. The tube was heated at 105 °C (oil bath temperature) for 22 h. After cooling to RT 3 mL water and dodecane as internal standard were added. The product was extracted with diethyl ether (2x) and purified by column chromatography or crystallization.

Acceptorless Dehydrogenation:

Typical Procedure:

In a 10 mL Schlenk tube 50 mg (0.18 mol% active metal) Pd@SiCN, 1.0 mmol substrate and 0.75 mL diglyme were evacuated and flushed with argon for three times. A slight argon flow of 4-6 mL/min was adjusted and the mixture was stirred for 20 h at 190 °C (oil bath temperature). After cooling to RT the catalyst was separated by centrifugation and washed with acetone two times. The organic phases were combined and the solvent was removed under reduced pressure at 60 °C giving the pure product. If required, further purification was achieved by either column chromatography or crystallization.

Synthesis of 2a:

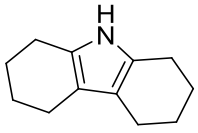

8H-2a: 2,3,4,5,6,7,8,9-octahydro-1*H*-carbazole

2.0 mL Catalyst **I** (0.02 mmol, 0.01 M in thf), cyclohexanol (1556 µL, 15.22 mmol), 2-aminocyclohexanol (875 mg, 7.61 mmol), 10 mL thf, KO^{t}Bu (943 mg, 8.40 mmol), 22 h at

105 °C. Purification by column chromatography 30:1 pentane : diethyl ether. Yield: 1.13 g = 6.42 mmol = 85 %. M($C_{12}H_{17}N$) = 175.27 gmol^{-1}.

^{1}H NMR (300 MHz, $CDCl_3$, 298 K): δ = 7.28 (s_br, 1H), 2.57-2.53 (m, 4H), 2.42-2.38 (m, 4H), 1.86-1.71 (m, 8H) ppm. ^{13}C NMR (75 MHz, $CDCl_3$, 298 K): δ = 124.9, 115.1, 23.7, 23.5, 22.8, 21.1 ppm. MS (EI, m/z): 174.9 (M^+).

elemental analysis (%) for $C_{12}H_{17}N$ calcd: C 82.23, H 9.78, N 7.99; found: C 82.08, H 9.71, N 7.09.

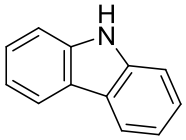

2a: 9*H*-carbazole

Yield: quantitative as light brown solid. M($C_{12}H_9N$) = 167.21 gmol^{-1}.

^{1}H NMR (300 MHz, $CDCl_3$, 298 K): δ = 8.13-8.10 (m, 2H), 8.10 (s_br, 1H), 7.46-7.44 (m, 4H), 7.31-7.24 (m, 2H) ppm. ^{13}C NMR (75 MHz, $CDCl_3$, 298 K): δ = 139.4, 125.8, 123.3, 120.3, 119.4, 110.5 ppm. MS (EI, m/z): 166.7 (M^+).

elemental analysis (%) for $C_{12}H_9N$ calcd: C 86.20, H 5.43, N 8.38; found: C 86.33, H 5.49, N 8.07.

The overall yield combining all three steps for product **2a** was 81 %.

Synthesis of 2b:

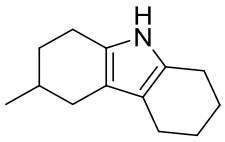

8H-2b: 3-methyl-2,3,4,5,6,7,8,9-octahydro-1*H*-carbazole

2.0 mL Catalyst **I** (0.02 mmol, 0.01 M in thf), 4-methylcyclohexanol (1.74 g, 15.22 mmol), 2-aminocyclohexanol (875 mg, 7.61 mmol), 10 mL thf, KO^{t}Bu (943 mg, 8.40 mmol), 22 h at 105 °C. Purification by column chromatography 30:1 → 10 : 1 pentane : diethyl ether. Yield: 1.039 g = 5.49 mmol = 72 % as light yellow solid. M($C_{13}H_{19}N$) = 189.15 gmol^{-1}.

^{1}H NMR (300 MHz, $CDCl_3$, 298 K): δ = 7.28 (s_br, 1H), 2.63-2.53 (m, 5H), 2.43-2.38 (m, 2H), 2.05-1.96 (m, 1H), 1.89-1.72 (m, 6H), 1.56-1.40 (m, 1H), 1.08 (d, *J* = 6.6 Hz, 3H) ppm. ^{13}C NMR (75 MHz, $CDCl_3$, 298 K): δ = 125.2, 124.7, 115.2, 115.0, 31.9, 30.0, 29.8, 23.6, 23.5, 22.8, 22.6, 22.0, 21.1 ppm. MS (EI, m/z): 189.2 (M^+).

elemental analysis (%) for $C_{13}H_{19}N$ calcd: C 82.48, H 10.12, N 7.40; found: C 81.02, H 9.48, N 6.95.

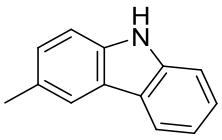

2b: 3-methyl-9*H*-carbazole

Yield: 97 % as colorless light brown solid. M($C_{13}H_{11}N$) = 181.09 gmol^{-1}.

^{1}H NMR (300 MHz, $CDCl_3$, 298 K): δ = 8.05 (d, *J* = 7.8 Hz, 1H), 7.93 (s_br, 1H), 7.88 (s, 1H), 7.41-7.40 (m, 2H), 7.32 (d, *J* = 8.4 Hz, 1H), 7.26-7.18 (m, 2H), 2.54 (s, 3H) ppm. ^{13}C NMR (75 MHz, $CDCl_3$, 298 K): δ = 141.6, 139.6, 128.3, 127.5, 126.0, 124.4, 124.1, 120.7, 120.7, 119.2, 111.4, 111.2, 21.7 ppm. MS (EI, m/z): 181.1 (M^+).

elemental analysis (%) for $C_{13}H_{11}N$ calcd: C 86.15, H 6.12, N 7.73; found: C 85.28, H 5.83, N 7.63.

The overall yield combining all three steps for product **2b** was 70 %.

Synthesis of 2c:

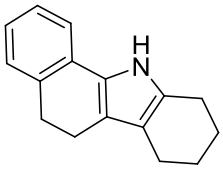

6H-2c: 6,7,8,9,10,11-hexahydro-5*H*-benzo[*a*]carbazole

2.0 mL Catalyst **I** (0.02 mmol, 0.01 M in thf), 1,2,3,4-tetrahydronaphthalen-1-ol (2.23 g, 15.22 mmol), 2-aminocyclohexanol (875 mg, 7.61 mmol), 10 mL thf, KO^{t}Bu (943 mg, 8.40 mmol), 22 h at 105 °C. Purification by column chromatography 30:1 pentane : diethyl ether. Yield: 0.973 g = 4.36 mmol = 57 % as colorless solid. M($C_{16}H_{17}N$) = 223.14 gmol^{-1}.

^{1}H NMR (300 MHz, $CDCl_3$, 298 K): δ = 7.85 (s_br, 1H), 7.20-7.14 (m, 2H), 7.10-7.07 (m, 1H), 7.04-6.99 (m, 1H), 2.94 (t, *J* = 7.5 Hz, 2H), 2.68-2.62 (m, 4H), 2.49 (t, *J* = 7.5 Hz, 2H),

1.92-1.77 (m, 4H) ppm. ^{13}C NMR (75 MHz, $CDCl_3$, 298 K): δ = 134.4, 129.6, 128.2, 128.1, 126.3, 125.8, 124.2, 118.6, 117.6, 116.1, 29.9, 23.5, 23.4, 23.0, 21.2, 20.0 ppm. MS (EI, m/z): 223.2 (M^+).

elemental analysis (%) for $C_{16}H_{17}N$ calcd: C 86.05, H 7.67, N 6.27; found: C 85.55, H 7.62, N 5.95.

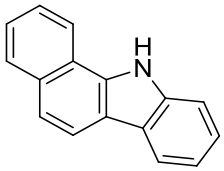

2c: 11*H*-benzo[*a*]carbazole

Yield: 96 % as light yellow solid. M($C_{16}H_{11}N$) = 217.09 gmol^{-1}.

^{1}H NMR (300 MHz, $CDCl_3$, 298 K): δ = 8.75 (s_br, 1H), 8.17-8.09 (m, 3H), 8.03 (d, *J* = 8.7 Hz, 1H), 7.68 (d, *J* = 8.7 Hz, 1H), 7.62-7.53 (m, 3H), 7.48-7.43 (m, 1H), 7.36-7.31 (m, 1H) ppm. ^{13}C NMR (75 MHz, $CDCl_3$, 298 K): δ = 138.4, 134.8, 132.4, 129.0, 125.5, 125.2, 124.8, 124.2, 121.1, 120.4, 120.2, 120.0, 119.9, 119.3, 118.4, 111.0 ppm. MS (EI, m/z): 217.1 (M^+).

elemental analysis (%) for $C_{16}H_{11}N$ calcd: C 88.45, H 5.10, N 6.45; found: C 88.54, H 5.26, N 6.40.

The overall yield combining all three steps for product **2c** was 53 %.

Synthesis of Tetrahydropyridines and Dehydrogenation to Quinolines

ADC Coupling:

The conditions of the tetrahydropyrrole synthesis were adopted. The best catalyst loading was found to be 0.5 mol% active metal. At the beginning, a small temperature screening was performed resulting in 140 °C as the best reaction temperature (**Tab. S4**). All products except **3a** were synthesized using the heterogeneous Ir@SiCN catalyst.

Tab. S4: Temperature screening

T (oil bath) [°C]	Yield [%]
110	32
120	51
130	55
140	85
150	23

Reaction conditions: 150 mg (0.5 mol% active metal) Ir@SiCN, cyclohexanol (1268 µL, 12.0 mmol), 3-amino-3-(3,4-dimethoxyphenyl)propan-1-ol (635 mg, 3.0 mmol), 3 mL diglyme, KO^{t}Bu (673 mg, 6.0 mmol), 24 h. The reaction mixture was cooled to RT and water (3 mL) and dodecane as internal standard were added. The mixture was extracted with diethyl ether and a GC sample was taken.

General Procedure:

In a glove box 150 mg Ir@SiCN (0.5 mol% active metal), cyclohexanol (12.0 mmol), 1,3-aminoalcohol (3.0 mmol), 3 mL diglyme and KO^{t}Bu (673 mg, 6.0 mmol) were added in a pressure tube and the tube was closed by a pressure equalization device. The mixture was stirred at 140 °C (oil bath temperature) for 24 h. After cooling to RT 3 mL water and dodecane as internal standard were added and the product was extracted by diethyl ether (2x). The products were purified either by column chromatography or crystallization.

Acceptorless Dehydrogenation

General Procedure

In a 10 mL Schlenk tube 50 mg (0.18 mol% active metal) Pd@SiCN, 1.0 mmol substrate and 0.75 mL diglyme were evacuated and flushed with argon for three times. A slight argon flow of 4-6 mL/min was adjusted and the mixture was stirred for 18 h at 200 °C (metal bath

temperature). After cooling to RT the catalyst was separated by centrifugation and washed with acetone two times. The organic phases were combined and the solvent was removed under reduced pressure at 60 °C giving the pure product. If required, further purification can be achieved either by column chromatography or crystallization.

Synthesis of 3a:

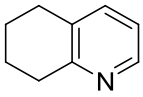

4H-3a: 5,6,7,8-tetrahydroquinoline

Synthesis by a modified procedure according to literature using the homogeneous PN_5P-Ir-Pincer catalyst **II** (**Fig. S11**)[42].

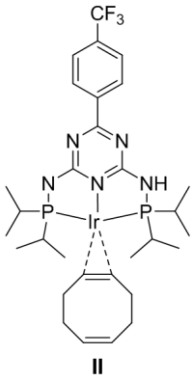

II

Fig. S11: Homogeneous PN_5P-Ir-Pincer catalyst used for the synthesis of 3a.

1.5 mL Catalyst **II** (0.015 mmol, 0.01 M in thf), cyclohexanol (1268 µL, 12 mmol), 3-amino-1-propanol (228 mg, 3 mmol), 10 mL thf, NaO^tBu (317 mg, 3.3 mmol), 22 h at 110 °C. Purification by column chromatography 10:1 pentane : diethyl ether. Yield: 0.271 g = 2.04 mmol = 68 % as light colorless oil. $M(C_9H_{11}N) = 133.09\ gmol^{-1}$.

^1H NMR (300 MHz, $CDCl_3$, 298 K): δ = 8.31-8.29 (m, 1H), 7.31-7.28 (m, 1H), 6.99-6.95 (m, 1H), 2.91-2.86 (m, 2H), 2.74-2.70 (m, 2H), 1.90-1.72 (m, 4H) ppm. ^{13}C NMR (75 MHz, $CDCl_3$, 298 K): δ = 157.2, 146.5, 136.6, 132.1, 120.7, 32.3, 28.6, 22.9, 22.5 ppm. MS (EI, m/z): 133.1 (M^+).

elemental analysis (%) for $C_9H_{11}N$ calcd: C 81.16, H 8.32, N 10.52; found: C 81.57, H 8.64, N 10.85.

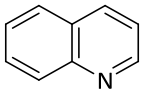

3a: quinoline

Yield: 92 % as yellow brown liquid by column chromatography with pentane : diethyl ether = 10 : 1. M(C_9H_7N) = 129.16 gmol^{-1}.

^{1}H NMR (300 MHz, $CDCl_3$, 298 K): δ = 8.93-8.91 (m, 1H), 8.16-8.10 (m, 2H), 7.83-7.80 (m, 1H), 7.74-7.69 (m, 1H), 7.57-7.57 (m, 1H), 7.41-7.37 (m, 1H) ppm. ^{13}C NMR (75 MHz, $CDCl_3$, 298 K): δ = 150.4, 148.3, 136.0, 129.5, 129.4, 128.2, 127.7, 126.5, 121.0 ppm. MS (EI, m/z): 129.1 (M^+).

elemental analysis (%) for C_9H_7N calcd: C 83.69, H 5.46, N 10.84; found: C 83.10, H 5.48, N 10.83.

The overall yield combining all three steps for product **3a** was 58 %.

Synthesis of 3b:

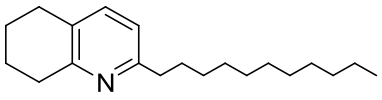

4H-3b: 2-undecyl-5,6,7,8-tetrahydroquinoline

Purification by column chromatography 40:1→5:1 pentane: Et_2O;
Yield: 0.793 g = 0.276 mmol = 84 % as light yellow oil. M($C_{20}H_{33}N$) = 287.26 gmol^{-1}.
^{1}H NMR (300 MHz, $CDCl_3$, 298 K): δ = 7.24 (d, *J* = 7.8 Hz, 1H), 6.87 (d, *J* = 7.8 Hz, 1H), 2.88 (t, *J* = 6.3 Hz, 2H), 2.73-2.67 (m, 4H), 1.92-1.84 (m, 2H), 1.82-1.74 (m, 2H), 1.71-1.61 (m, 2H), 1.37-1.20 (m, 16H), 0.87 (t, *J* = 6.6 Hz, 3H) ppm. ^{13}C NMR (75 MHz, $CDCl_3$, 298 K): δ = 159.4, 156.4, 137.0, 129.0, 119.7, 38.3, 32.6, 31.9, 30.4, 29.6, 29.6, 29.6, 29.5, 29.5, 29.3, 28.4, 23.2, 22.8, 22.7, 14.1 ppm. MS (EI, m/z): 286.3 (M^+).

elemental analysis (%) for $C_{20}H_{33}N$ calcd: C 83.56, H 11.57, N 4.87; found: C: 82.60, H: 11.67, N: 4.13.

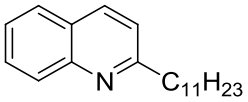

3b: 2-undecylquinoline

Dehydrogenation at 210 °C metal bath temperature for 36 h. Yield: 88 % as brown oil by column chromatography with pentane : Et_2O = 40 : 1. M($C_{20}H_{29}N$) = 283.23 gmol^{-1}.

^{1}H NMR (300 MHz, $CDCl_3$, 298 K): δ = 8.06 (d, *J* = 8.4 Hz, 1H), 8.06-8.04 (m, 1H), 7.79-7.76 (m, 1H), 7.71-7.65 (m, 1H), 7.50-7.45 (m, 1H), 7.30 (d, *J* = 8.4 Hz, 1H), 2.97 (t, *J* = 8.1 Hz, 2H), 1.86-1.76 (m, 2H), 1.36-1.19 (m, 16H), 0.88 (t, *J* = 6.3 Hz, 2H) ppm. ^{13}C NMR (75 MHz, $CDCl_3$, 298 K): δ = 163.1, 147.9, 136.2, 129.3, 128.8, 127.5, 126.7, 125.6, 121.4, 39.4, 31.9, 30.1, 29.7, 29.6, 29.6, 29.5, 29.4, 29.3, 22.7, 14.1 ppm. MS (EI, m/z): 283.2 (M^+).

elemental analysis (%) for $C_{20}H_{29}N$ calcd: C 84.75, H 10.31, N 4.94; found: C 84.25, H 10.20, N 4.44.

The overall yield combining all three steps for product **3b** was 72 %.

Synthesis of 3c:

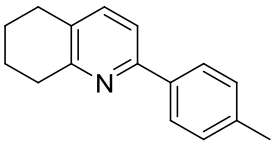

4H-3c: 2-*p*-tolyl-5,6,7,8-tetrahydroquinoline

Purification by column chromatography 30:1→ 5:1 pentane: Et_2O;
Yield: 0.527 g = 2.36 mmol = 79 % as white solid. M($C_{16}H_{17}N$) = 223.24 gmol^{-1}.
^{1}H NMR (300 MHz, $CDCl_3$, 298 K): δ = 7.89 (d, *J* = 8.1 Hz, 2H), 7.41 (dd, *J* = 7.8 Hz, *J* = 9.9 Hz, 2H), 7.27 (d, *J* = 7.8 Hz, 2H), 3.05-3.00 (m, 2H), 2.82-2.78 (m, 2H), 2.42 (s, 3H), 1.99-1.91 (m, 2H), 1.89-1.81 (m, 2H) ppm. ^{13}C NMR (75 MHz, $CDCl_3$, 298 K): δ = 157.0, 154.5, 138.1, 137.2, 137.0, 130.2, 129.2, 126.6, 117.5, 32.8, 28.4, 23.2, 22.8, 21.1 ppm. MS (EI, m/z): 223.2 (M^+).

elemental analysis (%) for $C_{16}H_{17}N$ calcd: C 86.05, H 7.67, N 6.27; found: C 55.99, H 7.94, N 5.97.

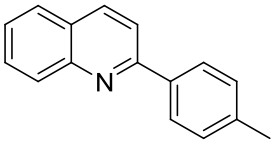

3c: 2-*p*-tolylquinoline

Yield: 94 % as light brown solid by recrystallization from diethyl ether. M($C_{16}H_{13}N$) = 219.28 $gmol^{-1}$.

^{1}H NMR (300 MHz, $CDCl_3$, 298 K): δ = 8.21-8.16 (m, 2H), 8.09 (d, *J* = 8.1 Hz, 2H), 7.88-7.80 (m, 2H), 7.75-7.70 (m, 1H), 7.54-7.49 (m, 1H), 3.34 (d, *J* = 8.4 Hz, 2H), 2.44 (s, 3H) ppm. ^{13}C NMR (75 MHz, $CDCl_3$, 298 K): δ = 157.33, 148.3, 139.4, 136.9, 136.8, 136.7, 136.7, 129.7, 129.6, 127.4, 127.1, 126.1, 118.9, 21.4 ppm. MS (EI, m/z): 219.2 (M^+).

elemental analysis (%) for $C_{16}H_{13}N$ calcd: C 87.64, H 5.98, N 6.39; found: C 87.30, H 6.12, N 6.36.

The overall yield combining all three steps for product **3c** was 72 %.

Synthesis of 3d:

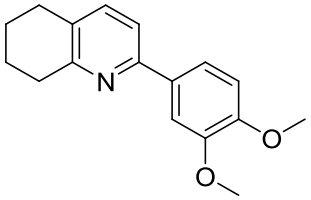

4H-3d: 2-(3,4-dimethoxyphenyl)-5,6,7,8-tetrahydroquinoline

Purification by column chromatography 5:1→1:1 pentane: Et_2O;
Yield: 0.687 g = 2.52 mmol = 85 % as colorless solid. M($C_{17}H_{19}NO_2$) = 269.14 $gmol^{-1}$.
^{1}H NMR (300 MHz, $CDCl_3$, 298 K): δ = 7.59-7.58 (m, 1H), 7.46-7.30 (m, 3H), 6.90-6.87 (m, 1H), 3.95 (s, 3H), 3.87 (s, 3H), 2.98-2.94 (m, 2H), 2.75-2.71 (m, 2H), 1.92-1.72 (m, 4H) ppm. ^{13}C NMR (75 MHz, $CDCl_3$, 298 K): δ = 156.8, 154.0, 149.3, 148.9, 137.1, 132.7, 129.9, 119.0, 117.1, 110.8, 109.7, 55.7, 55.7, 32.6, 28.3, 23.0, 22.6 ppm. MS (EI, m/z): 269.1 (M^+).

elemental analysis (%) for $C_{17}H_{19}NO_2$ calcd: C 75.81, H 7.11, N 5.20; found: C 75.41, H 7.37, N 4.91.

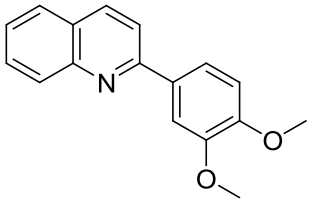

3d: 2-(3,4-dimethoxyphenyl)quinoline

Yield: 93 % as colorless solid by recrystallization from diethyl ether. M($C_{17}H_{15}NO_2$) = 265.11 $gmol^{-1}$.

^{1}H NMR (300 MHz, $CDCl_3$, 298 K): δ = 8.18-8.15 (m, 2H), 7.89-7.78 (m, 3H), 7.74-7.64 (m, 2H), 7.52-7.45 (m, 1H), 7.00-6.97 (m, 2H), 4.05 (s, 3H), 3.95 (s, 3H) ppm. ^{13}C NMR (75 MHz, $CDCl_3$, 298 K): δ = 156.7, 150.3, 149.3, 148.1, 136.6, 132.5, 129.5, 129.4, 127.4, 126.9, 125.9, 120.2, 118.5, 111.0, 110.3, 56.0, 56.0 ppm. MS (EI, m/z): 265.1 (M^+).

elemental analysis (%) for $C_{17}H_{15}NO_2$ calcd: C 76.96, H 5.70, N 5.28; found: C 76.82, H 5.85, N 5.14.

The overall yield combining all three steps for product **3d** was 77 %.

Synthesis of 3e:

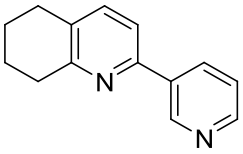

4H-3e: 2-(pyridin-3-yl)-5,6,7,8-tetrahydroquinoline

Purification by column chromatography 1:1 pentane: Et_2O → pure Et_2O;
Yield: 0.417 g = 1.98 mmol = 66 % as yellow oil. M($C_{14}H_{14}N_2$) = 210.27 $gmol^{-1}$.
^{1}H NMR (300 MHz, $CDCl_3$, 298 K): δ = 9.14-9.13 (m, 1H), 8.62-8.59 (m, 1H), 8.30-8.26 (m, 1H), 7.46-7.45 (m, 2H), 7.38-7.34 (m, 1H), 3.02-2.97 (m, 2H), 2.84-2.79 (m, 2H), 1.98-1.81 (m, 4H) ppm. ^{13}C NMR (75 MHz, $CDCl_3$, 298 K): δ = 157.8, 151.8, 149.4, 148.2, 137.6, 135.3, 134.2, 131.7, 123.5, 117.9, 32.8, 28.6, 23.1, 22.7 ppm. MS (EI, m/z): 210.2 (M^+).

elemental analysis (%) for $C_{14}H_{14}N_2$ calcd: C 79.97, H 6.71, N 13.32; found: C 79.06, H 6.79, N 12.44.

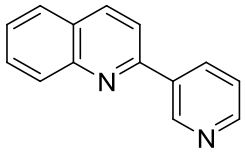

3e: 2-(pyridin-3-yl)quinoline

Yield: 97 % as red-brown oil. M($C_{14}H_{10}N_2$) = 206.24 $gmol^{-1}$.

^{1}H NMR (300 MHz, $CDCl_3$, 298 K): δ = 9.36-9.35 (m, 1H), 8.71-8.69 (m, 1H), 8.53-8.49 (m, 1H), 8.25 (d, *J* = 8.7 Hz, 1H), 8.17 (d, *J* = 8.7 Hz, 1H), 7.89-7.83 (m, 1H), 7.86 (s, 1H), 7.78-7.72 (m, 1H), 7.58-7.53 (m, 1H), 7.47-7.43 (m, 1H) ppm. ^{13}C NMR (75 MHz, $CDCl_3$, 298 K): δ = 154.6, 150.2, 148.8, 148.3, 137.1, 135.1, 134.9, 129.9, 129.7, 127.5, 127.3, 126.7, 123.6, 118.5 ppm. MS (EI, m/z): 206.2 (M^+).

HRMS (ESI): calcd. for $C_{14}H_{11}N_2$ $[M+H]^+$: 207.09168; found: 207.09170.

The overall yield combining all three steps for product **3e** was 62 %.

Synthesis of Tetrahydroacridines and Dehydrogenation to Acridines

ADC Coupling:

General Procedure:

In a glove box 150 mg Ir@SiCN (0.5 mol% active metal), cyclohexanol (12.0 mmol), 1,3-aminoalcohol (3.0 mmol), 3 mL diglyme and KO^{t}Bu (673 mg, 6.0 mmol) were added in a pressure tube and the tube was closed by a pressure equalization device. The mixture was stirred at 140 °C (oil bath temperature) for 24 h. After cooling to RT 3 mL water and dodecane as internal standard were added and the product was extracted by diethyl ether (2x). The products were purified either by column chromatography or crystallization.

Acceptorless Dehydrogenation

General Procedure

In a 10 mL Schlenk tube 50 mg (0.18 mol% active metal) Pd@SiCN, 1.0 mmol substrate and 0.75 mL diglyme were evacuated and flushed with argon for three times. A slight argon flow of 4-6 mL/min was adjusted and the mixture was stirred for 18 h at 200 °C (oil bath temperature). After cooling to RT the catalyst was separated by centrifugation and washed with acetone two times. The organic phases were combined and the solvent was removed under reduced pressure at 60 °C giving the pure product. If required, further purification can be achieved either by column chromatography or crystallization.

Synthesis of 4a:

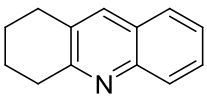

4H-4a: 1,2,3,4-tetrahydroacridine

Purification by column chromatography 1:20 → 1:5 pentane : Et_2O. Yield: 0.457 g = 2.50 mmol = 83 % as yellow solid. M($C_{13}H_{13}N$) = 183.10 gmol^{-1}.

^{1}H NMR (300 MHz, $CDCl_3$, 298 K): δ = 7.99-7.96 (m, 1H), 7.80 (s, 1H), 7.71-7.68 (m, 1H), 7.63-7.57 (m, 1H), 7.45-7.40 (m, 1H), 3.15-3.11 (m, 2H), 3.00-2.96 (m, 2H), 2.04-1.96 (m, 2H), 1.93-1.85 (m, 2H) ppm. ^{13}C NMR (75 MHz, $CDCl_3$, 298 K): δ = 159.3, 146.6, 134.9,

130.9, 128.4, 128.3, 127.2, 126.9, 125.5, 33.6, 29.3, 23.2, 22.9 ppm. MS (EI, m/z): 183.1 (M^+).

elemental analysis (%) for $C_{13}H_{13}N$ calcd: C 85.21, H 7.15, N 7.64; found: C 84.39, H 7.18, N 7.61.

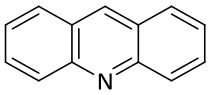

4a: acridine

Yield: 97 % as yellow solid. M($C_{13}H_9N$) = 179.22 $gmol^{-1}$.

^{1}H NMR (300 MHz, $CDCl_3$, 298 K): δ = 8.76 (s, 1H), 8.26-8.23 (m, 2H), 8.01-7.98 (m, 2H), 7.81-7.76 (m, 2H), 7.56-7.51 (m, 2H) ppm. ^{13}C NMR (75 MHz, $CDCl_3$, 298 K): δ = 149.0, 136.0, 130.3, 129.4, 128.2, 126.6, 125.7 ppm. MS (EI, m/z): 179.1 (M^+).

elemental analysis (%) for $C_{13}H_9N$ calcd: C 87.12, H 5.06, N 7.82; found: C 87.03, H 5.26, N 7.70.

The overall yield combining all three steps for product **4a** was 79 %.

Synthesis of 4b:

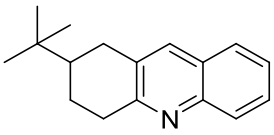

4H-4b: 2-*tert*-butyl-1,2,3,4-tetrahydroacridine

Purification by column chromatography 20:1 → 3:1 pentane : Et_2O. Yield: 0.66 g = 2.76 mmol = 92 % as light yellow solid. M($C_{17}H_{21}N$) = 239.17 $gmol^{-1}$.

^{1}H NMR (300 MHz, $CDCl_3$, 298 K): δ = 7.99-7.96 (m, 1H), 7.82 (s, 1H), 7.71-7.68 (m, 1H), 7.63-7.57 (m, 1H), 7.45-7.40 (m, 1H), 3.32-3.23 (m, 1H), 3.11-3.01 (m, 2H), 2.77-2.72 (m, 1H), 2.20-2.12 (m, 1H), 1.65-1.52 (m, 2H), 1.00 (s, 9H) ppm. ^{13}C NMR (75 MHz, $CDCl_3$, 298 K): δ = 159.4, 146.6, 135.2, 131.2, 128.4, 128.3, 127.2, 126.8, 125.5, 44.6, 34.4, 32.6, 30.8, 27.3, 24.6 ppm. MS (EI, m/z): 239.1 (M^+).

elemental analysis (%) for $C_{17}H_{21}N$ calcd: C 85.30, H 8.84, N 5.85; found: C 85.07, H 8.87, N 5.77.

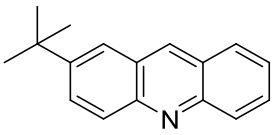

4b: 2-*tert*-butylacridine

Yield: 98 % as colorless solid by recrystallization from pentane/diethyl ether. M($C_{17}H_{17}N$) = 235.14 $gmol^{-1}$.

^{1}H NMR (300 MHz, $CDCl_3$, 298 K): δ = 8.71 (s, 1H), 8.24-8.17 (m, 2H), 7.99-7.97 (m, 1H), 7.92-7.86 (m, 2H), 7.78-7.72 (m, 1H), 7.54-7.49 (m, 1H), 1.46 (s, 9H) ppm. ^{13}C NMR (75 MHz, $CDCl_3$, 298 K): δ = 148.7, 148.2, 148.1, 135.7, 130.0, 129.8, 129.4, 128.9, 128.1, 126.7, 126.4, 125.4, 125.3, 35.0, 30.9 ppm. MS (EI, m/z): 235.1 (M^+).

HRMS (ESI): calcd. for $C_{17}H_{18}N$ $[M+H]^+$: 236.14337; found: 236.14338.

The overall yield combining all three steps for product **4b** was 87 %.

Synthesis of 4c:

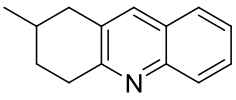

4H-4c: 2-methyl-1,2,3,4-tetrahydroacridine

Oil bath temperature: 135 °C. Purification by column chromatography 5:1 → 1:1 pentane : Et_2O. Yield: 0.416 g = 2.11 mmol = 70 % as yellow solid. M($C_{14}H_{15}N$) = 197.12 $gmol^{-1}$.
^{1}H NMR (300 MHz, $CDCl_3$, 298 K): δ = 7.98-7.95 (m, 1H), 7.73 (s, 1H), 7.68-7.65 (m, 1H), 7.61-7.56 (m, 1H), 7.43-7.38 (m, 1H), 3.26-3.17 (m, 1H), 3.14-2.95 (m, 2H), 2.60-2.51 (m, 1H), 2.10-1.90 (m, 2H), 1.65-1.51 (m, 1H), 1.10 (d, *J* = 6.3 Hz, 3H) ppm. ^{13}C NMR (75 MHz, $CDCl_3$, 298 K): δ = 158.9, 146.6, 134.8, 130.5, 128.4, 128.2, 127.1, 126.8, 125.4, 37.7, 33.1, 31.4, 29.0, 21.6 ppm. MS (EI, m/z): 197.1 (M^+).

HRMS (ESI): calcd. for $C_{14}H_{16}N$ $[M+H]^+$: 198.12772; found: 198.12773.

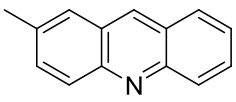

4c: 2-methylacridine

Yield: 96 % as yellow-orange solid; purification by column chromatography with diethyl ether as eluent. M($C_{14}H_{11}N$) = 193.09 $gmol^{-1}$.

^{1}H NMR (300 MHz, $CDCl_3$, 298 K): δ = 8.62 (s, 1H), 8.22 (d, *J* = 9.0 Hz, 1H), 8.13 (d, *J* = 9.0 Hz, 1H), 7.97-7.94 (m, 1H), 7.77-7.71 (m, 2H), 7.63-7.59 (m, 1H), 7.53-7.48 (m, 1H), 2.56 (s, 3H) ppm. ^{13}C NMR (75 MHz, $CDCl_3$, 298 K): δ = 148.5, 148.0, 135.4, 134.8, 133.2, 129.7, 129.4, 129.0, 128.1, 126.7, 126.2, 125.5, 21.8 ppm. MS (EI, m/z): 193.1 (M^+).

HRMS (ESI): calcd. for $C_{14}H_{12}N$ $[M+H]^+$: 194.09642; found: 194.09643.

The overall yield combining all three steps for product **4c** was 68 %.

Synthesis of 4d:

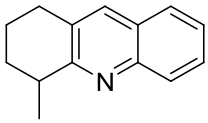

4H-4d: 4-methyl-1,2,3,4-tetrahydroacridine

Oil bath temperature: 135 °C. Purification by column chromatography 3:1 pentane : Et_2O. Yield: 0.427 g = 2.17 mmol = 72 % as yellow oil. M($C_{14}H_{15}N$) = 197.12 gmol^{-1}.
^{1}H NMR (300 MHz, $CDCl_3$, 298 K): δ = 8.03-8.00 (m, 1H), 7.79 (s, 1H), 7.71-7.68 (m, 1H), 7.63-7.57 (m, 1H), 7.46-7.40 (m, 1H), 3.28-3.17 (m, 1H), 3.03-2.93 (m, 2H), 2.18-2.09 (m, 1H), 2.03-1.91 (m, 1H), 1.89-1.69 (m, 2H), 1.49 (d, *J* = 6.9 Hz, 3H) ppm. ^{13}C NMR (75 MHz, $CDCl_3$, 298 K): δ = 163.1, 146.6, 134.9, 130.5, 128.3, 126.7, 125.5, 119.4, 114.8, 36.4, 31.2, 29.7, 21.7, 20.0 ppm. (EI, m/z): 197.1 (M^+).

HRMS (ESI): calcd. for $C_{14}H_{16}N$ $[M+H]^+$: 198.12380; found: 198.12773.

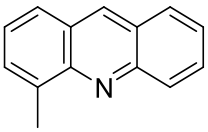

4d: 4-methylacridine

Yield: 93 % as yellow solid; purification by crystallization from pentane/diethyl ether. M($C_{14}H_{11}N$) = 193.09 gmol^{-1}.

^{1}H NMR (300 MHz, $CDCl_3$, 298 K): δ = 8.71 (s, 1H), 8.31-8.28 (m, 1H), 7.98 (d, *J* = 8.4 Hz, 1H), 7.84 (d, *J* = 8.4 Hz, 1H), 7.79-7.74 (m, 1H), 7.63-7.61 (m, 1H), 7.55-7.50 (m, 1H), 7.45-7.40 (m, 1H), 2.96 (s, 3H) ppm. ^{13}C NMR (75 MHz, $CDCl_3$, 298 K): δ = 148.6, 148.4, 137.2, 135.9, 130.0, 129.7, 129.5, 127.9, 126.6, 126.4, 126.2, 125.5, 125.5, 18.4 ppm. MS (EI, m/z): 194.1 (M^+).

elemental analysis (%) for $C_{14}H_{11}N$ calcd: C 87.01, H 5.74, N7.25; found: C 86.45, H 6.04, N 7.10. HRMS (ESI): calcd. for $C_{14}H_{12}N$ $[M+H]^+$: 194.09250; found: 194.09596.

The overall yield combining all three steps for product **4d** was 65 %.

Synthesis of 4e:

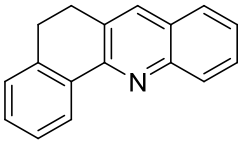

2H-4e: 5,6-dihydrobenzo[*c*]acridine:

Purification by column chromatography 1:20 pentane : Et_2O; Yield: 0.643 g = 2.78 mmol = 93 % as colorless solid. M($C_{17}H_{13}N$) = 231.10 $gmol^{-1}$.

^{1}H NMR (300 MHz, $CDCl_3$, 298 K): δ = 8.61-8.58 (m, 1H), 8.16-8.13 (m, 1H), 7.92 (s, 1H), 7.76-7.73 (m, 1H), 7.68-7.63 (m, 1H), 7.50-7.35 (m, 3H), 7.30-7.27 (m, 1H), 3.16-3.11 (m, 2H), 3.04-2.99 (m, 2H) ppm. ^{13}C NMR (75 MHz, $CDCl_3$, 298 K): δ = 153.4, 147.6, 139.4, 134.7, 133.6, 130.5, 129.6, 129.4, 128.6, 127.9, 127.8, 127.3, 129.9, 126.0, 125.9, 28.8, 28.4 ppm. MS (EI, m/z): 230.2 (M^+).

elemental analysis (%) for $C_{17}H_{13}N$ calcd: C 88.28, H 5.67, N 6.06; found: C 88.13, H 5.90, N 5.71.

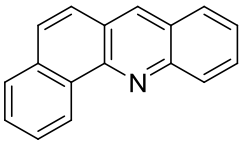

4e: benzo[*c*]acridine

Yield: 98 % as colorless solid by recrystallization from pentane/diethyl ether. M($C_{17}H_{11}N$) = 229.09 $gmol^{-1}$.

^{1}H NMR (300 MHz, $CDCl_3$, 298 K): δ = 9.56-9.53 (m, 1H), 8.59 (s, 1H), 8.40 (d, *J* = 8.7 Hz,1H), 7.99 (d, *J* = 8.4 Hz,1H), 7.88-7.66 (m, 6H), 7.61-7.56 (m, 1H) ppm. ^{13}C NMR (75 MHz, $CDCl_3$, 298 K): δ = 147.7, 147.6, 134.9, 133.9, 131.5, 129.7, 129.6, 129.0, 127.8, 127.7, 127.5, 127.2, 126.9, 125.8, 125.7, 125.2, 125.0 ppm. MS (EI, m/z): 229.1 (M^+).

elemental analysis (%) for $C_{17}H_{11}N$ calcd: C 89.06, H 4.84, N 6.11; found: C 88.66, H 5.02, N 5.93.

The overall yield combining all three steps for product **4e** was 88 %.

Synthesis of 4f:

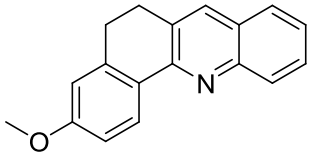

2H-4f: 3-methoxy-5,6-dihydrobenzo[*c*]acridine

Purification by column chromatography 5:1 → 1:2 pentane : Et_2O. Yield: 0.724 g = 2.77 mmol = 92 % as light yellow solid. M($C_{18}H_{15}NO$) = 261.12 $gmol^{-1}$.
^{1}H NMR (300 MHz, $CDCl_3$, 298 K): δ = 8.57 (d, *J* = 8.7 Hz, 1H), 8.14 (d, *J* = 8.7 Hz, 1H), 7.80 (s, 1H), 7.70-7.62 (m, 2H), 7.46-7.41 (m, 1H), 7.00-6.96 (m, 1H), 6.79-6.78 (m, 1H), 3.85 (s, 3H), 3.08-3.03 (m, 2H), 2.96-2.92 (m, 2H) ppm. ^{13}C NMR (75 MHz, $CDCl_3$, 298 K): δ = 160.7, 153.2, 147.5, 141.1, 133.3, 129.8, 129.0, 128.4, 127.6, 127.4, 126.8, 126.8, 125.4, 112.9, 112.7, 55.1, 28.7, 28.6 ppm. MS (EI, m/z): 261.1 (M^+).

elemental analysis (%) for $C_{18}H_{15}NO$ calcd: C 82.73, H 5.79, N 5.36; found: C 82.83, H 6.00, N 5.18.

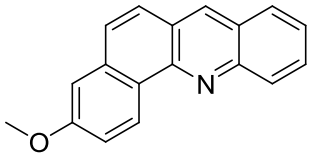

4f: 3-methoxybenzo[*c*]acridine

Yield: 98 % as colorless solid. M($C_{18}H_{13}NO$) = 259.10 $gmol^{-1}$.

^{1}H NMR (300 MHz, $CDCl_3$, 298 K): δ = 9.41 (d, *J* = 9.0 Hz, 1H), 8.60 (s, 1H), 8.34 (d, *J* = 8.4 Hz, 1H), 8.00 (d, *J* = 8.1 Hz, 1H), 7.83-7.71 (m, 2H), 7.64-7.54 (m, 2H), 7.39-7.35 (m, 1H), 7.26 (s, 1H), 3.99 (s, 3H) ppm. ^{13}C NMR (75 MHz, $CDCl_3$, 298 K): δ = 160.4, 147.9, 147.8, 135.5, 135.0, 129.6, 129.5, 127.8, 127.4, 127.1, 126.6, 126.4, 125.4, 124.4, 116.5, 109.2, 55.5 ppm. MS (EI, m/z): 259.1 (M^+).

elemental analysis (%) for $C_{18}H_{13}NO$ calcd: C 83.37, H 5.05, N 5.40; found: C: 82.78, H 5.05, N 5.21.

The overall yield combining all three steps for product **4f** was 79 %.

Synthesis of phenazine:

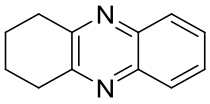

1,2,3,4-tetrahydrophenazine:

150 mg Ir@SiCN, cyclohexan-1,2-diol (2.79 g, 24.0 mmol), benzene-1,2-diamine (649 mg, 6.0 mmol), 5 mL diglyme, KO^{t}Bu (1374 mg, 12.0 mmol), 24 h at 140 °C (oil bath temperature). Purification by column chromatography 1:5 → pentane : Et_2O → pure Et_2O. Yield: 1.08 g = 5.87 mmol = 98 % as colorless solid. M($C_{12}H_{12}N_2$) = 184.10 gmol^{-1}.

^{1}H NMR (300 MHz, $CDCl_3$, 298 K): δ = 7.99-7.94 (m, 2H), 7.68-7.63 (m, 2H), 3.19-3.14 (m, 4H), 2.06-2.02 (m, 4H) ppm. ^{13}C NMR (75 MHz, $CDCl_3$, 298 K): δ = 154.1, 141.2, 128.9, 128.3, 33.2, 22.8 ppm. MS (EI, m/z): 184.1 (M^+).

elemental analysis (%) for $C_{12}H_{12}N_2$ calcd: C 78.23, H 6.57, N 15.21; found: C 78.26, H 6.59, N 15.18.

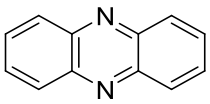

phenazine:

50 mg Pd@SiCN, 184 mg (1.0 mmol) and 0.5 mL diglyme were stirred for 20 h at 200 °C (oil bath temperature) under nitrogen atmosphere. A pressure equalization device was used to let the produced hydrogen out of the reaction vial. The catalyst was separated by centrifugation and washed with acetone two times. The organic phases were combined and the solvent was removed under reduced pressure at 60 °C giving the product in quantitative yield as light yellow solid.

M($C_{12}H_8N_2$) = 180.07 gmol^{-1}.

^{1}H NMR (300 MHz, $CDCl_3$, 298 K): δ = 8.22-8.16 (m, 4H), 7.81-7.75 (m, 4H) ppm. ^{13}C NMR (75 MHz, $CDCl_3$, 298 K): δ = 143.4, 130.4, 129.5 ppm. MS (EI, m/z):.180.1 (M^+).

7.4.4 Comparison to Commercial Catalysts

All available heterogeneous catalysts were applied in the acceptorless dehydrogenation of 2,3,4,5,6,7,8,9-octahydro-1*H*-carbazole **2a** (**Tab. S5**).

In a 10 mL Schlenk tube 0.5 mmol **2a** were solved in 1.0 mL diglyme and the catalyst (0.18 mol% active metal) was added. The reaction mixture was evacuated and flushed with argon for three times and a slight argon flow of 4-6 mL/min was adjusted. The Schlenk tube was placed in a pre-heated oil bath at 180 °C for 6-24 h. After cooling to RT in an argon atmosphere, dodecane as internal standard was added and a sample for GC and GC-MS analysis was taken.

Tab. S5: Acceptorless dehydrogenation of 2a

Catalyst	Yield[a] [%] 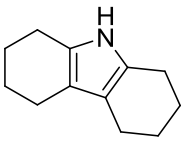	Yield[a] [%] 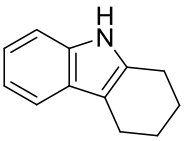	Yield[a] [%] 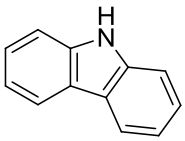
Pd@SiCN[b]	0	8	92
Pd/C (10 %)[b]	43	0	57
Pd/SiO_2 (5 %)[b]	78	0	22
Ru@SiCN	17	74	9
Ru/C (5 %)	97	3	0
Ru/Al_2O_3 (5 %)	97	0	3
Ir@SiCN	96	1	2
Ir/C (1 %)	97	3	0
$Ir/CaCO_3$ (5 %)	100	0	0
Ir/Al_2O_3 (1 %)	100	0	0

Reaction conditions: Catalyst (0.18 mol% active metal), 0.5 mmol (88 mg) 2a, 1 mL digylme, T (oil bath) = 180 °C (170 °C reaction temperature), Ar flow (4-6 mL/min), 24 h. a) Yields determined by GC. b) Reaction time: 5 h.

7.4.5 NMR Spectra

4H-1a:

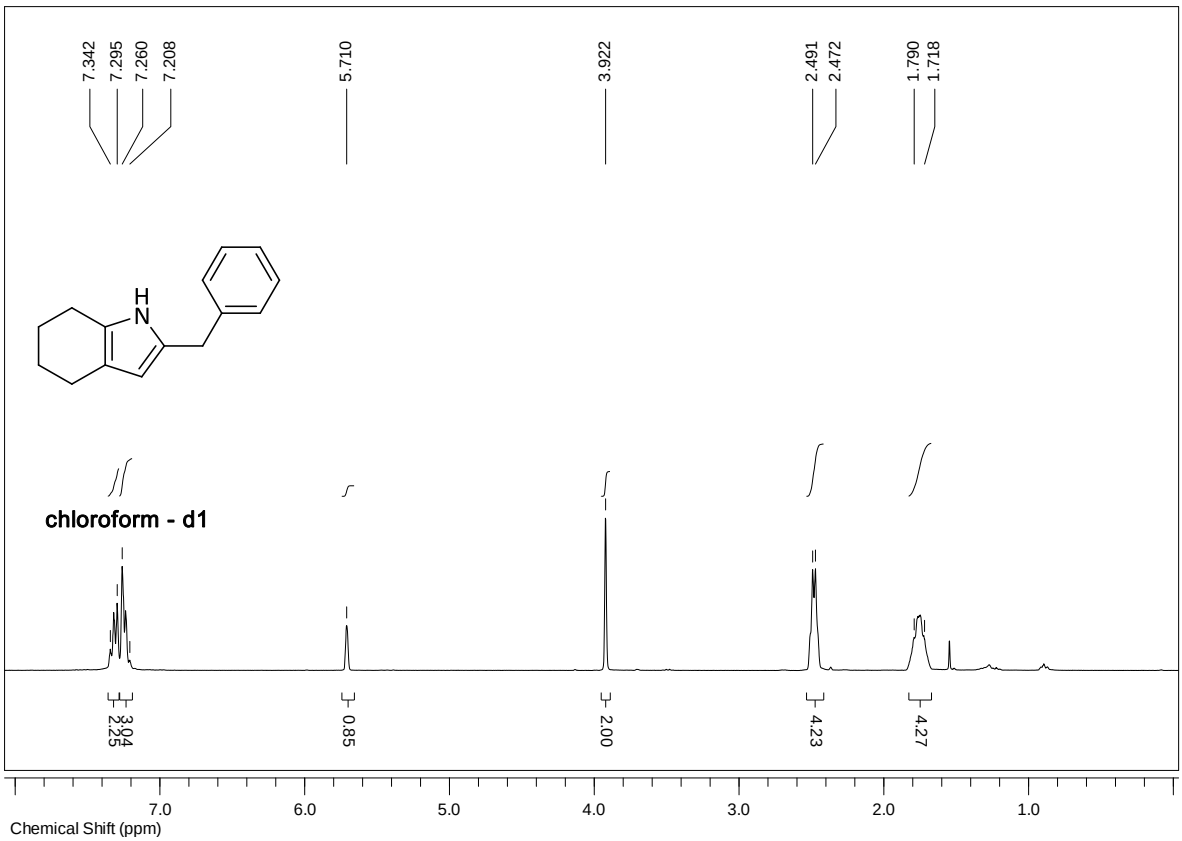

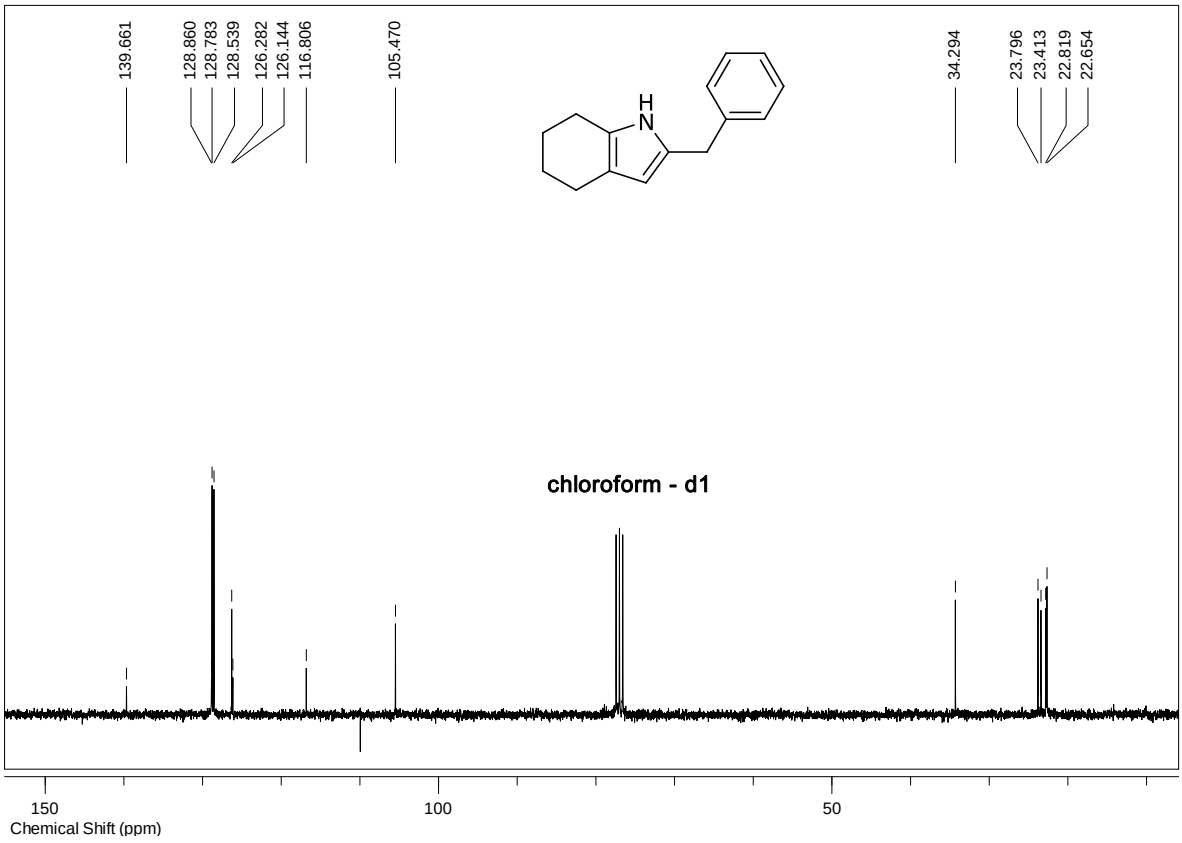

1a:

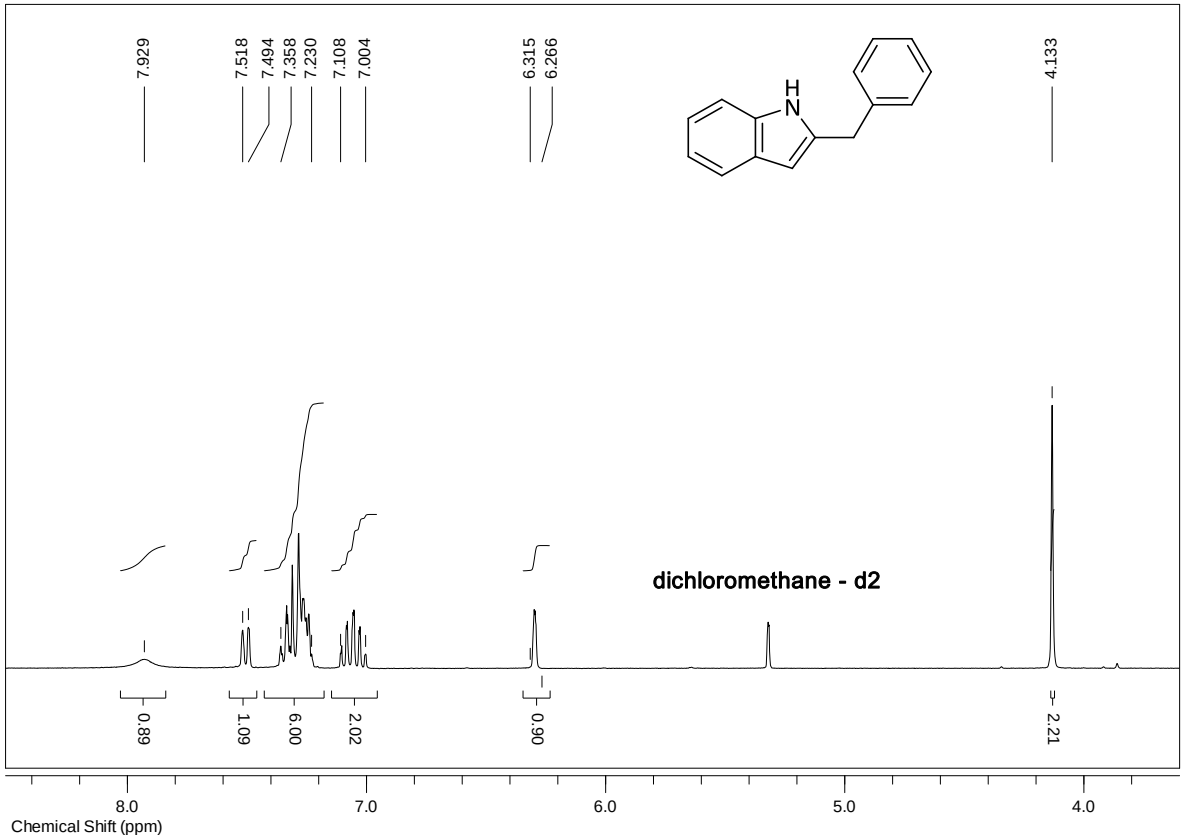
7.929
7.518
7.494
7.358
7.230
7.108
7.004
6.315
6.266
4.133
H
N
dichloromethane - d2
0.89
1.09
6.00
2.02
0.90
2.21
8.0
7.0
6.0
5.0
4.0
Chemical Shift (ppm)

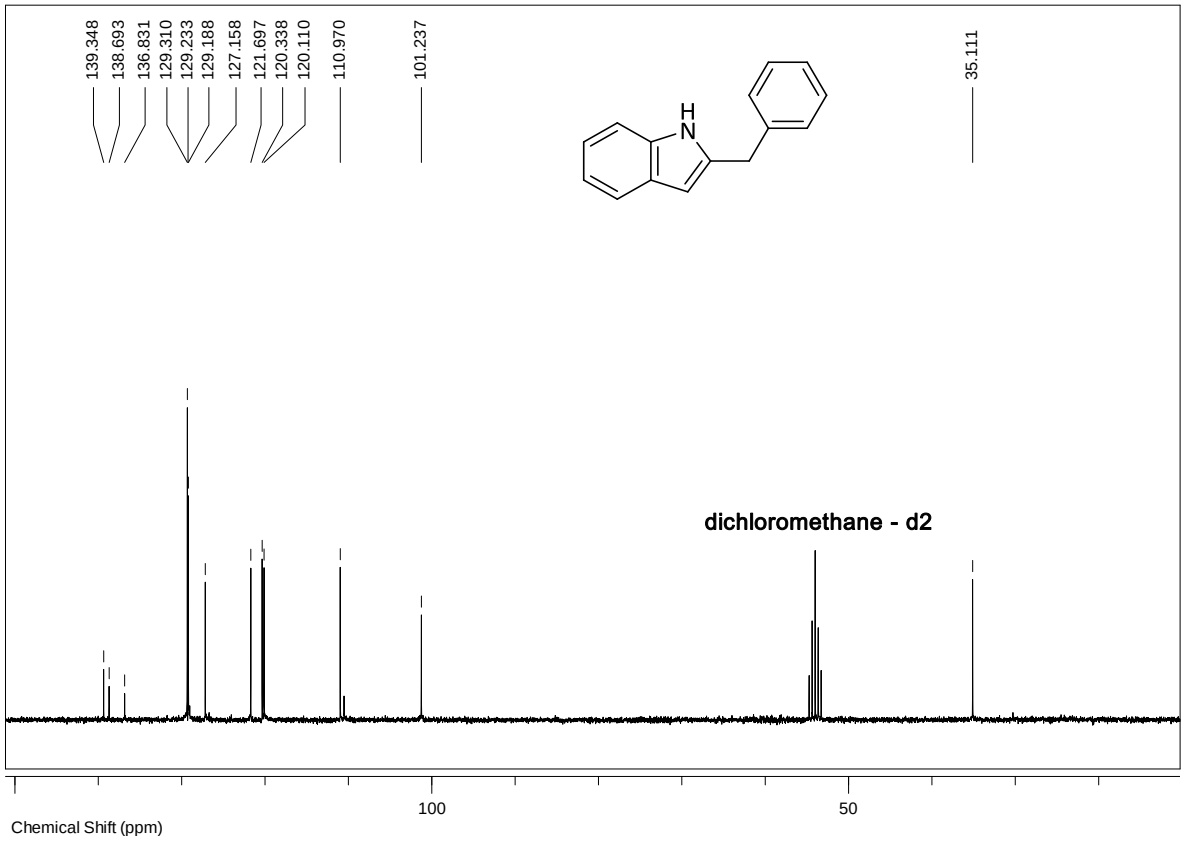
139.348
138.693
136.831
129.310
129.233
129.188
127.158
121.697
120.338
120.110
110.970
101.237
35.111
H
N
dichloromethane - d2
100
50
Chemical Shift (ppm)

4H-1b:

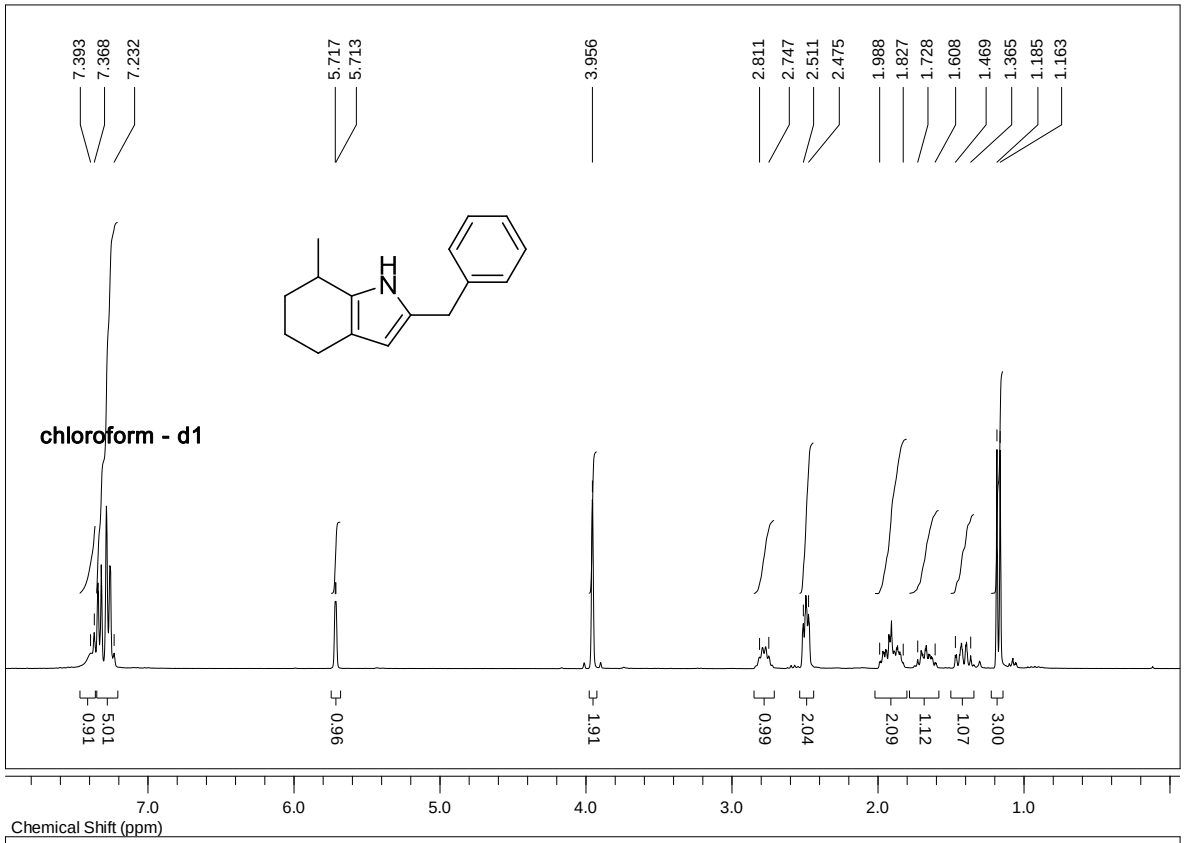
7.393
7.368
7.232
5.717
5.713
3.956
2.811
2.747
2.511
2.475
1.988
1.827
1.728
1.608
1.469
1.365
1.185
1.163
chloroform - d1
0.91
5.01
0.96
1.91
0.99
2.04
2.09
1.12
1.07
3.00
7.0
6.0
5.0
4.0
3.0
2.0
1.0
Chemical Shift (ppm)

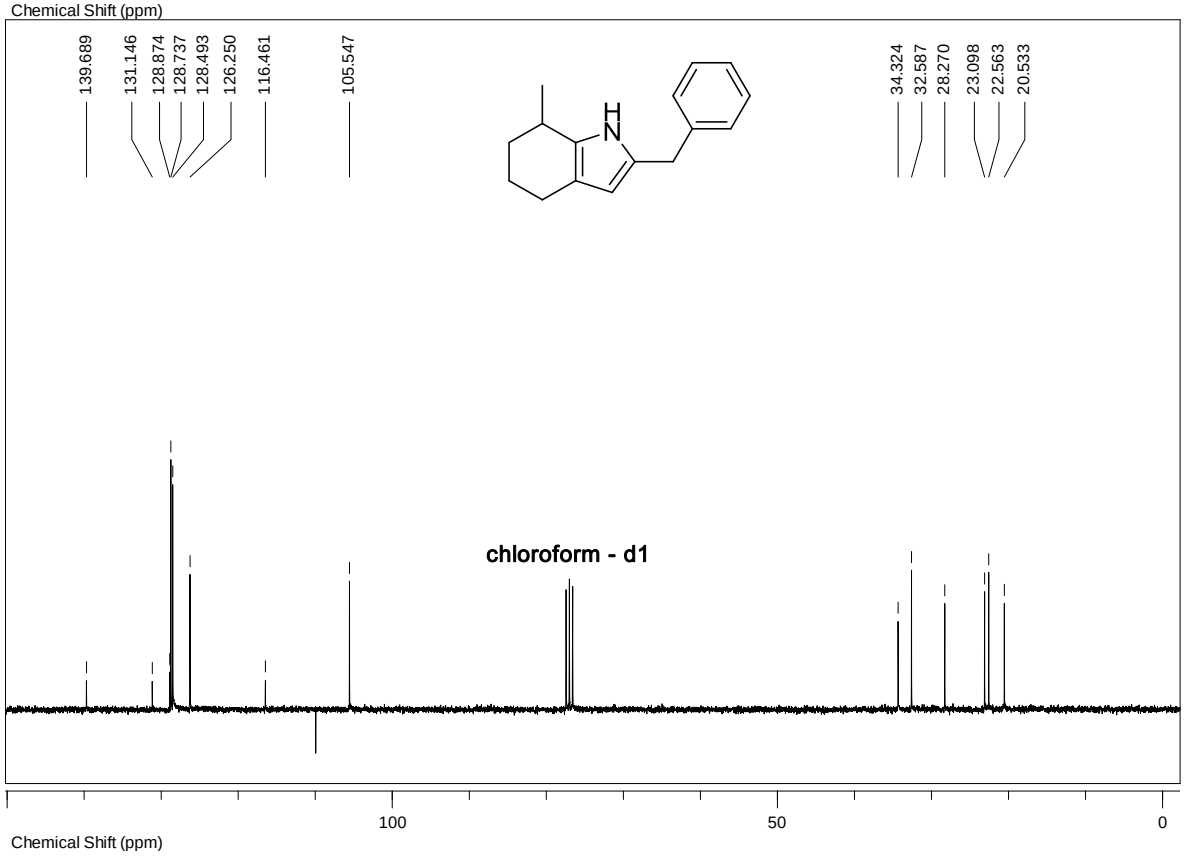
139.689
131.146
128.874
128.737
128.493
126.250
116.461
105.547
34.324
32.587
28.270
23.098
22.563
20.533
chloroform - d1
100
50
0
Chemical Shift (ppm)

1b:

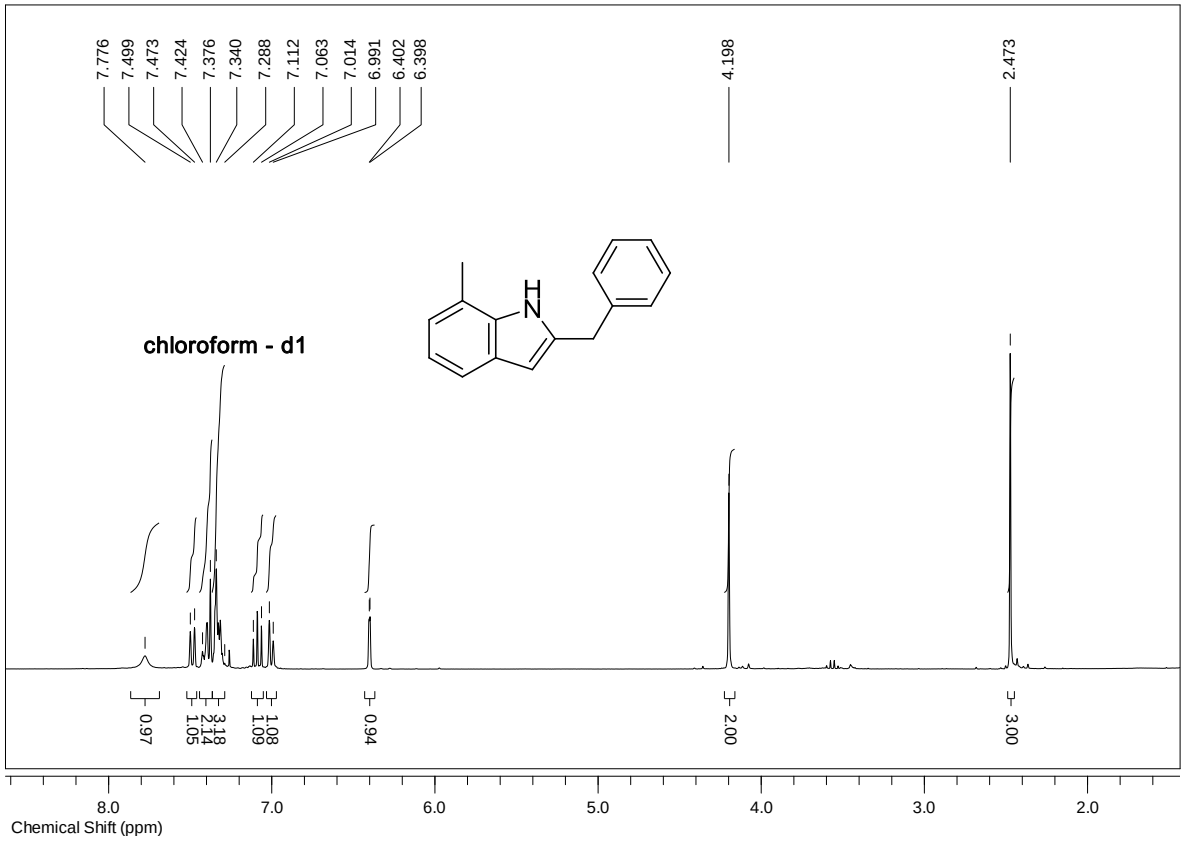
7.776
7.499
7.473
7.424
7.376
7.340
7.288
7.112
7.063
7.014
6.991
6.402
6.398
4.198
2.473
chloroform - d1
0.97
1.05
3.18
2.14
1.08
1.09
0.94
2.00
3.00
8.0
7.0
6.0
5.0
4.0
3.0
2.0
Chemical Shift (ppm)

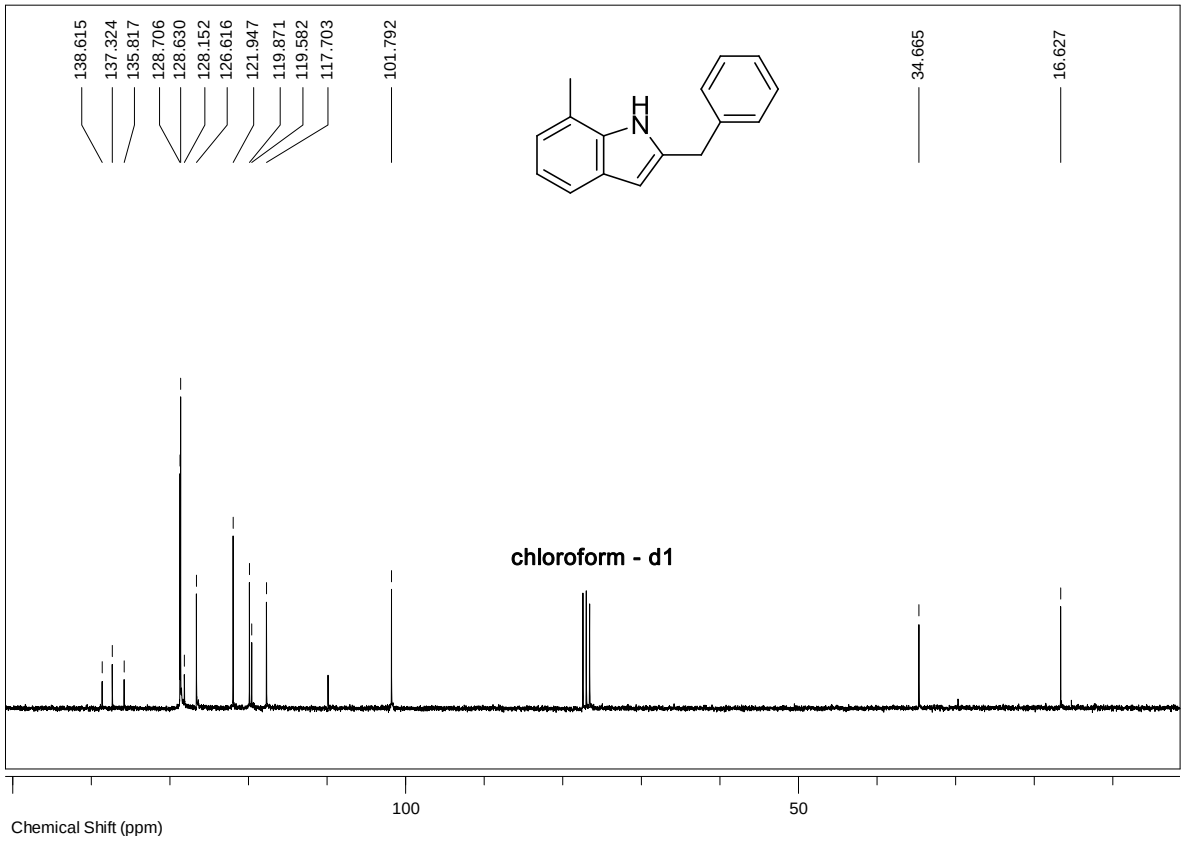
138.615
137.324
135.817
128.706
128.630
128.152
126.616
121.947
119.871
119.582
117.703
101.792
34.665
16.627
chloroform - d1
100
50
Chemical Shift (ppm)

4H-1c:

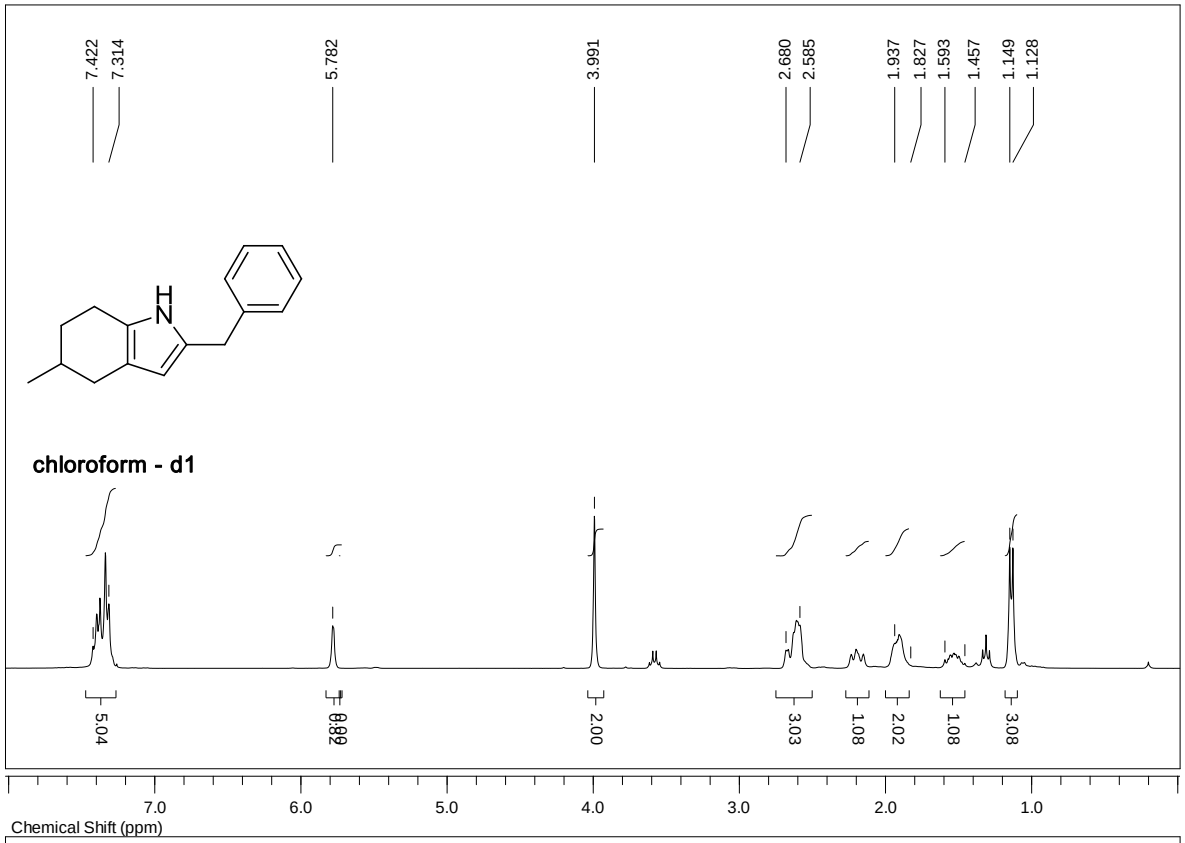
7.422
7.314
5.782
3.991
2.680
2.585
1.937
1.827
1.593
1.457
1.149
1.128
chloroform - d1
5.04
0.88
2.00
3.03
1.08
2.02
1.08
3.08
7.0
6.0
5.0
4.0
3.0
2.0
1.0
Chemical Shift (ppm)

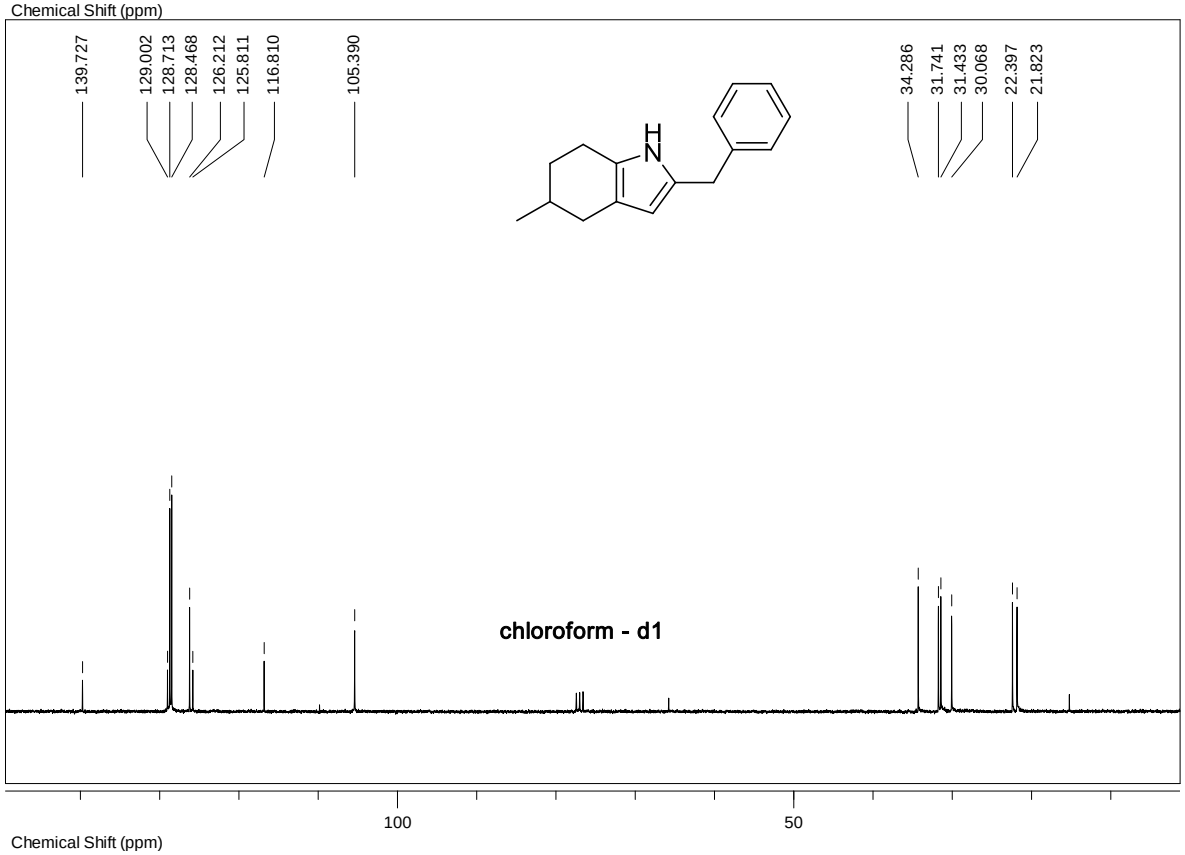
139.727
129.002
128.713
128.468
126.212
125.811
116.810
105.390
34.286
31.741
31.433
30.068
22.397
21.823
chloroform - d1
100
50
Chemical Shift (ppm)

1c:

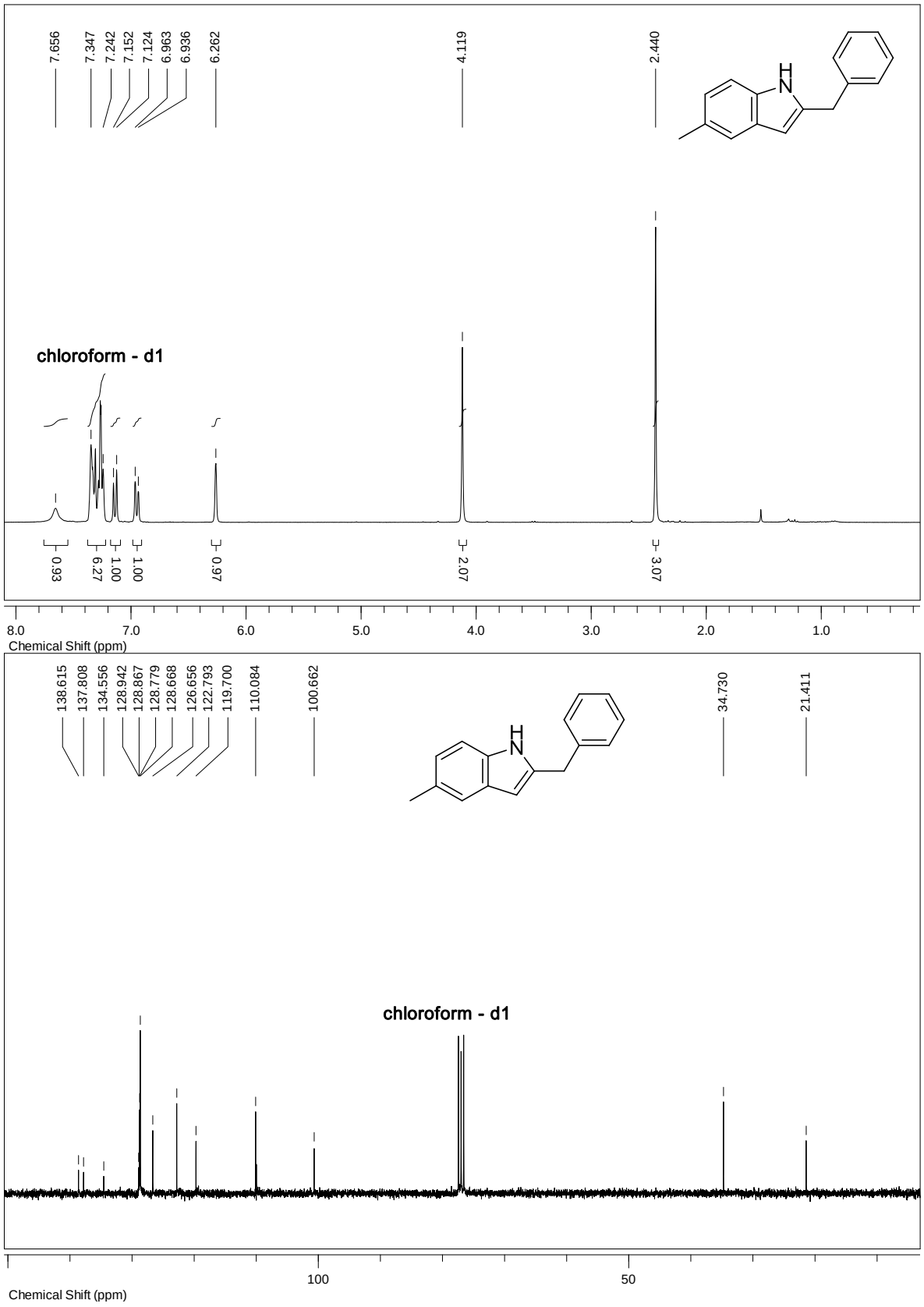
7.656
7.347
7.242
7.152
7.124
6.963
6.936
6.262
4.119
2.440
chloroform - d1
0.93
6.27
1.00
1.00
0.97
2.07
3.07
8.0
7.0
6.0
5.0
4.0
3.0
2.0
1.0
Chemical Shift (ppm)
138.615
137.808
134.556
128.942
128.867
128.779
128.668
126.656
122.793
119.700
110.084
100.662
34.730
21.411
chloroform - d1
100
50
Chemical Shift (ppm)

4H-1d:

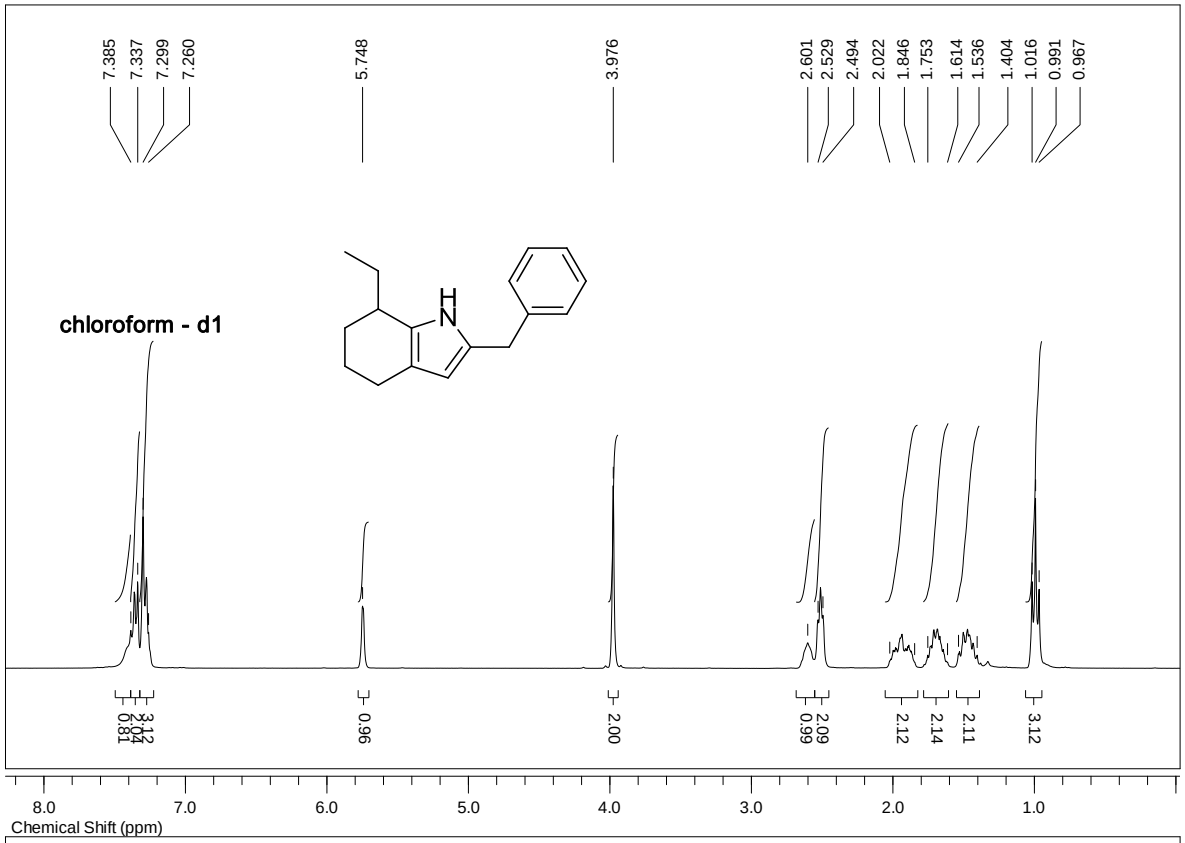
7.385
7.337
7.299
7.260
5.748
3.976
2.601
2.529
2.494
2.022
1.846
1.753
1.614
1.536
1.404
1.016
0.991
0.967
chloroform - d1
0.81
3.12
3.04
0.96
2.00
0.99
2.09
2.12
2.14
2.11
3.12
8.0
7.0
6.0
5.0
4.0
3.0
2.0
1.0
Chemical Shift (ppm)

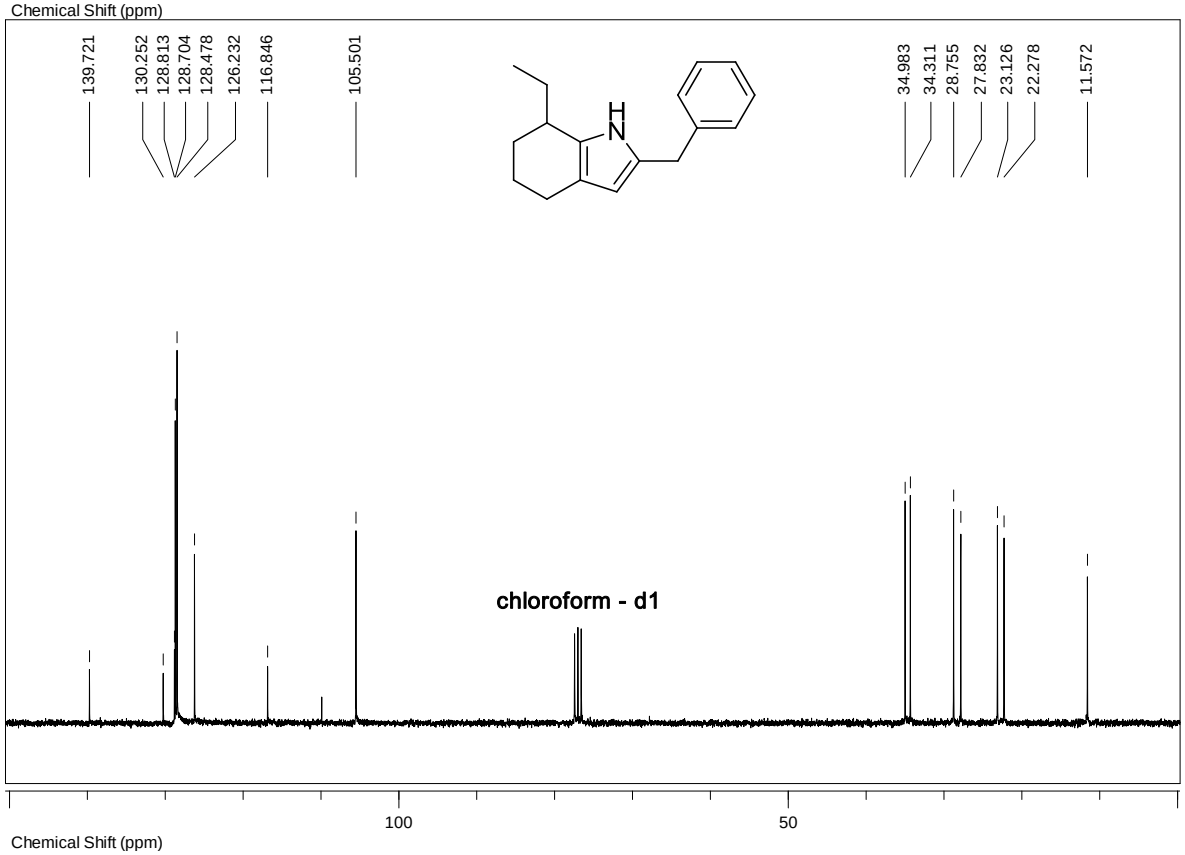
139.721
130.252
128.813
128.704
128.478
126.232
116.846
105.501
34.983
34.311
28.755
27.832
23.126
22.278
11.572
chloroform - d1
100
50
Chemical Shift (ppm)

1d:

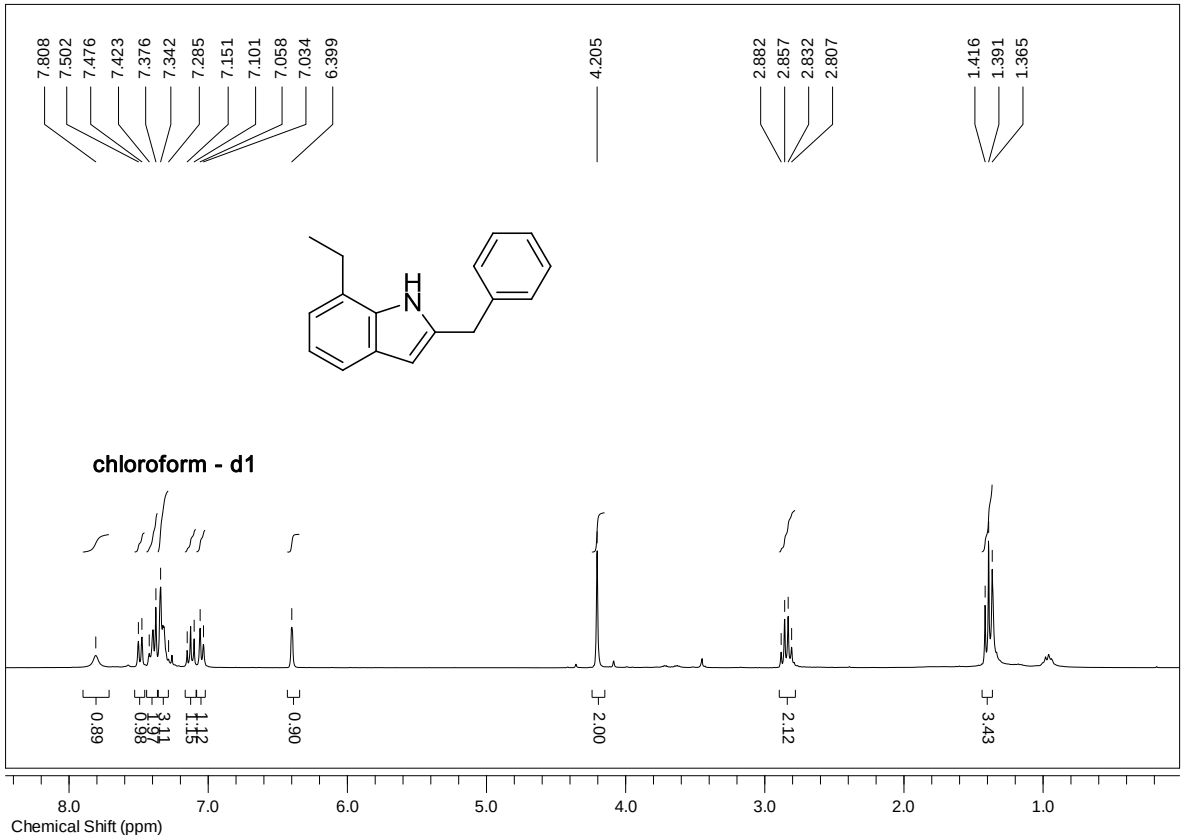
7.808
7.502
7.476
7.423
7.376
7.342
7.285
7.151
7.101
7.058
7.034
6.399
4.205
2.882
2.857
2.832
2.807
1.416
1.391
1.365
chloroform - d1
0.89
0.98
1.01
3.11
1.12
0.90
2.00
2.12
3.43
8.0
7.0
6.0
5.0
4.0
3.0
2.0
1.0
Chemical Shift (ppm)

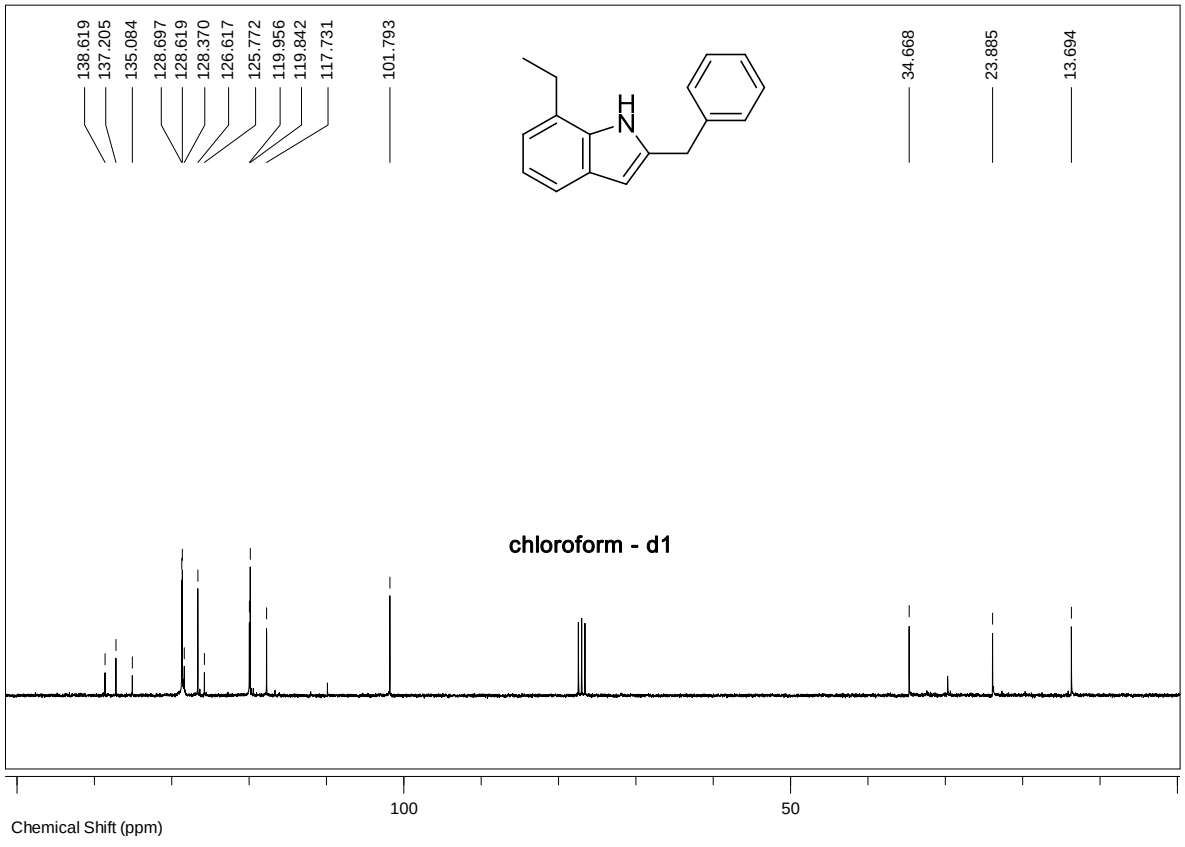
138.619
137.205
135.084
128.697
128.619
128.370
126.617
125.772
119.956
119.842
117.731
101.793
34.668
23.885
13.694
chloroform - d1
100
50
Chemical Shift (ppm)

4H-1e:

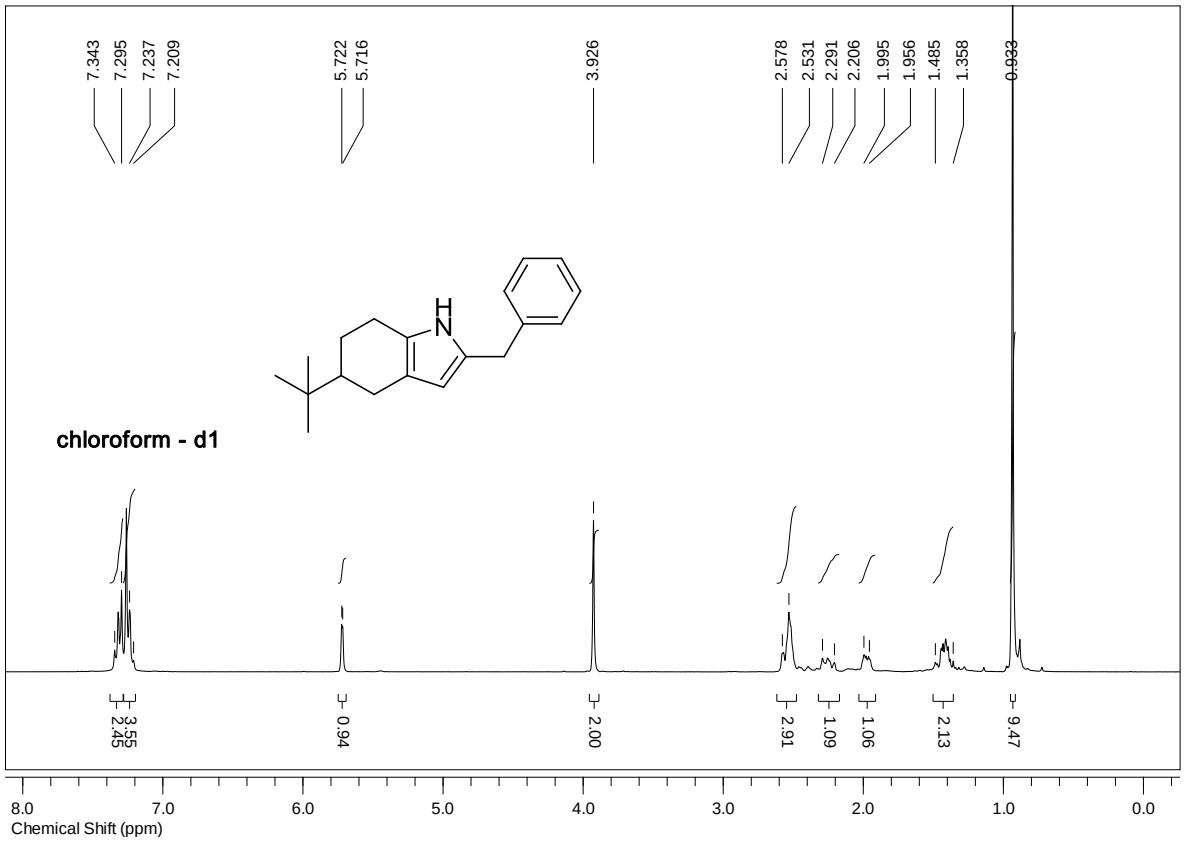
7.343
7.295
7.237
7.209
5.722
5.716
3.926
2.578
2.531
2.291
2.206
1.995
1.956
1.485
1.358
0.933
chloroform - d1
3.55
3.45
0.94
2.00
2.91
1.09
1.06
2.13
9.47
8.0
7.0
6.0
5.0
4.0
3.0
2.0
1.0
0.0
Chemical Shift (ppm)

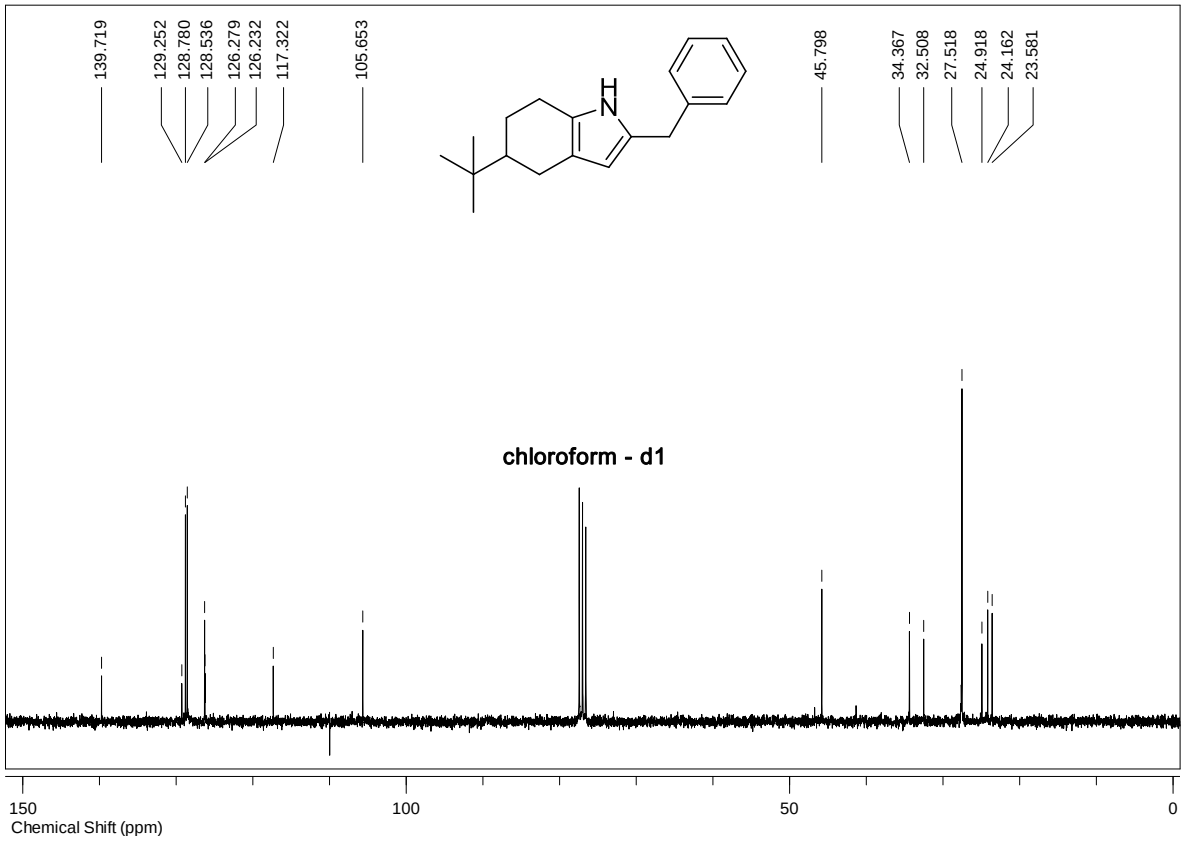
139.719
129.252
128.780
128.536
126.279
126.232
117.322
105.653
45.798
34.367
32.508
27.518
24.918
24.162
23.581
chloroform - d1
150
100
50
0
Chemical Shift (ppm)

1e:

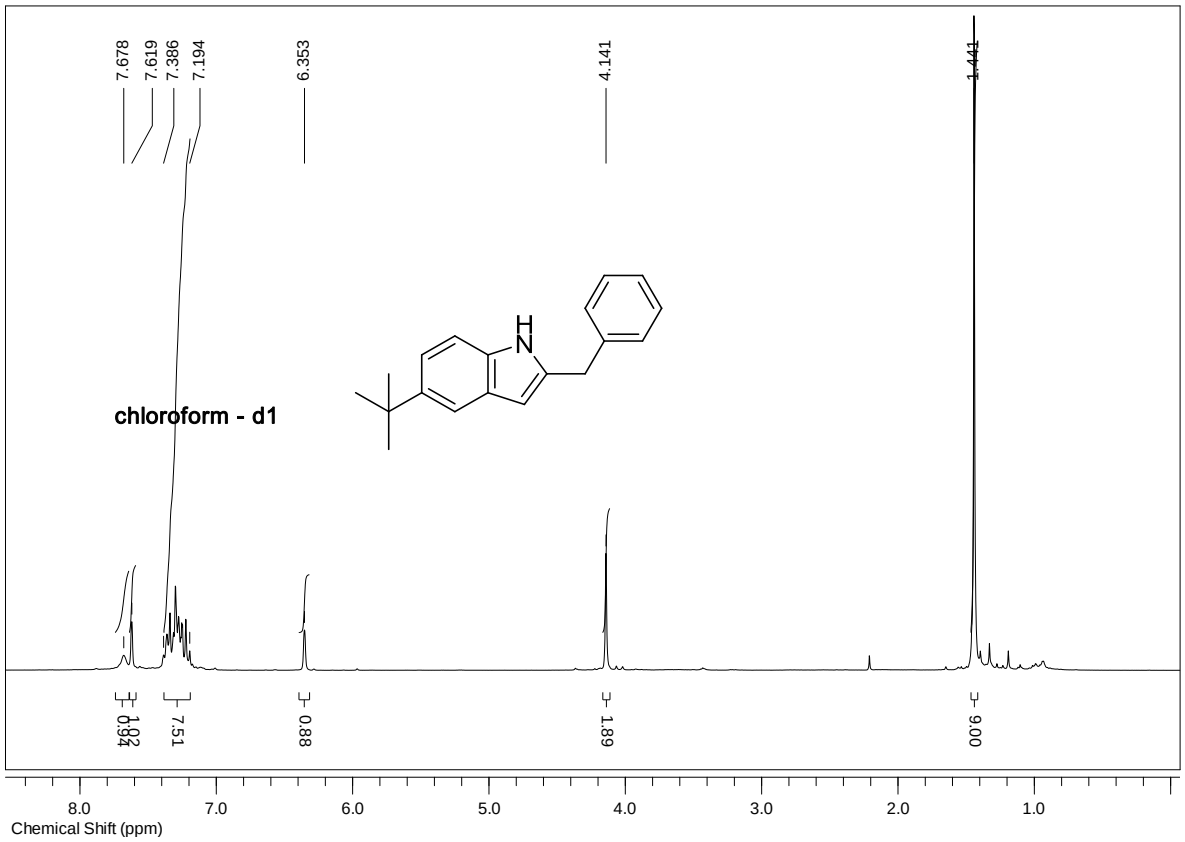
7.678
7.619
7.386
7.194
6.353
4.141
1.441
chloroform - d1
1.02
0.94
7.51
0.88
1.89
9.00
8.0
7.0
6.0
5.0
4.0
3.0
2.0
1.0
Chemical Shift (ppm)

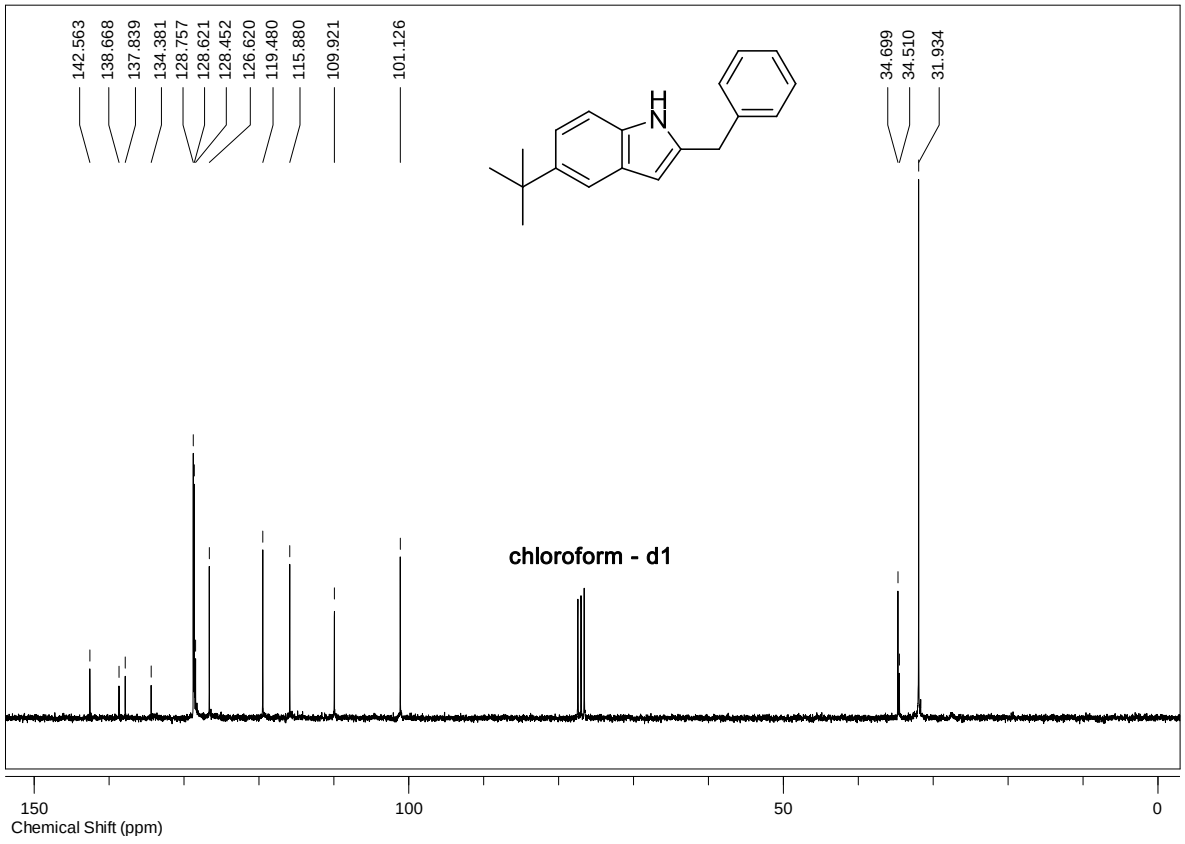
142.563
138.668
137.839
134.381
128.757
128.621
128.452
126.620
119.480
115.880
109.921
101.126
34.699
34.510
31.934
chloroform - d1
150
100
50
0
Chemical Shift (ppm)

4H-1f:

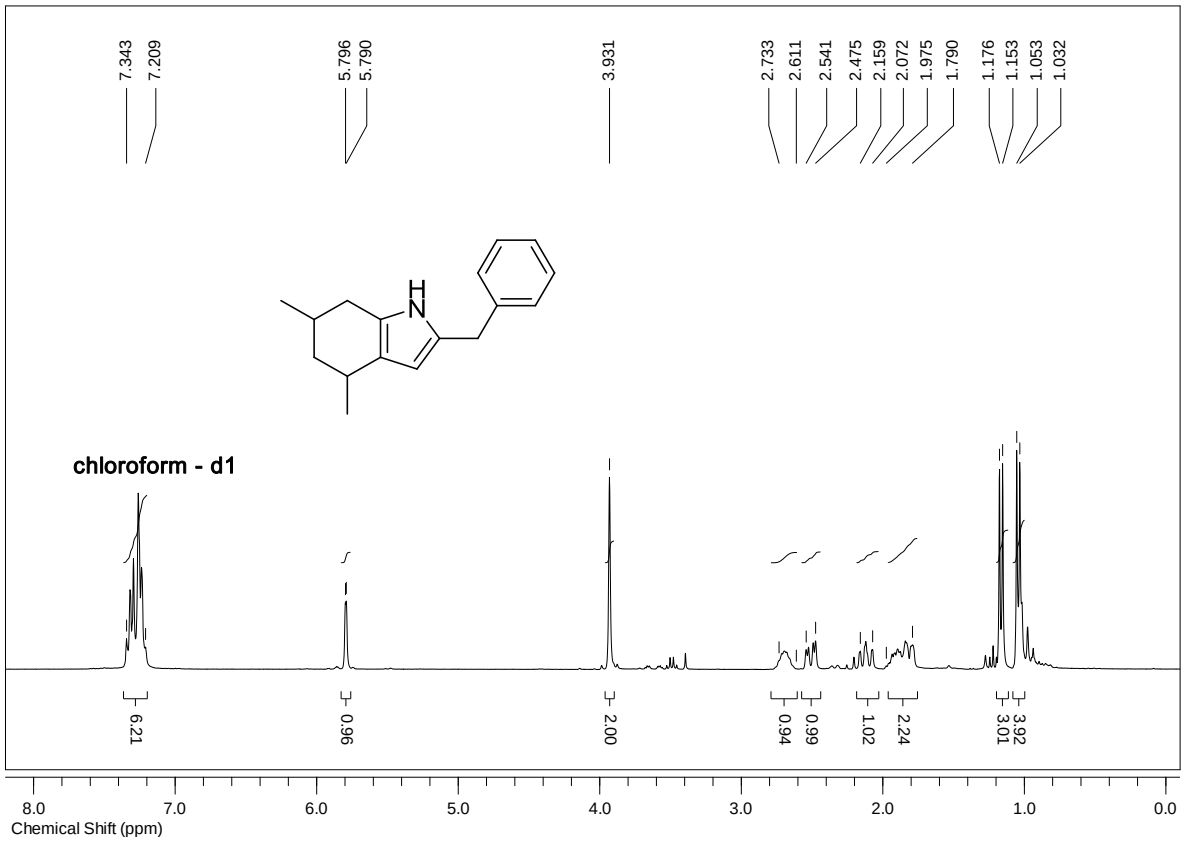
7.343
7.209
5.796
5.790
3.931
2.733
2.611
2.541
2.475
2.159
2.072
1.975
1.790
1.176
1.153
1.053
1.032
H
N
chloroform - d1
6.21
0.96
2.00
0.94
0.99
1.02
2.24
3.01
3.92
8.0
7.0
6.0
5.0
4.0
3.0
2.0
1.0
0.0
Chemical Shift (ppm)

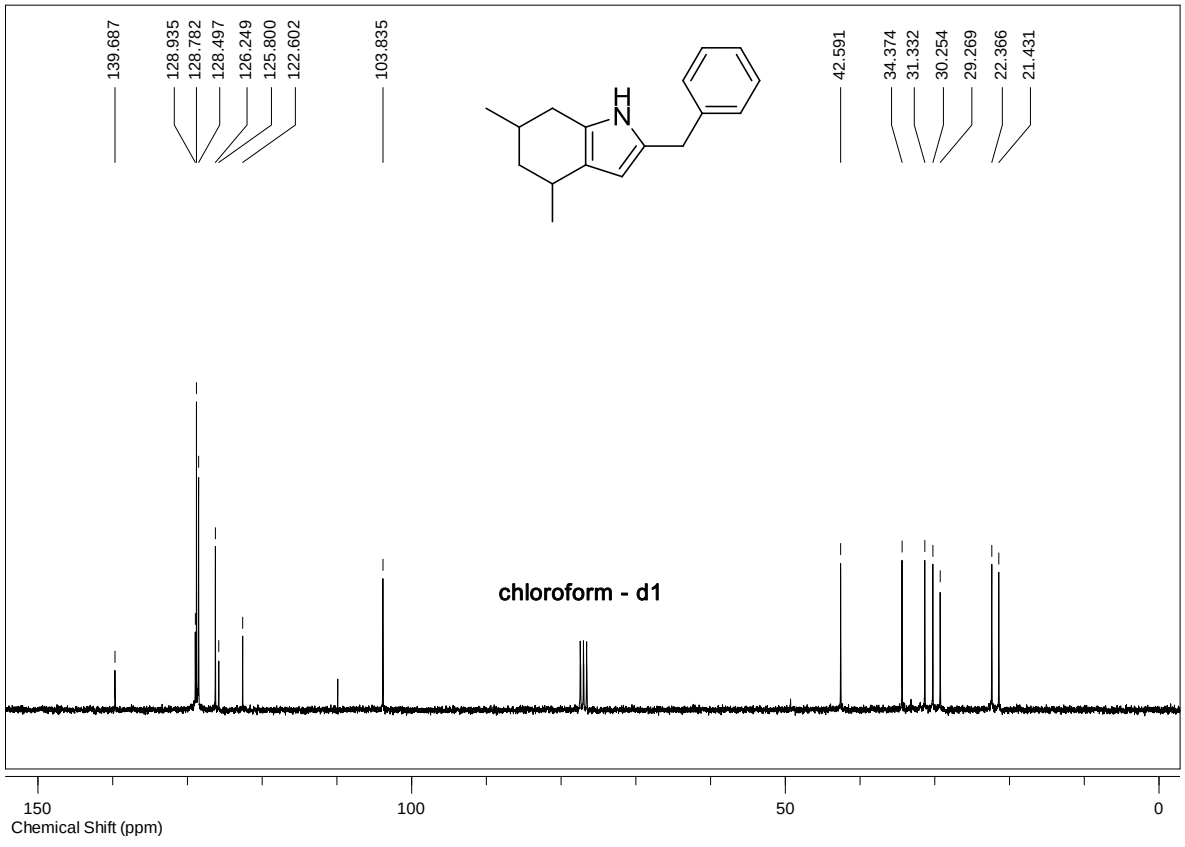
139.687
128.935
128.782
128.497
126.249
125.800
122.602
103.835
42.591
34.374
31.332
30.254
29.269
22.366
21.431
H
N
chloroform - d1
150
100
50
0
Chemical Shift (ppm)

1f:

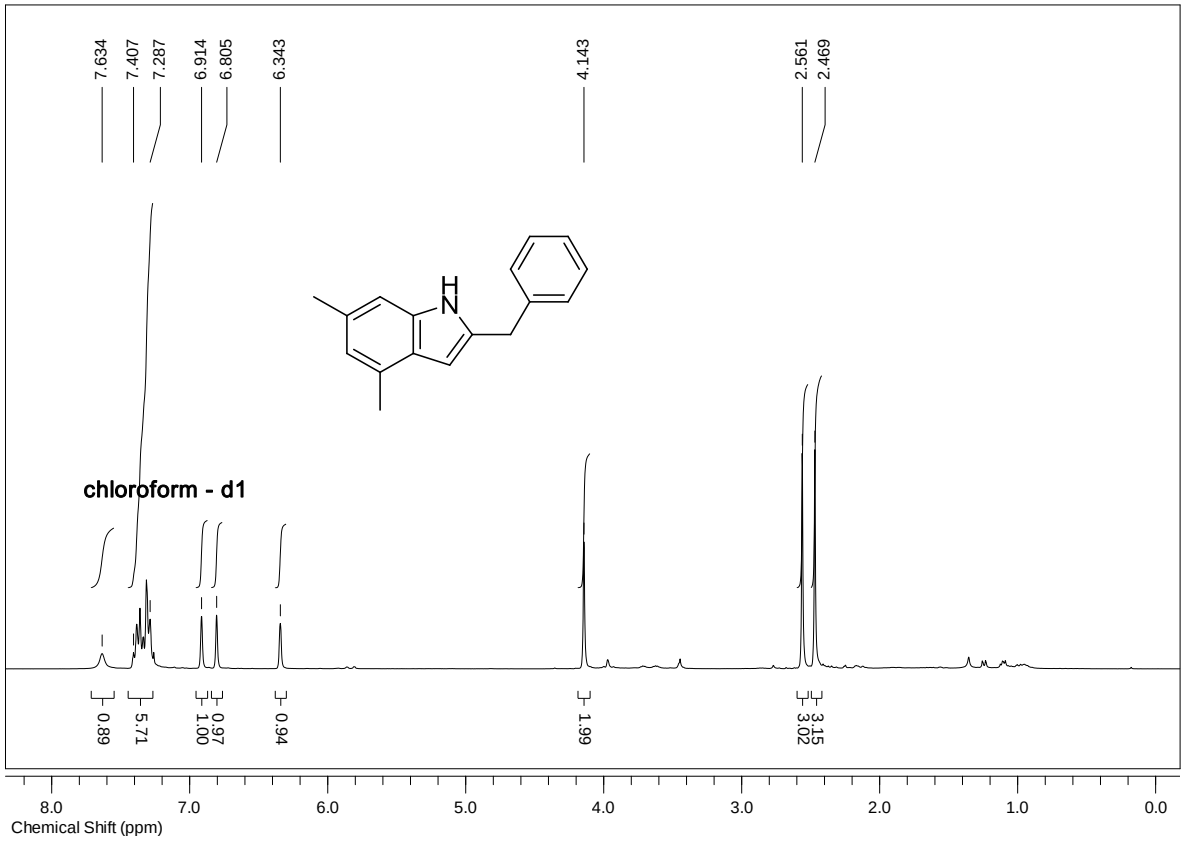
7.634
7.407
7.287
6.914
6.805
6.343
4.143
2.561
2.469
H
N
chloroform - d1
0.89
5.71
1.00
0.97
0.94
1.99
3.02
3.15
8.0
7.0
6.0
5.0
4.0
3.0
2.0
1.0
0.0
Chemical Shift (ppm)

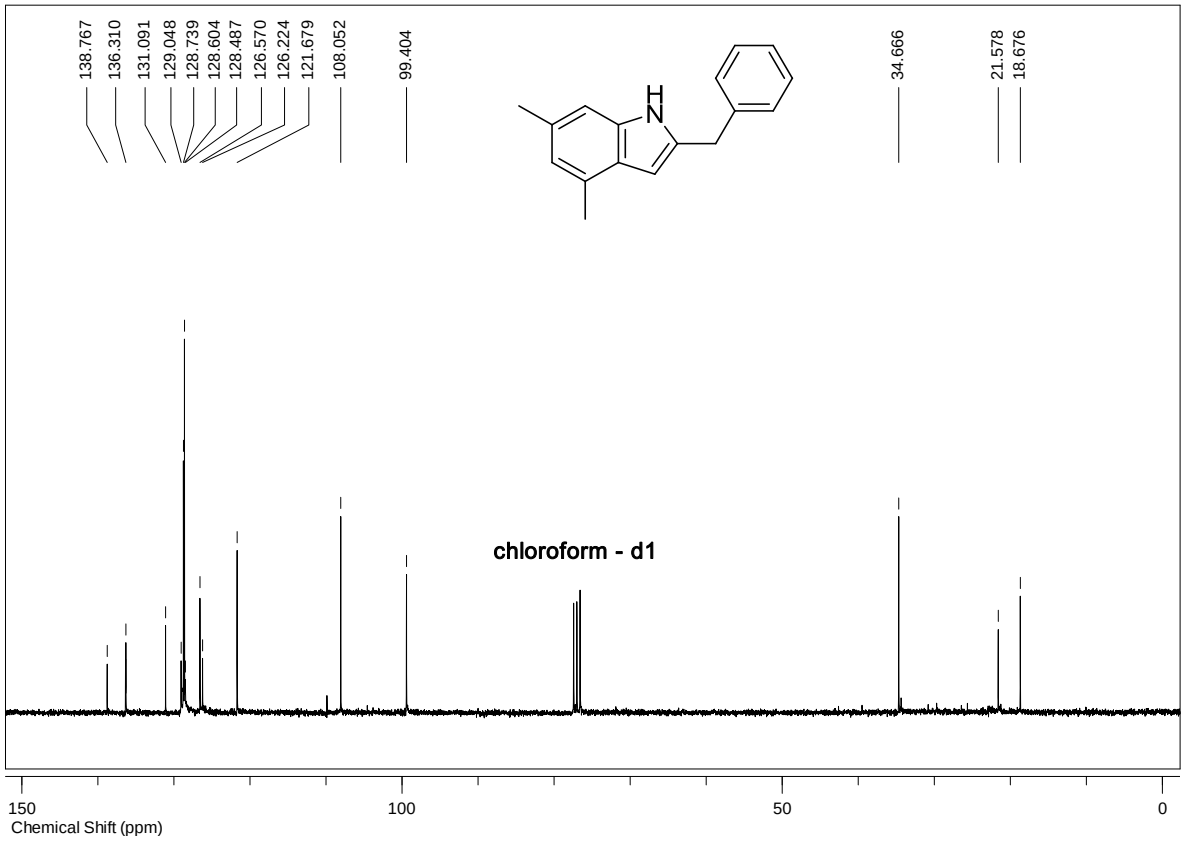
138.767
136.310
131.091
129.048
128.739
128.604
128.487
126.570
126.224
121.679
108.052
99.404
34.666
21.578
18.676
H
N
chloroform - d1
150
100
50
0
Chemical Shift (ppm)

2H-1g:

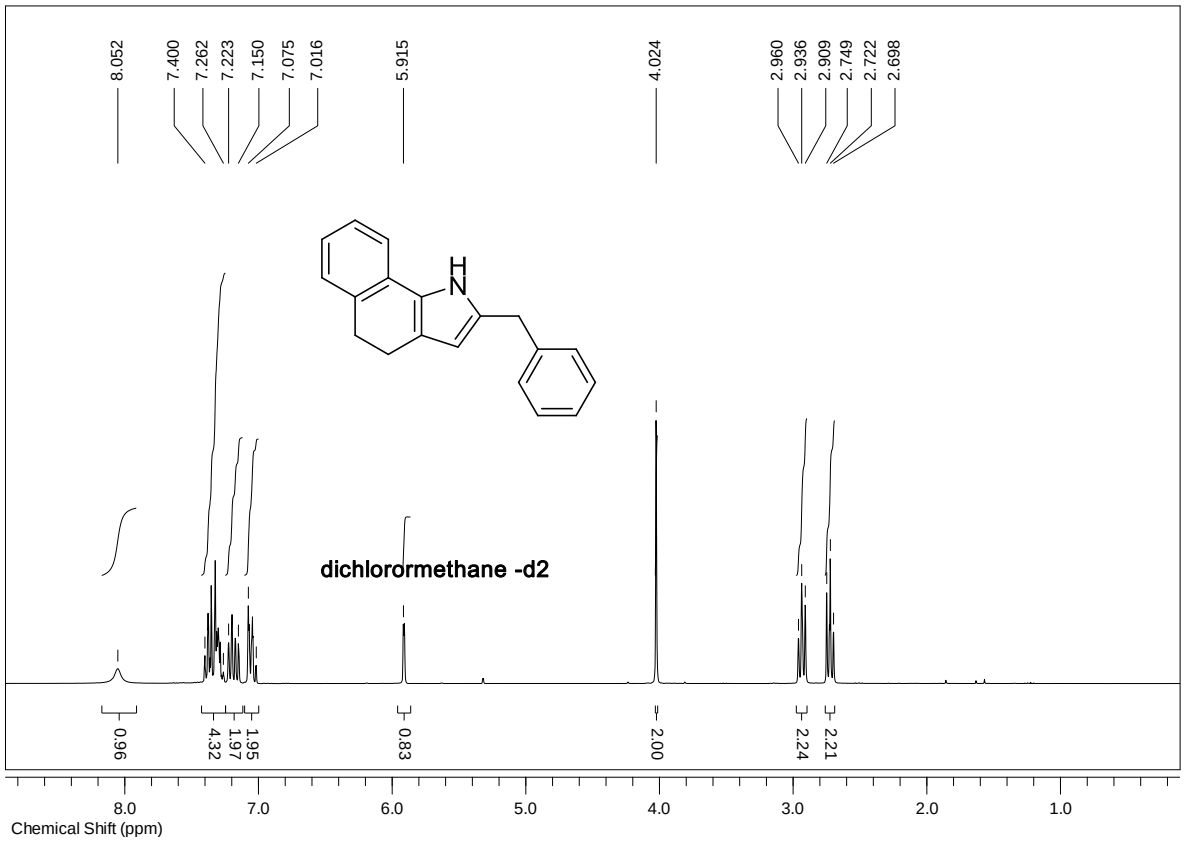
8.052
7.400
7.262
7.223
7.150
7.075
7.016
5.915
4.024
2.960
2.936
2.909
2.749
2.722
2.698
H
N
dichlorormethane -d2
0.96
4.32
1.67
1.65
0.83
2.00
2.24
2.21
8.0
7.0
6.0
5.0
4.0
3.0
2.0
1.0
Chemical Shift (ppm)

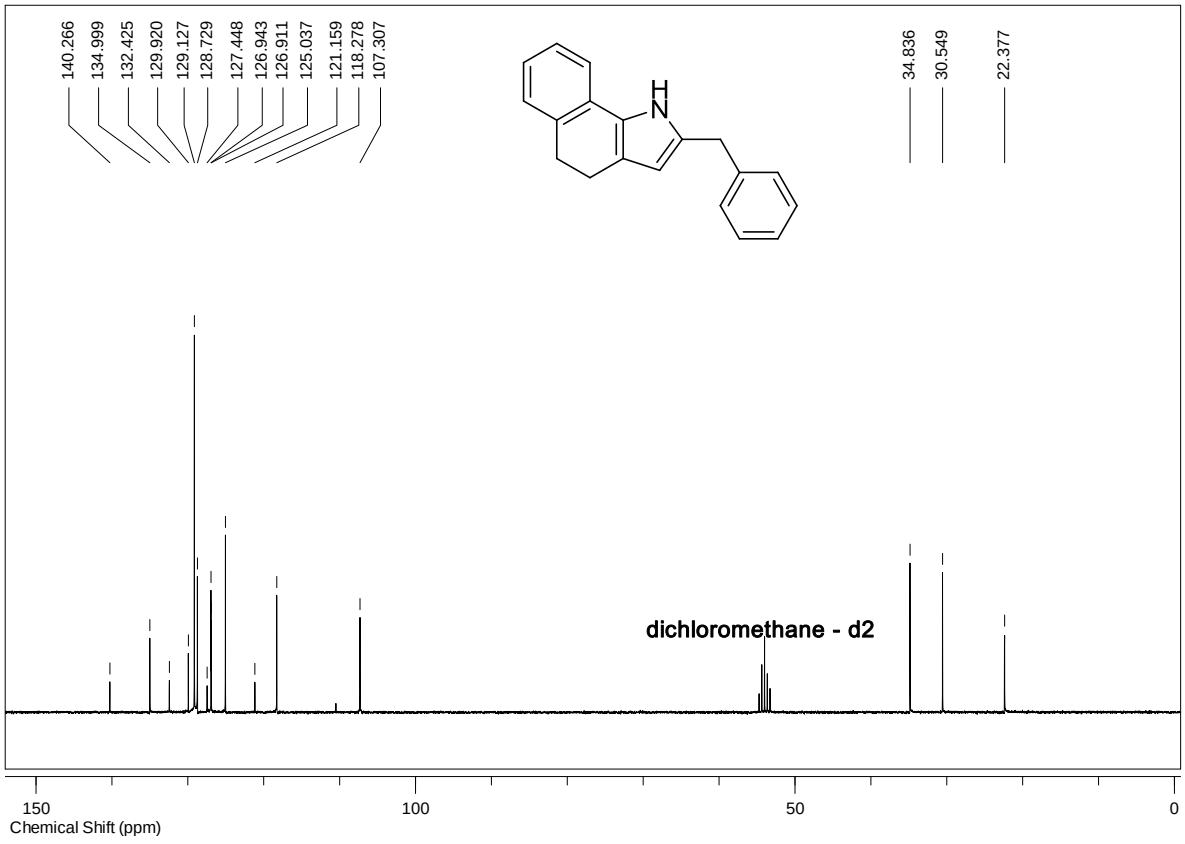
140.266
134.999
132.425
129.920
129.127
128.729
127.448
126.943
126.911
125.037
121.159
118.278
107.307
34.836
30.549
22.377
H
N
dichloromethane - d2
150
100
50
0
Chemical Shift (ppm)

1g:

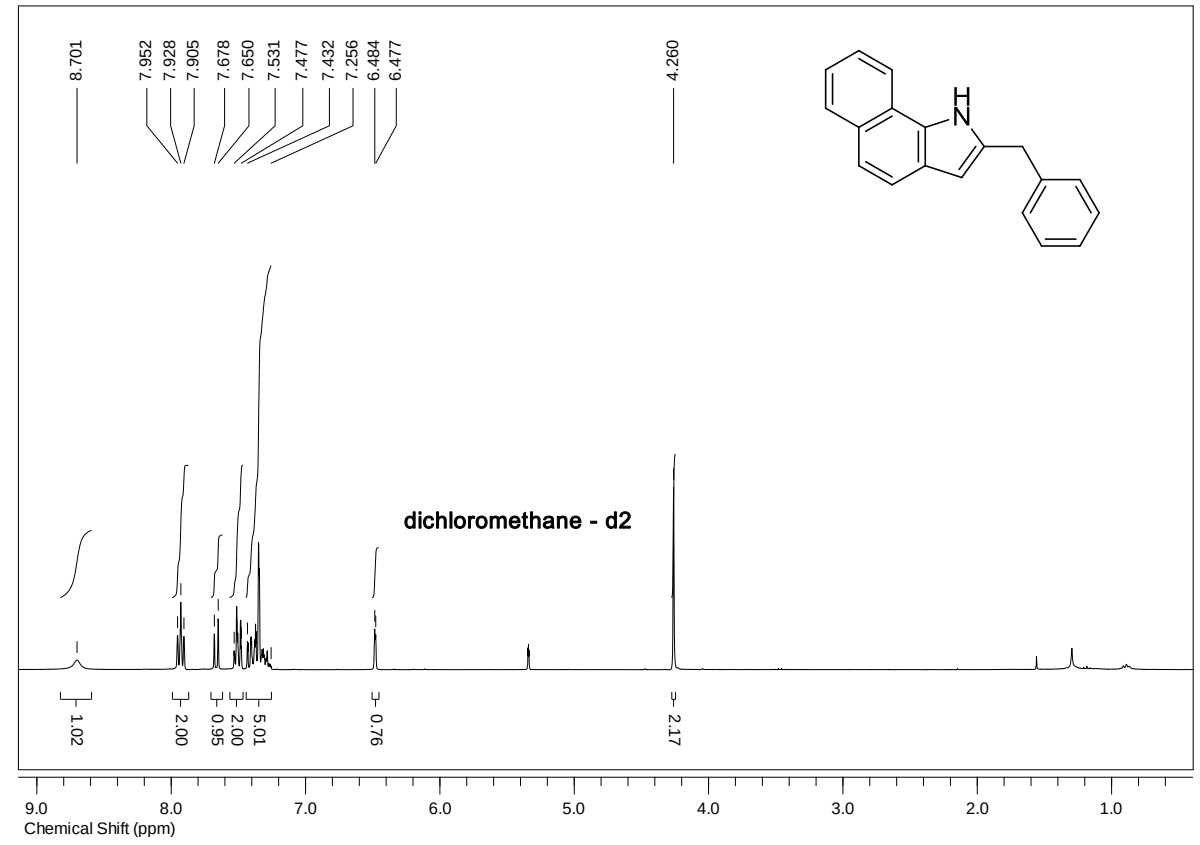
8.701
7.952
7.928
7.905
7.678
7.650
7.531
7.477
7.432
7.256
6.484
6.477
4.260
H
N
dichloromethane - d2
1.02
2.00
0.95
2.00
5.01
0.76
2.17
9.0
8.0
7.0
6.0
5.0
4.0
3.0
2.0
1.0
Chemical Shift (ppm)

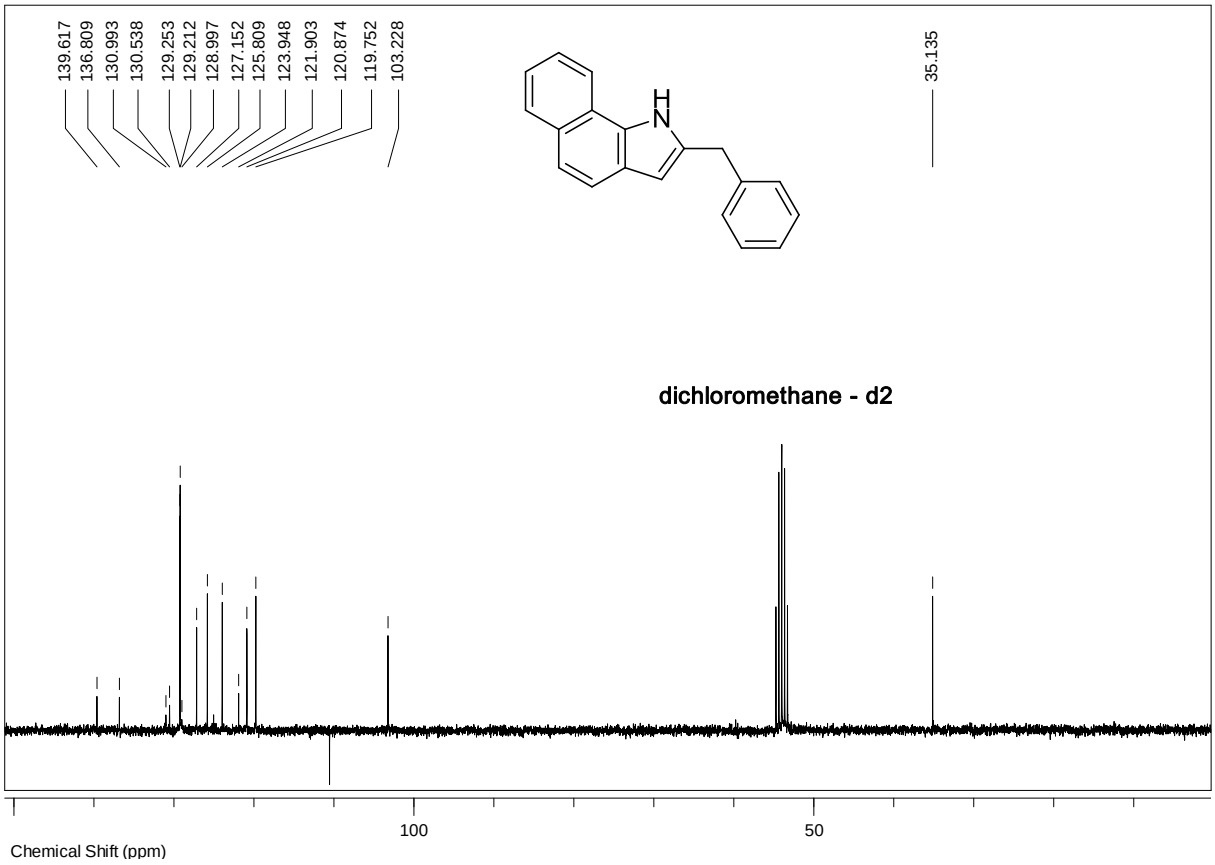
139.617
136.809
130.993
130.538
129.253
129.212
128.997
127.152
125.809
123.948
121.903
120.874
119.752
103.228
35.135
H
N
dichloromethane - d2
100
50
Chemical Shift (ppm)

2H-1h:

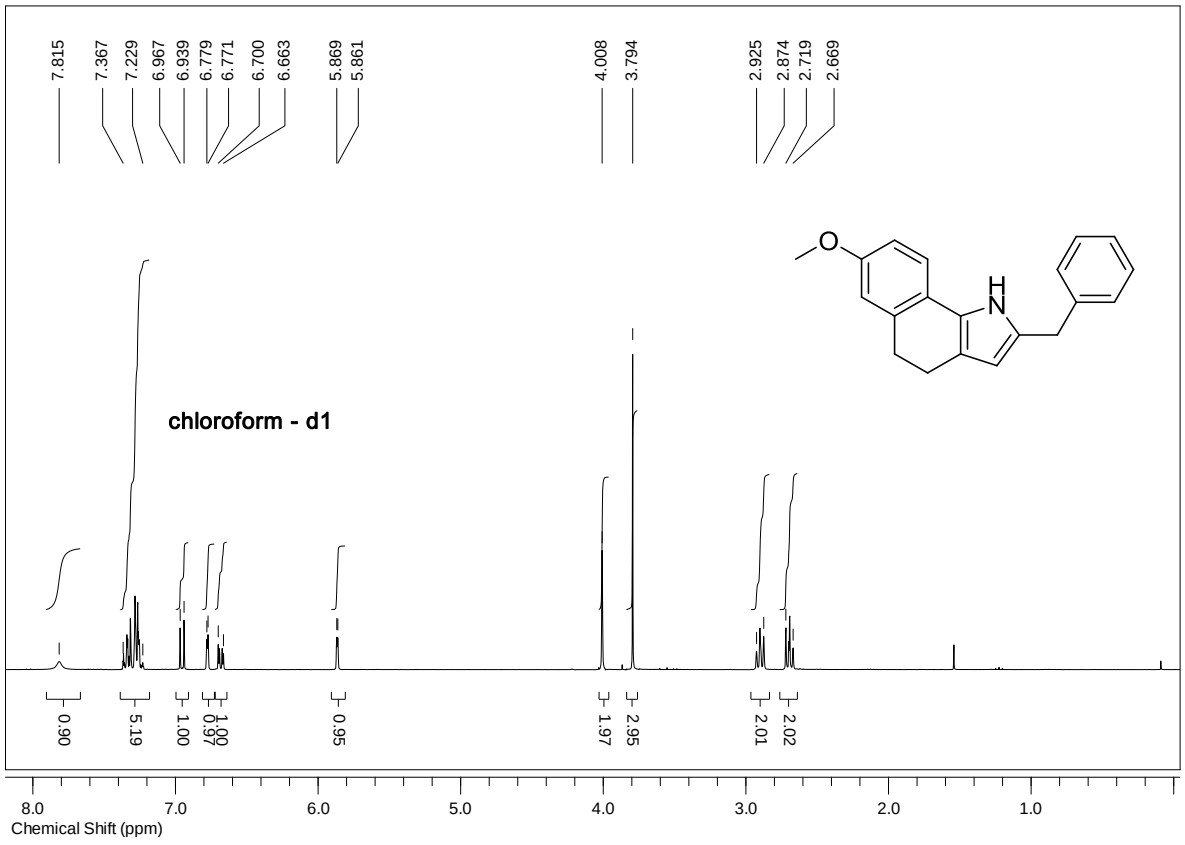
7.815
7.367
7.229
6.967
6.939
6.779
6.771
6.700
6.663
5.869
5.861
4.008
3.794
2.925
2.874
2.719
2.669
chloroform - d1
0.90
5.19
1.00
0.97
1.00
0.95
1.97
2.95
2.01
2.02
8.0
7.0
6.0
5.0
4.0
3.0
2.0
1.0
Chemical Shift (ppm)

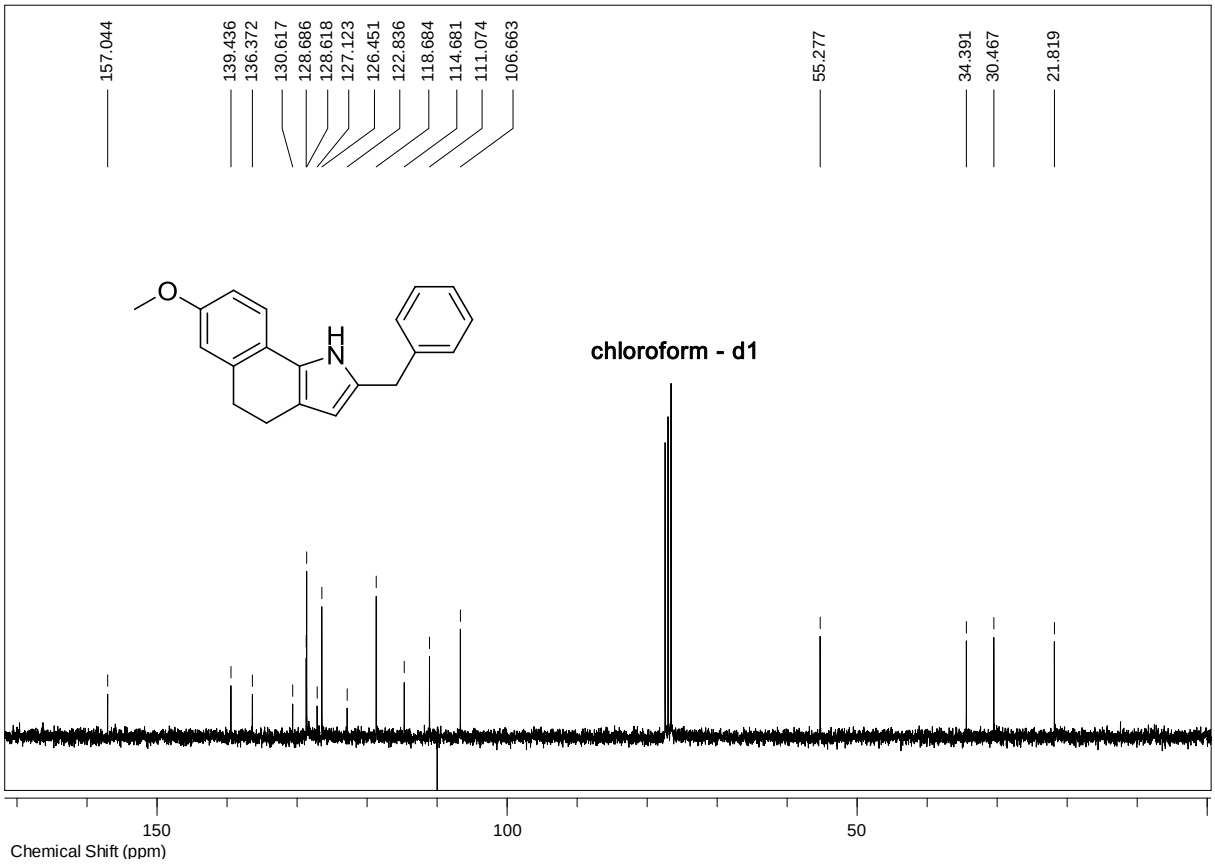
157.044
139.436
136.372
130.617
128.686
128.618
127.123
126.451
122.836
118.684
114.681
111.074
106.663
55.277
34.391
30.467
21.819
chloroform - d1
150
100
50
Chemical Shift (ppm)

1h:

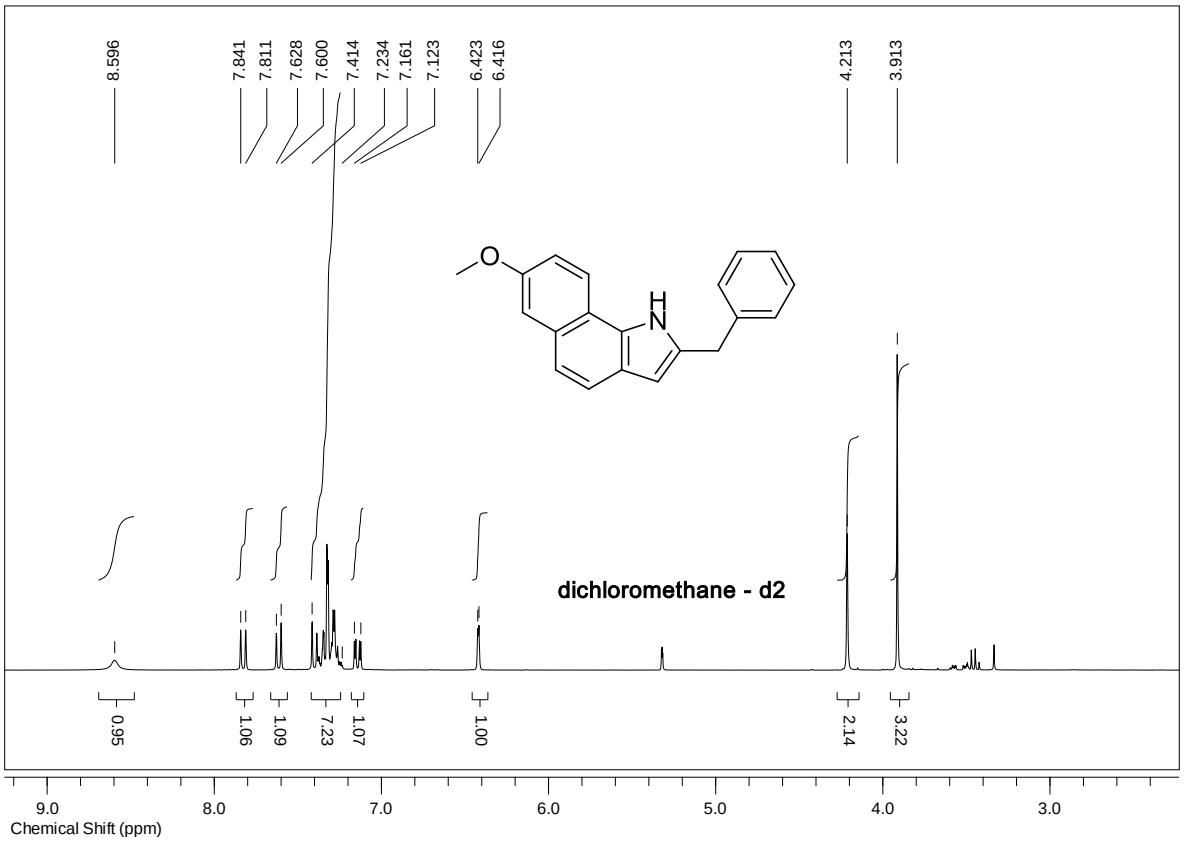
8.596
7.841
7.811
7.628
7.600
7.414
7.234
7.161
7.123
6.423
6.416
4.213
3.913
O
H
N
dichloromethane - d2
0.95
1.06
1.09
7.23
1.07
1.00
2.14
3.22
9.0
8.0
7.0
6.0
5.0
4.0
3.0
Chemical Shift (ppm)

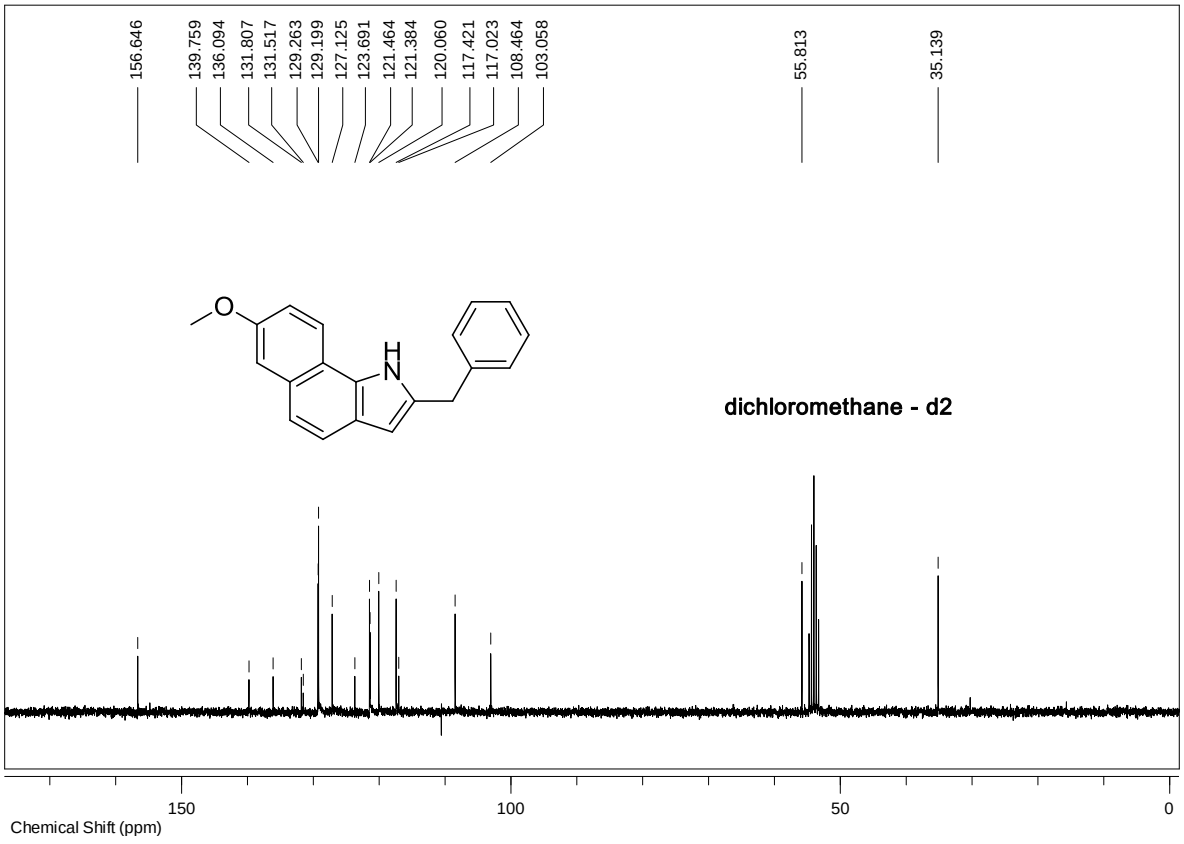
156.646
139.759
136.094
131.807
131.517
129.263
129.199
127.125
123.691
121.464
121.384
120.060
117.421
117.023
108.464
103.058
55.813
35.139
O
H
N
dichloromethane - d2
150
100
50
0
Chemical Shift (ppm)

4H-1i:

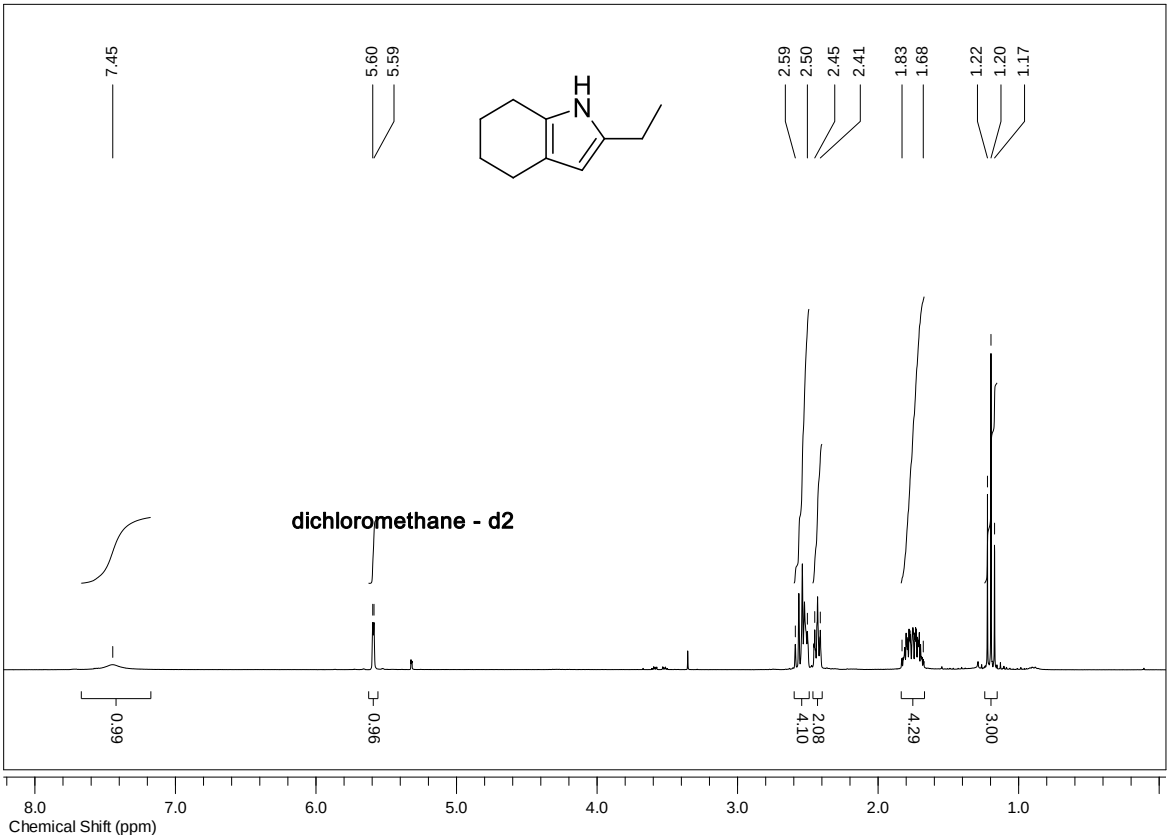
7.45
5.60
5.59
2.59
2.50
2.45
2.41
1.83
1.68
1.22
1.20
1.17
dichloromethane - d2
0.99
0.96
4.10
2.08
4.29
3.00
8.0
7.0
6.0
5.0
4.0
3.0
2.0
1.0
Chemical Shift (ppm)

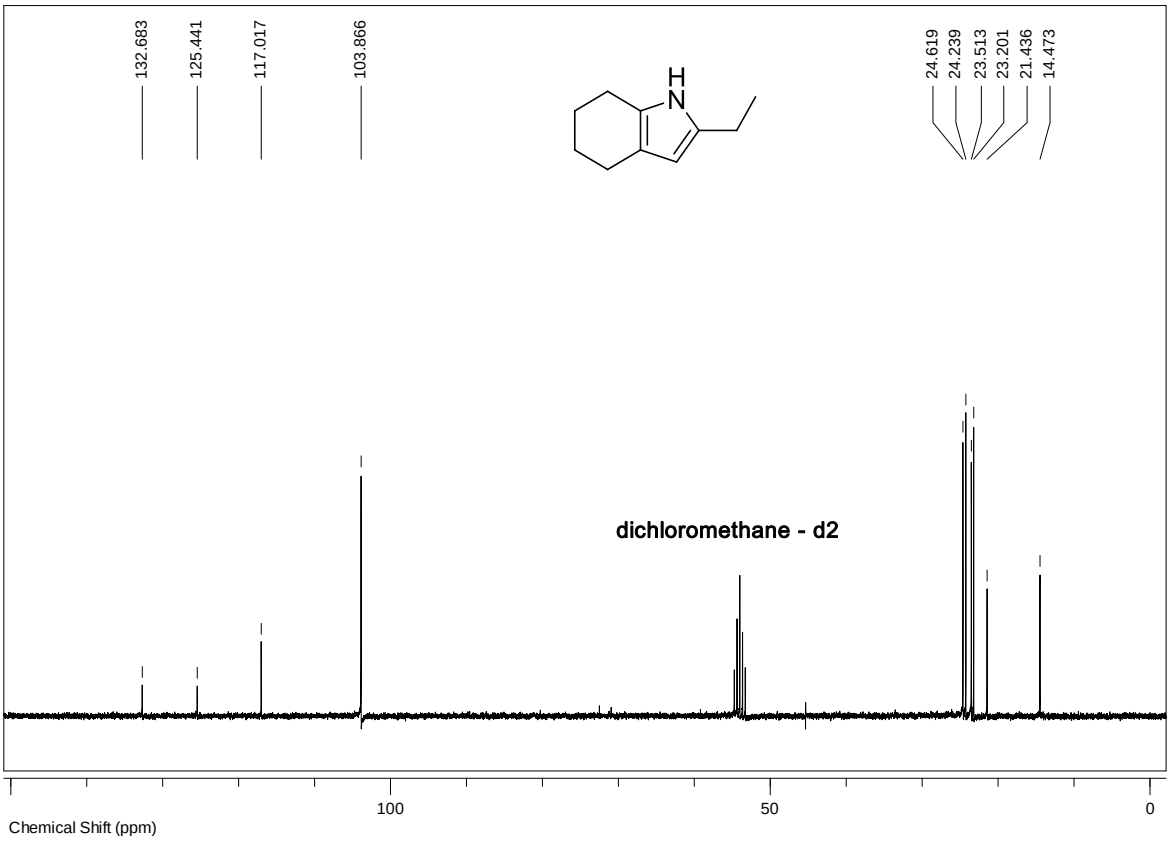
132.683
125.441
117.017
103.866
24.619
24.239
23.513
23.201
21.436
14.473
dichloromethane - d2
100
50
0
Chemical Shift (ppm)

1i:

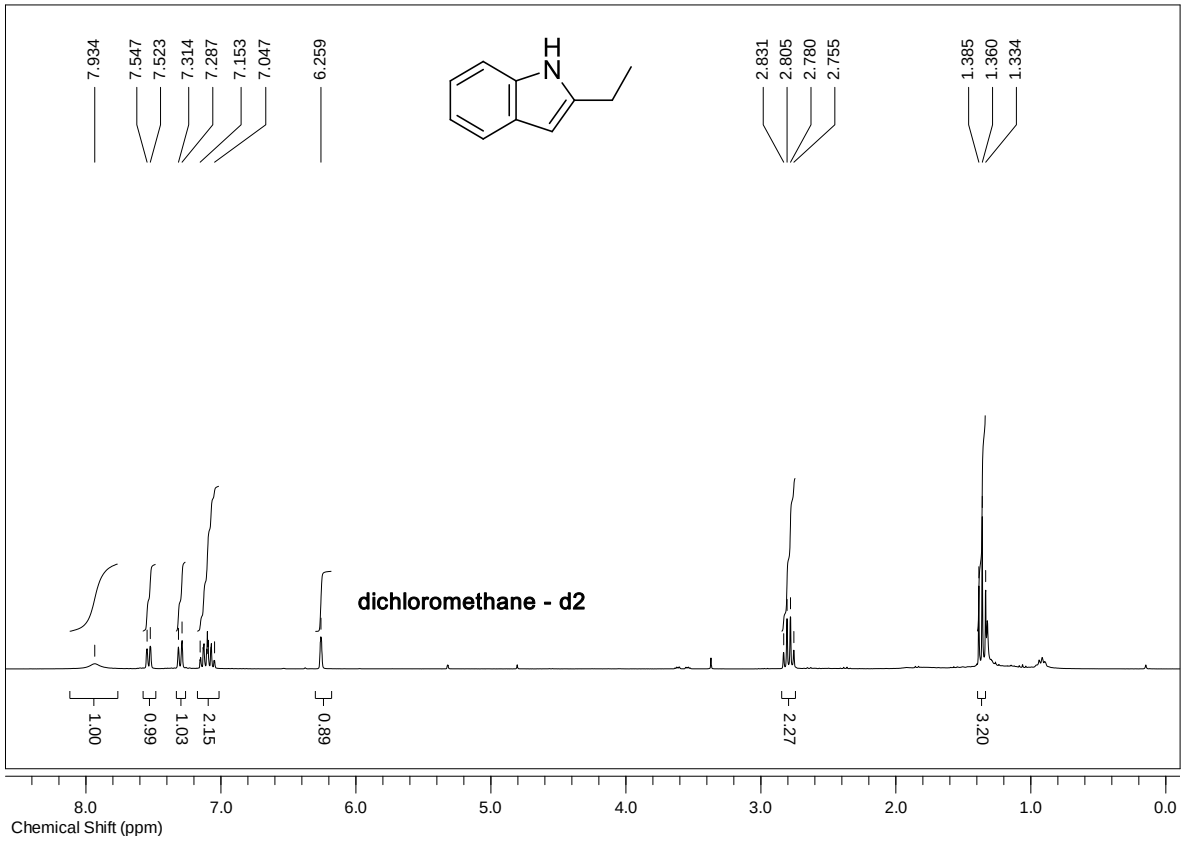
7.934
7.547
7.523
7.314
7.287
7.153
7.047
6.259
2.831
2.805
2.780
2.755
1.385
1.360
1.334
dichloromethane - d2
1.00
0.99
1.03
2.15
0.89
2.27
3.20
8.0
7.0
6.0
5.0
4.0
3.0
2.0
1.0
0.0
Chemical Shift (ppm)

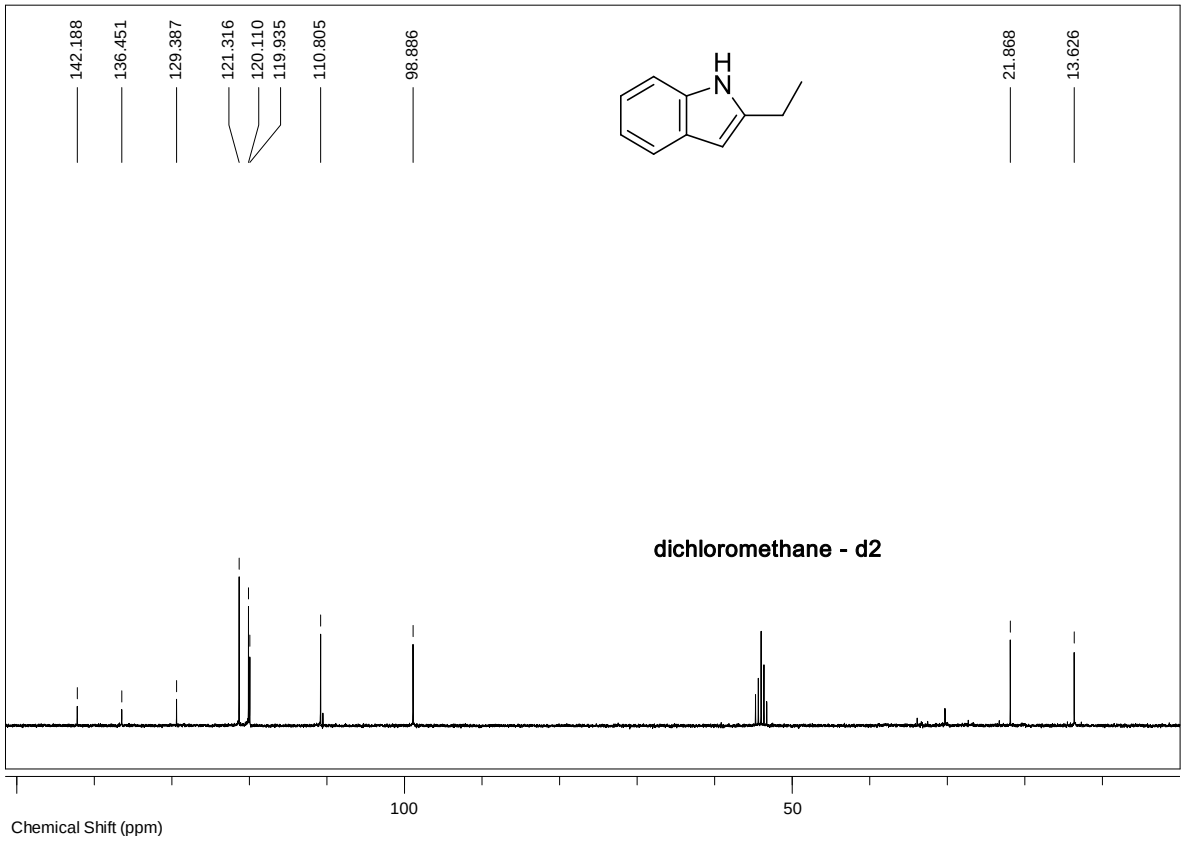
142.188
136.451
129.387
121.316
120.110
119.935
110.805
98.886
21.868
13.626
dichloromethane - d2
100
50
Chemical Shift (ppm)

4H-1j:

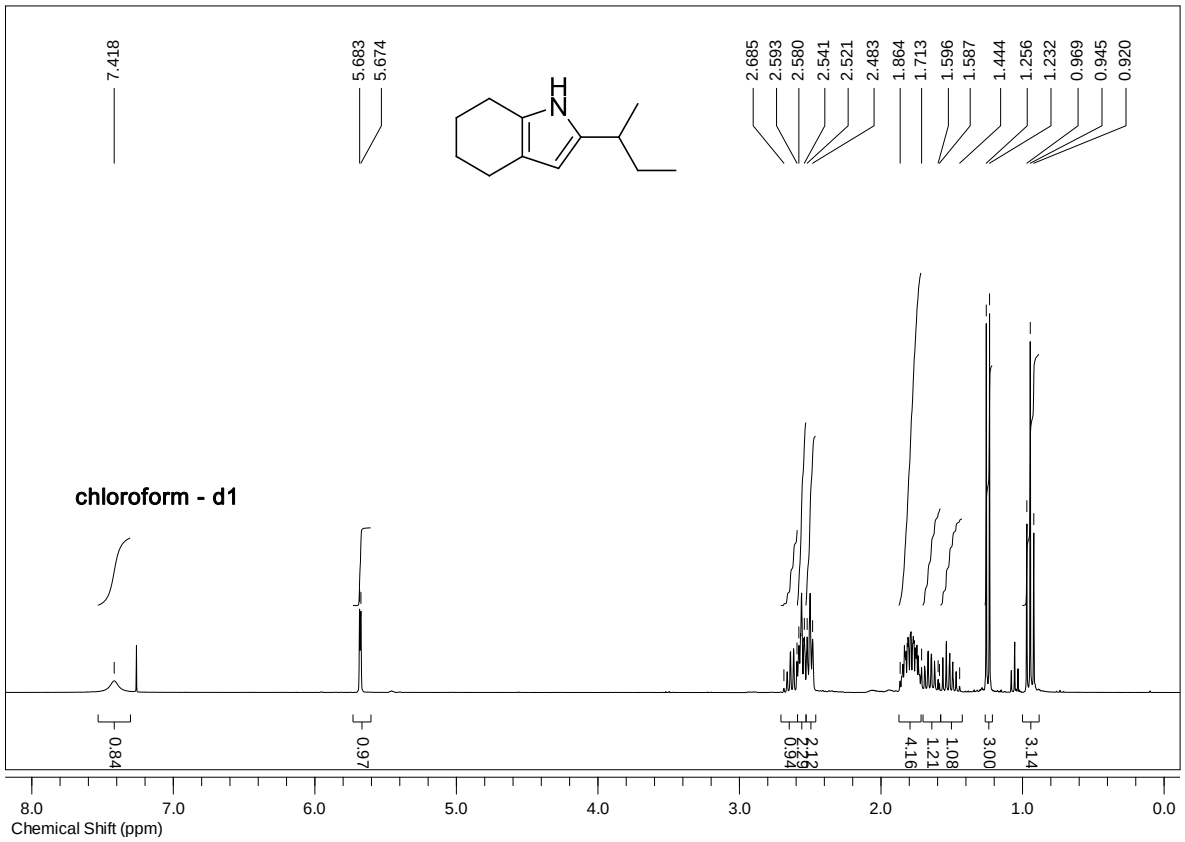
7.418
5.683
5.674
2.685
2.593
2.580
2.541
2.521
2.483
1.864
1.713
1.596
1.587
1.444
1.256
1.232
0.969
0.945
0.920
chloroform - d1
0.84
0.97
0.94
4.16
1.21
1.08
3.00
3.14
8.0
7.0
6.0
5.0
4.0
3.0
2.0
1.0
0.0
Chemical Shift (ppm)

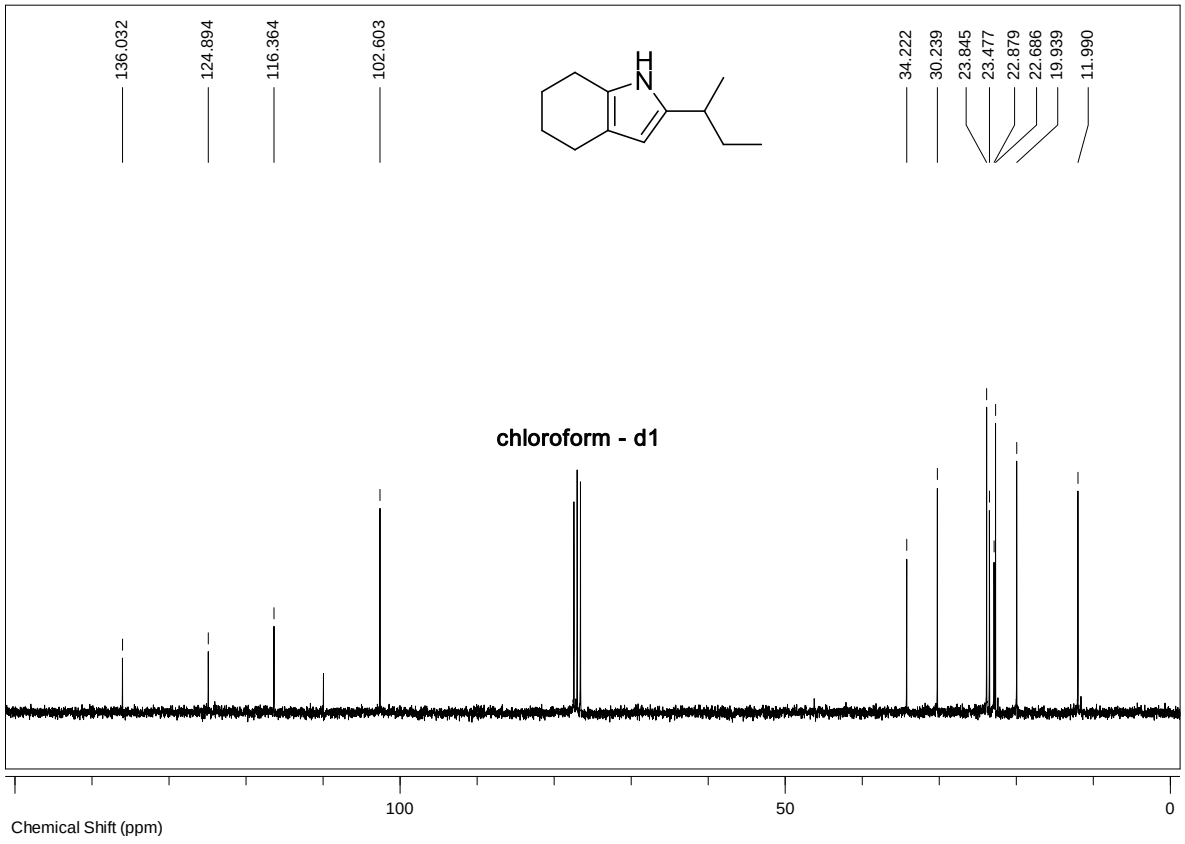
136.032
124.894
116.364
102.603
34.222
30.239
23.845
23.477
22.879
22.686
19.939
11.990
chloroform - d1
100
50
0
Chemical Shift (ppm)

1j:

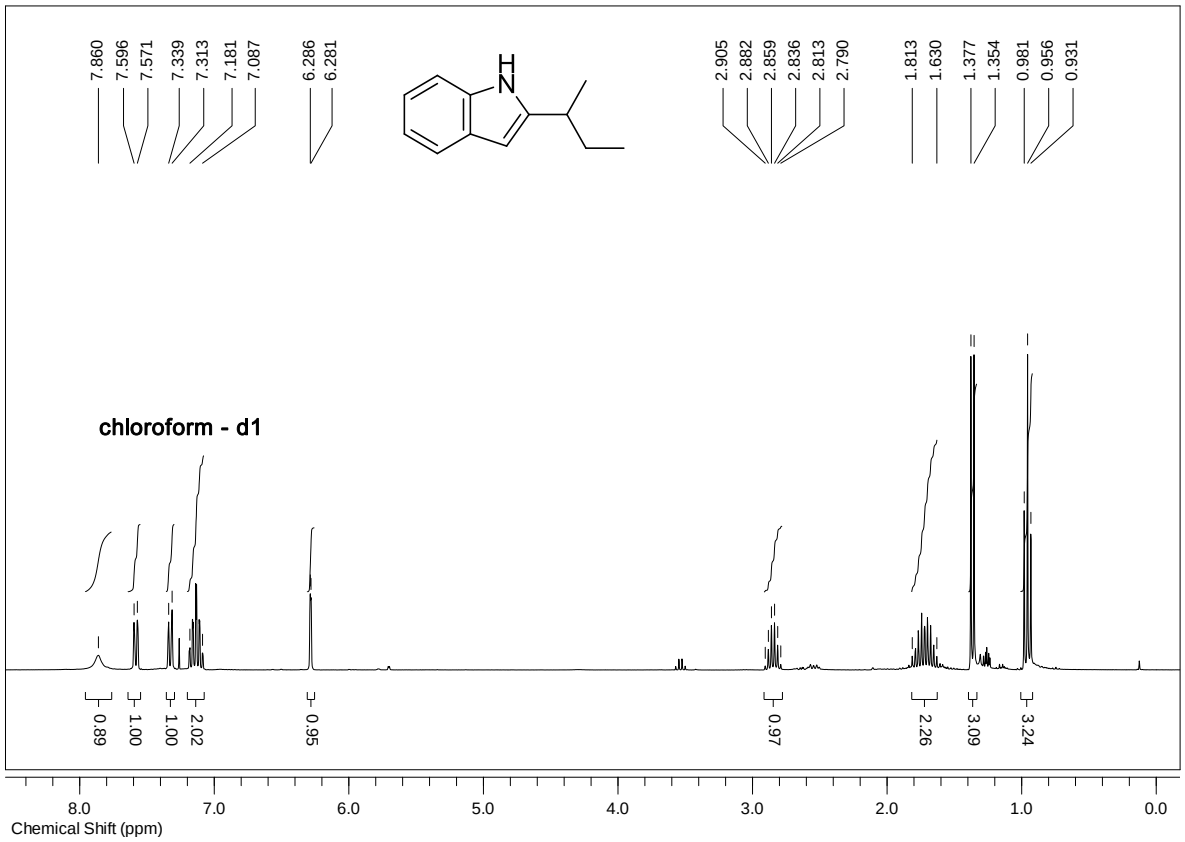
7.860
7.596
7.571
7.339
7.313
7.181
7.087
6.286
6.281
2.905
2.882
2.859
2.836
2.813
2.790
1.813
1.630
1.377
1.354
0.981
0.956
0.931
chloroform - d1
0.89
1.00
1.00
2.02
0.95
0.97
2.26
3.09
3.24
8.0
7.0
6.0
5.0
4.0
3.0
2.0
1.0
0.0
Chemical Shift (ppm)

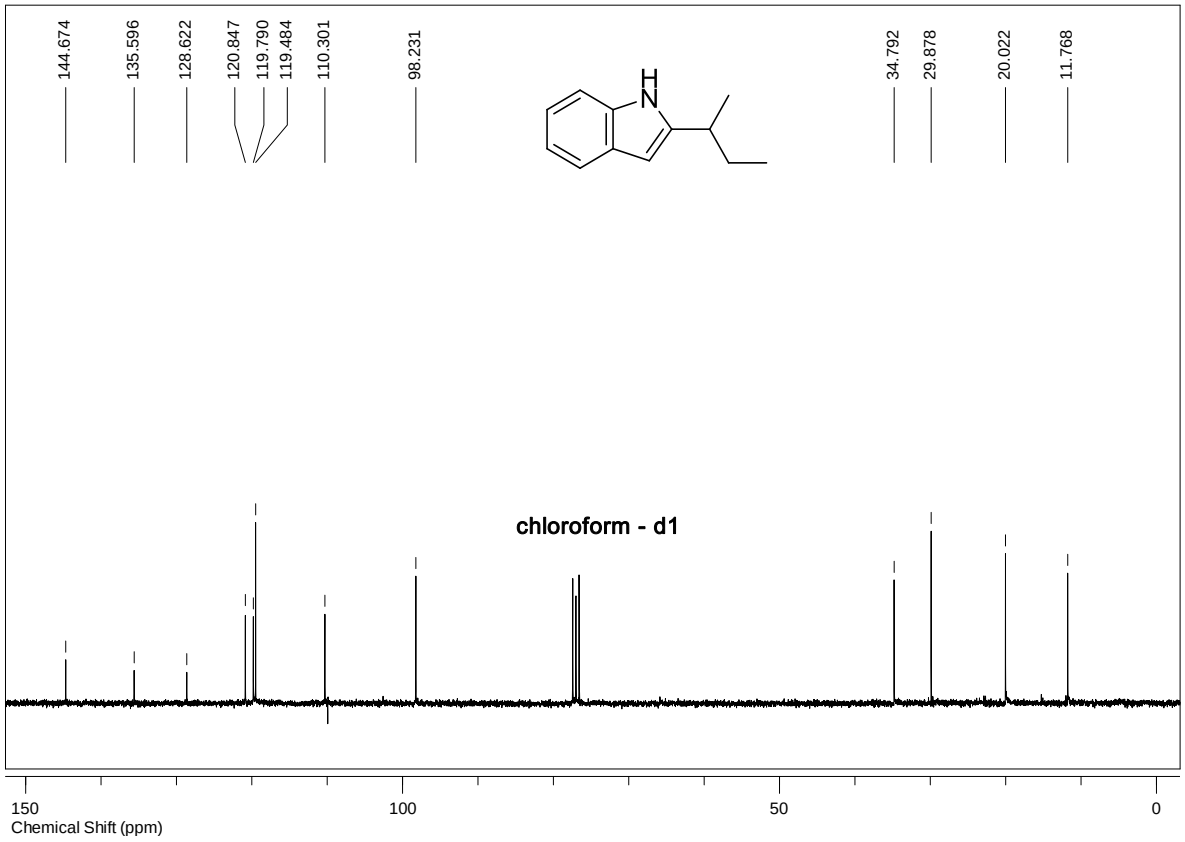
144.674
135.596
128.622
120.847
119.790
119.484
110.301
98.231
34.792
29.878
20.022
11.768
chloroform - d1
150
100
50
0
Chemical Shift (ppm)

4H-1k:

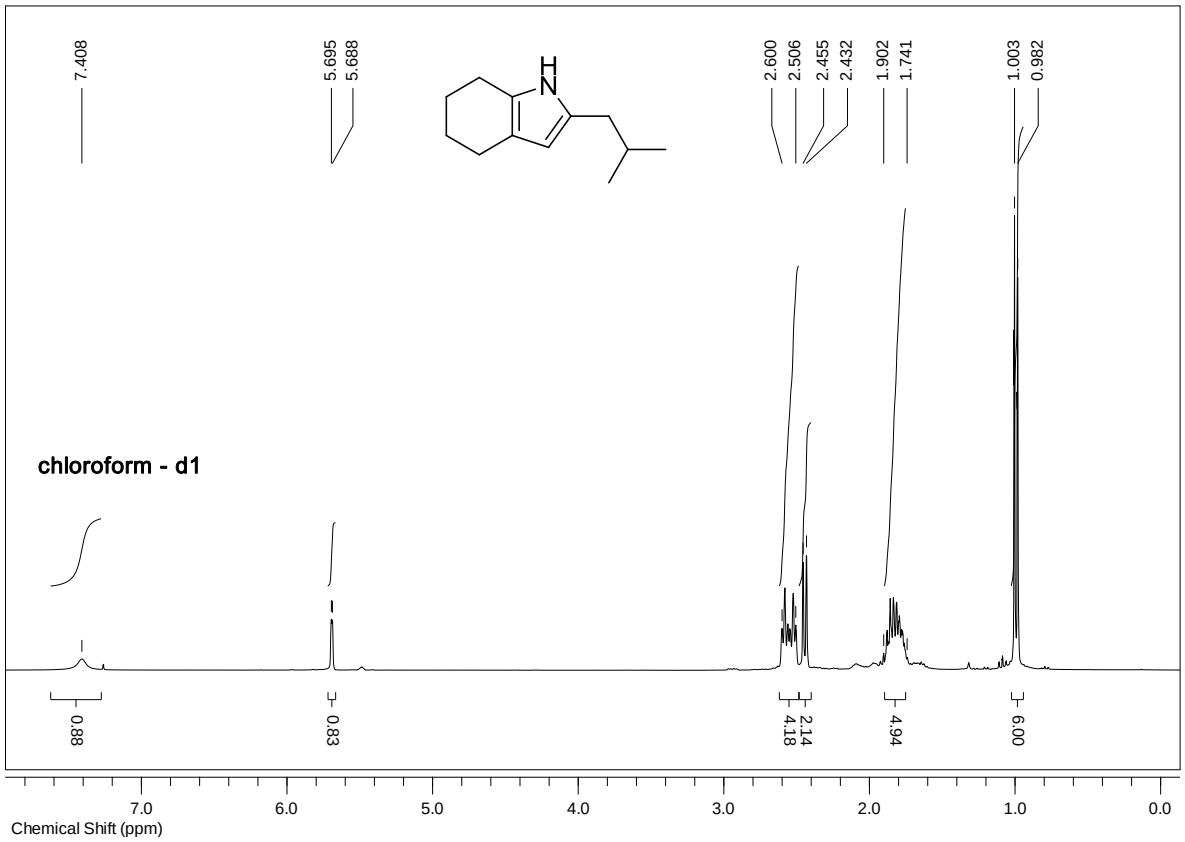
7.408
5.695
5.688
2.600
2.506
2.455
2.432
1.902
1.741
1.003
0.982
chloroform - d1
0.88
0.83
2.14
4.18
4.64
6.00
7.0
6.0
5.0
4.0
3.0
2.0
1.0
0.0
Chemical Shift (ppm)

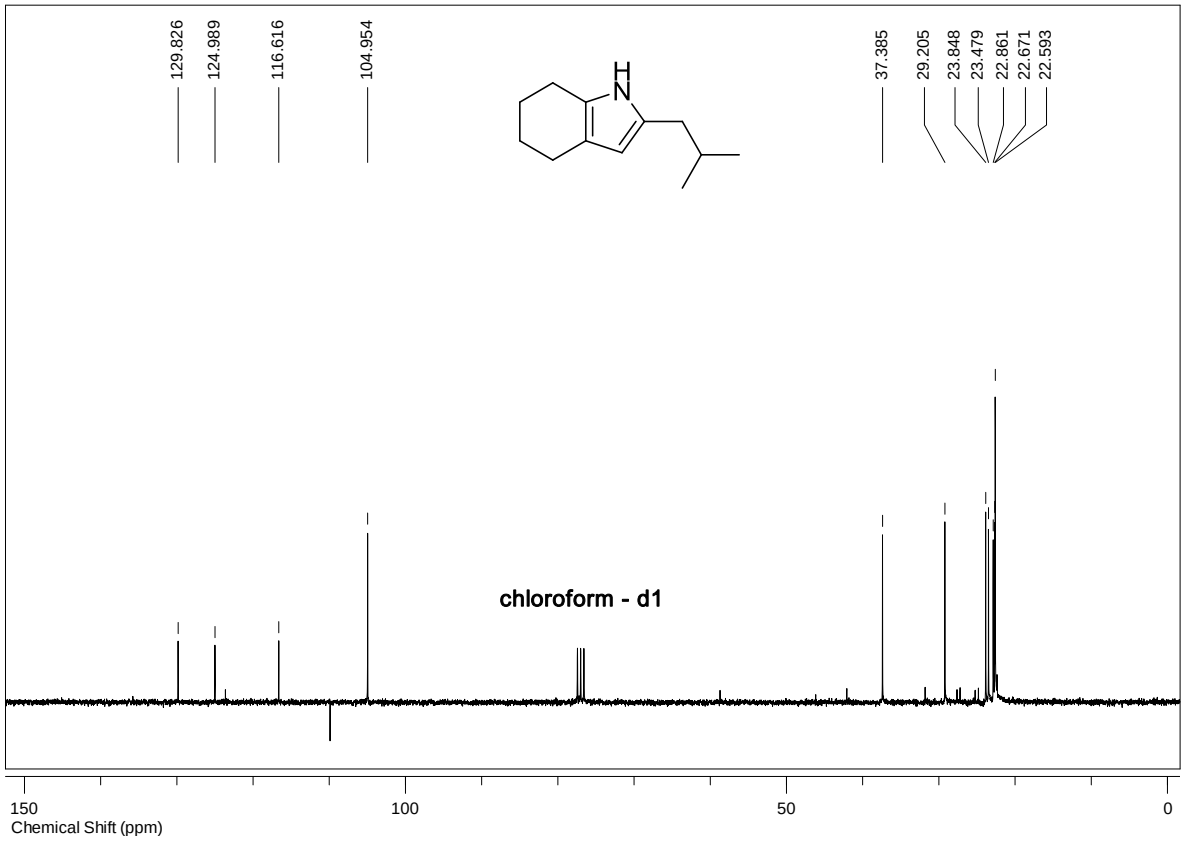
129.826
124.989
116.616
104.954
37.385
29.205
23.848
23.479
22.861
22.671
22.593
chloroform - d1
150
100
50
0
Chemical Shift (ppm)

1k:

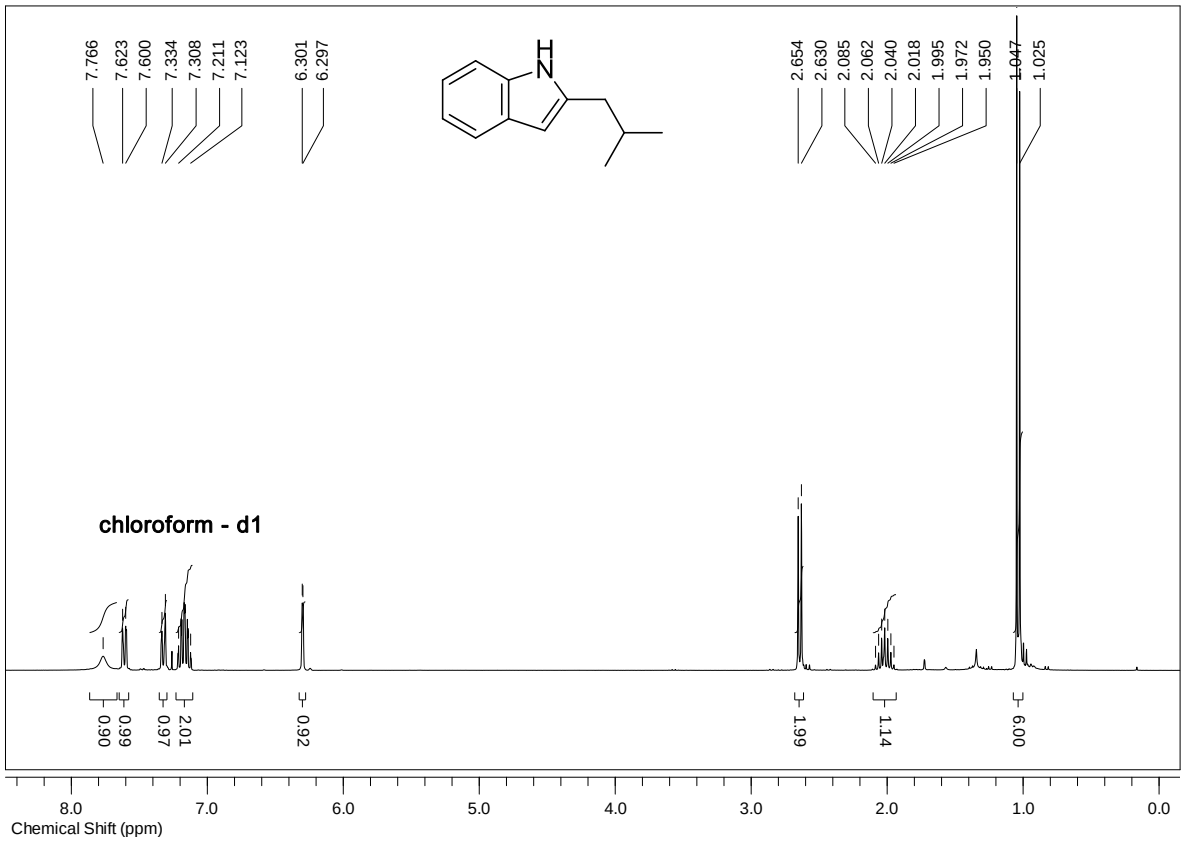
7.766
7.623
7.600
7.334
7.308
7.211
7.123
6.301
6.297
2.654
2.630
2.085
2.062
2.040
2.018
1.995
1.972
1.950
1.047
1.025
chloroform - d1
0.90
0.99
0.97
2.01
0.92
1.99
1.14
6.00
8.0
7.0
6.0
5.0
4.0
3.0
2.0
1.0
0.0
Chemical Shift (ppm)

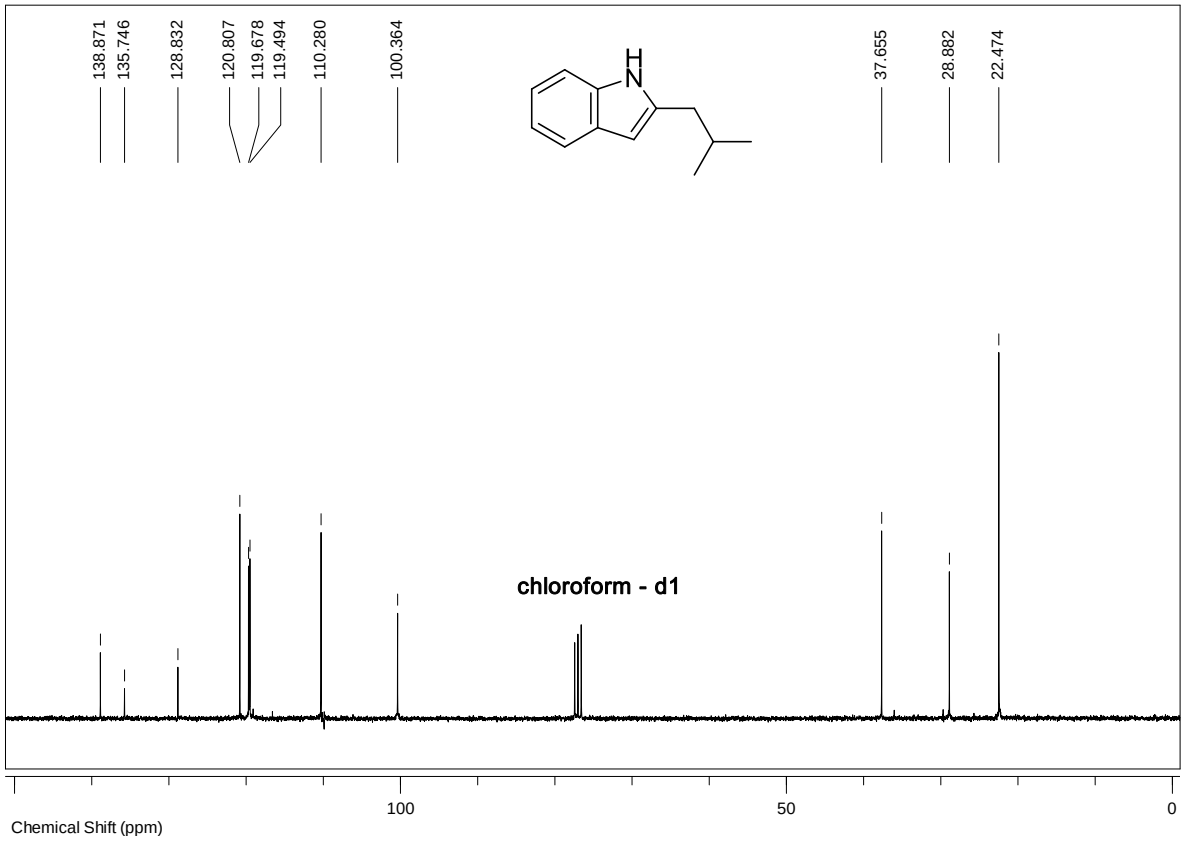
138.871
135.746
128.832
120.807
119.678
119.494
110.280
100.364
37.655
28.882
22.474
chloroform - d1
100
50
0
Chemical Shift (ppm)

4H-1l:

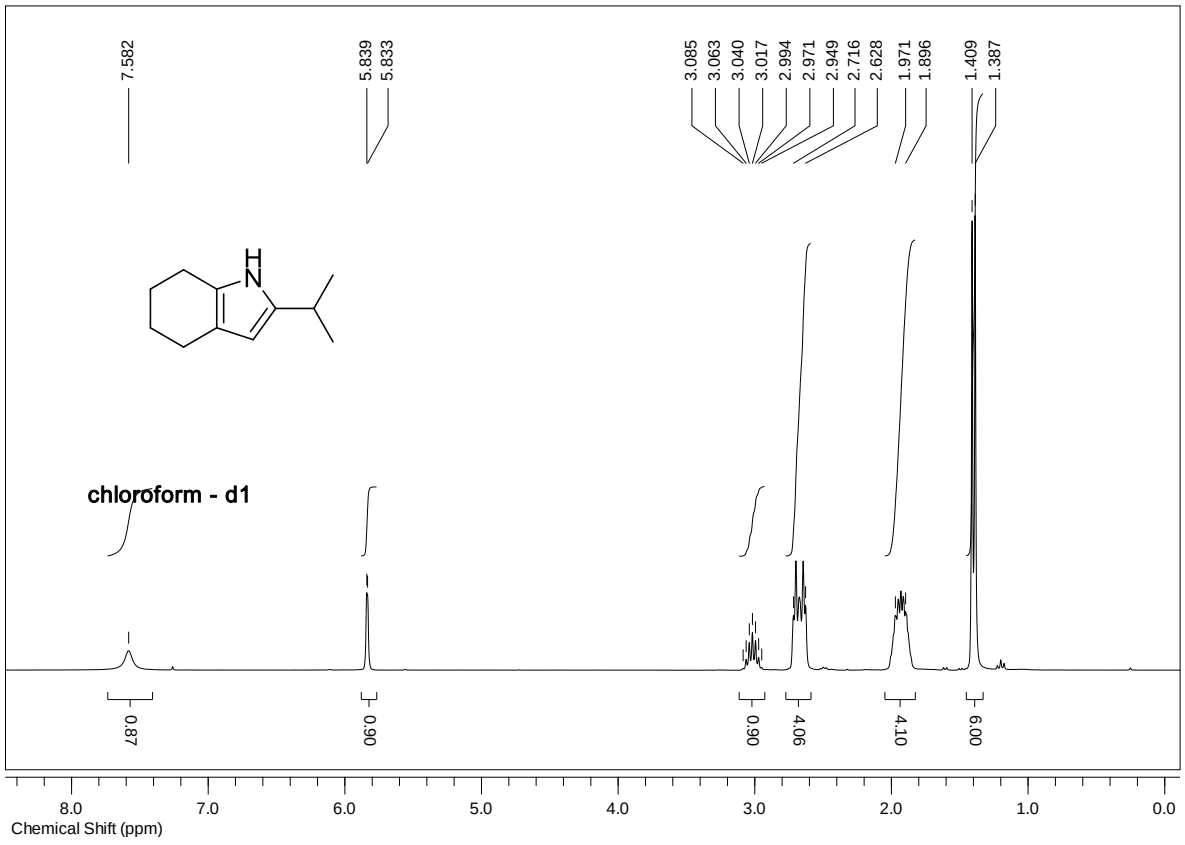
7.582
5.839
5.833
3.085
3.063
3.040
3.017
2.994
2.971
2.949
2.716
2.628
1.971
1.896
1.409
1.387
chloroform - d1
0.87
0.90
0.90
4.06
4.10
6.00
8.0
7.0
6.0
5.0
4.0
3.0
2.0
1.0
0.0
Chemical Shift (ppm)

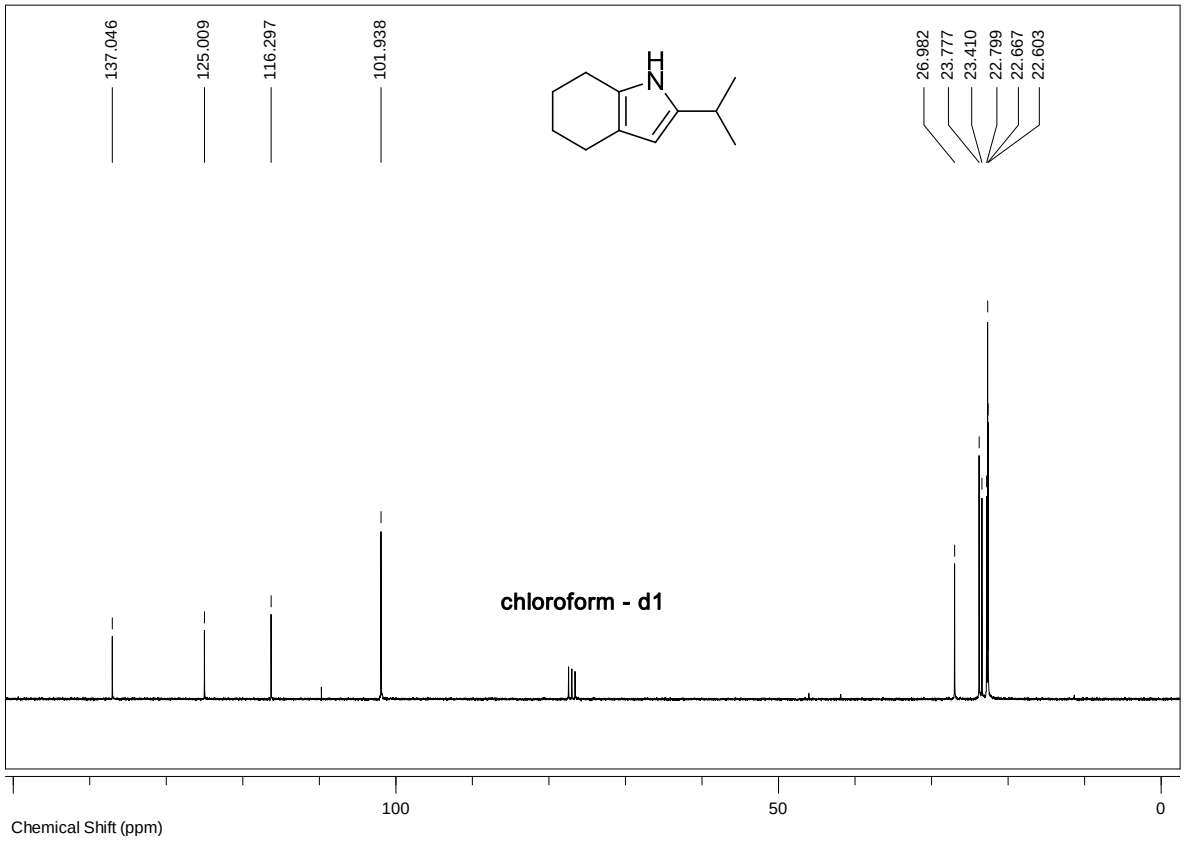
137.046
125.009
116.297
101.938
26.982
23.777
23.410
22.799
22.667
22.603
chloroform - d1
100
50
0
Chemical Shift (ppm)

1l:

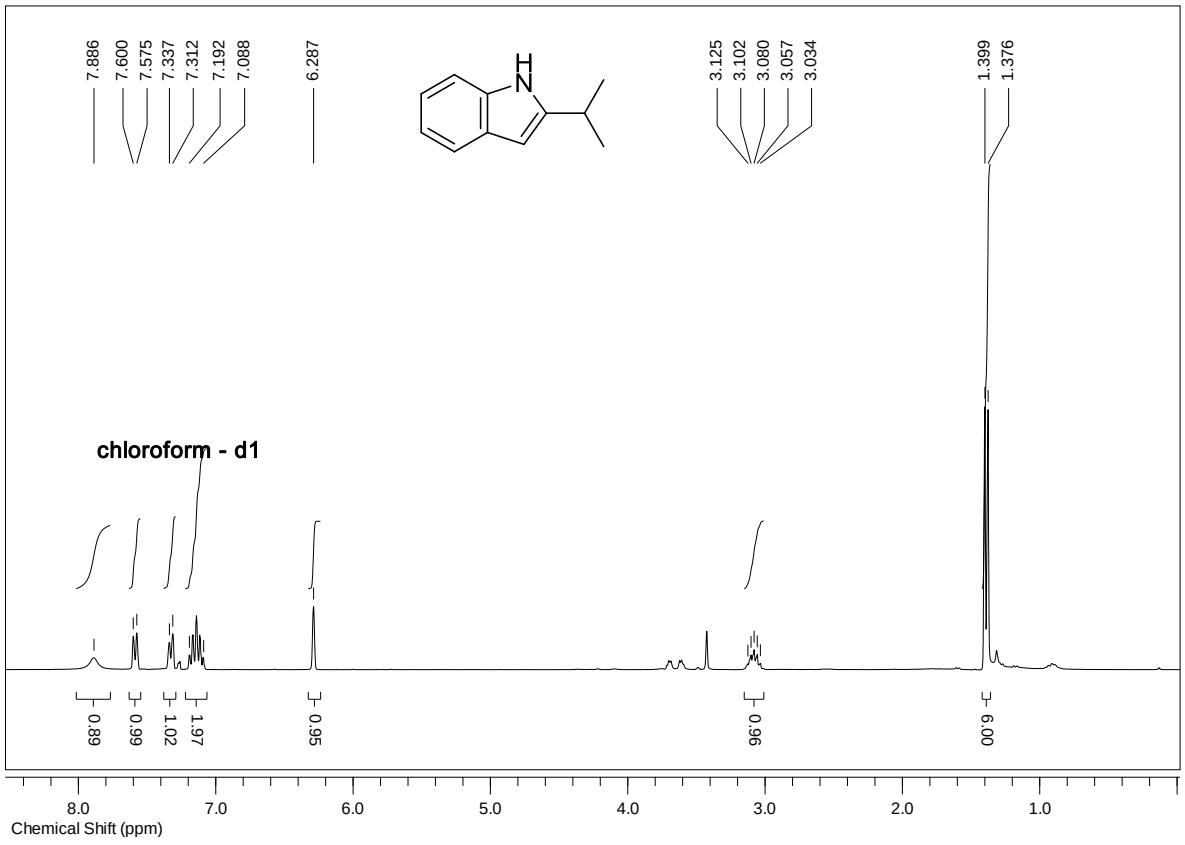
7.886
7.600
7.575
7.337
7.312
7.192
7.088
6.287
3.125
3.102
3.080
3.057
3.034
1.399
1.376
chloroform - d1
0.89
0.99
1.02
1.97
0.95
0.96
6.00
8.0
7.0
6.0
5.0
4.0
3.0
2.0
1.0
Chemical Shift (ppm)

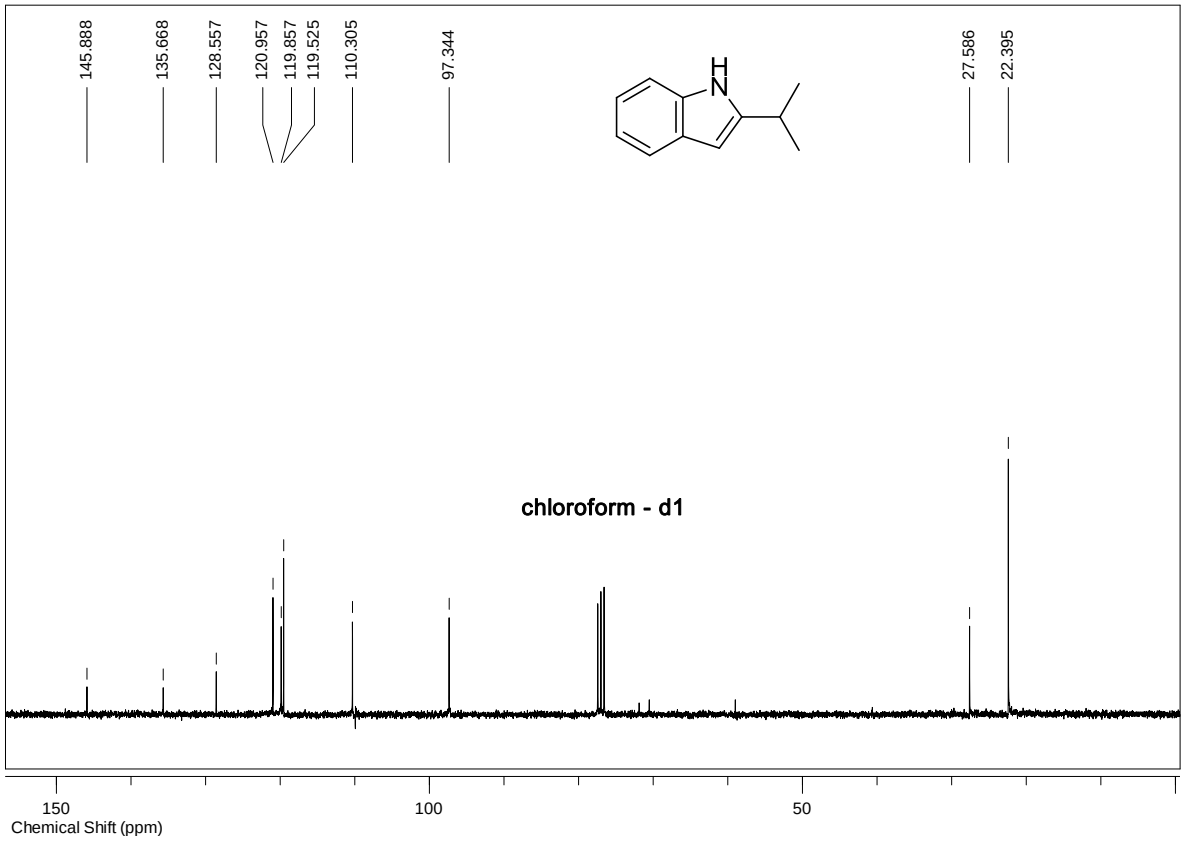
145.888
135.668
128.557
120.957
119.857
119.525
110.305
97.344
27.586
22.395
chloroform - d1
150
100
50
Chemical Shift (ppm)

4H-1m:

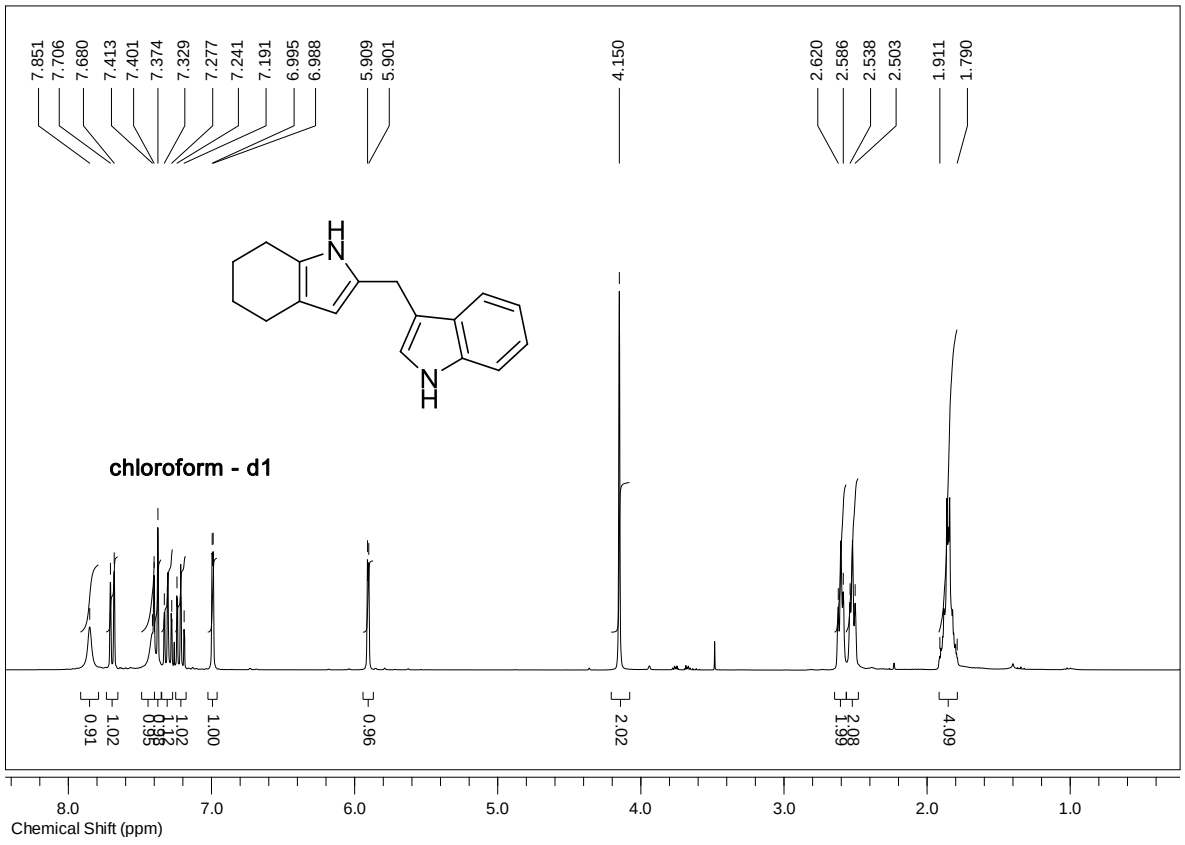
7.851
7.706
7.680
7.413
7.401
7.374
7.329
7.277
7.241
7.191
6.995
6.988
5.909
5.901
4.150
2.620
2.586
2.538
2.503
1.911
1.790
chloroform - d1
0.91
1.02
1.00
0.96
2.02
1.99
2.08
4.09
8.0
7.0
6.0
5.0
4.0
3.0
2.0
1.0
Chemical Shift (ppm)

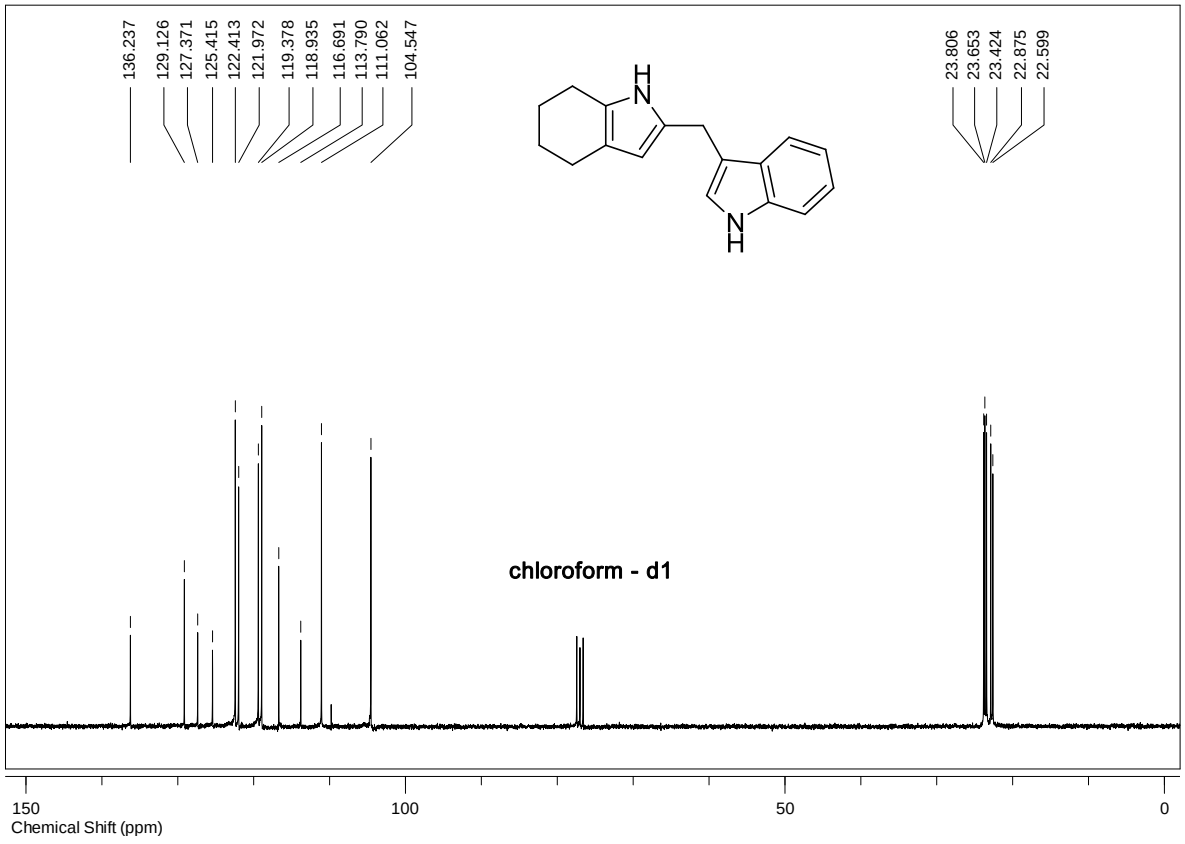
136.237
129.126
127.371
125.415
122.413
121.972
119.378
118.935
116.691
113.790
111.062
104.547
23.806
23.653
23.424
22.875
22.599
chloroform - d1
150
100
50
0
Chemical Shift (ppm)

1m:

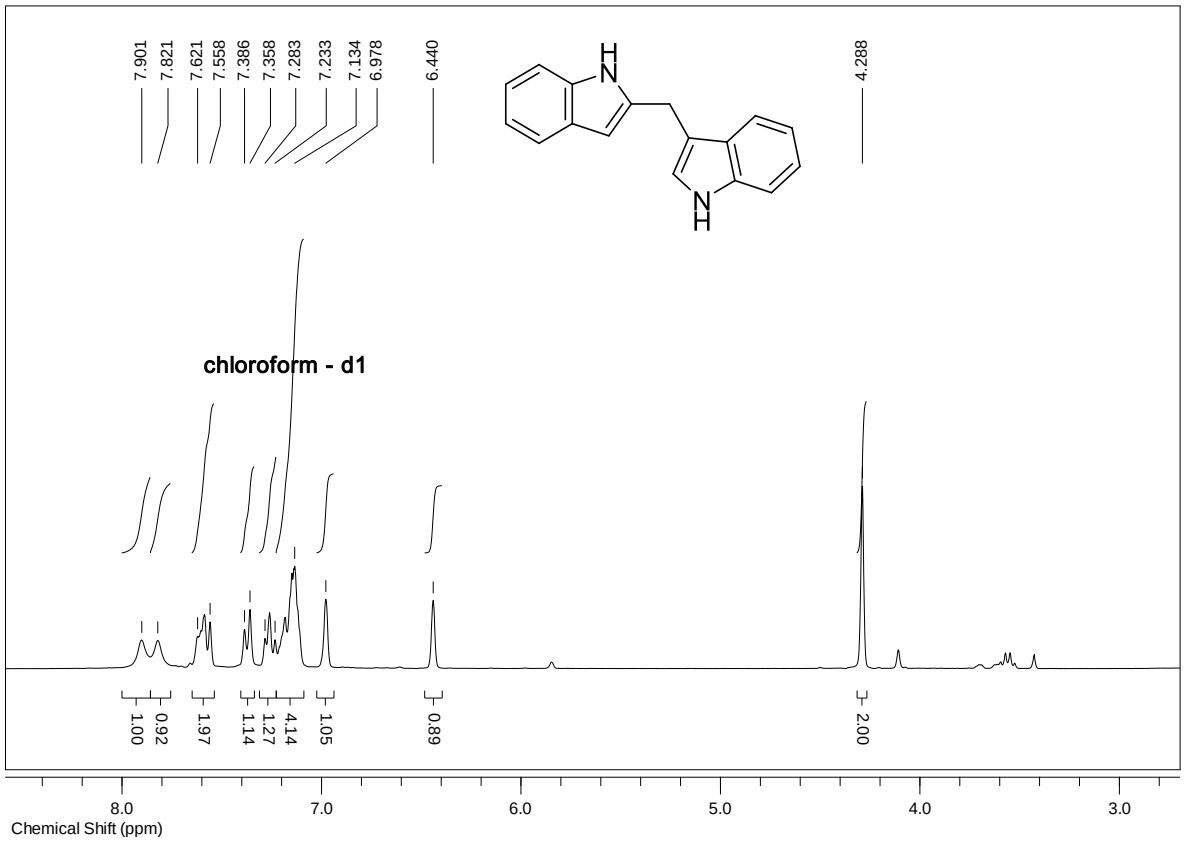
7.901
7.821
7.621
7.558
7.386
7.358
7.283
7.233
7.134
6.978
6.440
4.288
chloroform - d1
1.00
0.92
1.97
1.14
1.27
4.14
1.05
0.80
2.00
8.0
7.0
6.0
5.0
4.0
3.0
Chemical Shift (ppm)

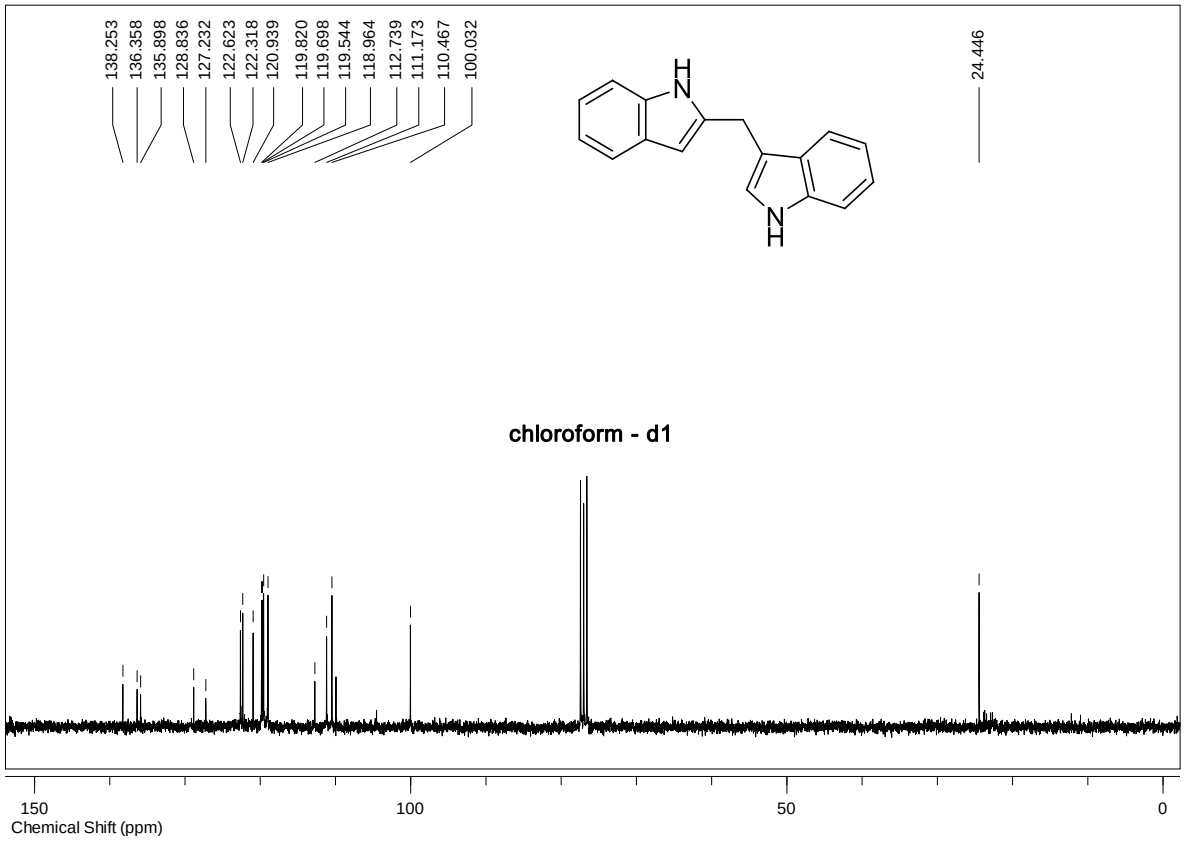
138.253
136.358
135.898
128.836
127.232
122.623
122.318
120.939
119.820
119.698
119.544
118.964
112.739
111.173
110.467
100.032
24.446
chloroform - d1
150
100
50
0
Chemical Shift (ppm)

4H-1n:

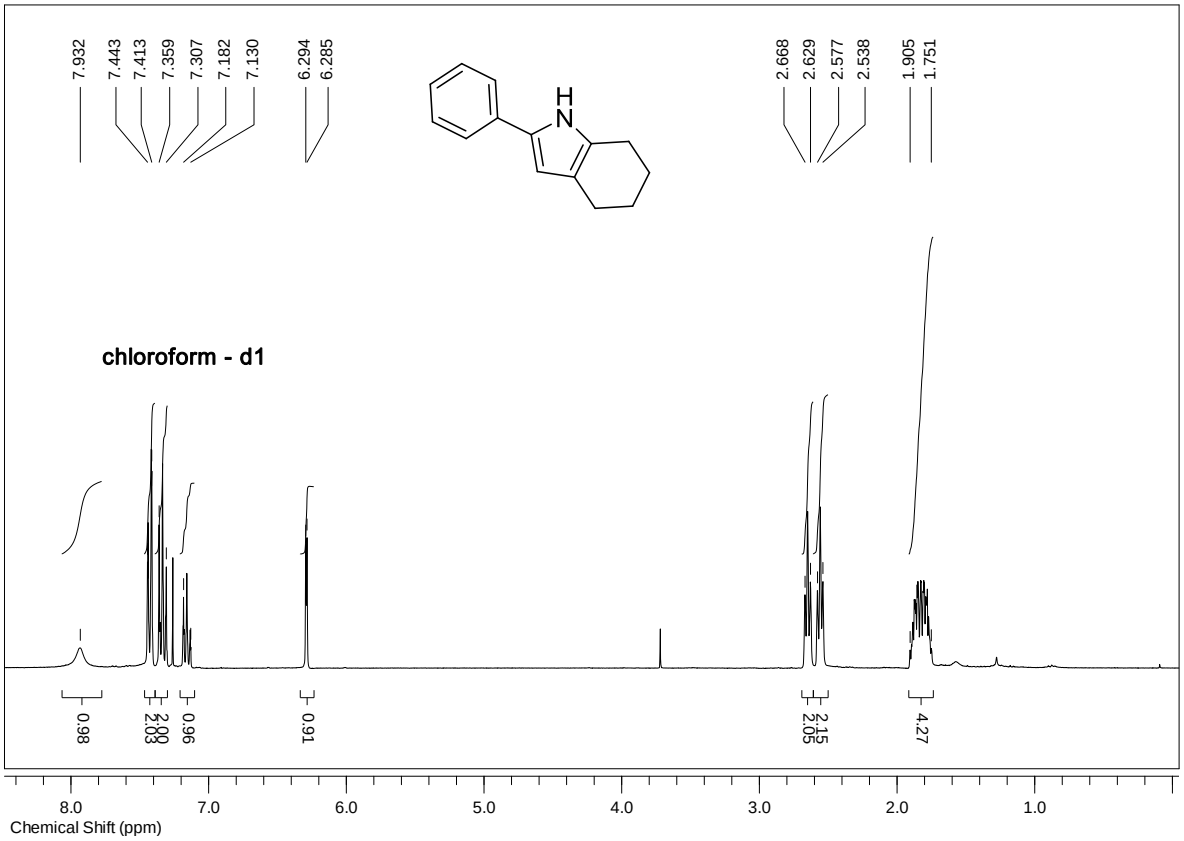
7.932
7.443
7.413
7.359
7.307
7.182
7.130
6.294
6.285
2.668
2.629
2.577
2.538
1.905
1.751
H
N
chloroform - d1
0.98
2.08
0.96
0.91
2.15
2.05
4.27
8.0
7.0
6.0
5.0
4.0
3.0
2.0
1.0
Chemical Shift (ppm)

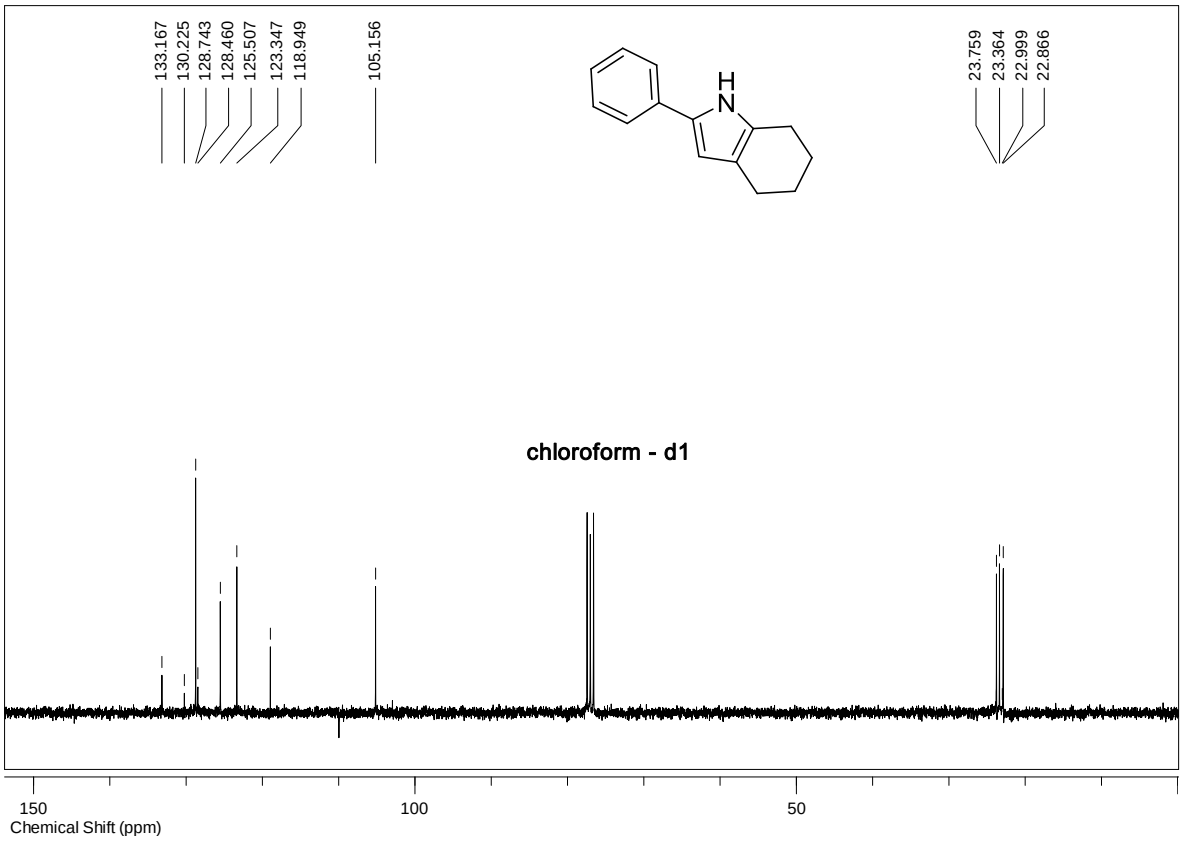
133.167
130.225
128.743
128.460
125.507
123.347
118.949
105.156
23.759
23.364
22.999
22.866
H
N
chloroform - d1
150
100
50
Chemical Shift (ppm)

1n:

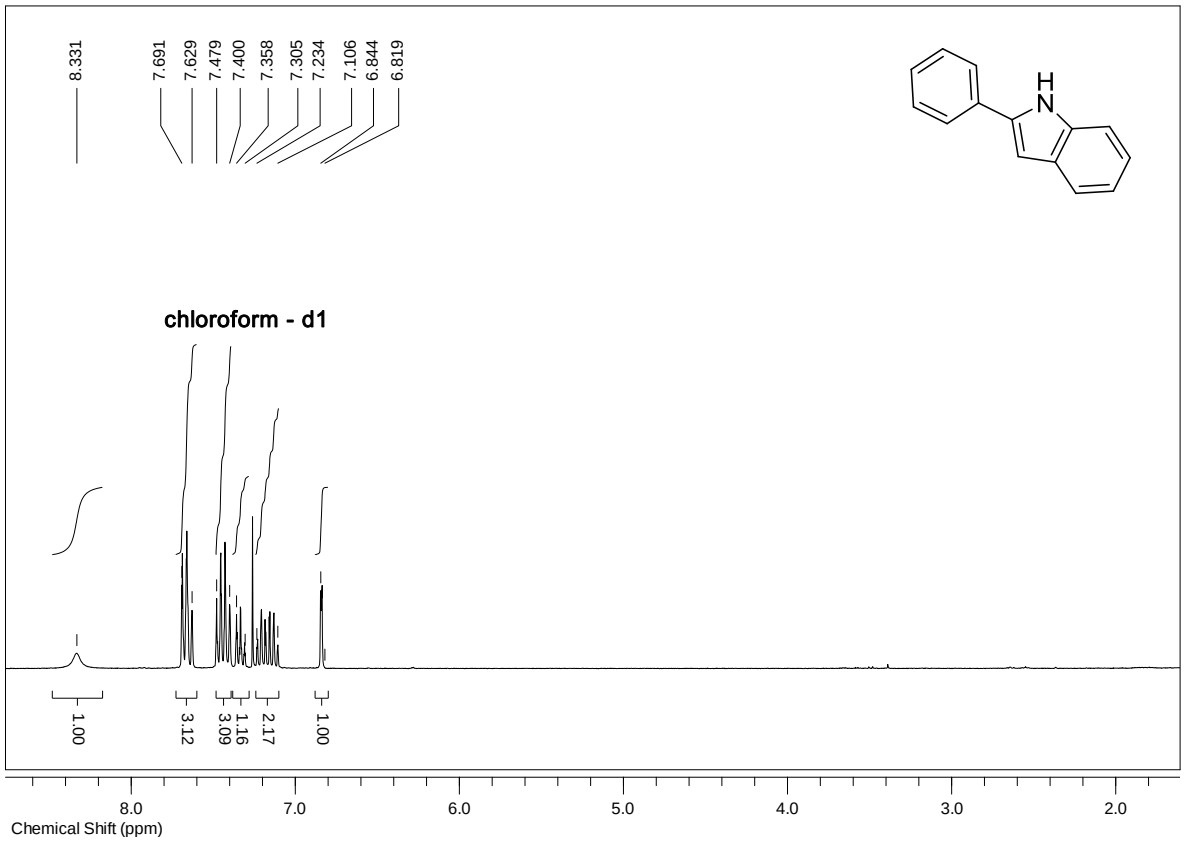
8.331
7.691
7.629
7.479
7.400
7.358
7.305
7.234
7.106
6.844
6.819
H
N
chloroform - d1
1.00
3.12
3.09
1.16
2.17
1.00
8.0
7.0
6.0
5.0
4.0
3.0
2.0
Chemical Shift (ppm)

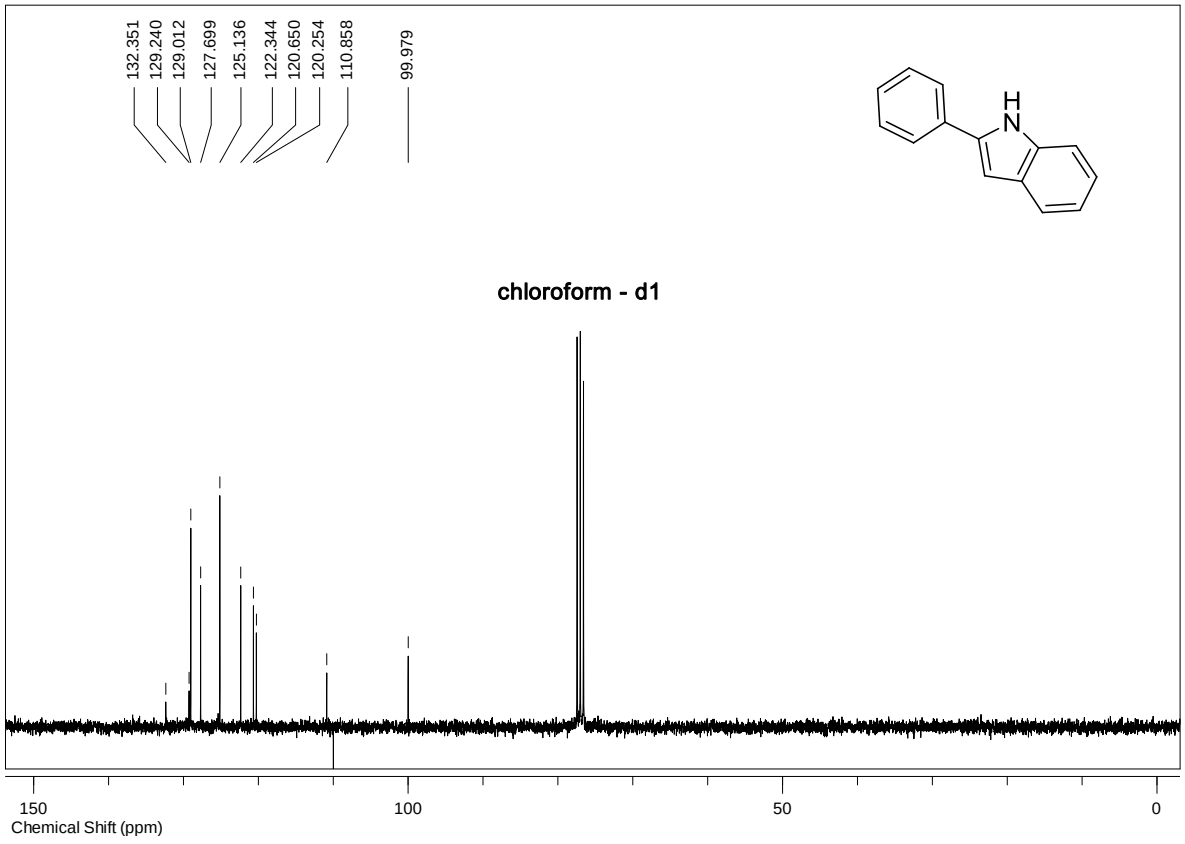
132.351
129.240
129.012
127.699
125.136
122.344
120.650
120.254
110.858
99.979
H
N
chloroform - d1
150
100
50
0
Chemical Shift (ppm)

4H-1o:

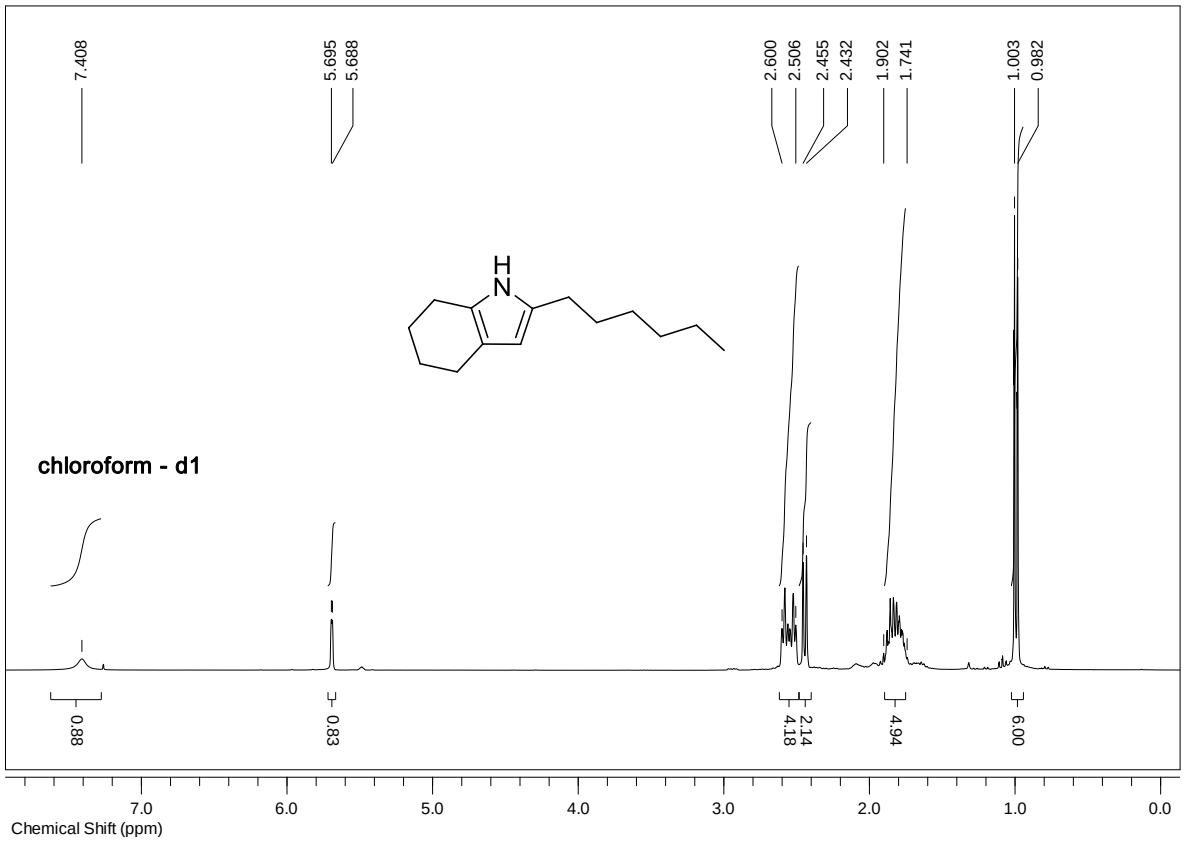
7.408
5.695
5.688
2.600
2.506
2.455
2.432
1.902
1.741
1.003
0.982
chloroform - d1
0.88
0.83
2.14
4.18
4.94
6.00
7.0
6.0
5.0
4.0
3.0
2.0
1.0
0.0
Chemical Shift (ppm)

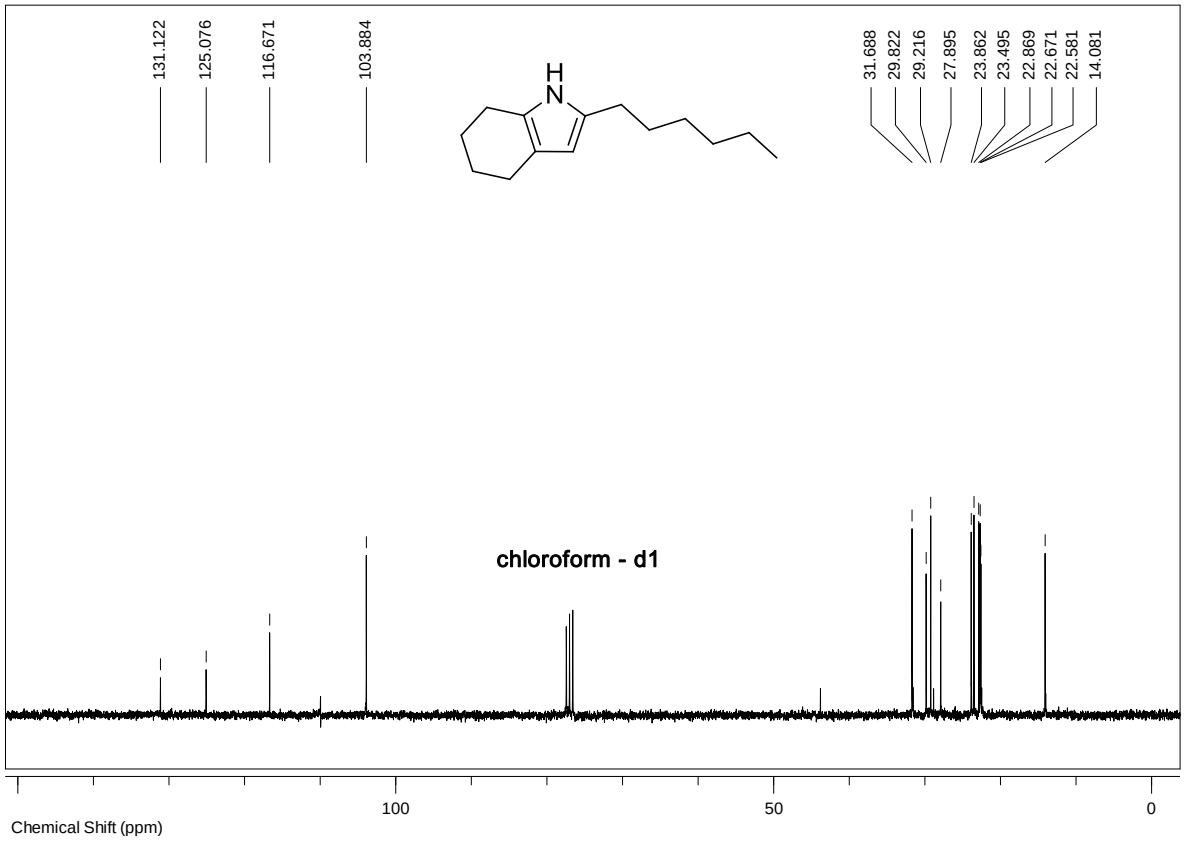
131.122
125.076
116.671
103.884
31.688
29.822
29.216
27.895
23.862
23.495
22.869
22.671
22.581
14.081
chloroform - d1
100
50
0
Chemical Shift (ppm)

1o:

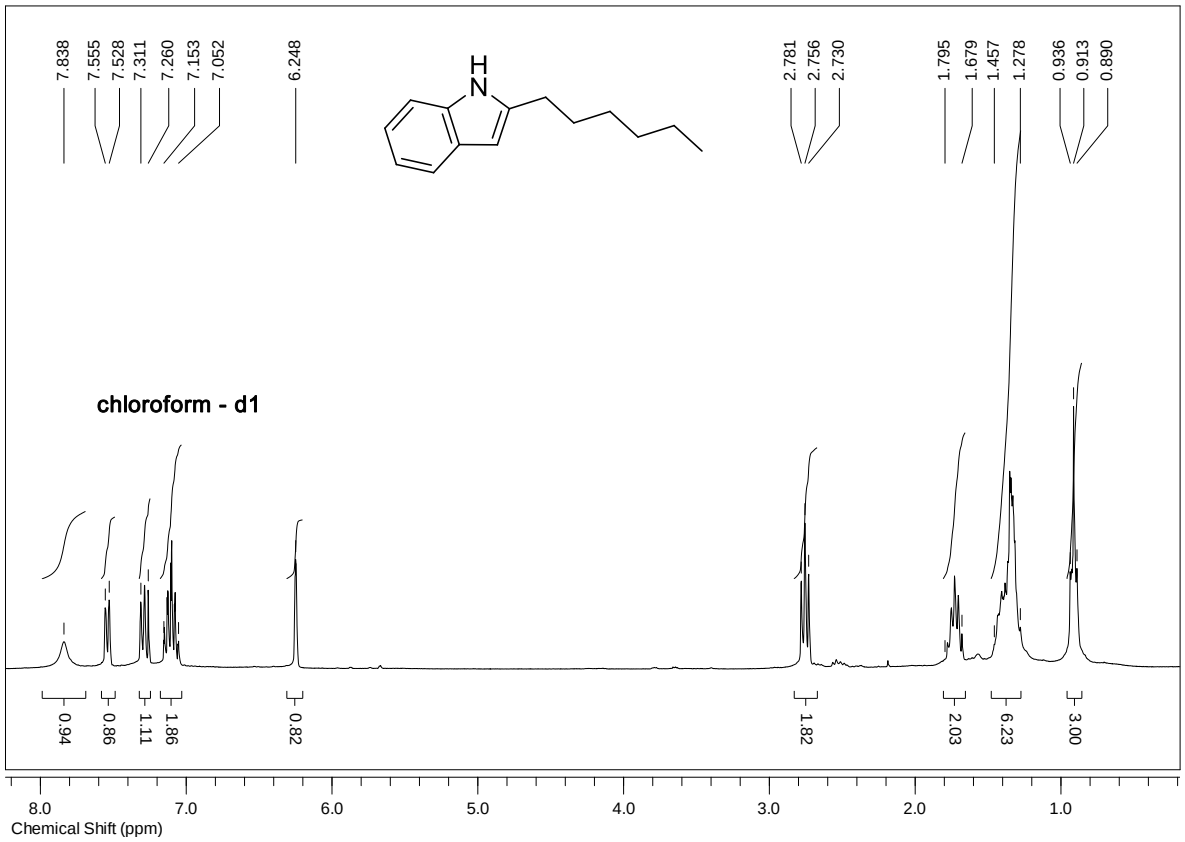
7.838
7.555
7.528
7.311
7.260
7.153
7.052
6.248
2.781
2.756
2.730
1.795
1.679
1.457
1.278
0.936
0.913
0.890
chloroform - d1
0.94
0.86
1.11
1.86
0.82
1.82
2.03
6.23
3.00
8.0
7.0
6.0
5.0
4.0
3.0
2.0
1.0
Chemical Shift (ppm)

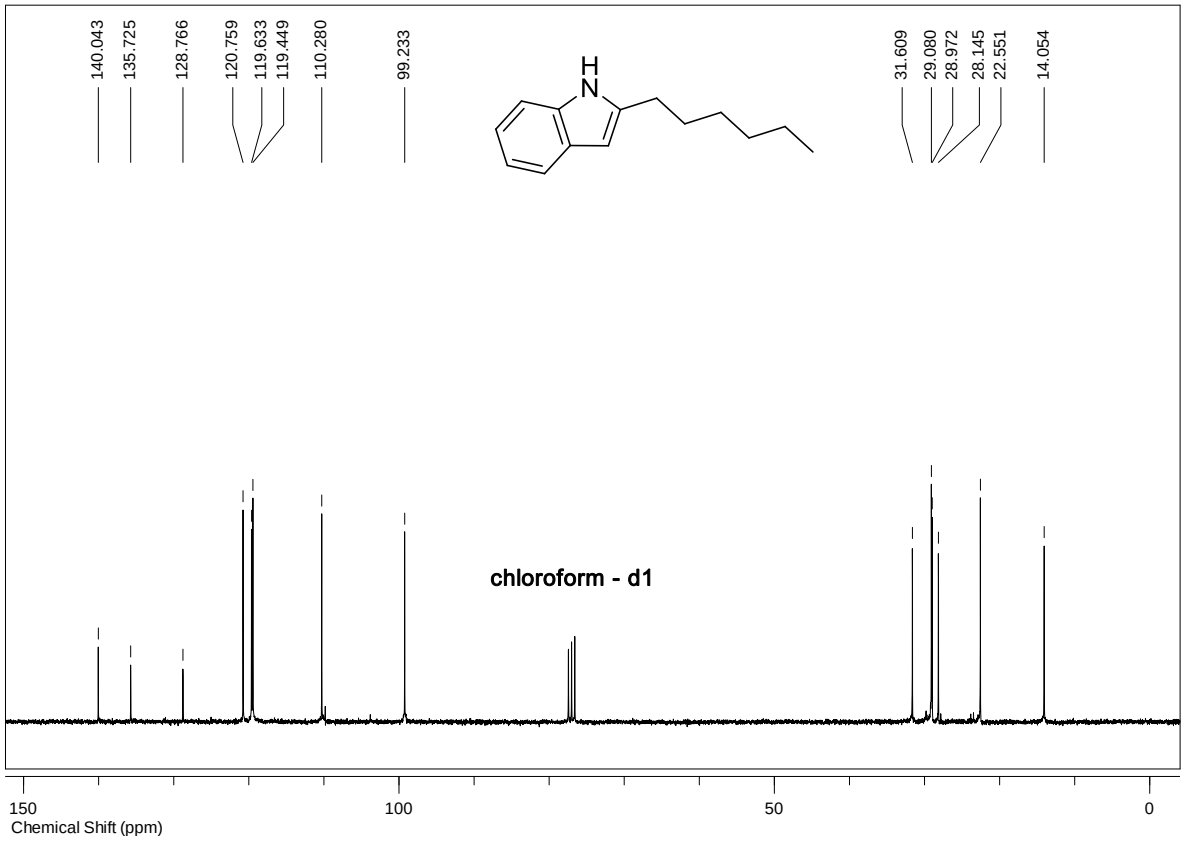
140.043
135.725
128.766
120.759
119.633
119.449
110.280
99.233
31.609
29.080
28.972
28.145
22.551
14.054
chloroform - d1
150
100
50
0
Chemical Shift (ppm)

4H-1p:

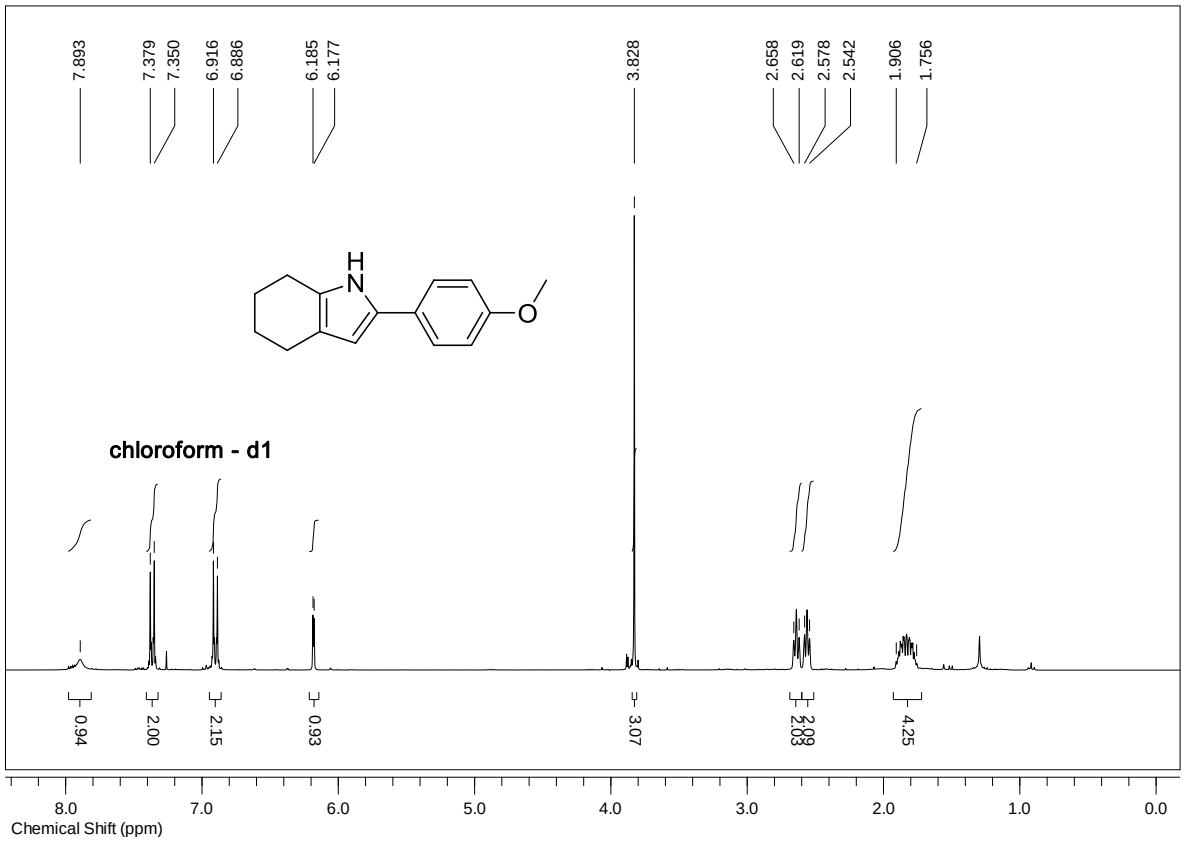
7.893
7.379
7.350
6.916
6.886
6.185
6.177
3.828
2.658
2.619
2.578
2.542
1.906
1.756
H
N
O
chloroform - d1
0.94
2.00
2.15
0.93
3.07
2.09
2.03
4.25
8.0
7.0
6.0
5.0
4.0
3.0
2.0
1.0
0.0
Chemical Shift (ppm)

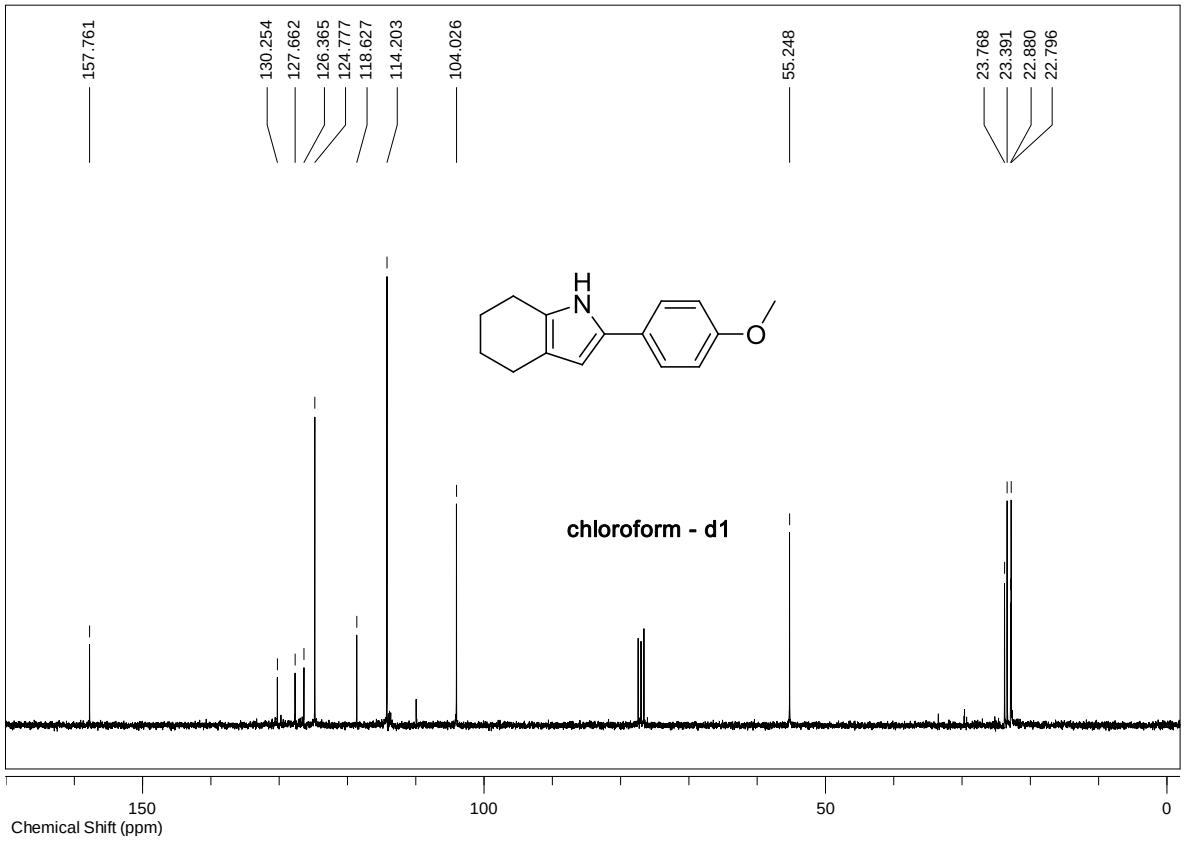
157.761
130.254
127.662
126.365
124.777
118.627
114.203
104.026
55.248
23.768
23.391
22.880
22.796
H
N
O
chloroform - d1
150
100
50
0
Chemical Shift (ppm)

1p:

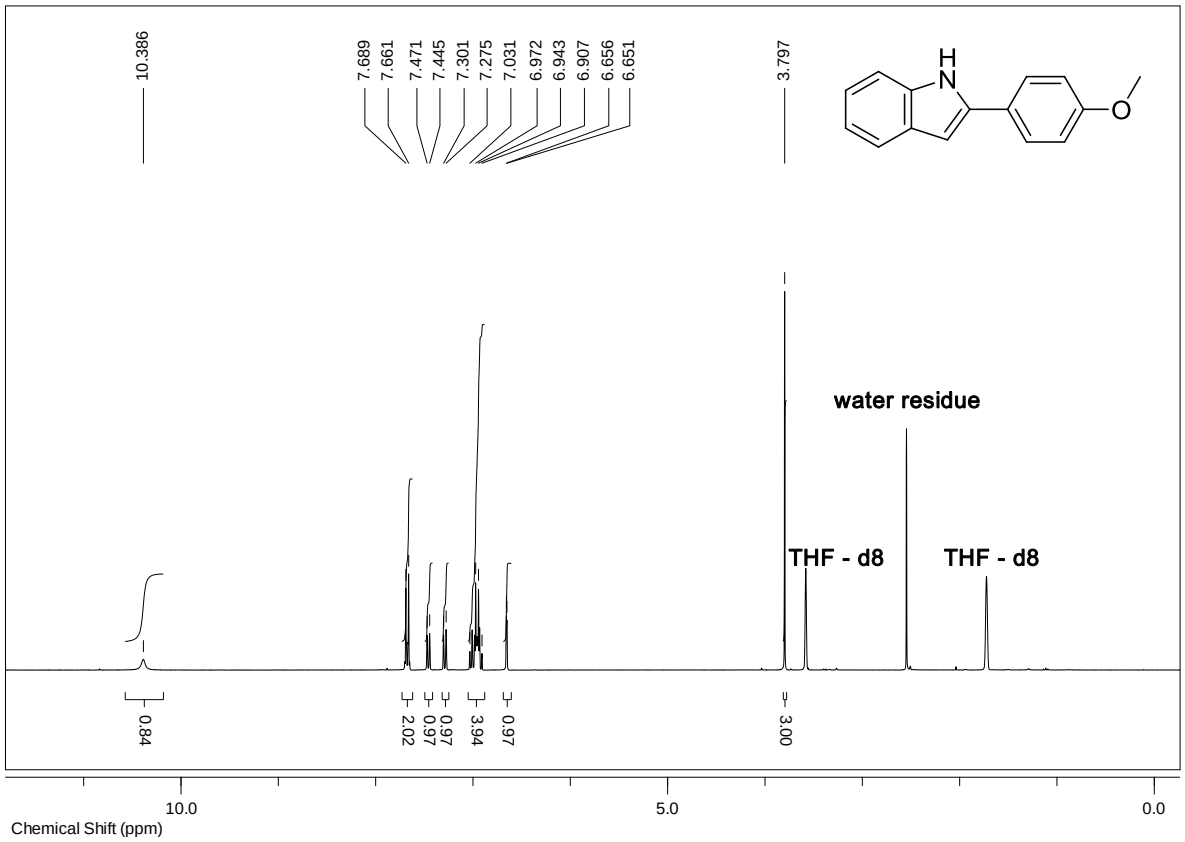
10.386
7.689
7.661
7.471
7.445
7.301
7.275
7.031
6.972
6.943
6.907
6.656
6.651
3.797
H
N
O
water residue
THF - d8
THF - d8
0.84
2.02
0.97
0.97
3.94
0.97
3.00
10.0
5.0
0.0
Chemical Shift (ppm)

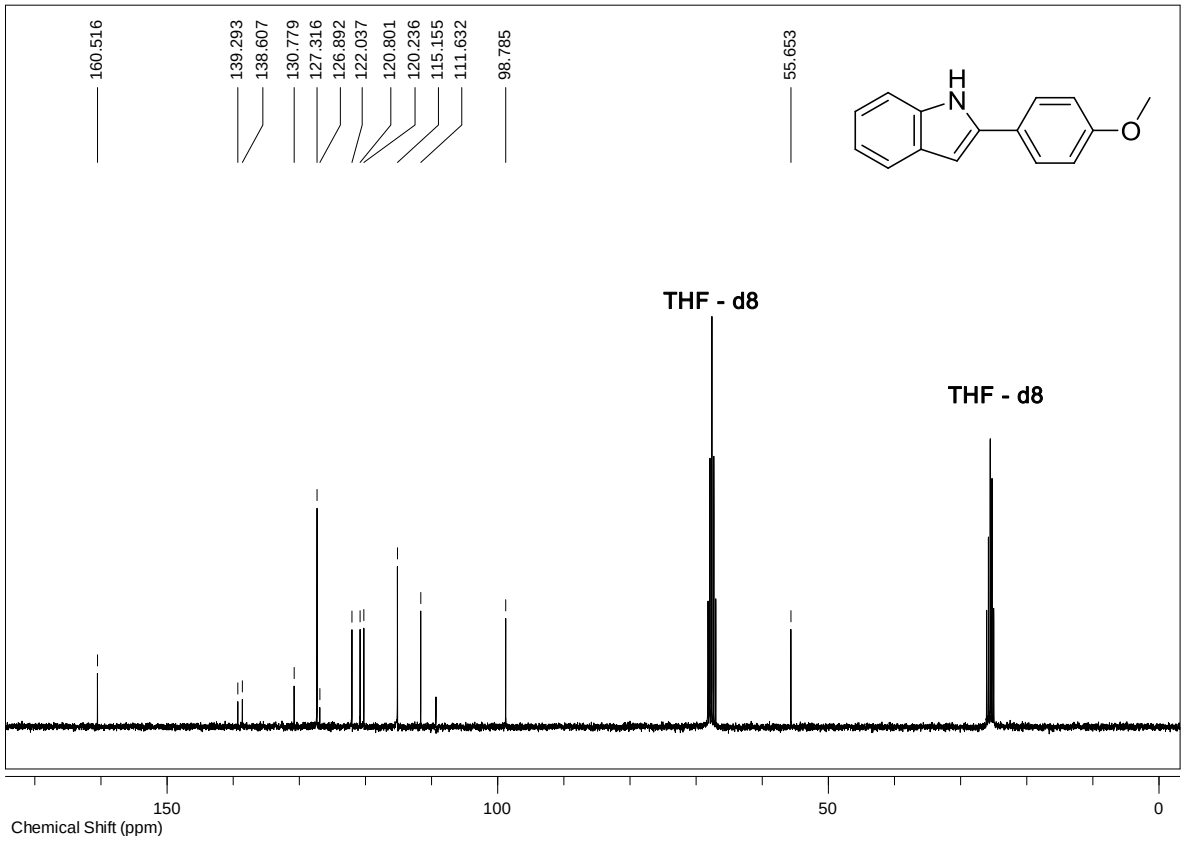
160.516
139.293
138.607
130.779
127.316
126.892
122.037
120.801
120.236
115.155
111.632
98.785
55.653
H
N
O
THF - d8
THF - d8
150
100
50
0
Chemical Shift (ppm)

4H-1q:

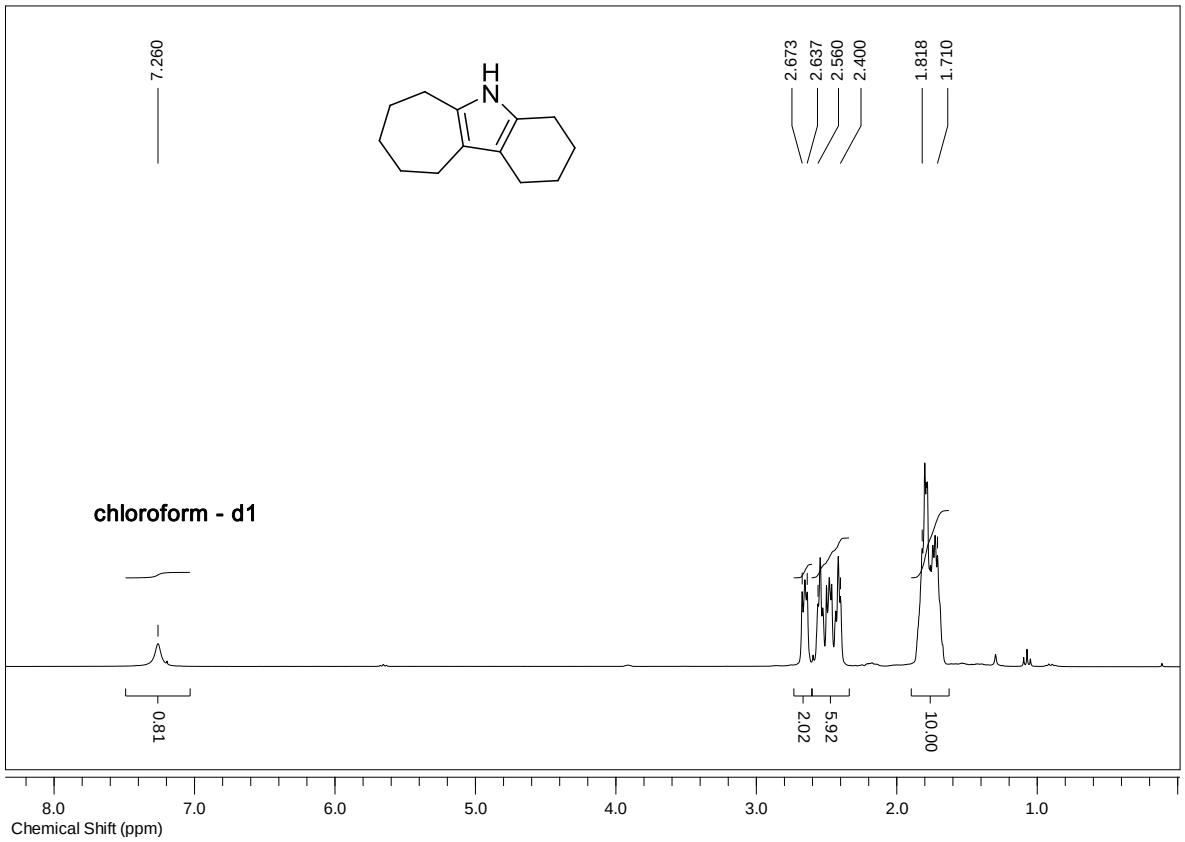
7.260
2.673
2.637
2.560
2.400
1.818
1.710
chloroform - d1
0.81
2.02
5.92
10.00
8.0
7.0
6.0
5.0
4.0
3.0
2.0
1.0
Chemical Shift (ppm)

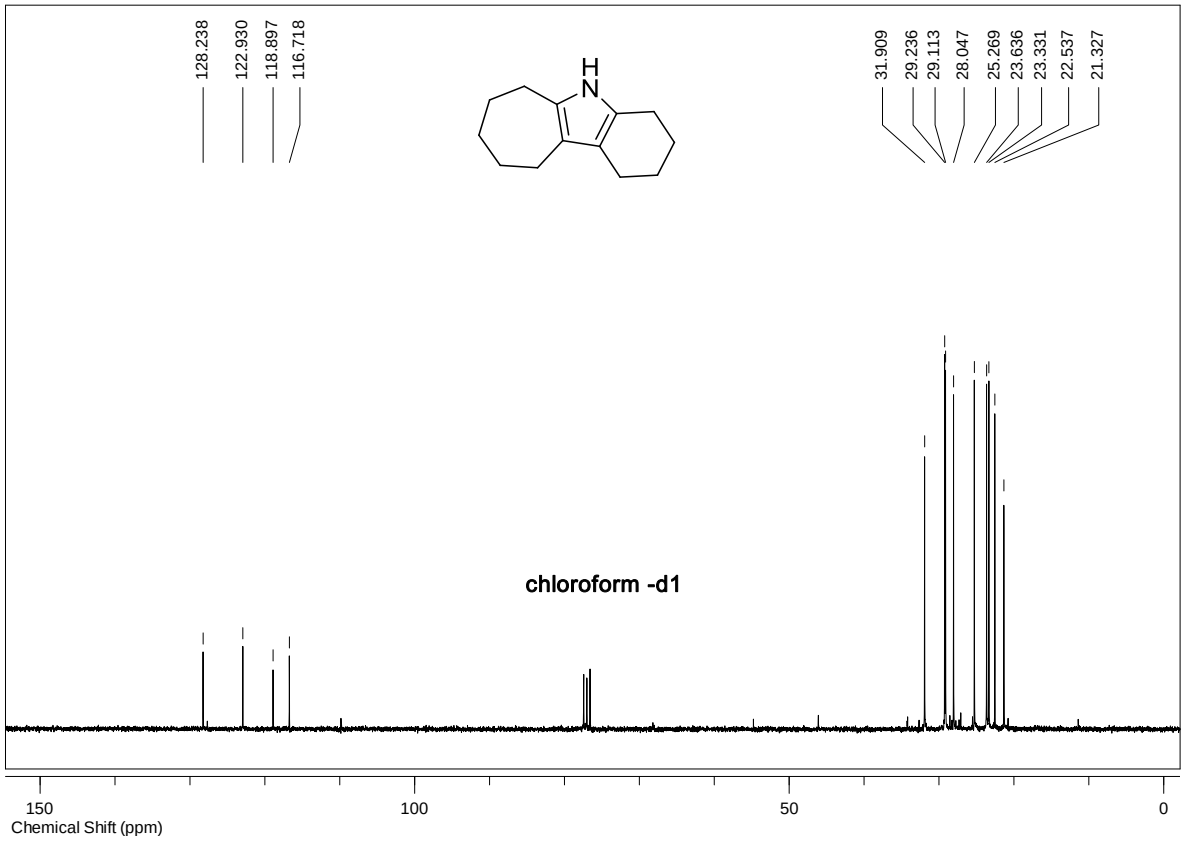
128.238
122.930
118.897
116.718
31.909
29.236
29.113
28.047
25.269
23.636
23.331
22.537
21.327
chloroform -d1
150
100
50
0
Chemical Shift (ppm)

1q:

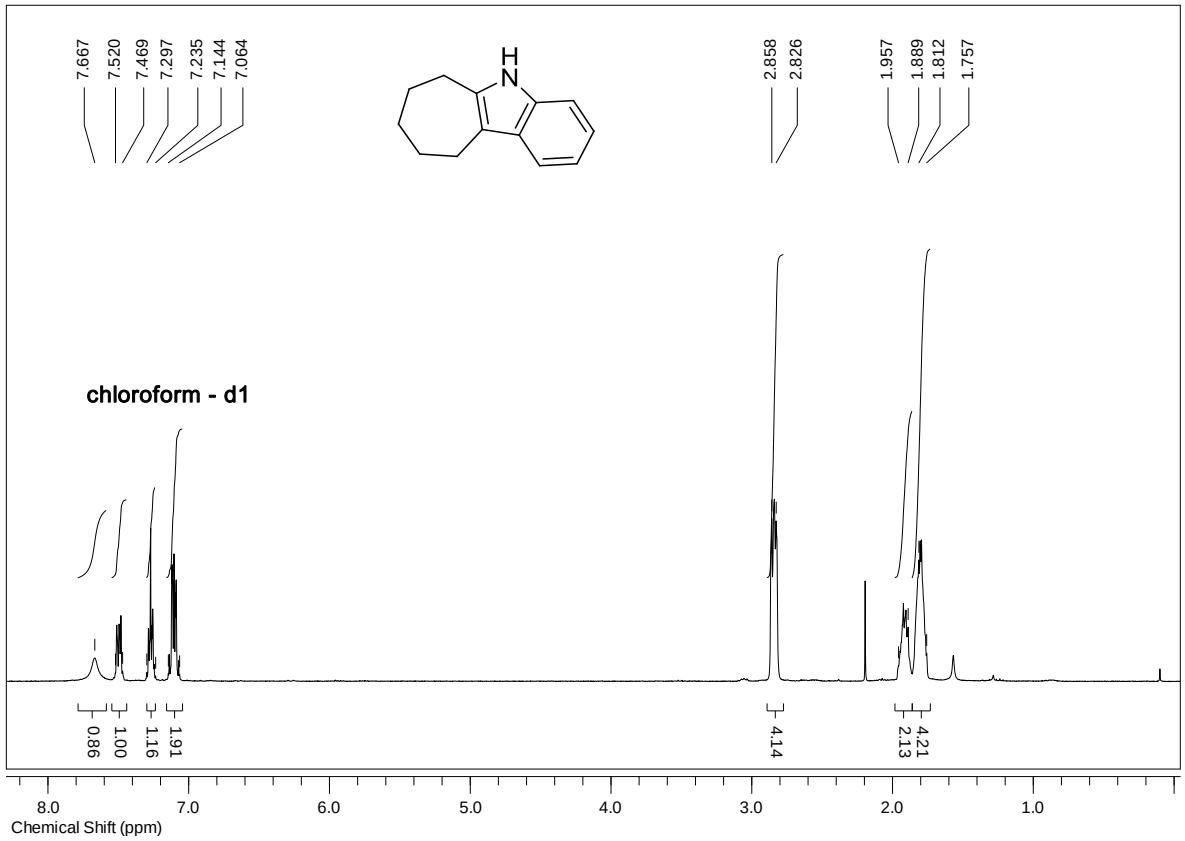
7.667
7.520
7.469
7.297
7.235
7.144
7.064
2.858
2.826
1.957
1.889
1.812
1.757
chloroform - d1
0.86
1.00
1.16
1.61
4.14
2.13
4.21
8.0
7.0
6.0
5.0
4.0
3.0
2.0
1.0
Chemical Shift (ppm)

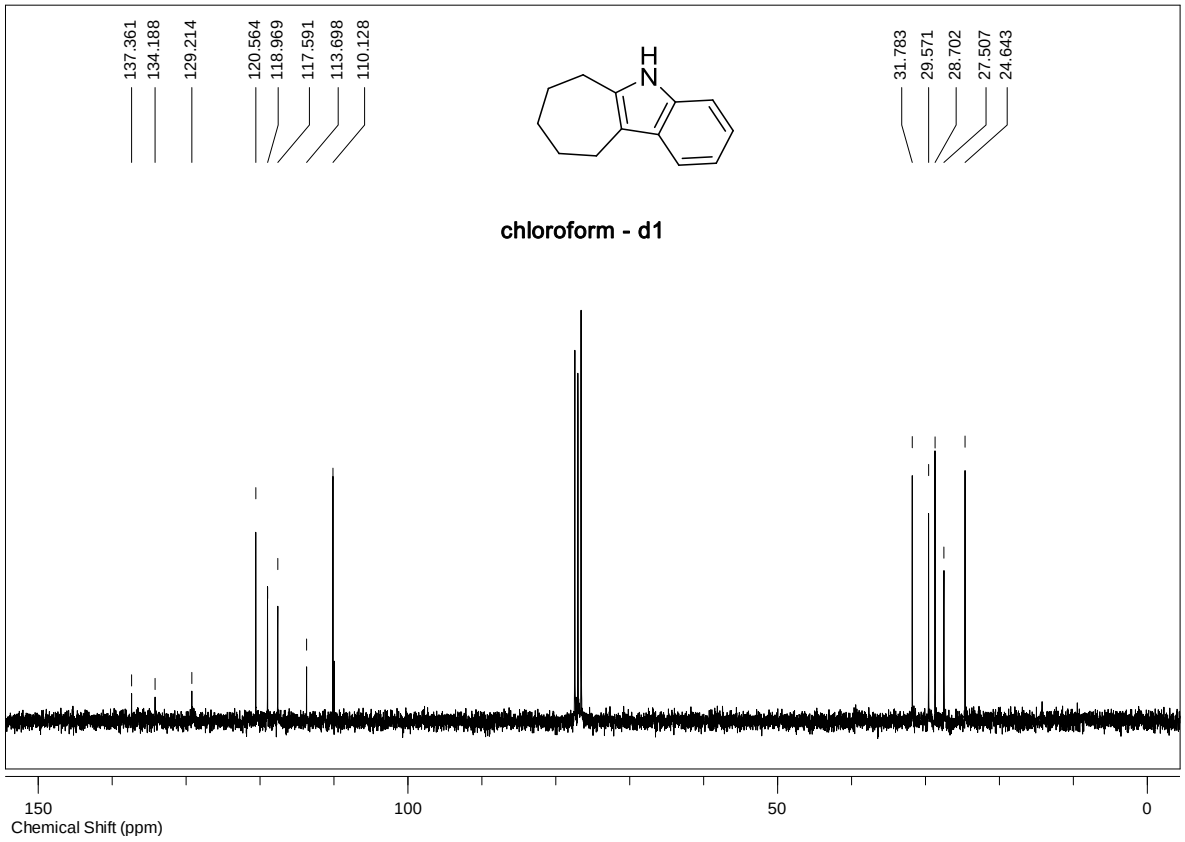
137.361
134.188
129.214
120.564
118.969
117.591
113.698
110.128
31.783
29.571
28.702
27.507
24.643
chloroform - d1
150
100
50
0
Chemical Shift (ppm)

4H-1r:

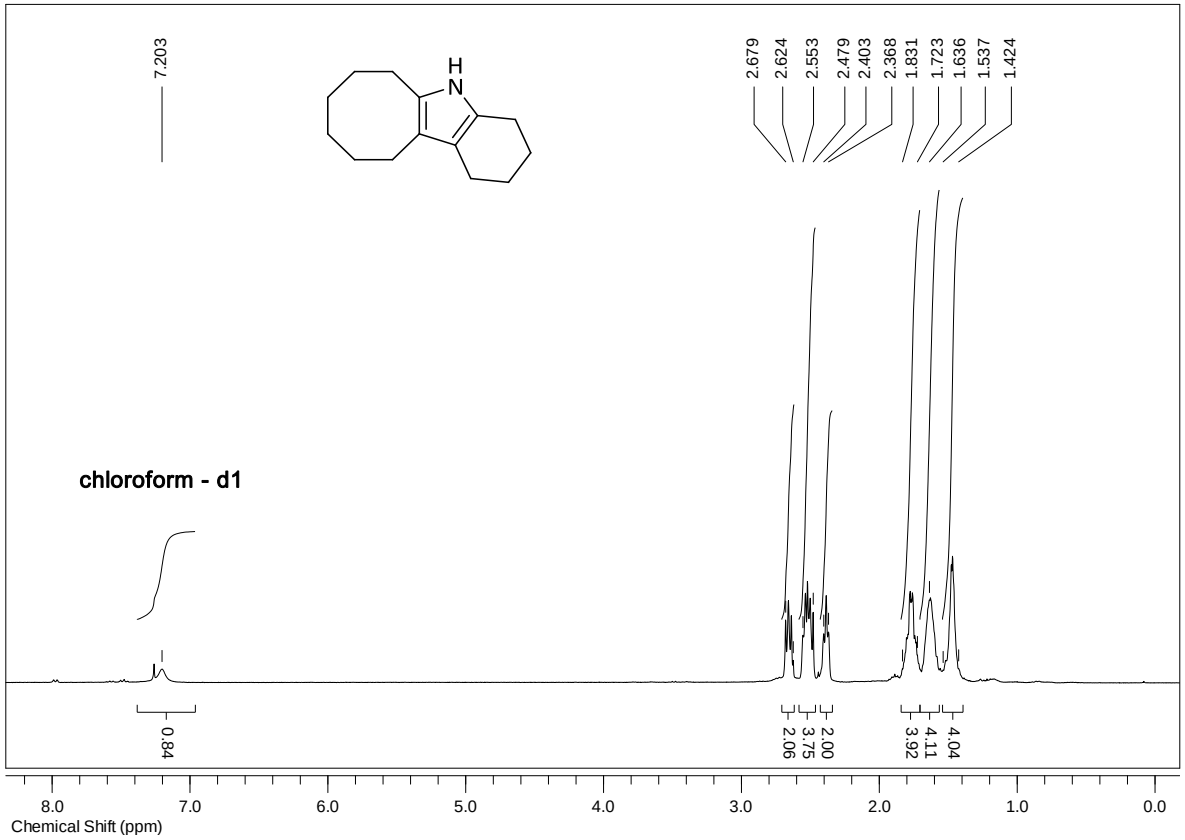
7.203
H
N
2.679
2.624
2.553
2.479
2.403
2.368
1.831
1.723
1.636
1.537
1.424
chloroform - d1
0.84
2.06
3.75
2.00
3.92
4.11
4.04
8.0
7.0
6.0
5.0
4.0
3.0
2.0
1.0
0.0
Chemical Shift (ppm)

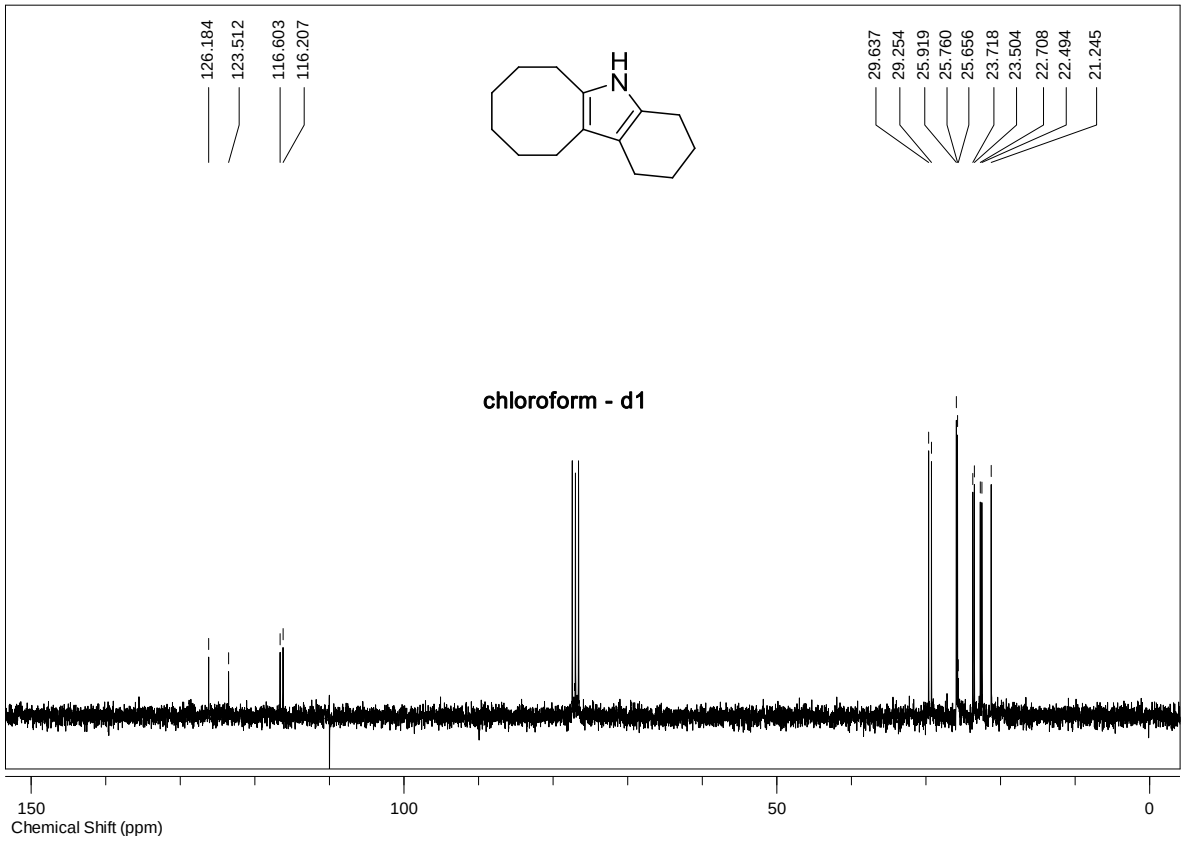
126.184
123.512
116.603
116.207
H
N
29.637
29.254
25.919
25.760
25.656
23.718
23.504
22.708
22.494
21.245
chloroform - d1
150
100
50
0
Chemical Shift (ppm)

1r:

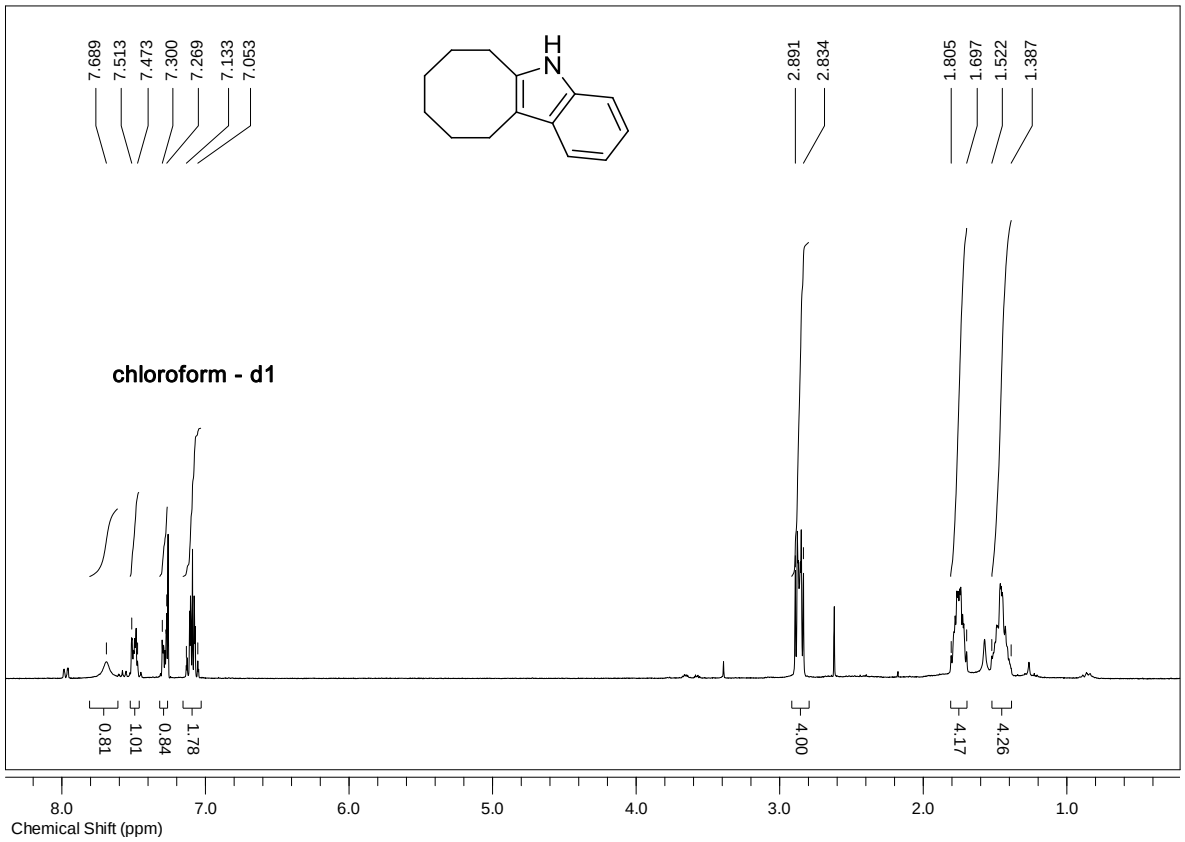
7.689
7.513
7.473
7.300
7.269
7.133
7.053
2.891
2.834
1.805
1.697
1.522
1.387
chloroform - d1
0.81
1.01
0.84
1.78
4.00
4.17
4.26
8.0
7.0
6.0
5.0
4.0
3.0
2.0
1.0
Chemical Shift (ppm)

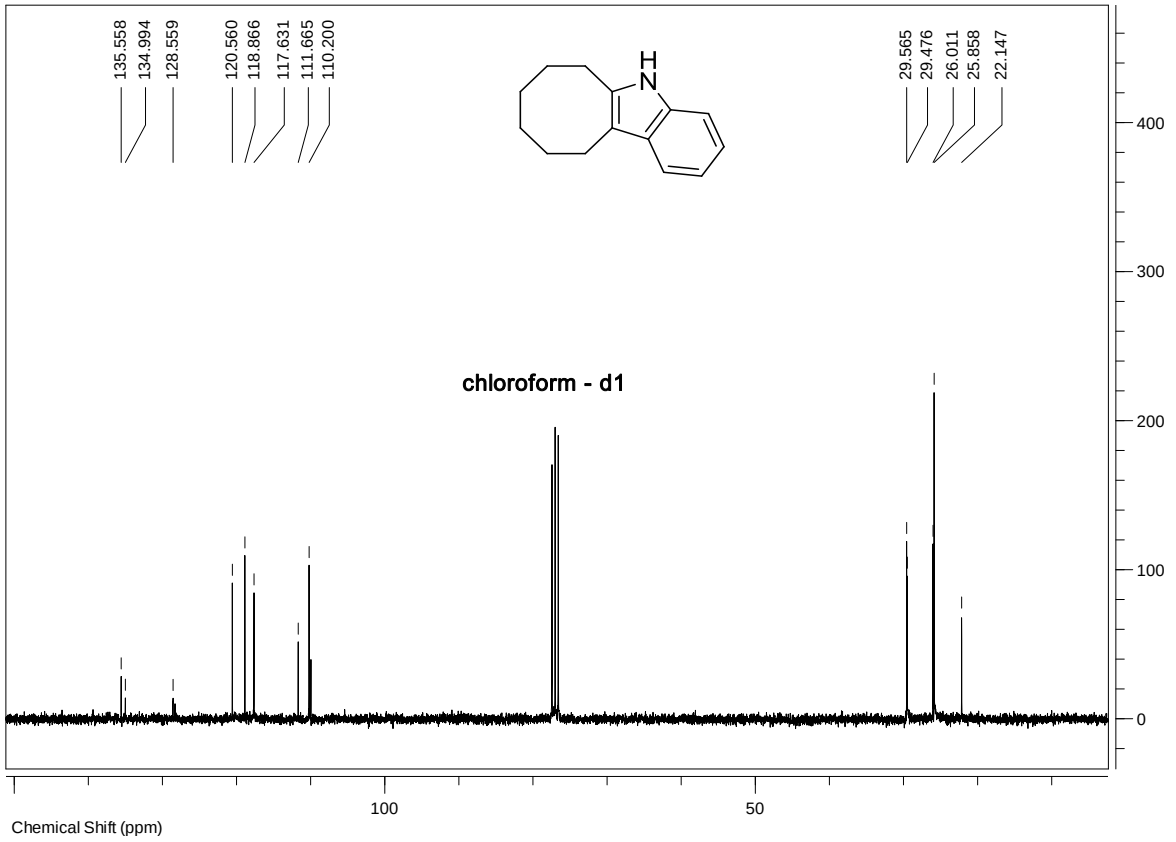
135.558
134.994
128.559
120.560
118.866
117.631
111.665
110.200
29.565
29.476
26.011
25.858
22.147
chloroform - d1
400
300
200
100
0
100
50
Chemical Shift (ppm)

4H-1s:

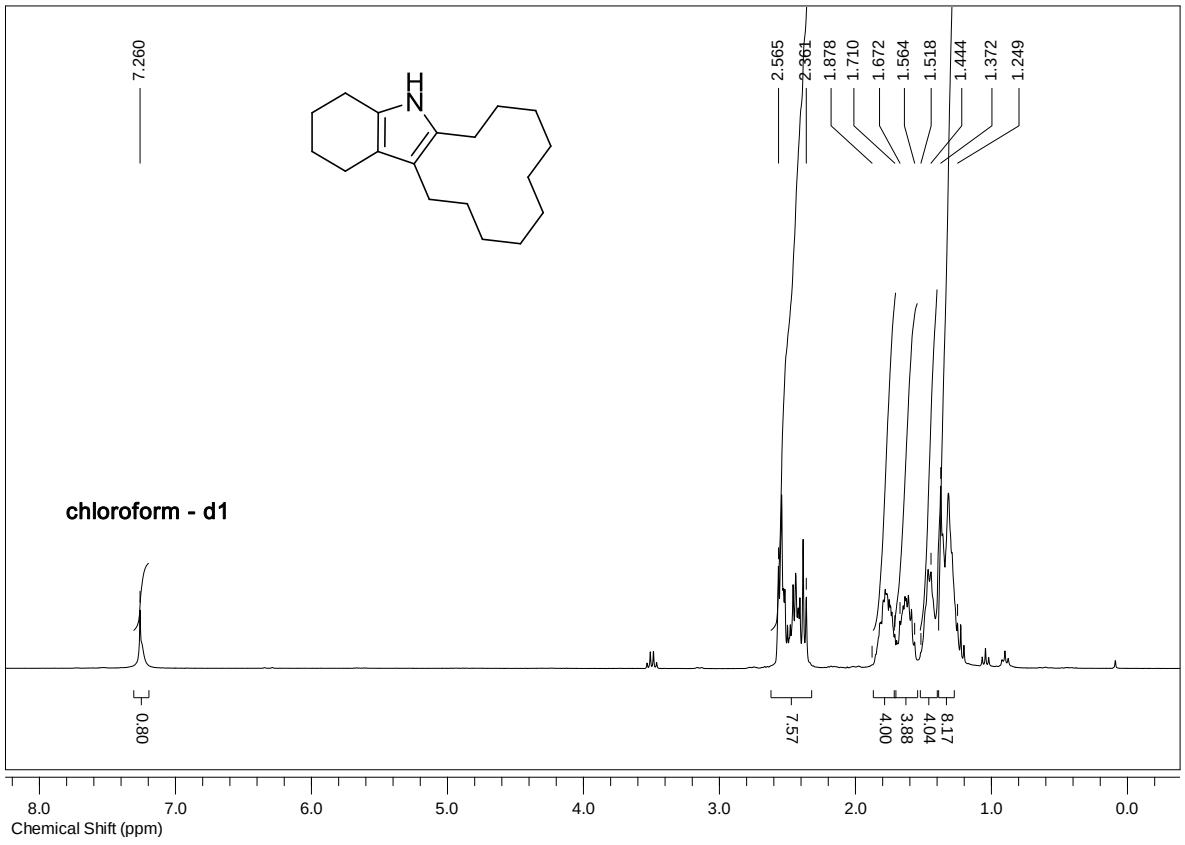
7.260
2.565
2.361
1.878
1.710
1.672
1.564
1.518
1.444
1.372
1.249
chloroform - d1
0.80
7.57
4.00
3.88
4.04
8.17
8.0
7.0
6.0
5.0
4.0
3.0
2.0
1.0
0.0
Chemical Shift (ppm)

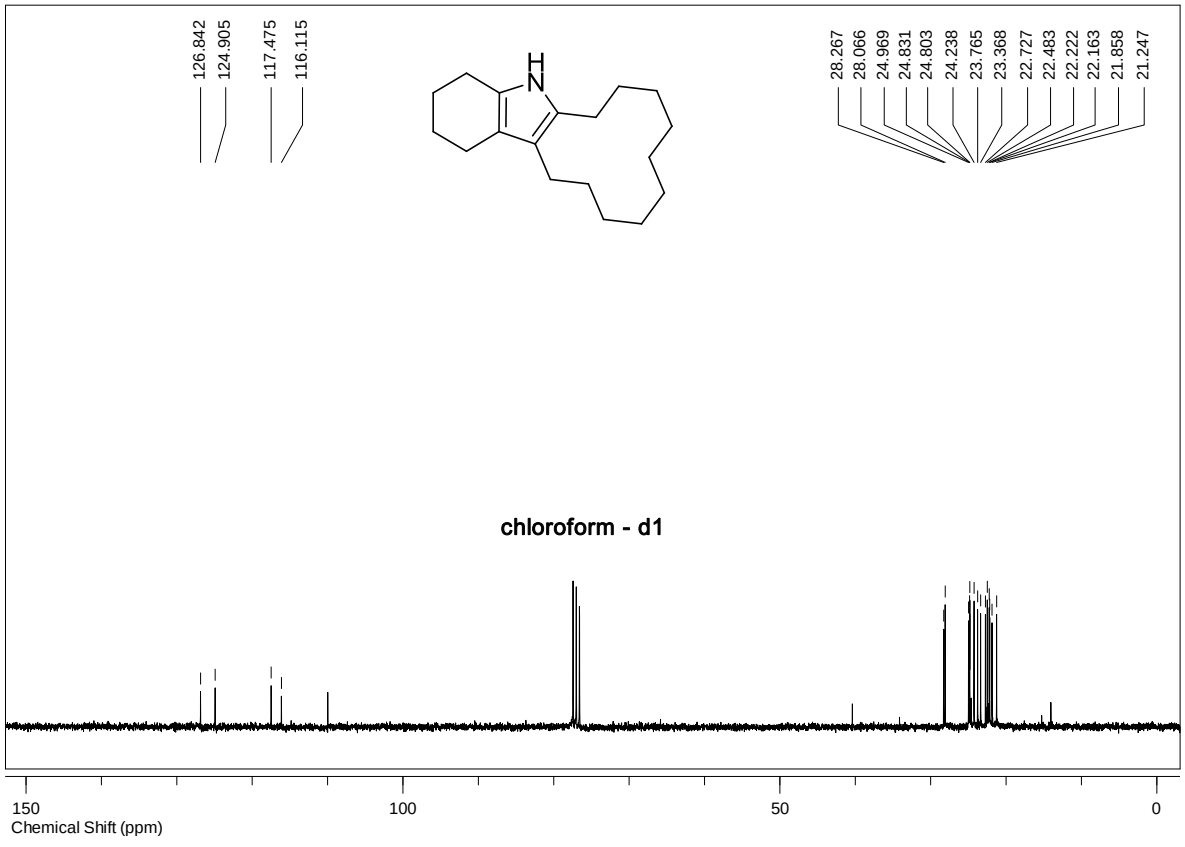
126.842
124.905
117.475
116.115
28.267
28.066
24.969
24.831
24.803
24.238
23.765
23.368
22.727
22.483
22.222
22.163
21.858
21.247
chloroform - d1
150
100
50
0
Chemical Shift (ppm)

1s:

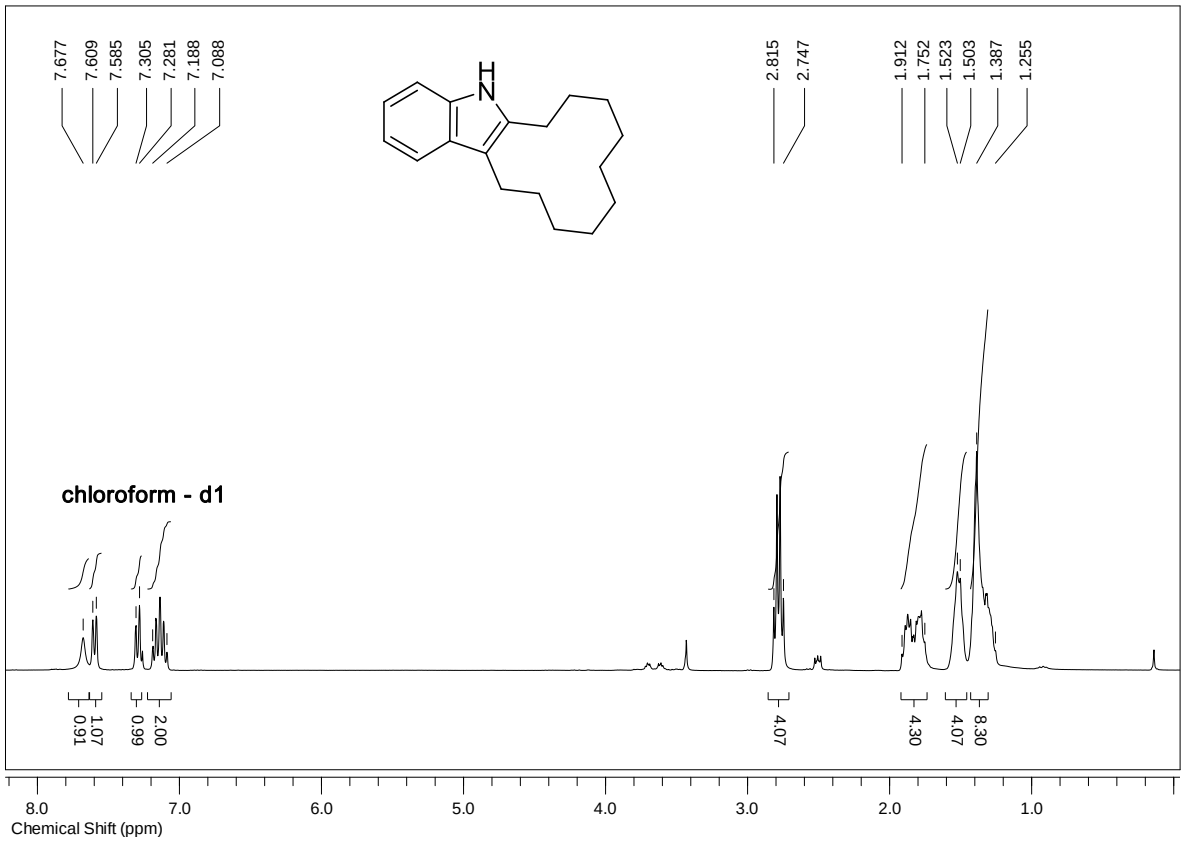
7.677
7.609
7.585
7.305
7.281
7.188
7.088
2.815
2.747
1.912
1.752
1.523
1.503
1.387
1.255
chloroform - d1
0.91
1.07
0.99
2.00
4.07
4.30
4.07
8.30
8.0
7.0
6.0
5.0
4.0
3.0
2.0
1.0
Chemical Shift (ppm)

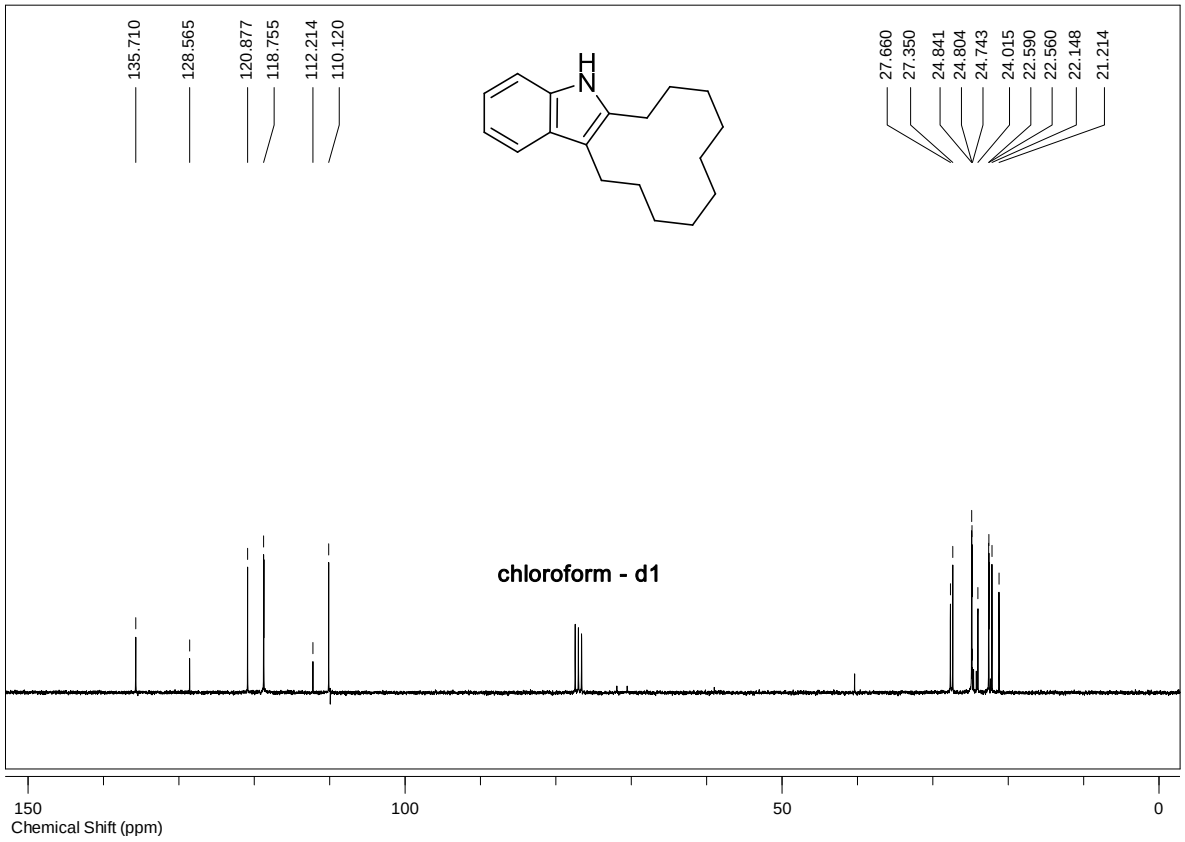
135.710
128.565
120.877
118.755
112.214
110.120
27.660
27.350
24.841
24.804
24.743
24.015
22.590
22.560
22.148
21.214
chloroform - d1
150
100
50
0
Chemical Shift (ppm)

8H-2a:

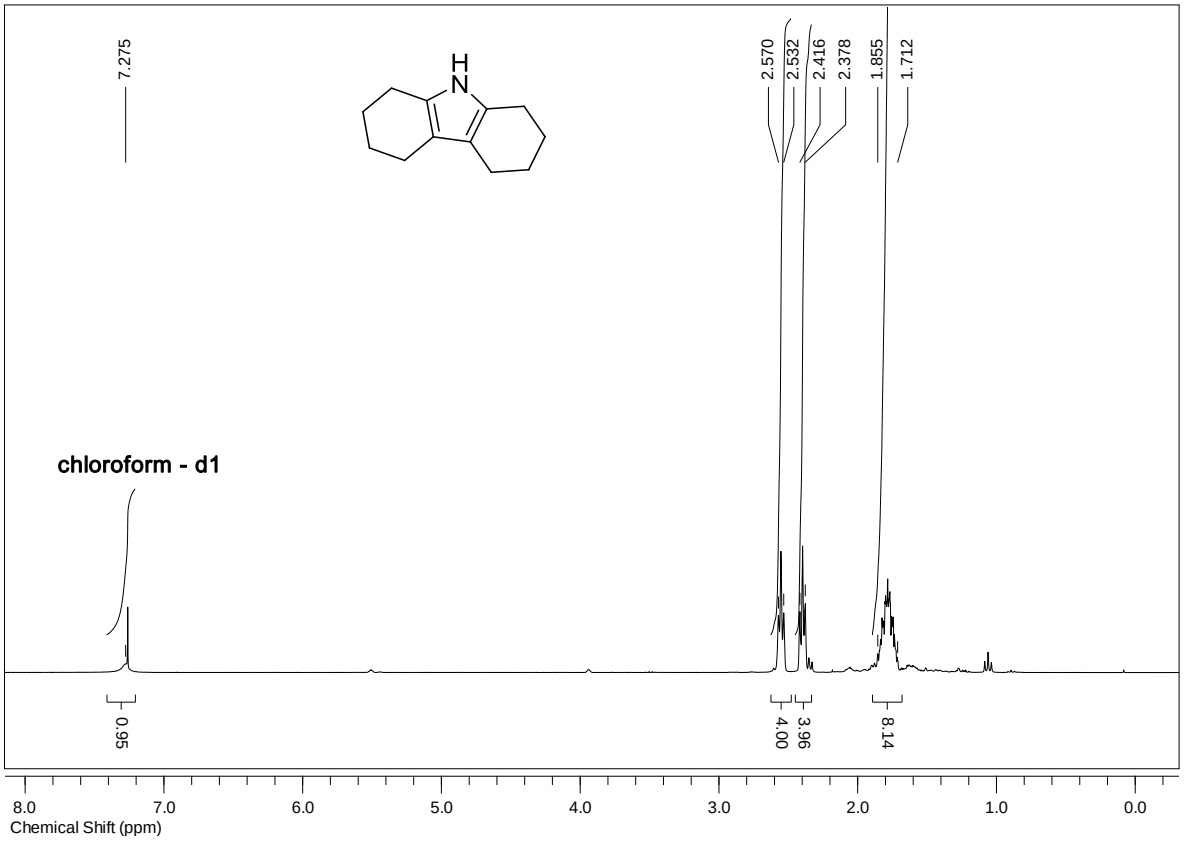
7.275
2.570
2.532
2.416
2.378
1.855
1.712
chloroform - d1
0.95
4.00
3.96
8.14
8.0
7.0
6.0
5.0
4.0
3.0
2.0
1.0
0.0
Chemical Shift (ppm)

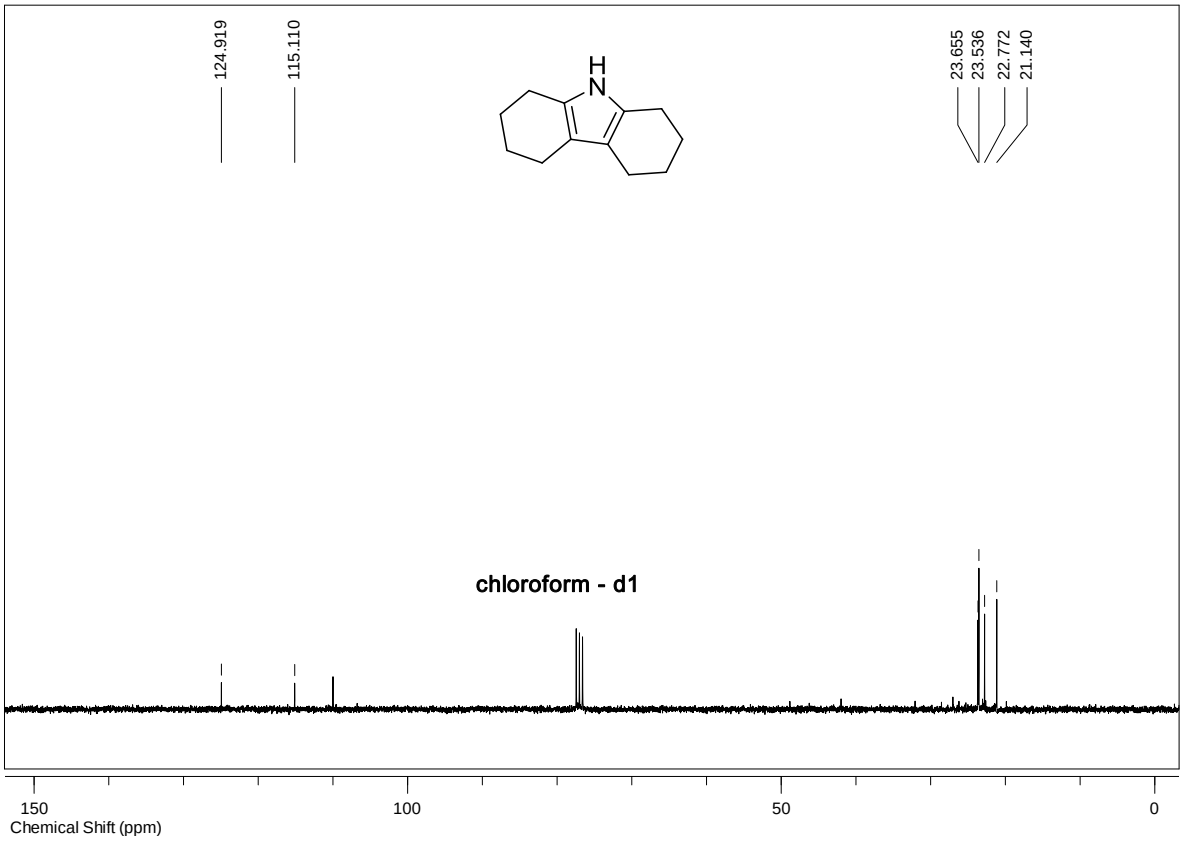
124.919
115.110
23.655
23.536
22.772
21.140
chloroform - d1
150
100
50
0
Chemical Shift (ppm)

2a:

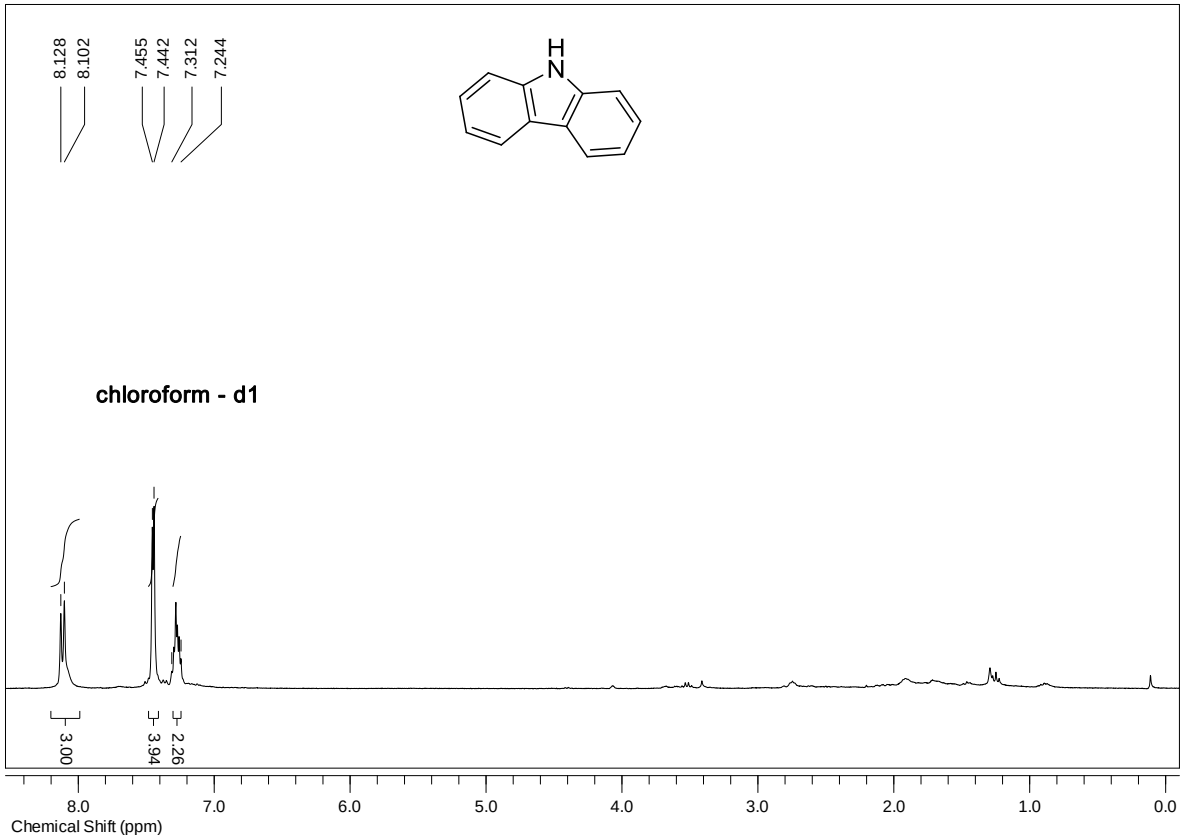
8.128
8.102
7.455
7.442
7.312
7.244
H
N
chloroform - d1
3.00
3.94
2.26
8.0
7.0
6.0
5.0
4.0
3.0
2.0
1.0
0.0
Chemical Shift (ppm)

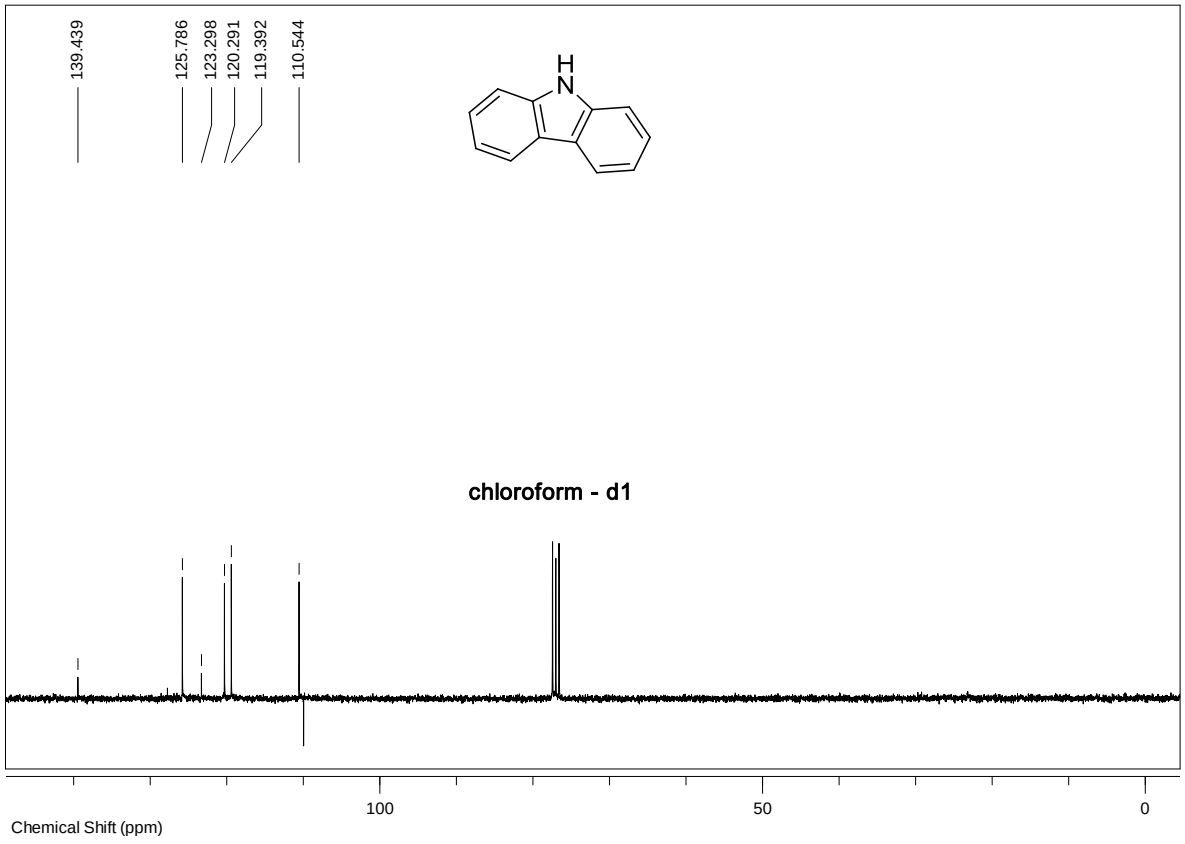
139.439
125.786
123.298
120.291
119.392
110.544
H
N
chloroform - d1
100
50
0
Chemical Shift (ppm)

8H-2b:

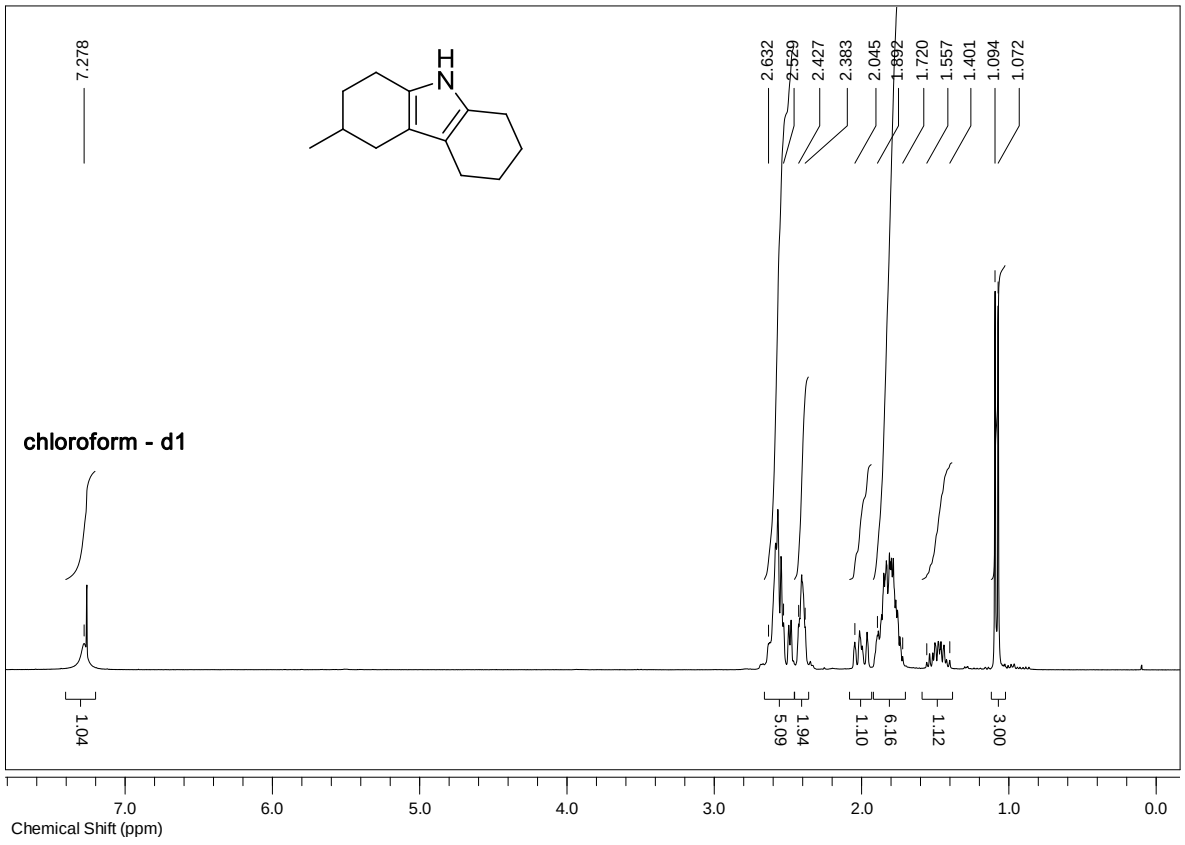
7.278
2.632
2.529
2.427
2.383
2.045
1.892
1.720
1.557
1.401
1.094
1.072
chloroform - d1
1.04
5.09
1.94
1.10
6.16
1.12
3.00
7.0
6.0
5.0
4.0
3.0
2.0
1.0
0.0
Chemical Shift (ppm)

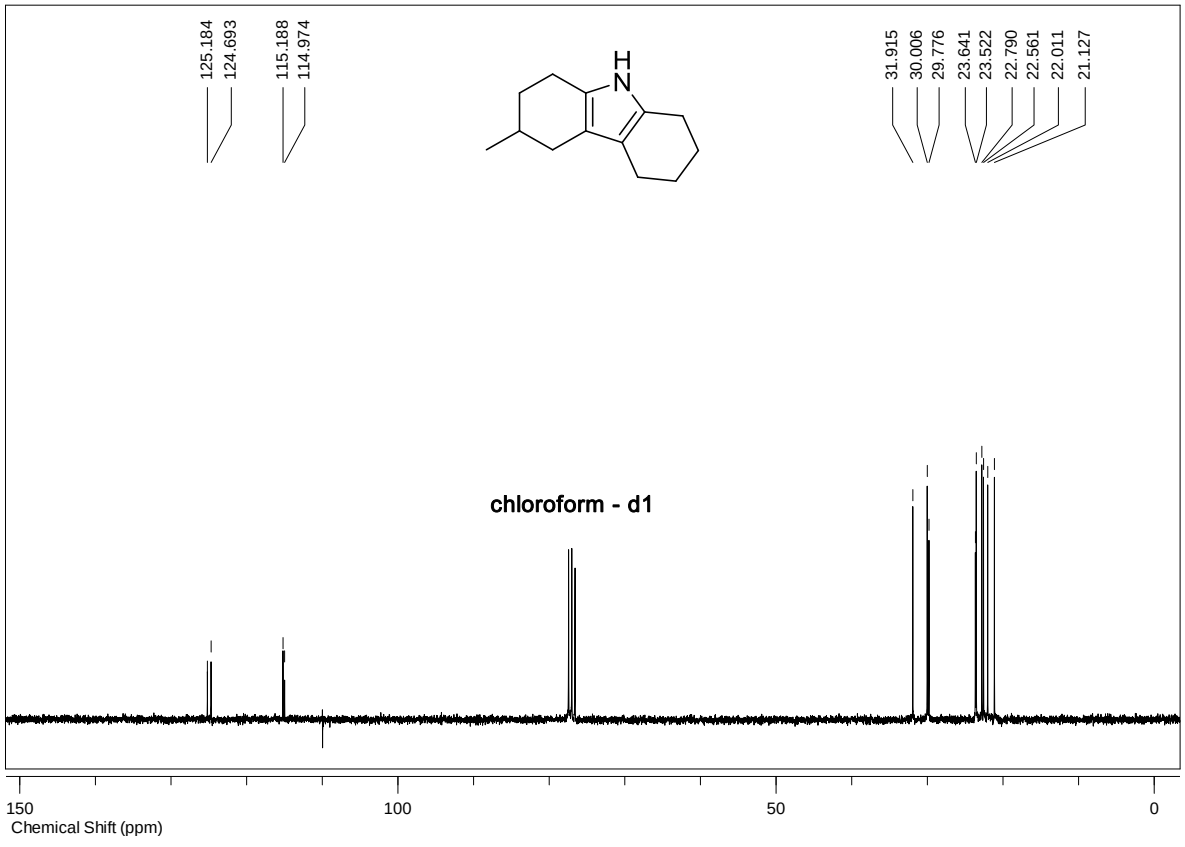
125.184
124.693
115.188
114.974
31.915
30.006
29.776
23.641
23.522
22.790
22.561
22.011
21.127
chloroform - d1
150
100
50
0
Chemical Shift (ppm)

2b:

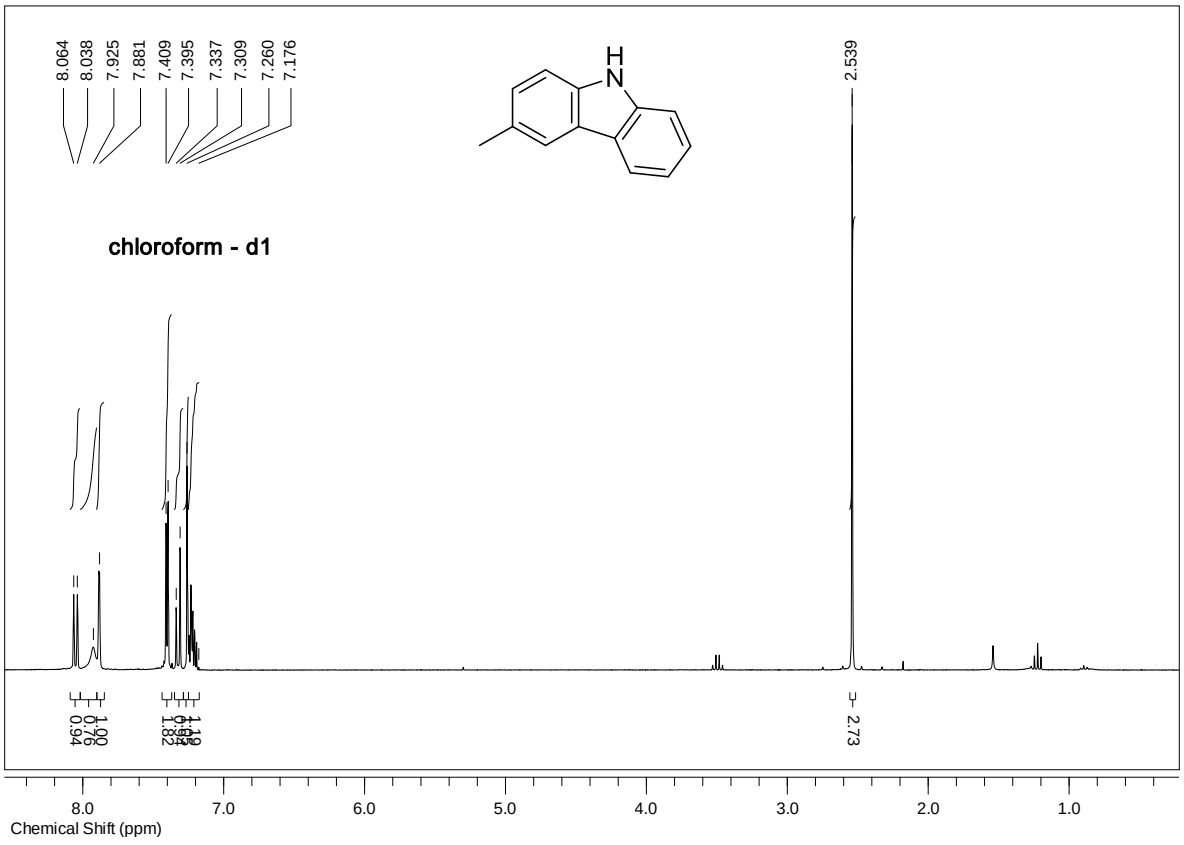
8.064
8.038
7.925
7.881
7.409
7.395
7.337
7.309
7.260
7.176
2.539
chloroform - d1
2.73
8.0
7.0
6.0
5.0
4.0
3.0
2.0
1.0
Chemical Shift (ppm)

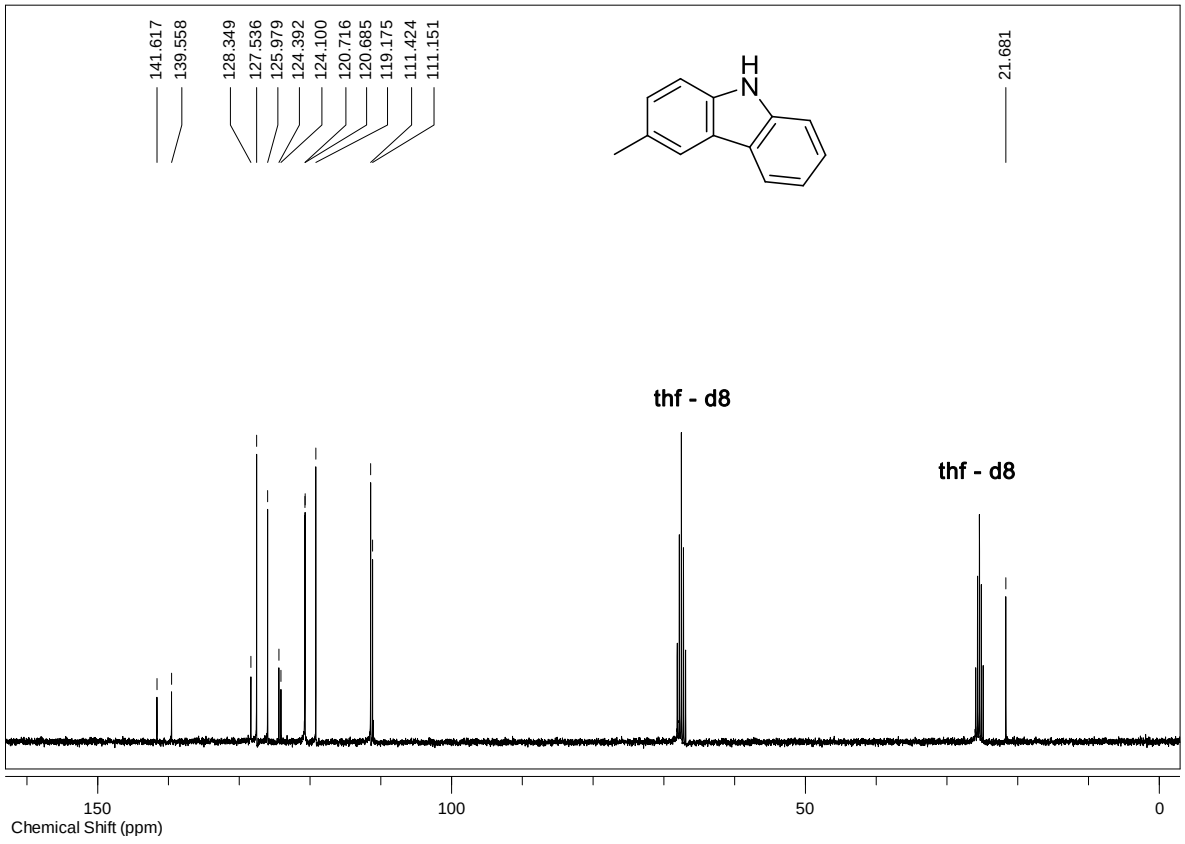
141.617
139.558
128.349
127.536
125.979
124.392
124.100
120.716
120.685
119.175
111.424
111.151
21.681
thf - d8
thf - d8
150
100
50
0
Chemical Shift (ppm)

6H-2c:

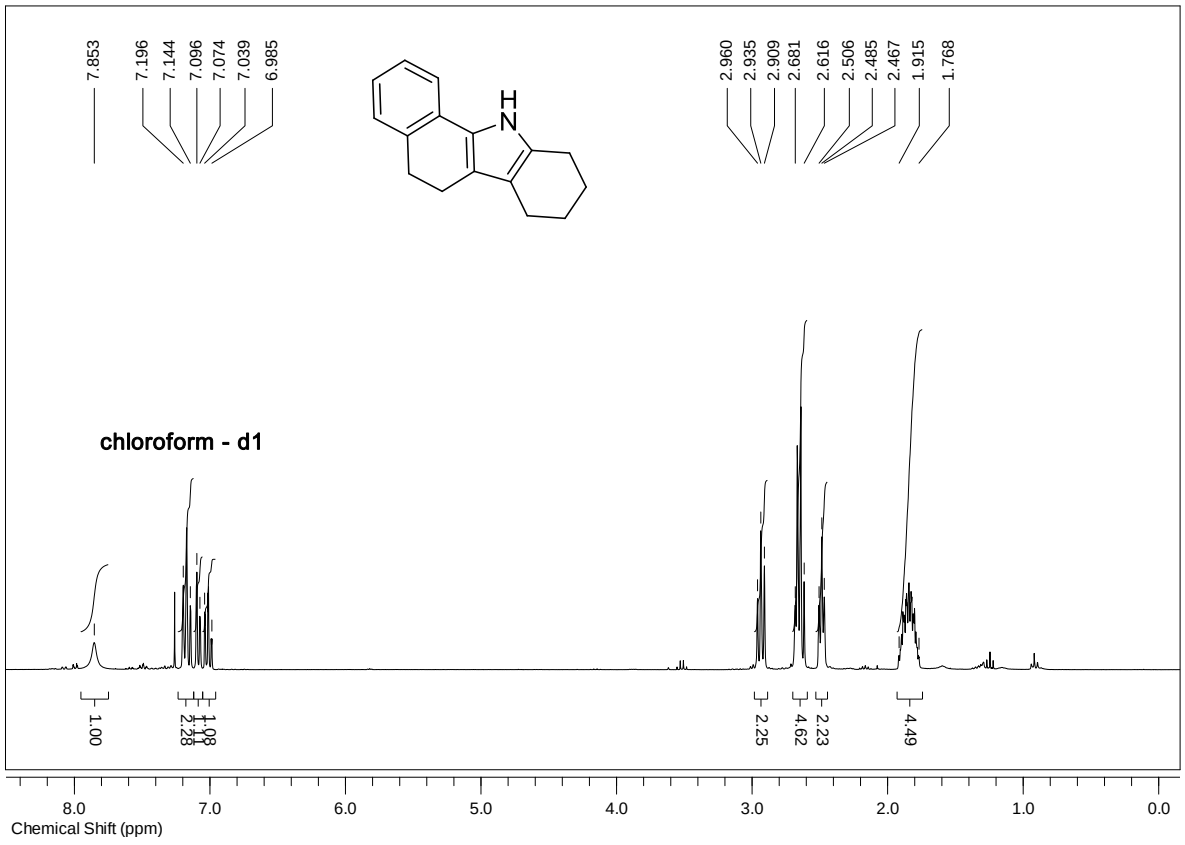
7.853
7.196
7.144
7.096
7.074
7.039
6.985
2.960
2.935
2.909
2.681
2.616
2.506
2.485
2.467
1.915
1.768
H
N
chloroform - d1
1.00
2.28
1.11
1.08
2.25
4.62
2.23
4.49
8.0
7.0
6.0
5.0
4.0
3.0
2.0
1.0
0.0
Chemical Shift (ppm)

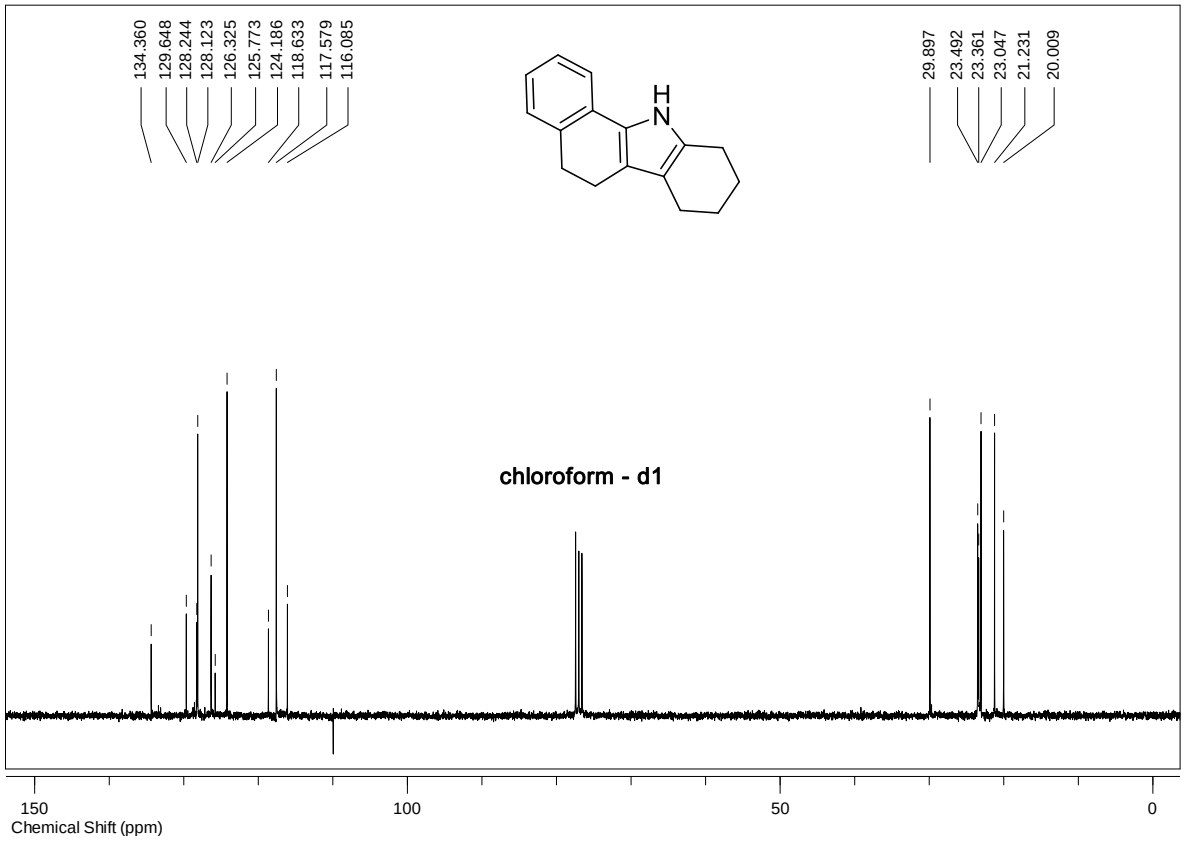
134.360
129.648
128.244
128.123
126.325
125.773
124.186
118.633
117.579
116.085
29.897
23.492
23.361
23.047
21.231
20.009
H
N
chloroform - d1
150
100
50
0
Chemical Shift (ppm)

2c:

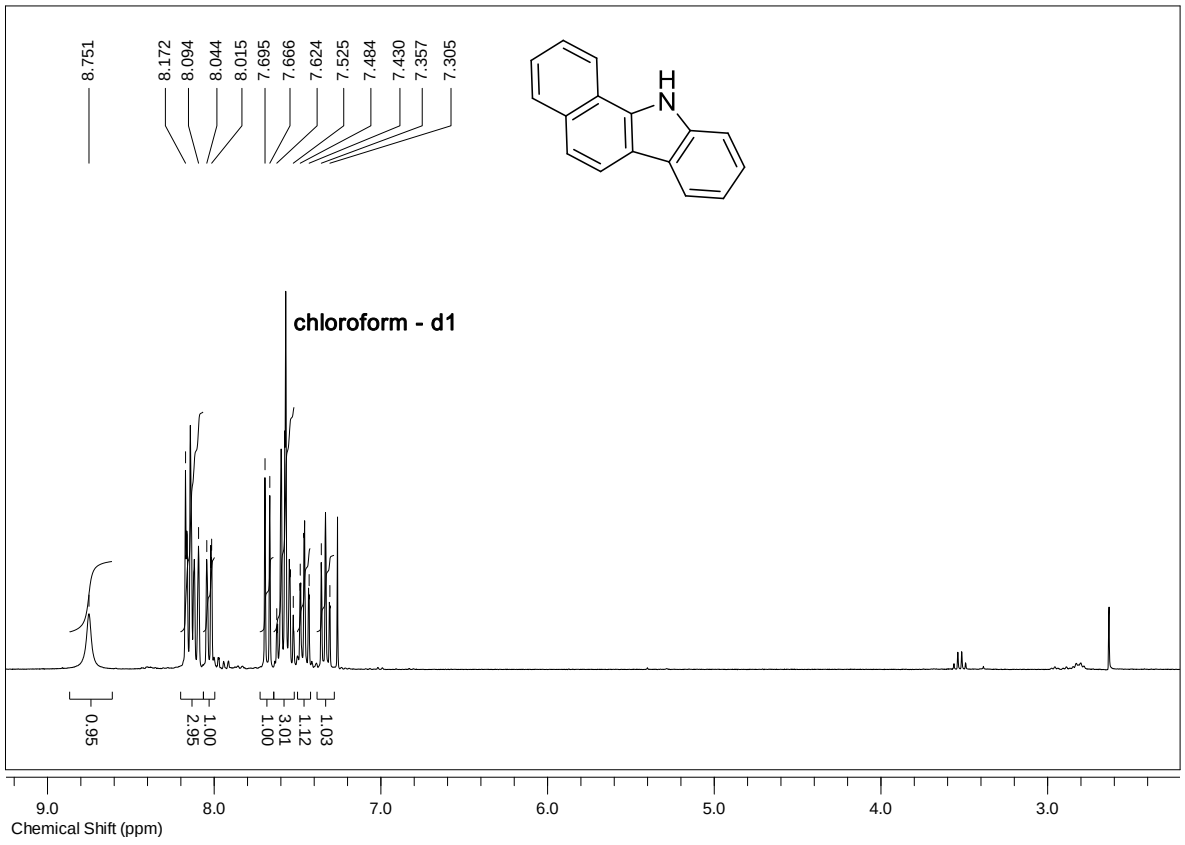
8.751
8.172
8.094
8.044
8.015
7.695
7.666
7.624
7.525
7.484
7.430
7.357
7.305
H
N
chloroform - d1
0.95
2.95
1.00
1.00
1.01
1.12
1.03
9.0
8.0
7.0
6.0
5.0
4.0
3.0
Chemical Shift (ppm)

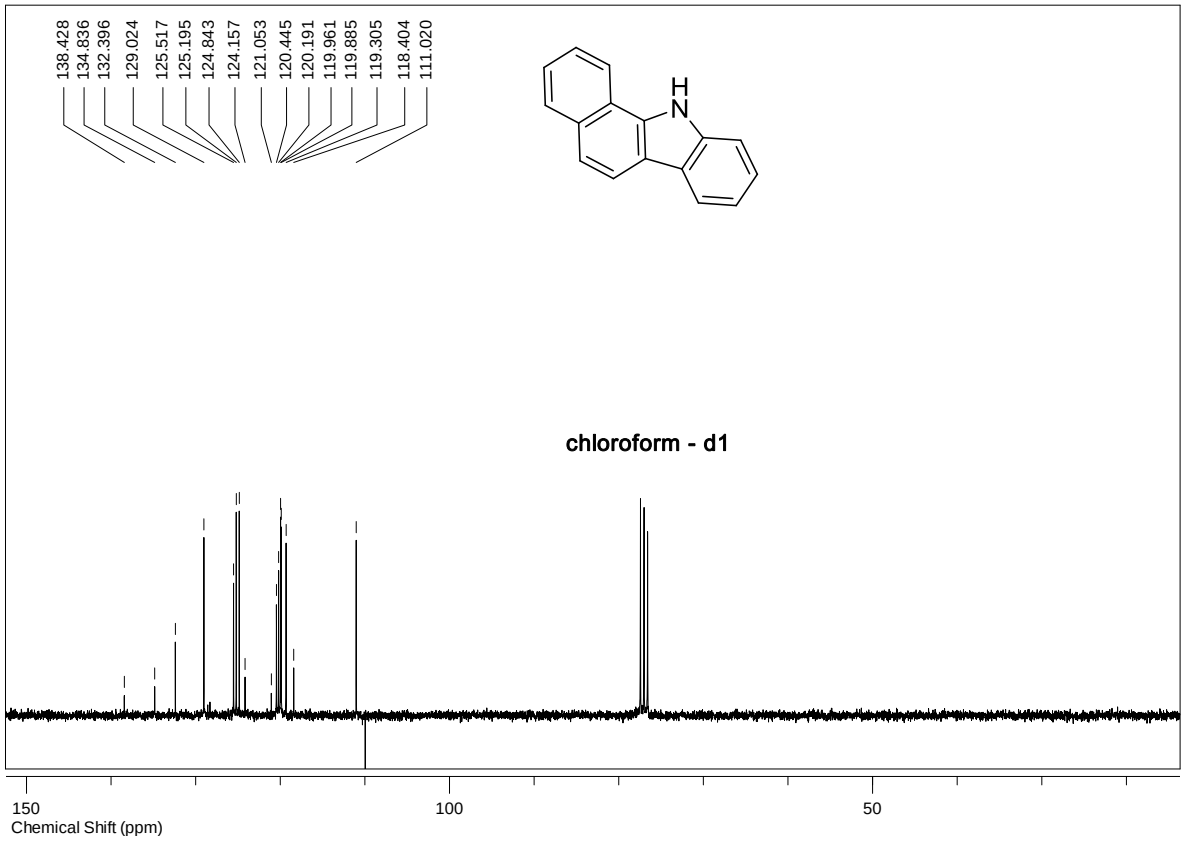
138.428
134.836
132.396
129.024
125.517
125.195
124.843
124.157
121.053
120.445
120.191
119.961
119.885
119.305
118.404
111.020
H
N
chloroform - d1
150
100
50
Chemical Shift (ppm)

4H-3a:

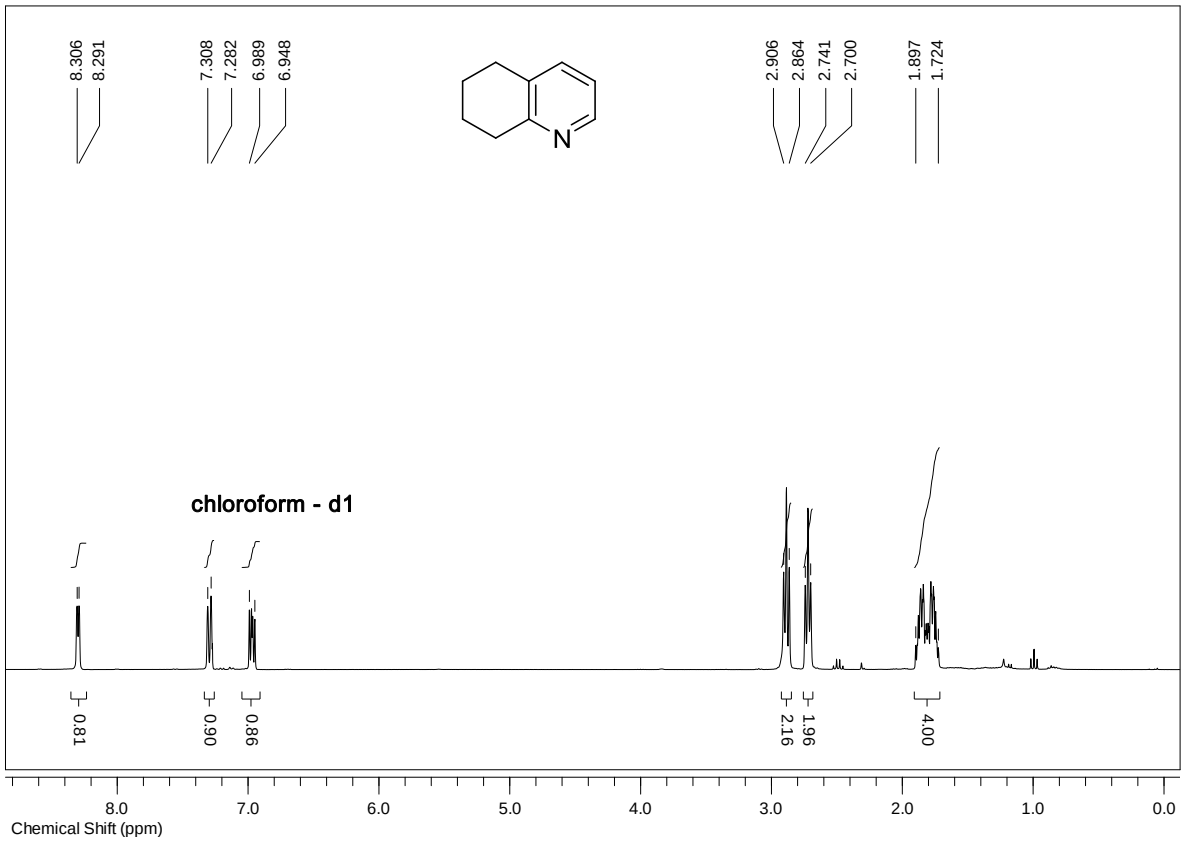
8.306
8.291
7.308
7.282
6.989
6.948
2.906
2.864
2.741
2.700
1.897
1.724
N
chloroform - d1
0.81
0.90
0.86
2.16
1.66
4.00
8.0
7.0
6.0
5.0
4.0
3.0
2.0
1.0
0.0
Chemical Shift (ppm)

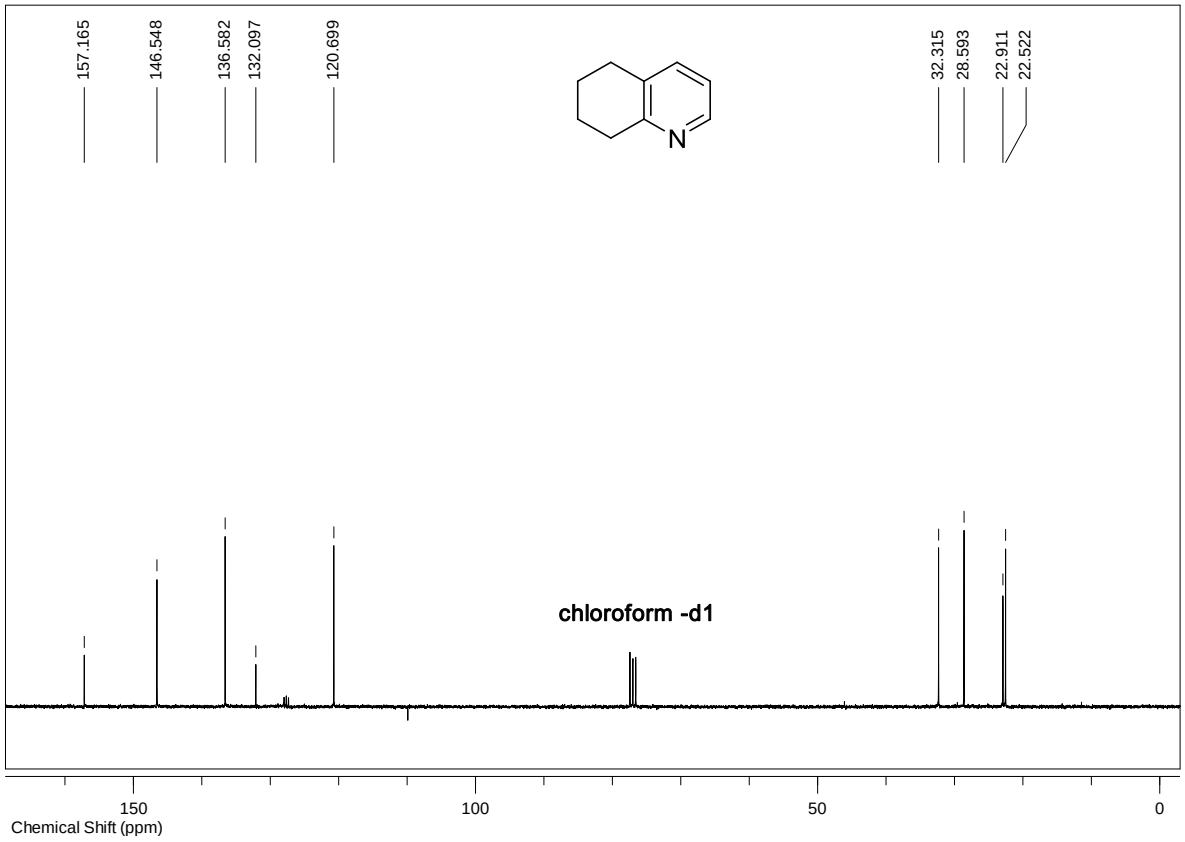
157.165
146.548
136.582
132.097
120.699
32.315
28.593
22.911
22.522
N
chloroform -d1
150
100
50
0
Chemical Shift (ppm)

3a:

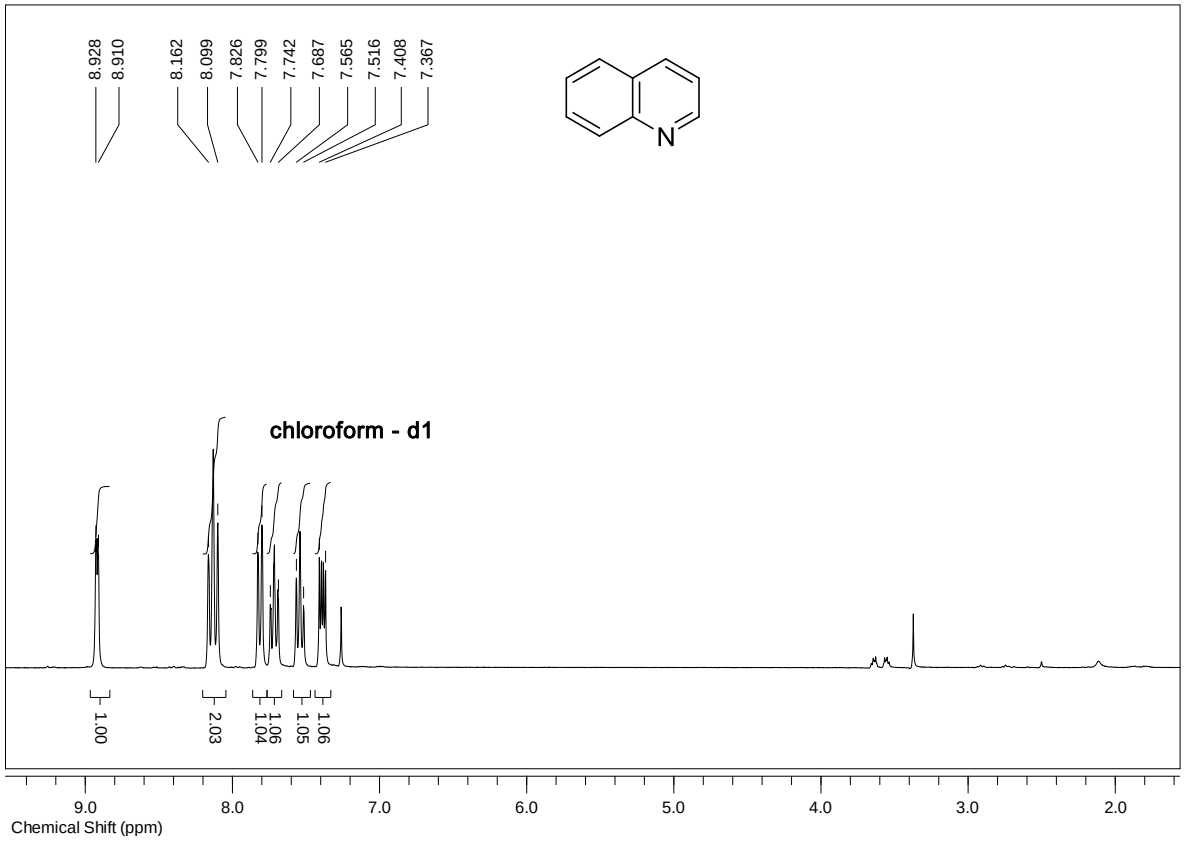
8.928
8.910
8.162
8.099
7.826
7.799
7.742
7.687
7.565
7.516
7.408
7.367
N
chloroform - d1
1.00
2.03
1.06
1.04
1.05
1.06
9.0
8.0
7.0
6.0
5.0
4.0
3.0
2.0
Chemical Shift (ppm)

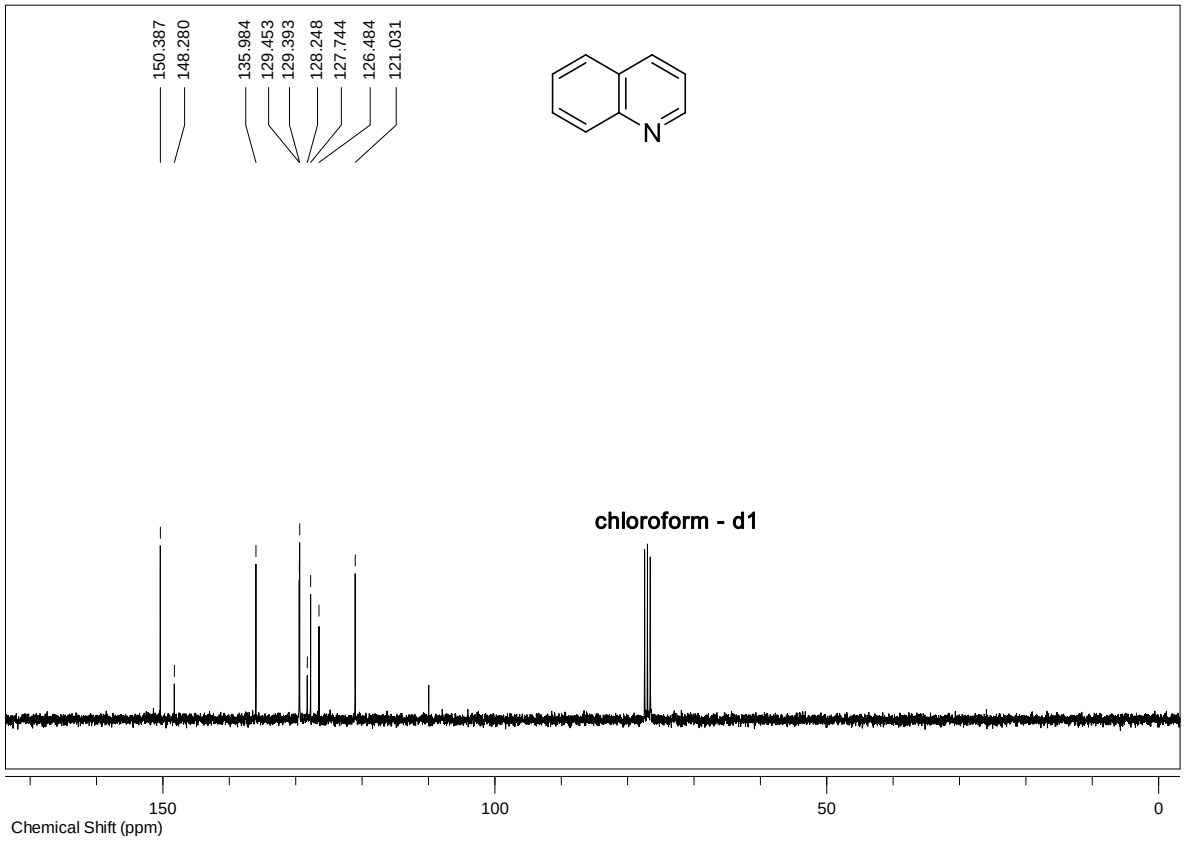
150.387
148.280
135.984
129.453
129.393
128.248
127.744
126.484
121.031
N
chloroform - d1
150
100
50
0
Chemical Shift (ppm)

4H-3b:

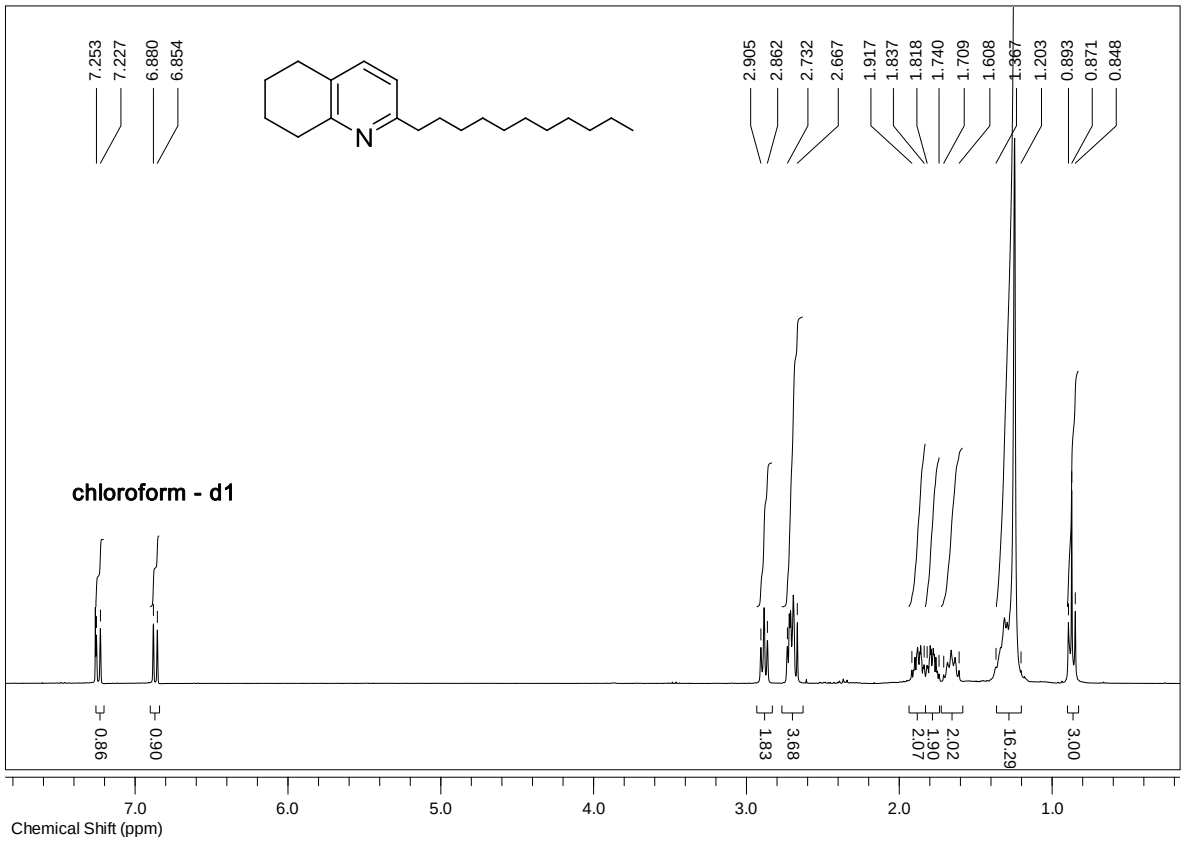
7.253
7.227
6.880
6.854
2.905
2.862
2.732
2.667
1.917
1.837
1.818
1.740
1.709
1.608
1.367
1.203
0.893
0.871
0.848
chloroform - d1
0.86
0.90
1.83
3.68
2.07
1.60
2.02
16.29
3.00
7.0
6.0
5.0
4.0
3.0
2.0
1.0
Chemical Shift (ppm)

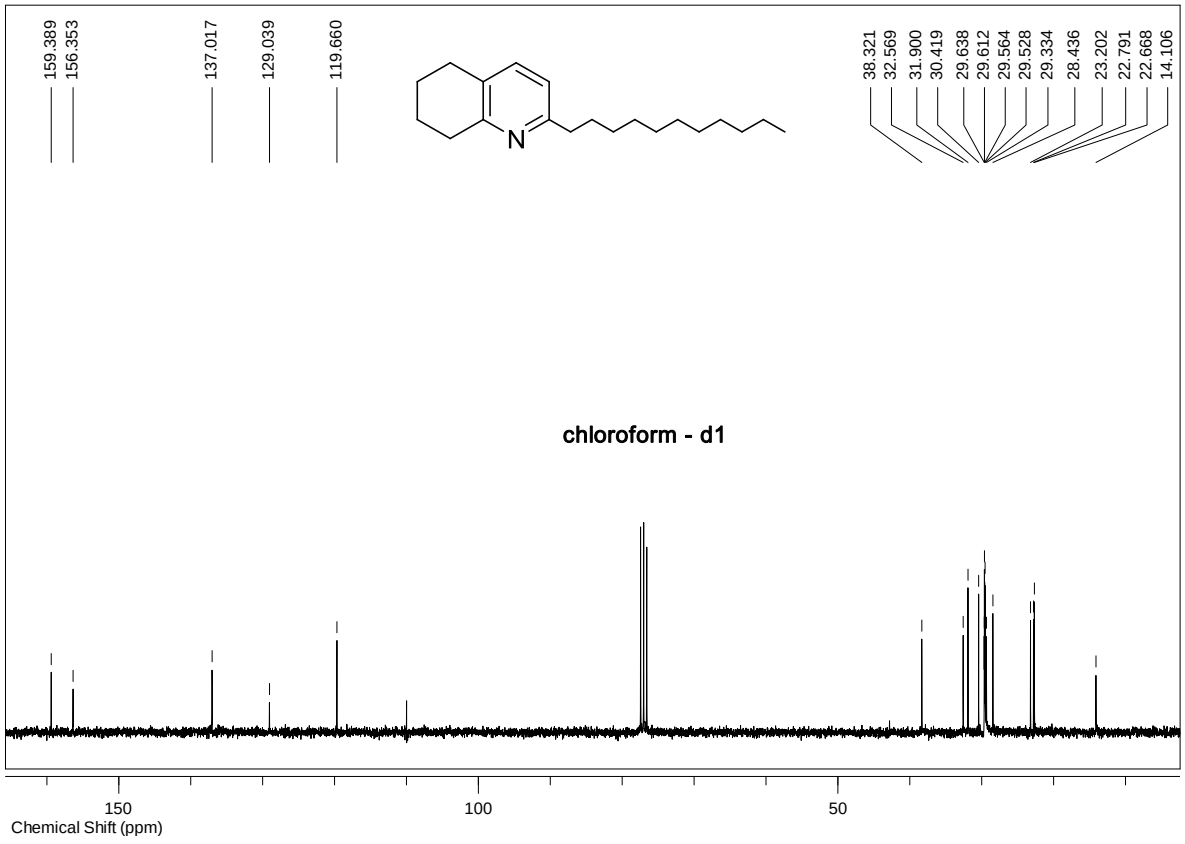
159.389
156.353
137.017
129.039
119.660
38.321
32.569
31.900
30.419
29.638
29.612
29.564
29.528
29.334
28.436
23.202
22.791
22.668
14.106
chloroform - d1
150
100
50
Chemical Shift (ppm)

3b:

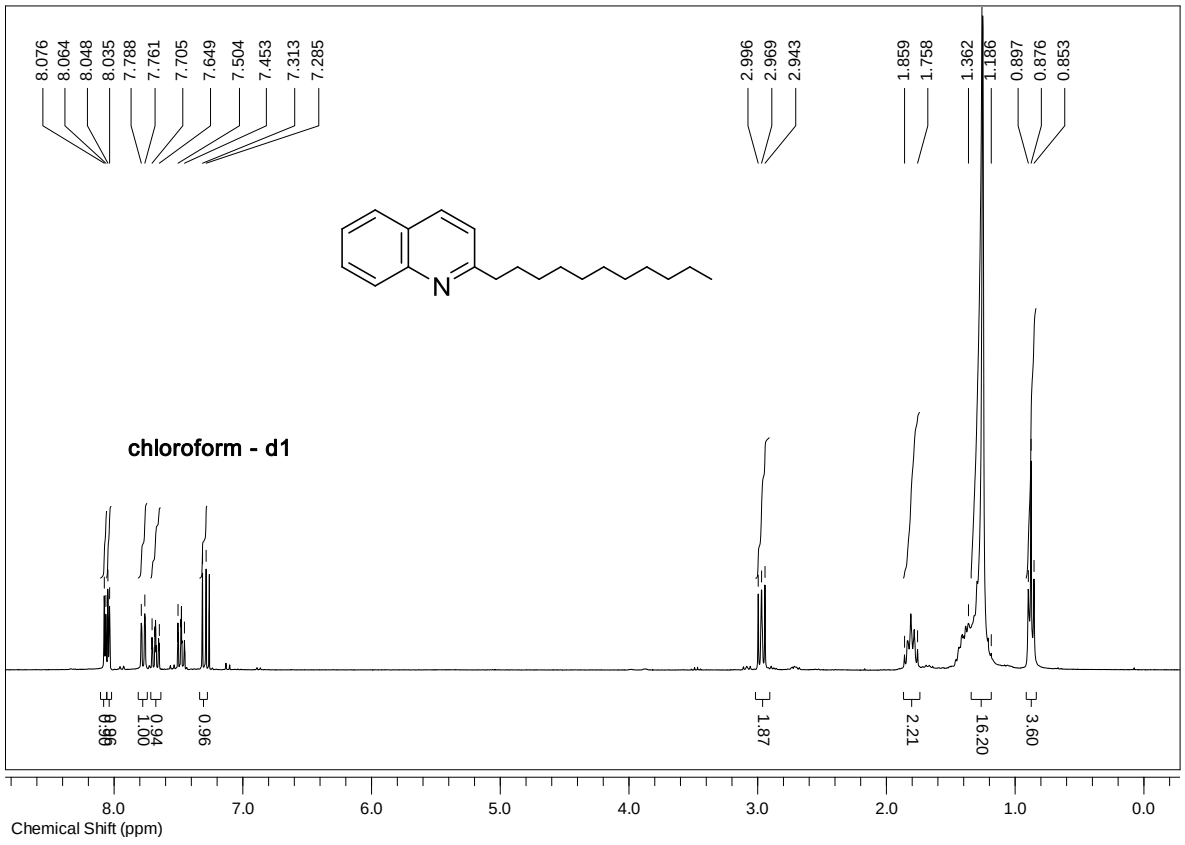
8.076
8.064
8.048
8.035
7.788
7.761
7.705
7.649
7.504
7.453
7.313
7.285
2.996
2.969
2.943
1.859
1.758
1.362
1.186
0.897
0.876
0.853
chloroform - d1
0.98
1.00
0.94
0.96
1.87
2.21
16.20
3.60
8.0
7.0
6.0
5.0
4.0
3.0
2.0
1.0
0.0
Chemical Shift (ppm)

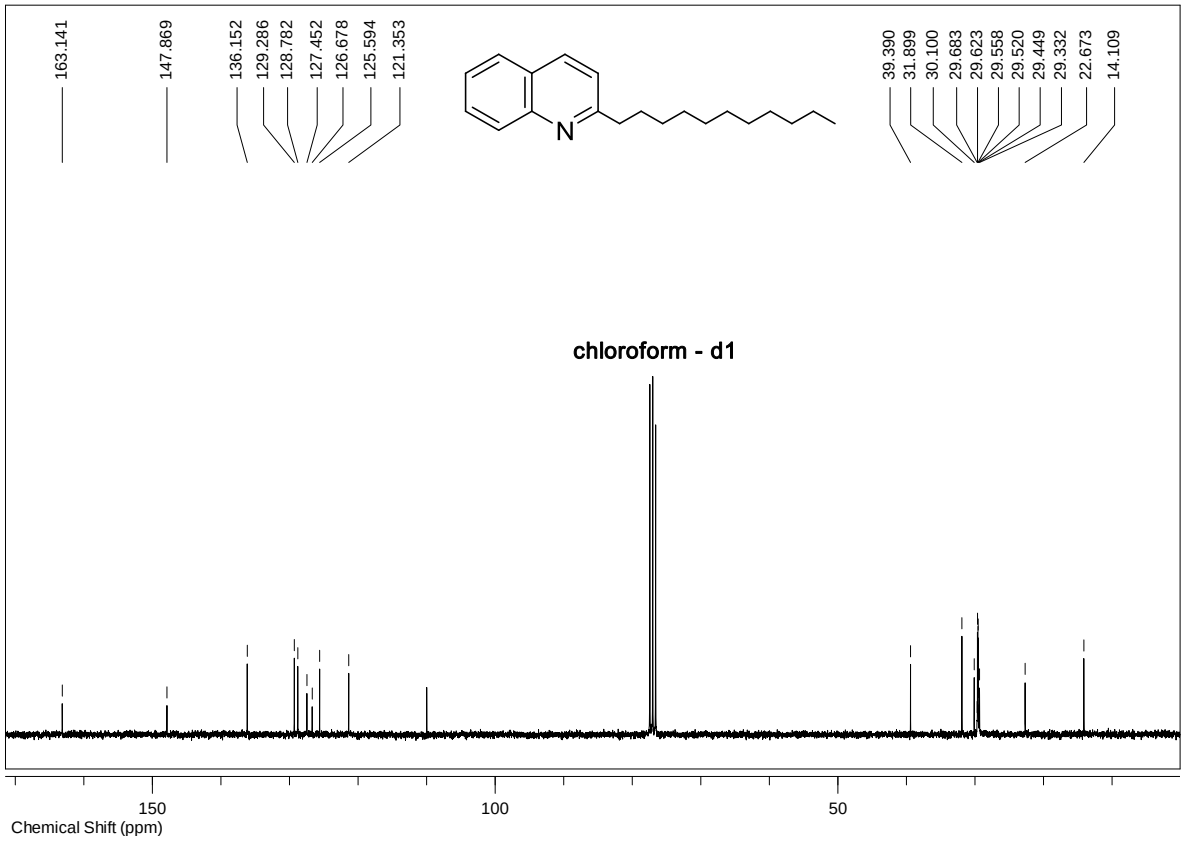
163.141
147.869
136.152
129.286
128.782
127.452
126.678
125.594
121.353
39.390
31.899
30.100
29.683
29.623
29.558
29.520
29.449
29.332
22.673
14.109
chloroform - d1
150
100
50
Chemical Shift (ppm)

4H-3c:

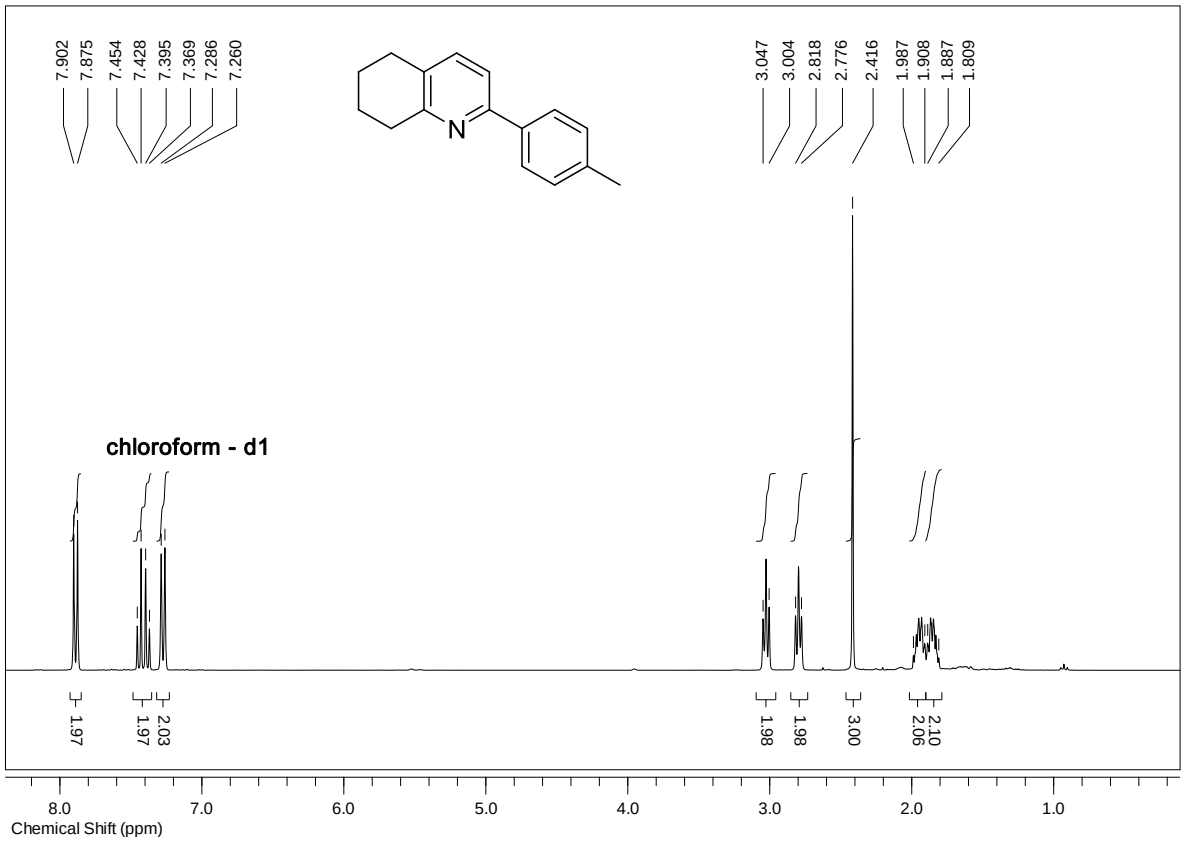
7.902
7.875
7.454
7.428
7.395
7.369
7.286
7.260
3.047
3.004
2.818
2.776
2.416
1.987
1.908
1.887
1.809
N
chloroform - d1
1.97
1.97
2.03
1.98
1.98
3.00
2.06
2.10
8.0
7.0
6.0
5.0
4.0
3.0
2.0
1.0
Chemical Shift (ppm)

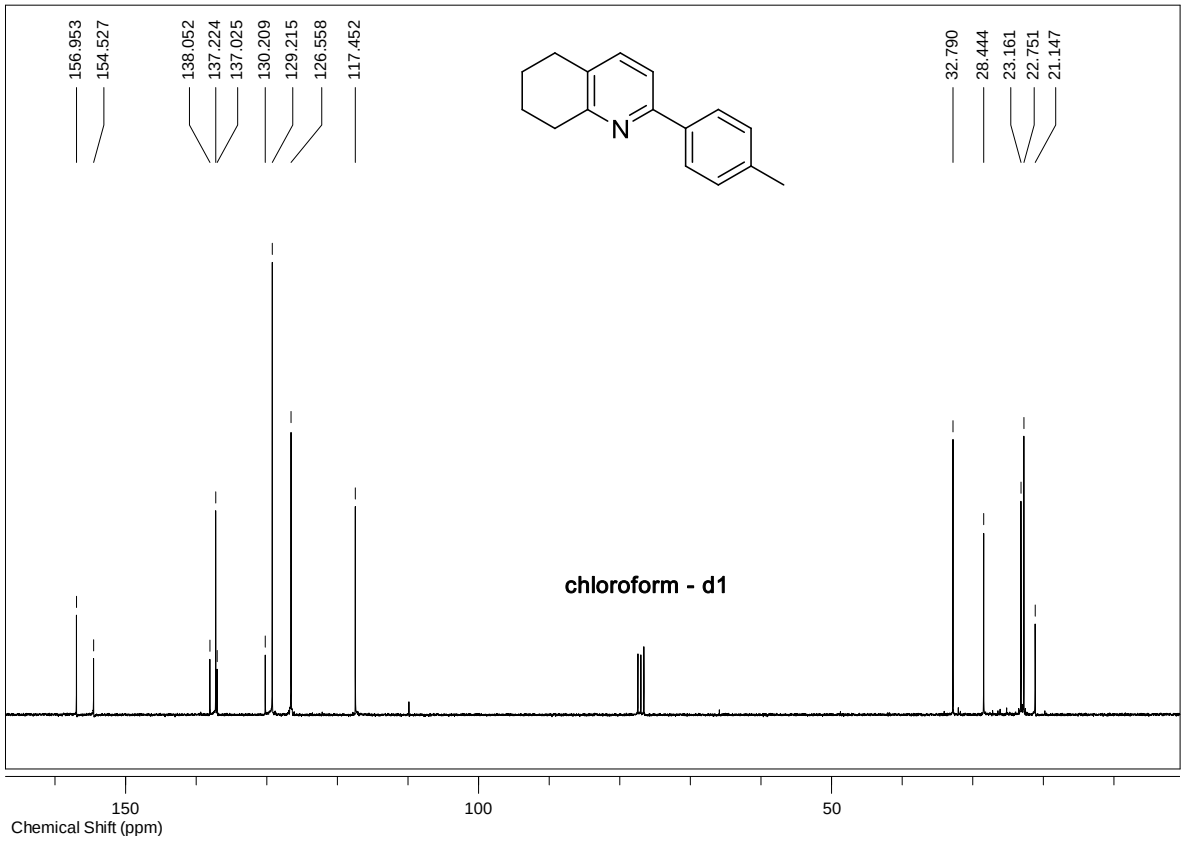
156.953
154.527
138.052
137.224
137.025
130.209
129.215
126.558
117.452
32.790
28.444
23.161
22.751
21.147
N
chloroform - d1
150
100
50
Chemical Shift (ppm)

3c:

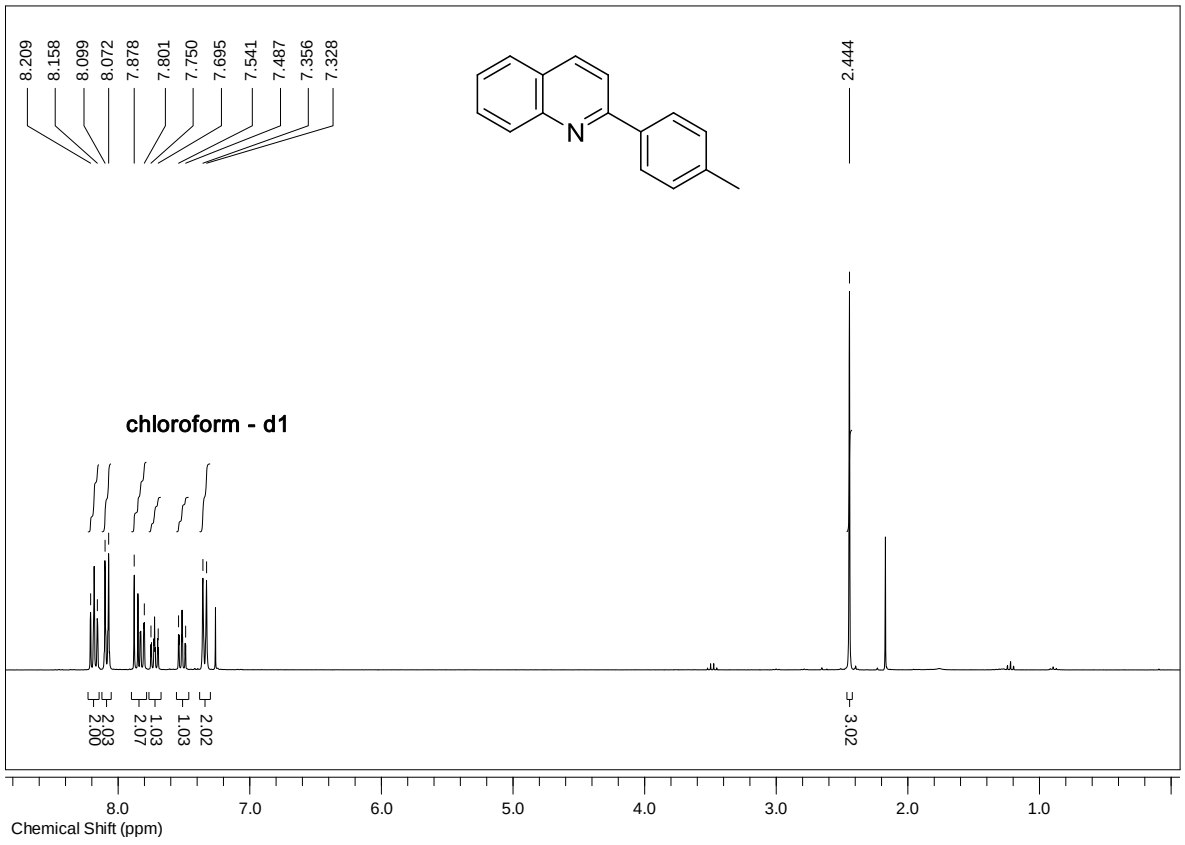
8.209
8.158
8.099
8.072
7.878
7.801
7.750
7.695
7.541
7.487
7.356
7.328
2.444
chloroform - d1
2.00
2.03
1.03
2.07
1.03
2.02
3.02
8.0
7.0
6.0
5.0
4.0
3.0
2.0
1.0
Chemical Shift (ppm)

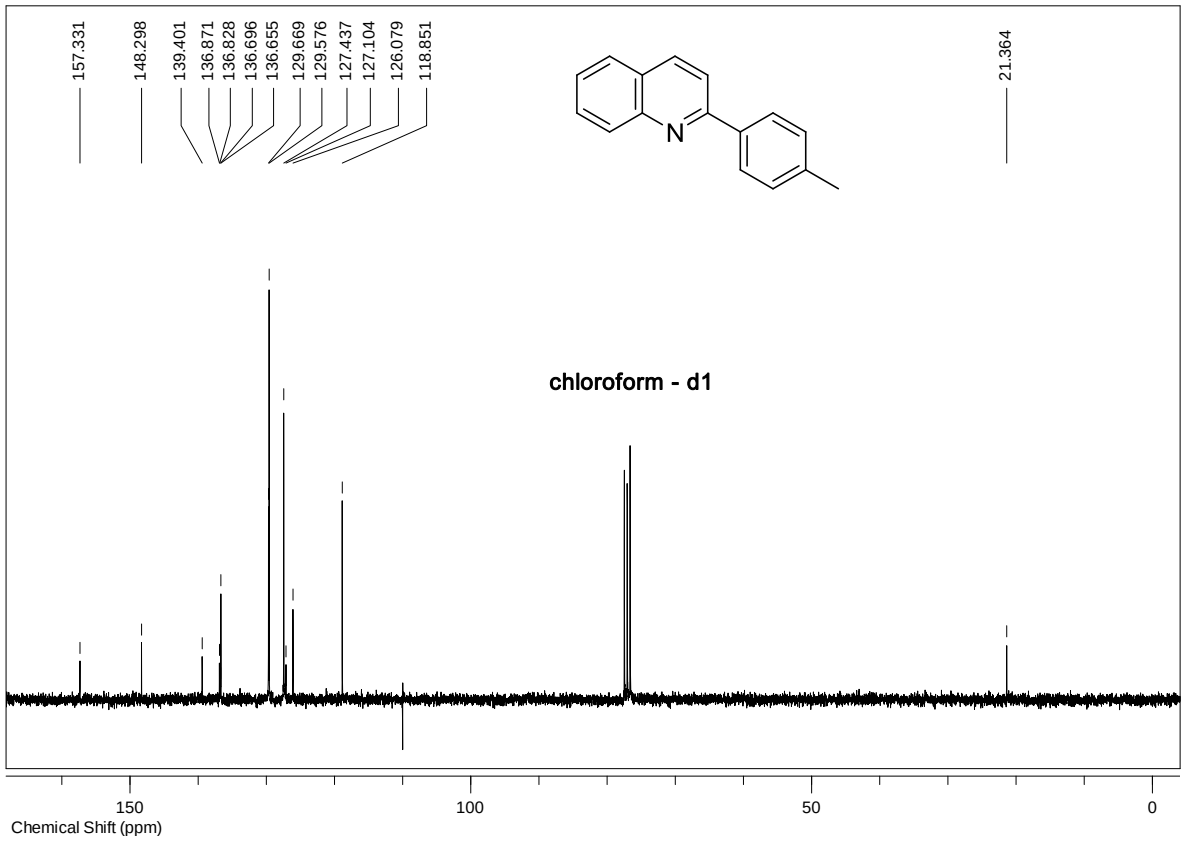
157.331
148.298
139.401
136.871
136.828
136.696
136.655
129.669
129.576
127.437
127.104
126.079
118.851
21.364
chloroform - d1
150
100
50
0
Chemical Shift (ppm)

4H-3d:

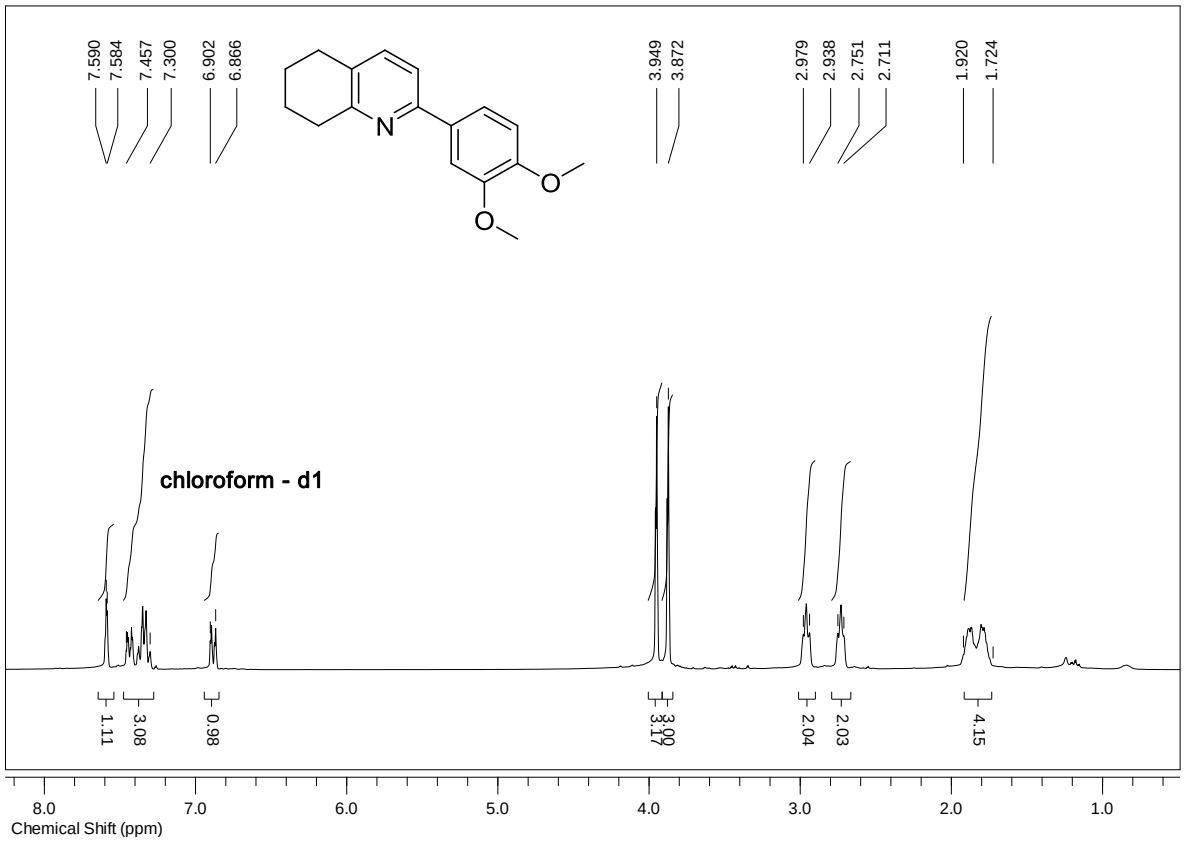
7.590
7.584
7.457
7.300
6.902
6.866
3.949
3.872
2.979
2.938
2.751
2.711
1.920
1.724
N
O
O
chloroform - d1
1.11
3.08
0.98
3.17
3.09
2.04
2.03
4.15
8.0
7.0
6.0
5.0
4.0
3.0
2.0
1.0
Chemical Shift (ppm)

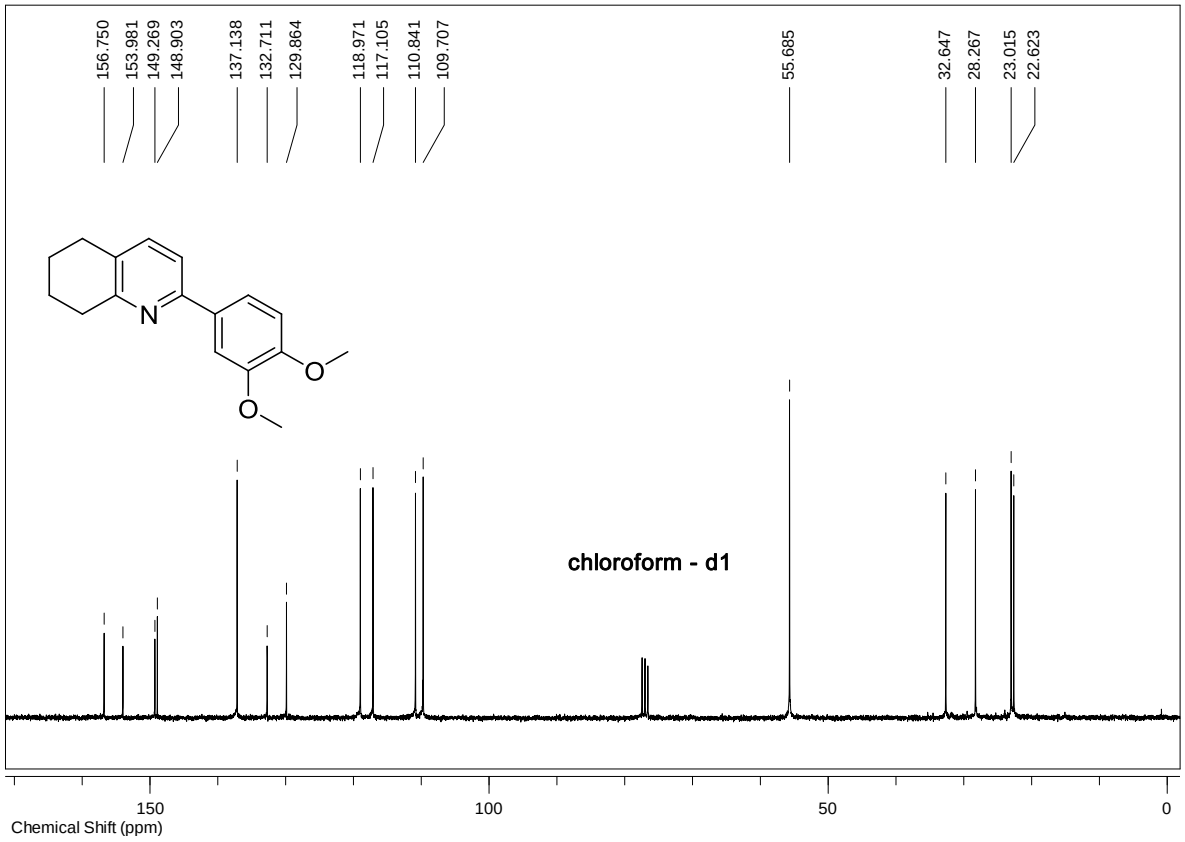
156.750
153.981
149.269
148.903
137.138
132.711
129.864
118.971
117.105
110.841
109.707
55.685
32.647
28.267
23.015
22.623
N
O
O
chloroform - d1
150
100
50
0
Chemical Shift (ppm)

3d:

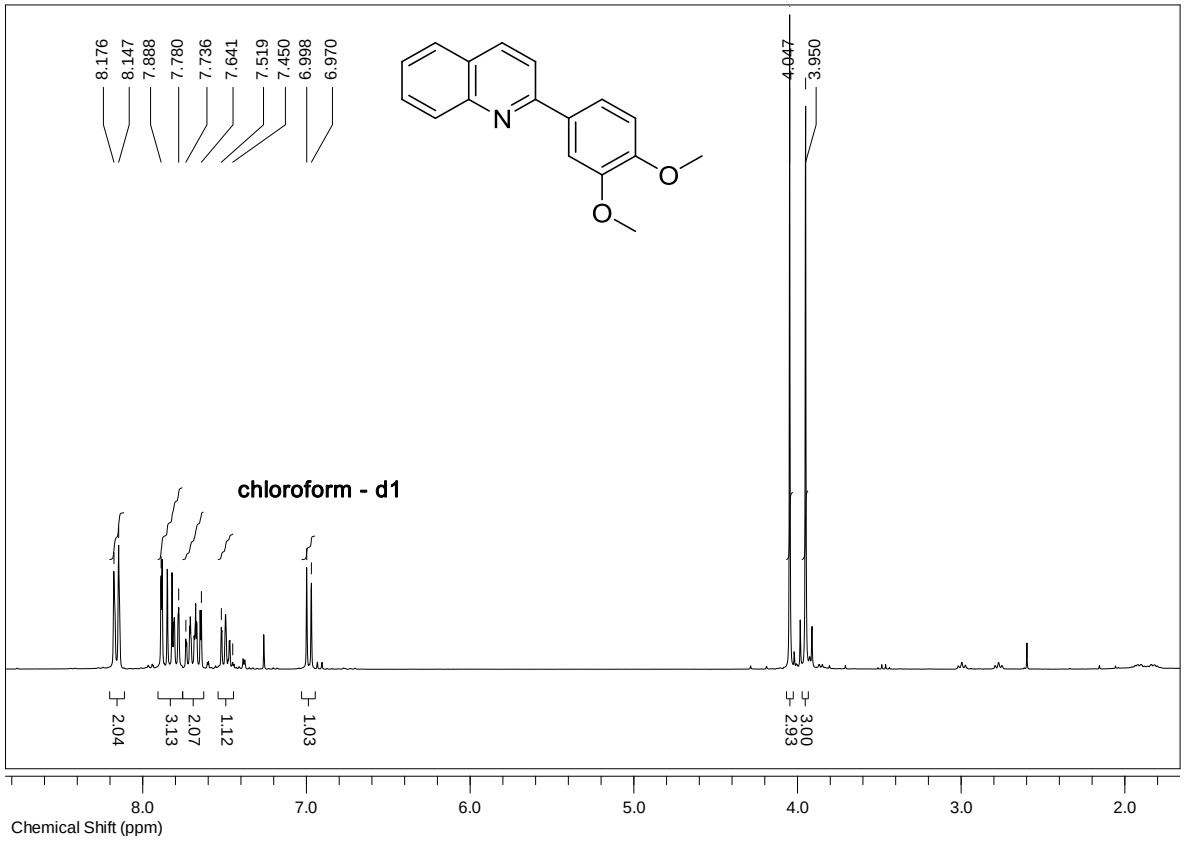
8.176
8.147
7.888
7.780
7.736
7.641
7.519
7.450
6.998
6.970
4.047
3.950
N
O
O
chloroform - d1
2.04
3.13
2.07
1.12
1.03
2.93
3.00
8.0
7.0
6.0
5.0
4.0
3.0
2.0
Chemical Shift (ppm)

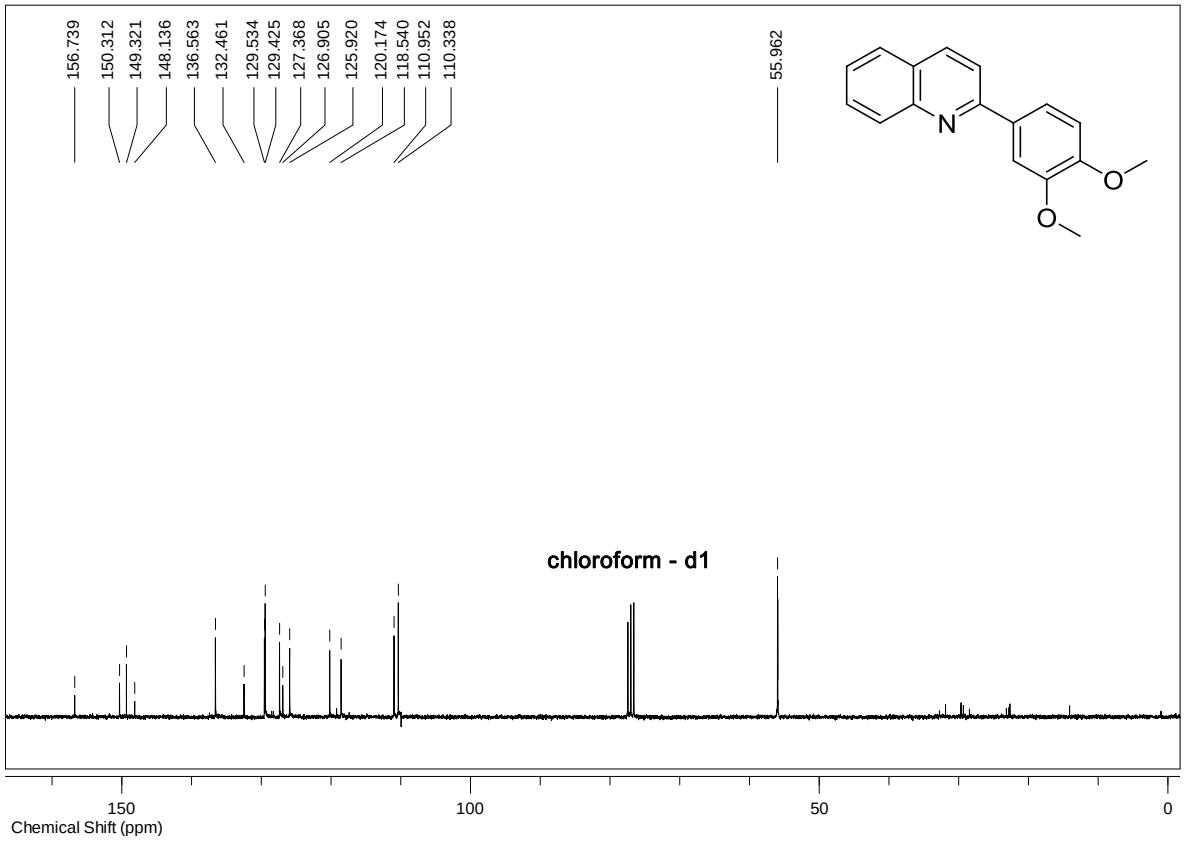
156.739
150.312
149.321
148.136
136.563
132.461
129.534
129.425
127.368
126.905
125.920
120.174
118.540
110.952
110.338
55.962
N
O
O
chloroform - d1
150
100
50
0
Chemical Shift (ppm)

4H-3e:

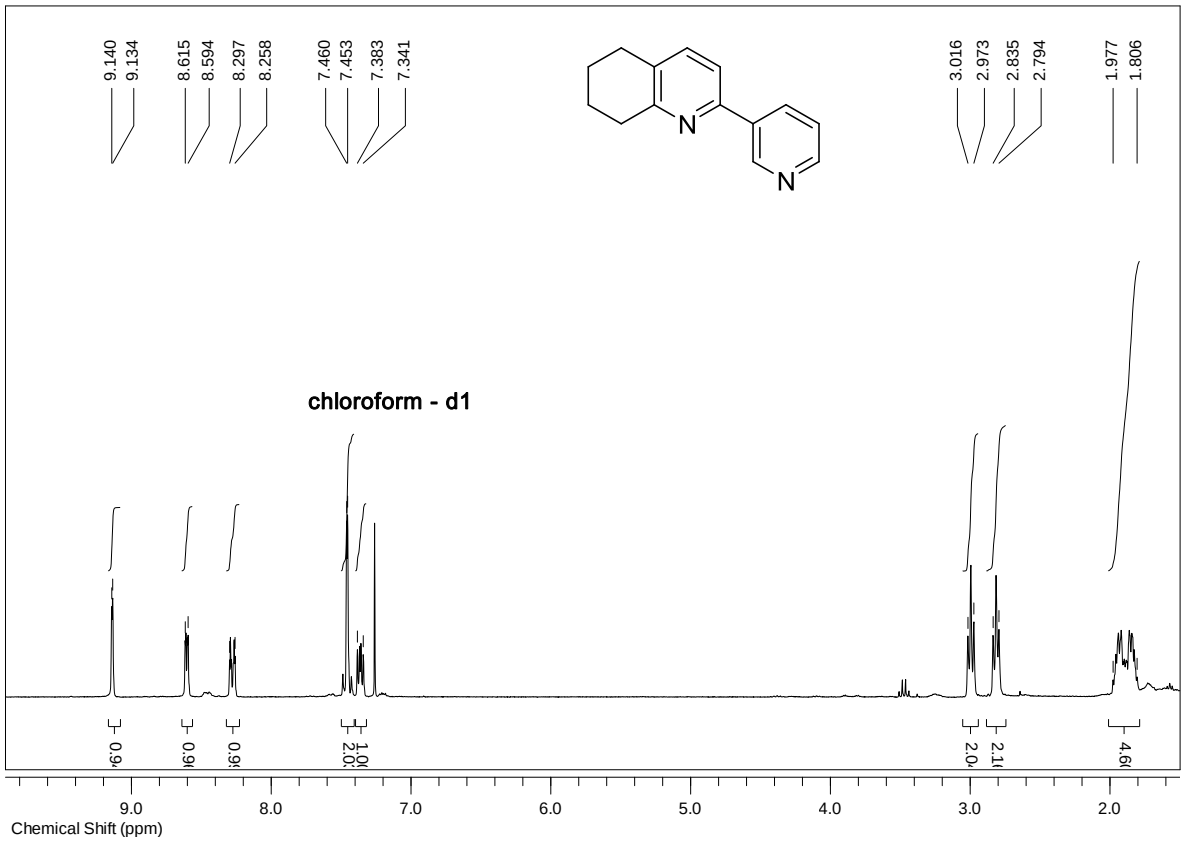
9.140
9.134
8.615
8.594
8.297
8.258
7.460
7.453
7.383
7.341
3.016
2.973
2.835
2.794
1.977
1.806
chloroform - d1
0.9
0.9
0.9
2.0
1.0
2.0
2.1
4.9
9.0
8.0
7.0
6.0
5.0
4.0
3.0
2.0
Chemical Shift (ppm)

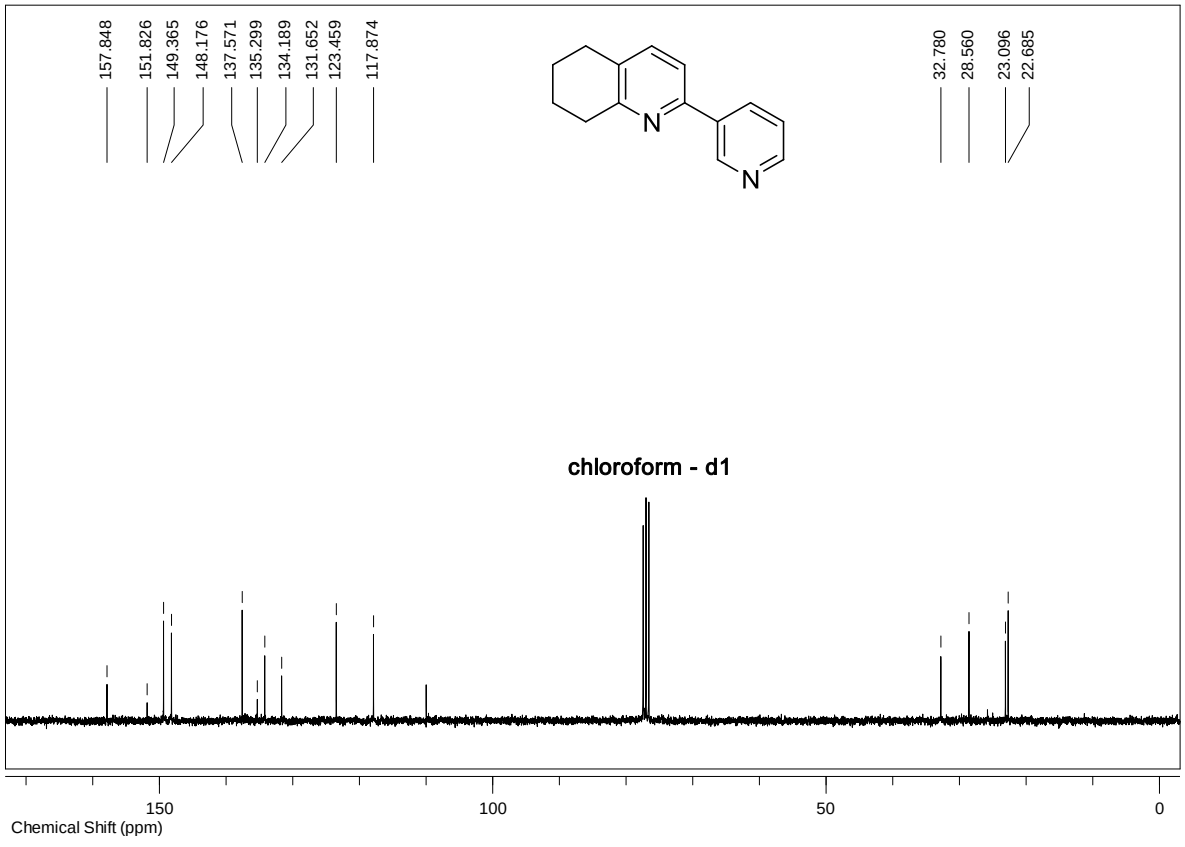
157.848
151.826
149.365
148.176
137.571
135.299
134.189
131.652
123.459
117.874
32.780
28.560
23.096
22.685
chloroform - d1
150
100
50
0
Chemical Shift (ppm)

3e:

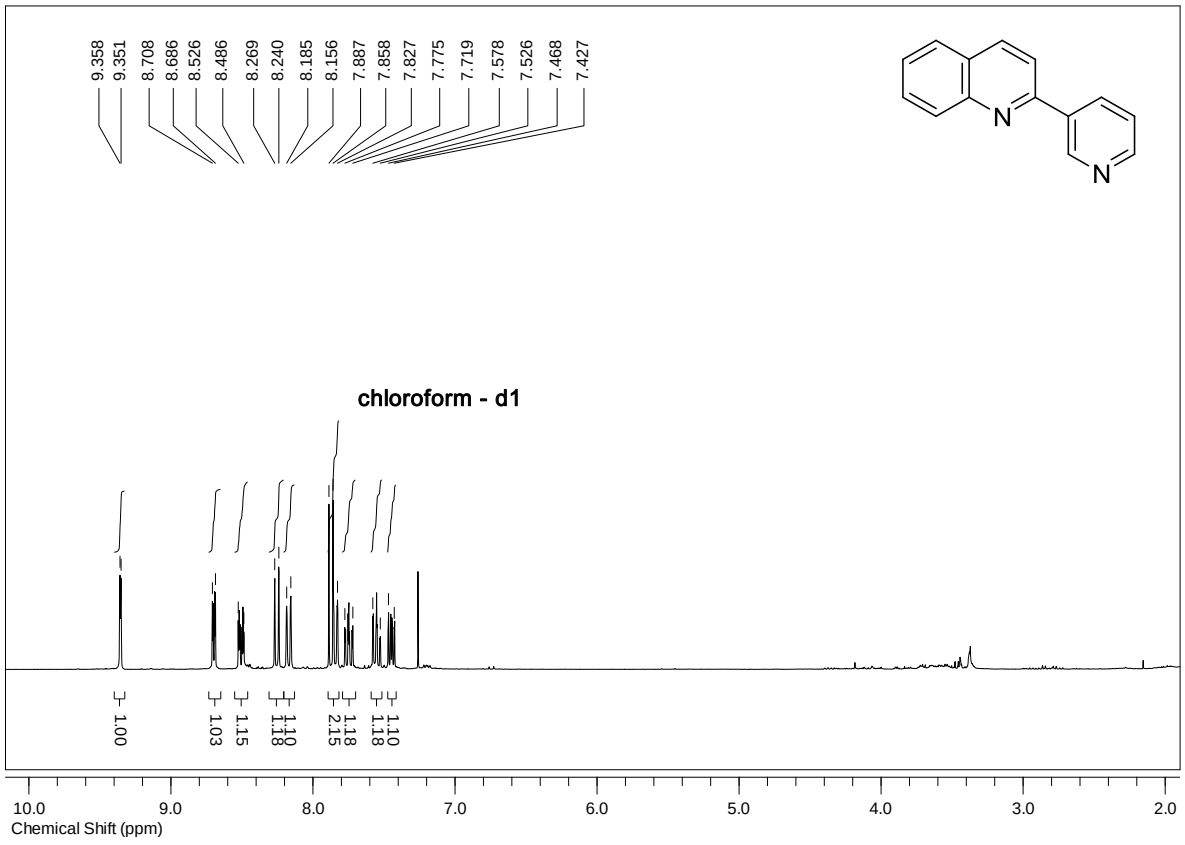
9.358
9.351
8.708
8.686
8.526
8.486
8.269
8.240
8.185
8.156
7.887
7.858
7.827
7.775
7.719
7.578
7.526
7.468
7.427
N
N
chloroforom - d1
1.00
1.03
1.15
1.10
1.18
2.15
1.18
1.10
10.0
9.0
8.0
7.0
6.0
5.0
4.0
3.0
2.0
Chemical Shift (ppm)

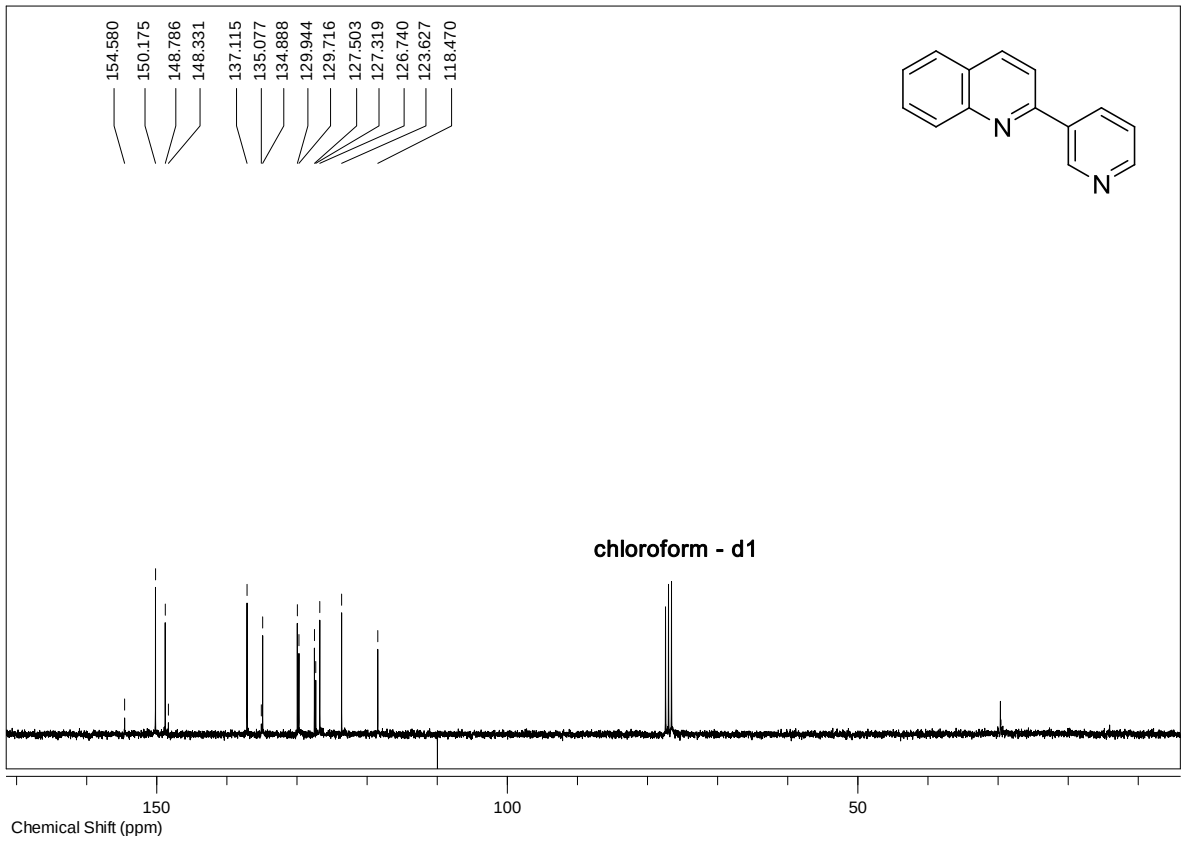
154.580
150.175
148.786
148.331
137.115
135.077
134.888
129.944
129.716
127.503
127.319
126.740
123.627
118.470
N
N
chloroform - d1
150
100
50
Chemical Shift (ppm)

4H-4a:

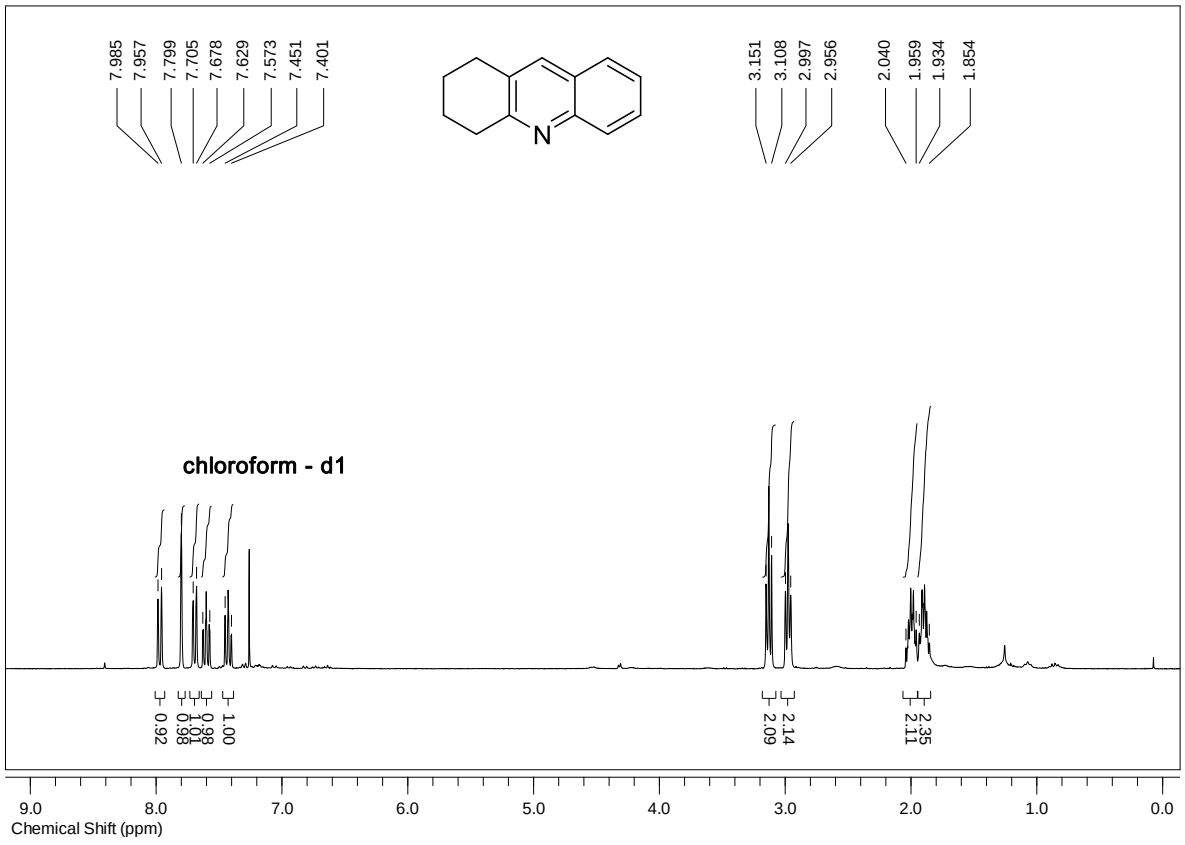
7.985
7.957
7.799
7.705
7.678
7.629
7.573
7.451
7.401
3.151
3.108
2.997
2.956
2.040
1.959
1.934
1.854
N
chloroform - d1
0.92
0.88
1.01
0.98
1.00
2.09
2.14
2.35
2.11
9.0
8.0
7.0
6.0
5.0
4.0
3.0
2.0
1.0
0.0
Chemical Shift (ppm)

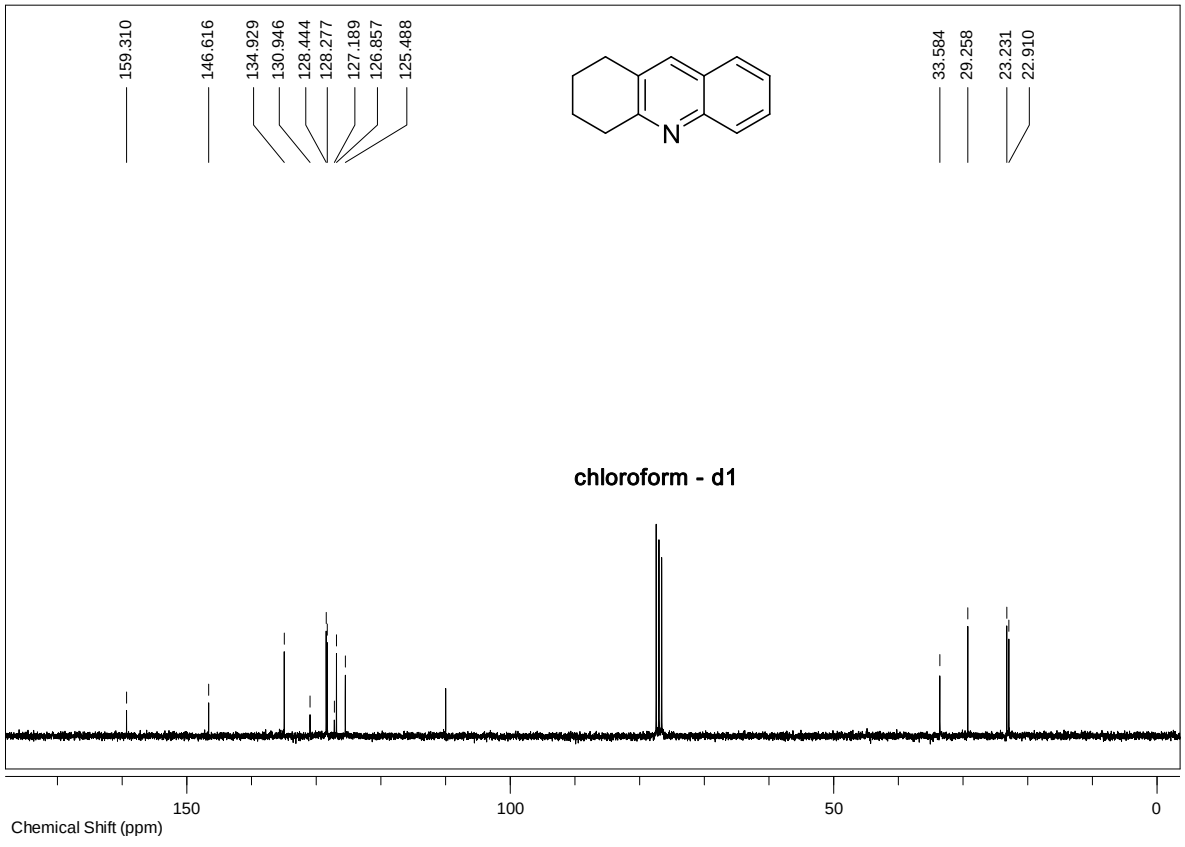
159.310
146.616
134.929
130.946
128.444
128.277
127.189
126.857
125.488
33.584
29.258
23.231
22.910
N
chloroform - d1
150
100
50
0
Chemical Shift (ppm)

4a:

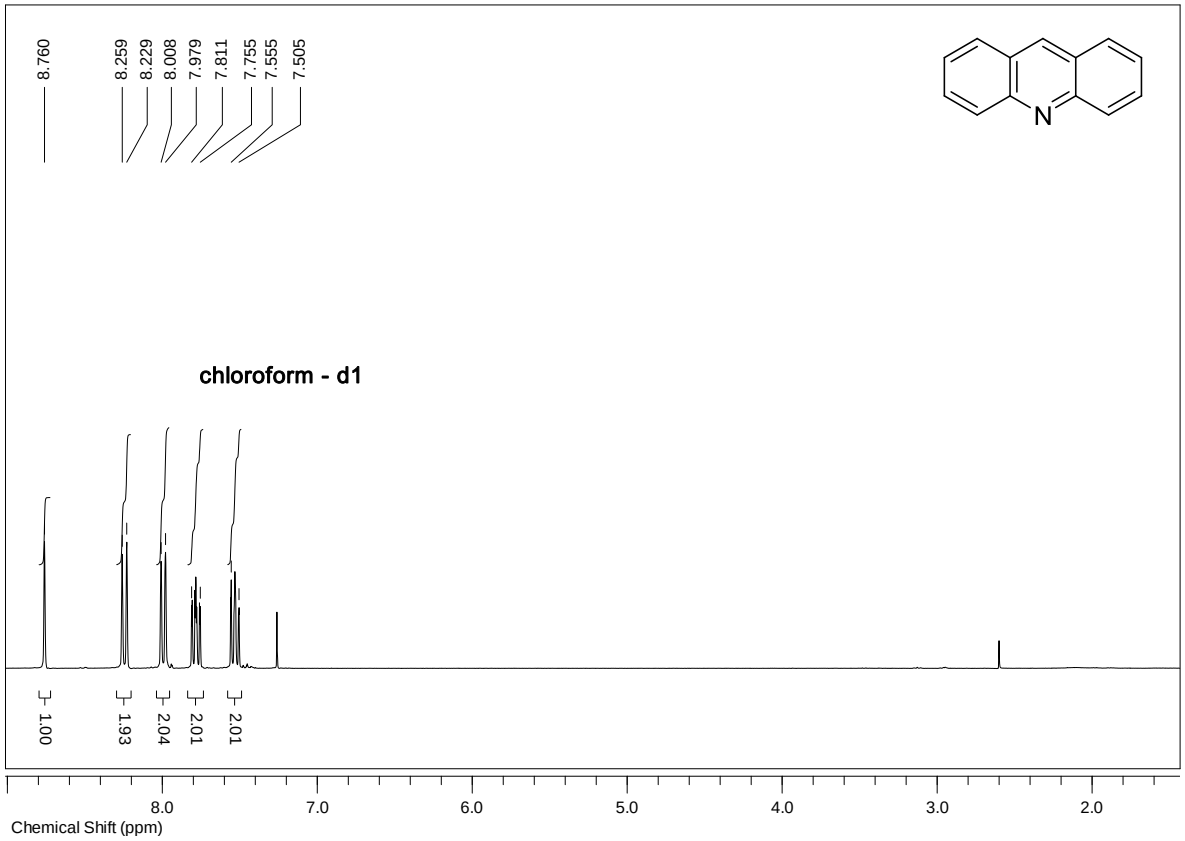
8.760
8.259
8.229
8.008
7.979
7.811
7.755
7.555
7.505
N
chloroform - d1
1.00
1.93
2.04
2.01
2.01
8.0
7.0
6.0
5.0
4.0
3.0
2.0
Chemical Shift (ppm)

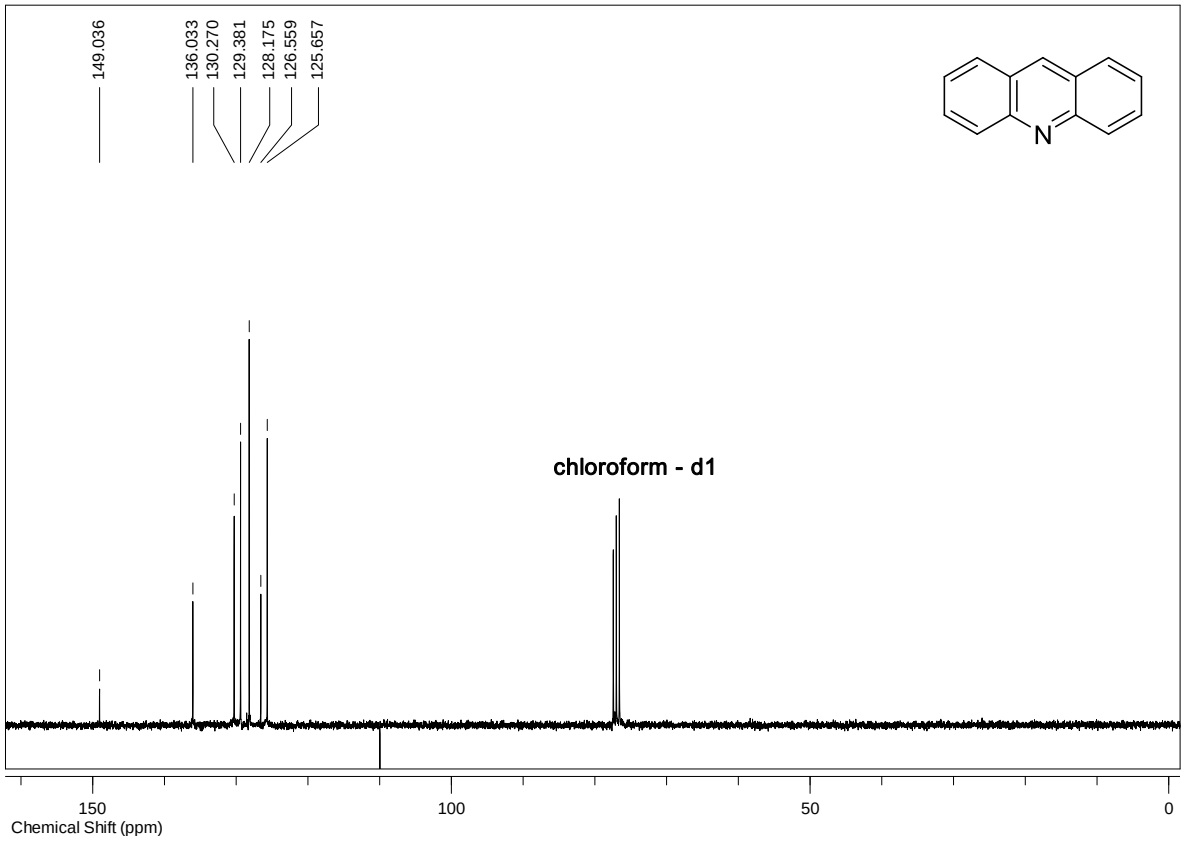
149.036
136.033
130.270
129.381
128.175
126.559
125.657
N
chloroform - d1
150
100
50
0
Chemical Shift (ppm)

4H-4b:

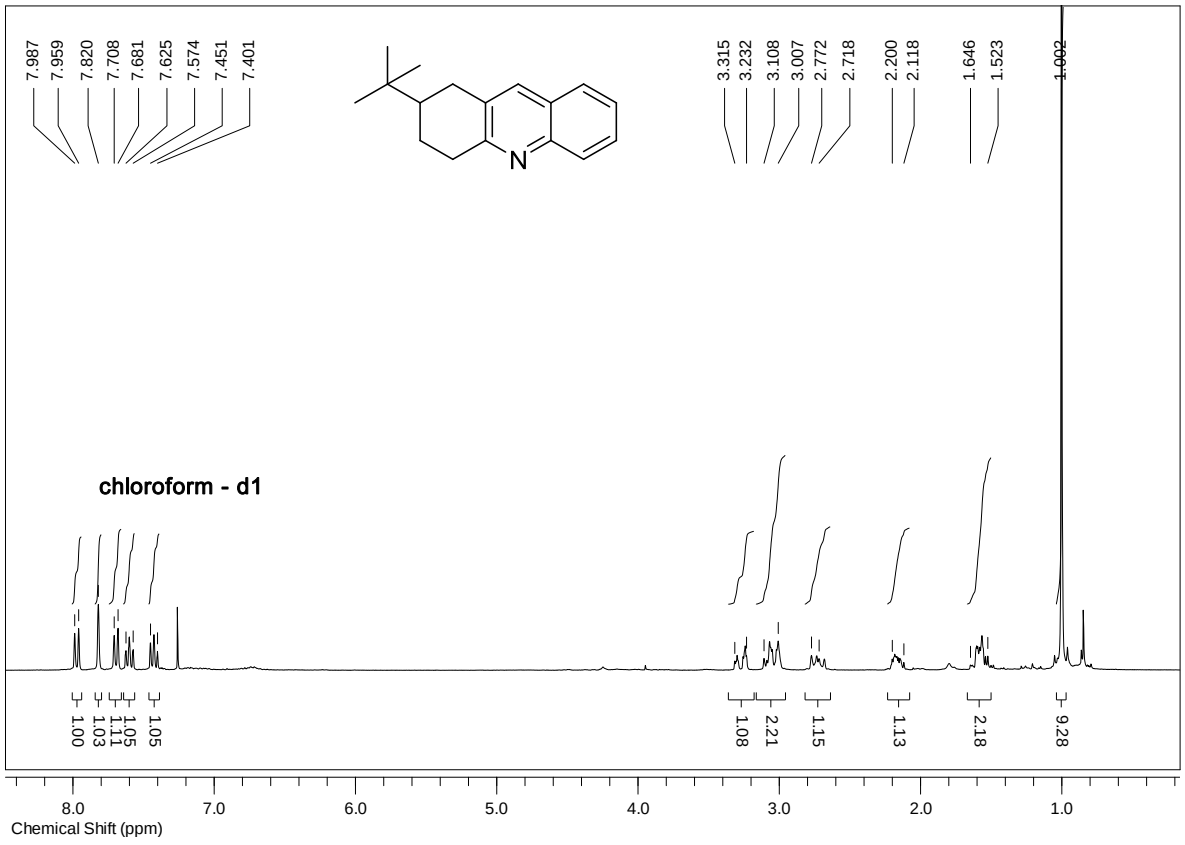
7.987
7.959
7.820
7.708
7.681
7.625
7.574
7.451
7.401
3.315
3.232
3.108
3.007
2.772
2.718
2.200
2.118
1.646
1.523
1.002
chloroform - d1
1.00
1.03
1.11
1.05
1.05
1.08
2.21
1.15
1.13
2.18
9.28
8.0
7.0
6.0
5.0
4.0
3.0
2.0
1.0
Chemical Shift (ppm)

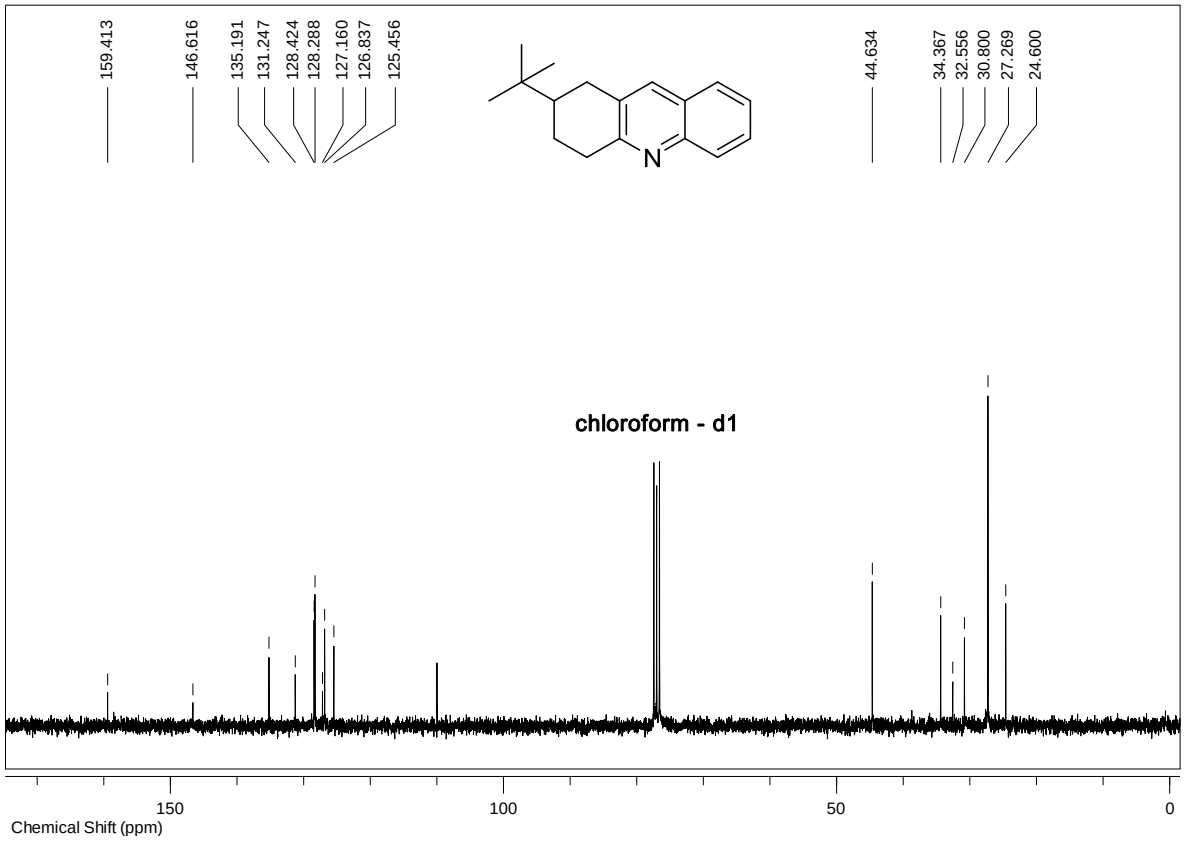
159.413
146.616
135.191
131.247
128.424
128.288
127.160
126.837
125.456
44.634
34.367
32.556
30.800
27.269
24.600
chloroform - d1
150
100
50
0
Chemical Shift (ppm)

4b:

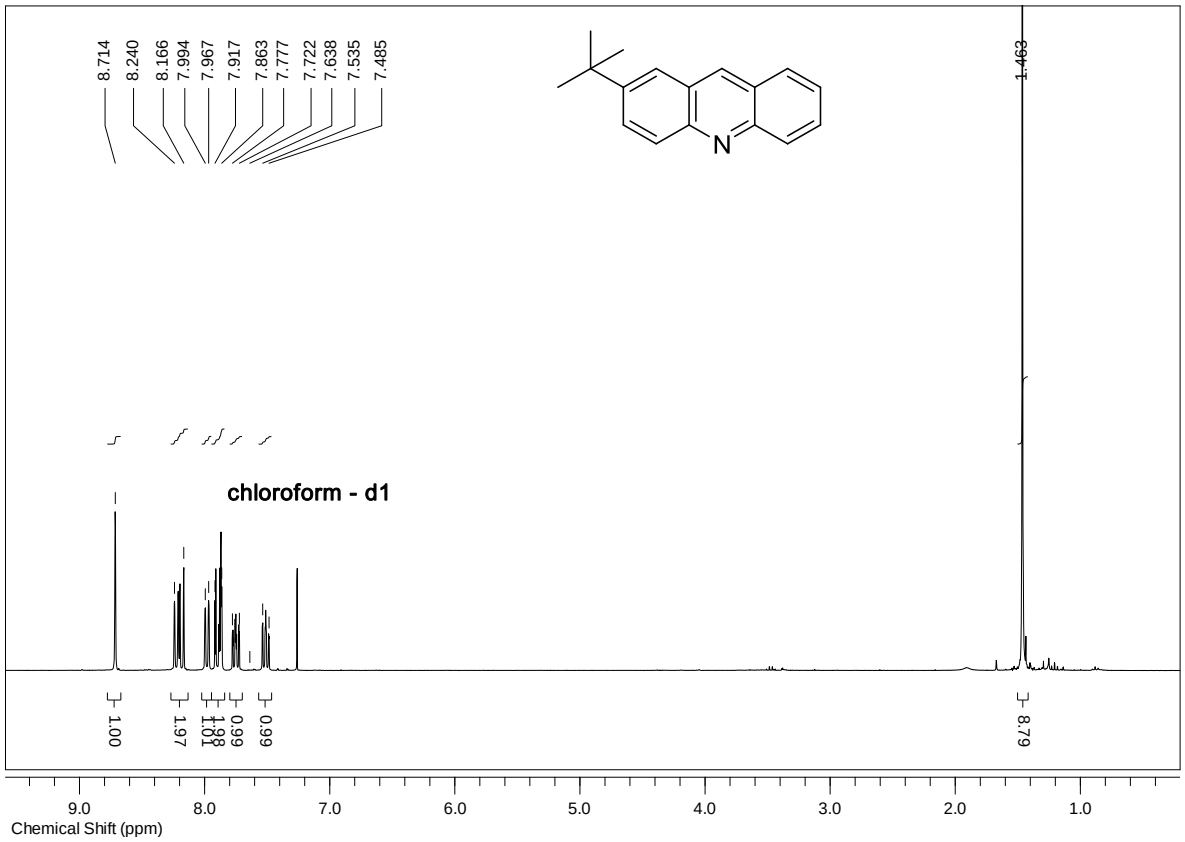
8.714
8.240
8.166
7.994
7.967
7.917
7.863
7.777
7.722
7.638
7.535
7.485
1.463
chloroform - d1
1.00
1.97
1.01
1.98
1.11
0.99
0.99
8.79
9.0
8.0
7.0
6.0
5.0
4.0
3.0
2.0
1.0
Chemical Shift (ppm)

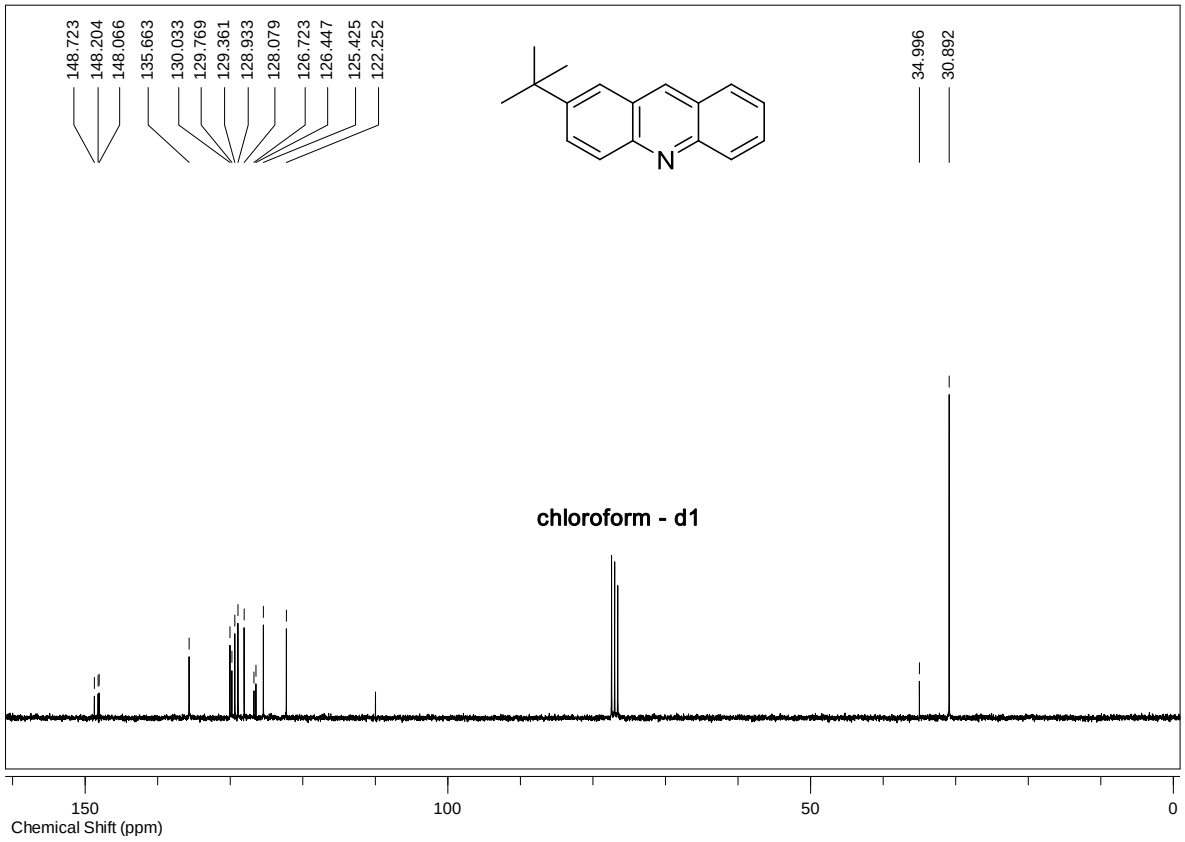
148.723
148.204
148.066
135.663
130.033
129.769
129.361
128.933
128.079
126.723
126.447
125.425
122.252
34.996
30.892
chloroform - d1
150
100
50
0
Chemical Shift (ppm)

4H-4c:

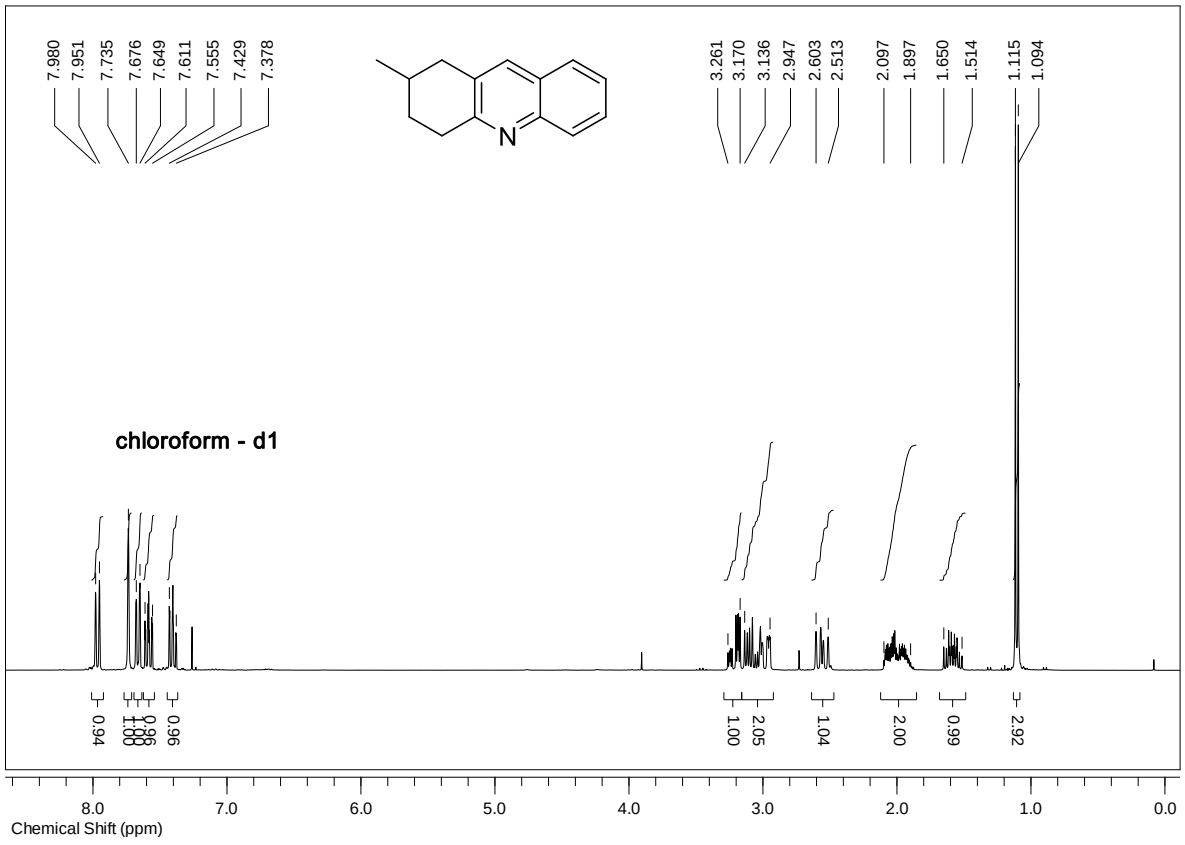
7.980
7.951
7.735
7.676
7.649
7.611
7.555
7.429
7.378
3.261
3.170
3.136
2.947
2.603
2.513
2.097
1.897
1.650
1.514
1.115
1.094
chloroform - d1
0.94
1.00
0.98
0.96
1.00
2.05
1.04
2.00
0.99
2.92
8.0
7.0
6.0
5.0
4.0
3.0
2.0
1.0
0.0
Chemical Shift (ppm)

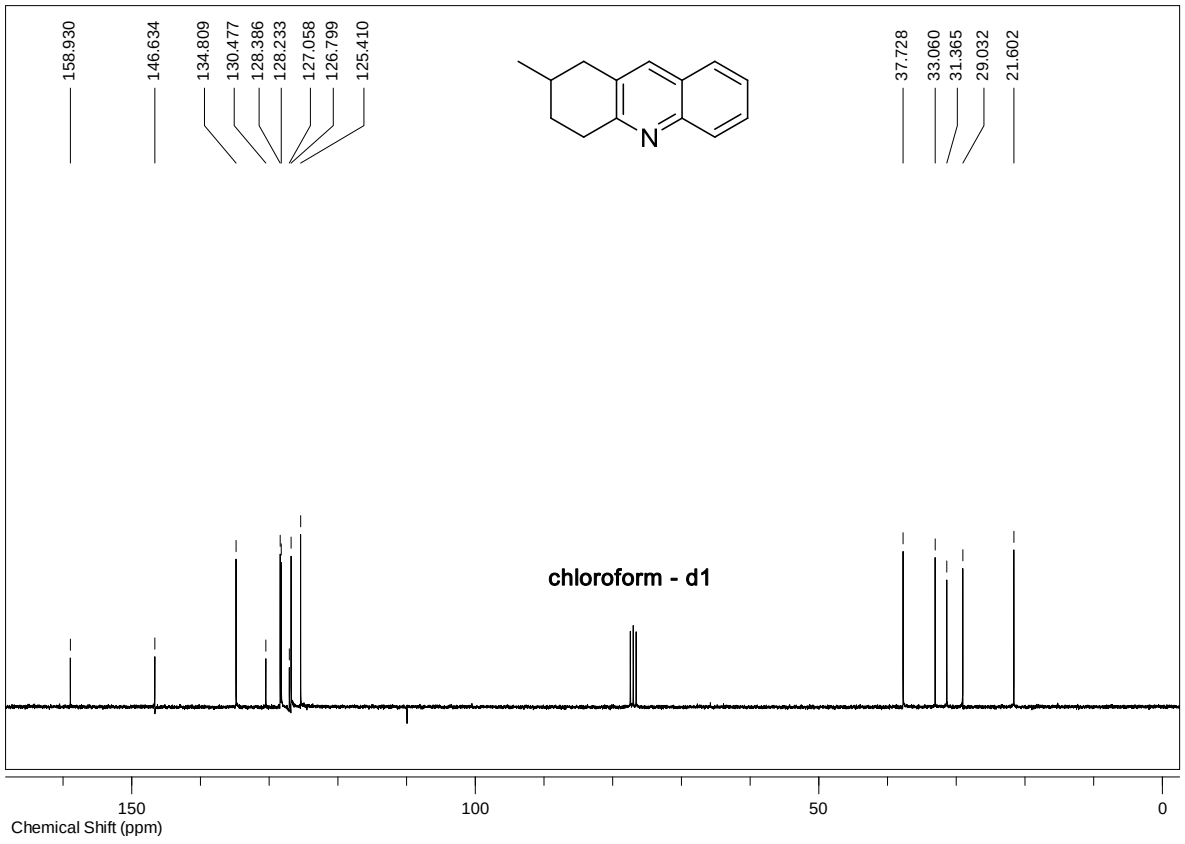
158.930
146.634
134.809
130.477
128.386
128.233
127.058
126.799
125.410
37.728
33.060
31.365
29.032
21.602
chloroform - d1
150
100
50
0
Chemical Shift (ppm)

4c:

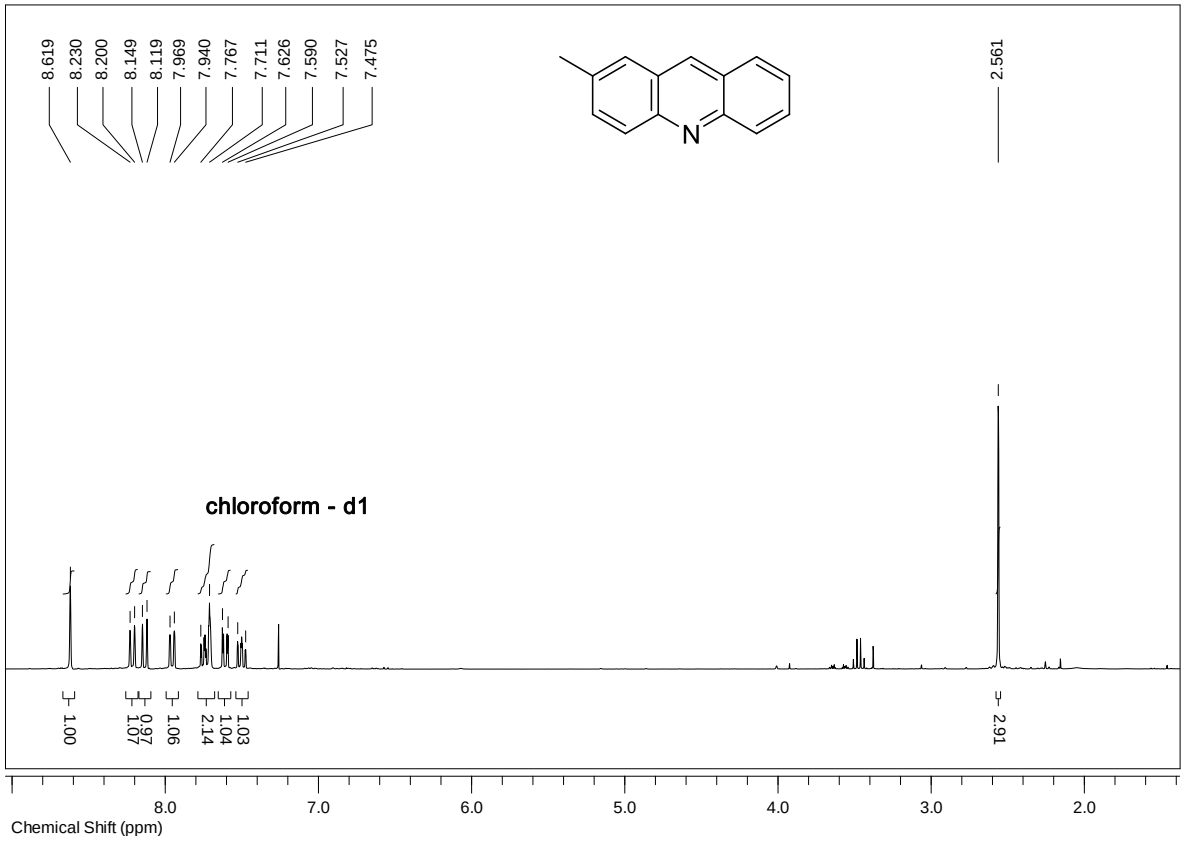
8.619
8.230
8.200
8.149
8.119
7.969
7.940
7.767
7.711
7.626
7.590
7.527
7.475
2.561
chloroform - d1
1.00
0.97
1.07
1.06
2.14
1.04
1.03
2.91
8.0
7.0
6.0
5.0
4.0
3.0
2.0
Chemical Shift (ppm)

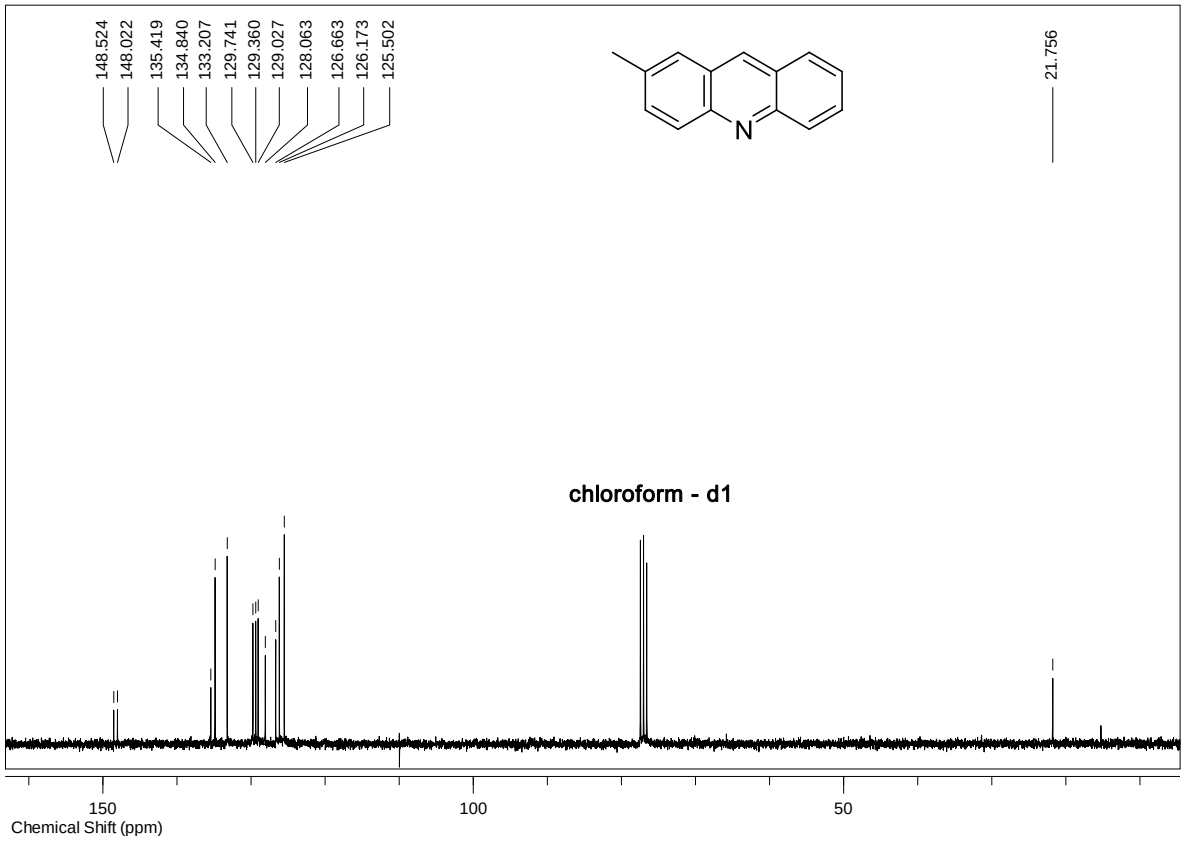
148.524
148.022
135.419
134.840
133.207
129.741
129.360
129.027
128.063
126.663
126.173
125.502
21.756
chloroform - d1
150
100
50
Chemical Shift (ppm)

4H-4d:

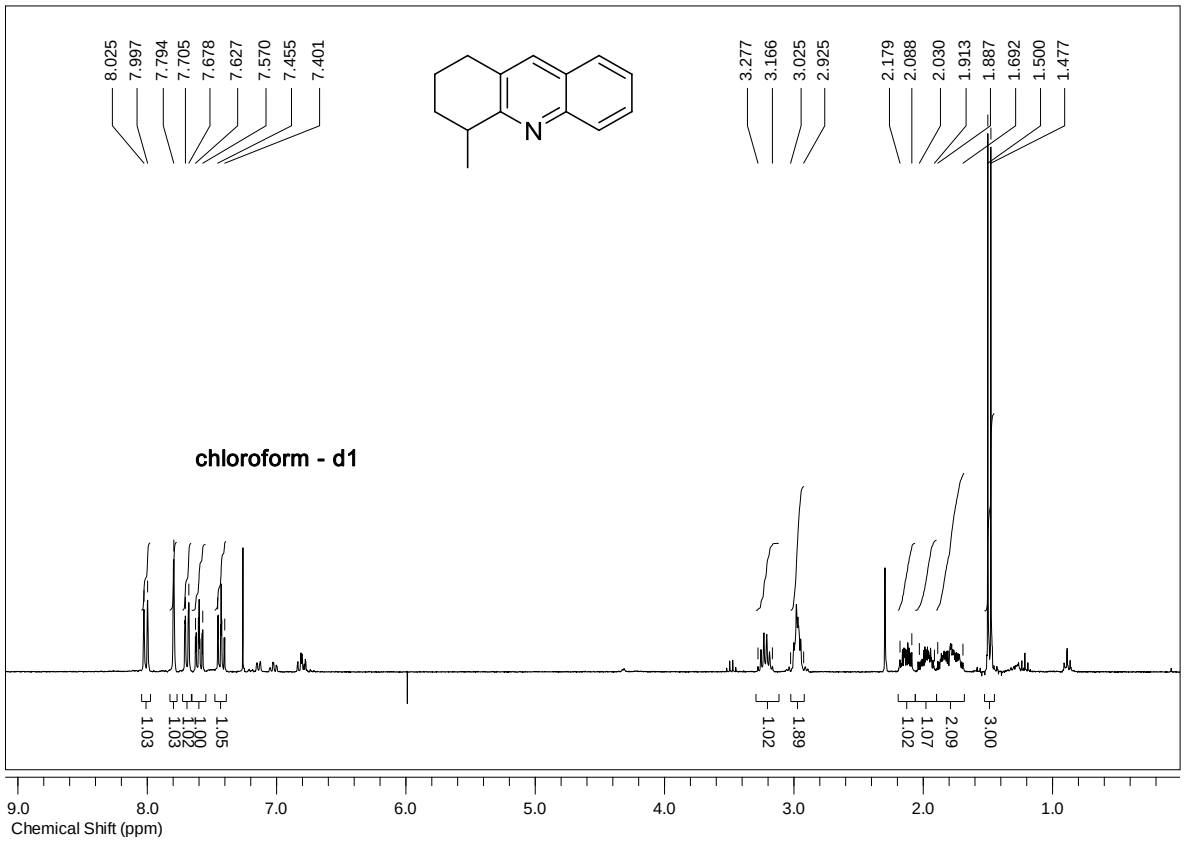
8.025
7.997
7.794
7.705
7.678
7.627
7.570
7.455
7.401
3.277
3.166
3.025
2.925
2.179
2.088
2.030
1.913
1.887
1.692
1.500
1.477
chloroform - d1
1.03
1.03
1.00
1.00
1.05
1.02
1.89
1.02
1.07
2.09
3.00
9.0
8.0
7.0
6.0
5.0
4.0
3.0
2.0
1.0
Chemical Shift (ppm)

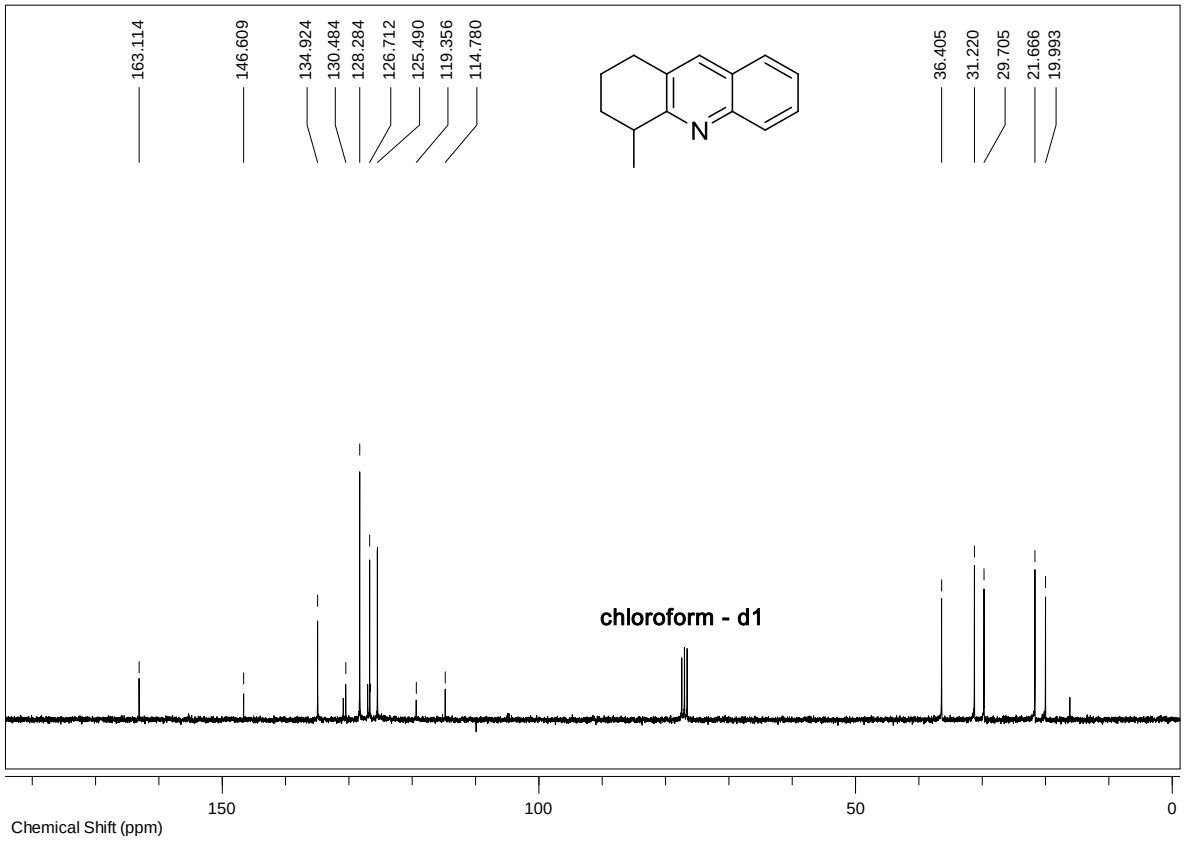
163.114
146.609
134.924
130.484
128.284
126.712
125.490
119.356
114.780
36.405
31.220
29.705
21.666
19.993
chloroform - d1
150
100
50
0
Chemical Shift (ppm)

4d:

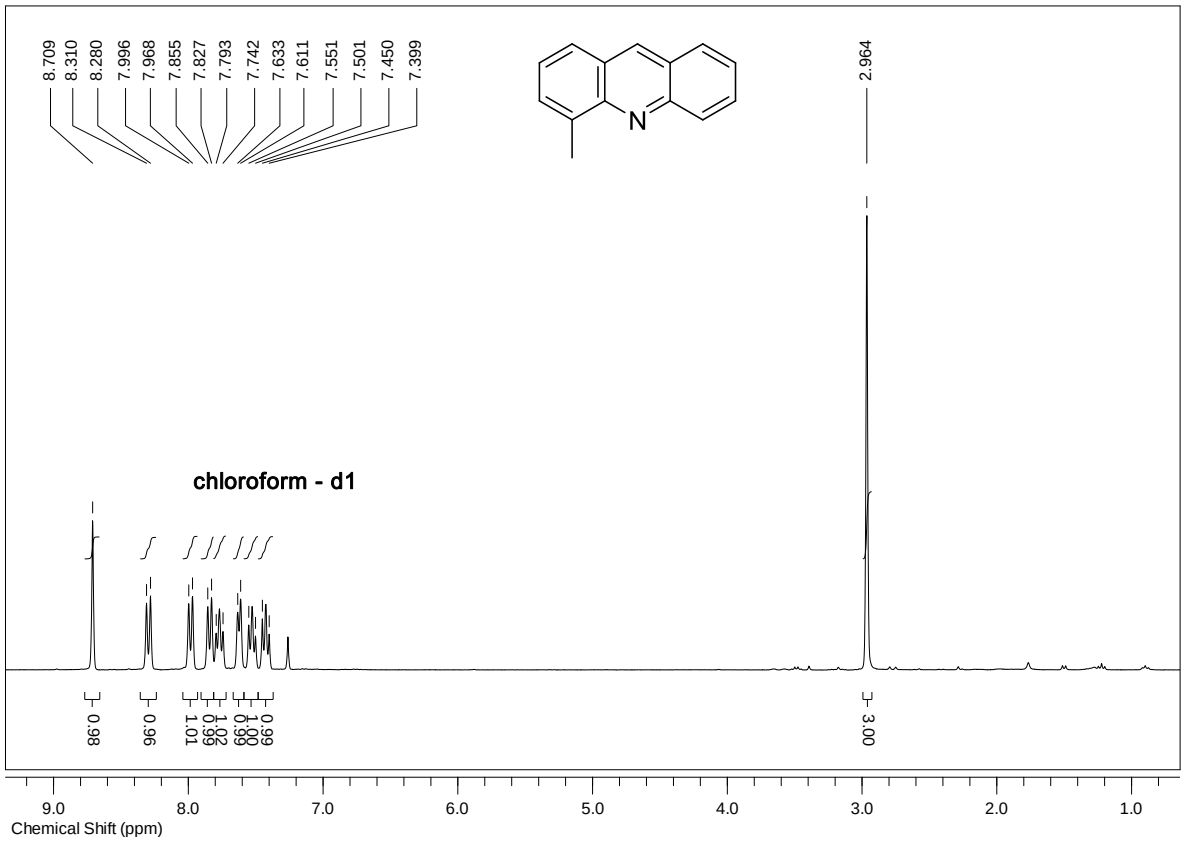
8.709
8.310
8.280
7.996
7.968
7.855
7.827
7.793
7.742
7.633
7.611
7.551
7.501
7.450
7.399
2.964
N
chloroform - d1
0.98
0.96
1.01
0.99
1.02
0.99
1.00
1.00
0.99
3.00
9.0
8.0
7.0
6.0
5.0
4.0
3.0
2.0
1.0
Chemical Shift (ppm)

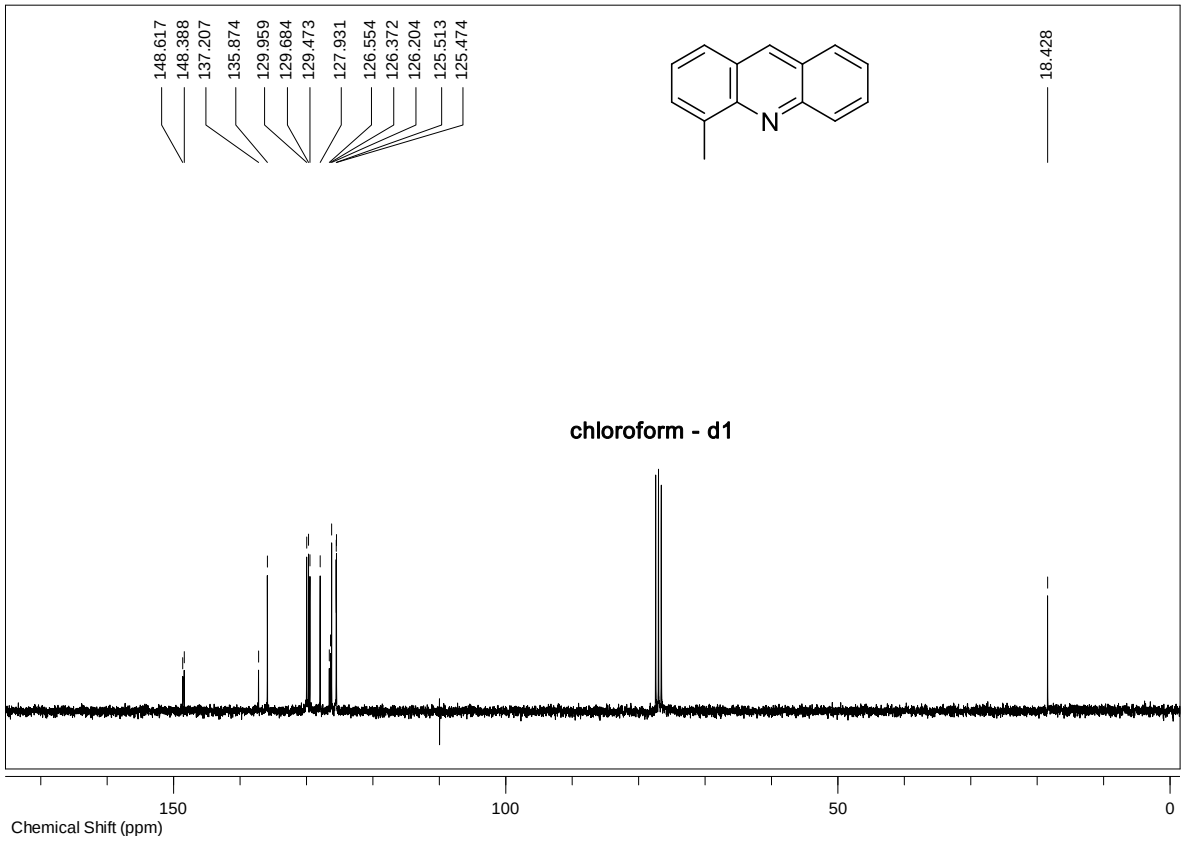
148.617
148.388
137.207
135.874
129.959
129.684
129.473
127.931
126.554
126.372
126.204
125.513
125.474
18.428
N
chloroform - d1
150
100
50
0
Chemical Shift (ppm)

2H-4e:

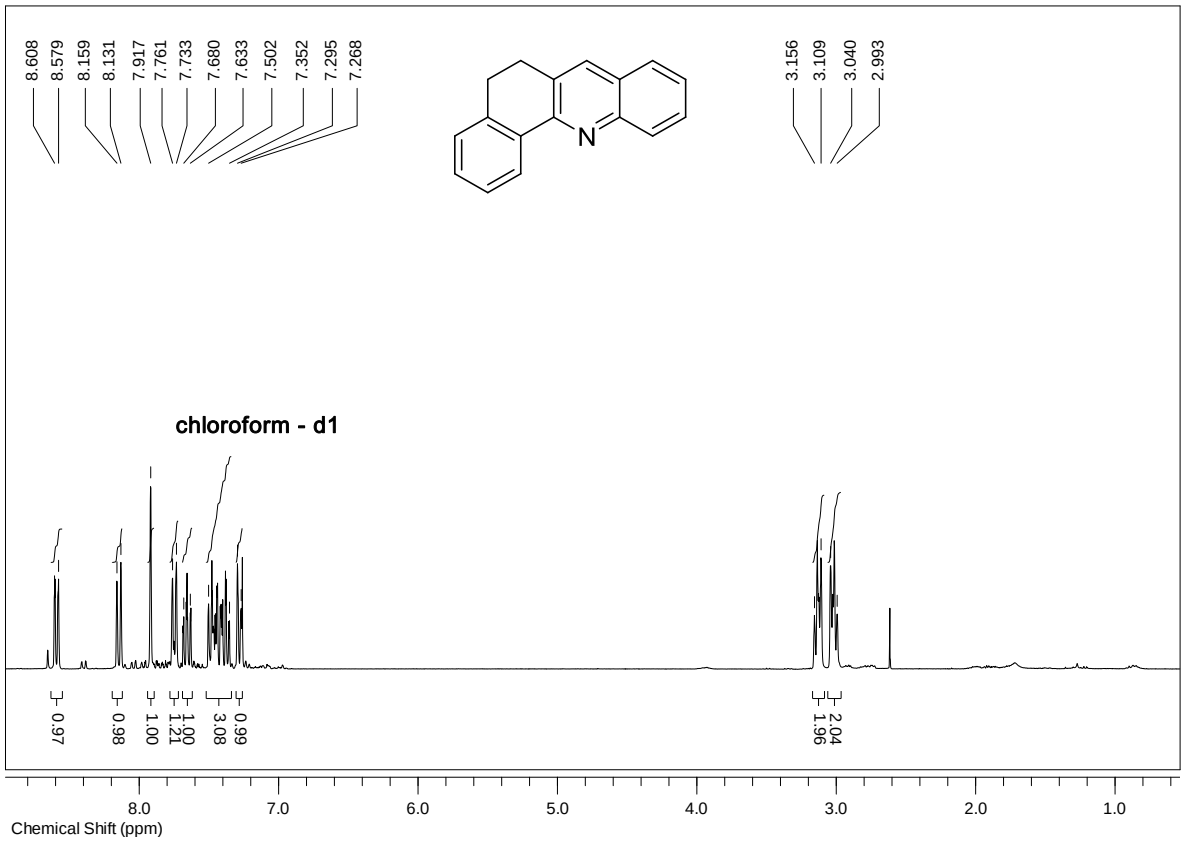
8.608
8.579
8.159
8.131
7.917
7.761
7.733
7.680
7.633
7.502
7.352
7.295
7.268
3.156
3.109
3.040
2.993
N
chloroform - d1
0.97
0.98
1.00
1.21
1.00
3.08
0.99
1.96
2.04
8.0
7.0
6.0
5.0
4.0
3.0
2.0
1.0
Chemical Shift (ppm)

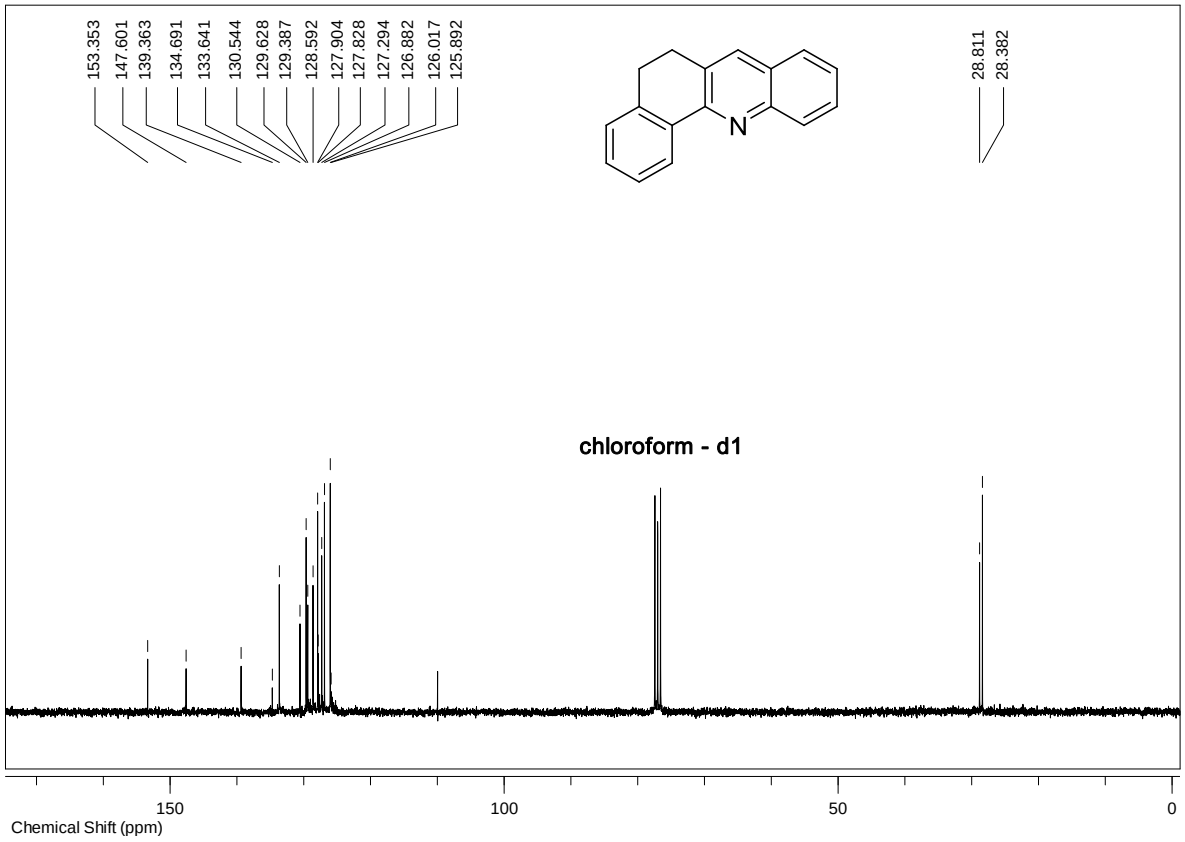
153.353
147.601
139.363
134.691
133.641
130.544
129.628
129.387
128.592
127.904
127.828
127.294
126.882
126.017
125.892
28.811
28.382
N
chloroform - d1
150
100
50
0
Chemical Shift (ppm)

4e:

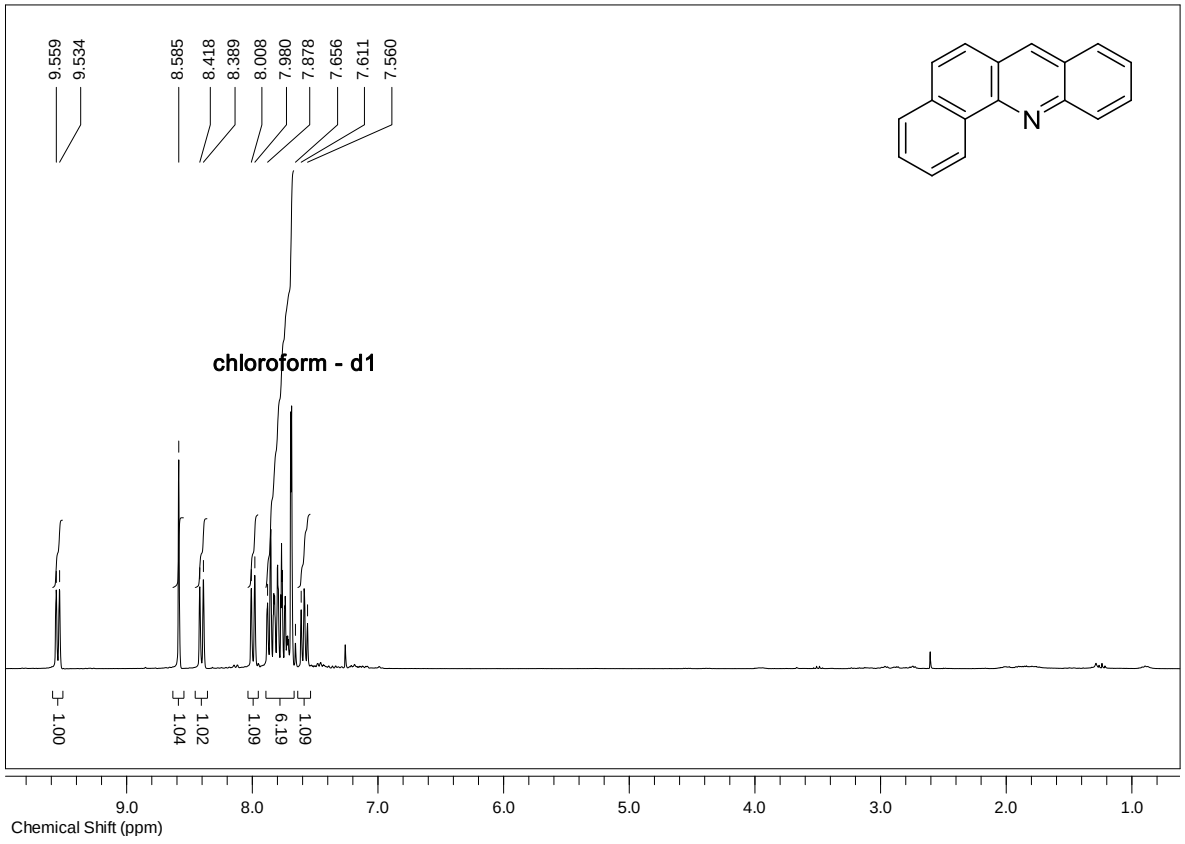
9.559
9.534
8.585
8.418
8.389
8.008
7.980
7.878
7.656
7.611
7.560
N
chloroform - d1
1.00
1.04
1.02
1.09
6.19
1.09
9.0
8.0
7.0
6.0
5.0
4.0
3.0
2.0
1.0
Chemical Shift (ppm)

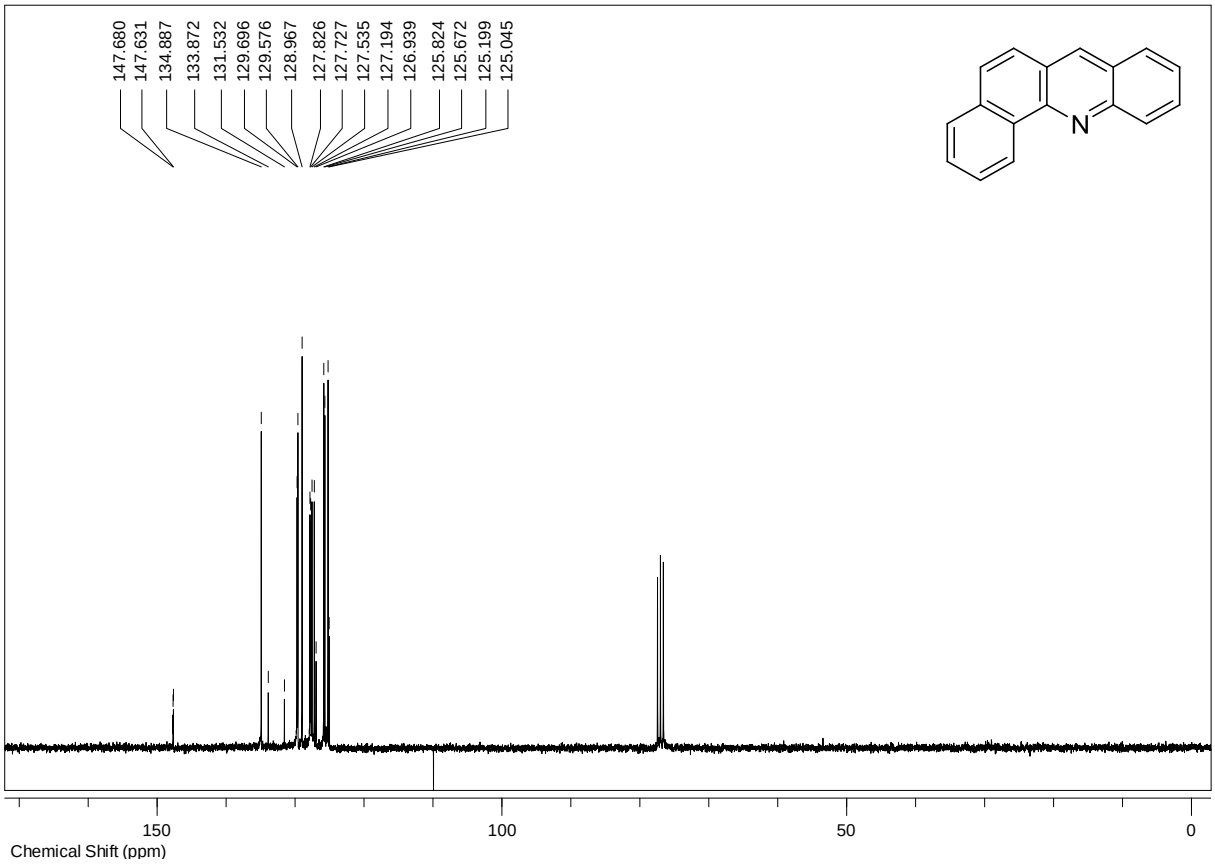
147.680
147.631
134.887
133.872
131.532
129.696
129.576
128.967
127.826
127.727
127.535
127.194
126.939
125.824
125.672
125.199
125.045
N
150
100
50
0
Chemical Shift (ppm)

2H-4f:

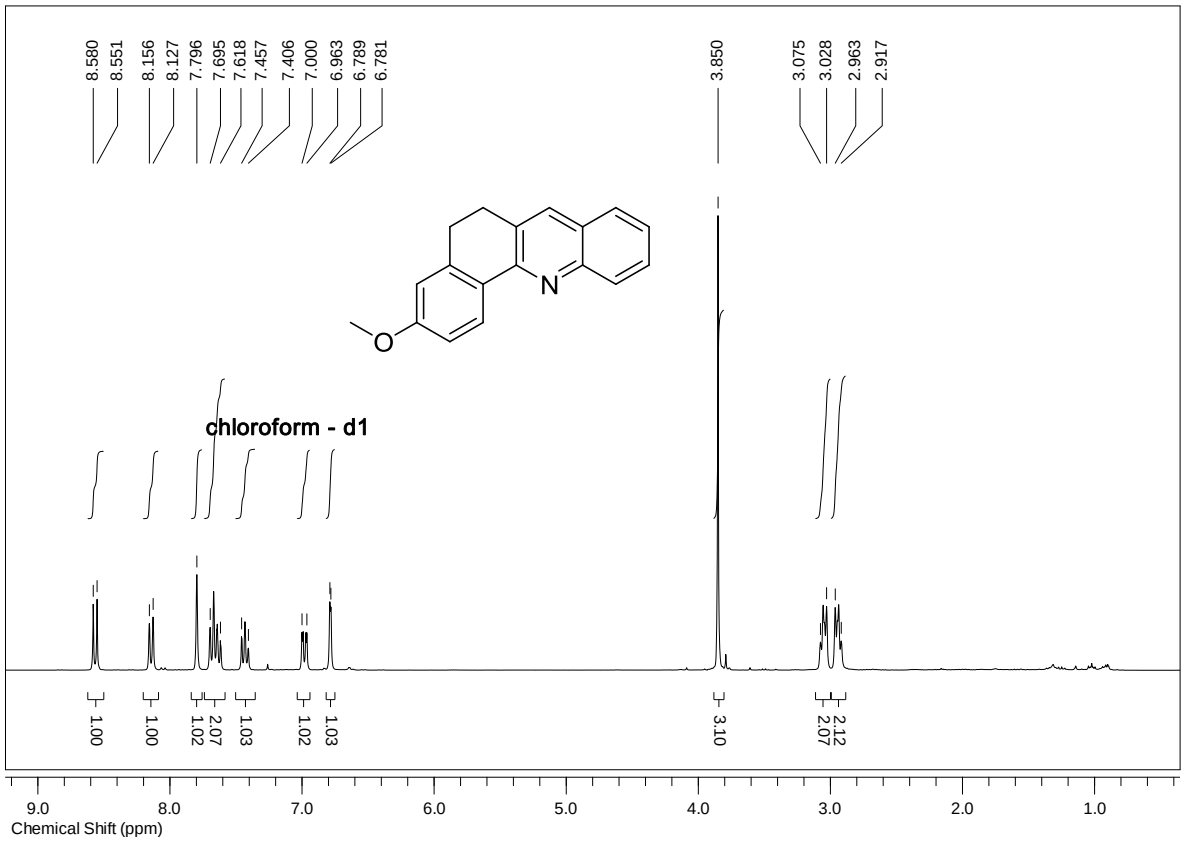
8.580
8.551
8.156
8.127
7.796
7.695
7.618
7.457
7.406
7.000
6.963
6.789
6.781
3.850
3.075
3.028
2.963
2.917
chloroform - d1
1.00
1.00
1.20
2.07
1.03
1.02
1.03
3.10
2.07
2.12
9.0
8.0
7.0
6.0
5.0
4.0
3.0
2.0
1.0
Chemical Shift (ppm)

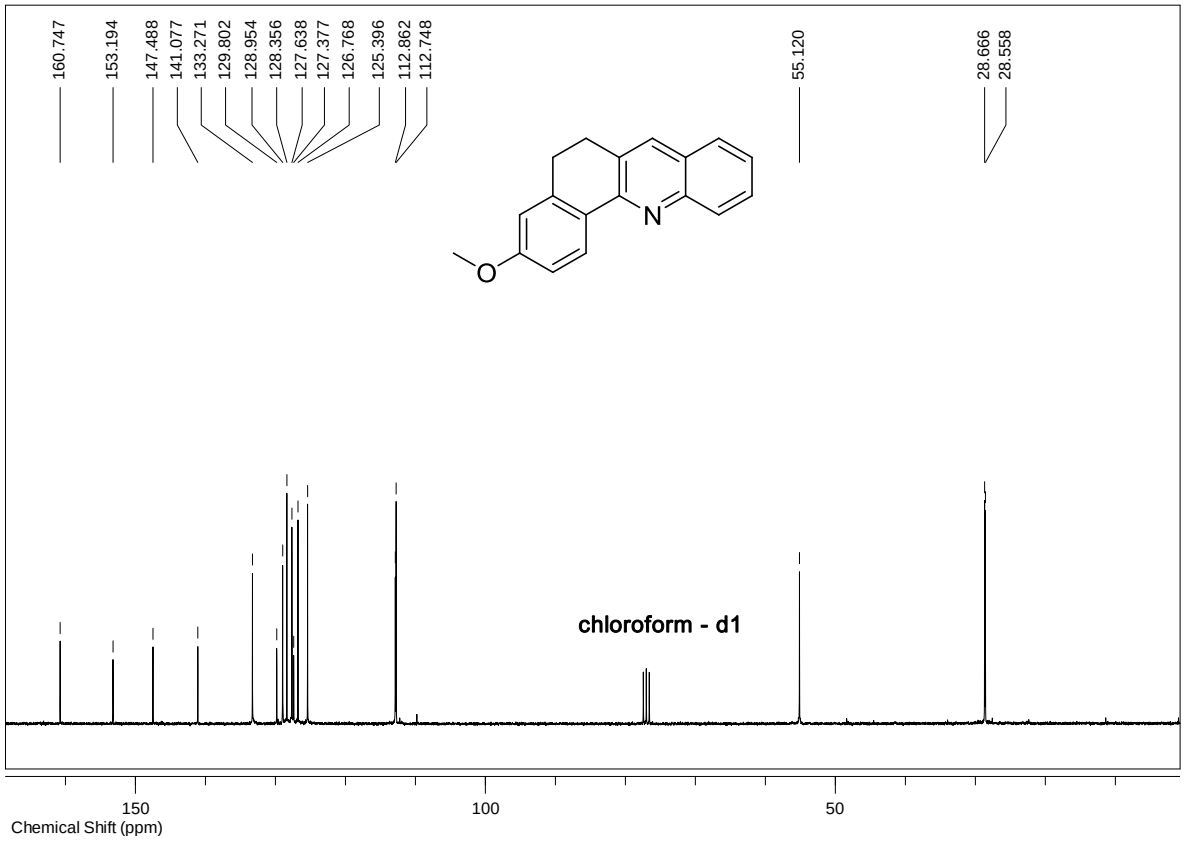
160.747
153.194
147.488
141.077
133.271
129.802
128.954
128.356
127.638
127.377
126.768
125.396
112.862
112.748
55.120
28.666
28.558
chloroform - d1
150
100
50
Chemical Shift (ppm)

4f:

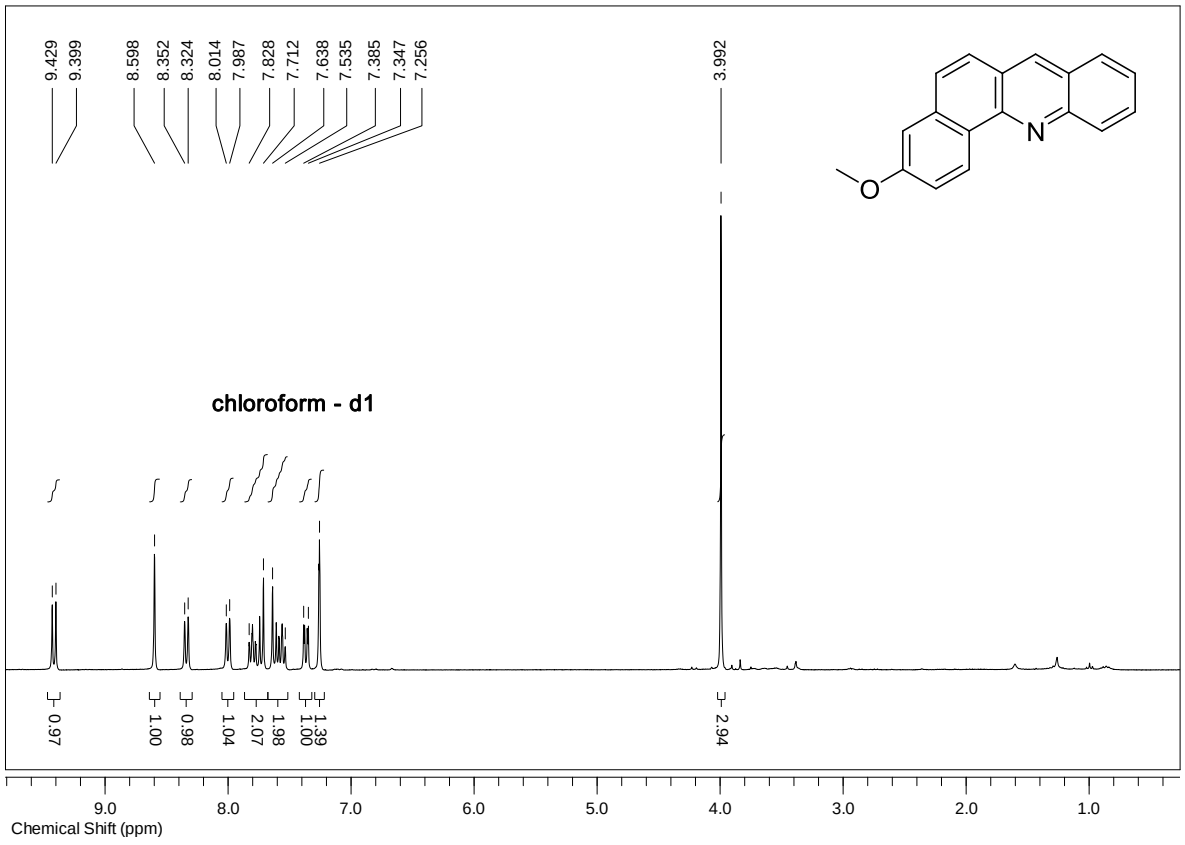
9.429
9.399
8.598
8.352
8.324
8.014
7.987
7.828
7.712
7.638
7.535
7.385
7.347
7.256
3.992
chloroform - d1
0.97
1.00
0.98
1.04
2.07
1.98
1.00
1.39
2.94
9.0
8.0
7.0
6.0
5.0
4.0
3.0
2.0
1.0
Chemical Shift (ppm)

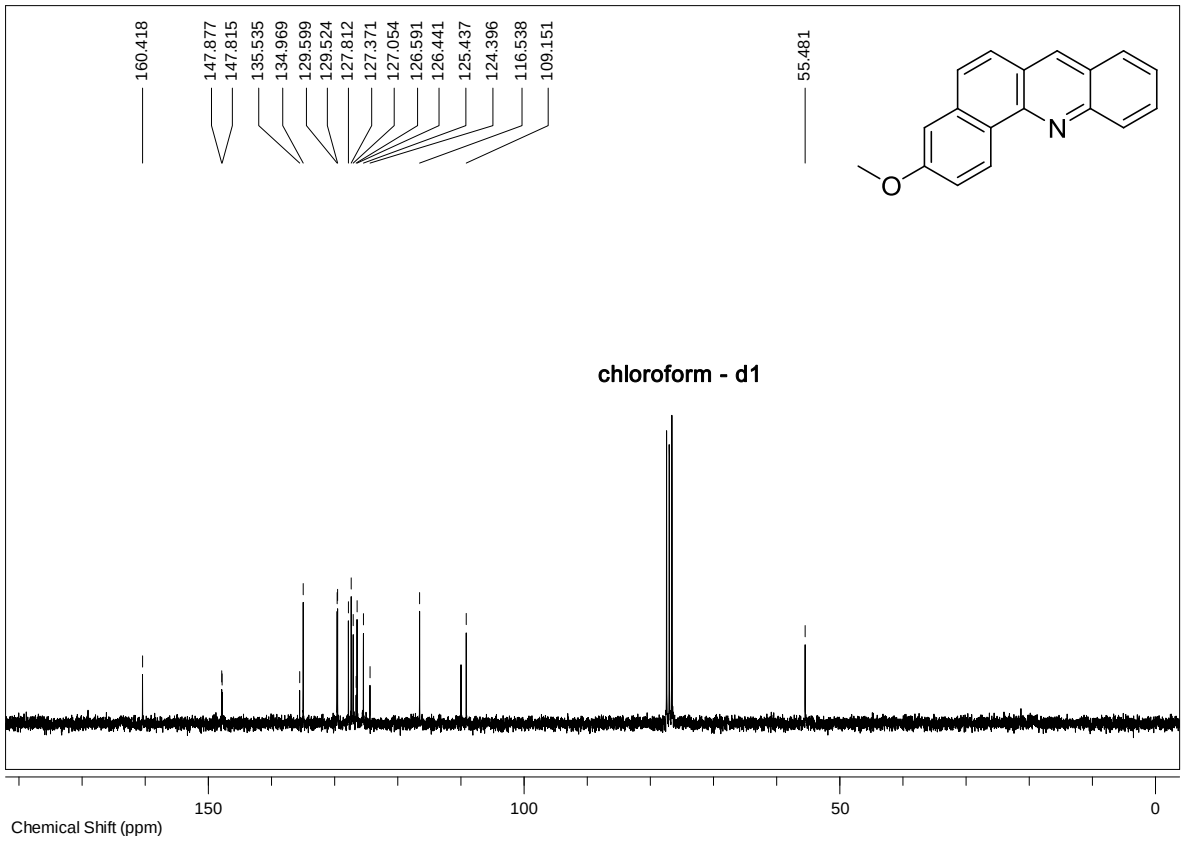
160.418
147.877
147.815
135.535
134.969
129.599
129.524
127.812
127.371
127.054
126.591
126.441
125.437
124.396
116.538
109.151
55.481
chloroform - d1
150
100
50
0
Chemical Shift (ppm)

7.4.6 References

[25] A. Altomare, M. C. Burla, M. Camalli, G. L. Cascarano, *C.* Giacovazzo, *A.* Guagliardi, A. G. G. Moliterni, *G.* Polidori, R. Spagna, *J. Appl. Crystallogr.* **115**, *32,* (1999).

[26] G. M. Sheldrick, *Acta Crystallogr., Sect. A: Found Crystallogr.* **112**, *64*, (2008).

[27] D. Forberg, J. Obenauf, M. Friedrich, S.-M. Hühne, W. Mader, G. Motz, R. Kempe, *Catal. Sci. Technol.* **4**, 4188 (2014).

[28] R. Kempe, P. Arndt, *Inorg. Chem.* **35**, 2644 (1996).

[29] A. Spannenberg, P. Arndt, R. Kempe, *Angew. Chem.* **110**, 824 (1998); *Angew. Chem., Int. Ed.* **37**, 832 (1998).

[30] M. Wojdyr, *J. Appl. Cryst.*, **43**, 1126 (2010).

[31] M. S. Daw, M. Baskes, *Phys. Rev. B* **29**, 6443 (1984).

[32] J. Terso, *Phys. Rev. B* **37**, 6991 (1988).

[33] J. Terso, *Phys. Rev. B* **39**, 1 (1989).

[34] J. Terso, *Phys. Rev. B* **41**, 3248 (1990).

[35] J. Kaiser, *et al.*, *Phys. Chem. Chem. Phys.* **14**, 6487 (2012).

[36] L. Leppert, R. Kempe, S. Kümmel, *Phys. Chem. Chem. Phys*. **17**, 26140 (2015).

[37] J. P. Perdew, K. Burke, M. Ernzerhof, *Phys. Rev. Lett*. **77**, 3865 (1996).

[38] Turbomole V 6.4 **2012**, a development of University of Karlsruhe and Forschungszentrum Karlsruhe GmbH, 1998-2007, available from www.turbomole.com.

[39] C. Adamo, V. Barone, *J. Chem. Phys*. **110**, 6158 (1999).

[40] A. D. Becke, *J. Chem. Phys.* **98**, 1372 (1993).

[41] S. Michlik, R. Kempe, *Nat. Chem*. **5**, 140 (2013).

[42] S. Michlik, R. Kempe, *Angew. Chem., Int. Ed*. **52**, 6326 (2013).

8. Single-Catalyst High Weight% Hydrogen Storage in a N-Heterocycle Synthesized From Lignin Hydrogenolysis Products and Ammonia

Daniel Forberg[a], Martin Friedrich[a], Nobuyoshi Miyajima[b], Rhett Kempe[a]

[a] Lehrstuhl für Anorganische Chemie II, Universität Bayreuth, Universitätsstraße 30, 95440 Bayreuth, Germany. E-Mail: kempe@uni-bayreuth.de

[b] Bayerisches Geoinstitut, Universität Bayreuth, 95440 Bayreuth, Germany.

Submitted to and out for review: *Nat. Commun.*

Now published: D. Forberg, T. Schwob. M. Zaheer, M. Friedrich, N. Miyajima, R. Kempe, . *Commun.* **2016**, *7*, 13201.

Abstract

Large-scale energy storage and the utilization of biomass as a sustainable carbon source are global challenges of this century. The reversible storage of hydrogen covalently bound in chemical compounds is a particularly promising energy storage technology. For this, compounds that can be sustainably synthesized and that permit high weight-% hydrogen storage would be highly desirable. Herein, we report that catalytically modified lignin, an indigestible, abundantly available and hitherto barely used biomass, can be harnessed to reversibly store hydrogen. A novel reusable bimetallic catalyst has been developed which is able to hydrogenate and dehydrogenate N-heterocycles most efficiently. Furthermore, a particular N-heterocycle has been identified which can be synthesized catalytically in one step from the main lignin hydrogenolysis product and ammonia, and in which the new bimetallic catalyst allows multiple cycles of high-weight-% hydrogen storage.

8.1 Introduction

The search for sustainable living under conditions in which there is an increasing energy demand calls for the replacement of the dominant fossil fuel-based technologies that are currently employed. Two central issues of this global challenge are energy storage and the use of indigestible and abundantly available biomass as a carbon source. The concept of a "hydrogen economy" including hydrogen-based energy storage was suggested over 40 years ago[1]. Hydrogen possesses a high energy density, is an environmentally friendly energy carrier and is suitable for mobile application[2,3]. Due to significant technical and safety concerns regarding cryogenic liquid and compressed hydrogen, chemical hydrogen storage is a highly attractive alternative especially for large scale energy storage[2,4]. Molecular hydrogen carriers based on the diversity of molecular compounds from which hydrogen can be liberated are particularly promising. H_2-release has been described for a variety of different classes of compounds, such as cycloalkanes, N-heterocycles, 1,2-BN-heterocycles, methanol or formic acid, ammonia borane, hydrous hydrazine, and hydrazine borane[5]. Methanol might be the most attractive or mature molecular hydrogen carrier for irreversible hydrogen storage. It can be produced sustainably from CO_2[6] and hydrogen liberation can occur efficiently under mild conditions[7,8]. In this low temperature reforming process, three equivalents of dihydrogen are liberated, with one originating from water, the oxygen atom of which contributes to CO_2 formation[9]. For the reversible storage of hydrogen, N-heterocycles have been earmarked as promising candidates[10]. The presence of N atoms in carbocyclic compounds allows dehydrogenation to take place at lower temperatures when compared to the corresponding cycloalkanes[11,12]. Exhaustive hydrogenation and acceptor-less dehydrogenation by the very same catalyst is a domain of homogeneous catalysis and has been reported for 2,6-dimethylpyridine[13] and 2,6-dimethyl-1,5-naphthyridine[14]. Interestingly, the latter, having a maximum hydrogen storage capacity of 6.0 weight-%, has been multiply hydrogenated and dehydrogenated using a molecular Ir catalyst. Reversible single-catalyst hydrogen storage based on catalytic peptide formation has been demonstrated very recently[15,16]. An important issue with regard to any hydrogen storage material/compound is its sustainable production and scalability[11]. We recently disclosed a sustainable catalytic synthesis concept in which a combination of condensation and hydrogen liberation steps allows the synthesis of aromatic N-heterocycles from different alcohols[17]. The synthesis of pyridines[18,19] proceeds with the liberation of three equivalents of H_2. Pyrimidines can be synthesized from alcohols and ammonia generating up to four equiv. of H_2[20]. Based on this concept of alcohol-to-heterocycle conversion, it seems feasible to

develop a reaction that converts key building blocks of the overabundant and indigestible biomass lignin to N-heterocycles suitable for reversible high-wt.-% hydrogen storage.

Herein, we report on the development of a robust reusable bimetallic catalyst able to completely hydrogenate and dehydrogenate N-heterocycles in a most efficient way. In addition, we also disclose a catalytic one-step synthesis of octahydrophenazine starting from the main lignin hydrogenolysis product[21,22] and ammonia. The novel reusable catalyst mediates reversible high-wt.-% hydrogen storage and depletion in this sustainably synthesized N-heterocycle.

8.2 Results and Discussion

First, we became interested in developing an efficient reusable catalyst capable of completely hydrogenating and dehydrogenating N-heterocycles under relatively mild conditions. N-ethylcarbazole (NEC)[10], which has a theoretical hydrogen storage capacity of 5.8 wt.-%, was chosen as a model N-heterocycle for catalyst identification. It is a solid with a melting point of 68 °C and a negligible toxicity, whereas the hydrogenated product, dodecahydro-N-ethylcarbazole (12H-NEC), is a liquid under ambient conditions with a boiling point above 220 °C. Thus, it can be handled similarly to diesel fuel[23]. Consequently, large-scale automated and especially decentralized energy applications for domestic or commercial buildings seem feasible by means of NEC and an appropriate catalyst[23,24]. The hydrogenation of NEC can be accomplished by heterogeneous ruthenium (Ru) catalysts[10,25] while palladium (Pd)-based solid catalysts have been reported to be efficient in the dehydrogenation of NEC[26]. Reusable single catalysts would extend the applicability of NEC-based hydrogen storage significantly. In their patents, Pez *et al.* performed the hydrogenation and dehydrogenation of NEC in a single reactor system using two different catalysts[10,27]. Given, that the most efficient catalysts for NEC-hydrogenation are Ru based and the most efficient ones for 12H-NEC-dehydrogenation are Pd based, potential novel single-catalysts for reversible hydrogen storage should comprise both metals. Synergistic effects of Pd catalysts, when combined with other transition metals, have been reported for hydrogenation reactions[28] and can be rationalized by assuming a lower hydride-binding energy in a metal alloy[29]. Recently, the silicon carbonitride (SiCN) matrix has been introduced as an attractive support for metal catalysts[30,31]. Amorphous SiCN is very robust thermally and chemically inert[32]. The N-atoms of such a support permit the generation of very small metal nanoparticles despite the high pyrolysis temperature and high metal loadings[33]. The polymer

based synthesis protocol for SiCN, operating by crosslinking polysilazanes and subsequent pyrolysis, allows the introduction of porosity in various ways. For instance, metal mediated nanoporosity[34] and meso-structuring via sacrificial polyolefin components have been reported[35,36,37,38].

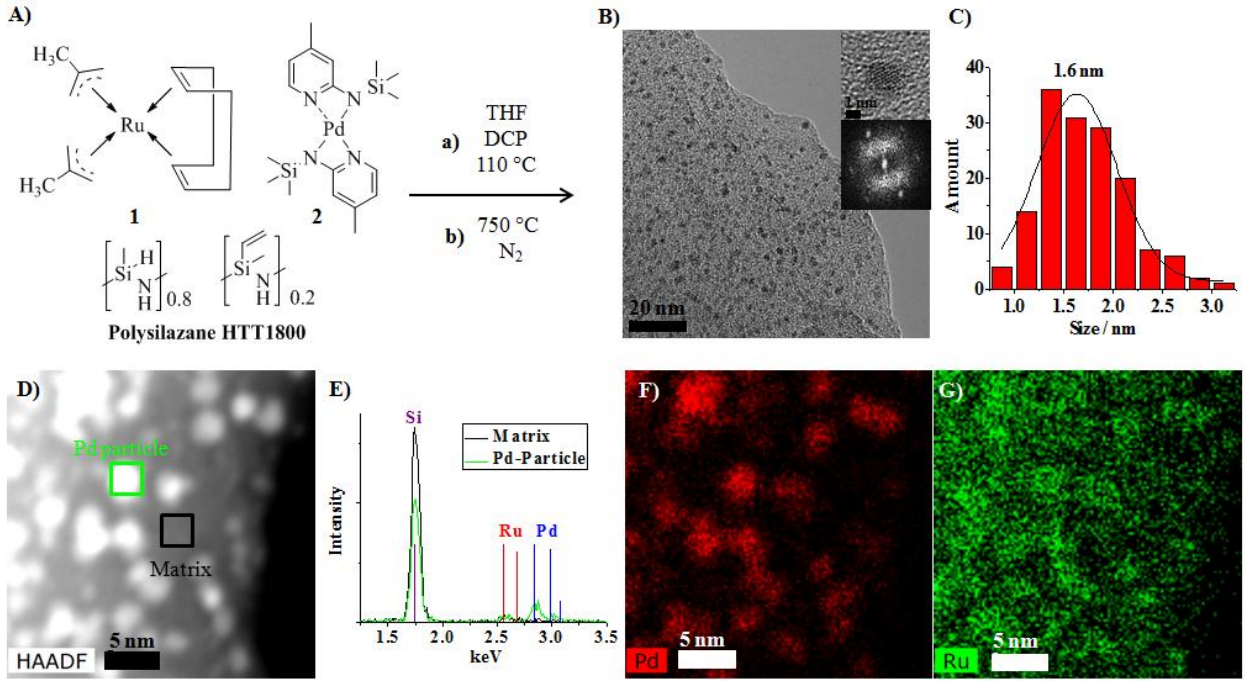

Figure 1 | Synthesis and characterization of the nanocomposite catalyst Pd_2Ru@SiCN. A, A solution of complex **1** and complex **2** in THF was mixed with the polysilazane HTT1800 and crosslinked at 110 °C for 24 h. The solvent was removed and the resulting black-brown metallopolymer was pyrolyzed under N_2 atmosphere at 750 °C. **B,** HR-TEM picture of the catalyst with magnification of one Pd nanoparticle and FFT. **C,** Pd particle size distribution. **D,** HAADF picture. **E,** EDX analysis of the matrix and Pd particle. **F,** EDX mapping of Pd. **G,** EDX mapping of Ru.

By mixing the commercially available Ru complex **1** and the aminopyridinato palladium complex **2**[39] with the commercially available polysilazane HTT1800, followed by crosslinking and pyrolysis, bimetallic nanocomposite catalysts are accessible (**Figure 1, A**). The variation of the molar ratio of both metals allows an optimization of the performance of the catalyst with regard to both, the hydrogenation and dehydrogenation steps. A Pd-to-Ru ratio of 2 was found to be optimal (Pd_2Ru@SiCN). N_2 sorption revealed metal mediated porosity with a bimodal pore size distribution centered at 1.5 (minor) and 4.6 nm (major) and a specific surface area (Brunauer-Emmett-Teller model [BET]) of 82 m^2/g for Pd_2Ru@SiCN. Transmission electron microscopy (TEM) revealed a nanocomposite in which the metal particles are homogenously distributed over the SiCN matrix (**Figure 1, B**). High Resolution TEM (HR-TEM) analysis resulted in a d-spacing of 224.1 ± 2.1 pm, which is in accordance

with the expected value of 224.6 pm for the (111) reflex of cubic crystalline Pd (**Figure 1, B** inset). The averaged Pd particle size was determined to be 1.6 nm by TEM (**Figure 1, C**). High-angle annular dark-field (HAADF) and energy dispersive X-ray spectroscopy (EDX) investigations confirmed the existence of metallic Pd nanoparticles and of homogenously distributed Ru clusters smaller than 1 nm in size and undetectable via X-ray diffraction (XRD) (**Figure 1, D-G**).

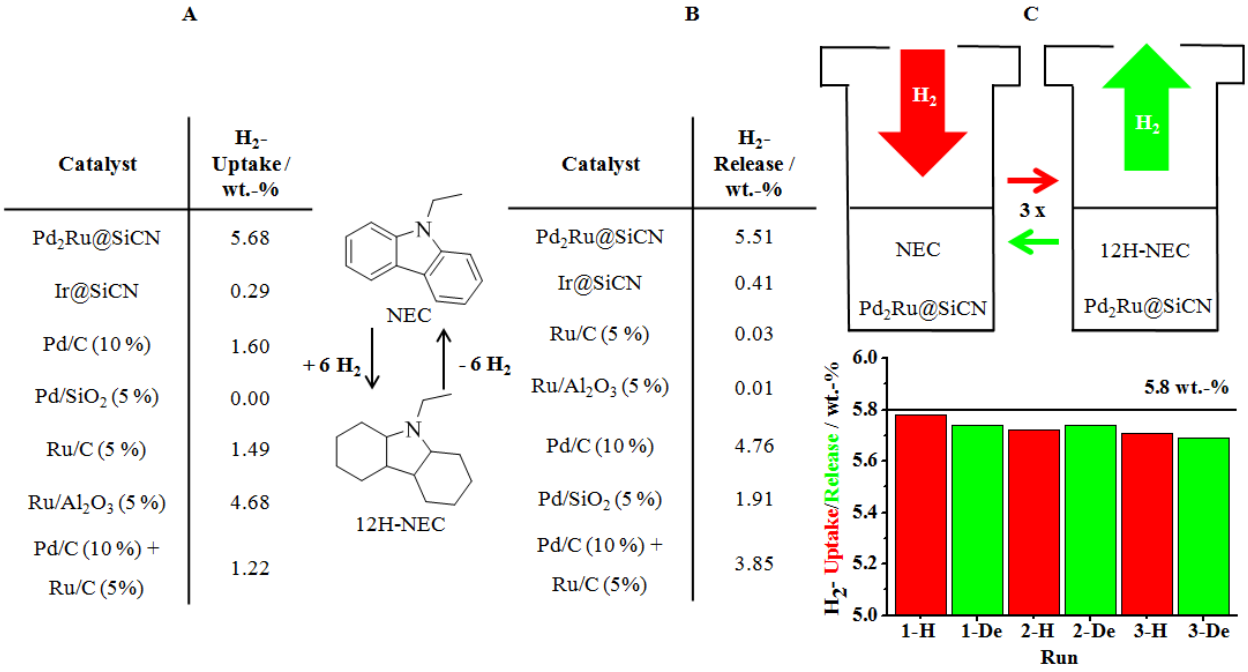

Figure 2 | Catalyst screening and reversible hydrogen storage in NEC. A, Hydrogenation of NEC to 12H-NEC; 110 °C, p(H_2) = 20 bar, 1 mmol NEC, 0.52 mol-% active metal, 36 h. **B,** Dehydrogenation of 12H-NEC to NEC; 180 °C, 2 mmol 12H-NEC, 0.52 mol-% active metal, 7 h. The hydrogen uptake and release values were calculated by gas chromatography (GC) and GC-mass spectrometry (MS) analysis. The maximum hydrogen uptake or release is 5.8 wt.-%. The exact product distribution is listed in the Supplementary Information. **C,** Catalyst reusability and reversible hydrogen storage in NEC: 1.0 g (5.12 mmol) N-ethylcarbazole, 200 mg Pd_2Ru@SiCN (0.52 mol-% active metal); Hydrogenation: 110 °C, 20 bar H_2, 36 h; Dehydrogenation: 180 °C, 20 h. The hydrogen uptake and release values were calculated by GC and GC-MS analysis and based on the preceding step.

A comparison of Pd_2Ru@SiCN with a variety of Pd, Ru and Ir catalysts including catalyst mixtures reveals the superiority of our bimetallic catalyst in hydrogen uptake and release (**Figure 2, A**). The Pd_2Ru@SiCN catalyst hydrogenated NEC quantitatively at 110 °C and only 20 bar H_2 pressure and thus exceeded the efficiency of other commercial Ru catalysts and of Ir@SiCN by far. We included an efficient heterogeneous Ir catalyst[40] in our comparison due to the reported perhydrogenation and perdehydrogenation activity of a

homogenous Ir catalyst.[14] The exhaustive dehydrogenation of 12H-NEC to NEC by the Pd_2Ru@SiCN catalyst could be performed at 180 °C reaction temperature within 7 h. Again, other catalysts are less efficient. It is worth noting, that the Pd_2Ru@SiCN catalyst is superior also to a 2:1 mixture of commercially available Pd and Ru catalysts. The reusability of the Pd_2Ru@SiCN catalyst was verified by three consecutive hydrogen storage cycles with NEC (**Figure 2, C**). NEC was hydrogenated to 12H-NEC at 110 °C and 20 bar H_2 pressure within a hydrogen storage capacity of > 5.7 wt.-%. Subsequently, the reaction vial was heated to 180 °C in an oil bath whereupon 5.7 wt.-% of hydrogen were released within 20 h. This procedure was repeated three times without any significant loss of catalytic activity or hydrogen storage capacity.

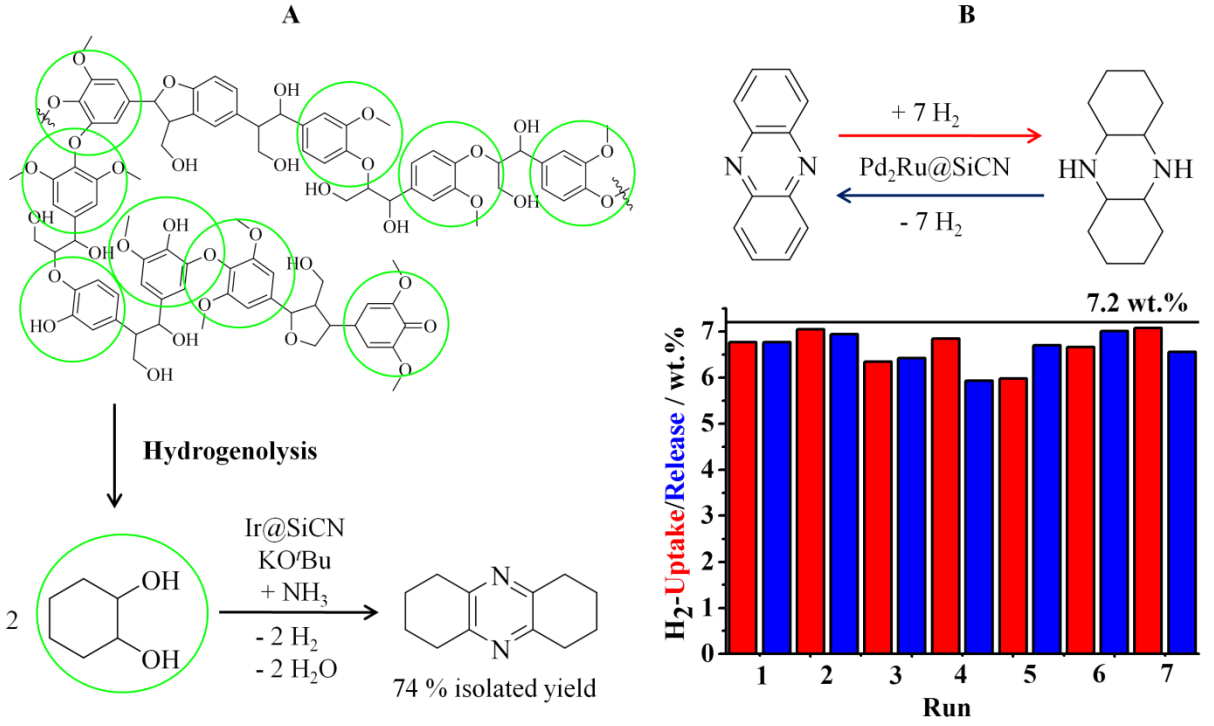

Figure 3 | Sustainable synthesis of octahydrophenazine from 1,2-cyclohexanediol and ammonia and its use as a reversible hydrogen carrier. A, A section of the lignin structure with alkoxybenzene subunits marked by green circles (top). Lignin can be converted to cyclohexane-1,2-diol using existing methodologies (hydrogenolysis). Synthesis of octahydrophenazine from cyclohexane-1,2-diol and ammonia (bottom). **B,** Catalyst reusability and reversible hydrogen storage with phenazine: 360 mg (2 mmol) phenazine, 70 mg Pd_2Ru@SiCN (0.36 mol-% active metal). Hydrogenation: 115 °C, 50 bar H_2, 2 mL dioxane, 0.5 mL water, 24 h. Dehydrogenation: 190 °C, 0.75 mL digylme, 24 h. The hydrogen uptake and release values were calculated by GC and GC-MS analysis and based on the preceding step. The maximum hydrogen uptake or release is 7.2 wt.-%. The values for the uptake and release of H_2 are based on those of the preceding step.

The storage of hydrogen with the NEC/12H-NEC system is limited to a capacity of 5.8 wt.-%[41]. Now, with an efficient catalysts system for reversible hydrogen storage in hand, we set out to identify an N-heterocycle with a higher storage capacity and amenable to a simple, sustainable synthesis. Lignin, a three-dimensional biopolymer, composes 15 – 30 % of the lignocellulosic biomass, which is abundant along with negligible food chain competition[42]. In addition, it is barely used. The main lignin building blocks are 1,2-dialkoxybenzenes (**Figure 3, green circles**) and their hydrogenolysis proceeds mostly in combination with hydrogenation[21] leading to cyclohexane-1,2-diol[22]. Cyclohexane-1,2-diol could be reacted with ammonia[43] applying the borrowing hydrogen[44] methodology leading to a 2-aminocyclohexanol intermediate which then can undergo dehydrogenation and condensation steps[17] to form perhydrophenazine(s) (**Figure 3, A**). Ir@SiCN (ref. 40) converts cyclohexane-1,2-diol and ammonia selectively to 1,2,3,4,6,7,8,9-octahydrophenazine in 74 % isolated yield (**Figure 3, A**). Octahydrophenazine can be quantitatively dehydrogenated to phenazine with the Pd_2Ru@SiCN catalyst and then used in consecutive hydrogen storage cycles (**Figure 3, B**) or used directly. Hydrogenation was performed by dissolving phenazine in a dioxane/water mixture at 115 °C and 50 bar H_2 pressure. After removal of the solvent, the residual tetradecahydrophenazine was dehydrogenated at 190 °C. The hydrogen uptake/release was demonstrated for seven consecutive cycles under identical conditions. Besides some minor variations of hydrogen uptake and/or release over these seven cycles, the Pd_2Ru@SiCN catalyst was still capable of mediating a hydrogen uptake of more than 7.0 wt.-% in the last cycle (**Figure 3, B**).

8.3 Conclusions

In summary, we demonstrated that lignin, an overabundant, indigestible and barely used type of biomass, can be catalytically modified to N-heterocyclic compounds suitable for reversible high-weight-% hydrogen storage. A novel robust, reusable, and highly efficient bimetallic catalyst for the exhaustive hydrogenation and dehydrogenation of such N-heterocycles was also developed to complete a conceptionally new lignin based energy storage system. We expect it to initiate an intensified quest by scientists for similar integrative energy storage systems, that can be produced and operated sustainably and in accordance with conservation-of-elements strategies. The new bimetallic hydrogenation–dehydrogenation catalyst is interesting in its own right and we expect it to find ample application to sustainable organic synthesis.

8.4 Experimental Section

Catalyst Synthesis:

Under an argon atmosphere, complex **1** (29 mg, 0.09 mmol), complex **2** (84 mg, 0.18 mmol) (**Figure 1, A**), and dicumylperoxide (5 mg, 2.9 wt.-%) were dissolved in 1.5 mL of tetrahydrofuran and the commercially available polysilazane HTT1800 (173 mg) was added. The reaction vial was placed in a preheated oil bath at 120 °C for 24 h. After removing of the solvent by reduced pressure, the brown-black solid was pyrolyzed under N_2 atmosphere: heating of 1 °C per minute to 300 °C, holding time 1 h at 300 °C, heating of 5 °C per minute to 750 °C, holding time 1 h at 750 °C and cooling of 4 °C per minute to room temperature.

Synthesis of 1,2,3,4,6,7,8,9-octahydrophenazine:

In a glass vial, Ir@SiCN catalyst (250 mg, 0.08 mol-% active metal) and cyclohexane-1,2-diol (2.32 g, 20 mmol) were dissolved in 12 mL of degassed water. The vial was placed in a 250 mL stainless steel autoclave and was flushed three times with ammonia. An ammonia pressure of 5 bar was adjusted and the reaction mixture was stirred at 105 °C. After 24 h the ammonia atmosphere was released and the reactor was again pressured with 5 bar ammonia and the reaction mixture was allowed to stir for another 24 h. The reactor was cooled to room temperature with an ice bath and the mixture was extracted two times with 100 mL diethylether. The organic phases were combined and were extracted with 150 mL of 0.1 M HCl. The water phase was neutralized with 2 M NaOH and extracted two times with 100 mL diethylether. The combined organic phases were dried over Na_2SO_4 and the solvent was removed under reduced pressure giving the light yellow product in 74 % yield.

Acknowledgments

We acknowledge financial support from the Deutsche Forschungsgemeinschaft, SFB 840, B1.

8.5 References

[1] Bockris, J. O'M. A hydrogen economy. *Science* **176**, 1323 (1972).

[2] Sartbaeva, A.; Kuznetsov, V. L.; Wells, S. A. & Edwards, P. P. Hydrogen nexus in a sustainable energy future. *Energy Environ. Sci.* **1**, 79-85 (2008).

[3] Schlapbach, L. & Züttel, A. Hydrogen-storage materials for mobile applications. *Nature* **414**, 353-358 (2001).

[4] Eberle, U.; Felderhoff, M. & Schüth, F. Chemical and physical solutions for hydrogen storage. *Angew. Chem. Int. Ed.* **48**, 6608-6630 (2009).

[5] Zhu, Q.-L. & Xu, Q. Liquid organic and inorganic chemical hydrides for high-capacity hydrogen storage, *Energy Environ. Sci.* **8**, 478-512 (2015).

[6] Behrens, M.; *et al*., The active site of methanol synthesis over $Cu/ZnO/Al_2O_3$ industrial catalysts. *Science* **336**, 893-897 (2012).

[7] Nielsen, M.; *et al*., Low-temperature aqueous-phase methanol dehydrogenation to hydrogen and carbon dioxide. *Nature* **495**, 85–89 (2013).

[8] Rodriguez-Lugo, R. E.; *et al*., A homogeneous transition metal complex for clean hydrogen production from methanol–water mixtures. *Nat. Chem*. **5**, 342–347 (2013).

[9] Balaraman, E.; Khaskin, E.; Leitus, G. & Milstein, D. Catalytic transformation of alcohols to carboxylic acid salts and H_2 using water as the oxygen atom source. *Nat. Chem.* **5**, 122-125 (2013).

[10] Pez, G. P.; *et al*., World Pat., WO 2005/000457A2, **2005**.

[11] Clot, E.; Eisenstein, O. & Crabtree, R. H. Computational structure–activity relationships in H_2 storage: how placement of N atoms affects release temperatures in organic liquid storage materials. *Chem. Commun.* **2007**, 2231-2233 (2007).

[12] Crabtree, R. H. Hydrogen storage in liquid organic hetrocycles. *Energy Environ. Sci*. **1**, 134-138 (2008).

[13] Chakraborty, S.; Brennessel, W. W. & Jones, W. D. A molecular iron catalyst for the acceptorless dehydrogenation and hydrogenation of N-heterocycles. *J. Am. Chem. Soc.* **136**, 8564-8567 (2014).

[14] Fujita, K.-I.; Tanaka, Y.; Kobayashi, M. & Yamaguchi, R. Homogeneous perdehydrogenation and perhydrogenation of fused bicyclic N-heterocycles catalyzed

by iridium complexes bearing a functional bipyridonate ligand. *J. Am. Chem. Soc.* **136**, 4829-4832 (2014).

[15] Hu, P.; Fogler, E.; Diskin-Posner, Y.; Iron, M. A. & Milstein, D. A novel liquid organic hydrogen carrier system based on catalytic peptide formation and hydrogenation. *Nat. Commun.* **6**, 1-7 (2015).

[16] Hu, P.; Yehoshoa, B.-D. & Milstein, D. Rechargeable hydrogen storage system based on the dehydrogenative coupling of ethylenediamine with ethanol. *Angew. Chem.* **55**, 1061-1064 (2016).

[17] Michlik, S. & Kempe, R. A sustainable catalytic pyrrole synthesis. *Nat. Chem.* **5**, 140-144 (2013).

[18] Michlik, S. & Kempe, R. Regioselectively functionalized pyridines from sustainable resources. *Angew. Chem.* **125**, 6450-6454 (2013); *Angew. Chem. Int. Ed.* **52**, 6326-6329 (2013).

[19] Srimani, D.; Yehoshoa, B.-D. & Milstein, D. Direct synthesis of pyridines and quinolines by coupling of γ-amino-alcohols with secondary alcohols liberating H_2 catalyzed by ruthenium pincer complexes. *Chem. Commun.* **49**, 6632-6634 (2013).

[20] Deibl, N.; Ament, K. & Kempe, R. A sustainable multicomponent pyrimidine synthesis. *J. Am. Chem. Soc.* **137**, 12804-12807 (2015).

[21] Zaheer, M. & Kempe, R. Hydogenolysis of aryl ethers: a key step in lignin valorization to valuable chemicals. *ACS Catal*. **5**, 1675-1684 (2015).

[22] Vispute, T. P.; Zhang, H.; Sanna, A.; Xiao, R. & Huber, G. W. Renewable chemical commodity feedstocks from integrated catalytic processing of pyrolysis oils. *Science* **330**, 1222-1227 (2010).

[23] Teichmann, D.; *et al*., Energy storage in residential and commercial buildings via Liquid Organic Hydrogen Carriers (LOHC). *Energy Environ. Sci.* **5**, 9044-9054 (2012).

[24] Teichmann, D.; Arlt, W.; Wasserscheid, P. & Freymann, R. A future energy supply based on Liquid Organic Hydrogen Carriers (LOHC). *Energy Environ. Sci.* **4**, 2767-2773 (2011).

[25] Eblagon, K. M.; Tam, K. & Tsang, S. C. E. Comparison of catalytic performance of supported ruthenium and rhodium for hydrogenation of 9-ethylcarbazole for hydrogen storage applications. *Energy Environ. Sci.* **5**, 8621-8630 (2012).

[26] Wechsler, D.; Cui, Y.; Dean, D.; Davis, B. & Jessop, P. G. Production of H_2 from combined endothermic and exothermic hydrogen carriers. *J. Am. Chem. Soc.* **130**, 17195-17203 (2008).

[27] Pez, G. P. *et al.*, Hydrogen storage by reversible hydrogenation of pi-conjugated substrates. US patent 7,351,395 (**2008**).

[28] Hermannsdörfer, J. *et al*., *Angew. Chem. Int. Ed.* **51**, 11473-11477 (2012).

[29] Leppert, L.; Kempe, R. & Kümmel, S. Hydrogen binding energies and electronic structure of Ni–Pd particles: a clue to their special catalytic properties. *Phys. Chem. Chem. Phys.* **17**, 26140-26148 (2015).

[30] Kamperman, M. *et al*., Integrating structure control over multiple length scales in porous high temperature ceramics with functional platinum nanoparticles. *Nano Lett.* **9**, 2756-2762 (2009).

[31] Glatz, G. *et al.*, Copper containing SiCN precursor ceramics (Cu@SiCN) as selective hydrocarbon oxidation catalysts using air as an oxidant. *Chem. Eur. J.* **16**, 4231-4238 (2010).

[32] *Polymer derived Ceramics - From Nano-Structure to Applications*, ed. Colombo, P.; Riedel, R.; Soraru, G. D. & Kleebe, H.-J. DEStech Publications, Pennsylvania, **2010**.

[33] The N atoms in the support restrain fast metal aggregation via coordinative saturation of single metal ions or atoms and clusters. Zaheer, M.; Schmalz, T.; Motz, G. & Kempe, R. Polymer derived non-oxide ceramics modified with late transition metals. *Chem. Soc. Rev*. **41**, 5102-5116 (2012).

[34] Zaheer, M. *et al*., Robust microporous monoliths with integrated catalytically active metal sites investigated by hyperpolarized ^{129}Xe NMR. *Chem. Mater.* **24**, 3952-3963 (2012).

[35] Kamperman, M.; Garcia, C. B. W.; Du, P.; Ow, H. & Wiesner, U. Ordered mesoporous ceramics stable up to 1500 °C from diblock copolymer mesophases. *J. Am. Chem. Soc.* **126**, 14708-14709 (2004).

[36] Jones, B.H. & Lodge, T.P. High-temperature nanoporous ceramic monolith prepared from a polymeric bicontinuous microemulsion template. *J. Am. Chem. Soc.* **131**, 1676-1677 (2009).

[37] Pillai, S. K. T. *et al*., SiCN nanofibers with a diameter below 100 nm synthesized via concerted block copolymer formation, microphase separation, and crosslinking. *Small* **9**, 984-989 (2013).

[38] Ewert, J.-K. *et al*., Enhanced capacitance of nitrogen-doped hierarchically porous carbide-derived carbon in matched ionic liquids. *J. Mater. Chem. A* **3**, 18906-18912 (2015).

[39] Spannenberg, A.; Arndt, P. & Kempe, R. Yttrate-mediated ligand transfer and direct synthesis as a route to amidopalladium complexes. *Angew. Chem., Int. Ed.* **37**, 832-835 (1998).

[40] Forberg, D. *et al*., The synthesis of pyrroles via acceptorless dehydrogenative condensation of secondary alcohols and 1,2-amino alcohols mediated by a robust and reusable catalyst based on nanometer-sized iridium particles. *Catal. Sci. Technol.* **4**, 4188-4192 (2014).

[41] The current DOE target is 5.5 wt.-% for the year 2017. For details, please visit their website. Targets for onboard automotive hydrogen storage systems, US Department of Energy, Office of Energy. Efficiency and Renewable Energy, http://energy.gov/eere/fuelcells/hydrogen-storage.

[42] Tuck, C. O.; Pérez, E.; Horváth, I. T.; Sheldon, R. A. & Poliakoff, M. Valorization of biomass: deriving more value from waste. *Science* **337**, 695-699 (2012).

[43] Gunanathan, C. & Milstein, C. Selective synthesis of primary amines directly from alcohols and ammonia. *Angew. Chem.* **120**, 8789-8792 (2008); *Angew. Chem. Int. Ed.* **47**, 8661-8664 (2008).

[44] Watson, A. J. A. & Williams, J. M. J. The give and take of alcohol activation. *Science* **329**, 635-636 (2010).

8.6 Supporting Informations

8.6.1 General Considerations

All reactions were carried out in a dry argon or nitrogen atmosphere using standard Schlenk or glove box techniques. Halogenated solvents were dried over P_2O_5, and nonhalogenated solvents were dried over sodium benzophenone ketyl. Deuterated solvents were ordered from Cambridge Isotope Laboratories, vented, stored over molecular sieves and distilled. All chemicals were purchased from commercial sources with purity over 95 % and used without further purification. Polysilazane "KiON HTT1800" was purchased from Clariant Advanced Materials GmbH, Frankfurt (Germany) and used without further purification. NMR spectra were received using an INOVA 300 MHz spectrometer at 298 K. Chemical shifts are reported in ppm relative to the deuterated solvent. Elemental analyses were carried out on a Vario elementar EL *III*. X-ray crystal structure analyses were performed with a STOE-STADIVARI diffractometer [λ(Mo-K_α) = 0.71073 Å] equipped with an Oxford Cryostream low-temperature unit. Structure solution and refinement were accomplished with SIR-97 and SHELXL-201[1,2]. GC analyses were carried out on an Agilent 6890N Network GC system equipped with a HP-5 column (30 m x 0.32 μm x 0.25 μm) using *n*-dodecane as internal standard. GC/MS analyses were carried out on an Agilent 7890A/MSD 5975C system equipped with a HP-5MS column (30 m x 0.32 μm x 0.25 μm). Ceramization was carried out under nitrogen atmosphere in a high temperature furnace (Gero, Germany). All X-ray powder diffractograms were recorded by using a STOESTADE-P-diffractometer (CuK_α-radiation, 1.54178 Å) in θ-2θ-geometry and with a position sensitive detector. Transmission electron microscopy (TEM) was carried out by using a Varian LEO 9220 (200 kV) instrument. The sample was suspended in chloroform and sonicated for 5 min. Subsequently a drop of the suspended sample was placed on a grid (Plano S 166-3) and allowed to dry. High resolution transmission electron microscopy (HR-TEM) was carried out by using a Philips CM300 FEG/UT (300 kV) instrument. The sample was suspended in chloroform and sonicated for 2 min. Subsequently a drop of the suspended sample was placed on a grid with lacy carbon film and allowed to dry. EDX measurements were carried out by using a Zeiss Field-Emission-Scanning-Electron-Microscope (FESEM) „LEO 1530 GEMINI". The acceleration voltage was 1 – 5 kV. FT-IR measurements were performed using a Perkin-Elmer FTIR-spectrum 100. Milling of the catalyst was performed in a ball mill "Pulverisette 0" (Fritsch, Germany) for 15 min. ChemBET measurements were carried out by using a ChemBET Pulsar TPR/TPD instrument from Quantachrome. N_2 sorption was measure using a Nova2000e

(Quantachrome). ICP-OES measurements were carried out by using a Vista-pro radical model from Varian. The catalysts Pd/SiO_2 (5 %) and Ru/C (5 %) were purchased from ABCR, Pd/C (10 %) was purchased from Merck and the Ru/Al_2O_3 (5 %) catalyst was obtained from Alfar Aesar. All these catalysts were used without further activation or purification. The STEM-EDX analysis was performed at a FEI Titan G2 80-200 S/TEM equipped with a Super-X EDX system, operating at 200 kV, at "Bayerisches Geoinstitut" (University of Bayreuth).

8.6.2 Catalyst Synthesis

Synthesis of the Pd_2Ru@SiCN catalyst:

The bis(2-methylallyl)(1,5-cyclooctadiene)ruthenium(II) complex was purchased from the company "Sigma Aldrich" and used without further purification.

Synthesis of 4-methyl-2-((trimethylsilyl)amino)pyridine $Ap^{TMS}H$

4-Methyl-2-((trimethylsilyl)-amino)pyridine $Ap^{TMS}H$ was synthesized according to a published procedure in 92 % yield[3].

Synthesis of complex $Pd(Ap^{TMS}{}_2)$ (**2**)

The palladium complex **2** was synthesized according to a published procedure in 53 % yield[4].

^{1}H NMR (300 MHz, $CDCl_3$, 298 K): δ = 7.31 (d, 1H, *J* = 8.7 Hz), 5.84 (d, 1H, *J* = 8.7 Hz), 5.71 (s, 1H), 2.10 (s, 3H), 0.19 (s, 9H) ppm. ^{13}C NMR (75 MHz, $CDCl_3$, 298 K): δ = 175.9, 148.8, 143.1, 110.9, 108.1, 21.6, 1.7 ppm.

Pyrolysis

Under vigorous stirring 173 mg HTT1800 was added drop wise to a solution of 84 mg (0.18 mmol) $[PdAp^{TMS}{}_2]$, 29 mg (0.09 mmol) bis(2-methylallyl)(1,5-cyclooctadiene)ruthenium(II) and 5 mg dicumylperoxid (2.9 wt.-%) in 1.5 mL thf. The reaction vial was immediately placed in a pre-heated oilbath at 120 °C for 24 h. After cooling down the solvent was removed under reduced pressure and the brown-black solid was pyrolyzed under N_2 atmosphere with the following heating program:

$$25\ °C \xrightarrow{1\ °C/min} 300\ °C\ (1\ h) \xrightarrow{5\ °C/min} 750\ °C\ (1\ h) \xrightarrow{4\ °C/min} 25\ °C$$

The ceramic yield was 77 %. After ball milling for 15 minutes, the catalyst was pre-treated by stirring in an aqueous solution of NaOH (c = 1 mol/l) at 60 °C for 12 h.

ICP-OES-analysis

50 mg of the sample was solved in 1.5 mL HNO_3 (65 %, distilled), 4.5 mL HCl (32 %, p.a.) and 1 mL HF (40 %) and heated in the microwave at 170 °C for 7 min (80 % power), at 180 °C for 7 min (85 % power) and at 195 °C for 20 min (90 % power).

Result: 7.56 wt.-% Pd content

3.95 wt.-% Ru content

The metal contents are slightly lower than expected (8.92 wt.-% Pd, 4.26 wt.-% Ru).

ChemBET measurements

30 mg of the Pd_2Ru@SiCN catalyst was pre-treated under helium and nitrogen atmosphere at 400 °C for 3 hours. After cooling the sample to RT, hydrogen gas (5 % in N_2) was added portion wise using a 250 µL injection loop. Analysis of the results was performed with the free version of the program fytik 0.9.8[5]. The metal content of the sample was calculated to be 8.92 wt.-% palladium and 4.26 wt.-% ruthenium.

Metal dispersion on the surface of Pd_2Ru@SiCN catalyst (The main component palladium was chosen for calculation): 8.57 %

N_2 sorption

The BET surface area was calculated to be 82 m^2/g (**Fig. S1**). The NLDFT equilibrium model (N_2 at 77 K) with slit/cylindrical pores on Carbon surface was chosen due to the lowest fitting error.

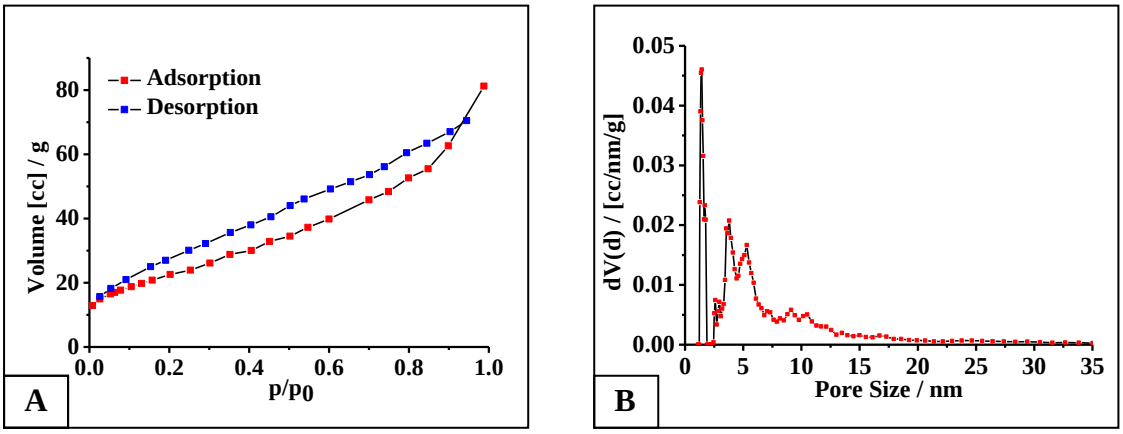

Fig. S8-1: N_2 sorption analysis of the Pd_2Ru@SiCN catalyst; (A) Nitrogen sorption isotherme; **(B)** calculated pore size distribution.

Powder XRD analysis

The result of the powder XRD analysis is shown in **Fig. S8-2**. A median particle diameter of 1.6 nm was calculated by Debye-Scherrer-equation.

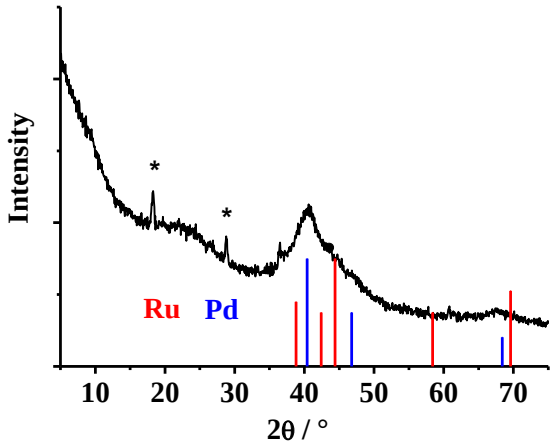

Fig. S8-2: Powder XRD analysis of the Pd_2Ru@SiCN catalyst (red: Reflexes of hexagonal crystalline ruthenium; reference card: 00-001-1253; blue: Reflexes of cubic crystalline palladium; reference card: 00-001-1201; * SiO_2).

Size of the Pd nanoparticles

The size of the palladium nanoparticles were measured with the programm “ImageJ”. The median particle diameter was measured to be 1.6 nm (**Fig. S8-3**).

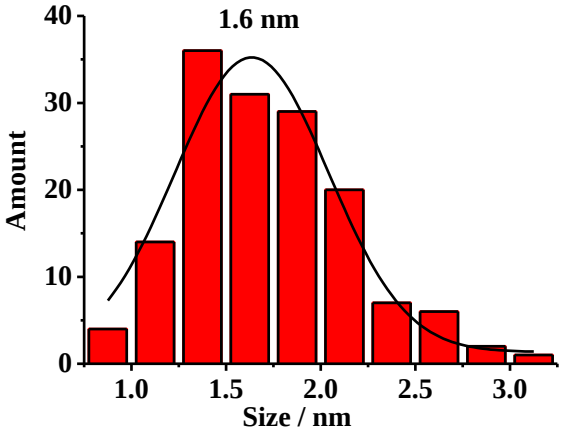

Fig. S8-3: Histogramm of the measured palladium nanoparticles.

TPR measurements

Temperature programmed reduction (TPR) measurements were performed using a ChemBET Pulsar TPR/TPD instrument from Quantachrome. 12 mg of the sample were oxidized on air by heating with 5 K/min to 500 °C for 3 h. Afterwards the sample was transferred to an u-tube and pre-treated under nitrogen atmosphere at 200 °C for 0.5 h. The sample was cooled down under nitrogen atmosphere and flushed with hydrogen (5 % in N_2). TPR analysis was performed by heating the sample with 5 K/min to 525 °C and the results were analyzed using the program fytik 0.9.8[5] (**Fig. S8-4**).

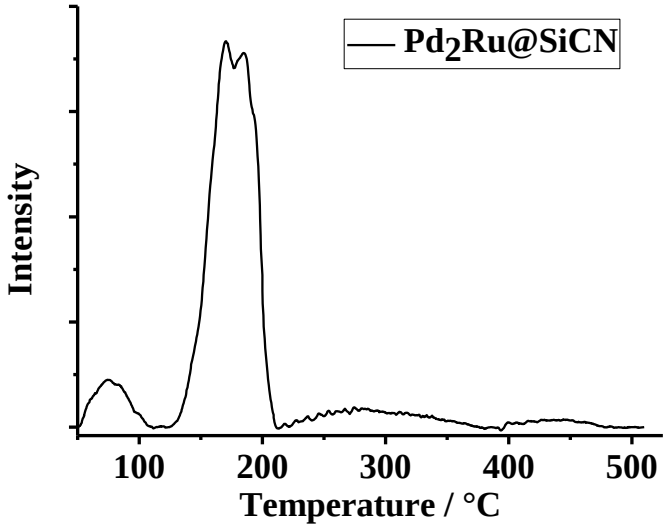

Fig. S8-4: TPR analysis of the Pd_2Ru@SiCN catalyst.

Synthesis of the Ir@SiCN catalyst:

The used Ir@SiCN catalyst was synthesized, characterized and used as reported[6].

8.6.3 Catalyst Screening

For our catalytic reactions we use the following nomenclature for the intermediate products:

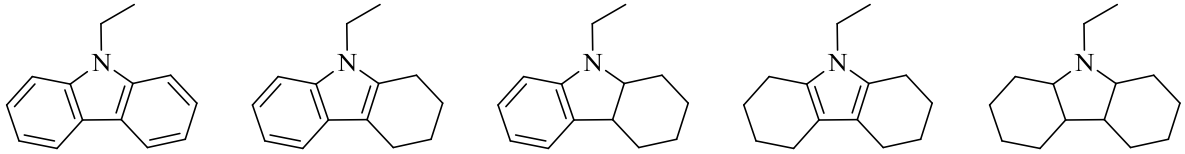

NEC 4H-NEC 6H-NEC 8H-NEC 12H-NEC

Hydrogenation of NEC

In a typical procedure, the catalyst and NEC are filled in a glass reaction vial which is placed in 250 mL stainless steel autoclave. The autoclave is flushed with hydrogen gas three times, pressured with hydrogen gas and then heated to the desired temperature. After the reaction time, the autoclave was placed in an ice bath, the hydrogen pressure was released and a sample for GC and GC-MS analysis was taken.

Dehydrogenation of 12H-NEC

In a typical procedure the catalyst and 12H-NEC are filled in a 10 mL schlenk tube and the mixture was evacuated and flushed with argon three times. The tube was placed in a pre-heated oil bath and a slight argon flow of 4-6 mL/min was adjusted. After the desired reaction time the tube was cooled to RT under argon atmosphere and a sample for GC and GC-MS analysis was taken.

Analysis of the results:

The maximum hydrogen uptake or hydrogen release for the NEC/12H-NEC system is 5.8 wt.-%. All H_2-uptake and H_2-release values were calculated by GC and GC-MS taking all the intermediate products into account.

Dodecahydro-N-ethylcarbazole (12H-NEC) was synthesized on large scale according to published procedure[7].

Optimization of Pd : Ru ratio

The Ru : Pd ratio was optimized in the hydrogenation of NEC and dehydrogenation of 12H-NEC (**Tab. S1**).

Tab. S1: Optimization of the Pd : Ru ratio

Hydrogenation				**Yields / %**			
No.	**Pd : Ru**	**NEC**	**4H-NEC**	**6H-NEC**	**8H-NEC**	**12H-NEC**	**H_2-Uptake/ wt.-%**
1	2 : 1	24	35	2	6	33	2.90
2	1 : 1	71	19	1	1	8	0.93
3	1 : 2	67	21	1	1	10	1.04
Dehydrogenation				**Yields / %**			
No.	**Pd : Ru**	**NEC**	**4H-NEC**	**6H-NEC**	**8H-NEC**	**12H-NEC**	**H_2-Release / wt.-%**
4	2 : 1	6	45	19	26	4	3.13
5	1 : 1	3	10	8	68	11	2.15
6	1 : 2	0	10	2	11	77	0.64

Reaction conditions: Hydrogenation of N-ethylcarbazole (NEC): 1 mmol N-ethylcarbazole, 20 mg catalyst (0.26 mol-% active metal), 110 °C, 20 bar H_2 pressure, neat, 36 h. Dehydrogenation of 9-ethyl-dodecahydrocarbazole (12H-NEC): 2 mmol 12H-NEC, 20 mg catalyst (0.13 mol-% active metal), 172 °C, 1 mL diglyme, 20 h, Ar flow (4-6 mL/min). Yields were determined by GC and GC-MS. H_2-storage was calculated taking all the intermediate products into account.

Comparison to other catalysts

40 mg of the designed Pd_2Ru@SiCN catalyst contains 2.88 e^{-6} mol active palladium and 1.44 e^{-6} mol active ruthenium on the surface. So we tested the commercial catalysts in the dehydrogenation of 12H-NEC with the particular amounts of palladium or ruthenium or mixtures of them (**Tab. S2, Tab. S3**).

Tab. S2: Catalyst screening for the hydrogenation of N-ethylcarbazole (NEC)

		Yields / %[a)]					
No.	**Catalyst**	**NEC**	**4H-NEC**	**6H-NEC**	**8H-NEC**	**12H-NEC**	**H_2-Uptake / wt.-%**
1	Pd_2Ru@SiCN[b)]	24	35	2	6	33	2.90
2	Pd_2Ru@SiCN	0	1	1	1	97	5.68
3	Ir@SiCN	90	7	0	2	1	0.29
4	Ru/C (5 %)[c)]	59	17	0	12	12	1.49
5	Ru/Al_2O_3 (5 %)[c)]	0	0	0	58	42	4.68
6	Pd/C (10 %)[c)]	52	30	0	1	17	1.60
7	Pd/SiO_2 (5 %)[c)]	0	0	0	0	0	0.00
8	Pd/C (10 %) + Ru/C (5%)[d)]	65	20	0	3	12	1.22

Reaction conditions: 1 mmol N-ethylcarbazole, 0.52 mol-% active metal (referring to 40 mg Pd_2Ru@SiCN), 110 °C, 20 bar H_2 pressure, neat, 36 h. Yields were determined by GC and GC-MS. H_2-storage was calculated taking all the intermediate products into account. a) Yields were determined by GC and GC-MS. b) 20 mg catalyst (0.26 mol-% active metal); c) The amount of ruthenium was 4.32 e^{-6} mol referring to the total active metal content of the Pd_2Ru@SiCN catalyst. d) Mixture of 6 mg Pd/C and 6 mg Ru/C (0.17 mol-% active ruthenium and 0.35 mol-% active palladium)

Tab. S3: Catalyst screening for the dehydrogenation of 9-ethyl-dodecahydrocarbazole (12H-NEC)

		Yields / %[a]					
No.	**Catalyst**	**NEC**	**4H-NEC**	**6H-NEC**	**8H-NEC**	**12H-NEC**	**H_2-Release / wt.-%**
1	Pd_2Ru@SiCN[b]	6	45	19	26	4	3.13
2	Pd_2Ru@SiCN	84	16	0	0	0	5.51
3	Ir@SiCN	0	1	10	9	80	0.41
4	Pd/C (10 %)[c]	17	69	0	12	2	3.89
5	Pd/SiO_2 (5 %)[c]	0	14	3	21	62	1.03
6	Ru/C (5 %)[c]	0	0	1	3	96	0.03
7	Ru/Al_2O_3 (5 %)[c]	0	0	1	1	98	0.01
8	Pd/C (10 %) + Ru/C (5 %)[d]	18	66	0	13	3	3.85

Reaction conditions: 2 mmol 12H-NEC, 0.52 mol-% active metal (referring to 40 mg Pd_2Ru@SiCN), 180 °C, neat, 7 h, Ar flow (4-6 mL/min). Yields were determined by GC and GC-MS. H_2-storage was calculated taking all the intermediate products into account. a) Yields were determined by GC and GC-MS. b) 20 mg catalyst (0.26 mol-% active metal); c) The amount of palladium was 4.32 e^{-6} mol referring to the total active metal content of the Pd_2Ru@SiCN catalyst. d) Mixture of 6 mg Pd/C and 6 mg Ru/C (0.17 mol-% active ruthenium and 0.35 mol-% active palladium).

8.6.4 Reversible Hydrogen Storage

Reversible hydrogen storage and catalyst reusability with the NEC system:

Hydrogenation: 1.0 g (5.12 mmol) NEC and 200 mg Pd_2Ru@SiCN (0.52 mol-% active metal) were given in a 250 mL stainless steel autoclave and flushed with hydrogen three times. A hydrogen pressure of 20 bar was adjusted and the reactor was heated to 110 °C for 36 h. After cooling to room temperature with an ice bath, a sample for GC and GC-MS was taken and the mixture was transferred to a 40 mL schlenk tube for dehydrogenation.

Dehydrogenation: The schlenk tube was evacuated and flushed with argon three times and placed in a preheated oil bath at 190 °C. The reaction temperature was measured to be 180 °C. A slight argon flow of 4-6 mL/min was adjusted. After 20 h the mixture was cooled to room temperature and a sample for by GC and GC-MS was taken. Afterwards the mixture was again transferred to a 250 mL stainless steel autoclave for hydrogenation. The exact product distributions can be found in **Tab. S4**.

Tab. S4: Catalyst reusability and catalytic H_2 storage with NEC

	Yields / %					
No.	**NEC**	**4H-NEC**	**6H-NEC**	**8H-NEC**	**12H-NEC**	**H_2-Release/Uptake / wt.-%**
1-H	0	0	0	1	99	5.78
2-De	98	2	0	0	0	5.74
3-H	0	1	0	1	98	5.72
4-De	100	0	0	0	0	5.74
5-H	0	0	1	3	96	5.71
6-De	99	1	0	0	0	5.69

Reaction conditions: 1.0 g (5.12 mmol) N-ethylcarbazole, 200 mg Pd/Ru@SiCN (0.52 mol-% active metal); Hydrogenation: 110 °C, 20 bar H_2, 36 h; Dehydrogenation: 181 °C, Ar flow (4-6 mL/min), 20 h; The hydrogen uptake and release values were calculated by GC and GC-MS analysis. The maximum hydrogen uptake or release is 5.8 wt.-%. Yields were determined by GC and GC-MS. H_2-storage was calculated taking all the intermediate products into account. The H_2-storage or release values are based on the H_2-storage or release of the former step.

Hydrogen release experiment

1.25 mmol 12H-NEC and 40 mg Pd_2Ru@SiCN were given in a 10 mL schlenk tube and the mixture was evacuated and flushed with argon for three times. Afterwards the argon pressure was released and the schlenk tube was placed in a pre-heated oil bath at 190 °C for 20 h. The hydrogen was collected by a water column.

Result: 172 mL (7.7 mmol) H_2 which refers to 88 % (5.10 wt.%) H_2 release could be collected. The GC and GC-MS results suggested a H_2 release of 89 % (5.16 wt.%).

Reversible hydrogen storage and catalyst reusability with the phenazine system

For our catalytic reactions we use the following nomenclature for the intermediate products:

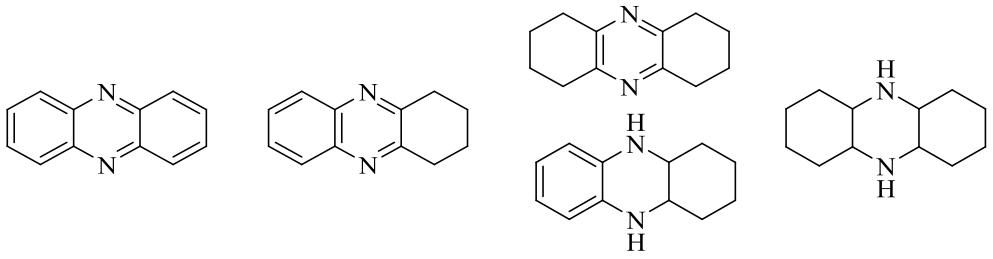

Phen 4H-Phen 8H-Phen 14H-Phen

Hydrogenation: A reaction vial containing a solution of 360 mg (2 mmol) phenazine and 70 mg Pd_2Ru@SiCN (0.46 mol-% active metal) in 2 mL dioxane and 0.5 mL water was given in a 250 mL stainless steel autoclave. The autoclave was flushed with hydrogen three times and a hydrogen pressure of 50 bar was adjusted. The reactor was heated to 115 °C for 24 h. After cooling to room temperature with an ice bath a sample for GC and GC-MS was taken and the mixture was transferred to a 20 mL schlenk tube.

Dehydrogenation: The solvents were removed under reduced pressure and 0.75 mL diglyme was added. The tube was evacuated and flushed with argon for three times and a slight argon flow of 4-6 mL/min was adjusted. The tube was placed in a preheated metal bath at 200 °C (190 °C reaction temperature). After 24 h the mixture was cooled to room temperature under argon atmosphere and a sample for GC and GC-MS analysis was taken. Afterwards the mixture was solved in dioxane/water again and transferred to a 250 mL stainless steel autoclave for hydrogenation.

The exact product distributions can be found in **Tab. S5**.

Tab. S5: Catalyst reusability and reversible hydrogen storage with phenazine

	Yields / %				
No.	**Phen**	**4H-Phen**	**8H-Phen**	**14H-NPhen**	**H_2-Release/Uptake / wt.-%**
1-H	0	0	15	85	6.77
1-De	100	0	0	0	6.77
2-H	0	0	5	95	7.05
2-De	94	6	0	0	6.94
3-H	0	4	17	79	6.35
3-De	99	1	0	0	6.42
4-H	0	0	9	91	6.85
4-De	77	0	23	0	5.81
5-H	0	0	5	95	5.93
5-De	93	0	7	0	6.70
6-H	0	0	6	94	6.66
6-De	99	1	0	0	7.01
7-H	0	1	3	96	7.08
7-De	90	0	10	0	6.56

Reaction conditions: 360 mg (2 mmol) phenazine, 70 mg Pd_2Ru@SiCN (0.46 mol-% active metal); Hydrogenation: 115 °C, 50 bar H_2, 2 mL dioxane, 0.5 mL water, 24 h; Dehydrogenation: 190 °C, 0.75 mL digylme, slight Ar flow (4-6 mL/min). The maximum hydrogen uptake or release is 7.2 wt.-%.The hydrogen uptake and release values were calculated by GC and GC-MS analysis. Yields were determined by GC and GC-MS. H_2-storage was calculated taking all the intermediate products into account. The H_2-storage or release values are based on the H_2-storage or release of the former step.

8.6.5 Catalytic Synthesis of Phenazine

Step 1: Reaction of cyclohexane-1,2-diol with ammonia and acceptorless dehydrogenation to 1,2,3,4,6,7,8,9-octahydrophenazine

In a 250 mL stainless steel autoclave 250 mg Ir@SiCN[6] was added to a solution of 2.32 g (20 mmol) cyclohexane-1,2-diol in 12 mL of degassed water. The reactor was flushed three times with ammonia, pressured to 5 bar and the reaction mixture was stirred at 105 °C. After 24 h the ammonia atmosphere was released and the reactor was again pressured with 5 bar ammonia and the reaction mixture was allowed to stir for another 24 h. After cooling to room temperature with an ice bath the mixture was extracted two times with 100 mL diethylether. The organic phase was reduced to the half and extracted with 150 mL of 0.1 M HCl. The water phase was basified with NaOH and extracted two times with 100 mL diethylether. The organic phase was dried over Na_2SO_4 and the solvent was removed giving the light yellow product in 74 % yield.

^{1}H NMR (300 MHz, $CDCl_3$, 298 K): δ = 2.88-2.84 (m, 8H), 1.86-1.90 (m, 8H) ppm. ^{13}C NMR (75 MHz, $CDCl_3$, 298 K): δ = 149.3, 31.6, 22.8 ppm.

elemental analysis (%) for $C_{12}H_{16}N_2$ calcd: C 76.55, H 8.57, N 14.88; found: C 75.54, H 8.54, N 14.16.

Step 2: Acceptorless dehydrogenation to phenazine

A mixture of 25 mg (0.33 mol-% active metal) Pd_2Ru@SiCN catalyst, 0.5 mL digylme and 188 mg (1.0 mmol) 1,2,3,4,6,7,8,9-octahydrophenazine was given in a 10 mL schlenk tube and evacuated and flushed with argon for two times. The schlenk tube was placed in a preheated metal bath at 200 °C (190 °C reaction temperature) for 20 h and a slight argon flow of 4-6 mL/min was adjusted. After cooling down under Ar atmosphere the catalyst was separated by centrifugation and washed three times with acetone. The centrifugates were combined and the solvent was removed under reduced pressure at 60 °C giving the yellow crystalline product in 99 % yield.

^{1}H NMR (300 MHz, $CDCl_3$, 298 K): δ = 8.29-8.23 (m, 4H), 7.88-7.82 (m, 4H) ppm. ^{13}C NMR (75 MHz, $CDCl_3$, 298 K): δ = 143.5, 130.5, 129.7 ppm.

NMR Spectra

1,2,3,4,6,7,8,9-octahydrophenazine

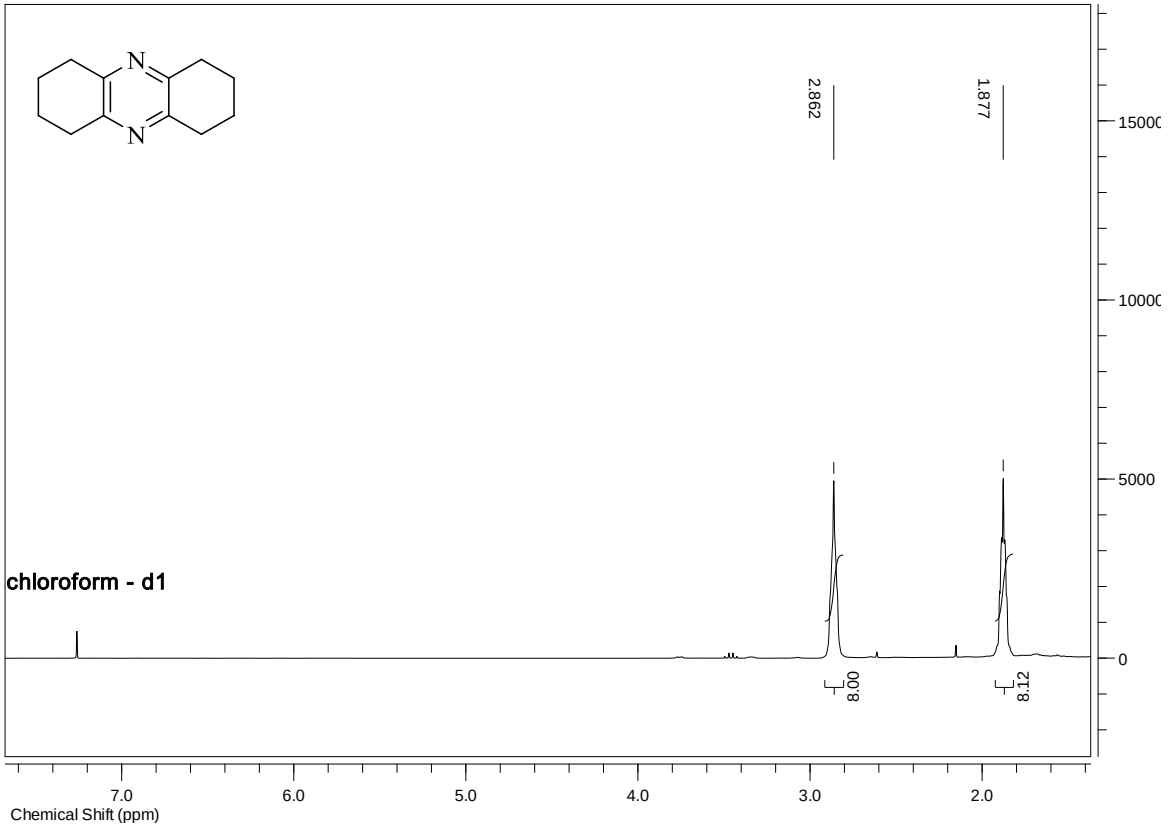

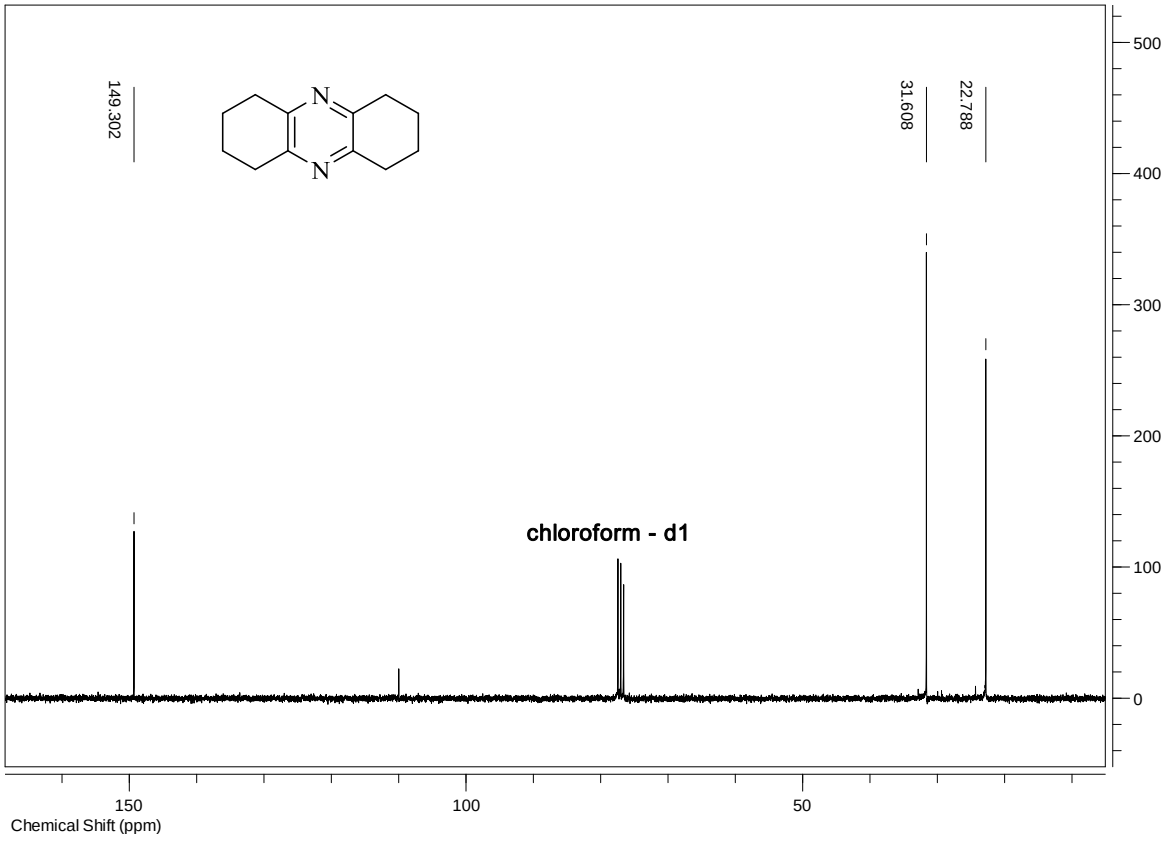

Phenazine

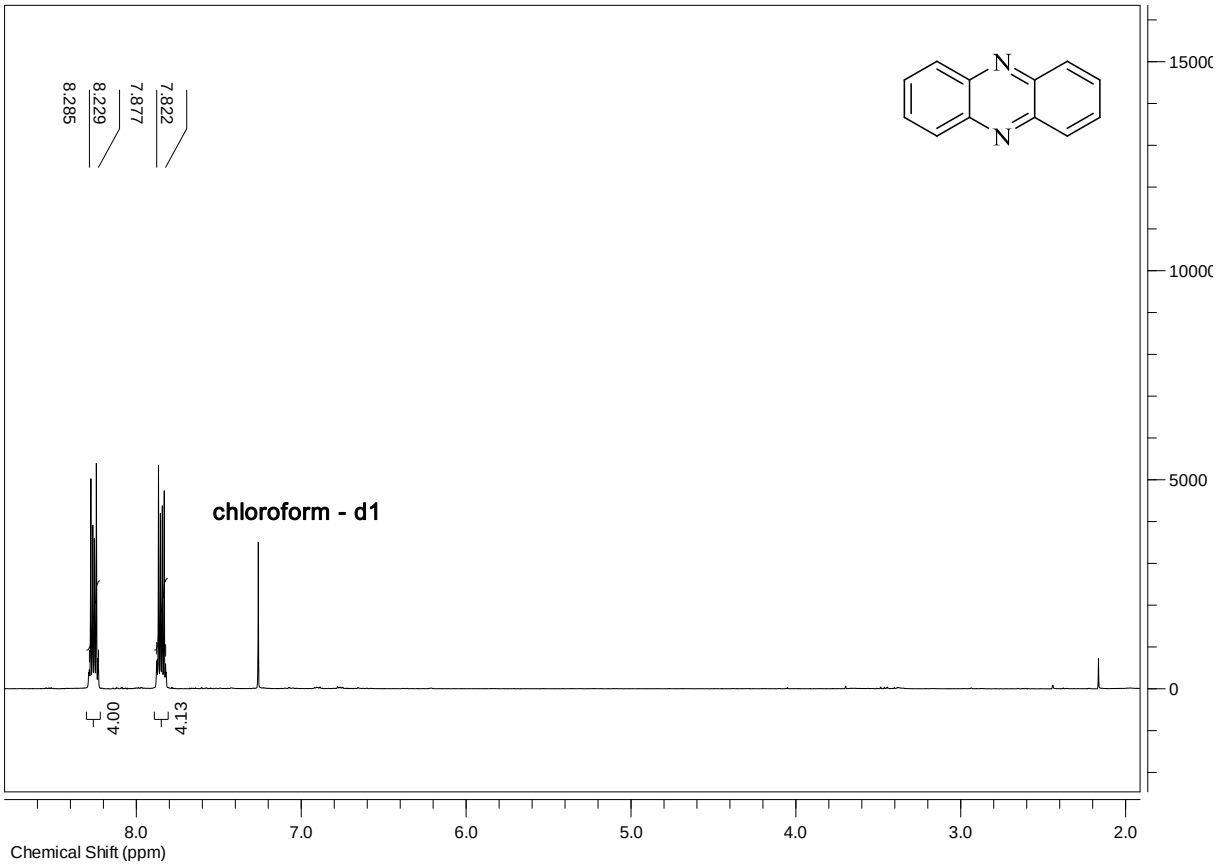
8.285
8.229
7.877
7.822
chloroform - d1
4.00
4.13
15000
10000
5000
0
8.0
7.0
6.0
5.0
4.0
3.0
2.0
Chemical Shift (ppm)

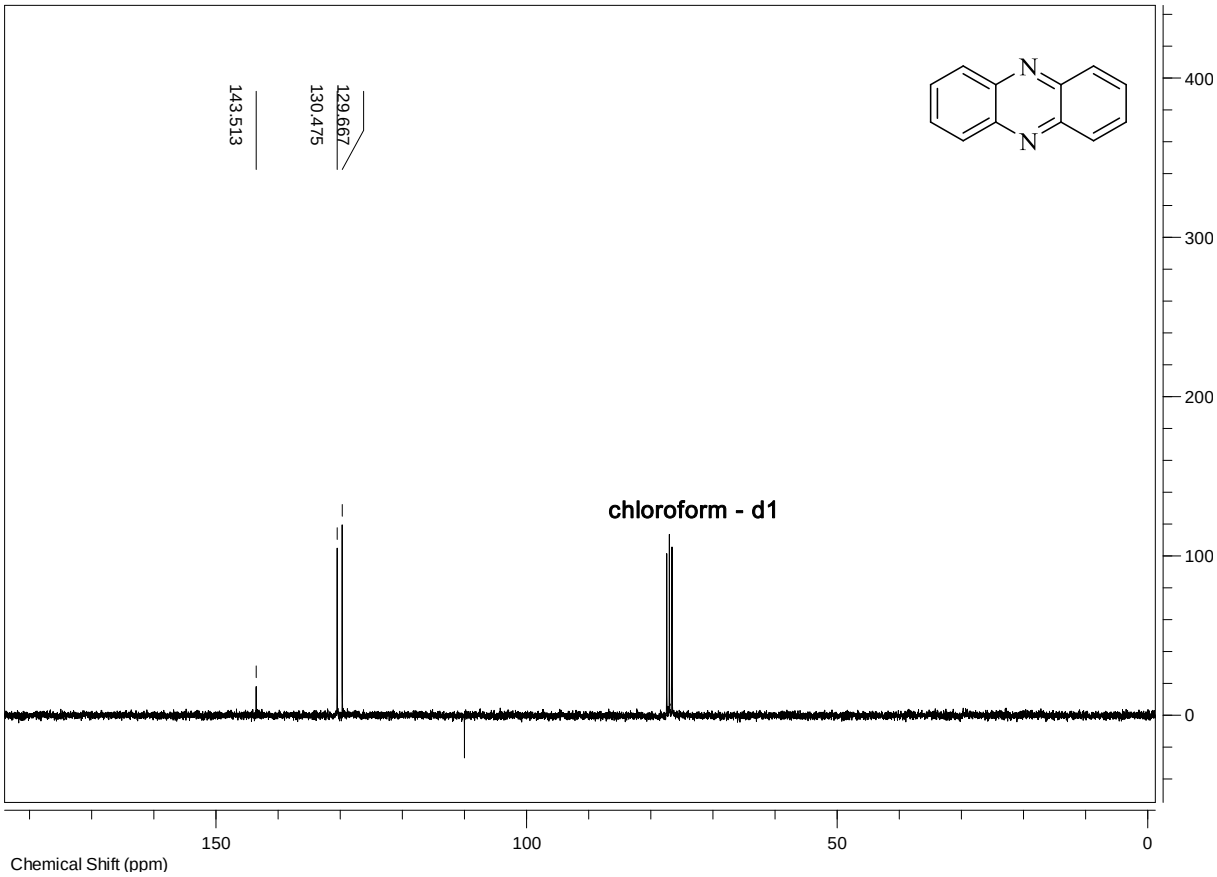
143.513
130.475
129.667
chloroform - d1
400
300
200
100
0
150
100
50
0
Chemical Shift (ppm)

8.6.6 References

[1] Altomare, *A.*, *et al. J. Appl. Crystallogr.* **32**, 115, (1999).

[2] Sheldrick, G. M. *Acta Crystallogr., Sect. A: Found Crystallogr.* **64**, 112, (2008).

[3] Kempe, R. & Arndt, P. Mononuclear titanium complexes that contain aminopyridinato ligands. *Inorg. Chem.* **35**, 2644-2649, (1996).

[4] Spannenberg, A.; Arndt, P. & Kempe, R. Yttrate-mediated ligand transfer and direct synthesis as a route to amidopalladium complexes. *Angew. Chem., Int. Ed.* **37**, 832-835 (1998).

[5] Wojdyr, M. Fityk: a general-purpose peak fitting program. *J. Appl. Cryst*. **43**, 1126-1128, (2010).

[6] Forberg, D.; Obenauf, J.; Friedrich, M.; Hühne, S.-M.; Mader, W.; Motz, G. & Kempe, R. The synthesis of pyrroles via acceptorless dehydrogenative condensation of secondary alcohols and 1,2-amino alcohols mediated by a robust and reusable catalyst based on nanometer-sized iridium particles. *Catal. Sci. Technol.* **4**, 4188-4192 (2014).

[7] Eblagon, K. M.; Rentsch, D.; Friedrichs, O.; Remhof, A.; Zuettel, A.; Ramirez-Cuesta, A. J. & Tsang, S. C. Hydrogenation of N-ethylcarbazole as prototype of a liquid hydrogen carrier. *Int. J. Hydrogen Energy* **35**, 11609– 11621 (2010).

9. List of Publications

The following publications have been published or are submitted or are to be submitted during the work on this thesis:

1. Daniel Forberg, Johannes Obenauf, Martin Friedrich, Sven-Martin Hühne, Werner Mader, Günter Motz, Rhett Kempe, *Catal. Sci. Technol.* **2014**, *4*, 4188-4192.

   The synthesis of pyrroles *via* acceptorless dehydrogenative condensation of secondary alcohols and 1,2-amino alcohols mediated by a robust and reusable catalyst based on nanometer-sized iridium particles.

2. Daniel Forberg, Muhammad Zaheer, Martin Friedrich, Wilfried Assenmacher, Werner Mader, Tobias Schmidt, Rodrigo Q. Albuquerque, Stephan Kümmel, Rhett Kempe, *submitted to Science and out for review.*

   The Sustainable Synthesis of Indoles, Carbazoles, Quinolines and Acridines via Catalytic Condensation of Phenols and Aminoalcohols or Aminophenols.

3. Daniel Forberg, Martin Friedrich, Nobuyoshi Miyajima, Rhett Kempe, *submitted to Nat. Commun. and out for review.*

   Single-catalyst high weight% hydrogen storage in a N-heterocycle synthesized from lignin hydrogenolysis products and ammonia.

10. Acknowledgements

I would like to thank my academic supervisor,

Prof. Dr. Rhett Kempe,

for giving me the opportunity to work on this very interesting subject. I am grateful for his constant interest in the progress of the work, for the numerous scientific discussions, and for the scientific independence he has granted me.

Furthermore, I want to thank Dr. Christine Denner for the great mentoring during the past five years, the REM and EDX measurements, the careful correction of this manuscript and for the help regarding my job application.

A great thank you goes to all my lab-mates, Julia-Katharina Ewert, Muhammad Zaheer, Saravanna Pillai, Sonja Fehn, Sabrina Sacchau, Stefan Schwarz, Tobias Schwob, and Gabriela Wietzel for the trouble-free time and great support in lab. Especially Stefan Schwarz requires a commendation for all the friday afternoon “saidlas” in the lab and the interesting scientific discussions resulting from them.

My special acknowledgment goes to Martin Friedrich for the measurements, discussions, and helpful support regarding TEM and HR-TEM measurements.

For the careful correction of this manuscript and the herein included publications as well as for many scientific discussions and technical hints I would like the thank Dr. Torsten Irrgang.

Of course I want to thank all other members of the ACII group for the great time, interesting discussions and helpful practical advises: Toni Hille, Nicklas Deibl, Stefan Michlik, Dr. Winfried Kretschmer, Dr. Awal Noor, Dr. Sadaf Qayyum, Sina Rößler, Susanne Ruch, Andreas Gollwitzer, Thomas Dietel, Dominik Tilgner, Sven Hafke, Markus Weise, and Alexander Wachter.

Moreover, I thank all the hard working stuff in the mechanic and glassblowing workshops. Anna Dietel, Simone Ott, Walter Kremnitz, and Heidi Maisel are acknowledged for providing dried solvents and other lab equipment as well as for many chemicals from the storage room and the enormous patience they had with me.

Furthermore, I want to thank all colleges from the other chairs here in Bayreuth for the good collaboration, appropriation of chemicals, and fast measurements of all samples: Dr. Günter Motz (Keramik), Dr. Wolfgang Milius (ACI), Sebastian Koch (ACI), Florian Puchtler (ACI), Thomas Wittmann (ACIII), Karl Kempf (OCI), Carmen Kunnert (PCI), Dr. Markus Drechsler (TEM), Sandra Ganzleben (MCI), and Dr.Gunter Ilgen (BayCEER).

Of course, I also want to acknowledge my friends here in Bayreuth for supporting me, useful and non-useful discussion during the coffee breaks and at the world famous Frankenstadion as well as some good advises: Christian Schulz, Toni Hille, Thomas Wittmann, Benedikt Neugirg, Jonas Schubert, Ottokar Klimm, and Mathias Schlenk.

My special thank go to my parents and to my family, who always motivated me and whose support I could always rely on. My grandma, Ingrid Fischer, gets an extra acknowledgement for moral and financial support during my study and my doctor thesis. Thank you grandma all this would not have been possible without you.

Finally and most importantly, I thank Judith Mehlhorn for her enormous patience, constant support and endless love as well as for the proof reading of the thesis. I love you Mausi.

11. Declaration/Erklärung

Der (Eidesstattliche) Versicherungen und Erklärungen

(§ 5 Nr. 4 PromO)

Hiermit erkläre ich, dass keine Tatsachen vorliegen, die mich nach den gesetzlichen Bestimmungen über die Führung akademischer Grade zur Führung eines Doktorgrades unwürdig erscheinen lassen.

(§ 8 S. 2 Nr. 5 PromO)

Hiermit erkläre ich mich damit einverstanden, dass die elektronische Fassung meiner Dissertation unter Wahrung meiner Urheberrechte und des Datenschutzes einer gesonderten Überprüfung hinsichtlich der eigenständigen Anfertigung der Dissertation unterzogen werden kann.

(§ 8 S. 2 Nr. 7 PromO)

Hiermit erkläre ich eidesstattlich, dass ich die Dissertation selbständig verfasst und keine anderen als die von mir angegebenen Quellen und Hilfsmittel benutzt habe.

(§ 8 S. 2 Nr. 8 PromO)

Ich habe die Dissertation nicht bereits zur Erlangung eines akademischen Grades anderweitig eingereicht und habe auch nicht bereits diese oder eine gleichartige Doktorprüfung endgültig nicht bestanden.

(§ 8 S. 2 Nr. 9 PromO)

Hiermit erkläre ich, dass ich keine Hilfe von gewerblichen Promotionsberatern bzw. -vermittlern in Anspruch genommen habe und auch künftig nicht nehmen werde.

…….

Ort, Datum, Unterschrift